



UNIVERSITAT DE  
BARCELONA

## Design and synthesis of heterocyclic compounds potentially antitumor by enzymatic inhibition

Enric Lizano Gispert



Aquesta tesi doctoral està subjecta a la llicència *Reconeixement- NoComercial – SenseObraDerivada 4.0. Espanya de Creative Commons.*

Esta tesis doctoral está sujeta a la licencia *Reconocimiento - NoComercial – SinObraDerivada 4.0. España de Creative Commons.*

This doctoral thesis is licensed under the *Creative Commons Attribution-NonCommercial-NoDerivs 4.0. Spain License.*



UNIVERSITAT DE  
BARCELONA

UNIVERSITAT DE BARCELONA

FACULTAT DE FARMÀCIA I CIÈNCIES DE L'ALIMENTACIÓ  
DEPARTAMENT DE FARMACOLOGIA, TOXICOLOGIA I QUÍMICA  
TERAPÈUTICA

**DESIGN AND SYNTHESIS OF HETEROCYCLIC COMPOUNDS  
POTENTIALLY ANTITUMOR BY ENZYMATIC INHIBITION**

ENRIC LIZANO GISPERT  
2020



UNIVERSITAT DE BARCELONA

FACULTAT DE FARMÀCIA I CIÈNCIES DE L'ALIMENTACIÓ  
DEPARTAMENT DE FARMACOLOGIA, TOXICOLOGIA I QUÍMICA  
TERAPÈUTICA

**DESIGN AND SYNTHESIS OF HETEROCYCLIC COMPOUNDS  
POTENTIALLY ANTITUMOR BY ENZYMATIC INHIBITION**

PROGRAMA DE DOCTORAT DE QUÍMICA ORGÀNICA

Memòria presentada per Enric Lizano Gispert per optar al títol de  
doctor per la Universitat de Barcelona

Directora de la tesis

Doctorand

Dra. M. Dolors Pujol Dilmé

Enric Lizano Gispert

ENRIC LIZANO GISPERT, 2020







UNIVERSITAT DE  
BARCELONA

## DESIGN AND SYNTHESIS OF HETEROCYCLIC COMPOUNDS POTENTIALLY ANTITUMOR BY ENZYMATIC INHIBITION

Memòria presentada per **Enric Lizano Gispert**, graduat en Farmàcia per la Universitat de Barcelona, per optar al grau de doctor per la Universitat de Barcelona

El projecte de tesi doctoral es troba inscrit en el **Departament de Farmacologia, Toxicologia i Química Terapèutica** de la Facultat de Farmàcia. El treball experimental i la redacció de la memòria que es presenta han estat dirigits per la doctora **M. Dolors Pujol Dilmé**

Barcelona 5 de Març de 2020

Directora de la tesi

Doctorand

Dra. M. Dolors Pujol Dilmé

Enric Lizano Gispert



## AGRAÏMENTS

Aquest treball és el resultat de quatre anys de perseverança i dedicació a un projecte que m'ha aportat tan coneixements científics, propis de la recerca duta a terme, com coneixements transversals i habilitats essencials com la constància, la comprensió, la empatia, el treball en equip i sobretot molta paciència.

Tot i que al llarg d'aquests anys hi han hagut moments de patiment i de preocupació, aquesta experiència em quedarà marcada pels grans moments de felicitat, d'alegria i per la gran família que tenim dins del laboratori, que sense la seva col·laboració no hagués estat possible.

A la primera persona a la que voldria agrair per la seva dedicació i esforç, donant-me la oportunitat de poder realitzar aquesta tesis doctoral i per tant, sense ella res hagués estat possible: la Dra. Dolors Pujol. Gràcies a la seva gran capacitat investigadora i per la seva gran qualitat humana, he pogut realitzar una enriquidora experiència tant científica com personal. Vull transmetre-li de tot cor tota la meva admiració per la seva empatia, constància, paciència, el seu esforç, per la capacitat d'escoltar, d'ensenyar i sobretot per no rendir-se mai. També voldria agrair-li tots els consells i la ajuda que m'ha donat, sempre disposada a escoltar-me i a mirar el millor per mi. Gràcies de tot cor per totes les oportunitats que m'has donat i per ajudar-me a créixer professionalment i personalment.

En segon lloc, m'agradaria agrair-li al Dr. Francis S. Willard, a la Dra. Marta Piñeiro per donar-me la oportunitat d'haver treballat als laboratoris Eli Lilly & Company a Indianapolis i posar a la meua disposició els mitjans necessaris per formar-me en el camp de la biologia quantitativa. Al Dr. Francis Willard, agrair-li la seva confiança i la seva actitud positiva, sempre obert a nous reptes. A la Dra. Marta Piñeiro agrair-li el seu temps i la seva confiança.

Al llarg d'aquests anys de doctorat he tingut el plaer de compartir el dia a dia en el laboratori de Química farmacèutica amb la Dra. Laura Grau, la Dra. Lorena Navarro, la Dra. Patricia Mateo, la Dra. Lucia Acedo, la Marta Vilaplana, el Miquel Viñas i el Dani Jahani. A la Dra. Laura Grau agrair-li tot el que m'ha ensenyat. A la Dra. Lorena Navarro, per ser un referent dins i fora del laboratori i proporcionar sempre un ambient agradable, una gran professional i una gran persona. A la Dra. Patricia Mateo, agrair-li totes les experiències viscudes i pels seus consells, ja que amb il·lusió, motivació i el treball en equip, tot és més amè i gratificant. A la Dra. Lucia Acedo per la seva visió de la vida i la tranquil·litat enfront als reptes. A la Marta Vilaplana, companya desde l'inici d'aquest viatge, per la seva alegria, per la seva motivació i inquietuts, per tots els moments que hem viscut, ajudant-nos a superar els obstacles quan ha estat necessari i sobretot a riure plegats, sense ella al costat aquest viatge hagués estat ben diferent.

Al Miquel Viñas, animar-lo a seguir pel mateix camí, amb la seva intel·ligència i serenor segur que arribaràs on et proposis. Al Dani, animar-lo també a continuar treballant ben dur en el laboratori i donar-li els millors desitjos.

De la mateixa manera, m'agradaria recalcar la participació en aquest treball de Jorge Baladón, Amelia Morantin, Ariadna Martin, Josep Grima, Marina Cervera, Alexandre Chabrit i a la Elena Haro, sense els quals no hagués pogut obtenir tots els resultats inclosos en aquesta memòria.

Gràcies a la Dra. Núria Mur, al Dr. Arturo Vinuesa, a la Dra. Lorena Navarro i a la Dra. Vanessa Prieur per haver realitzat el valuós treball previ, ajudant a encaminar aquest projecte.

Agrair a la meva família i en especial als meus pares, Marcel Lizano, Ana M. Gispert, als meus germans, Marcel i Anna, i als que considero també germans, a la Maria i a l'Adrià, pels valors que m'han transmès, la educació que m'han donat, estant sempre presents, ajudant-me a seguir endavant amb optimisme, seguretat i sempre conscients de que voler és poder. Sou el far que em guia.

A la Núria Boixareu, per la seva paciència, pel seu afecte, per estar sempre al meu costat i fer d'aquesta vida una alegria constant. I a la Dolors Balagué, partícep d'aquest llarg camí, per cuidar-me, escoltar-me i ajudar-me sempre a créixer.

Gràcies,

*"Where there is a will, there is a way"*  
Pauline Kael

## ABBREVIATIONS

ABC: ATP binding cassette  
AC: Adenylyl cyclase  
ACN: Acetonitril/ Acetonitrile  
AcOEt: Acetat d'etil / Ethyl acetate  
ADN/DNA: Àcid desoxiribonucleic / Deoxyribonucleic acid  
ALDH: Aldehyde dehydrogenase (ALDH)  
APTS: Àcid *para*-toluensulfònic / *para*-toluenesulfonic acid  
ATP: Adenosine triphosphate  
ARN/RNA: Àcid ribonucleic / Ribonucleic acid  
BIM: BCL2-like 11  
BINAP: (2,2'-*bis*(difenilfosfino)-1,1'-binaftil)/(2,2'-*bis*(diphenylphosphino)-1,1'-binaphthyl)  
BNIP3: BCL2 interacting protein 3  
CAF: Cancer associated fibroblast  
CCs: Cancer cells  
CD73: Cluster of differentiation 73  
CDI: 1,1'-Carbonyldiimidazol / 1,1'-Carbonyldiimidazole  
CDK: Cyclin dependent kinases  
CDR: Cancer drug resistance  
CRC: Concentration response curve  
CRE: cAMP response element  
CREB: cAMP response element binding  
CSA: Cyclosporine A  
CSC: Cancer stem cells  
CSF-1R: Colony stimulating factor-1 receptor  
CTF: C-terminal fragment  
DAG: Diacylglycerol  
DALYs: Disability-adjusted life years  
DCM: Diclorometà / Dichloromethane  
DDR: DNA damage repair  
DEAD: Dietilazodicarboxilat / Diethyl azodicarboxylate  
DHFR: Dihydrofolate reductase  
DMF: Dimetilformamida / Dimethylformamide  
DMSO: Dimetilsulfòxid / Dimethyl sulfoxide  
DOX: Doxorubicin  
ECD: Extracellular domain  
ECM: Extracellular matrix  
EGFR: Epidermal growth factor receptor  
EMT: Epithelial mesenchymal transition  
EOM: Etiloximetil / Ethyloximethyl  
Eq: Equivalents  
ESI: Ionització per electrospai / Electrospray ionization  
EtOH: Etanol / Ethanol  
FDA: *Food and Drug Administration*  
GAIN: GPCR autoproteolytic-inducing  
GPCRs: G protein coupled receptors  
GPS: GPCR proteolytic site  
GRKs: GPCR kinases  
GTP: Guanosine triphosphate  
h: Hores / Hours  
HCC: Hepatocellular carcinoma  
HER<sub>2</sub>: Human epidermal growth factor receptor 2

HGNC: *Human Gene Nomenclature Committee*  
HIV/AIDS: Human immunodeficiency virus infection / acquired immune deficiency syndrome  
hNNMT: Human nicotinamide *N*-methyltransferase  
HRMS: High resolution mass spectrometry  
HUGO: *Human Genome Organization*  
IC<sub>50</sub>: Half maximal inhibitory concentration  
ID: Intracellular domain  
IP<sub>3</sub>: Inositol trisphosphate  
LDA: Diisopropilamida de liti / Lithium diisopropylamide  
LTβ: Lymphotoxin-β  
*m*-CPBA: àcid *meta*-chloroperoxibenzoic / *meta*-chloroperoxybenzoic acid  
MDR-1: Multidrug resistance 1  
MeOH: Metanol / Methanol  
MNA: 1-Methylnicotinamide  
MOM: Metiloximetil/ Methyloximethyl  
Mp: Meltig point  
MTB: *Mycobacterium tuberculosis*  
MW: Microones / Microwave  
NAD: Nicotinamide adenine dinucleotide  
NBS: *N*-bromosuccinimida / *N*-bromosuccinimide  
NCS: *N*-clorosuccinimida / *N*-chlorosuccinimide  
ncRNA: non-codingRNA  
NIS: *N*-iodosuccinimida / *N*-iodosuccinimide  
NSCLC: Non-small-cell lung carcinoma  
NTF: N-terminal fragment  
PASS: *Prediction of Activity Spectra for Substance*  
P-gp: P-glycoprotein  
PIP2: Phosphatidylinositol 4,5-bisphosphate  
PKA: cAMP-dependent protein kinase  
PKC: Protein kinase C  
QSAR: *Quantity Structure-Activity Relationship*  
QSPR: *Quantity Structure-Property Relationship*  
QSRR: *Quantity Structure-Reactivity Relationship*  
RBP2: Retinoblastoma-binding protein 2  
Rf: Factor de retenció / retention factor  
RGS: Regulators of G protein signaling  
RMN/NMR: Resonància magnètica nuclear / Nuclear magnetic resonance  
ROS: Reactive oxygen species  
SP: Single point  
t.a./r.t.: Temperatura ambient / room temperature  
TAM: Tumor associated macrophage  
TB: Tuberculosis  
TDs: Tropical diseases  
TFA: Àcid trifluoroacètic / Trifluoroacetic acid  
TGF: Tumor growth factor  
THF: Tetrahydrofuran / Tetrahidrofurà  
TKIs: Tyrosine kinase inhibitors  
TLC: Thin layer chromatography  
TM: Transmembrane  
TME: Tumor microenvironment  
TNF: Tumor necrosis factor  
WHO: *World Health Organization*



## RESUM

La present tesi doctoral està enfocada a la investigació i desenvolupament de nous compostos dirigits a diferents dianes implicades en el càncer i en malalties tropicals. La resistència al tractament, tant en càncer com en malalties tropicals, és una barrera que en els últims anys està portant a la comunitat científica a investigar noves tècniques de diagnòstic, a millorar en la seqüenciació genòmica, així com en el desenvolupament de nous tractaments com la síntesis de noves petites molècules per exemple. L'entramat dels processos fisiològics que condueixen a la resistència als fàrmacs i/o a la radioteràpia és complexa i per aquets motiu la personalització dels tractaments és un concepte creixent i necessari per millorar el pronòstic dels pacients.

Per tant, es busca la síntesis de compostos que actuïn sobre més d'una diana i amb selectivitat per disminuir els efectes adversos i augmentar l'eficàcia del tractament.

D'aquesta manera, s'han posat a punt dues rutes sintètiques diferents: la primera, agafant com a nucli principal l'1-espiro[benzodioxole-2,4'-piperidina], a partir del qual s'obté una gran varietat de compostos. La segona ruta, la preparació de derivats de pirrolo[2,3-*b*]pirazines, obtenint així anàlegs de purines i pirimidines. Aquests compostos s'han desenvolupat mitjançant reaccions clàssiques de la química orgànica, han estat purificats mitjançant tècniques de separació (cromatografia) i s'ha dut a terme l'elucidació estructural corresponent per a cadascun d'ells.

Amb la finalitat d'avaluar els compostos en diferents dianes terapèutiques, els laboratoris Eli Lilly han dut a terme un cribratge d'elevat rendiment en múltiples dianes implicades en càncer, malalties tropicals, diabetis, entre d'altres. A més, s'han realitzat assajos biològics quantitius per tal de caracteritzar els aGPCRs, receptors involucrats en diferents desordres com el càncer i malalties cardiovasculars, aportant informació necessària per a la seva cristal·lització i poder estudiar-los com a noves dianes.

## ABSTRACT

This doctoral thesis is focused on the investigation and development of new compounds directed to different cancer and tropical diseases targets. Drug resistance, as well in cancer as in tropical diseases, is a hurdle which in the latest years it is driving the scientific community to investigate in new diagnostic techniques, to improve in genomic sequencing, as well as to develop new treatments through the synthesis of new small molecules, for example. The physiologic framework, that drives to resistance, is complex and for this reason, personalized treatments is an increasing concept and needed in order to improve the prognostic of the patients.

Therefore, we are looking for compounds acting on multiple targets, with selectivity to diminish the adverse effects and increase the treatments efficacy.

Two different synthetic routes have been carried out: the first, taking as a main nucleus the 1-spiro[benzodioxole-2,4'-piperidine], from which a wide variety of derivatives was obtained. The second route is the preparation of pirrolo[2,3-*b*]pyrazine derivatives, then obtaining a purine and pyrimidine analogues. All compounds were developed through classical chemistry reactions, purified by means of separation techniques (chromatography), and their structural elucidation was accomplished for every one of them. In order to test the compounds in different therapeutic targets, Eli Lilly laboratories have undertaken a high throughput screening in several targets related with cancer, tropical diseases, diabetes, amongst others. In addition, quantitative biological assays have been made to characterize aGPCRs, the receptors involved in different disorders such as cancer or cardiovascular diseases, providing information needed for their crystallization and their study as a new targets.

# INDEX

1. INTRODUCTION .....	1
1.1. CANCER .....	1
1.1.1. EPIDEMIOLOGY OF CANCER .....	2
1.1.2. PREVENTION AND TREATMENT.....	5
1.1.3. DIFFICULTIES IN CANCER TREATMENT .....	6
1.1.3.1. CELL MECHANISMS FOR DRUG RESISTANCE .....	9
1.2. DRUGS REPURPOSING.....	19
1.3. PREDICTION OF ACTIVITY PROGRAMS.....	21
1.4. TROPICAL DISEASES (TDs).....	25
1.4.1. CHAGAS DISEASE .....	26
1.4.2. MALARIA .....	28
1.4.3. TUBERCULOSIS .....	30
1.5. PREVIOUS WORK .....	32
1.5.1. SPIRO DERIVATIVES .....	32
1.5.2. PIRROLOPYRAZINES.....	33
2. OBJECTIVES.....	35
2.1. FIRST OBJECTIVE.....	35
2.2. SECOND OBJECTIVE .....	37
2.3. THIRD OBJECTIVE.....	38
3. THEORICAL DISCUSSION .....	39
3.1. CHEMICAL DISCUSSION .....	39
3.1.1. Preparation of 1-spiro[benzodioxole-2,4'-piperidine] .....	39
3.1.1.1. Preparation of <i>N</i> -acetyl-spiro[1,3-benzodioxole-2,4'-piperidine] ( <b>1</b> ) .....	39
3.1.1.2. Preparation of 1',5-diacetyl-spiro[benzo[1,3]dioxole-2,4'-piperidine] ( <b>2</b> ) and 5-acetyl-spiro[benzo[1,3]dioxole-2,4'-piperidine] ( <b>3</b> ) .....	40
3.1.1.3. Preparation of 1'-acetyl-5-(1-(hydroxyimino)ethyl)spiro[benzo[1,3]dioxole-2,4'-piperidine] ( <b>4</b> ).....	40
3.1.1.4. Preparation of 1'-acetyl-5-(1-hydroxyethyl)spiro[benzo[1,3]dioxole-2,4'-piperidine]( <b>5</b> ) ..	42
3.1.1.5. Preparation of 1'-acetyl-5-bromospiro[benzo[1,3]dioxole-2,4'-piperidine] ( <b>6</b> ).....	42
3.1.1.6. Preparation of <b>7</b> .....	43
3.1.1.7. Preparation of <b>8</b> to <b>11</b> .....	45
3.1.1.8. Preparation of 1-acetyl-5-nitro-spiro[benzodioxole-2,4'-piperidine] ( <b>12</b> ) and <b>13</b> .....	49
3.1.1.9. Preparation of 5-nitro-1'-(4-nitrophenyl)spiro[benzo[1,3]dioxole-2,4'-piperidine] ( <b>14</b> ) ...	50
3.1.1.10. Preparation of spiro[benzo[1,3]dioxole-2,4'-piperidine] ( <b>16</b> ) and the 1'-(4-nitrophenyl)spiro[benzo[1,3]dioxole-2,4'-piperidine] ( <b>17</b> ).....	51
3.1.1.11. Preparation of <b>18</b> and <b>20</b> .....	53

3.1.1.12. Preparation of 1-(1'-(4-nitrophenyl)spiro[benzo[1,3]dioxole-2,4'-piperidine]-5-yl)ethan-1-ol ( <b>21</b> ) and 1-(1'-(4-aminophenyl)espiro[benzo[1,3]dioxole-2,4'-piperidine]-5-yl)ethan-1-ol ( <b>22</b> ).	55
3.1.1.13. Preparation of <b>23</b> to <b>26</b> .....	57
3.1.1.14. Preparation of <b>27</b> to <b>36</b> .....	59
3.1.1.15. Preparation of ureas <b>37-42</b> .....	64
3.1.1.16. Preparation of 1'-acetyl-1-(3 <i>H</i> -spiro[benzoxazole-2,4'-piperidine]) ( <b>43</b> ) and 1',3,6-triacetyl-1-(spiro[benzoxazole-2,4'-piperidine]) ( <b>44</b> ) .....	70
3.1.2. Preparation of pyrrole[2,3- <i>b</i> ]pyrazines .....	71
3.1.2.1. Preparation of 2-amino-3,5-dibromopyrazine ( <b>91c</b> ).....	74
3.1.2.2. Preparation of pyrrole[2,3- <i>b</i> ]pyrazine.....	78
3.1.2.3. Preparation of derivatives 2,6-diphenyl-5 <i>H</i> -pyrrole[2,3- <i>b</i> ]pyrazines <b>47-52</b> .....	81
3.1.2.4. Preparation of arylated derivatives at positions C-3 and C-7 .....	83
3.1.2.5. Protection of pyrrole NH, arylation of pyrrole[2,3- <i>b</i> ]pyrazines .....	85
3.1.3. Characterization results of the synthesized compounds .....	93
3.1.3.1. Analysis of 1-spiro[benzodioxole-2,4'-piperidines] .....	93
3.1.3.1. Analysis of pyrrole[2,3- <i>b</i> ]pyrazines .....	97
3.2. BIOLOGICAL DISCUSSION .....	100
3.2.1. ONCOLOGY.....	100
3.2.2. IMMUNOLOGY .....	110
3.2.3. TROPICAL DISEASES AND NEGLECTED.....	112
3.2.4. NEURODEGENERATION AND PAIN .....	119
3.2.5. ENDOCRINE/CARDIOVASCULAR .....	123
3.2.6. ELANCO ANIMAL HEALTH.....	126
3.3. DISCOVERING NEW TARGETS- Quantitative Biology in Eli Lilly & Company .....	127
3.3.1. G-PROTEIN COUPLED RECEPTORS (GPCRs) .....	127
3.3.2. ADHESION GPCRs .....	129
3.3.3. CHARACTERIZATION of 33 ADHESION GPCRs .....	136
4. EXPERIMENTAL PART .....	141
4.1. ORGANIC CHEMISTRY LABORATORY MATERIALS AND METHODS.....	141
4.2. Preparation of 1-spiro[benzodioxole-2,4'-piperidine].....	142
4.2.1. Preparation of <i>N</i> -acetyl-spiro[1,3-benzodioxole-2,4'-piperidine] ( <b>1</b> ) .....	142
4.2.2. Preparation of 1',5-diacetyl-spiro[benzo[1,3]dioxole-2,4'-piperidine] ( <b>2</b> ).....	143
4.2.3. Preparation of 5-acetyl-spiro[benzo[1,3]dioxole-2,4'-piperidine] ( <b>3</b> ).....	144
4.2.4. Preparation of 1'-acetyl-5-(1-(hydroxyimino)ethyl)spiro[benzo[1,3]dioxole-2,4'-piperidine] ( <b>4</b> ).....	145
4.2.5. Preparation of 1'-acetyl-5-(1-hydroxyethyl)spiro[benzo[1,3]dioxole-2,4'-piperidine]( <b>5</b> ) ...	146
4.2.6. Preparation of 1'-acetyl-5-bromospiro[benzo[1,3]dioxole-2,4'-piperidine] ( <b>6</b> ).....	147
4.2.7. Preparation of 1'-acetyl-5-( <i>p</i> -tolyl)spiro[benzo[1,3]dioxole-2,4'-piperidine] ( <b>7</b> ) .....	148

4.2.8. Preparation of 1'-acetyl-5-(4-nitrophenyl)spiro[benzo[1,3]dioxole-2,4'-piperidine] ( <b>8</b> ) ....	149
4.2.9. Preparation of 1'-acetyl-5-((4-aminophenyl)amino)spiro[benzo[1,3]dioxole-2,4'-piperidine] ( <b>9</b> ).....	150
4.2.10. Preparation of 4-((1'-acetylspiro[benzo[1,3]dioxole-2,4'-piperidine]-5-yl)amino)benzonitrile ( <b>10</b> ).....	151
4.2.11. Preparation of 1'-acetyl-5-((3-phenoxyphenyl)amino)spiro[benzo[1,3]dioxole-2,4'-piperidine] ( <b>11</b> ) .....	152
4.2.12. Preparation of 1'-acetyl-5-nitrospiro[benzo[1,3]dioxole-2,4'-piperidine] ( <b>12</b> ).....	153
4.2.13. Preparation of 5-nitrospiro[benzo[1,3]dioxole-2,4'-piperidine] ( <b>13</b> ).....	154
4.2.14. Preparation of 5-nitro-1'-(4-nitrophenyl)spiro[benzo[1,3]dioxole-2,4'-piperidine] ( <b>14</b> ) ..	155
4.2.15. Preparation of 1'-(4-aminophenyl)spiro[benzo[1,3]dioxole-2,4'-piperidine]-5-amine ( <b>15</b> ) .....	156
4.2.16. Preparation of 1'-(4-nitrophenyl)spiro[benzo[1,3]dioxole-2,4'-piperidine] ( <b>16</b> ) .....	157
4.2.17. Preparation of 5-acetyl-1'-(4-nitrophenyl)spiro[benzo[1,3]dioxole-2,4'-piperidine] ( <b>17</b> )	158
4.2.18. Preparation of 5-acetyl-1'-(4-nitrophenyl)spiro[benzo[1,3]dioxole-2,4'-piperidine] ( <b>17</b> )	159
4.2.19. Preparation of 1-(1'-(4-nitrophenyl)spiro[benzo[1,3]dioxole-2,4'-piperidine]-5-yl)ethanone oxime ( <b>18</b> ) .....	159
4.2.20. Preparation of N-(1'-(4-nitrophenyl)spiro[benzo[1,3]dioxole-2,4'-piperidine]-5-yl)acetamide ( <b>19</b> ).....	160
4.2.21. Preparation of 1'-(4-nitrophenyl)spiro[benzo[1,3]dioxole-2,4'-piperidine]-5-amine ( <b>20</b> )	161
4.2.22. Preparation of 1-(1'-(4-nitrophenyl)spiro[benzo[1,3]dioxole-2,4'-piperidine]-5-yl)ethanol ( <b>21</b> ).....	163
4.2.23. Preparation of 1-(1'-(4-aminophenyl)spiro[benzo[1,3]dioxole-2,4'-piperidine]-5-yl)ethanol ( <b>21</b> ).....	164
4.2.24. Preparation of 5-acetyl-1'-(4-aminophenyl)spiro[benzo[1,3]dioxole-2,4'-piperidine] ( <b>23</b> ) .....	165
4.2.25. Preparation of 2-(4-(5-acetylspiro[benzo[1,3]dioxole-2,4'-piperidine]-1'-yl)phenyl)isoindoline-1,3-dione ( <b>24</b> ) .....	166
4.2.26. Preparation of 2-(4-(5-(1-hydroxyethyl)spiro[benzo[1,3]dioxole-2,4'-piperidine]-1'-yl)phenyl)isoindoline-1,3-dione ( <b>25</b> ) .....	167
4.2.27. Preparation of 3-((4-(5-acetylspiro[benzo[1,3]dioxole-2,4'-piperidine]-1'-yl)phenyl)amino)furan-2,5-dione ( <b>26</b> ).....	168
4.2.28. Preparation of 5-acetyl-1'-(phenylsulfonyl)spiro[benzo[1,3]dioxole-2,4'-piperidine] ( <b>27</b> )	169
4.2.29. Preparation of 5-acetyl-1'-tosylspiro[benzo[1,3]dioxole-2,4'-piperidine] ( <b>28</b> ).....	170
4.2.30. Preparation of 1-(1'-(phenylsulfonyl)spiro[benzo[1,3]dioxole-2,4'-piperidine]-5-yl)ethan-1-ol ( <b>29</b> ).....	171
4.2.31. Preparation of 5-(1-chloroethyl)-1'-tosylspiro[benzo[1,3]dioxole-2,4'-piperidine] ( <b>32</b> )...	172
4.2.32. Preparation of <i>N,N</i> -diethyl-2-(1-(1'-(phenylsulfonyl)spiro[benzo[1,3]dioxole-2,4'-piperidine]-5-yl)ethoxy)ethan-1-amine ( <b>33</b> ).....	173
4.2.33. Preparation of <i>N,N</i> -dimethyl- <i>N</i> -(1-(1'-tosylspiro[benzo[1,3]dioxole-2,4'-piperidine]-5-yl)ethyl)ethane-1,2-diamine ( <b>34</b> ) .....	174

4.2.34. Preparation of <i>N,N</i> -dimethyl- <i>N</i> -(1-(1'-(phenylsulfonyl)spiro[benzo[1,3]dioxole-2,4'-piperidine]-5-yl)ethyl)ethane-1,2-diamine ( <b>34</b> ).....	175
4.2.35. Preparation of <i>N</i> -(1-(1'-tosylspiro[benzo[ <i>d</i> ][1,3]dioxole-2,4'-piperidine]-5-yl)ethyl)hexan-1-amine ( <b>35</b> ).....	176
4.2.36. Preparation of 2-((4-(5-(1-(2-hydroxyethoxy)ethyl)spiro[benzo[1,3]dioxole-2,4'-piperidine]-1'-yl)phenyl)amino)ethanol ( <b>36</b> ).....	177
4.2.37. Preparation of 1-(4-(5-acetylspiro[benzo[1,3]dioxole-2,4'-piperidine]-1'-yl)phenyl)-3-(2-fluoro-5-(trifluoromethyl)phenyl)urea ( <b>37</b> ).....	178
4.2.38. Preparation of 1-(2-fluoro-5-(trifluoromethyl)phenyl)-3-(4-(5-(1-hydroxyethyl)spiro[benzo[1,3]dioxole-2,4'-piperidine]-1'-yl)phenyl)urea ( <b>38</b> ).....	179
4.2.39. Preparation of 1-ethyl-3-(4-(5-(1-hydroxyethyl)spiro[benzo[1,3]dioxole-2,4'-piperidine]-1'-yl)phenyl)urea ( <b>39</b> ).....	180
4.2.40. Preparation of 1-(pyridin-3-yl)-3-(4-(5-(3-(pyridin-3-yl)ureido)spiro[benzo[1,3]-dioxole-2,4'-piperidine]-1'-yl)phenyl)urea ( <b>40</b> ).....	181
4.2.41. Preparation of 1-ethyl-3-(4-(5-(3-ethylureido)spiro[benzo[1,3]dioxole-2,4'-piperidine]-1'-yl)phenyl)urea ( <b>41</b> ).....	182
4.2.42. Preparation of 1-(4-((1'-acetylspiro[benzo[1,3]dioxole-2,4'-piperidine]-5-yl)-amino)phenyl)-3-(4-chloro-3-(trifluoromethyl)phenyl)urea ( <b>42</b> ).....	183
4.2.43. Preparation of 1'-acetyl-3 <i>H</i> -spiro[benzoxazole-2,4'-piperidine] ( <b>43</b> ).....	184
4.2.44. Preparation of 1'-acetyl-3 <i>H</i> -spiro[benzoxazole-2,4'-piperidine] ( <b>43</b> ).....	185
4.2.45. Preparation of 1,1'-(3 <i>H</i> -spiro[benzoxazole-2,4'-piperidine]-1',5'-diyl)bis(ethanone) ( <b>44</b> )	185
4.2.46. Preparation of 1'-acetyl-5-(4-nitrophenoxy)spiro[benzo[1,3]dioxole-2,4'-piperidine] ( <b>64</b> )	186
4.2.47. Preparation of 1'-acetyl-5-(piperazin-1-yl)spiro[benzo[1,3]dioxole-2,4'-piperidine] ( <b>67</b> )	187
4.2.48. Preparation of 1'-acetyl-5-(3-acetyl-1 <i>H</i> -indol-1-yl)spiro[benzo[1,3]dioxole-2,4'-piperidine] ( <b>69</b> ).....	188
4.2.49. Preparation of spiro[benzo[1,3]dioxole-2,4'-piperidine] ( <b>71</b> ).....	188
4.2.50. Preparation of 1'-(4-nitrophenyl)spiro[benzo[1,3]dioxole-2,4'-piperidine]-5-yl acetate ( <b>72</b> )	189
4.2.51. Preparation of 5-(1-bromoethyl)-1'-(4-nitrophenyl)spiro[benzo[1,3]dioxole-2,4'-piperidine] ( <b>74</b> ).....	190
4.3. Preparation of pyrrolo[2,3- <i>b</i> ]pyrazines.....	192
General procedure <b>A</b> (Sonogoshira coupling).....	192
General procedure <b>B</b> (Cyclization).....	192
General procedure <b>C</b> (Suzuki-Miyaura coupling).....	192
General procedure <b>D</b> (halogenation of C-7).....	192
4.3.1. Halogenation of 2-aminopyrazine.....	193
4.3.2. Preparation of 2-bromo-6-phenyl-5 <i>H</i> -pyrrolo[2,3- <i>b</i> ]pyrazine ( <b>45a</b> ).....	195
4.3.3. Preparation of 2-bromo-6-(4-fluorophenyl)-5 <i>H</i> -pyrrolo[2,3- <i>b</i> ]pyrazine ( <b>45b</b> ).....	196
4.3.4. Preparation of 2-bromo-6-(4-chlorophenyl)-5 <i>H</i> -pyrrolo[2,3- <i>b</i> ]pyrazine ( <b>45c</b> ).....	196

4.3.5. Preparation of 6-phenyl-2-( <i>p</i> -tolyl)-5 <i>H</i> -pyrrolo[2,3- <i>b</i> ]pyrazine (47) .....	197
4.3.6. Preparation of 2-(4-methoxyphenyl)-6-phenyl-5 <i>H</i> -pyrrolo[2,3- <i>b</i> ]pyrazine (48).....	198
4.3.7. Preparation of 6-phenyl-2-(4-(trifluoromethyl)phenyl)-5 <i>H</i> -pyrrolo[2,3- <i>b</i> ]pyrazine (49)....	198
4.3.8. Preparation of 6-(4-fluorophenyl)-2-( <i>p</i> -tolyl)-5 <i>H</i> -pyrrolo[2,3- <i>b</i> ]pyrazine (50) .....	199
4.3.9. Preparation of 6-(4-fluorophenyl)-2-( <i>m</i> -tolyl)-5 <i>H</i> -pyrrolo[2,3- <i>b</i> ]pyrazine (51) .....	200
4.3.10. Preparation of 6-(4-chlorophenyl)-2-( <i>p</i> -tolyl)-5 <i>H</i> -pyrrolo[2,3- <i>b</i> ]pyrazine (52).....	201
4.3.11. Preparation of 6-phenyl-7-( <i>m</i> -tolyl)-2-( <i>p</i> -tolyl)-5 <i>H</i> -pyrrolo[2,3- <i>b</i> ]pyrazine (53a).....	202
4.3.13. Preparation of 7-bromo-6-phenyl-2,3-di- <i>p</i> -tolyl-5 <i>H</i> -pyrrolo[2,3- <i>b</i> ]pyrazine (54).....	203
4.3.14. Preparation of 7-bromo-6-phenyl-2,3-di- <i>p</i> -tolyl-5 <i>H</i> -pyrrolo[2,3- <i>b</i> ]pyrazine (54).....	204
4.3.15. Preparation of 5-(ethoxymethyl)-6-(4-fluorophenyl)-2-( <i>p</i> -tolyl)-5 <i>H</i> -pyrrolo[2,3- <i>b</i> ]pyrazine (55a).....	204
4.3.16. Preparation of 5-(ethoxymethyl)-6-(4-fluorophenyl)-2-( <i>p</i> -tolyl)-5 <i>H</i> -pyrrolo[2,3- <i>b</i> ]pyrazine (55a).....	205
4.3.17. Preparation of 5-(ethoxymethyl)-6-(4-fluorophenyl)-2-( <i>m</i> -tolyl)-5 <i>H</i> -pyrrolo[2,3- <i>b</i> ]pyrazine (55b).....	206
4.3.18. Preparation of 5-benzyl-6-(4-fluorophenyl)-2,7-di- <i>p</i> -tolyl-5 <i>H</i> -pyrrolo[2,3- <i>b</i> ]pyrazine (56) .....	207
4.3.19. Preparation of 6-(4-fluorophenyl)-2,7-di- <i>p</i> -tolyl-5 <i>H</i> -pyrrolo[2,3- <i>b</i> ]pyrazine (57a).....	208
4.3.20. Preparation of 6-(4-fluorophenyl)-2,7-di- <i>p</i> -tolyl-5 <i>H</i> -pyrrolo[2,3- <i>b</i> ]pyrazine (57a).....	209
4.3.21. Preparation of 6-(4-fluorophenyl)-2-( <i>m</i> -tolyl)-7-( <i>p</i> -tolyl)-5 <i>H</i> -pyrrolo[2,3- <i>b</i> ]pyrazine (57b) .....	210
4.3.22. Preparation of 2-(4-methoxyphenyl)-5-(4-nitrophenyl)-6-phenyl-5 <i>H</i> -pyrrolo[2,3- <i>b</i> ]pyrazine (58).....	211
4.3.23. Preparation of 5-bromo-3-(phenylethynyl)pyrazin-2-amine (92).....	212
4.3.24. Preparation of 5-bromo-3-((4-fluorophenyl)ethynyl)pyrazin-2-amine (97) .....	213
4.3.25. Preparation of 5-bromo-3-((4-chlorophenyl)ethynyl)pyrazin-2-amine (98).....	213
4.3.26. Preparation of 6-phenyl-2-(phenylethynyl)-5 <i>H</i> -pyrrolo[2,3- <i>b</i> ]pyrazine (100) .....	214
4.3.27. Preparation of 7-iodo-6-phenyl-2-( <i>p</i> -tolyl)-5 <i>H</i> -pyrrolo[2,3- <i>b</i> ]pyrazine (101).....	215
4.3.28. Preparation of 7-bromo-6-phenyl-2-( <i>p</i> -tolyl)-5 <i>H</i> -pyrrolo[2,3- <i>b</i> ]pyrazine (102a) .....	216
4.3.29. Preparation of 7-bromo-6-phenyl-2-(4-(trifluoromethyl)phenyl)-5 <i>H</i> -pyrrolo[2,3- <i>b</i> ]pyrazine (102b).....	217
4.3.30. Preparation of 3,7-dibromo-6-phenyl-2-( <i>p</i> -tolyl)-5 <i>H</i> -pyrrolo[2,3- <i>b</i> ]pyrazine and the 7-bromo-3-chloro-6-phenyl-2-( <i>p</i> -tolyl)-5 <i>H</i> -pyrrolo[2,3- <i>b</i> ]pyrazine (103 and 105).....	218
4.3.31. Preparation of 7-bromo-3-chloro-6-phenyl-2-( <i>p</i> -tolyl)-5 <i>H</i> -pyrrolo[2,3- <i>b</i> ]pyrazine (105). 218	
4.3.32. Preparation of 7-bromo-5-(methoxymethyl)-6-phenyl-2-(4-(trifluoromethyl)-phenyl)-5 <i>H</i> -pyrrolo[2,3- <i>b</i> ]pyrazine (106) .....	219
4.3.33. Preparation of 7-bromo-3-chloro-5-(ethoxymethyl)-6-phenyl-2-( <i>p</i> -tolyl)-5 <i>H</i> -pyrrolo[2,3- <i>b</i> ]pyrazine (107) .....	220
4.3.34. Preparation of 7-bromo-5-(ethoxymethyl)-6-phenyl-2,3-di- <i>p</i> -tolyl-5 <i>H</i> -pyrrolo[2,3- <i>b</i> ]pyrazine (108) .....	221

4.3.35. Preparation of 7-bromo-5-(ethoxymethyl)-6-(4-fluorophenyl)-2-( <i>p</i> -tolyl)-5 <i>H</i> -pyrrolo[2,3- <i>b</i> ]pyrazine ( <b>109a</b> ) .....	221
4.3.36. Preparation of 7-bromo-5-(ethoxymethyl)-6-(4-fluorophenyl)-2-( <i>m</i> -tolyl)-5 <i>H</i> -pyrrolo[2,3- <i>b</i> ]pyrazine ( <b>109b</b> ) .....	222
4.3.37. Preparation of 5-(ethoxymethyl)-6-(4-fluorophenyl)-2,7-di- <i>p</i> -tolyl-5 <i>H</i> -pyrrolo[2,3- <i>b</i> ]pyrazine ( <b>110a</b> ) .....	223
4.3.38. Preparation of 5-(ethoxymethyl)-6-(4-fluorophenyl)-2-( <i>m</i> -tolyl)-7-( <i>p</i> -tolyl)-5 <i>H</i> -pyrrolo[2,3- <i>b</i> ]pyrazine ( <b>110b</b> ) .....	224
4.3.39. Preparation of 5-benzyl-6-(4-fluorophenyl)-2-( <i>p</i> -tolyl)-5 <i>H</i> -pyrrolo[2,3- <i>b</i> ]pyrazine ( <b>111</b> )	225
4.3.40. Preparation of 5-benzyl-6-phenyl-2-(phenylethynyl)-5 <i>H</i> -pyrrolo[2,3- <i>b</i> ]pyrazine ( <b>112</b> ) ...	226
4.3.41. Preparation of 5-benzyl-7-bromo-6-(4-fluorophenyl)-2-( <i>p</i> -tolyl)-5 <i>H</i> -pyrrolo[2,3- <i>b</i> ]pyrazine ( <b>113</b> ).....	227
4.3.42. Preparation of 5-benzyl-7-bromo-6-phenyl-2-(phenylethynyl)-5 <i>H</i> -pyrrolo[2,3- <i>b</i> ]pyrazine ( <b>114</b> ).....	228
4.3.43. Preparation of 5-benzyl-6-phenyl-2-(phenylethynyl)-7-( <i>p</i> -tolyl)-5 <i>H</i> -pyrrolo[2,3- <i>b</i> ]pyrazine ( <b>115</b> ).....	229
4.3.44. Preparation of 7-bromo-2-(4-methoxyphenyl)-5-(4-nitrophenyl)-6-phenyl-5 <i>H</i> -pyrrolo[2,3- <i>b</i> ]pyrazine ( <b>116</b> ) .....	230
4.4. MATERIALS AND METHODS OF QUANTITATIVE BIOLOGY LABORATORY.....	231
5. CONCLUSIONS .....	237
6. REFERENCES AND NOTES .....	240
7. ANNEX 1 .....	250
7.1. A REVIEW OF THE ADHESION GPCRS FROM THE AVAILABLE LITERATURE UNTIL NOW .....	250
7.2. BIBLIOGRAPHY.....	270

# 1. INTRODUCTION

## 1.1. CANCER

Cancer is a wide term used to describe a collection of genetic diseases produced by different causes. All these diseases share a common start characterized by an uncontrolled cell division and growth (either the process is accelerated or slowed down). As a result, new cells are formed unrequired, old and damaged cells survive, producing an accumulation of cells called tumor (in tissues, they are able to form solid tumors (sarcoma) unlike blood cancers (leukemia)). There are more than 100 types of cancer, usually they are named after the tissue or organ where it forms (i.e. pancreatic or colon) or it can describe the kind of cell where cancer is formed (lymphoma-lymphocytes).<sup>1</sup>

The meaning of malignant tumor entails a related characteristics, unlike normal cells, allowing them to spread and become invasive into surrounding tissues or into other parts of the body through blood or lymph nodes (metastasis). As well, these features enable cancer cells (CC) to ignore signal pathways that normally keep cells differentiated, controlled and functionally and also, to hide from immune system or using it to protect themselves against killing cells. Another property is the microenvironment made around tumors, which helps them to arise in multiple ways, for example creating new blood vessels (angiogenesis), keeping a lower pH or increasing nutrients and oxygen. Besides, another important feature to highlight, is the capacity of some cancer cells to revert to a cancer stem cell (CSC), that is, undifferentiated quiescent cells with availability to differentiate into diverse cancer cells, increasing tumor heterogeneity and complexity.<sup>2</sup>

The process called carcinogenesis, where normal cells become cancer cells, can be summarized in three points. The starting point, due to mutations in DNA, cells get the properties commented above. Then, the first accumulation of cells (primary tumor) and local invasion occurs. Finally, it ends up with tumor progression (metastasis). The benign tumors do not produce metastasis, so when they are removed, generally they do not grow up again, unlike malignant cancers.<sup>3</sup>

These genetic causes could be inherited from parents (hereditary cancer) and/or obtained along lifetime due to errors in division process and/or DNA damage affected by environmental exposures (i.e. radiations, tobacco smoke). However, not all genetic changes will conclude to cancer, actually, three kind of genes can be sorted as principal drivers of cancer when they become altered: proto-oncogenes, tumor suppressor genes and DNA repair genes.<sup>1</sup>

· *Proto-oncogenes*: genes encoding proteins with multiple cell functions, giving as a main result, a set of proteins involved in cell division stimulation, inhibiting cell differentiation, and arresting cell death. Therefore, when these genes are mutated, they can become oncogenes, hence, an uncontrolled cell proliferation occurs.<sup>4</sup> Currently 40 genes are known to be oncogenes, for example, K-RAS is related with non-small cell lung cancer (NSCLC), colorectal cancer, and pancreatic cancer.<sup>1</sup>

---

<sup>1</sup> <https://www.cancer.gov> (07/08/2019)

<sup>2</sup> C. Alibert; B. Goud; J. B. Manneville. *Biol. Cell.* **2017**, *109*, 167-189

<sup>3</sup> <https://www.who.int> (07/08/2019)

<sup>4</sup> <https://www.cancer.org> (07/10/2019)



· *Tumor suppressor genes*: They are the opposite to proto-oncogenes. Thus, encoding a set of proteins involved in slowing down cell division, repairing DNA damages, or promoting programmed cell death (apoptosis). When these genes are mutated, the break that controls the pace of cell division is turned off. For example, if DNA is damaged, the tumor suppressor p53 will stop cell cycle before S phase (replication of DNA), giving time to the cell to repair the error. When this damage is extremely, p53 will drive cell to apoptosis process, ensuring tissues wellness. Therefore, when this gene results mutated, all these protective functions can be switched off.<sup>4</sup>

· *DNA repair genes*: They are those genes encoding proteins whose function is to fix DNA damages occurred previously to cell division. If mutations affect these genes, the cell capacity to repair errors could be overwhelmed, triggering cancer.<sup>5</sup>

These brief reviewed cancer concepts have taken more than centuries to understand for human being. From dawn of history people have written about cancer. The first related manuscript (Edwin Smith Papyrus) was found in Egypt and dates back to 3000 BC. It describes different kinds of breast cancer and concludes with the quote "there is no treatment".<sup>6</sup> The word cancer was created by the Greek Hippocrates, using in his texts the word "carcinos" (that is, crab in Greek) to describe tumors. Since then, the number of books, articles, manuscripts, texts, where cancer is treated has increased along the history of humanity.<sup>4</sup> This stands out the complexity and specificity of carcinogenesis and remains a challenge to find an effective medicine for each tumor.

### 1.1.1. EPIDEMIOLOGY OF CANCER

#### INTERNATIONAL EXTENSION

Cancer is still one of the main causes of mortality and morbidity in the world, increasing from the estimated amount of 14 million diagnosed in 2012 to the most recent data from 2018 with an amount of 18.1 millions of cancers detected and 9.6 millions of mortality (Figure 1). The predictions made by GLOBOCAN project foresee an amount of 29.5 millions of cancers for 2040.<sup>7</sup>

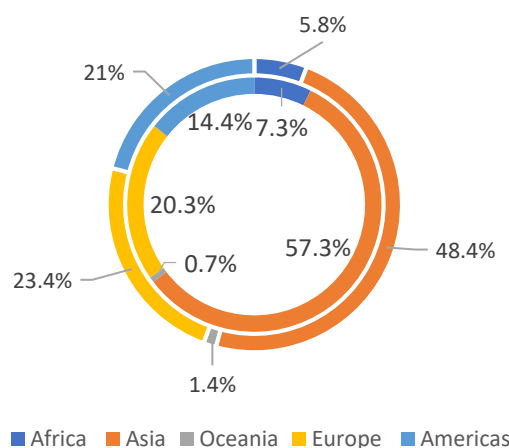


**Figure 1.** Global estimated distribution of cancer incidence (out) and mortality (in) by continents

<sup>5</sup> R. D. Wood; M. Mitchell; J. Sgouros; T. Lindahl. *Science* **2001**, 291, 1284-1289

<sup>6</sup> S. I. Hajdu. *Cancer* **2011**, 117, 1097-1102

<sup>7</sup> <https://gco.iarc.fr> (08/10/2019)

Among both sexes, the most common diagnosed cancer in 2018 is lung cancer, 11.6% of all cases and most important, the main cause of cancer death (18.4%). Then, in what incidence respects, the breast cancer (11.6%), colorectal cancer (10.2%) and prostate cancer (7.1%) are the following most important. For mortality, colorectal cancer (9.2%), stomach cancer (8.2%) and liver cancer (8.2%) (Figure 2).<sup>7</sup>

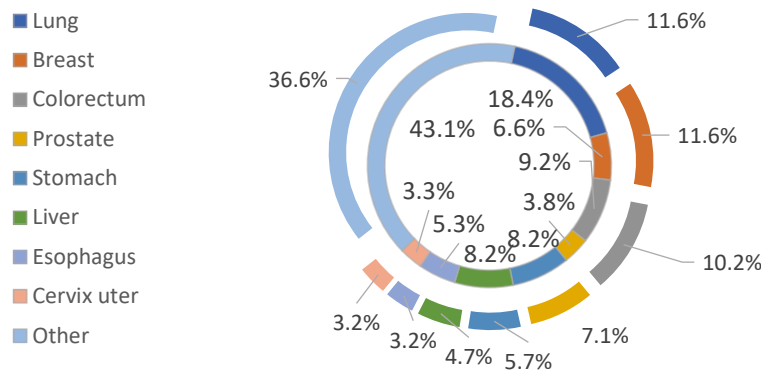


**Figure 2.** Global estimated distribution, incidence (out) and mortality (in), for most common cancers (both sexes)

Differentiating between males and females, most incidence cancers in males are lung (14.5%), prostate (13.5%), colorectum (10.9%), stomach (7.2%) and liver (6.3%). The ones with highest mortality rate are lung (22%), liver (10.2%), stomach (9.5%), colorectum (9%) and prostate (6.7%) (Figure 3). In females, most incidence cancers are breast (24.2%), colorectum (9.5%), lung (8.4%), cervix uteri (6.6%) and stomach (4.1%). The ones with highest mortality rate are breast (15%), lung (13.8%), colorectum (9.5%), cervix uteri (7.5%) and stomach (6.5%) (Figure 4).<sup>7</sup>

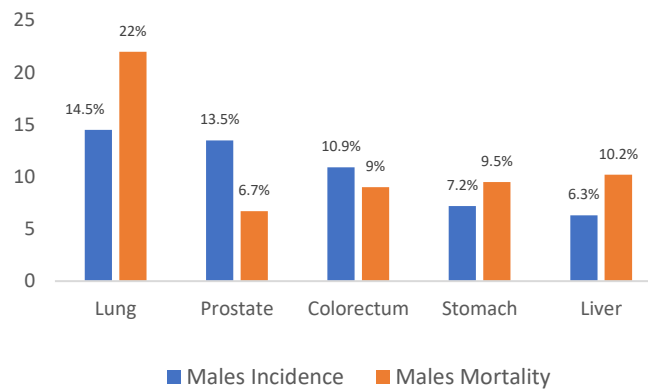


**Figure 3.** Global estimated distribution of incidence and mortality for most common cancers in males (2018)

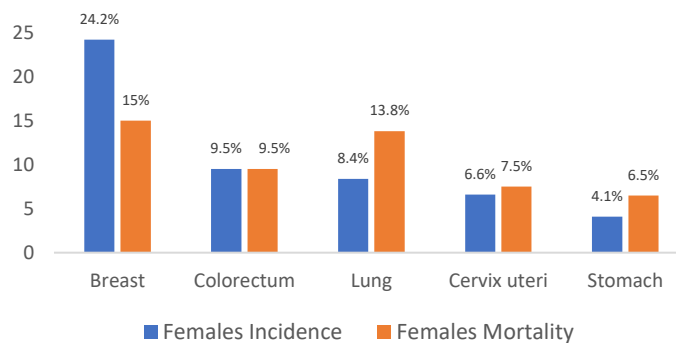


**Figure 4.** Global estimated distribution of incidence and mortality for most common cancers in females (2018)

According to a report, the therapeutic and supportive care cost in 2017 was 133 billion dollars and it is foreseen to exceed 150 billion dollars by 2020.<sup>8</sup> This data is related with therapies and it is necessary, as well, to consider costs of hospitalizations, services out of hospital, physician/supplier services, pharmacist, psychologist, medical equipment, home health care, and others.

*NATIONAL EXTENSION*

In Spanish state, cancer is on top three of death causes, located after heart diseases.

In 2018 an amount of 270.363 incidences has been estimated (114.392 female and 155.971 male) and 110.779 deaths (43.448 females and 67.331 males). In both sexes, most frequent cancer is colorectum (14%), then prostate (12%), lung (10%), breast (12%) and skin cancers (8%). The cancers with highest rate of death in 2018 are lung (20.3%), colorectum (14.1%), pancreas (6.3%), breast (6%) and prostate (5.5%) (figure 5).<sup>9</sup>

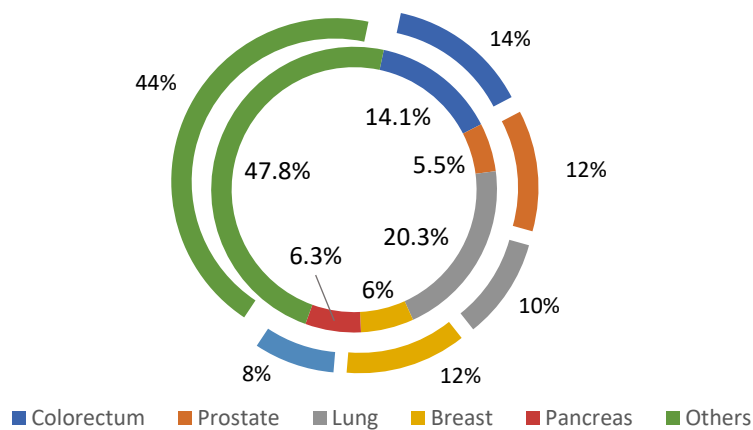


**Figure 5.** Spanish estimated distribution of incidence (out) and mortality (in) for most common cancers (both sexes)

If we differentiate between female and male, breast cancer (29%), colorectum (13%), lung (6%), cervix uteri (6%) and ovarium (4.3%) are the most incidence cancers in females, and the ones with most deaths rate are breast (15%), colorectum (15%), lung (11%), pancreas (7%) and ovarium (5%) (Figure 6). While in males, most incident cancers in 2018 are prostate (20%), lung (18%), colorectum (15%), urinary bladder (9%) and stomach (4%) and the ones with highest rate of mortality are lung (26%), colorectum (14%), prostate (9%), urinary bladder (6%) and pancreas (10.2%) (Figure 7).<sup>9</sup>

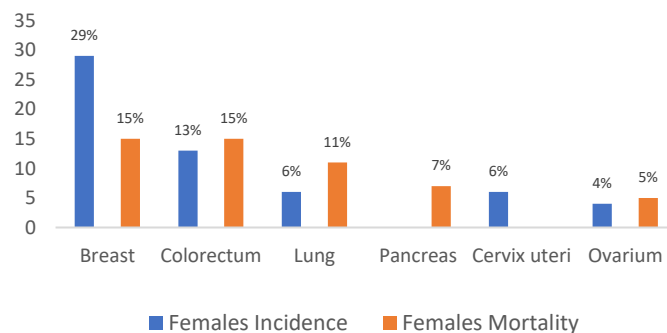


**Figure 6.** Spanish estimated distribution of incidence and mortality for most common cancers in females (2018)

<sup>8</sup> <https://www.iqvia.com> (08/10/2019)

<sup>9</sup> <https://www.aecc.es> (08/10/2019)

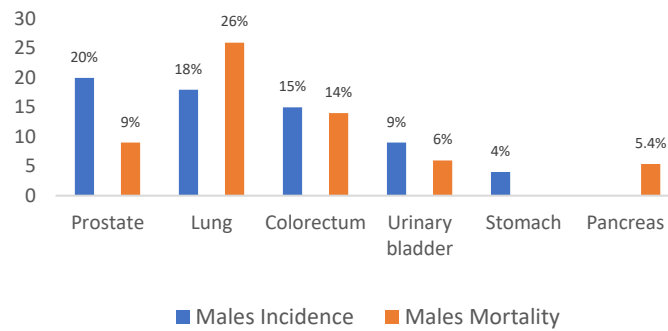


**Figure 7.** Spanish estimated distribution of incidence and mortality for the most common cancers in males (2018)

Cancer is responsible for a very considerable number of deaths, however, recent studies shows how patients survival has increased in latest years (survival expectance in Spain is 53% at 5 years), standing out Non-Hodgkin lymphoma and prostate cancer due to improvement in treatment and early diagnostic.<sup>10</sup>

Another highlight is the outstanding importance of evitable factors, responsible of 33% of cancer deaths. These factors are tobacco (33% responsible of cancer incidence worldwide, and 22% of cancer deaths), infections (25% responsible in developing countries), alcohol (responsible of 12% of cancer worldwide), inappropriate diets and sedentism.<sup>3</sup> Probably, with a good prevention, education and early diagnostic, the statistics of cancer deaths would see reduced, yet it would be need to break some hurdles regarding treatments to ensure an enhancement in survival rate.

### 1.1.2. PREVENTION AND TREATMENT

The treatment of cancer is a complex process since depends on many factors such as type of cancer, affected tissues, cancer stage, patient genetics, drug resistance, amongst others. The first remedy to fight against cancer is its prevention.

#### *PREVENTION*

In prevention we can differ between primary and secondary. Primary prevention embraces the behave of human being to avoid those factors that could lead to cancer, such as alcohol, obesity, radiation, sunlight, tobacco, infectious agents, chemical agents, and others. Actually, the probability to develop lung cancer is increased up to 50% for people that live in cities with high rates of pollution.<sup>7</sup> To reduce contact with these factors an improvement in sanitary education would be need.

Then, secondary prevention encompasses two main terms, early diagnostic and screenings. Such processes are really important in order to catch tumor in a primary stage, because in that way the prognostic to cure cancer would be better. Again, an improvement in sanitary education is required to teach people about early signals of cancer and to attend doctor as fast as possible. Thus, a clinical examination (analysis, laboratory test, genetic tests, radiological imaging, and others), diagnosis and classification would be done and the access to treatment, if needed, would be granted.

Screenings help to detect cancers when no previous signals or symptoms appeared, for example, in colorectum cancer is estimated an increased 90% of cure if a good detection is made before

<sup>10</sup> <https://seom.org> (08/10/2019)

late stages of disease, when symptoms comes out.<sup>11</sup> These processes are more complex and require a huge effort in organization and efficiency.

In both prevention stages there is one test getting relevance, genetic proves. In the beginning, to read the genome costed around 2700 millions of dollars worldwide, nowadays it is possible to get it for 600 dollars.<sup>12</sup> Cancer is not inherited for the parents, is the genetic error what drives to cancer, but the increased risk, the predisposition to get some type of cancers, is inherited. It is not possible to cure cancer through this test but provides valuable knowledge about predisposed genes, specifically for each human being (personalized therapy).

In the second stage, when cancer is already detected, it is also important to get back up from genetic tests. In other words, if genetics of cancer cells is known, the efficiency of treatment would be enhanced, choosing correctly through a wide breadth of drugs and therefore the probability of survival would be improved as well.

### *TREATMENT*

Based on the factors commented above, a specific treatment is chosen. Treatments can be sorted by surgery (removing tumor from the body), radiation (high doses of radiation to kill cancer cells), chemotherapy (drugs), immunotherapy (treatment to boost immune system to fight cancer), targeted therapies (targeting changes that helps cancer cells to grow and progress), hormone therapy (for breast or prostate), stem cell transplant (when radiotherapy and/or chemotherapy has destroyed their own) and precision medicine (based on genetic knowledge).<sup>4</sup> Even with this wide portfolio of options, cancer is one of the biggest challenge due to its complexity.

### **1.1.3. DIFFICULTIES IN CANCER TREATMENT**

One of the hardest difficulties is the similarity between normal cells and cancer cells, fact that complicates the treatment (high rate of adverse effects) and therefore more selectivity is needed. Probably, through a better conception of biology and tumor genetics, chasing those differences present in cancer cells, will improve chemotherapeutic treatments. Taking this into account, what makes cancer very tricky is his ability to spread (metastasis) and the resistance to treatments. Linking these three factors gives as a result a cancer cells with an enhanced capacity to survive.

### *METASTASIS*

Defined as the ability of cancer cells to spread in the body, to nearby tissues or to other parts through blood or lymphatic system. When it occurs is called stage IV. The metastatic cancer cells are the same than in primary tumor. It is well known that depending on the type of cancer it will spread preferably to certain parts of the body than others. For example, breast cancer has metastasis in bone, brain, liver and lung. Lung cancer in adrenal gland, bone, brain, liver and the other lung.<sup>1</sup>

The mechanistic processes through which metastasis develops embrace some steps summarized in:<sup>13</sup>

- Invading near tissue, blood vessels or/and lymph, changing epithelial cell structure (cell polarity and cell adhesion)

---

<sup>11</sup> F. T. Kolligs. *Visc. Med.* **2016**, 32, 158–164

<sup>12</sup> <https://ghr.nlm.nih.gov> (09/10/2019)

<sup>13</sup> F. Zijl; G. Krupitza; W. Mikulitsa. *Mutat. Res.* **2011**, 728, 23–34

- Moving to other parts of the body
- Stopping in small vessels, invading them and moving into the tissue. Their ability to promote angiogenesis helps to improve these steps
- If the conditions are suitable, a new primary tumor grows

Not all cancer cells that undertake metastasis will survive, but if metastasis success, cells could stay in a quiescent state for a long period of time, reappearing even when treatment is done. Bearing in mind this processes, metastasis of cancer is one of the main factors leading to patient death. When a stage IV is diagnosed it is tricky to foresee the outcomes after treatment, sometimes it would be a good prognostic but in other cases treatment will shrink the tumor but not enough to cure it. Nowadays, treatments focused in metastasis have shown progress but there are still some limitations such as the recurrence after treatment, the tough side effects and most important, drug resistance. Hereto, new mechanism of action to prevent and to break metastasis are needed. There are two concepts to stand out in metastasis, the epithelial mesenchymal transition (EMT) and cancer stem cells, two concepts really linked and still in debate to know which one precede the other.<sup>14</sup>

#### RESISTANCE

Cancer drug resistance is responsible of 90% of deaths in cancer, as well as for the more relapses after treatment (Figure 8). Two kinds of resistance can be sorted, intrinsic and acquired.<sup>15</sup>

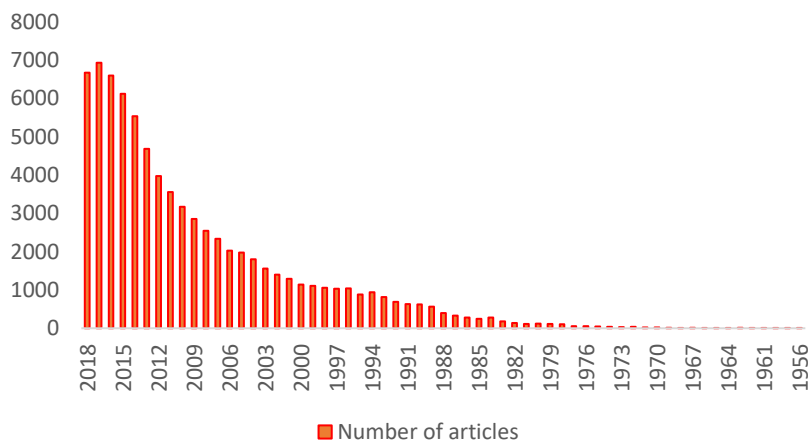


**Figure 8.** Timeline of cancer drug resistance articles from PubMed

#### · INTRINSIC

It refers at resistance present in patient before the treatment is administered and it can be given by different mechanisms. The intrinsic resistance triggers to diminish treatment efficacy, what brings back the relevance of knowing patient and cancer genetics.

Several studies have shown how genetics in a tumor can differ significantly between cells, what means intratumoral heterogeneity.<sup>16</sup> This concept is linked with time, because as much time pass between initial tumor and detection, more probability to find high heterogeneity. Cancer stem cells (CSCs) are one of these subpopulations being in a quiescent state with an enhanced capacity

<sup>14</sup> T. N. Seyfried; L. C. Huysentruyt. *Crit. Rev. Oncog.* **2013**, *18*, 43–73

<sup>15</sup> J. Rueff; A. S. Rodrigues. *Methods Mol. Biol.* **2016**, *1395*, 1-18

<sup>16</sup> S. Turajlic; A. Sottoriva; T. Graham; C. Swanton. *Nat. Rev. Genet.* **2019**, *20*, 404-416

to resist therapy due to their characteristics. CSCs have a high tumorigenic potential since they act as normal stem cells, ergo they possess capacity of self-renewing and capacity to generate differentiated subpopulations of cells, increasing heterogeneity.<sup>17</sup>

Another possibility that could confer intrinsic resistance is the pre-existence of mutations in a gene(s) involved in cell division, proliferation and apoptosis. For example, in gastric cancer, patients with HER<sub>2</sub> overexpression showed a reduced outcome after treatment with *cisplatin*. The HER<sub>2</sub> gene upregulates the factor called Snail, which promotes, the mentioned before, epithelial mesenchymal transition (EMT), conferring more resistance to chemotherapy and radiotherapy.<sup>18</sup> It has been mentioned that EMT and CSCs are linked with metastasis and now these two last points relate them with the resistance as well. Finally, another mechanism that can decrease efficiency of treatment are those pathways that organism undertakes to get rid of environmental toxins or to detoxify cells. An example of this case is the ATP binding cassette (ABC), transporters that regulate drug efflux, reducing drugs concentration inside the cells.<sup>19</sup>

**Table 1.** Examples of intrinsic resistance in cancer

Drug	Cancer	Mutation	Outcome
<i>Cisplatin</i>	Gastric cancer	HER <sub>2</sub> +/Snail + HER <sub>2</sub> -/Snail + HER <sub>2</sub> -/Snail -	Patients with double positive genes have less survival rate followed by -/+ and highest survival rate for -/- profile <sup>18</sup>
<i>TKIs</i>	Chronic myeloid leukemia and EGFR NSCLC	Polymorphism BCL2-like 11(BIM)	Upregulation of BIM is required for <i>TKIs</i> to induce apoptosis in kinase-driven cancers. The polymorphism confers a lack in the pro-apoptotic domain <sup>20</sup>
<i>Gemcitabine</i>	Pancreatic cancer	Down regulation of BCL2 interacting protein 3 (BNIP3)	Overexpression of BNIP3 induces cell death <sup>21</sup>

#### · ACQUIRED

In acquired resistance the efficacy of treatment slows down along it due to new mutations in proto-oncogenes, alterations in drug targets (mutations, up or down-regulation) or/and the influence of tumor microenvironment. For example, *methotrexate*, which is among the most used known drugs for clinical cancer treatments, in acute leukemia treated with *methotrexate* an amplification of dihydrofolate reductase (DHFR) gene was observed.<sup>22</sup>

DHFR is the target of *methotrexate*, then if the concentration of DHFR is higher than the inhibitor, the cell cycle and the tumor growth will keep in progress.

In the treatment of osteosarcoma, the resistance is due to decreased transport through the reduced folate carrier (RFC).<sup>23</sup>

<sup>17</sup> M. Najafi; B. Farhood; K. Mortezaee. *J. Cell. Physiol.* **2019**, *234*, 8381-8395

<sup>18</sup> D. Huang; H. Duan; H. Huang; X. Tong; Y. Han; G. Ru; L. Qu; C. Shou; Z. Zhao. *Sci. Rep.* **2016**, *6*, 1-12

<sup>19</sup> M. Kartal-Yandim; A. Adan-Gokbulut; Y. Baran. *Crit. Rev. Biotechnol.* **2016**, *36*, 716-726

<sup>20</sup> C. Holohan; S. Van Schaeybroeck; D.B. Longley; P.G. Johnston. *Nat. Rev. Cancer* **2013**, *13*, 714-726

<sup>21</sup> M. Akada; T. Crnogorac-Jurcevic; S. Lattimore; P. Mahon; R. Lopes; M. Sunamura; S. Matsuno; N.R. Lemoine. *Clin. Cancer. Res.* **2005**, *11*, 3094-3101

<sup>22</sup> J. R. Bertino; E. Göker; R. Gorlick; W. W. Li; D. Banerjee. *Stem Cells* **1996**, *14*, 5-9

<sup>23</sup> W. Guo; J. H. Healey; P. A. Meyers; M. Ladanyi; A. G. Huvos; J. R. Bertino; R. Gorlick. *Clin. Cancer Res.* **1999**, *51*, 621-627

Some mechanisms are shared by both types of resistance, actually, to differ between intrinsic and acquired resistance is a temporal criteria, so may be, acquired resistance combines resistant subpopulations prior to treatment (intrinsic resistance) with a new mechanisms adapted

**Table 2.** Examples of acquired resistance in cancer

Drug	Cancer	Resistance	Outcome
<i>Cetuximab</i>	Head and neck cancer	EMT process through Snail activation	Methylation of EGFR (target of <i>cetuximab</i> ) and dimerization with lymphotoxin- $\beta$ (LT $\beta$ ) <sup>24</sup>
<i>Tamoxifen</i>	Breast cancer (estrogen receptor + (ER+))	Epigenetic alterations	Retinoblastoma-binding protein 2 (RBP2) activates the PI3K/AKT pathway, promoting the cell survival <sup>25</sup>
<i>Dovitinib, Vatalanib</i>	Glioblastoma	Tumor microenvironment	Tumor associated macrophages (TAMs) increase the secretion of colony stimulating factor-1 receptor (CSF-1R), then the survival and progression is increased <sup>26</sup>

### 1.1.3.1. CELL MECHANISMS FOR DRUG RESISTANCE

It is vital to understand the tumor resistance mechanism for each type of cancer in order to optimize treatment. Here, these mechanisms are summarized in decreased intracellular drug concentration, target alteration, epigenetic alterations, tumor microenvironment, tumor heterogeneity, deregulation of cell death, and EMT-CSCs.

#### DECREASED INTRACELLULAR DRUG CONCENTRATION

The decreased drug uptake and the augmented drug efflux is responsible for diminishing intracellular concentration of chemotherapeutics. Actually, it is the main reason of resistance.

As it is well known, to reach therapeutic effectiveness, anticancer drugs must get their targets with an adequate concentration. The underlying mechanisms acting to decrease the final concentration of drugs inside the cell has been studied for a long time and a clarification of them is summarized in numerous articles.<sup>27,28</sup>

It is proposed that an alteration in plasmatic membrane acts as a hurdle, as a defense mechanism to protect cancer cells. This alteration (changes in components and/or organization in membrane) is caused with the malignant transformation in cancer cells, for example, glucosylceramide was found increased in multidrug resistance cancer cell lines and absent in drug sensitive cells.<sup>29</sup>

Therefore, the quantity and the kind of transporters is linked with membrane components. In one side, drug influx is reduced due to different factors, one of the most important are the transporters such as solute carriers, for example, antifolates drugs enter inside cell through them

<sup>24</sup> D. S. Hsu; W. L. Hwang; C. H. Yuh; C. H. Chu; Y. H. Ho; P. B. Chen; H. S. Lin; H. K. Lin; S. P. Wu; C. Y. Lin; W. H. Hsu; H. Y. Lan; H. J. Wang; S. K. Tai; M. C. Hung; M. H. Yang. *Clin. Cancer Res.* **2017**, *23*, 4388-4401

<sup>25</sup> H. J. Choi; H. S. Joo; H. Y. Won; K. W. Min; H. Y. Kim; T. Son; Y. H. Oh; J. Y. Lee; G. Kong. *J. Nat. Cancer Inst.* **2018**, *110*, 400-410

<sup>26</sup> D. Yan; J. Kowal; L. Akkari; A. J. Schuhmacher; J. T. Huse; B. L. West; J. A. Joyce. *Oncogene* **2017**, *36*, 6049-6058

<sup>27</sup> R. R. Begicevic; M. Falasca. *Int. J. Mol. Sci.* **2017**, *18*, 2362-2386

<sup>28</sup> Y. H. Choi; A. M. Yu. *Curr. Pharm. Des.* **2014**, *20*, 793-807

<sup>29</sup> A. Lucci; W. I. Cho; T. Y. Han; A. E. Giuliano; D. L. Morton; M. C. Cabot. *Anticancer Res.* **1998**, *18*, 475-480



and it is been reported how in some cancers the alteration of this influx transporters decrease antifolates efficacy.<sup>30</sup> Another associated problem is the pH in tumor microenvironment, because intracellular pH is increased and extracellular decreased down to 6.5-7.1, thus, antineoplastic drugs with a weak basic character remain protonated outside the cell.<sup>31</sup>

In the other side, efflux transporters play a pivotal role in cancer drug resistance. The hugest family is the ABC transporters (superfamily of 49 ABC genes) like the well described P-glycoprotein (P-gp), also called multidrug resistance protein 1 (MDR-1).<sup>32</sup> In kidney, colon, liver, lung and rectum cancer an overexpression of P-gp has been described previous to treatment<sup>33</sup> (intrinsic resistance) and after treatment like in chronic myelogenous leukemia (acquired resistance).<sup>34</sup> The P-gp contains two transmembrane domains, through which drugs and toxins are removed from inside the cell, and two nucleotide binding domains to bind and hydrolyze the ATP in order to change the conformation and pump off the substrates.

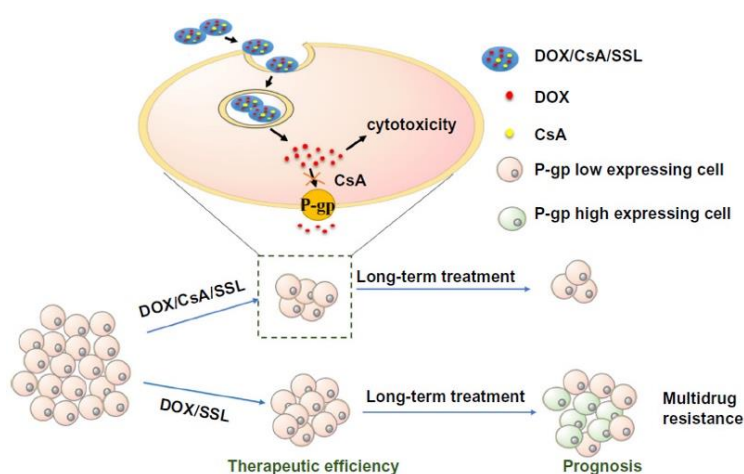


**Figure 9.** Illustration of possible advantages using *Doxorubicin* (DOX) + *Cyclosporine A* (CsA) (P-gp inhibitor) in a loaded liposomal (SSL) in a tumor treatment<sup>35</sup>

Consequently, the overexpression and mutations of P-gp has correlated with a poor prognosis and poor therapeutic response, diminishing sensitivity to drugs. Then, in order to improve the outcomes, it will be necessary to perform studies to recognize ABC cancer profile previous to treat it. Also, new strategies like a combined chemotherapy (inhibitor of growth and inhibitor of MDR-1) might rise in order to improve the treatment efficacy (Figure 9).<sup>35</sup>

#### TARGET ALTERATION

This mechanism of resistance appears for those treatments called target therapies, which acts inhibiting the activity of specific target (enzymes, receptors, and others).

In the beginning of a treatment it can be an advantage to use the differences between normal cells and CCs to decrease adverse effects, increasing selectivity, but it can draw CCs to CDR.

<sup>30</sup> L. H. Matherly; M. R. Wilson; Z. Hou. *Drug Metab. Dispos.* **2014**, *42*, 632-649

<sup>31</sup> D. T. Manallack. *Perspect. Medicin. Chem.* **2007**, *17*, 25-38

<sup>32</sup> F. J. Sharom. *Pharmacogenomics* **2008**, *9*, 105-127

<sup>33</sup> A. Adamska; M. Falasca. *World J. Gastroenterol.* **2018**, *24*, 3222-3238

<sup>34</sup> X. X. Peng; K. T. Amit; H. C. Wu; Z. S. Chen. *Chin. J. Cancer* **2012**, *31*, 110-118

<sup>35</sup> Z. Lin; M. Chen; X. Yang; Z. Cui; X. Zhang; L. Yuan; Q. Zhang. *Int. J. Nanomedicine* **2014**, *9*, 3425-3437

One of the best examples to understand this mechanism is resistance developed in treatments with tyrosine kinase inhibitors of EGFR in non-small cell lung cancer (NSCLC). Since treatment with *erlotinib*, *gefitinib* or *afatinib* was introduced into the market the efficacy in progression-free survival and overall survival were increased compared with traditional treatment, but most of the patients develop acquired resistance through mechanisms, such as mutations in target gene (altering the binding site), epigenetic alterations (upregulation or downregulation) or/and alterations in signal pathways.<sup>36</sup> If methods of drug target alteration are known it could bring support for diagnosis, for developing new strategies and drugs to treat resistant cancer cells.

#### EPIGENETIC ALTERATIONS

The epigenetic alterations refer to changes in gene expression that are heritable within cellular division, then, not those alterations present in primary DNA. Epigenetic includes DNA methylation, histone modification (acetylation or methylation) and non-coding RNA (miRNA and lncRNA) as principals.<sup>37</sup> The epigenetic changes control genes expression, for example when a histone is acetylated the chromatin opens, giving as a result a transcriptionally accessible state, thus, transcription factors between other proteins (inhibitors or activators) can regulate gene expression. A good example is the downregulation of gene expression, through hypermethylation of tumor suppressor genes or by contrast, the hypomethylation of oncogenes, ergo overexpression.

##### · DNA damage repair (DDR)

The epigenetic alterations are also related with enhanced DNA damage repair (DDR). This process of fixing damaged DNA is improved in cancer cells, reversing the efficacy of treatment. For example, treatment with *5-fluorouracil* induces upregulation of p53 target genes in damaged DNA, thus the success to repair it is increased, diminishing cell arrest and programmed cell death. It could be an appealing strategy to attack both, DDR and DNA, but it should contemplate the risk of increased mutations due to genomic instability.<sup>38</sup> Another related example is the hypomethylation of MDR1 promoter, giving a P-gp overexpression in stomach cancer and in invasive ductal carcinoma.<sup>39,40</sup> Therefore, increasing their aggressiveness. This example helps to emphasize the fact that resistance mechanisms are connected to each other, is a multifactorial process that has to be studied in every cancer, in every patient, for every drug.

##### · Human Nicotinamide N-Methyltransferase (hNNMT)

The hNNMT is a phase II metabolizing enzyme, catalyzing the methylation of nicotinamide into 1-methylnicotinamide (MNA) as a main reaction. Its expression is altered in some cancers depending on stress situation, because in those tissues with reduced nutrient availability it is found to be overexpressed, producing then more NAD<sup>+</sup> and MNA<sup>41</sup> (Figure 10), as well as, it has

---

<sup>36</sup> J. Gao; H. R. Li; C. Jin; J. H. Jiang; J. Y. Ding. *Clin. Transl. Oncol.* **2019**, *21*, 1287-1301

<sup>37</sup> M. Kacevska; M. Ivanov; M. Ingelman-Sundberg. *Pharmacogenomics* **2012**, *13*, 1373–1385

<sup>38</sup> M. D. Wyatt; D. M. Wilson. *Cell. Mol. Life Sci.* **2009**, *66*, 788–799

<sup>39</sup> G. Sharma; S. Mirza; R. Parshad; A. Srivastava; S. D. Gupta; P. Pandya; R. Ralhan. *Clin. Biochem.* **2010**, *43*, 373–379

<sup>40</sup> A. A. Muggenrud; J. A. Rønneberg; F. Wärnberg; J. Botling; F. Busato; J. Jovanovic; H. Solvang; I. Bukholm; A. L. Børresen-Dale; V. N. Kristensen; T. Sørli; J. Tost. *Breast Cancer Res.* **2010**, *12*, 1-10

<sup>41</sup> J. Jung; L. J. Kim; X. Wang; Q. Wu; T. Sanvoranart; C. G. Hubert; B. C. Prager; L. C. Wallace; X. Jin; S. C. Mack; J. N. Rich. *J.C.I. Insight* **2017**, *2*, e90019

found to be altered in some cancer stem cells.<sup>42</sup> The aberrant expression of hNNMT is related with poor prognosis in some cancers like in gastric, colorectal, gastric, prostate, breast and liver.<sup>43,44</sup> His activity in cancer drug resistance is linked with the inhibition of drug induced apoptosis, increased proliferation, survival and cell cycle progression. For example, due to its increased activity and expression, histones are hypomethylated rising protumorigenic genes. The final product of the reaction, MNA, reduces reactive oxygen species (ROS) and apoptosis, mechanism through which a resistance to 5-FU in colorectal cancer was described.<sup>45</sup> Recently, hNNMT has been correlated with SIRT1 (sirtuins family are NAD<sup>+</sup> dependent deacetylases), which regulates cell functions like DNA repair, cell survival and metabolism via deacetylation of histones and deacetylation of p53 (inhibition of p53, inhibition of apoptosis), inducing cell survival in a stress situation. As nicotinamide is an inhibitor of SIRT1, an nicotinamide concentration is decreased in those cancers where hNNMT is overexpressed, SIRT1 activity is overstimulated.<sup>43</sup> Finally, a recent study showed how hNNMT can be the key as a metabolic regulator in cancers associated with fibroblasts, differentiating cells to cancer associated fibroblast and therefore promoting cancer progression.<sup>46</sup> All these examples lead to a conclusion to undertake a new strategy in order to know the genomics of cancer and in those where hNNMT is overexpressed to use a combined therapy against both, the specific cancer cell, plus inhibiting hNNMT. Then, probably, prognosis and survival rate would arise.

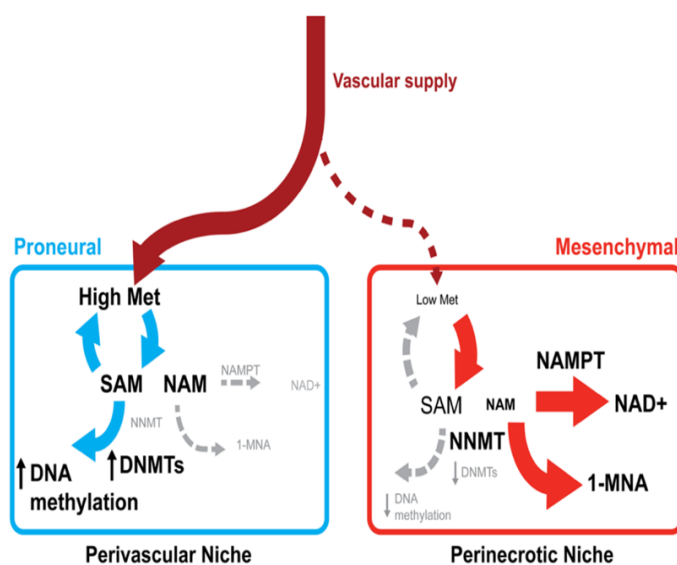


**Figure 10.** Differences in hNNMT expression between a glioblastoma stem cell in an enriched niche and glioblastoma stem cell in a non-enriched niche <sup>41</sup>

<sup>42</sup> F. P. Andrea; A. Safwat; M. Kassem; L. Gautier; J. Overgaard; M. R. Horsman. *Radiother. Oncol.* **2011**, *99*, 373-378

<sup>43</sup> Y. Wang; J. Zeng; W. Wu; S. Xie; H. Yu; G. Li; T. Zhu; F. Li; J. Lu; G. Y. Wang; X. Xie; J. Zhang. *Breast Cancer Res.* **2019**, *21*, 1-17

<sup>44</sup> <https://www.proteinatlas.org> (11/10/2019)

<sup>45</sup> X. Xinyou; L. Huixing; W. Yanzhong; Z. Yanwen; Y. Haitao; L. Guiling; R. Zhi; L. Fengying; W. Xiuhong; Z. Jun. *Oncotarget* **2016**, *7*, 45837-45848

<sup>46</sup> M. A. Eckert; F. Coscia; A. Chryplewicz; J. W. Chang; K. M. Hernandez; S. Pan; S. M. Tienda; D. A. Nahotko; G. Li; I. Blaženović; R. R. Lastra; M. Curtis; S. D. Yamada; R. Perets; S. M. McGregor; J. Andrade; O. Fiehn; R. E. Moellering; M. Mann; E. Lengyel. *Nature* **2019**, *569*, 723-728

· Non-coding RNAs (ncRNAs)

There are five types of ncRNAs, microRNAs (miRNAs), long noncoding RNAs (lncRNAs), small interfering RNAs (siRNAs), antisense RNAs (asRNAs) and circular RNAs (circRNAs).<sup>47</sup> About 98% of transcriptional output is ncRNA in humans.<sup>48</sup>

Due to their regulation function in gene expression, ncRNAs play an important role in initiation, metastasis, cancer stem cells and in latest years more evidence is coming up about its influence in cancer drug resistance.<sup>49</sup> The more related ones are lncRNA, miRNA and circRNA and the mechanisms through which they regulate resistance is via ABC transporters, cell arrest and apoptosis, CSC and EMT, autophagy and others.<sup>50</sup>

To understand how these RNA molecules affect in cancer, an example for each type is described. The miRNAs (18-22 nt in length) acts as an inhibitor of post-transcriptional gene expression binding to their complementary mRNAs, controlling different cellular process as apoptosis, cellular differentiation and proliferation. The profile expression in tumor tissues is different compared with normal tissues and their dysregulation has related with resistance and relapse.<sup>51,52</sup>

Before defining miRNAs as a tumor suppressor or oncogene it will be necessary to put in context the biological cell environment, because it is what decant them to one or other profile.<sup>53</sup>

For example, miR663 was found to be upregulated in breast cancer and to create resistance to *doxorubicin* by inhibiting apoptosis.<sup>54</sup>

The lncRNAs (200-10000 nt length) regulate gene expression through different mechanism, for example blocking the binding site to transcriptional activators, chromatin modification, post-translational regulation, and others. Their role in cells depends, like miRNAs, in the context.

An example is the resistance to *trastuzumab* in HER-2 positive breast cancer where it was found an overexpression of lncRNA-ATB, which promotes epithelial mesenchymal transition and this leads to drug resistance.<sup>55</sup>

The circRNAs unlike the already described RNAs makes a covalent closed loop. Their role also depends on cellular context. For example, upregulation of circ\_001569 in osteosarcoma has linked with *cisplatin* resistance by activating Wnt/beta-catenin pathway and therefore promoting cell proliferation.<sup>56</sup>

With these summarized implications it is visible how complex and wide can be the different roles of ncRNA in cancer resistance. Therefore, a genomic studies and functional considerations will be need it to understand the role of each ncRNA in each cancer, targeting them as a strategy in a combined therapy.

---

<sup>47</sup> S. Qu; Y. Zhong; R. Shang; X. Zhang; W. Song; J. Kjems; H. Li. *RNA Biol.* **2017**, *14*, 992-999

<sup>48</sup> J. S. Mattick. *EMBO Rep.* **2001**, *2*, 986-991

<sup>49</sup> E. Anastasiadou; L. S. Jacob; F. J. Slack. *Nature Reviews Cancer* **2018**, *18*, 5-18

<sup>50</sup> W. Z. Hu; C. L. Tan; Y. J. He; G. Q. Zhang; Y. Xu; J. H. Tang. *Onco. Targets Ther.* **2018**, *11*, 1529-1541

<sup>51</sup> I. Berindan-Neagoe; P. Monroig; B. Pasculli; G. A. Calin. *C.A. Cancer J. Clin.* **2014**, *64*, 311-336

<sup>52</sup> H. Lan; H. Lu; X. Wang; H. Jin. *Biomed. Res. Int.* **2015**, *v2015*, 1-17

<sup>53</sup> M. Carlo; M. D. Croce. *Nat. Rev. Genet.* **2009**, *10*, 704-714

<sup>54</sup> H. Hu; S. Li; X. Cui; X. Lv; Y. Jiao; F. Yu; H. Yao; E. Song; Y. Chen; M. Wang; L. Lin. *J. Biol. Chem.* **2013**, *288*, 10973-10985

<sup>55</sup> S. J. Shi; L. J. Wang; B. Yu; Y. H. Li; Y. Jin; X. Z. Bai. *Oncotarget* **2015**, *6*, 11652-11663

<sup>56</sup> H. Zhang; J. Yan; X. Lang; Y. Zhuang. *Oncol. Lett.* **2018**, *16*, 5856-5862

## TUMOR MICROENVIRONMENT (TME)

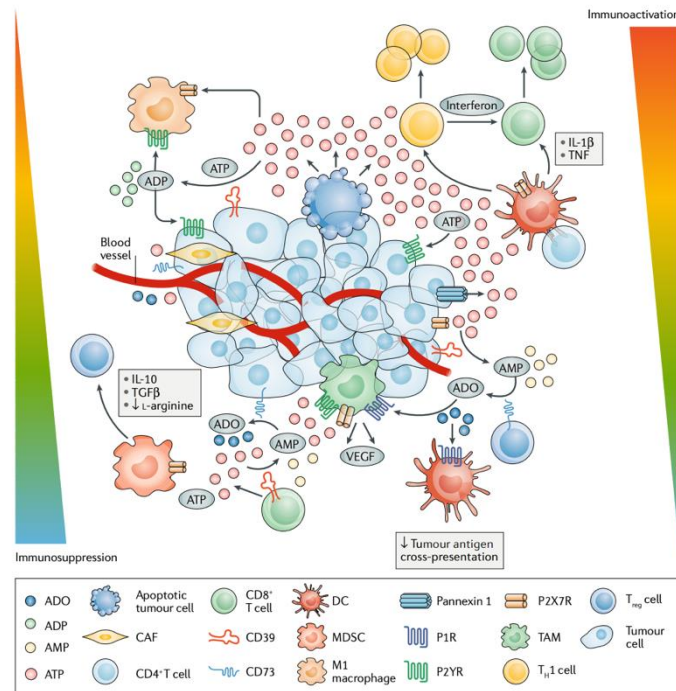


Figure 11. Illustration of tumor microenvironment<sup>69</sup>

The tumor microenvironment is not only made by homogenous cancer cells, it embraces vessels, immune cells (as tumor associated macrophages), fibroblasts, extracellular matrix (ECM), signal molecules, and others (Figure 11). All these factors aid the tumor to grow and survive.<sup>57</sup>

To keep this environment and the communication between cells a remodeling of ECM is necessary. ECM is a complex network made by macromolecules which offers a structural and biochemical support to cells, controlling cell growth, proliferation, motility, pH, hydration, and others. Therefore, as an inflection point, ECM can contribute to cancer proliferation, evasion of suppression, apoptosis resistance, induced angiogenesis, initiation of metastasis, dysregulation of cellular homeostasis and avoidance of immune response.<sup>58</sup> An example in CDR is described for HER2 therapies in breast cancer with a *PIK3CA* mutation, where an upregulation of collagen/integrin/Src signaling was found, endowing resistance to *trastuzumab* and *pertuzumab*.<sup>59</sup>

Another example is the intrinsic resistance mechanism previously mentioned, the changes in extracellular pH. In latest years a combined treatment including proton-pump inhibitors has increased.<sup>60</sup> When treatment starts, TME can change significantly giving as a result a resistance to therapy (chemotherapy or targeted).

<sup>57</sup> <https://www.nature.com> (14/10/2019)

<sup>58</sup> M. W. Pickup; J. K. Mouw; V. M. Weaver. *EMBO Rep.* **2014**, *15*, 1243-1253

<sup>59</sup> A. B. Hanker; M. V. Estrada; G. Bianchini; P. D. Moore; J. Zhao; F. Cheng; J. P. Koch; L. Gianni; D. R. Tyson; V. Sánchez; B. N. Rexer; M. E. Sanders; Z. Zhao; T. P. Stricker; C. L. Arteaga. *Cancer Res.* **2017**, *77*, 3280-3292

<sup>60</sup> Z. N. Lu; B. Tian; X. L. Guo. *Cancer Chemother. Pharmacol.* **2017**, *80*, 925-937

As an indispensable component of TME it is necessary to highlight myofibroblasts (or cancer associated fibroblasts (CAFs)) and tumor associated macrophages (TAMs). The CAFs are able to promote tumor growth and progression, to activate angiogenesis, to stimulate growth factors, to promote ECM and to keep the stemness, between other important roles.<sup>61</sup> An example of them in CDR is the described in head and neck cancers with *cisplatin* resistance, where they produce an exosomal miR-196a which promotes cell growth, survival and inhibition of apoptosis.<sup>62</sup> In non-small cell lung cancer cells, CAFs promote a signal pathway that upregulates P-gp and therefore endowing resistance.<sup>63</sup>

In reference to TAMs, they are anti-inflammatory and protumorigenic cells, facilitating tumor growth, metastasis and they can promote resistance by themselves or stimulating the growth of CSC through inflammatory signals.<sup>64</sup> An example of its role in CDR is found in hepatocellular carcinoma, where TAMs by means of autophagy creates resistance to *oxaliplatin* treatment.<sup>65</sup>

Finally, it is necessary to describe the implications of ATP in TME. In cancer cells, generation of energy, consuming high quantities of glucose and accumulation of lactate (aerobic glycolysis, Warburg effect) differs compared with normal cells in which glucose is oxidized in the mitochondria. Therefore, high levels of ATP have found to be essential for cancer cells and much more in resistance cancer cells where energy is necessary to fight stress. In one study, ATP concentration was found two times higher inside resistant cancer cells compared with primary tumor cells.<sup>66</sup> In intratumoral space, extracellular ATP (eATP) can be increased by apoptosis or autophagy of cancer cells, thus eATP works as a signal (purinergic signal) with ability to promote cell growth, proliferation and inducing EMT. This eATP can be internalized in cells increasing the intracellular ATP, hence, increasing activity of ABC transporters.<sup>67</sup>

This ATP is the principal source of adenosine for CCs (CD73 catalyzes the conversion of ATP to adenosine). Adenosine is essential in order to promote immunosuppression.<sup>68</sup>

All these summarized processes, underline the elaborated network that TME can be and actually TME is only one aspect of the following point, the tumor heterogeneity, because TME enriches the possible genetic differences in a tumor.<sup>69</sup>

#### TUMOR HETEROGENEITY

The heterogeneity of tumors embraces different concepts, the main one is probably genetic differences between tumor subpopulations (different cancer cells) and also different kinds of cells (immune cells, cancer stem cells, and others). Then, temporal heterogeneity, that is, temporal

---

<sup>61</sup> M. Wang; J. Zhao; L. Zhang; F. Wei; Y. Lian; Y. Wu; Z. Gong; S. Zhang; J. Zhou; K. Cao; X. Li; W. Xiong; G. Li; Z. Zeng; C. Guo. *J. Cancer* **2017**, *8*, 761–773

<sup>62</sup> X. Qin; H. Guo; X. Wang; X. Zhu; M. Yan; X. Wang; Q. Xu; J. Shi; E. Lu; W. Chen; J. Zhang. *Genome Biol.* **2019**, *20*, 1-21

<sup>63</sup> Q. Zhang; J. Yang; J. Bai; J. Ren. *Cancer Sci.* **2018**, *109*, 944-955

<sup>64</sup> A. J. Petty; Y. Yang. *Immunotherapy* **2017**, *9*, 289–302

<sup>65</sup> X. T. Fu; K. Song; J. Zhou; Y. H. Shi; W. R. Liu; G. M. Shi; Q. Gao; X. Y. Wang; Z. B. Ding; J. Fan. *Cancer Cell Int.* **2019**, *19*, 1-11

<sup>66</sup> Y. Zhou; F. Tozzi; J. Chen; F. Fan; L. Xia; J. Wang; G. Gao; A. Zhang; X. Xia; H. Brasher; W. Widger; M. L. M. Ellis; Z. Weihua. *Cancer Res.* **2012**, *72*, 304-314

<sup>67</sup> Y. Qian; X. Wang; Y. Liu; Y. Li; R. A. Colvin; L. Tong; S. Wu; X. Chen. *Cancer Lett.* **2014**, *351*, 242-251

<sup>68</sup> X. Wang; Y. Li; Y. Qian; Y. Cao; P. Shriwas; H. Zhang; X. Chen. *Oncotarget* **2017**, *8*, 87860-87877

<sup>69</sup> F. D. Virgilio; A. C. Sarti; S. Falzoni; E. De Marchi; E. Adinolfi. *Nat. Rev. Cancer* **2018**, *10*, 601-618

changes in cells composition. As well, it can be heterogeneity in nutrients and oxygen depending on the angiogenesis and vessels surrounding the tumor.<sup>70</sup>

The heterogeneity of a tumor is one of the biggest hurdles for a good efficacy in a treatment. In a cancer with a late diagnosis, the probability of high heterogeneity is increased, then chemotherapy and/or radiotherapy will kill some subpopulations, but the resistance ones will survive and they are able to communicate using extracellular vesicles containing ncRNAs and pass those genetic characteristics that confers resistance to other CCs.<sup>71</sup>

To avoid these decreased outcomes in treatments, more genetic studies (sequential cell-studies, samples of every part of tumor, and others) will afford good information about heterogeneity and then a personalized therapy can be prepared.

#### *DEREGULATION OF CELL DEATH*

Three main paths of programmed death can be sorted: apoptosis, autophagic programmed cell death and necrotic cell death.

Most of cancer therapies attack DNA or cell cycle (CDKs, p53, TNF family, and others) driving cells to a programmed cell death. As it has been explained, in some cancers the tumor suppressors or protooncogenes are altered and therefore they are able to avoid the apoptosis. Multiple mechanisms are used by cancer cells to avoid all pathways that can draw them to apoptosis, such as altering the expression of pro-apoptotic genes (downregulation) or anti-apoptotic genes (upregulation) or post-translational regulation (altering protein functions, destroying pro-apoptotic proteins).<sup>72</sup>

#### · Autophagy

The autophagy is an essential process, producing energy by means of degradation or recycling dysfunctional cellular components and/or proteins, so it is a self-renewal process which helps to keep homeostasis.<sup>73</sup>

In normal cells, autophagy can play a protective paper against cancer, destroying those cells, toxins, altered proteins, carcinogens, that can promote cancer, but when autophagy is altered (mutations) the energy in the cell is as well altered and processes as DNA replication can be affected.<sup>74</sup>

In cancer, autophagy can be a doubled-edged sword as well, because it can promote tumor growth and survival or either lead cancer cell to a programmed cell death. Since in cancer, stress and inflammatory states are present, autophagy helps to produce the amount of energy necessary to counter it.<sup>75</sup>

---

<sup>70</sup> I. Dagogo-Jack; A. T. Shaw. *Nat. Rev. Clin. Oncol.* **2018**, *15*, 81-94

<sup>71</sup> N. A. Yousafzai; H. Wang; Z. Wang; Y. Zhu; L. Zhu; H. Jin; X. Wang. *Am. J. Cancer Res.* **2018**, *8*, 2210–2226

<sup>72</sup> K. Fernald; M. Kurokawa. *Trends. Cell. Biol.* **2013**, *23*, 620–633

<sup>73</sup> N. Mizushima; M. Komatsu. *Cell.* **2011**, *147*, 728-741

<sup>74</sup> Z. J. Yang; C. E. Chee; S. Huang; F. A. Sinicrope. *Mol. Cancer. Ther.* **2011**, *10*, 1533–1541

<sup>75</sup> Y. J. Li; Y. H. Lei; N. Yao; C. R. Wang; N. Hu; W. C. Ye; D. M. Zhang; Z. S. Chen. *Chin. J. Cancer* **2017**, *36*, 1-10

The modulators of autophagy are called *Atgs* and in situations of stress, hypoxia they are stimulated.<sup>76</sup> It has been described how autophagy can drive to drug resistance in cancers like hepatocellular carcinoma, where was found that downregulation of miR-199a-5p induced by *cisplatin* treatment activates autophagy. Then, when autophagy is inhibited in MDR, the outcome of the treatment is improved.<sup>77</sup> Hence, autophagy can protect cancer cells destroying damaged DNA and fighting against stressful situation.

This is the pro-survival edge of autophagy, in what pro-death activity respects, cell intrinsic autophagy can help chemotherapeutics inhibiting genetic instability, because when DNA is damaged, autophagy is able to destroy erroneous sequences or even lead to a cell death, since controlling the protein quality is a described function of autophagy. Besides, in those cancer cells where apoptosis is altered, the autophagic process is able to drive cells to death, thus, targeting autophagy could be a resource to treat this type of cancers, due to autophagy overactivation drives to a programmed cell death.<sup>78</sup>

The activity of autophagy, acting as a pro-death or pro-survival, it depends on tumor type and the kind of treatment.<sup>79</sup> In each cancer should be studied the altered pathways to know if it will be useful to inhibit or stimulate autophagy in a combined therapy and much more in MDR cancers (Figure 12).

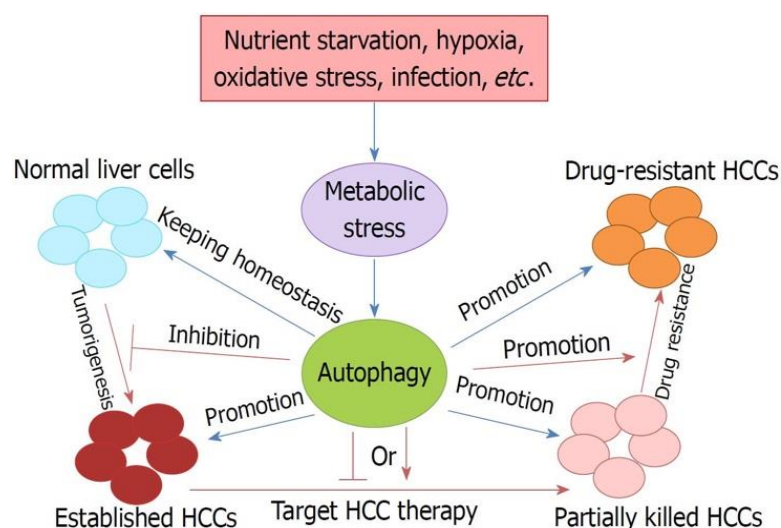


**Figure 12.** Illustration of autophagy roles in hepatocellular carcinoma (HCC)<sup>76</sup>

#### CANCER STEM CELLS (CSCs) AND EPITHELIAL MESENCHYMAL TRANSITION (EMT)

The subpopulation of CSCs and the phenotypic plasticity conferred by EMT provides cancer more aggressiveness with ability to decrease treatment efficacy, acquiring resistance to it.

To obtain these phenotypic characteristics, cancer cells undertake a reprogramming process.<sup>80</sup>

<sup>76</sup> Y. Cao; Y. Luo; J. Zou. J. Ouyang; Z. Cai; X. Zeng; H. Ling; T. Zeng. *Clin. Chim. Acta* **2019**, 489, 10-20

<sup>77</sup> N. Xu; J. Zhang; C. Shen; Y. Luo; L. Xia; F. Xue; Q. Xia. *Biochem. Biophys. Res. Commun.* **2012**, 423, 826-831

<sup>78</sup> B. Y. K. Law; V. W. K. Wai. *Intechopen* **2016**, 20, 435-454

<sup>79</sup> F. Huang; B. R. Wang; Y. G. Wang. *World J. Gastroenterol.* **2018**, 24, 4643-4651

<sup>80</sup> X. Liu; D. Fan. *Curr. Pharm. Des.* **2015**, 21, 1279-1291



· EMT

EMT is a highly conserved cellular process transforming epithelial cells to mesenchymal cells by means of losing cell polarity and cell-cell adhesion. It is involved in embryogenesis, wound healing and tumorigenesis (metastasis, recurrence, progression and resistance to therapy).

The mechanism used by EMT to endow cancer with drug resistance are not clear, but morphological changes produce alteration of functional proteins related with epithelial cells and mesenchymal cells. For example, it is known that some of ABC promoter genes have binding sites for EMT transcription factors.<sup>81</sup> The described miRNAs also contribute to EMT, regulating several signals cascades.

These are some of transcription factors that can be a good target to treat or prevent drug resistance: Snail, Slug, TGF-beta, ZEB, helix-loop-helix, amongst others. For example, in one study was showed how inhibiting TGF-beta can reverse EMT phenotype and increase chemotherapy efficacy (figure 13).<sup>82,83,84</sup>

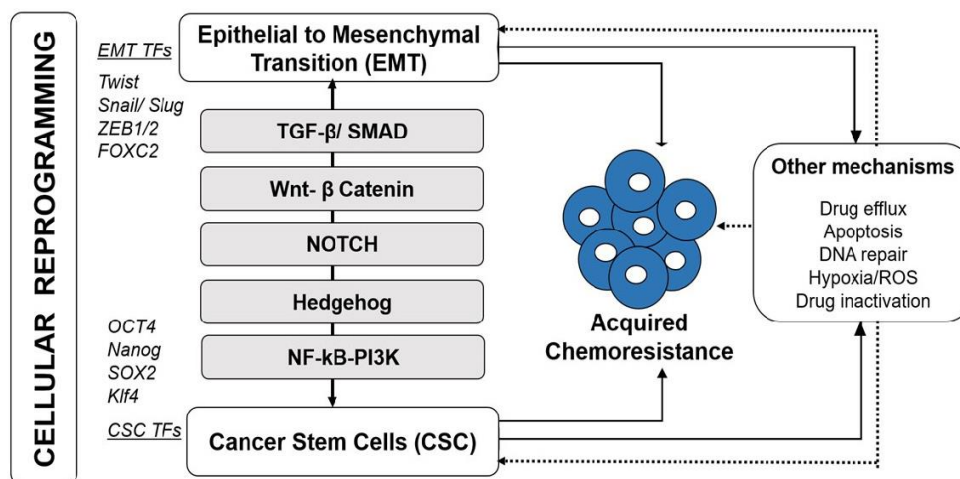


Figure 13. Illustration of connectivity network between EMT and CSC driving to resistance<sup>89</sup>

· CSCs

The CSCs are a subpopulation of tumor with the same characteristics of stem cells, that is, capacity of self-renewal, quiescence, plasticity and potency to differentiate cell populations, endowing CSCs with high tumorigenic potential. Besides, there are numerous studies showing the capacity of this cells to resist radiotherapy and chemotherapy.<sup>85,86</sup> Here we summarize some described mechanism to get CDR by CSC.

<sup>81</sup> Z. S. Jiang; Y. Z. Sun; S. M. Wang; J. S. Ruan. *J. Cancer* **2017**, *8*, 2319-2327

<sup>82</sup> Y. T. Tang; Y. Y. Huang; J. H. Li; S. H. Qin; Y. Xu; T. X. An; C. C. Liu; Q. Wang; L. Zheng. *BMC Genomics* **2018**, *19*, 1-14

<sup>83</sup> M. Mutlu; U. Raza; Ö. Saatci; E. Eyüpoğlu; E. Yurdusev; Ö. Şahin. *J. Mol. Med.* **2016**, *94*, 629-644

<sup>84</sup> N. E. Bhola; J. M. Balko; T. C. Dugger; M. G. Kuba; V. Sánchez; M. Sanders; J. Stanford; R. S. Cook; C. L. Arteaga. *J. Clin. Invest.* **2013**, *123*, 1348-1358

<sup>85</sup> T. B. Steinbichler; J. Dudás; S. Skvortsov; U. Ganswindt; H. Riechelmann; I. I. Skvortsova. *Semin. Cancer Biol.* **2018**, *53*, 156-167

<sup>86</sup> E. Batlle; H. Clevers. *Nat. Med.* **2017**, *23*, 1124-1134

One of the properties that confers more tumorigenicity is the quiescence state, which allows CSCs to avoid therapies since the main treatments attack proliferative cells. Also, if DNA results damaged, they have an improved DNA repair mechanism and more time to repair it.<sup>87</sup> After treatment, stress in cancer cells is increased and when levels of ROS are high, these can drive cell to death, but in CSCs the enzyme aldehyde dehydrogenase (ALDH) is overexpressed and thus the levels of ROS are kept low.<sup>88</sup>

The relation between EMT and CSCs is clear, they share a common regulatory mechanism and transcriptional factors which are the pivotal key to start the metastasis, recurrence and resistance. The EMT allows plasticity and stemness properties to maintain and to acquire CSCs features, meanwhile the CSCs uses EMT to get resistance, progression and tumor survival (Figure 13).<sup>89</sup> Resistant cells are more like mesenchymal cells.

All the reviewed mechanisms (Figure 14)<sup>90</sup> are a sample of how cancer is able to get resistance to treatment, of how cancer is a complex network adapting its functions to survive and progress in a Darwinian way. More efforts are needed to fight against resistance and relapses in cancer, standing out requirements of going further in mechanisms, enhancing the individual treatments with a good genetic back up and developing new drugs, finding new targets and repurposing drugs.

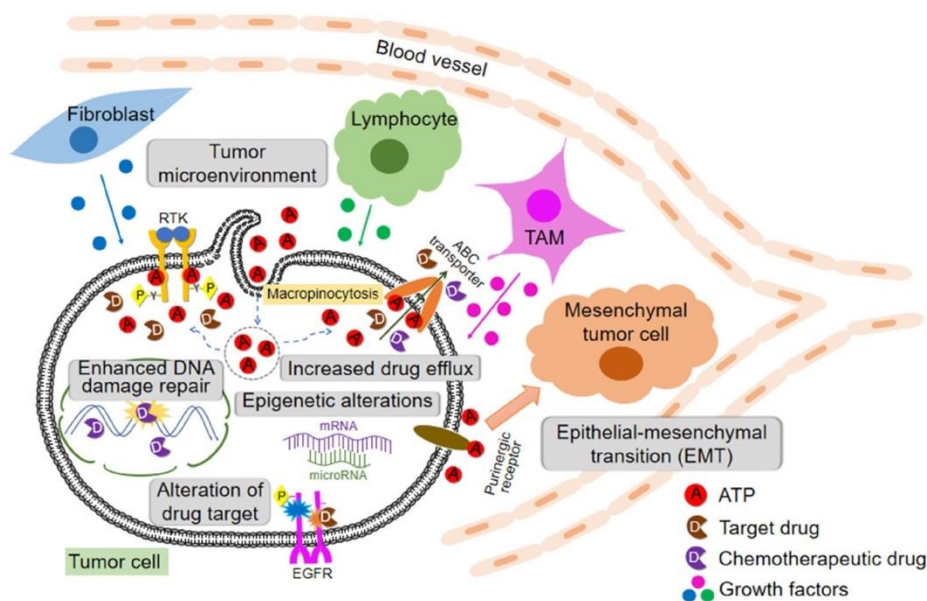


**Figure 14.** Illustration of the reviewed mechanisms responsible of drug resistance in cancer<sup>90</sup>

## 1.2. DRUGS REPURPOSING

Nowadays, developing new drugs is getting more difficult and long periods are needed. The time to obtain a new drug from the initial breakthrough is around 10-15 years, only with clinical trials 6-8 years are needed to ensure security and efficacy.

<sup>87</sup> S. Skvortsov; P. Debbage; P. Lukas; I. Skvortsova. *Semin. Cancer Biol.* **2015**, *31*, 36-42

<sup>88</sup> X. Xu; S. Chai; P. Wang; C. Zhang; Y. Yang; Y. Yang; K. Wang. *Cancer Lett.* **2015**, *369*, 50-57

<sup>89</sup> L. Ponnusamy; P. K. S. Mahalingaiah; Y. W. Chang; K. P. Singh. *Cancer Drug Resist.* **2019**, *2*, 297-312

<sup>90</sup> X. Wang; H. Zhang; X. Chen. *Cancer Drug Resist.* **2019**, *2*, 141-160

Then, the cost to produce it (measured by the Tufts University Center for the study of Drug Development) is around 2.6 billion dollars (2013), growing 8.5% every year.<sup>91</sup>

Given this situation, it is increasing the process called drug repurposing, a strategy to identify new activities and applications for already approved medicines or investigational medicines. This entails some advantages in terms of cost, time and safe. Since some drugs will have passed the clinical trials, they are concluded as safety for human use. The efficacy of these drugs has to be proved for the new use, but at least, the risks of fail is lower. Also, those drugs that have failed because of efficiency- efficacy but with a good safety profile, can be as well, repurposed.

In terms of cost, the investment it is also lower given that most of steps will be already done, so it can decrease from 3 billion dollars to 200-300 million dollars.<sup>92</sup> Indeed, time will be reduced as well, depending if drug is already on the market or in preclinical stage.

Taking all of this together, the advantages of this approach are clear, such as quickest return of benefits, low risk, and in research could bring new targets and new mechanisms of action. But there are some hurdles that decreases efficiency of drug repurposing, the patents.

In what patents belong, industry can find some problems in patenting new activities due to the main source of information will be already in the available literature. Only if new activity affords differences compared with public data, then the company will be able to patent it.

Exists a special patent for those drugs in the market out of patent when a new activity has found for them, the called new method-of-use. But it can be tricky to control it when generics of them are already in the market.<sup>93</sup>

Repurposing drugs has been practicing along history of research and development, probably not in a voluntary way, but affording good results as in *Thalidomide* case, which was used as a sedative and was withdrawn off the market in 1961 due to birth skeletal defects. A few years after, was found to be effective for erythema nodosum leprosum and finally, in 1999, for multiple myeloma.<sup>94</sup>

In latest years more techniques and methods have been developed in order to enhance the repurposing and activity prediction of thousand compounds. These tools can be computational, experimental or mixed, but the aim is the same, find a relationship drug-disease.

The most common computational approaches are based on comparison between genetic expression after treatment and genetics of diseases.<sup>95</sup>

Therefore, more open access resources should be available and exploded in order to downsize and correlate all information about the existence drugs and diseases (Table 3).

---

<sup>91</sup> J. A. DiMasi; H. G. Grabowski; R. W. Hansen. *J. Health Econ.* **2016**, *47*, 20-33

<sup>92</sup> N. Nosengo. *Nature* **2016**, *534*, 314-316

<sup>93</sup> S. Pushpakom; F. Iorio; P. A. Eyers; K. J. Escott; S. H. A. Wells; A. Doig; T. Williams; J. Latimer; C. McNamee; A. Norris; P. Sanseau; D. Cavalla; M. Pirmohamed. *Nat. Rev. Drug Discov.* **2019**, *18*, 41-58

<sup>94</sup> C. M. Telleria. *J. Cancer Sci. Ther.* **2012**, *4*, 9-11

<sup>95</sup> H. X. J. Li; H. Xie; Y. Wang. *Int. J. Biol. Sci.* **2018**, *14*, 1232-1244

**Table 3.** Examples of repurposed drugs with new applications in cancer

DRUG	FIRST INDICATION	REPURPOSED FOR
<i>Pemetrexed</i>	Mesothelioma	Lung cancer <sup>96</sup>
<i>Tretinoin</i>	Acne	Leukemia <sup>97</sup>
<i>Gemcitabine</i>	Antiviral	Cancer (bladder, breast, and others) <sup>98</sup>
<i>Disulfiram</i>	Alcoholism	Melanoma <sup>99</sup>
<i>Thalidomide (isomer)</i>	Morning sickness	Leprosy, multiple myeloma <sup>94</sup>
<i>Aspirin</i>	Analgesic, antipyretic and anti-inflammatory	Colon cancer prevention <sup>100</sup>
<i>Quinine</i>	Malaria	Arthritis rheumatoid <sup>101</sup>

Recently, Fuster et al.<sup>102</sup> have shown that treatment with the drug *dabigatran*, a direct-acting oral anticoagulant, delays the onset of Alzheimer's disease. Studies continue but is very likely that this drug is repurposed for the treatment of said disease.

### 1.3. PREDICTION OF ACTIVITY PROGRAMS

In the last years, more computational methods have been developed in order to link compounds, targets and diseases, as a basis of drug discovery, leading to an improvement in the selection through thousands of candidates (Figure 15).<sup>103</sup> These tools also help to understand mechanisms, unexpected activities, possible adverse effects, amongst others. Here, we summarize some of these tools, sorted by structure-based and ligand-based approaches, that can help to save cost and time in drug development.<sup>104</sup>

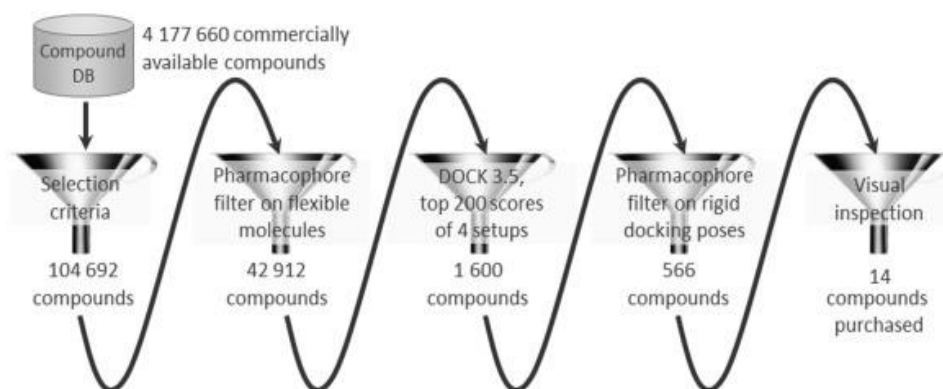


**Figure 15.** Example of virtual screening cascade to identify a new potential drug with the number of compounds that pass in each filter<sup>103</sup>

<sup>96</sup> A. Saxena; D. Becker; I. Preeshagul; K. Lee; E. Katz; B. Levyc. *Oncologist* **2015**, *20*, 934–945

<sup>97</sup> E. Damery; D. A. Solimando; J. A. Waddell. *Hosp. Pharm.* **2016**, *51*, 628–632

<sup>98</sup> <https://www.cancerresearchuk.org> (17/10/2019)

<sup>99</sup> <https://www.fda.gov> (17/10/2019)

<sup>100</sup> P. Patrignani; C. Patrono. *J. Am. Coll. Cardiol.* **2016**, *68*, 967–976

<sup>101</sup> J. An; M. Minie; T. Sasaki; J. J. Woodward; K. B. Elkon. *Annu. Rev. Med.* **2017**, *68*, 317–330

<sup>102</sup> M. Cortes-Canteli; A. Kruyer; I. Fernandez-Nueda; A. Marcos-Diaz; C. Ceron; A. T. Richards; V. Fuster. *JACC*, **2019**, *74*, 1910–1923

<sup>103</sup> N. Tidten-Luksch; R. Grimaldi; L. S. Torrie; J. A. Frearson; W. N. Hunter; R. Brenk. *PLoS One* **2012**, *7*, e35792

<sup>104</sup> S. S. Ou-Yang; J. Y. Lu; X. Kong; Z. Liang; C. Luo; H. Jiang. *Acta Pharmacol. Sin.* **2012**, *33*, 1131–1140

### STRUCTURE-BASED APPROACH (Interaction drug-target)

The target structure (macromolecule) has to be known through crystallization, NMR or/and homology models.<sup>105</sup>

#### a) COMPUTATIONAL DOCKING

Computational docking is based on the structure in order to predict the best conformation and orientation of a small molecule in a specific target (Figure 16).<sup>106</sup> It can be used testing a variety of ligands for one target or one ligand in front of different targets.<sup>107</sup>

In order to work with this tool a 3D structure of the molecule is needed and some proteins are still not available, for example G protein-coupled receptors (GPCRs), which are the largest class of membrane proteins in humans with vital roles in cells and approximately 475 approved drugs by FDA target GPCRs.<sup>108</sup> Also, some GPCRs are still considered orphan, probably crystallization of these receptors to obtain the 3D structure will open a new world of opportunities (new targets, new drugs).

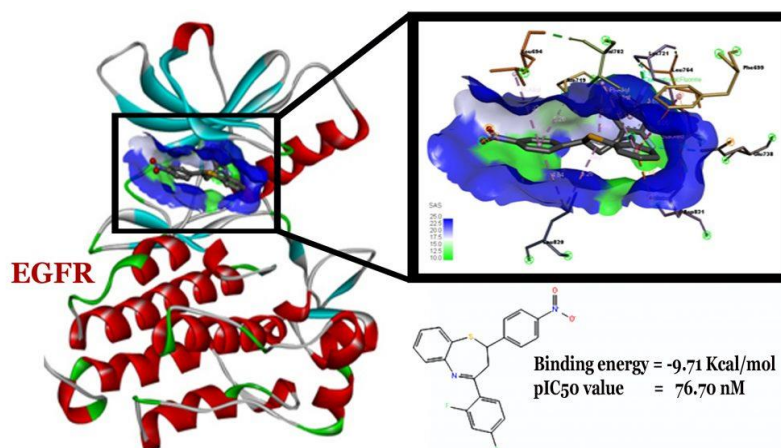


**Figure 16.** Example of computational docking in anti-cancer drug development targeting EGFR<sup>106</sup>

### LIGAND BASED APPROACH

These tools are applied when the targets 3D structure is not well known.

#### a) PHARMACOPHORE MODEL

Pharmacophore is the part of a molecule responsible for a specific biological or pharmacological activity. The pharmacophore model is based on ligand approach, that is, superposing different active compounds and extracting shared chemical features that confers the activity.

<sup>105</sup> L. Chen; J. K. Morrow; H. T. Tran; S. S. Phatak; L. Du-Cuny; S. Zhang. *Curr. Pharm. Des.* **2012**, *18*, 1217–1239

<sup>106</sup> C. H. M. M. P. Rao; R. P. Yejella; S. A. Rehman; C. Rajeswari; S. H. Basha. *Journal of Peer Scientist* **2018**, *1*, e1000008

<sup>107</sup> L. Scotti; M. F. J. Junior; H. M. Ishiki; F. F. Ribeiro; R. K. Singla; J. M. Barbosa; M. S. Da Silva; M. T. Scotti. *Curr. Drug Targets* **2017**, *18*, 592-604

<sup>108</sup> A. S. Hauser; S. Chavali; I. Masuho; L. J. Jahn; K. A. Martemyanov; D. E. Gloriam; M. M. Babu. *Cell*. **2018**, *172*, 41–54

In order to build a good model, it will be necessary the called “training set of ligands”, what means, choosing a wide spectrum of molecules (some with activity and others without) to establish references for the approach, this step is the most important.

Then, a good conformation generation must be created, taking in consideration the bounds with target, low energy conformation, and others. The last steps are superimposition or alignment of molecules and finally the results of common chemical features which affords activity.<sup>109</sup>

This method can draw some mistakes depending on the library of compounds chosen for the training set. Summarizing, this approach provides compounds information (hydrogen bonds, hydrophobicity, aromaticity, and others) allowing to create a relation between structural features-specific target.

#### b) SAR-QSAR

Quantitative Structure Activity Relationships (QSAR) is based on the idea that when a structure of a molecule changes also his properties or activity change. It is based on mathematical and statistical calculations of relations between psychochemical properties and biological activity.<sup>110</sup>

Since QSAR equations are created by descriptors (spatial, structure, thermodynamic, conformational, and others), it is important to define them properly, because it is the mechanism through which the molecule properties become numbers in the program. It is centered on structure-activity relationship, therefore, when a compound is tested in a SAR model it means that it is being compared with a wide spectra of active and non-active compounds (references) for a specific target. Finally, it gives as a result a mathematical formula correlating structure and activity.<sup>111</sup>

Nowadays, some derivations exist, for example QSPR (quantitative structure-property relationship) or QSRR (quantitative structure-reactivity relationship).

#### OPEN DATA BASES APPROACH

The number of potential targets, new mechanisms of action and molecular mechanism are increasing and therefore, valuable information that has to be processed. Since this data is online in open sources, tools to predict activities (between other properties) are increasing as well, enabling the research community to optimize the process of drug discovery (Table 4). Some computational tools, like machine learning or neural networks helps to maintain data bases in constant actualization through algorithms that regulates its bases.<sup>112</sup>

In the following table some open sources are summarized, and the Prediction of Activity Spectra for Substance (PASS) is developed as an example.

---

<sup>109</sup> S. Y. Yang. *Drug Discov Today* **2010**, *15*, 444-450

<sup>110</sup> G. Gini. *Methods Mol. Biol.* **2016**, *1425*, 1-20

<sup>111</sup> J. Verma; V. M. Khedkar; E. C. Coutinho. *Curr. Top. Med. Chem.* **2010**, *10*, 95-115

<sup>112</sup> J. Y. Trosset; C. Cave. *Methods Mol. Biol.* **2019**, *1953*, 189-193

**Table 4.** Examples of open source data base

DATABASE	DESCRIPTION	SOURCE
ChEMBL	Source of chemical, bioactivity and genomic data to support transition of genomic information to new drugs	<a href="https://www.ebi.ac.uk/chembl/">https://www.ebi.ac.uk/chembl/</a>
Chemspider	67 million structures from hundreds of data sources	<a href="http://www.chemspider.com">http://www.chemspider.com</a>
Open Targets Platform	Visualization of potential drug targets associated with disease	<a href="https://www.targetvalidation.org">https://www.targetvalidation.org</a>
Human Protein Atlas	Tissue atlas, distribution of proteins in tissues. Cell atlas, expression and distribution of proteins within human cells. Pathology atlas, mRNA and protein expression data from 17 different forms of cancer	<a href="https://www.proteinatlas.org">https://www.proteinatlas.org</a>
Genomics Data Commons	Data repository that allows data sharing in cancer genomic studies in support of precision medicine	<a href="https://gdc.cancer.gov">https://gdc.cancer.gov</a>
PASS	Source to predict biological activity of any compound. Predicts biological activity (pharmacological effects, mechanism of action, toxicity, interactions, and others)	<a href="http://www.way2drug.com/PASSonline/">http://www.way2drug.com/PASSonline/</a>

· PASS

This open source allows to predict over 3500 different biological activities and only structural formula is needed, then virtual drugs can be screened before synthesized.

In order to obtain the results, this platform is based on relationship activity-structure of 250.000 compounds with some biological activity.<sup>113</sup> In the case of cancer, detecting cytotoxicity in different cell lines by different compounds is a good example about how these tools can improve research. Prediction of cytotoxicity for 24 breast cancer cell lines, 49 compounds were selected between 1 million, based on cytotoxicity and interactions with cancer targets. Of this 49, only eight showed a significant  $IC_{50}$ .<sup>114</sup>

Combining these tools, it is afforded a valuable network of information with capacity to predict activities of potential drugs, considering other parameters like interaction with transporters, metabolic processes and signal pathways, which are related with tissue and cells.<sup>115</sup> In cancer, specifically in drug resistance, these tools can be really useful. For example, when tumor heterogeneity is described through genetic tests, data can be collected in these platforms and

<sup>113</sup> <http://www.way2drug.com> (18/10/2019)

<sup>114</sup> V. Konova; A. Lagunin; P. Pogodin; E. Kolotova; A. Shtil; V. Poroikov. *SAR QSAR Environ. Res.* **2015**, *26*, 595-604

<sup>115</sup> A. A. Lagunin; V. I. Dubovskaja; A. V. Rudik; P. V. Pogodin; D. S. Druzhilovskiy; T. A. Glorizova; D. A. Filimonov; N. G. Sastry; V. V. Poroikov. *PLoS One* **2018**, *13*, e0191838

therefore new or already commercial drugs (repurposing drugs) can be tested affording new results and enhancing a wide spectrum of drugs to treat cancer. With this example, stands out the need to take all processes together, clinical and research, because clinic feedbacks will improve research. Hence, open sources should collect data becoming for clinical trials, hospitals, laboratories, and others. Unfortunately, there are still lots of sources of valuable information without a software batching it, for example, treatments and outcomes of patients in hospitals where, in most cases, data is collected but not processed.

#### 1.4. TROPICAL DISEASES (TDs)

Tropical diseases englobe all those diseases mostly, or only, present in tropical countries. These countries, positioned between Tropic of Cancer and Tropic of Capricorn, are approximately occupied for 40% of worlds population and it is estimated a growth in the following years.<sup>116</sup> Tropical diseases are causing approximately 57 million deaths worldwide, affecting 149 countries.<sup>117</sup> They are called tropical in reference to infectious diseases prospering in humid-warm conditions. Some of them are chagas disease, malaria, dengue, dracunculiasis (guinea-worm disease), leishmaniasis, lymphatic filariasis, neglected tropical diseases, onchocerciasis, schistosomiasis, and others (Figure 17).<sup>118</sup> Most of them can drive to death, while others can produce malformation, injuries in cognitive development, disfigure, blind, and others.<sup>119</sup>

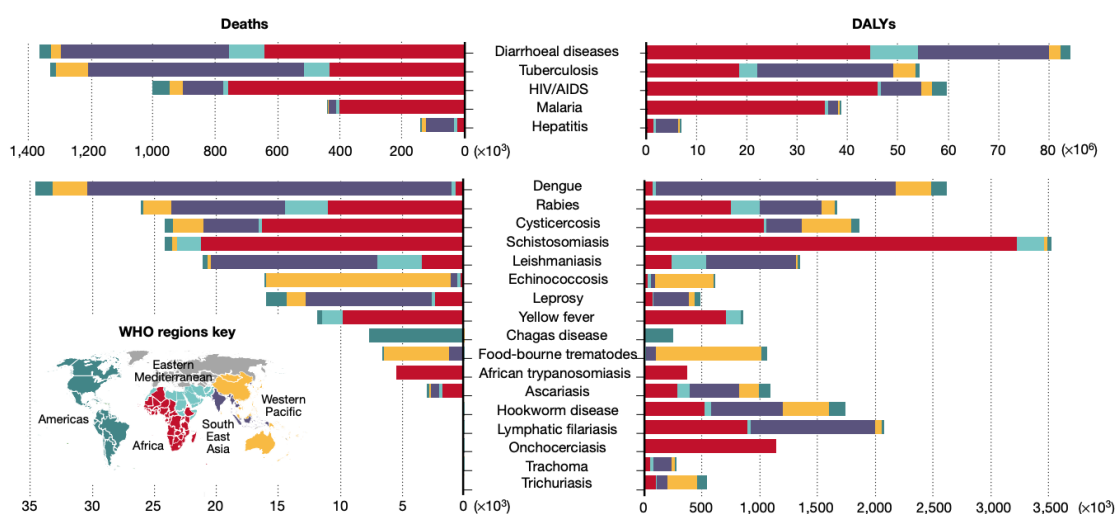


Figure 17. Illustration of deaths and disability-adjusted life years (DALYs) due to tropical diseases<sup>118</sup>

Since population continue growing and migration movements as well, the impact of TDs has increased. New diseases like Ebola have appear and controlled diseases like dengue, has recurred. Also, due to climate changes in temperate climate zones, and through migrations, some TDs have thrived to new countries.

<sup>116</sup> <http://worldpopulationreview.com> (22/10/2019)

<sup>117</sup> <https://www.cdc.gov> (22/10/2019)

<sup>118</sup> M. De Rycker; B. Baragaña; S. L. Duce; I. H. Gilbert. *Nature* **2018**, 559, 498–506

<sup>119</sup> <https://www.who.int> (22/10/2019)



Some of these diseases are considered neglected because they are associated with poverty, lack of sanitary infrastructures, lack of sanitary education and therefore no prevention and/or treatment are applied. In the past few years some of these diseases decreased considerably but there are still countries out of socioeconomic growth and thus, they are out of resources that afford help.

In the London Declaration on neglected TDs (2012), over 80 organizations, mainly pharmaceutical companies, agreed to control, eliminate or eradicate 10 diseases by 2020. Also, WHO establish a “roadmap” to accelerate the work to reduce global impact of TDs.

These objectives were set because WHO showed clear evidence about the capacity to eradicate or eliminate symptoms of TDs affecting more than 1 billion people. Basically, the aims proposed were to increase research in order to find new treatments, also to facilitate drug access, to improve collaboration and organization worldwide, as well to provide educational support and infrastructures to prevent diseases.<sup>120</sup>

Here, we summarize some of these diseases: chagas, malaria and tuberculosis, three of the most prevalent TDs.

### 1.4.1. CHAGAS DISEASE

Chagas disease, also known as American trypanosomiasis, is a potentially life-threatening illness caused by protozoan parasite *Trypanosoma cruzi* (*T. cruzi*). Among neglected tropical diseases half a billion of people are at risk of contracting chagas disease and 6-7 million people are estimated to be infected by it, particularly in South America.

#### TRANSMISION

In order to move to different hosts, parasite uses triatomine bug, typical from America, as a vector. Probably, the most common way to transmit parasites is through feces and urine of infected bugs, which are more active along the night seeking for mammalian blood and then transmitting parasites through its bite (Figure 18).<sup>121</sup>

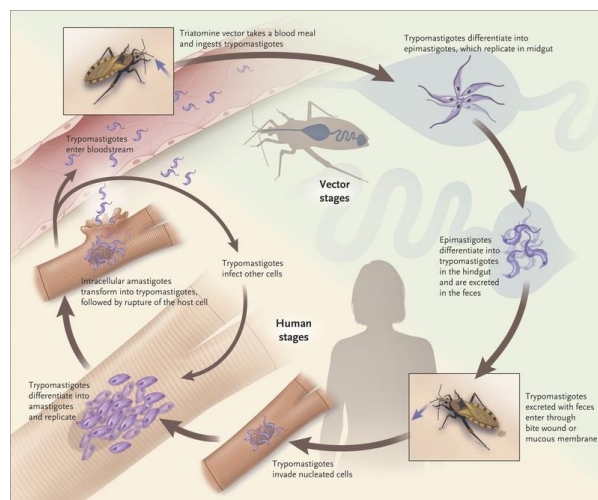


Figure 18. Illustration of *T. cruzi* life cycle<sup>121</sup>

<sup>120</sup> <https://unitingtocombatntds.org> (22/10/2019)

<sup>121</sup> C. Bern. *N. Engl. J. Med.* **2015**, *373*, 456-466

### DISEASE PHASES

The initial acute phase use to appear 2 months after infection. During acute phase, an elevated quantity of parasites circulates in blood. Symptoms can be either absent or some fever, headache, enlarged lymph glands, pallor, muscle pain, difficulty in breathing, swelling, and abdominal or chest pain can appear. Along chronic phase, parasites are concealed in heart and digestive muscles, so around 30% of patients suffer from cardiac alterations and up to 10% suffer from digestive, neurological or a mix of them. After some years, due to parasite attacks in heart muscle and nervous system, it can produce heart diseases, like heart failure or arrhythmias, drawing patients to death.<sup>119</sup>

### PREVENTION

Prevention in chagas disease embraces those practices that prevents contact with vector, such as spraying the house with insecticide, good hygiene practices, screenings and blood testing to detect infected people as soon as possible, the use of bed-nets, and others.<sup>119</sup>

### TREATMENT

Nowadays there are only two drugs to treat chagas, *benznidazole* and *nifurtimox* (Figure 19). Drugs developed 40 years ago. Both of them attacks DNA inhibiting its replication. If treatment starts in acute phases the rate of cure is around 76%, much higher compared with the 37% in chronic phases. For infants infected congenital, the cure rate of treatment is 96% when it starts sooner and 62% when it starts in chronic phase.<sup>122</sup>

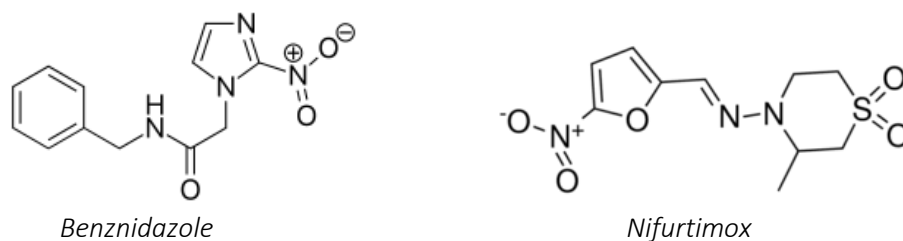


**Figure 19.** Chemical structure of *Benznidazole* and *Nifurtimox*

Chagas parasites are *Kinetoplastid*, a flagellated protozoan. They are defined by the presence of DNA-containing region, the 'kinetoplast', in their single large mitochondrion. They have similar genomic organization and cellular structures and undergo morphological changes during their life cycles inside insects and vertebrate hosts. Approximately 50% of these genomes encode for hypothetical proteins that do not resemble orthologs in human genome, plus several human protein classes are not represented in *kinetoplastid* genomes. All these differences suggest that may be there are essential proteins that can be exploited as selective targets for therapy.<sup>123</sup>

<sup>122</sup> S. Meymandi; S. Hernandez; S. Park; D. R. Sanchez; C. Forsyth. *Curr. Treat. Options Infect. Dis.* **2018**, *10*, 373–388

<sup>123</sup> J. A. Padilla; I. Cotillo; J. Presa; J. Cantizani; I. Peña; A. I. Bardera; J. J. Martín; A. Rodriguez. *PLoS Negl. Trop. Dis.* **2015**, *9*, e0003493

### 1.4.2. MALARIA

Around 300 million people suffer this disease annually around the world, and among this, 3 million people die due to complications. Particularly, young children living in low-income countries are the ones suffering it.

Nowadays, up to 200 million new cases are reported every year and every 2 minutes a child under five dies because of Malaria, that is approximately 60% of total deaths caused by the disease. Most affected areas are African regions (92% cases, 93% deaths).<sup>124</sup>

#### TRANSMISSION

This disease is induced by protozoas parasites of the gender *Plasmodium*, of which the most dangerous are *P. falciparum* (most common in Africa) and *P. vivax* (most common in America) species. The vector used for these parasites are the female of *Anopheles* mosquitoes.

Therefore, mosquitoes transmit malaria biting an infected host, getting parasites in their infective form (sporozoite) and transporting them to a new host (Figure 20).<sup>125</sup> Also, since infectious state of the parasites are found in red blood cells, it is possible to transfer disease through infected blood (needles, transfusions, along the birth (congenital malaria), and others).

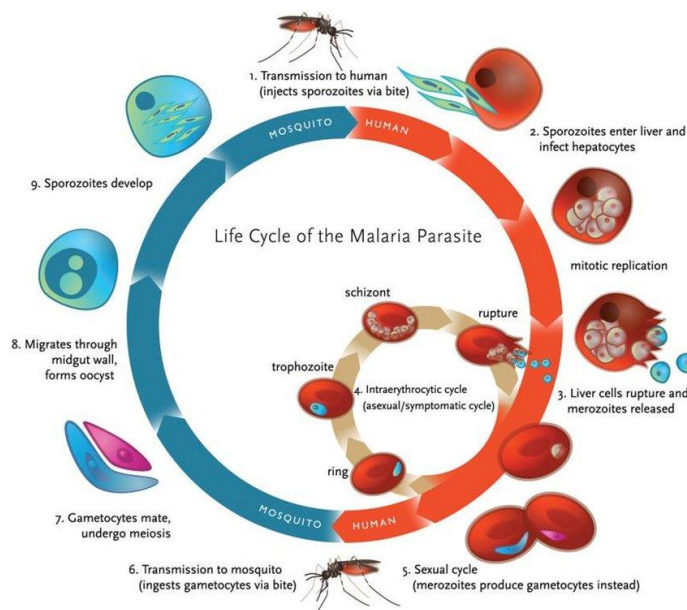


Figure 20. Illustration of *Plasmodium* life cycle<sup>125</sup>

#### DISEASE PHASES

When mosquito bites a new host, it spreads sporozoites present in their saliva into blood. Then, they arrive in liver where infect hepatocytes in order to replicate and grow. After 6-15 days, the rupture of liver cells occurs and thousands of merozoites are released into blood infecting red blood cells and starting the asexual cycle inside erythrocytes, replicating (mitosis) and progressing to different stages. First, ring stage, followed by trophozoite and schizont. Every schizont produces around 16 new merozoites, rupturing erythrocytes and producing clinical disease symptoms.

<sup>124</sup> <https://data.unicef.org> (23/10/2019)

<sup>125</sup> N. Vale; L. Aguiar; P. Gomes. *Front. Pharmacol.* **2014**, 5, 1-1

Some of these merozoites can progress to gametocytes (sexual cycle), which circulating through blood can be suctioned by a mosquito. Inside mosquitoes, gametocytes undergo meiosis and forms oocyst, which progress to sporozoites.<sup>125</sup>

Symptomatology usually appears between 7 to 30 days after the bite, but in some cases, it can take more time (months or a year), for example in travelers where a prophylaxis treatment was administered, delaying manifestations. Also, it will be important the kind of parasite, due to differences in their stages. *P. falciparum* is the shorter one and *P. malarie* the longest. *P. vivax* and *P. ovale* are able to produce dormant parasites in liver.

The common manifestations are fever, vomits, headaches and malaise. Since symptoms are not particularly tough and specific for malaria it can be difficult to recognize it, but another hint is the characteristic timing of symptomatology which appears in cycles of 48 hours with intervals of fatigue and fits of sweating and high temperature.<sup>119</sup>

The most dangerous parasite is *P. falciparum*, because without early treatment it can spread fast and promote organ failure and/or breathing complications.

#### PREVENTION

Prevention is focused in four points: awareness of risk, bite prevention, check if prevention tablets are needed and diagnosis.<sup>126</sup>

First, population sensitization to check where and how they can get infected is the first step to prevent it. People who has to travel in risk areas should visit doctor to know if prophylaxis is needed. Also, people who lives in this risk zones has to be aware of how malaria is transmitted. Second, mosquitoes bite prevention is a good barrier to avoid malaria. Actions like sleep under a net, use of insecticides and wear long clothes covering all body can protect against bites. Third, prophylaxis, which is not 100% protective against malaria, can be different relying upon country. The used drugs are *atovaquone/proguanil*, *chloroquine*, *doxycycline*, *mefloquine*, *primaquine* and *tafenoquine* (Figure 21).<sup>127</sup> Finally, if symptomatology appears, in order to make a correct diagnosis, patient should visit a doctor to confirm malaria through blood test.

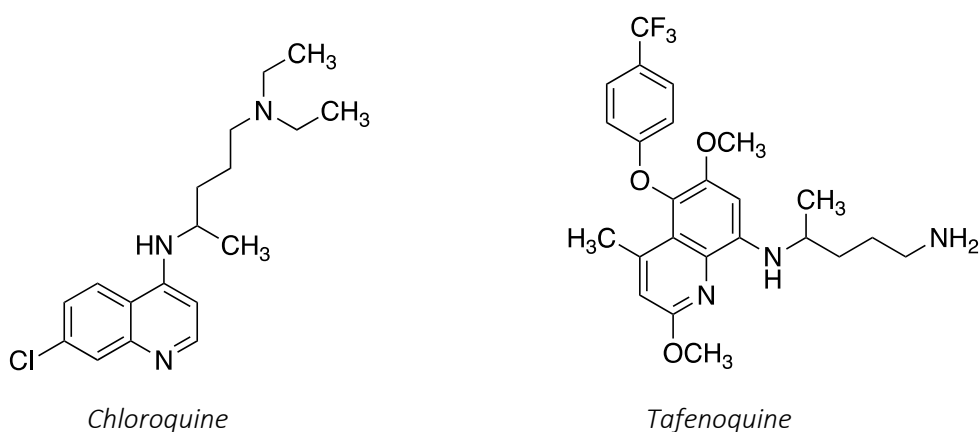


Figure 21. Chemical structure of *Chloroquine* and *Tafenoquine*

<sup>126</sup> G. Berberian; M. T. Rosanova; C. Torroija; M. L. Praino. *Arch. Argent. Pediatr.* **2014**, *112*, 468-473

<sup>127</sup> J. Talapko; I. Škrlec; T. Alebić; M. Jukić; A. Včev. *Microorganisms* **2019**, *7*, e179

## TREATMENT

When malaria is detected, treatment should start soon, because as earlier it starts, better outcomes are obtained. The used first line of drugs are *artemisinin*-based combination therapies and *chloroquine phosphate*. Also, drugs used for prophylaxis can be used as treatment.<sup>128</sup>

Depending on context (kind of parasite, country, prophylaxis, age, and others), dose, treatment-duration and drug-combinations will be decided.<sup>129</sup> Given that malaria is still a threat and more cases of resistance are described, the need of developing new drugs against malaria is desired.

### 1.4.3. TUBERCULOSIS

Tuberculosis (TB) is an infectious disease caused by *Mycobacterium tuberculosis* bacterium (MTB). TB kills around 1.7 million people every year, actually around 25% of all population is infected with TB, but a small portion of them will trigger sickness, especially those people with decreased immune system.<sup>130</sup>

The highest rates of infected people belong to India followed by China, Indonesia, Philippines, Pakistan, Nigeria, Bangladesh and South Africa.<sup>119</sup>

## TRANSMISION

Given that bacterium attacks mainly in lungs, TB spreads using air particles expelled when a person infected in lungs cough, sneezes or talks. It is not possible to get infected shaking hands or sharing drink/food. Then, when bacterium arrives in a new host lung, it is able to move to other parts of the body through blood.<sup>131</sup>

## DISEASE PHASES

As it has been explained, main part of people infected by TB do not get sick, so this phase is called latent. People with latent TB don not have symptoms and their immune system is fighting against bacterium. Therefore, in this phase, transmission of TB is not possible, because is not infectious. People who has HIV/AIDS are more likely to get TB easily than people with an effective immune system.<sup>117</sup>

In disease phase, *MTB* is invading alveolar sacs in lungs where it replicates and grow. Then, in phagosomes created by macrophages, in order to eliminate the invader, the bacterium, through its mycolic acid, it is able to resist, to stay inside the phagolysosome, replicating and finally killing immune cells (Figure 22).<sup>132</sup> At this stage, bacterium is infectious and can be transmitted to other hosts and also to spread to other parts of the body.<sup>133</sup> The most common symptoms in this phase are sickness, pain in chest, cough (with blood or sputum), fever and sweating.<sup>117</sup>

---

<sup>128</sup> S. Basu; P. K. Sahi. *Indian. J. Pediatr.* **2017**, *84*, 521-528

<sup>129</sup> <https://www.europeanpharmaceuticalreview.com> (24/10/2019)

<sup>130</sup> <https://ec.europa.eu> (22/10/2019)

<sup>131</sup> K. Dheda; C. E. Barry; G. Maartens. *Lancet.* **2016**, *387*, 1211-1226

<sup>132</sup> C. J. Cambier; S. Falkow; L. Ramakrishnan. *Cell* **2014**, *159*, 1497-1509

<sup>133</sup> E. N. Houben; L. Nguyen; J. Pieters. *Curr. Opin. Microbiol.* **2006**, *9*, 76-85

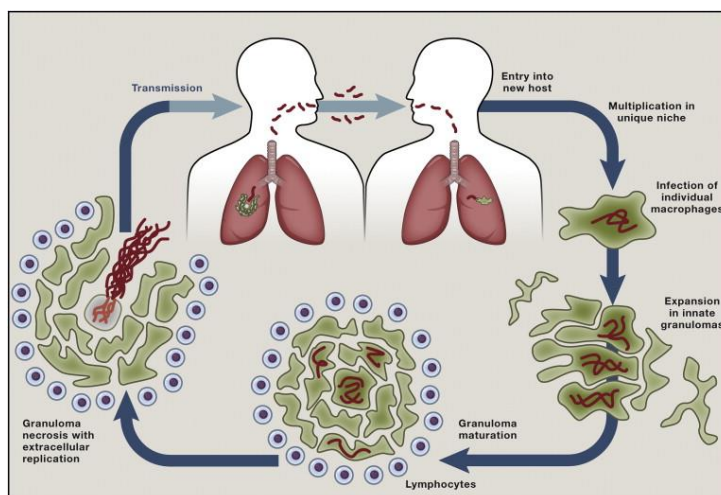


Figure 22. Illustration of *M. Tuberculosis* life cycle<sup>132</sup>

### PREVENTION

In those countries where socioeconomics are poor, the called Bacille Calmette-Guérin vaccine is administrated in order to prevent disease, but it does not protect against pulmonary TB in adults.<sup>134</sup> The riskier people are those with an inefficient immune system, young people and children. Sanitary education to avoid infected people and to treat latent patients, as soon as possible, can diminish the deaths by TB.

### TREATMENT

In latent stage, patients should be treated with *isoniazid*, *rifapentine*, or *rifampin*, personalizing dose, frequency and total dosage depending on age and context, because if patient has contracted TB through people who has a resistance strain to some drugs, treatment will be changed.<sup>135</sup>

In TB disease, treatment has to be followed strictly as prescribed, if not, risk of developing bacterium with resistance or to get sick again, increases. When multidrug resistance appears, cost and time of treatment increases considerably, and it is trickier to cure the disease.

The treatment for TB disease includes as first line, *isoniazid*, *rifampin*, *ethambutol* and *pyrazinamide*. If first line treatment fails, there are other drugs approved to treat TB, such as *bedaquiline* or *linezolid* (Figure 23).<sup>117</sup> Given that TB is still a big threat worldwide and hurdles to treat drug-resistance TB are increasing, development of new drugs is needed.

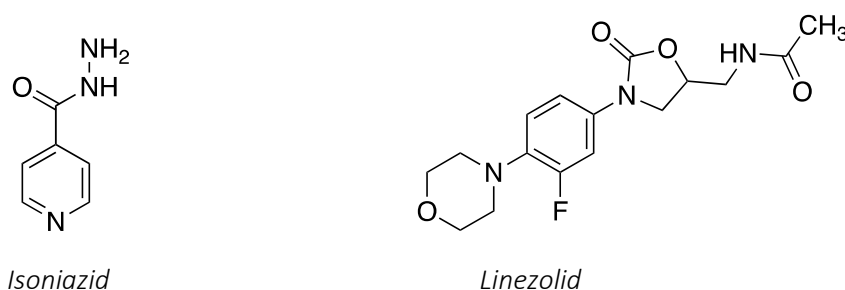


Figure 23. Chemical structure of *Isoniazid* and *Linezolid*

<sup>134</sup> J. Tang; W. C. Yam; Z. Chen. *Tuberculosis* **2016**, *98*, 30-41

<sup>135</sup> T. Degen; T. Bregenzer. *Praxis* **2016**, *105*, 457-61

## 1.5. PREVIOUS WORK

### 1.5.1. SPIRO DERIVATIVES

While many nitrogen heterocyclic systems appear among the most cited in the literature, the spiro-derivatives are usually scarcer. The spirobenzodioxolepiperidine core does not appear described in the literature, with the exception of an article afforded by our research group.<sup>136</sup> In this article, several spiro derivatives were synthesized and its biological activities were evaluated to study its adrenergic activity. As it is well known, aryloxypropanolamines are the most important  $\beta$ -adrenergic antagonists and therefore *propranolol* was also tested, as a positive control (Figure 24).

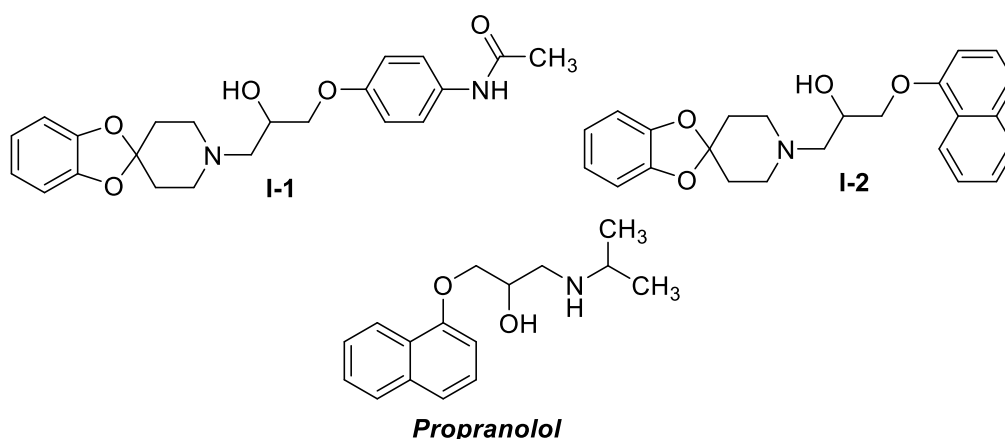


Figure 24. Structures of I-1, I-2 and *propranolol*

The spiro derivatives (I-1 and I-2) were evaluated in vitro for their  $\alpha$ -blocking activity against noradrenaline (in rat vas deferens). Also, their  $\beta$ -blocking activity against isoprenaline was tested,  $\beta_1$  in tracheal smooth muscle and  $\beta_2$  stimulating electrically left atrium of guinea pigs. Among all, the I-1 and I-2 spiro derivatives showed *propranolol*-like activity (Table 5).<sup>136</sup>

Table 5. Activities values for I-1, I-2 and *propranolol*

Compound	$\beta$ -Adrenergic antagonism		$\beta_1/\beta_2$	$\alpha$ -Adrenergic antagonism
	pA <sub>2</sub> ( $\beta_1$ )	pA <sub>2</sub> ( $\beta_2$ )		
I-1	8.42 + 0.31	7.59 + 0.25	6.8	Inactive
I-2	8.15 ± 0.15	6.96 + 0.21	15.5	Inactive
<i>Propranolol</i>	8.60 + 0.32	8.47 ± 0.25	1.4	Inactive

Regarding the spiropiperidine structure, there are not many approved drugs containing this ring. However, it should be noted that in the research part of therapeutic chemistry, studies with spiropiperidines begin to appear. Specifically related to the search for drugs for the treatment of different diseases, such as cancer, cardiovascular and central nervous system diseases, also in inflammation, infectious diseases, metabolic disorders, amongst others.<sup>137</sup>

<sup>136</sup> M.D. Pujol; G. Rosell; G. Guillaumet. *Eur. J. Med. Chem.* **1996**, *31*, 889-894

<sup>137</sup> L. Yet. *Privileged Structures in Drug Discovery: Medicinal Chemistry and Synthesis*, **2018**, 194-236

### 1.5.2. PIRROLOPYRAZINES

The 5*H*-pyrrolo[2,3-*b*]pyrazines nucleus, also known as aloisine, is described in the literature as a potent scaffold structure for protein kinase inhibition, such as, CDKs,<sup>138,139</sup> GSK,<sup>138</sup> Syk,<sup>140</sup> ERK2,<sup>141</sup> JAK,<sup>142</sup> among others (Figure 25).<sup>143</sup>

The *Aloisine A* is one of the products to highlight due to its high inhibitory activity in front of CDK1, CDK2, CDK5, GSK, JNK and less inhibitory activity for CK1, CK2, CDK4, MAPKK, PKA, PKG, PKCs and c-raf (Table 6). Therefore, inhibits the cell cycle in both G1 and G2 phases.<sup>138,139</sup>

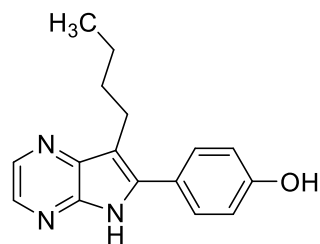


Figure 25. *Aloisine A*

Table 6. IC<sub>50</sub> of *Aloisine A* in different targets

Target	IC <sub>50</sub> (ATP-competitive inhibitor)
CDK1/cyclin B	150 nM
CDK2/cyclin A, CDK2/cyclin E	120 nM, 400 nM
CDK5/p25, CDK5/p35	200 nM, 160 nM
GSK-3α, GSK-3β	500 nM, 650 nM
JNK	3-10 μM
CK1, CK2, CDK4/cyclin D1, MAPKK, PKA, PKG, PKCs and c-raf	≥ 100 μM

Another related product to stand out is a patented compound by Sanofi that has showed a potent inhibitory activity for Syk kinase. Thus, can be useful in the treatment of inflammatory diseases (arthritis, asthma), cardiovascular diseases, cancer, amongst others (Figure 26).<sup>144</sup>

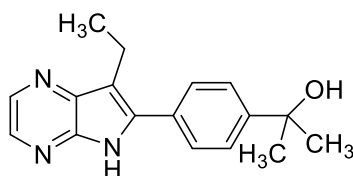


Figure 26. Pyrrolopyrazine with inhibition activity for Syk kinase

<sup>138</sup> Y. Mettey; M. Gompel. V. Thomas, M. Garnier; M. Leost; I. C. Picot; M. Noble; J. Endicott; J. Vierfond; L. Meijer. *J. Med. Chem.* **2003**, *46*, 222-236

<sup>139</sup> C. Corbel; R. Haddoub; D. Guiffant; O. Lozach; D. Gueyrard; J. Lemoine; M. Ratin; L. Meijer; S. Bach; P. Goekjian. *Bioorg. Med. Chem.* **2009**, *17*, 5572–5582

<sup>140</sup> F. Padilla; N. Bhagirath; S. Chen; E. Chiao; D. M. Goldstein; J. C. Hermann; J. Hsu; J. J. Kennedy-Smith; A. Kuglstatler; C. Liao; W. Liu; L. E. Lowrie; K. C. Luk; S. M. Lynch; J. Menke; L. Niu; T. D. Owens; C. O-Yang; A. Railkar; R. C. Schoenfeld; M. Slade; S. Steiner; Y. C. Tan; A. G. Villaseñor; C. Wang; J. Wanner; W. Xie; D. Xu; X. Zhang; M. Zhou; M. C. Lucas. *J. Med. Chem.* **2013**, *56*, 1677-1692

<sup>141</sup> D. J. Burdick; S. Wang; C. Heise; B. Pan; J. Drummond; J. P. Yin; L. Goeser; S. Magnuson; J. Blaney; J. Moffat; W. Wang; H. Chen. *Bioorg. Med. Chem. Lett.* **2015**, *25*, 4728-4732

<sup>142</sup> J. de Vicente; R. Lemoine; M. Bartlett; J. C. Hermann; M. Hekmat-Nejad; R. Henningsen; S. Jin; A. Kuglstatler; H. Li; A. J. Lovey; J. Menke; L. Niu, V. Patel; A. Petersen; L. Setti; A. Shao; P. Tivitmahaisoon; M. D. Vu, M. Soth. *Bioorg. Med. Chem. Lett.* **2014**, *24*, 4969-4975

<sup>143</sup> G. C. Senadi; B. C. Guo; Yu. C. Chang; W.P. Hu; J. J. Wang. *Adv. Synth. Catal.* **2017**, *360*, 491-501

<sup>144</sup> SANOFI. *Una pirrolopirazina como inhibidor de Syk-quinasa*. España; patente de invención; ES2437318; 23-10-2013



In the PhD thesis of Dra. Núria Mur<sup>145</sup> and Dr. Arturo Vinuesa<sup>146</sup>, which were developed in our group and were presented in 2011 and 2016 respectively, a series of novel purine derivatives were prepared. Then, because of the good outcomes from the purine derivatives, progress was made trying to incorporate purine derivatives such as deazapurines, from the removal of a nitrogen atom from purine, as the name indicates. Therefore, a series of novel deazapurines were prepared in the PhD thesis of Dra. Vanessa Prieur<sup>147</sup> and Dra. Lorena Navarro,<sup>148</sup> also developed in our group and presented in 2015 and 2018 respectively.

The synthesized purines and deazapurines derivatives were evaluated biologically affording interesting activities such as: antitumoral activity (CDKs inhibitors, cytotoxicity in several cancer cell lines), PCKS9 inhibition, Alzheimer disease, tropical diseases, amongst others.

Given these results, in order to deepen with these nitrogenated heterocycles, one objective of the current thesis is focused on the pyrrolo[2,3-*b*]pyrazine system (Figure 27).

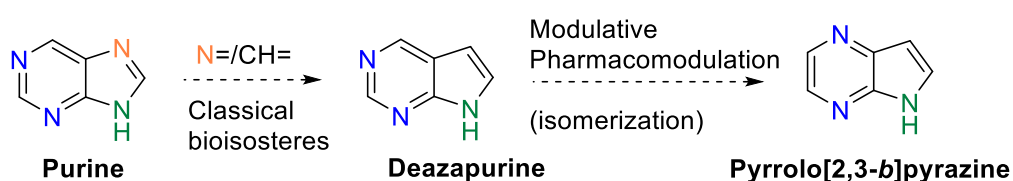


**Figure 27.** Chemical structure of purine, deazapurine and pyrrolo[2,3-*b*]pyrazine

<sup>145</sup> N. Mur. *Disseny i síntesi de nous compostos de naturalesa heterocíclica amb potencial activitat anticancerígena. Síntesi de nous inhibidors de CDKs*. Tesis doctoral. Universitat de Barcelona, **2011**

<sup>146</sup> A. Vinuesa. *Diseño, síntesis y evaluación biológica de nuevos compuestos nitrogenados potencialmente antitumorales*. Tesis Doctoral. Universidad de Barcelona y Universidad de San Jorge, **2016**

<sup>147</sup> V. Prieur. *Pyrolo[2,3-*d*]pyrimidines: Conception, Synthèse, Fonctionnalisation*. Tesis doctoral. Université d'Orléans (Francia). Universitat de Barcelona, **2015**

<sup>148</sup> L. Navarro. *Síntesis de nuevos compuestos con potencial actividad antitumoral y/o antiinflamatoria*. Tesis doctoral. Universitat de Barcelona, **2018**

## 2. OBJECTIVES

Considering the bibliographic precedents described in the introduction and the chemistry preparation and biological evaluation undertaken by our research group, hereunder, different structures with potential multitarget activity are shown. The structure design of the following compounds was prepared by means of an iteration process (Figure 28):

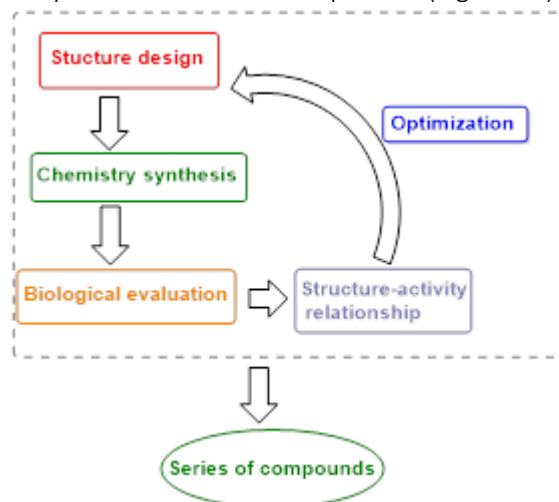
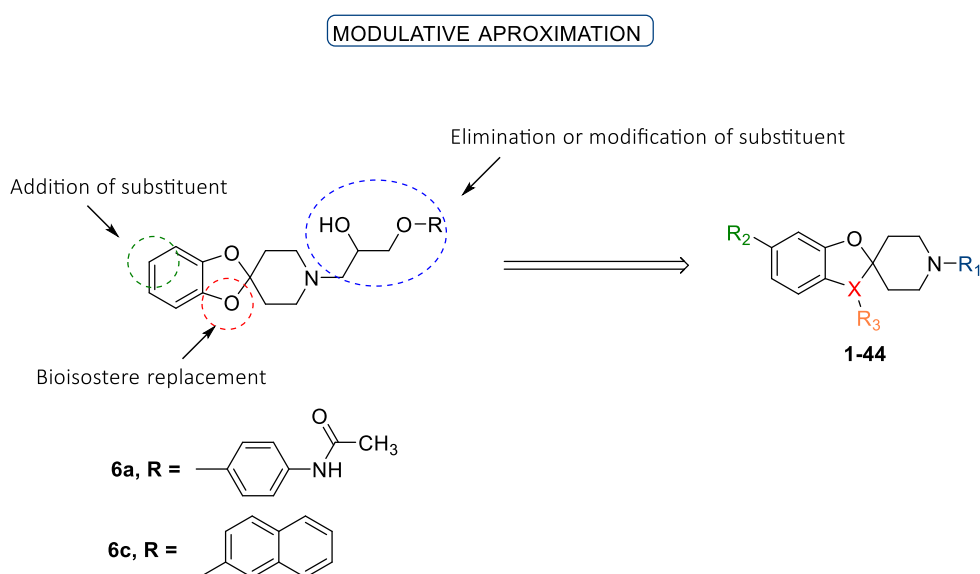


Figure 28. Iteration process followed for the design of new structures

### 2.1. FIRST OBJECTIVE

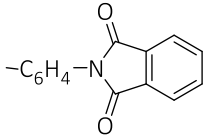
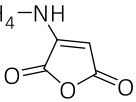
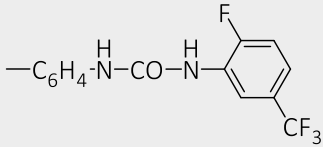
As described before, the spiroderivatives are an attractive systems with scant information in the literature. For this reason, the preparation of compounds **1-42** with structure of spirobenzodioxolepiperidine and **43, 44** with structure of spirobenzoxazolepiperidine forms the first objective of this work (Table 7). From the active compounds **6a** and **6c** described in the bibliography by M. D. Pujol and col. a modulative approximation is proposed, modifying the substituents of the piperidine ring, adding substituents to the position 5 of the spirobenzodioxolepiperidine and a bioisostere replacement in the dioxole ring (Figure 29).

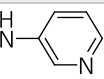
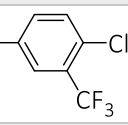


M.D. Pujol; G Rosell; G. Guillaumet. *Eur. J. Med. Chem.* 1996, 31, 889-894

Figure 29. Modulative approximation for compounds **1-44**

Table 7. The proposed 44 spiro derivative compounds

COMPOUNDS	R <sub>1</sub>	R <sub>2</sub>	R <sub>3</sub>	X
1	-COCH <sub>3</sub>	-H	-	O
2	"	-COCH <sub>3</sub>	-	"
3	-H	"	-	"
4	-COCH <sub>3</sub>	-CN(OH)-CH <sub>3</sub> ( <i>E</i> )	-	"
5	"	-CH(OH)-CH <sub>3</sub>	-	"
6	"	-Br	-	"
7	"	-C <sub>6</sub> H <sub>4</sub> -CH <sub>3</sub> ( <i>p</i> )	-	"
8	"	-C <sub>6</sub> H <sub>4</sub> -NO <sub>2</sub> ( <i>p</i> )	-	"
9	"	-C <sub>6</sub> H <sub>4</sub> -NH <sub>2</sub> ( <i>p</i> )	-	"
10	"	-C <sub>6</sub> H <sub>4</sub> -CN ( <i>p</i> )	-	"
11	"	-C <sub>6</sub> H <sub>4</sub> -O-C <sub>6</sub> H <sub>5</sub> ( <i>m</i> )	-	"
12	"	-NO <sub>2</sub>	-	"
13	-H	"	-	"
14	-C <sub>6</sub> H <sub>4</sub> -NO <sub>2</sub> ( <i>p</i> )	"	-	"
15	-C <sub>6</sub> H <sub>4</sub> -NH <sub>2</sub> ( <i>p</i> )	-NH <sub>2</sub>	-	"
16	-C <sub>6</sub> H <sub>4</sub> -NO <sub>2</sub> ( <i>p</i> )	-H	-	"
17	"	-COCH <sub>3</sub>	-	"
18	"	-C=N(OH)-CH <sub>3</sub> ( <i>E</i> )	-	"
19	"	-NHCOCH <sub>3</sub>	-	"
20	"	-NH <sub>2</sub>	-	"
21	"	-CH(OH)-CH <sub>3</sub>	-	"
22	-C <sub>6</sub> H <sub>4</sub> -NH <sub>2</sub> ( <i>p</i> )	"	-	"
23	"	-COCH <sub>3</sub>	-	"
24		"	-	"
25	"	-CH(OH)-CH <sub>3</sub>	-	"
26		-COCH <sub>3</sub>	-	"
27	-SO <sub>2</sub> -C <sub>6</sub> H <sub>5</sub>	"	-	"
28	-SO <sub>2</sub> -C <sub>6</sub> H <sub>5</sub> -CH <sub>3</sub> ( <i>p</i> )	"	-	"
29	-SO <sub>2</sub> -C <sub>6</sub> H <sub>5</sub>	-CH(OH)-CH <sub>3</sub>	-	"
30	-SO <sub>2</sub> -C <sub>6</sub> H <sub>5</sub> -CH <sub>3</sub> ( <i>p</i> )	"	-	"
31	-SO <sub>2</sub> -C <sub>6</sub> H <sub>5</sub>	-CH(Cl)-CH <sub>3</sub>	-	"
32	-SO <sub>2</sub> -C <sub>6</sub> H <sub>5</sub> -CH <sub>3</sub> ( <i>p</i> )	"	-	"
33	-SO <sub>2</sub> -C <sub>6</sub> H <sub>5</sub>	-CH(CH <sub>3</sub> )-O-(CH <sub>2</sub> ) <sub>2</sub> -N(CH <sub>2</sub> CH <sub>3</sub> ) <sub>2</sub>	-	"
34	"	-CH(CH <sub>3</sub> )-NH-(CH <sub>2</sub> ) <sub>2</sub> -N(CH <sub>3</sub> ) <sub>2</sub>	-	"
35	-SO <sub>2</sub> -C <sub>6</sub> H <sub>5</sub> -CH <sub>3</sub> ( <i>p</i> )	-CH(CH <sub>3</sub> )-NH-(CH <sub>2</sub> ) <sub>5</sub> -CH <sub>3</sub>	-	"
36	-NH-(CH <sub>2</sub> ) <sub>2</sub> -OH	-CH(OH)-CH <sub>3</sub>	-	"
37		-COCH <sub>3</sub>	-	"
38	"	-CH(OH)-CH <sub>3</sub>	-	"

39	-C <sub>6</sub> H <sub>4</sub> -NH-CO-NH-Et	"	-	"
40		-NH <sub>2</sub>	-	"
41	-C <sub>6</sub> H <sub>4</sub> -NH-CO-NH-Et	-C <sub>6</sub> H <sub>4</sub> -NH-CO-NH-Et	-	"
42	-COCH <sub>3</sub>		-	"
43	-COCH <sub>3</sub>	-H	-H	N
44	-COCH <sub>3</sub>	-COCH <sub>3</sub>	-COCH <sub>3</sub>	N

## 2.2. SECOND OBJECTIVE

The pirrolo[2,3-*b*]pyrazine system, a derivative from the purines, has not studied as much as purines, neither the synthesis or its biological activities. Therefore, the second objective is to set up a synthesis in order to prepare the pirrolo[2,3-*b*]pyrazine system as optimally as possible (Figure 30).

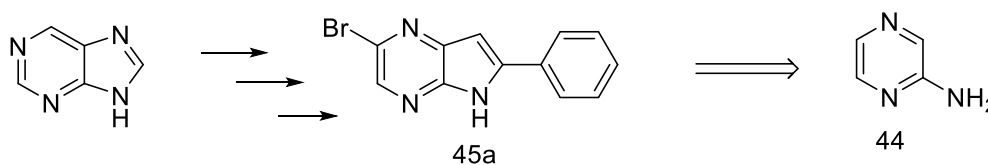


Figure 30. Pyrazine derivative **45a** and its starting material 2-aminopyrazine

If the desired pirrolo[2,3-*b*]pyrazine system is obtained, a synthesis to prepare diarylates, triarylates and tetrarylates compounds consist the second part of this objective. Thus, starting from the good scaffolds **45a-c** the preparation of products **47-58** is proposed (Table 8).

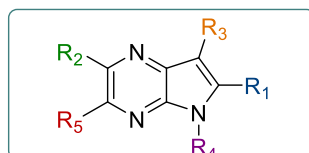


Table 8. The proposed 13 pirrolo-pyrazine derivative compounds

COMPOUNDS	R <sub>1</sub>	R <sub>2</sub>	R <sub>3</sub>	R <sub>4</sub>	R <sub>5</sub>
47	-C <sub>6</sub> H <sub>5</sub>	-C <sub>6</sub> H <sub>5</sub> -CH <sub>3</sub> ( <i>p</i> )	-H	-H	-H
48	"	-C <sub>6</sub> H <sub>5</sub> -OCH <sub>3</sub> ( <i>p</i> )	"	"	"
49	"	-C <sub>6</sub> H <sub>5</sub> -CF <sub>3</sub> ( <i>p</i> )	"	"	"
50	-C <sub>6</sub> H <sub>5</sub> -F ( <i>p</i> )	-C <sub>6</sub> H <sub>5</sub> -CH <sub>3</sub> ( <i>p</i> )	"	"	"
51	"	-C <sub>6</sub> H <sub>5</sub> -CH <sub>3</sub> ( <i>m</i> )	"	"	"
52	-C <sub>6</sub> H <sub>5</sub> -Cl ( <i>p</i> )	-C <sub>6</sub> H <sub>5</sub> -CH <sub>3</sub> ( <i>p</i> )	"	"	"
53a	-C <sub>6</sub> H <sub>5</sub>	"	-C <sub>6</sub> H <sub>5</sub> -CH <sub>3</sub> ( <i>p</i> )	"	"
54	"	"	-Br	"	-C <sub>6</sub> H <sub>5</sub> -CH <sub>3</sub> ( <i>p</i> )
55a	-C <sub>6</sub> H <sub>5</sub> -F ( <i>p</i> )	"	-H	-MO-Et	-H
55b	"	-C <sub>6</sub> H <sub>5</sub> -CH <sub>3</sub> ( <i>m</i> )	"	"	"
56	"	-C <sub>6</sub> H <sub>5</sub> -CH <sub>3</sub> ( <i>p</i> )	-C <sub>6</sub> H <sub>5</sub> -CH <sub>3</sub> ( <i>p</i> )	-Bn	"
57	"	"	"	-H	"
58	-C <sub>6</sub> H <sub>5</sub>	-C <sub>6</sub> H <sub>5</sub> -OCH <sub>3</sub> ( <i>p</i> )	-H	-C <sub>6</sub> H <sub>5</sub> -NO <sub>2</sub> ( <i>p</i> )	"

### 2.3. THIRD OBJECTIVE

The third objective of this work is focused on the multi-target drug discovery (MTDD). Then, all these proposed products are aimed to be tested in several targets to seek a new leads in different diseases, mainly in cancer resistance and in tropical diseases. Thus, targets like human nicotinamide methyl transferase (hNNMT), arginase, CDKs, between other enzymes playing a key role in cancer resistance are the central focus. Those drugs acting in several targets with significant activity can be selected for further biological studies and they can be used as a model to optimize the design of new structures as well.

The search of multitarget drugs is based on the fact that in order to produce the required efficacy and, at the same time, minimizing adverse side effects, an equilibrated modulation of several targets, related with complex diseases as cancer, can be beneficial for the treatments, instead of one drug- one disease, due to the complexity of the biological pathways (Figure 31).

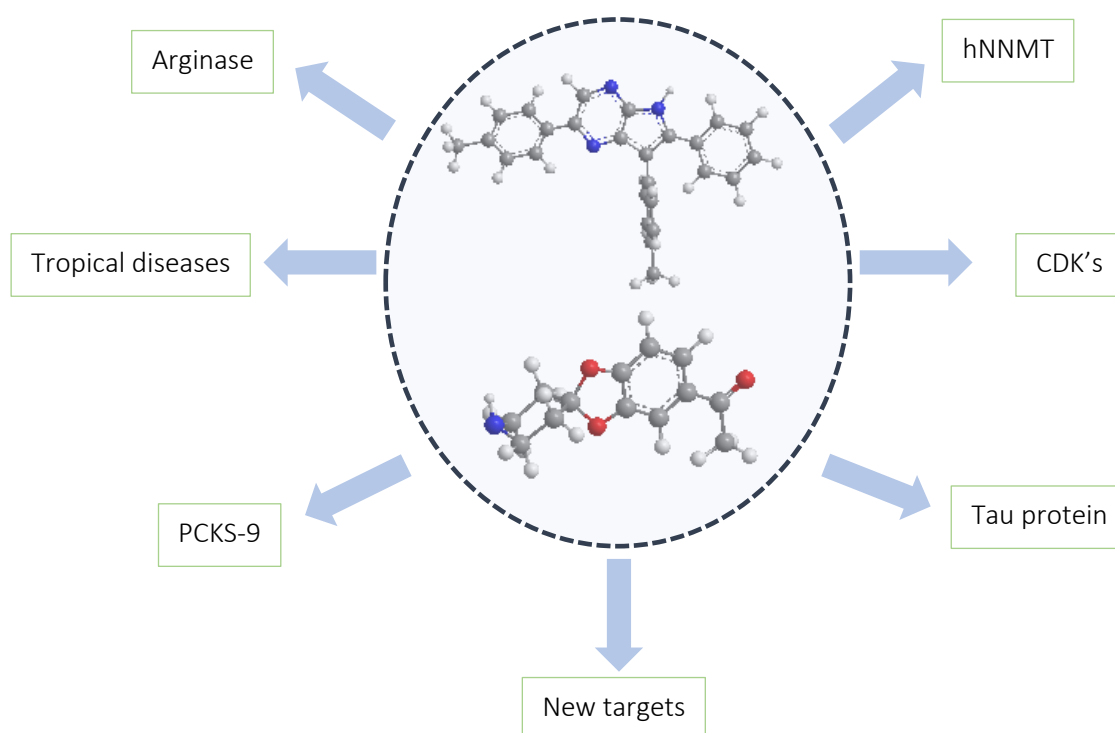


**Figure 31.** Multitarget drugs examples for spiropiperidines and pirrolopyrazines derivatives

The second part of this objective is focused on discover new targets. Thus, the design of cellular assay systems to measure the signal transduction of an orphan receptors is sought. In order to undertake these assays, a transient transfection of mammalian cells and the measurement of various second messengers (cAMP, IP3, kinase activity) in response to activated receptor point mutants and literature-described peptides is proposed. Analysis of the mechanism of receptor activation and protein signal- transduction pathway will be quantified.

### 3. THEORETICAL DISCUSSION

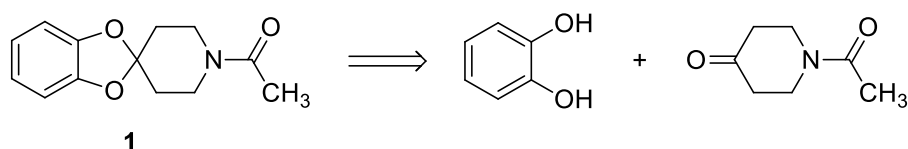
#### 3.1. CHEMICAL DISCUSSION

##### 3.1.1. Preparation of 1-spiro[benzodioxole-2,4'-piperidine]

###### 3.1.1.1. Preparation of *N*-acetyl-spiro[1,3-benzodioxole-2,4'-piperidine] (**1**)

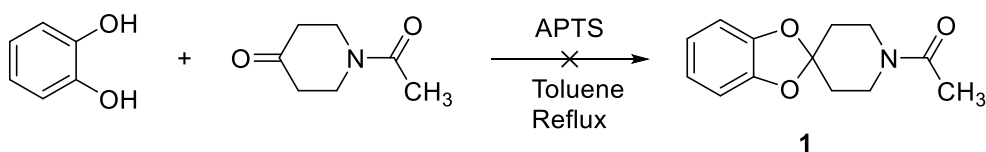
The spirobenzodioxolepiperidine system is not described in the bibliography, with the exception of one reference afforded by our research group.<sup>136</sup>

In order to prepare this dioxygenated nucleus, the following retrosynthetic scheme was proposed (Scheme 1):



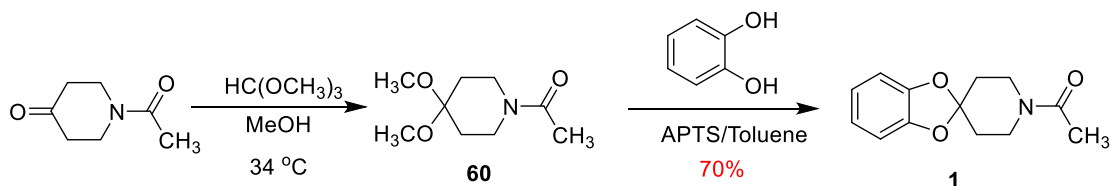
Scheme 1

In the first assay, through direct condensation of the catechol with *N*-acetyl-4-piperidone, in toluene and under acid conditions (APTS), the expected spiranic system was not obtained (Scheme 2).



Scheme 2

These results, led to consider a different conditions of reaction, such as the transacetalization of the acetal **60**, starting from the acetone, for the catechol (Scheme 3).



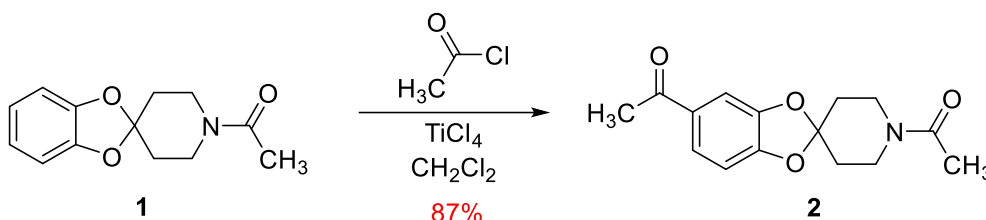
Scheme 3

The treatment of 4-piperidone with methyl orthoformate, warming up until the distillation of methyl formate (boiling point = 31.5 °C), leads to acetal **60**, which is stable under these conditions and then it becomes the spiranic derivative **1** by treatment with catechol in toluene and through acid catalysis (APTS). The global yield of the two steps was 70%.

### 3.1.1.2. Preparation of 1',5-diacetyl-spiro[benzo[1,3]dioxole-2,4'-piperidine] (2) and 5-acetyl-spiro[benzo[1,3]dioxole-2,4'-piperidine] (3)

The spirobenzodioxolepiperidine **1** it becomes the diacetylated derivative **2** by treatment with acetyl chloride, in dichloromethane, using titanium tetrachloride as a catalyst.

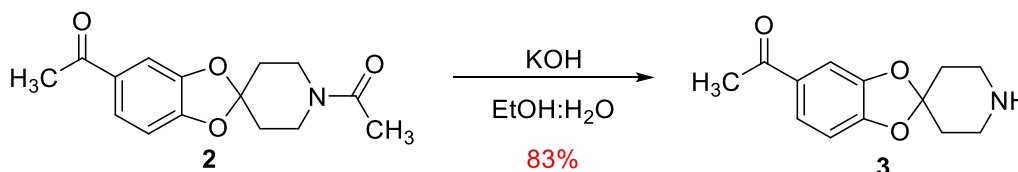
Applying this classic methodology of aromatic rings acetylation,<sup>149</sup> the compound **2** was obtained in 87% yield (Scheme 4).



Scheme 4

Then, the diacetylated derivative **2** by treatment with KOH 2N in ethanol-water (2:8), leads to the hydrolyzed spiro piperidine **3** in 83% yield.

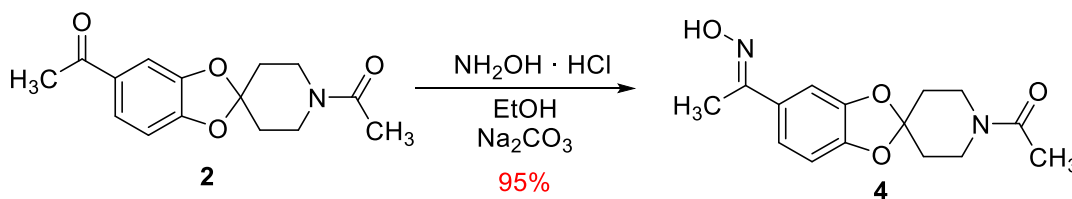
The hydrolysis conditions were previously developed in this work, obtaining the best results when the mixture of reaction was heated to 100 ± 10 °C, compared with the assays performed at room temperature (yields < 15%) (Scheme 5).



Scheme 5

### 3.1.1.3. Preparation of 1'-acetyl-5-(1-(hydroxyimino)ethyl)spiro[benzo[1,3]dioxole-2,4'-piperidine] (4)

The diacetylated compound **2** was treated with hydroxylamine hydrochloride in ethanol and with the presence of sodium carbonate leading to oxime **4** in 95% yield (Scheme 6).

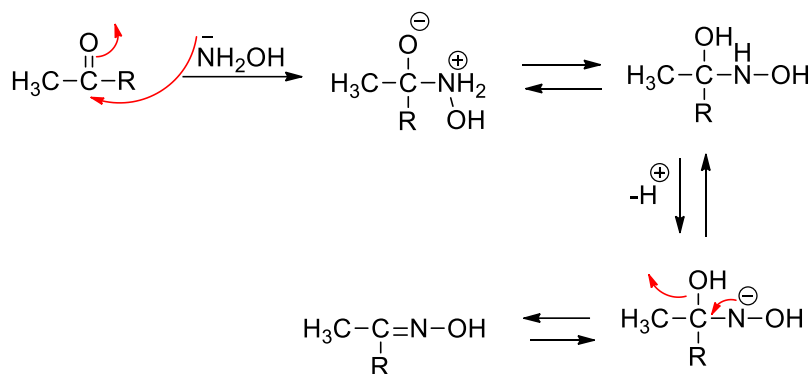


Scheme 6

In this reaction a carbinolamine intermediate is made, which by dehydration, leads to the expected oxime.<sup>150</sup> A possible mechanism for this reaction is indicated (Scheme 7):

<sup>149</sup> I. A. Khotina; V. A. Izumrudov; N. V. Tchebotareva; A. L. Rusenov. *Macromol. Chem. Phys.* **2001**, *202*, 2360-2366

<sup>150</sup> A. Williams; M. L. Bender. *J. Am. Chem. Soc.* **1966**, *88*, 2508-2513



Scheme 7

In the performed conditions, the isomer (*E*) of oxime **4** is mostly obtained. The spectroscopy data of <sup>1</sup>H-NMR show a singlet at 2.09 ppm assignable to the CH<sub>3</sub> of the amide group and other singlet at 2.17 ppm which integrates 3 protons assignable to the CH<sub>3</sub> of the oxime function (Figure 32).

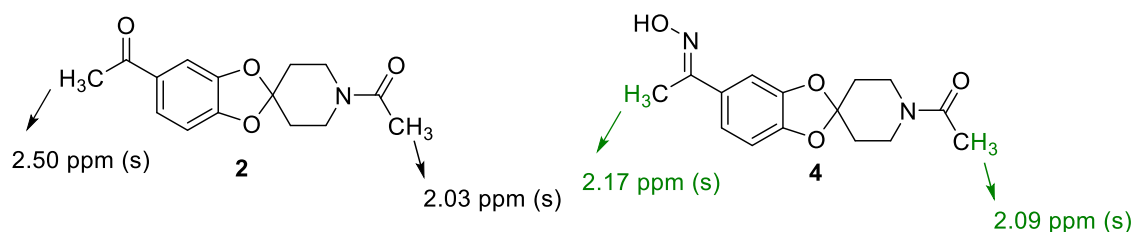


Figure 32. <sup>1</sup>H-NMR spectroscopy data of compounds **2** and **4**

The CH<sub>3</sub> group near to the oxime function, appears slightly shielded compared with the corresponding CH<sub>3</sub> of the methylketone of derivative **2**. Besides, it has to be mentioned that in the both NMR spectrums, proton and C-13, only these two singlets appear, which are from the isomer (*E*). The isomer (*Z*) was not detected.

The formation of isomer (*E*) can be attributed to the conditions used for the reaction. Also, the study of previously reported works related with the formation of oximes starting from carbonyl derivatives, bring out the fact that, while the treatment of aldehydes leads to the oxime of configuration (*Z*), the ketones allow to achieve mostly isomer (*E*) (Figure 33). In this case, the conditions to obtain the isomer (*E*) were used and this stereochemistry it can be confirmed by NOE (Nuclear overhauser effect) experiments, which clearly shows that there is no interaction between the oxime proton and the aromatic protons of the spiranic system.

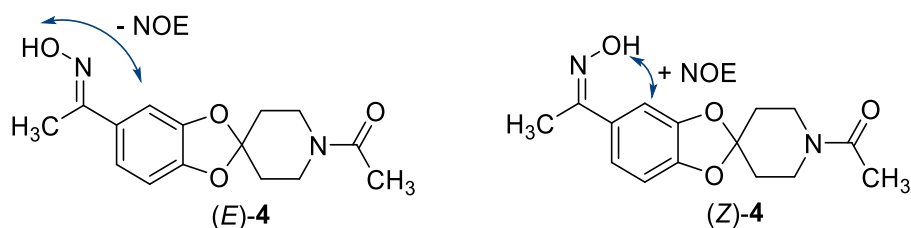
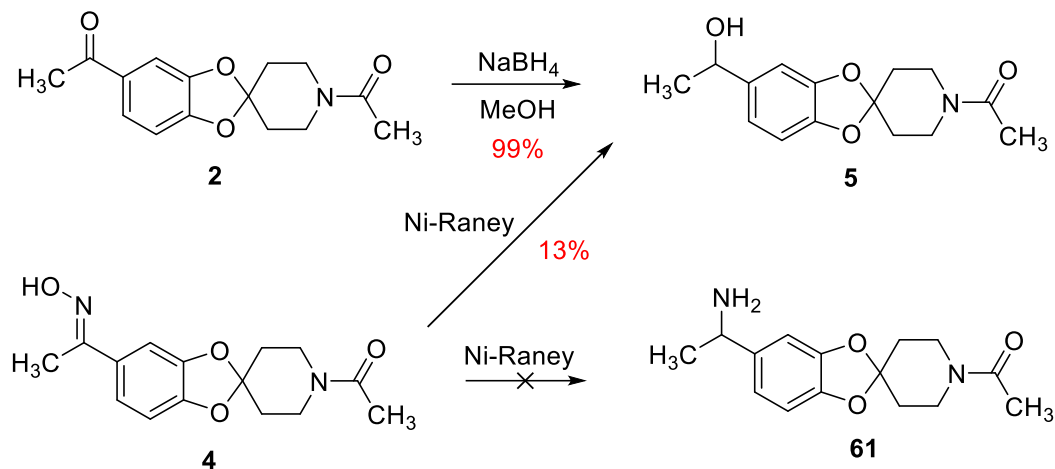


Figure 33. Isomers (*E*) and (*Z*) of compound **4** with the proposed intramolecular hydrogen interaction



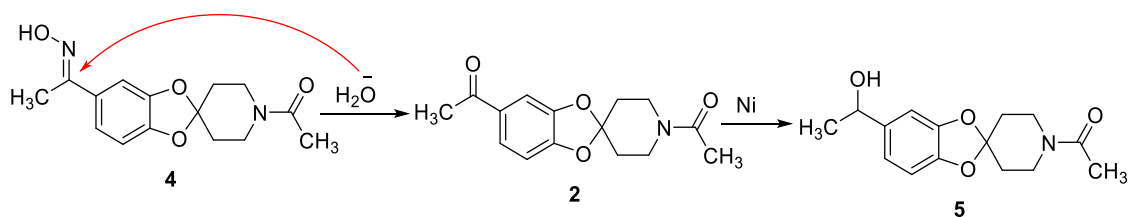
### 3.1.1.4. Preparation of 1'-acetyl-5-(1-hydroxyethyl)spiro[benzo[1,3]dioxole-2,4'-piperidine](5)

The reduction of spiranic derivative **2** with NaBH<sub>4</sub>, in methanol, leads to the secondary alcohol **5** in a regioselective manner as expected (Scheme 8).



Scheme 8

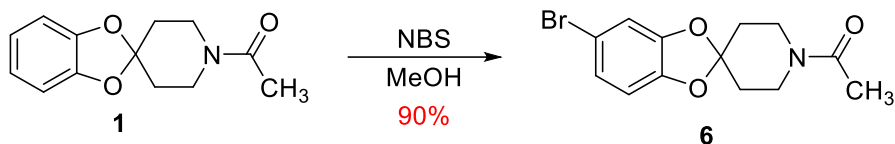
Likewise, the treatment of oxime **4** with Ni-Raney allows to obtain **5** in 13% yield, with no traces of the primary amine **61**, the aimed to obtain. In this case, the formation of **5** it could be possible due to the presence of water proceeding from Ni-Raney, which can induce the hydrolysis of the oxime, recovering the initial ketone,<sup>151</sup> and so the nickel ends reducing the ketone to the corresponding alcohol (Scheme 9).



Scheme 9

### 3.1.1.5. Preparation of 1'-acetyl-5-bromospiro[benzo[1,3]dioxole-2,4'-piperidine] (6)

In this work it was set up the halogenation of spiranic system **1** by using NBS in methanol and keeping the stirring at room temperature for 3 hours, leading then to the expected compound in 90% yield (Scheme 10).

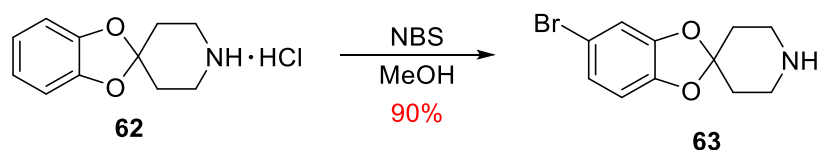


Scheme 10

It is necessary to stand out that in order to halogenate the C-5 of the spiranic system it was required the previous protection of the nitrogen atom of piperidine, such as the described case, where an acetyl group serves as a protecting group.

<sup>151</sup> S. Bher; S. Guha. *Synt. Commun.* **2005**, *35*, 1183-1188

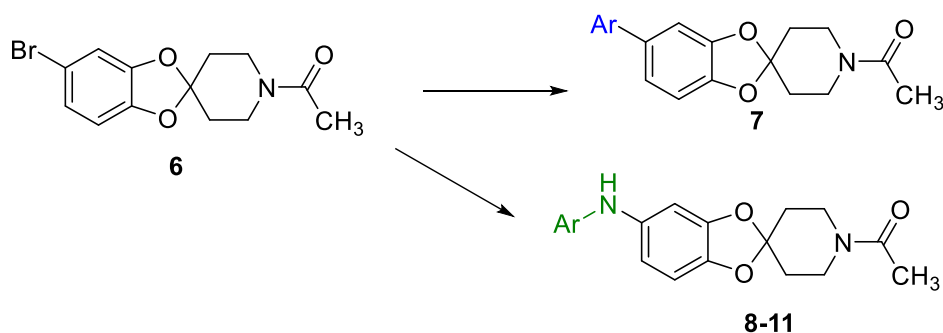
However, in the present case, a soft halogenation conditions are applied, because it is also possible to brominate the methyl group, an  $\alpha$ -carbonyl position. Previously, in our research group, the halogenation of the spiro piperidine hydrochloride system was made, as it is indicated hereunder (Scheme 11).<sup>136</sup>



Scheme 11

### 3.1.1.6. Preparation of 7

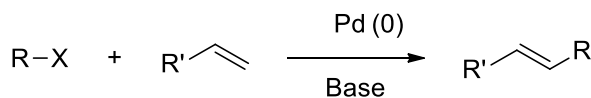
From the bromo derivative **6** it is possible to access to the spiro-derivatives **7-11** through cross-coupling reactions catalyzed by Pd-complex (Scheme 12).



Scheme 12

The formation of carbon-carbon (C-C) bonds is of vital importance for the preparation of different chemical products, many of them with application in therapeutic chemistry.

The cross-coupling reactions are very versatile and allow to prepare a wide number of compounds with different structural complexity, appearing as the most referenced reactions from the last decade. The conditions of this kind of reactions are usually softly than other type of radical reactions or in some cases of nucleophilic aromatic substitutions. Specifically in 2010, three scientist working in this field were winners of Nobel prize, Richard F. Heck, Ei-ichi Negishi and Akira Suzuki. Each one applied a methodology that allows to achieve a certain compounds. Thus, the Heck reaction involves the use of an unsaturated halide in presence of a base and a Pd catalyst, allowing to obtain alkenes and stilbenes above all, which are very useful for the preparation of drugs and other organic compounds (Scheme 13).<sup>152</sup>



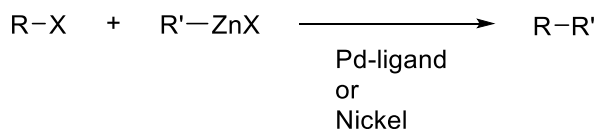
Scheme 13

E. Negishi also describes the preparation of compounds through the formation of C-C bonds under cross-coupling conditions catalyzed by palladium or nickel derivatives.<sup>153</sup> The reaction

<sup>152</sup> R. F. Heck; J. P. Nolley. *J. Org. Chem.* **1972**, *37*, 2320-2322

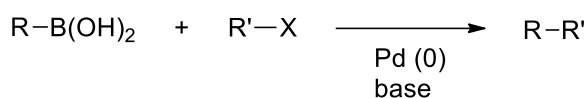
<sup>153</sup> A. O. King; N. Okukado; E. Negishi. *J. Chem. Soc. Chem. Commun.* **1977**, *19*, 683-684

involves the use of halides or organic triflate and organozincates as it is indicated in the following scheme (Scheme 14):



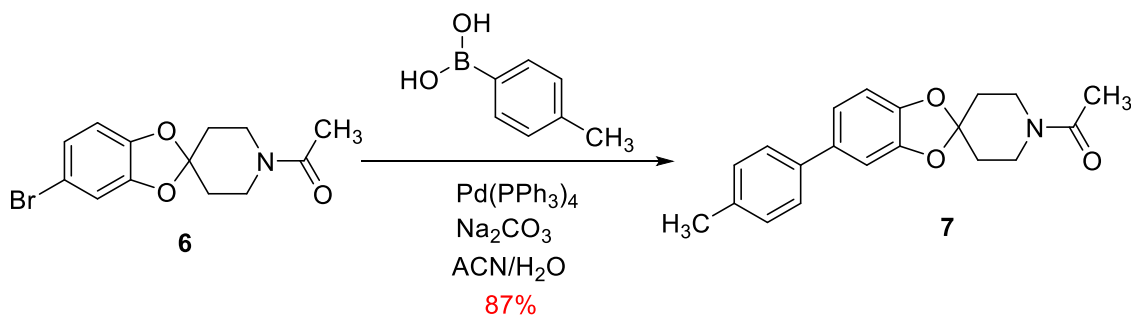
Scheme 14

Finally, A. Suzuki, which also afforded its methodology to make C-C bonds, distinguishing himself of the latter for the use of aryl or alkyl boronic acids which couple with organic halides, using palladium (0) as a catalyst in presence of a base.<sup>154</sup> Hereunder, a general scheme of this reaction is showed (Scheme 15).



Scheme 15

In these reactions, solvents, ligands, bases and catalyst are known to have very significant role in order to improve the effectiveness of these reactions. In this work it has been tried that the amount of transition metals was minimal so that the process was compatible and respectful with the environment. In this work, the arylation of the spiranic derivative **6** was carried out, using *p*-tolylboronic acid and palladium-triphenylphosphine complex (tetrakis) as a catalyst, through the Suzuki-Miyaura cross-coupling conditions (Scheme 16). Thus, the desired product **7** was obtained in 87% yield.



Scheme 16

The presence of two doublets in the <sup>1</sup>H-NMR spectrum, which integrate 2 protons each one at 7.11 and at 7.30 ppm assignable at protons of the positions 3'', 5'' and 2'', 6'', and as well as the presence of a singlet at 2.28 ppm belonging to the CH<sub>3</sub> group of the phenyl, incorporated in the position 5 of the spiranic system, allow to confirm the proposed structure for compound **7** (Figure 34).

<sup>154</sup> N. Miyaura; A. Suzuki. *J. Chem. Soc. Chem. Commun.* **1979**, 19, 866-867

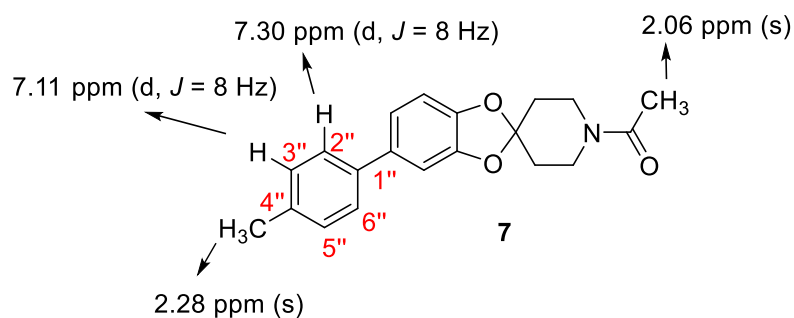
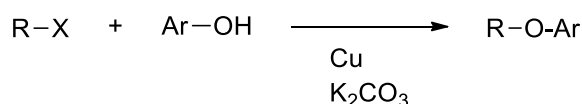


Figure 34.  $^1\text{H-NMR}$  data of derivative spiro **7**

### 3.1.1.7. Preparation of **8** to **11**

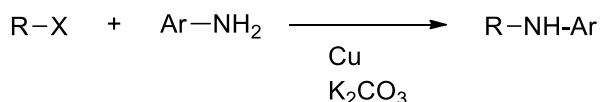
The cross-coupling reactions in addition to the C-C bonds formation, as described before, they also enable to prepare compounds with C-heteroatom bonds (C-N, C-O).

In order to make C-O bonds and more precisely diaryl-ethers, the cross-coupling conditions replaced the ones from the Ullmann reaction,<sup>155</sup> which allow to make diaryl-ethers (Scheme 17) using a base ( $\text{K}_2\text{CO}_3$ ) and big quantities of Cu or Cu salts, in addition to harsh conditions such as high temperatures ( $>200\text{ }^\circ\text{C}$ ). The mechanism for the Ullmann reaction is not fully accepted, but the most popular argues that this reaction takes place through a radical mechanism.



Scheme 17

The same conditions can be applied to prepare diaryl-amines (Scheme 18).



Scheme 18

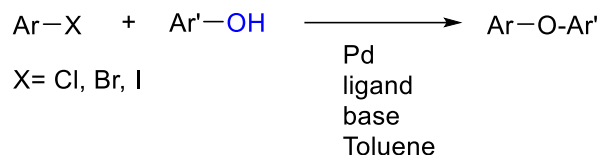
More recently, the Buchwald-Hartwig conditions allow to prepare diaryl-ethers and diaryl-amines through cross-coupling conditions.<sup>156</sup> The reagents can be phenols or anilines and organic halides, using in both cases palladium derivatives as catalyst.

<sup>155</sup> F. Monnier; M. Taillefer. *Angew. Chem.* **2009**, *48*, 6954-6971

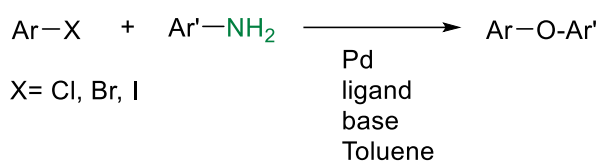
<sup>156</sup> a) J. P. Wolfe; S. Wagaw; S. L. Buchwald. *J. Am. Chem. Soc.* **1996**, *118*, 7215-7216 b) J. P. Wolfe; S. L. Buchwald. *J. Org. Chem.* **1997**, *62*, 1264-1267 c) J. P. Wolfe; R. A. Rennels; S. L. Buchwald. *Tetrahedron* **1996**, *52*, 7525-7546 d) J. P. Wolfe; S. L. Buchwald. *J. Org. Chem.* **2000**, *65*, 1144-1157 e) G. Mann; J. F. Hartwig; M. S. Driver; C. Fernández-Rivas. *J. Am. Chem. Soc.* **1998**, *120*, 827-828 f) J. F. Hartwig. *Synlett* **1996**, 329-340 g) M. S. Driver; J. F. Hartwig. *J. Am. Chem. Soc.* **1996**, *118*, 7217-7218 h) J. F. Hartwig. *Angew. Chem. Int. Ed.* **1998**, *37*, 2046-2067 i) J. Ahman; S. L. Buchwald. *Tetrahedron Lett.* **1997**, *38*, 6363-6366 j) J. P. Wolfe; J. Ahman; J. P. Sadighi; R. A. Singer; S. L. Buchwald. *Tetrahedron Lett.* **1997**, *38*, 6367-6370 k) S. L. Buchwald; X. Huang. *Org. Lett.* **2001**, *3*, 3417-3419 l) S. Lee; M. Jorgensen; J. F. Hartwig. *Org. Lett.* **2001**, *3*, 2729-2732 m) D. Y. Lee; J. F. Hartwig. *Org. Lett.* **2005**, *7*, 1169-1172

It is necessary to add ligands monophosphine-type such as triphenylphosphine or diphosphines, like BINAP, and also it is required the presence of a base. The most appropriate solvent is usually toluene or xylene, due to the high boiling point that enable, if it was necessary, to work at high temperatures (Scheme 19).

a) Diaryl-ethers

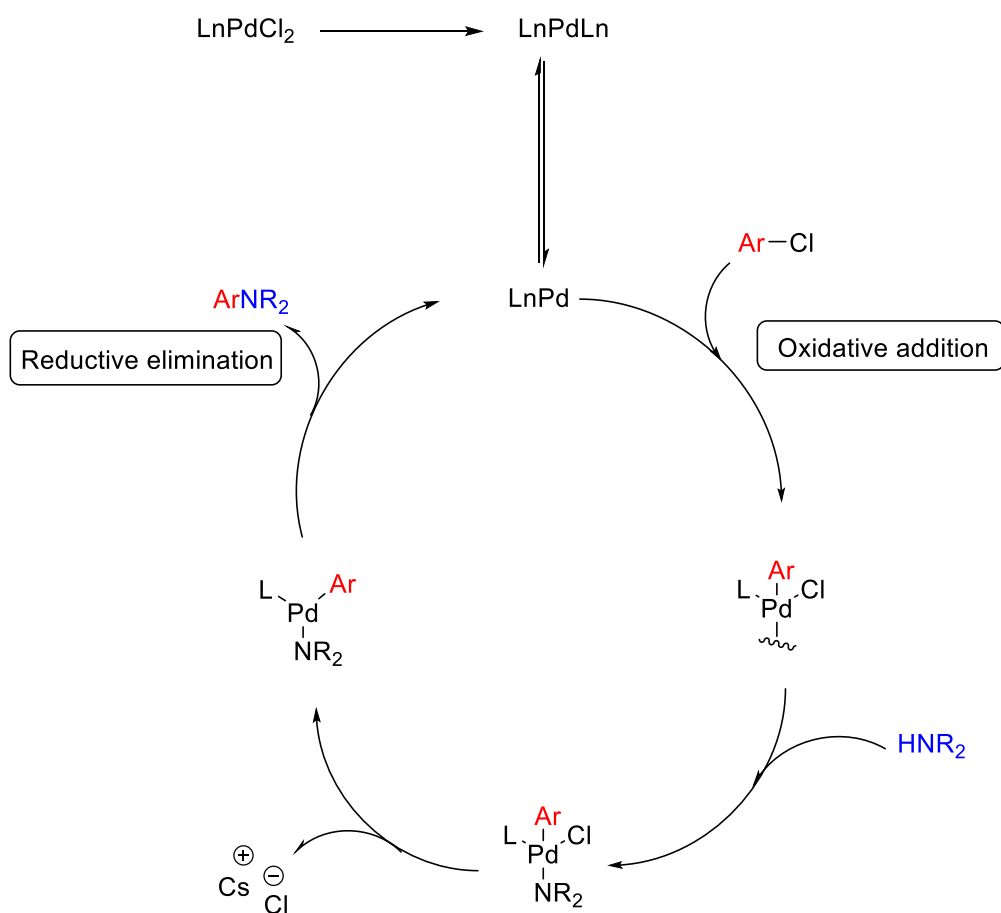


b) Diaryl-amines



Scheme 19

A proposed mechanism to explain this cross-coupling reaction is indicated in the following example (Scheme 20).

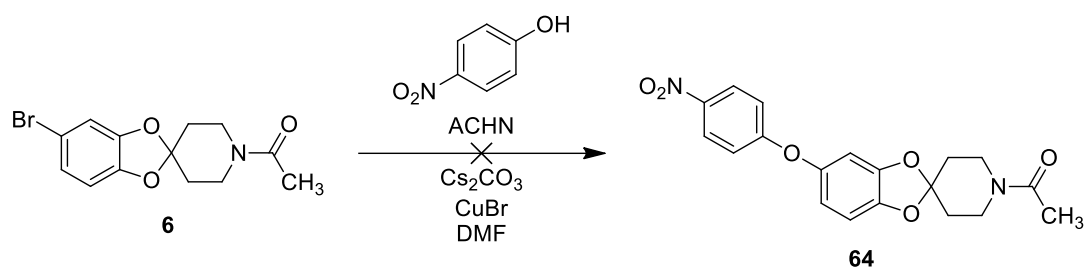


Scheme 20

The cycle is started by an oxidative addition of the aryl halide to the ligand-palladium complex. Then, the aniline is incorporated and the transmetalation with the organometallic reagent present in the medium occurs. This intermediate contains both components that makes the coupling (Ar and NR<sub>2</sub>).

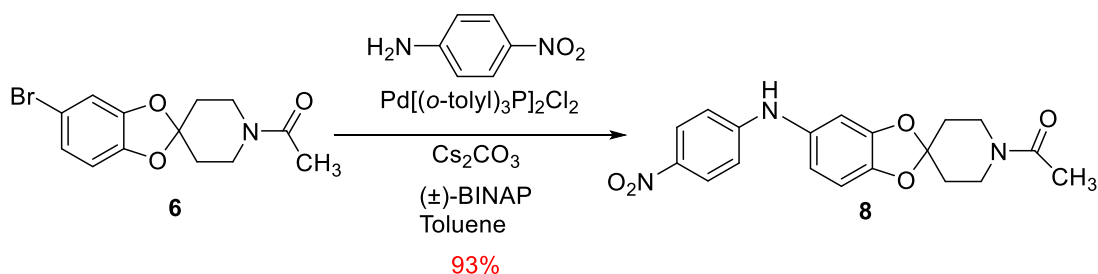
Finally, the reductive elimination was produced leading to the final cross-coupling product and the Pd was recyclable without loss of activity (Pd (0)) allowing to restart the catalytic cycle.

In this work, the reaction between the bromo-spiro **6** and *p*-nitrophenol was settled in order to obtain the corresponding diaryl-ether. Different tests were carried out but in any case it was possible to isolate the expected ether **64** (Scheme 21). The starting material **6** was recovered unaltered.



Scheme 21

The lack of reactivity can be attributed to the little nucleophile power of the phenol due to the presence of the nitro group, a big electron withdrawing. While, the cross-coupling reaction between 5-bromospiro (**6**) and 4-nitroaniline under palladium catalysis (Pd-II) and in presence of Cs<sub>2</sub>CO<sub>3</sub>, as a base, leads to diaryl-amine **8** in 93% yield (Scheme 22). The reaction was clean, and no byproduct was observed.

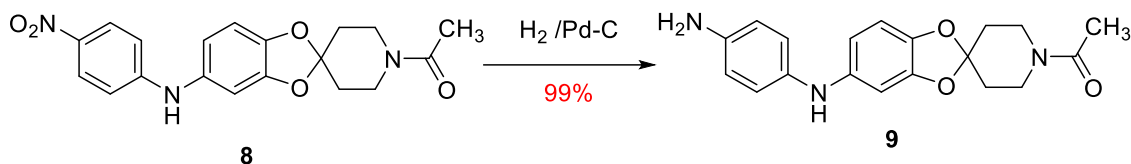


Scheme 22

The used conditions for this cross-coupling reaction were previously set up and optimized for our research group.<sup>157</sup> In that way, Pd[P(*o*-tolyl)<sub>3</sub>]<sub>2</sub>Cl<sub>2</sub> is used as a catalyst, BINAP (2,2'-*bis*(diphenylphosphino)-1,1'-binaphthyl) as a ligand, cesium carbonate as a base and drops of toluene as solvent. The reagents can be weighted and manipulated in contact with the air, while the catalyst and the ligand are manipulated strictly under argon atmosphere.

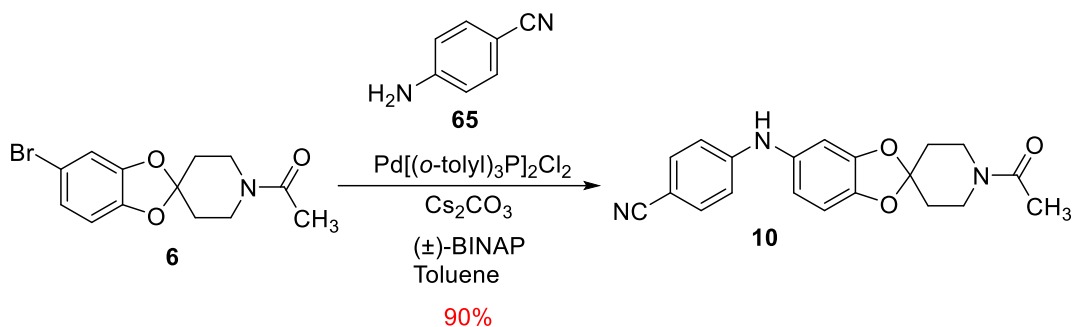
Then, the nitro-derivative **8** was subjected to reduction using a hydrogen stream and carbon-palladium catalysis. Under these conditions, the expected aniline **9** was achieved in almost quantitative yield (Scheme 23).

<sup>157</sup> M. Romero; Y. Harrak; J. Basset; L. Ginet; P. Constants; M. D. Pujol. *Tetrahedron* **2006**, *62*, 9010-9016



Scheme 23

The diarylamine **10** was prepared by cross-coupling between bromo-spiro **6** and 4-aminobenzonitrile (**65**), using the conditions, previously described, for the preparation of **8** (Scheme 24). Thus, the synthesis of diaryl-amine **10** was afforded in 90% yield.



Scheme 24

The shielding of the protons in the  $^1\text{H-NMR}$  spectrum of positions 4 (6.67 ppm) and 6 (6.56 ppm) of the spiranic system of compound **10** in comparison with the bromo derivative **6** (CH-4 a 6.81 ppm and CH-6 a 6.82 ppm), indicate the substitution of the bromo atom for an electron donor group. Besides, the presence of two new doublets that integrates two protons each one at 6.78 ppm and 7.37 ppm, belonging to the CH of the 4-cyanophenyl, allow to confirm the proposed structure for the spiro derivative **10** (Figure 35).

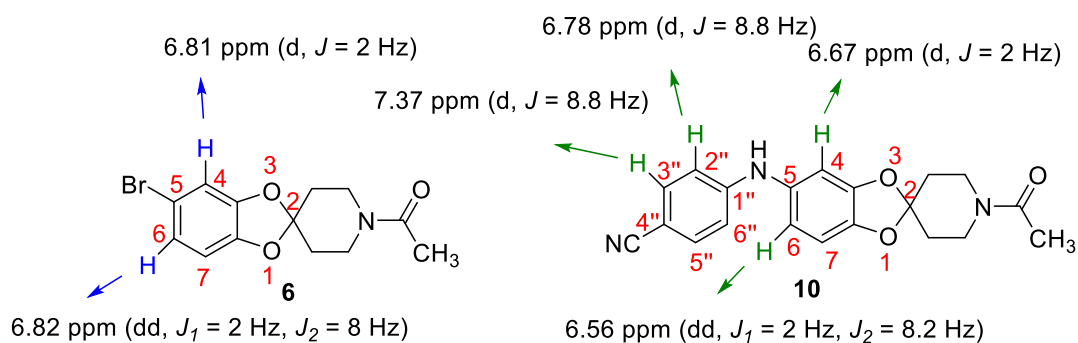
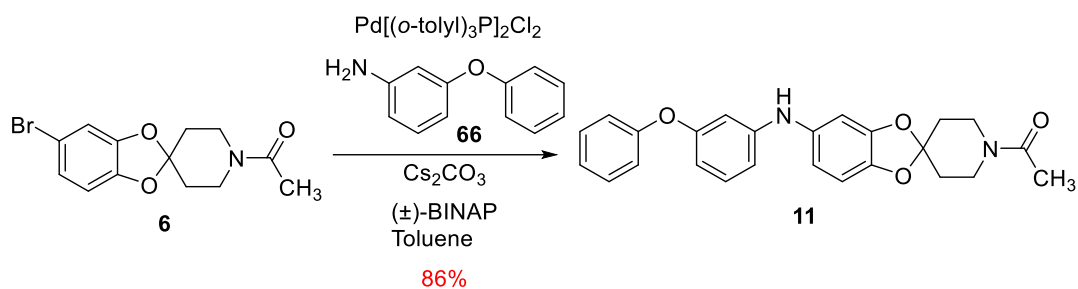


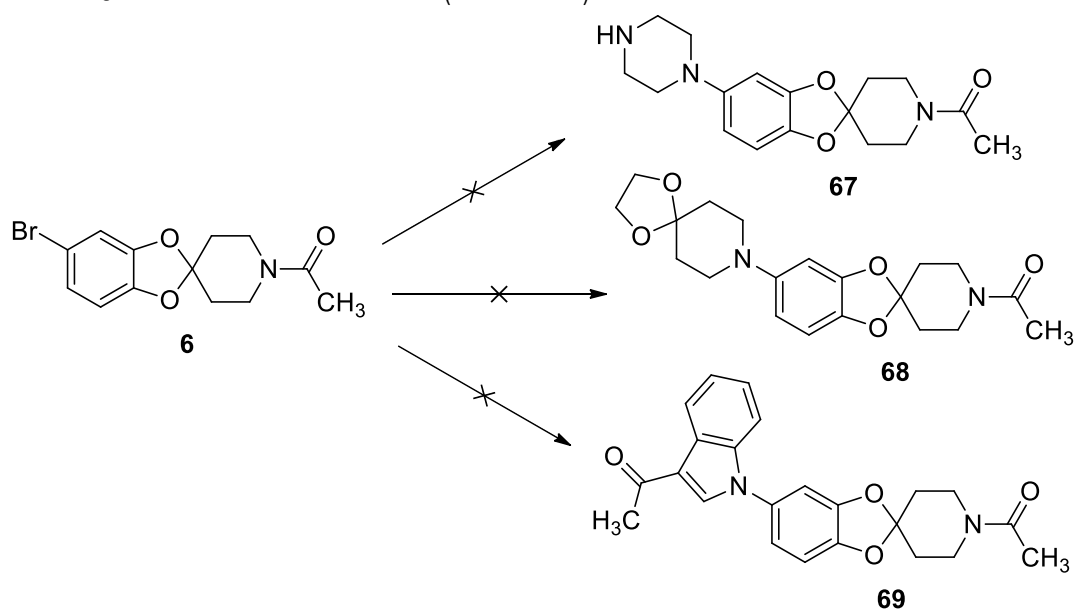
Figure 35.  $^1\text{H-NMR}$  spectroscopy data of compound **10**

Following the same methodology, the amination of the spiro derivative **6** it allows the preparation of the amide **11** in 86% yield. In this case, it starts from bromo-spiro **6** which couples with 3-phenoxyaniline (**66**) (Scheme 25).



Scheme 25

As well as, in this work, several assays were carried out to obtain the amination of bromospiro derivative **6** such as the indicated here. (Scheme 26).



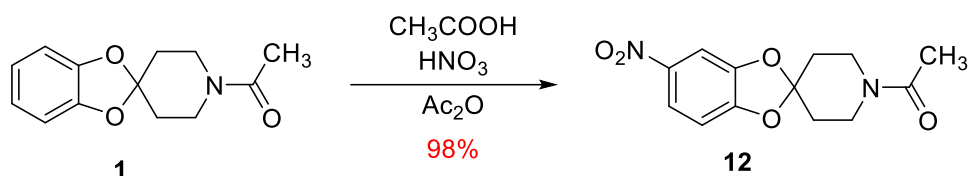
Scheme 26

In none of the assays, using the previously described cross-coupling conditions and even changing it, the desired products were observed. In the beginning it was thought that the free -NH of the piperazine could interfere in the cross-coupling reaction. Therefore, new assays without the presence of free -OH or -NH were carried out, but the desired products were not obtained either. In these cases, the unaltered starting material was recovered or in assays where drastic conditions were applied, the dehalogenated compound was obtained.

#### 3.1.1.8. Preparation of 1-acetyl-5-nitro-spiro[benzodioxole-2,4'-piperidine] (**12**) and **13**

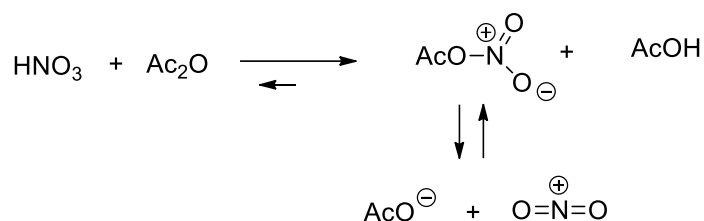
The preparation of nitro-derivative **12** was obtained by treatment of N-acetylspirobenzodioxolepiperidine **1** with nitric acid and acetic acid in acetic anhydride. Under these conditions the nitro-spiro **12** was obtained in 98% yield (Scheme 27).





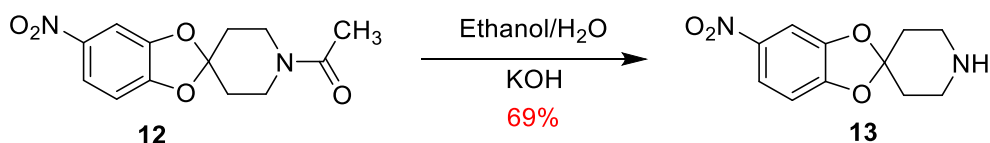
Scheme 27

It is worth mentioning that in previous assays it was found out that the sulfonitric mixture ( $\text{H}_2\text{SO}_4 + \text{HNO}_3$ ) did not allow the desired nitration and gave as a result degraded products. In view of these results, it was opted to apply softly conditions as the mixture of nitric and acetic acids, that affords the formation of nitronium acetate (Scheme 28).<sup>158</sup>



Scheme 28

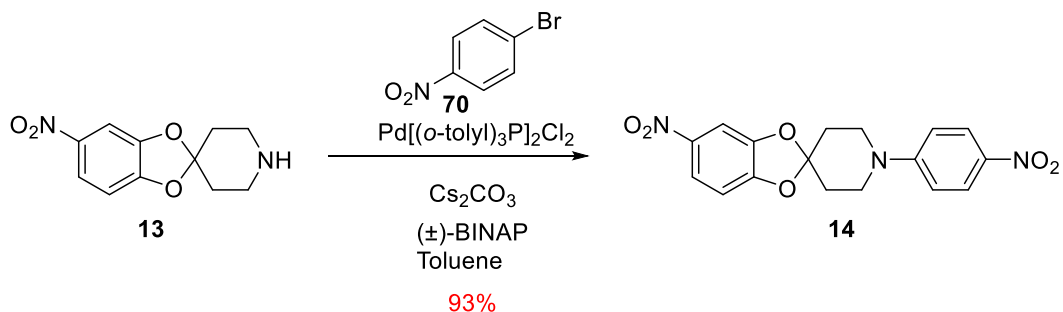
The hydrolysis of the acetamide function of **12** using KOH in a solution of ethanol:water (2:8) at room temperature, leads to the spirobenzodioxolepiperidine **13** in 69% yield. (Scheme 29).



Scheme 29

#### 3.1.1.9. Preparation of 5-nitro-1'-(4-nitrophenyl)spiro[benzo[1,3]dioxole-2,4'-piperidine] (**14**)

The spirobenzodioxolepiperidine **13** was treated with 4-bromonitrobenzene (**70**) under cross-coupling conditions previously indicated. So,  $\text{Pd}[\text{P}(o\text{-tolyl})_3]_2\text{Cl}_2$  as a catalyst, BINAP as ligand, cesium carbonate as a base and drops of toluene as solvent. In these conditions the dinitro-derivative **14** was obtained in 93% yield (Scheme 30).



Scheme 30

<sup>158</sup> a) J. G. Hoggett; R. B. Moodie; J. R. Penton; K. Schofield. *Nitration and Aromatic Reactivity* Cambridge: London, **1971**, p 76. b) Taylor, R. *Electrophilic Aromatic Substitution* Wiley: New York, **1990**, p 269

The emergence in the  $^1\text{H-NMR}$  spectrum of two doublets at 6.83 and 8.08 ppm integrating two protons each one, it allows us to confirm the proposed structure for the spiro-derivative **14** (Figure 36).

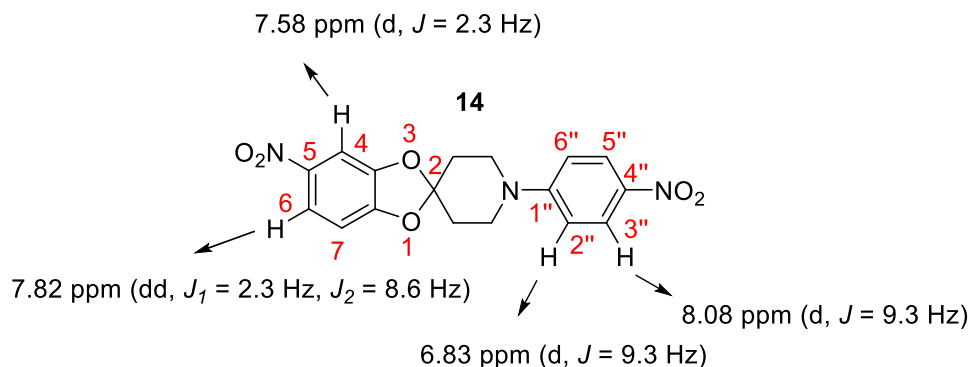
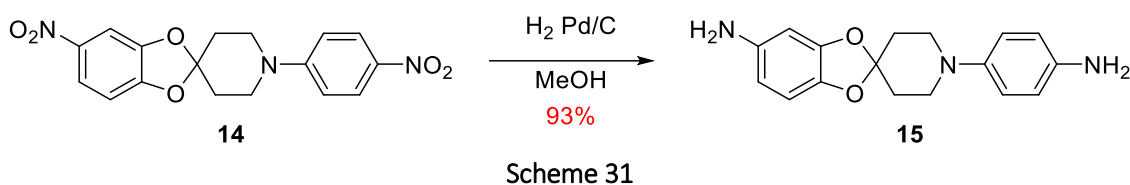


Figure 36.  $^1\text{H-NMR}$  spectroscopy data of compound **14**

The reduction of both nitro groups through catalytic hydrogenation, leads to the double aniline **15** in 93% yield (Scheme 31).



The shielding suffered by protons in the  $^1\text{H-NMR}$  spectrum, in the positions 3'' and 5'', and as well the ones in the positions 4 and 6 in comparison with the spectrum signals of the nitrate starting material, enable to confirm the proposed structure for the spiro-derivative **15** (Figure 37).

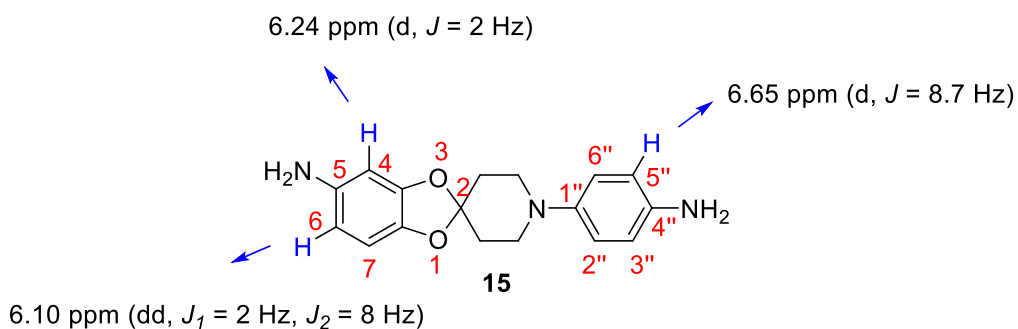
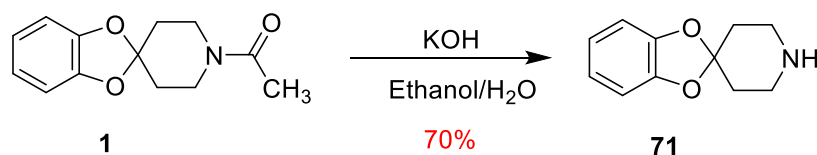


Figure 37.  $^1\text{H-NMR}$  spectroscopy data of compound **15**

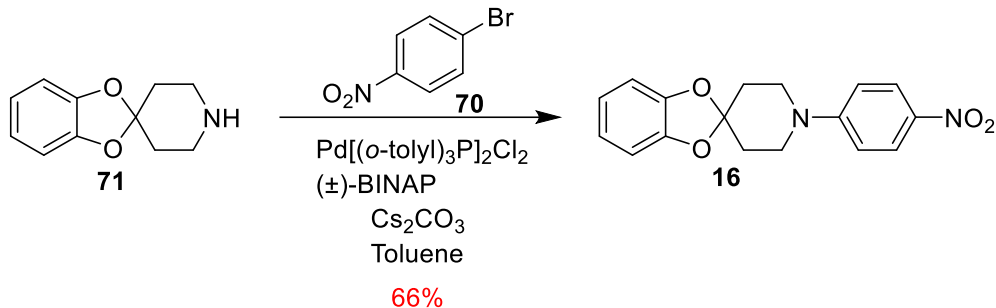
### 3.1.1.10. Preparation of spiro[benzo[1,3]dioxole-2,4'-piperidine] (**16**) and the 1'-(4-nitrophenyl)spiro[benzo[1,3]dioxole-2,4'-piperidine] (**17**)

Hydrolysis of the amide **1** using KOH in ethanol and water leads to the piperidine **71** in a 70% yield (Scheme 32).



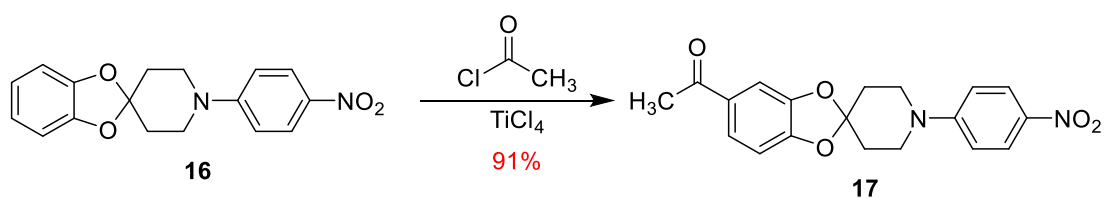
### Scheme 32

Then, the arylation of **71**, under cross-coupling conditions, catalyzed by Pd (II), allows to obtain the spiro-derivative **16** in 66% yield (Scheme 33).



### Scheme 33

The acylation of the spiroderivative **16** using acetyl chloride and titanium tetrachloride, in DCM, under classical conditions, allows to obtain the corresponding acetyl spiro **17** in 91% yield (Scheme 34).



### Scheme 34

The presence of a singlet in the <sup>1</sup>H-NMR at 2.46 ppm integrating three protons and the set of other signals, enables to assign the structure of the spiro-derivative **17** (Figure 38).

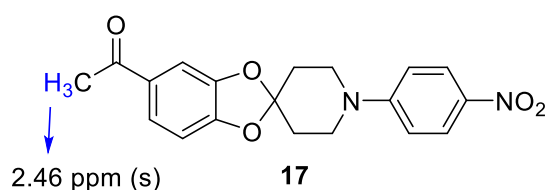
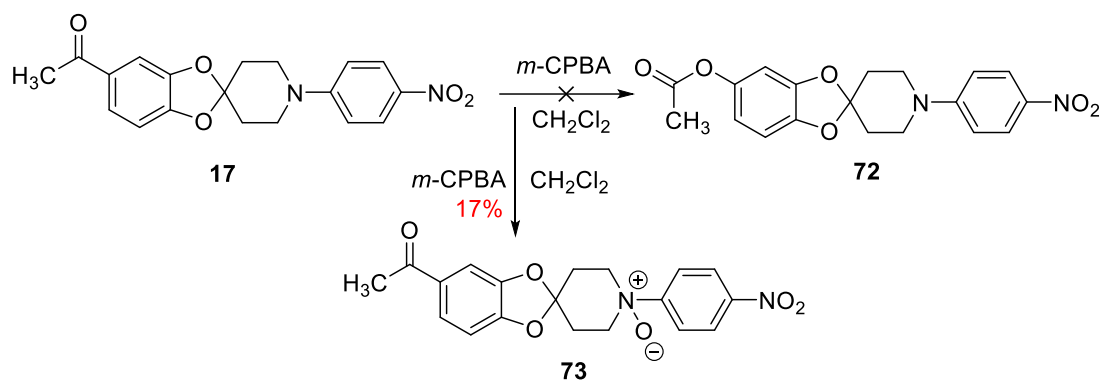


**Figure 38.** <sup>1</sup>H-NMR spectroscopy data of compound **17**

In the first moment, the treatment of **17** with *m*-CPBA was the procedure chosen in order to achieve the formation of an ester from the starting ketone by oxidative conditions of Baeyer-Villiger reaction (Scheme 35).<sup>159</sup>

<sup>159</sup> C. M. Crudden; A. C. Chen; L. A. Calhoun. *Angew. Chimie. Int. Ed.* **2000**, *39*, 2851-2855

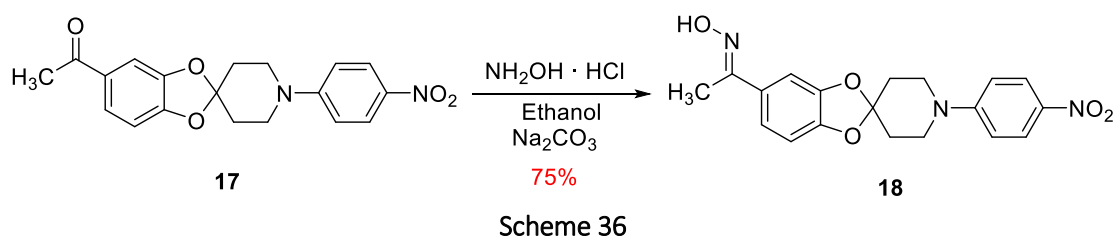


In the applied conditions it was not possible to prepare the expected ester **72**, but the corresponding *N*-oxide **73** was obtained. The *m*-CPBA produces oxidation of the tertiary amine<sup>160</sup> and as a result the corresponding *N*-oxide is obtained which presents solubility problems and would not allow the oxidation of the acylated position. The mass spectroscopy analysis with a molecular signal at 372.1243 g/mol (expected 372.1200 g/mol) allows to confirm the proposed structure for the *N*-oxide **73**.

#### 3.1.1.11. Preparation of **18** and **20**

The treatment of the methylketone **17** with hydroxylamine hydrochloride in presence of sodium carbonate, leads to the expected oxime **18** in 75% yield of isolated product (Scheme 36).

By NMR techniques it was confirmed only obtention of the isomer (*E*), that as it has been mentioned previously, is due to the applied conditions of reaction.



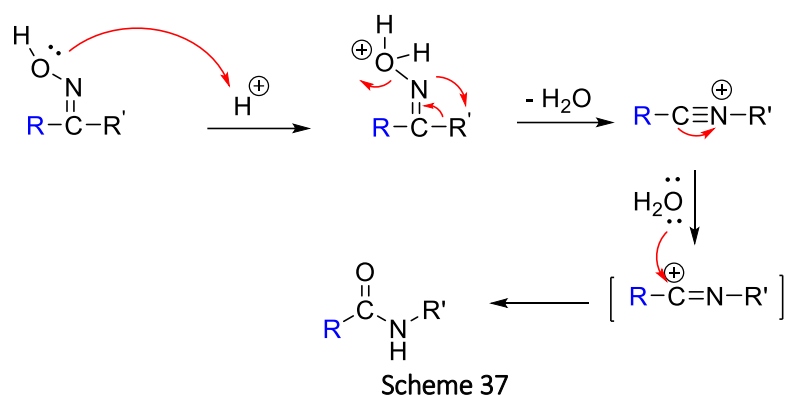
It is well known that oximes are synthetic intermediates that can be transformed into amides or lactones through Beckmann transposition.<sup>161</sup> In order for the transposition to take place it requires presence of an acid as sulfuric acid or  $\text{AlCl}_3 \cdot \text{H}_2\text{O}$ .<sup>162</sup>

A proposal mechanism for this transposition is indicated below (Scheme 37), where the most important characteristic lies in the stereochemistry disposition of the R and R' groups regarding the oxime. In the practice the migrating group is the one in *anti* disposition regarding the hydroxyl group (here it is the R' group).

<sup>160</sup> N. K. Jana; J. G. Verkade. *Org. Lett.* **2003**, *5*, 3787-3790

<sup>161</sup> a) R. E. Gawly. *Org. React.* **1988**, *35*, 39-40 b) M. B. Smith; J. March. *In Advanced Organic Chemistry* 5th ed., John Wiley & Sons, New York, **2001**, 1415-1416

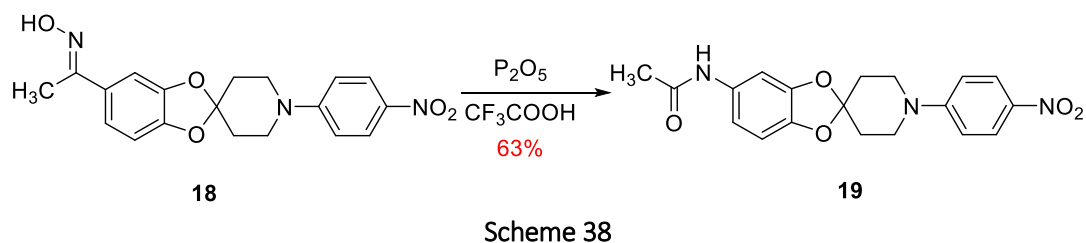
<sup>162</sup> M. Boruah; D. Konwar. *J. Org. Chem.* **2002**, *67*, 7138-7139



In the first step, the protonation of the -OH group through acid-base reaction occurs. Next, in a concerted way, the group R' (*anti*) migrates producing the loss of a molecule of water and an intermediate nitrile or carbene type is made. Then, these intermediates incorporate a molecule of water that allows the obtention of the amide or lactone.

These reactions are very useful in organic chemistry for the preparation of synthesis intermediates and products with industry applications. For this reason, there are a lot of undertaken studies in order to find the conditions that allow to apply this reaction to functionalize structures which will not support the strong acid conditions of the classic Beckmann transposition.

In our case, the P<sub>2</sub>O<sub>5</sub> and trifluoroacetic acid ( $pK_a = 0.3$ ) were introduced instead of sulfuric acid ( $pK_a = -5.2$ ) from the original reaction. These softly conditions enable to reach the desired amide **19** in 63% yield (Scheme 38).



The shielding experimented by the methyl group of the amide (23.8 ppm) in the <sup>13</sup>C-NMR regarding the starting oxime (12.1 ppm), confirms the proposed structure for the amide **19** (Figure 39).

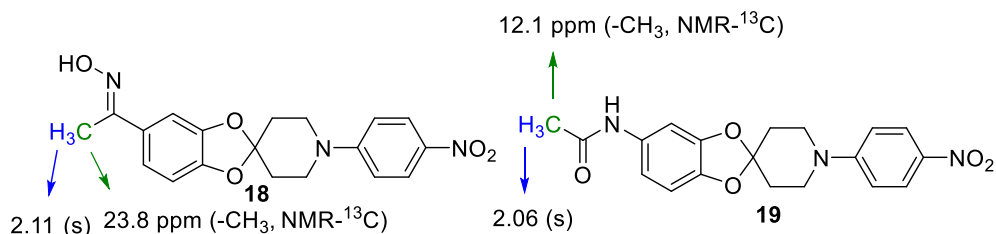
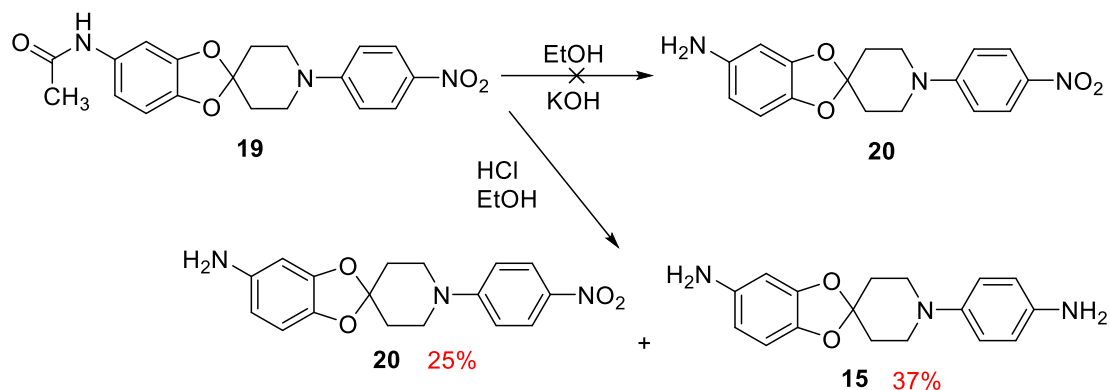


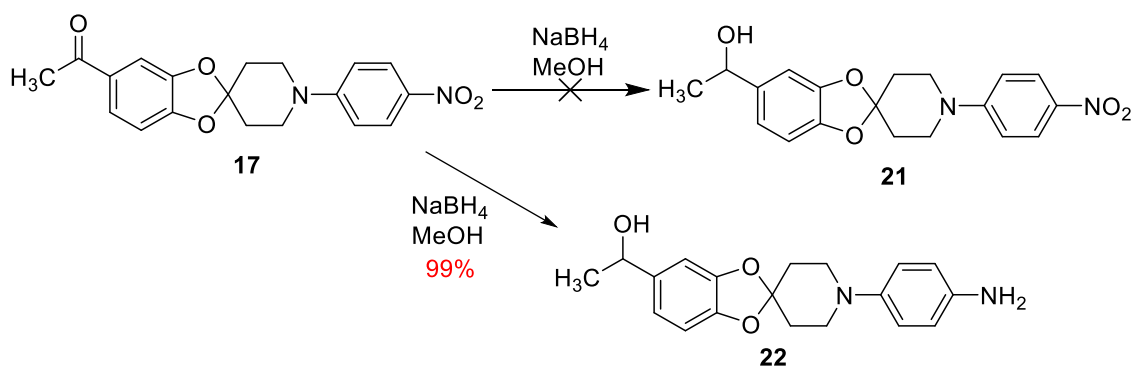
**Figure 39.** <sup>1</sup>H-NMR and <sup>13</sup>C-NMR spectroscopy data of compounds **18** and **19**

Hydrolysis of amide **19** in basic conditions at room temperature do not lead to the expected aniline **20**. However, when acid conditions were applied, such as the addition of chloride acid 2N, drives to a mixture of anilines **20** and **15** in 25 and 37% yield respectively (Scheme 39).

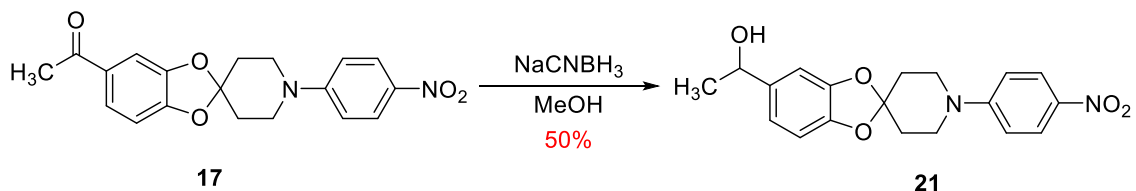


The analytic data of aniline **15** fully agree with the data afforded for the resulting product of the catalytic hydrogenation of 1-(*p*-nitrophenyl)-5-aminospiro[benzodioxole-2,4'-piperidine] (**14**).

3.1.1.12. Preparation of 1-(1'-(4-nitrophenyl)spiro[benzo[1,3]dioxole-2,4'-piperidine]-5-yl)ethan-1-ol (**21**) and 1-(1'-(4-aminophenyl)spiro[benzo[1,3]dioxole-2,4'-piperidine]-5-yl)ethan-1-ol (**22**)  
The treatment of ketone **17** with NaBH<sub>4</sub> does not allow to obtain the expected secondary alcohol **21**, however it did allow isolation of a product coming from the reduction of both, the ketone function and the nitro group, in 99% yield (Scheme 40).



The utilization of NaCNBH<sub>3</sub>, instead of NaBH<sub>4</sub> it affords with success the chemoselective reduction of the ketone in presence of nitro group, obtaining in this way, the nitroalcoholspiro derivative **21** in 50% yield (Scheme 41).



In <sup>1</sup>H-NMR spectrum appears a doublet at 1.39 ppm attributable to the methyl group and a quadruplet signal at 4.75 ppm attributable to the proton of benzylic position, signals that allow to confirm the proposed structure for the secondary alcohol **21** (Figure 40).

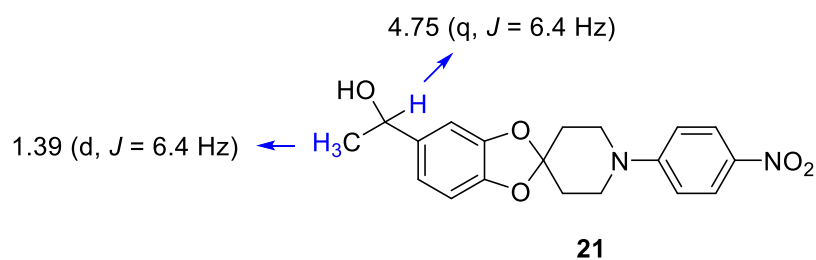
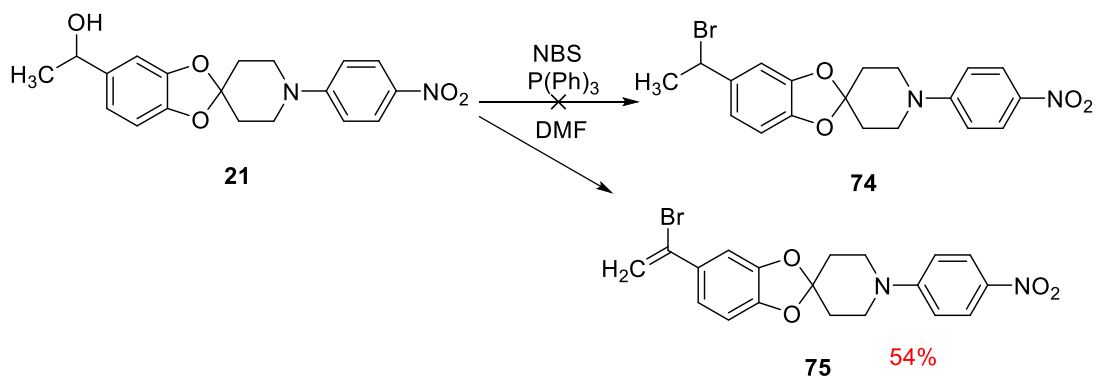


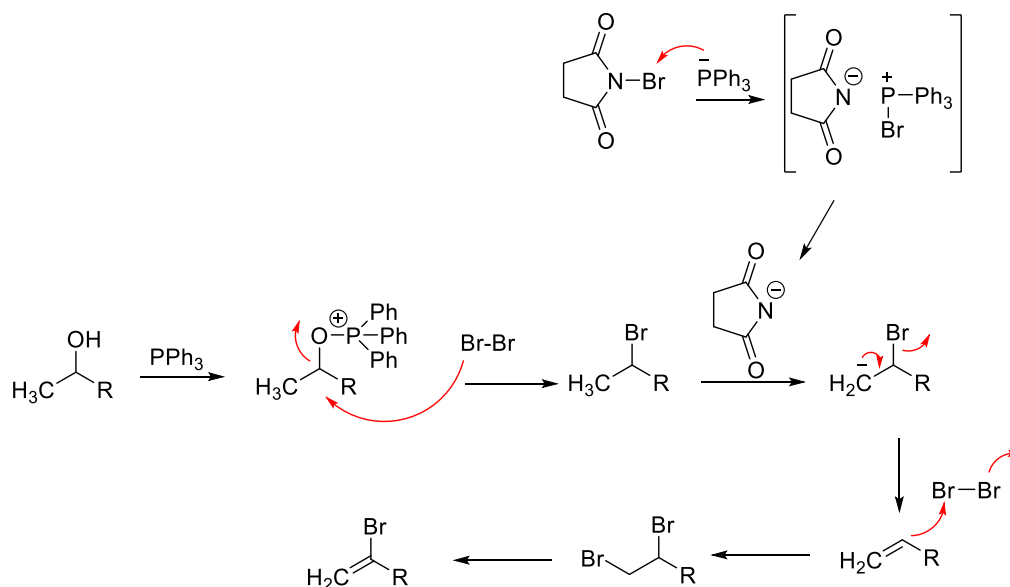
Figure 40.  $^1\text{H-NMR}$  spectroscopy data of compound **21**

Alcohol **21** was undertaken by the action of NBS in DMF in order to substitute the hydroxyl group for a bromo atom.<sup>163</sup> Even trying to modify the conditions, it was not possible to obtain the expected product **74**. With the applied conditions, it was possible to isolate the bromovinyl derivative **75** in 54% yield (Scheme 42).



Scheme 42

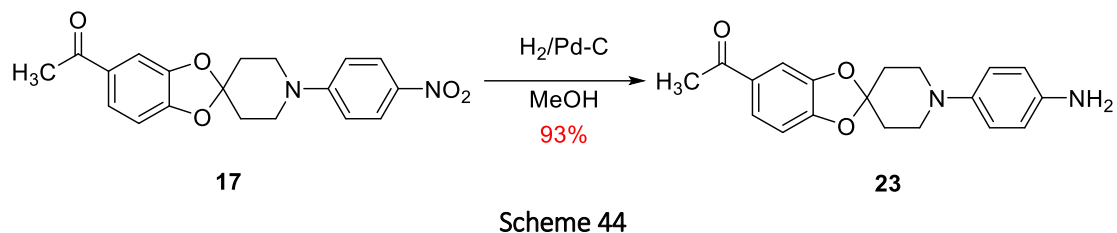
The following mechanism is proposed for the formation of **75** (Scheme 43):



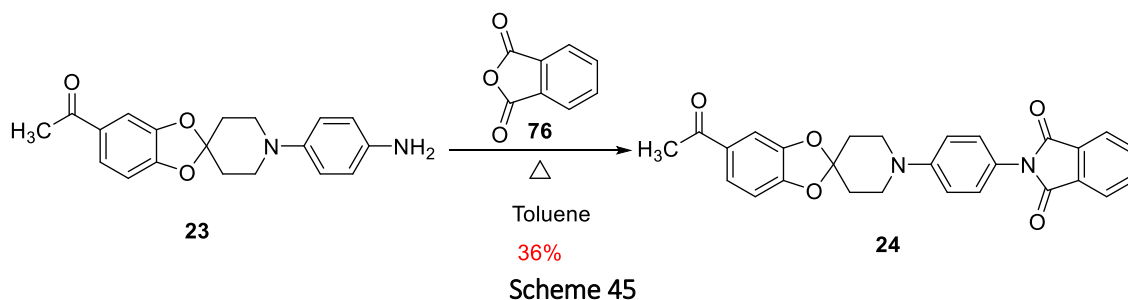
<sup>163</sup> S. Zhao; Y. Wu; Q. Sun; T. M. Cheng; R. T. Li. *Synthesis* **2015**, 47, 1154-1162

### 3.1.1.13. Preparation of spiroderivatives **23** to **26**

The treatment of nitro-derivative **17** with hydrogen stream under carbon-palladium catalysis, drives chemoselectively to the expected aniline **23** in 93% yield (Scheme 44).



The addition of the aniline **23** to the phthalic anhydride (**76**) allows to obtain the *N*-substituted phthalimide **24** in 36% yield (Scheme 45).



In the <sup>1</sup>H-NMR spectrum of **24** are distinguish two double doublets at 7.78 and 7.94 ppm integrating 2 protons each one, being attributable to the protons of positions  $\alpha$  and  $\beta$  with respect to the carbonyl groups. These data together with the C-13 NMR allow to confirm the proposed structure for imide **24** (Figure 41).

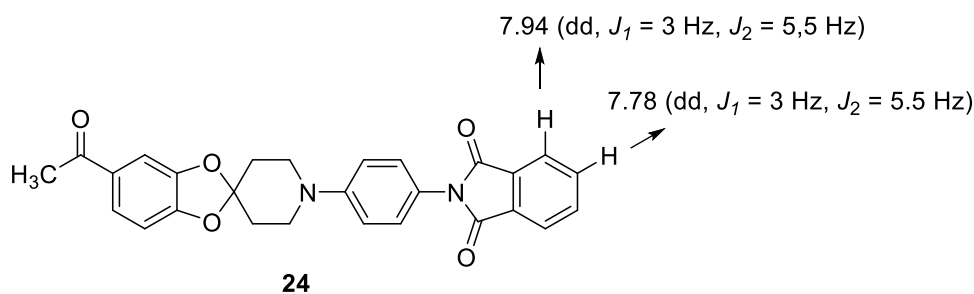
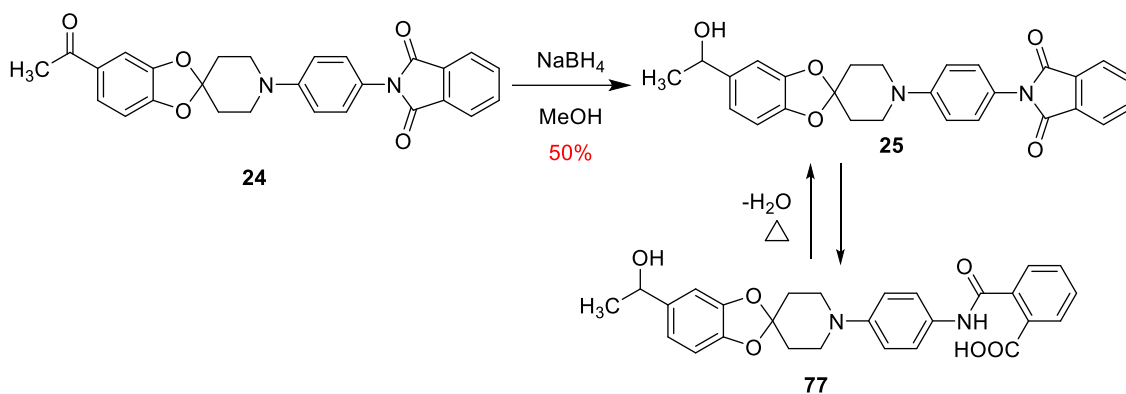


Figure 41. <sup>1</sup>H-NMR spectroscopy data of compound **24**

The methylketone **24** is reduced to secondary alcohol **25** by treatment with NaBH<sub>4</sub> in methanol (Scheme 46).

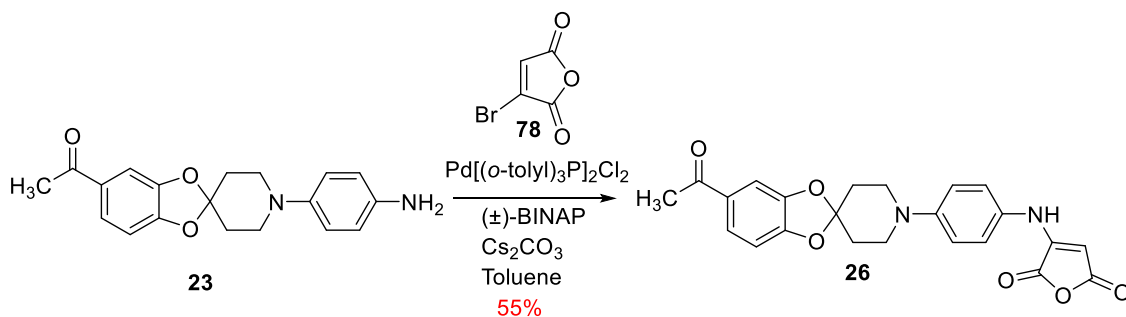




Scheme 46

In these conditions the expected alcohol **25** is obtained in only 50% yield. In the same reaction and under the described conditions the product from partial hydrolysis of the imide is detected. The corresponding monoamide is converted into the expected imide by heating the reaction in the presence of dehydrating agents (P<sub>2</sub>O<sub>5</sub>). It should be noted that alcohol **25** constitutes a racemic mixture of both enantiomers and in this case, they have not been split up or either prepared enantioselectivity none of them. The preparation of the enantiomers will be carried out if the racemic mixture shows interesting biological activity.

The addition of the aniline **23** to the bromomaleic anhydride (**78**) using the cross-coupling conditions, enables to obtain the derivative **26** in 55% yield (Scheme 47).



Scheme 47

The presence of a singlet at 7.34 ppm in the <sup>1</sup>H-NMR spectrum attributable to the proton of the methylene group, together with the signals of the carbonyl groups from the anhydride in the <sup>13</sup>C-NMR at 167.8 ppm allow to confirm the proposed structure for compound **26** (Figure 42).

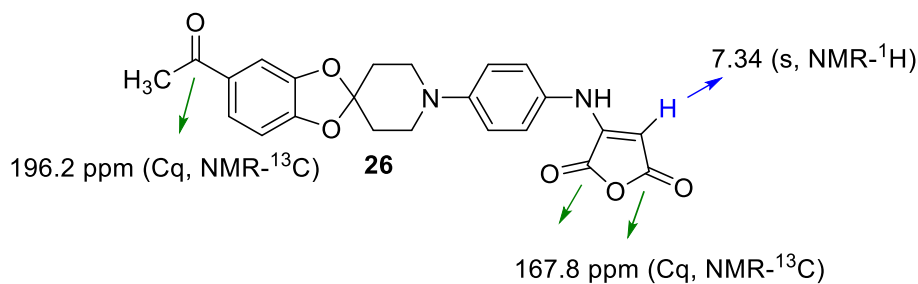
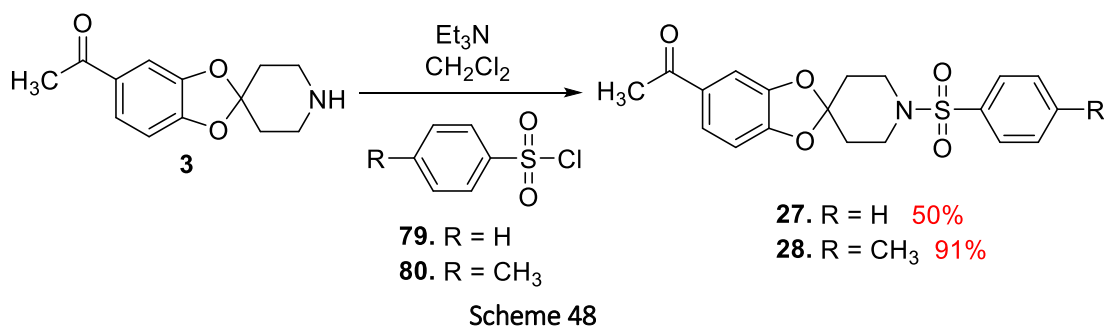


Figure 42. <sup>1</sup>H-NMR spectroscopy data of compound **26**

### 3.1.1.14. Preparation of **27** to **36**

The sulfonamides can be prepared classically by treatment of an amine with the corresponding chlorosulfonic acid in presence of a base, that through the uptake of the formed hydrochloric acid enables the evolution of the reaction.

In this work, the secondary amine **3** is treated with benzenesulfonyl chloride in one case and *p*-toluenesulfonyl chloride in other, using trimethylamine as a base in dichloromethane. Temperature control is very important, especially in the addition of the reagents, with temperatures below 5 °C being the ones affording the best results (Scheme 48).



The sulfonamides **27** and **28** were obtained in 50 and 91% yields respectively. The data from proton NMR allow to identify these compounds (Figure 43).

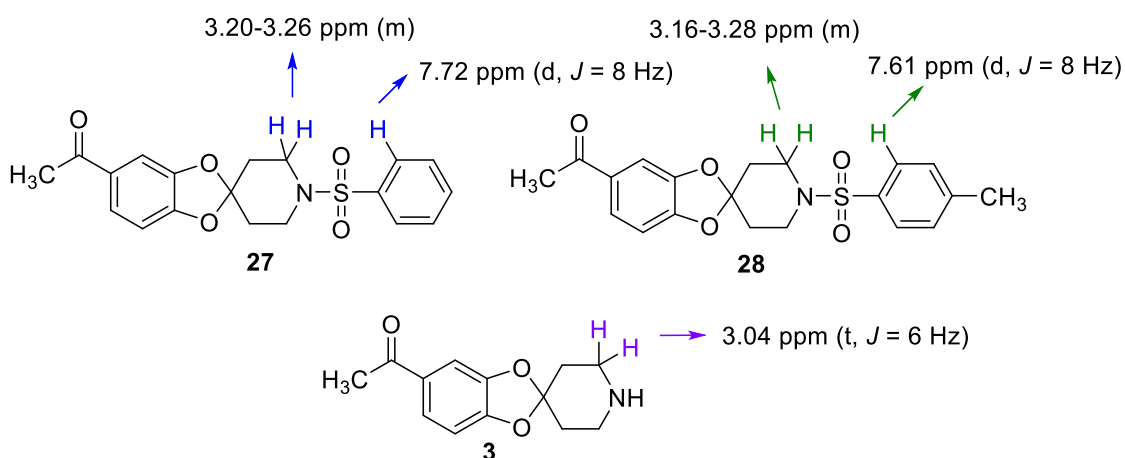
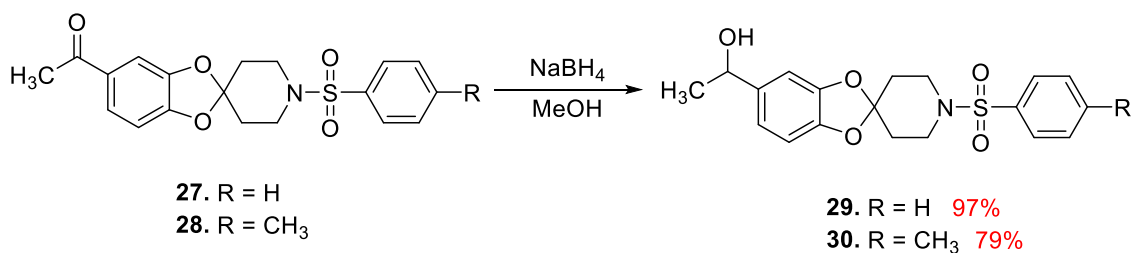


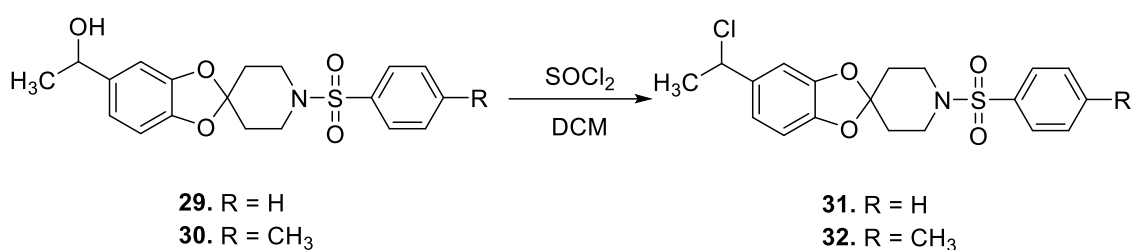
**Figure 43.** <sup>1</sup>H-NMR spectroscopy data of compounds **27** and **28**

It is important to highlight the shielding of the signals corresponding to the methylene groups from the piperidine which change from 3.04 ppm to 3.20-3.26 ppm (**27**) and 3.16-3.28 ppm (**28**) in the sulfamoylate derivatives. The reduction of methylketones **27** and **28** with NaBH<sub>4</sub>, in methanol, drives to the alcohols **29** and **30** in 97 and 79% yields respectively (Scheme 49).



Scheme 49

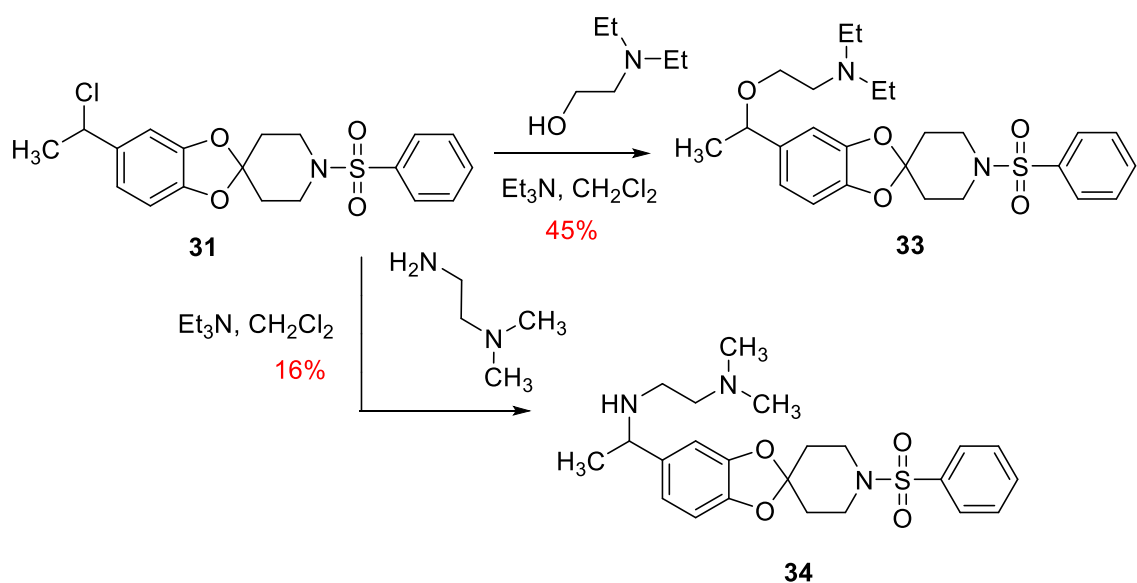
In both cases, the presence of quadruplet signals at 4.68 and 4.77 ppm in the <sup>1</sup>H-NMR spectrum of compounds **29** and **30** respectively, allows to confirm the proposed structures. With the purpose to convert the hydroxyl group of alcohols **29** and **30** into a good leaving group, these were treated with thionyl chloride using dichloromethane as a solvent (Scheme 50).



Scheme 50

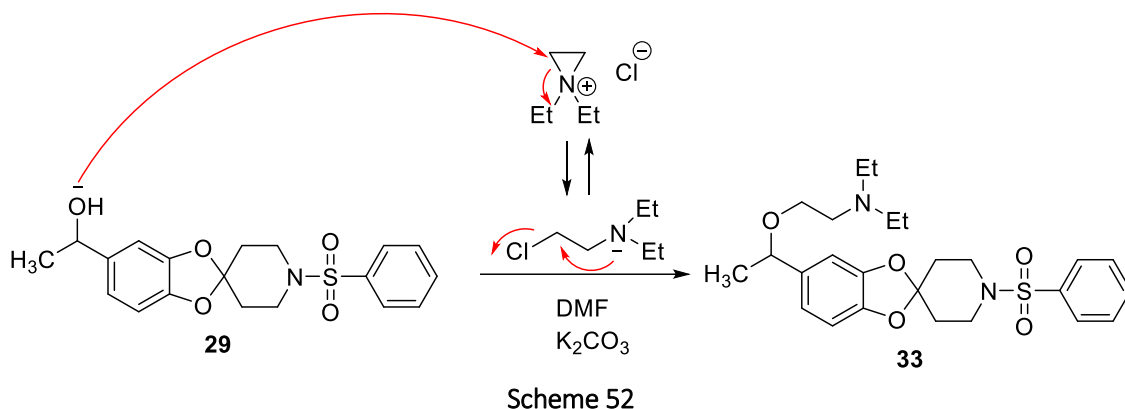
The chlorinated derivatives **31** and **32** were obtained in high purity and were used without purification in the following reactions.

The treatment of the chloro-derivative **31** with *N,N*-diethyl-2-hydroxyethylamine in presence of trimethylamine dissolved in dichloromethane, leads to the expected aminoalcohol **33** in 45% yield after purification (Scheme 51). The same conditions were applied, using *N,N*-diethyl-2-hydroxyethylamine, allowing the obtention of diamine **34** in 16% yield of the purified product (Scheme 51).

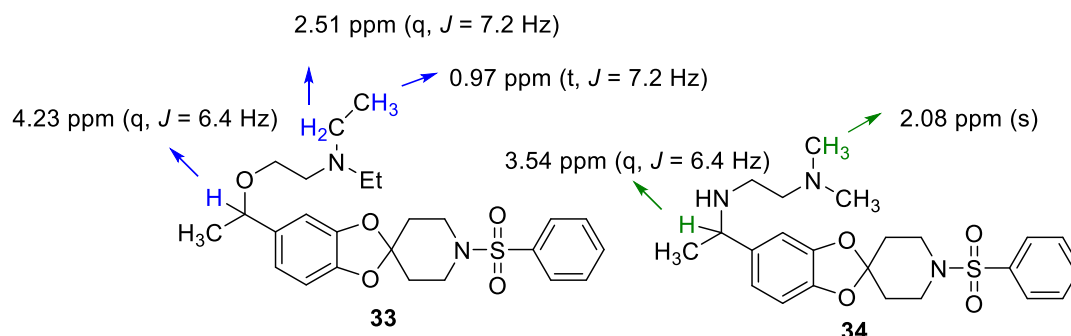


Scheme 51

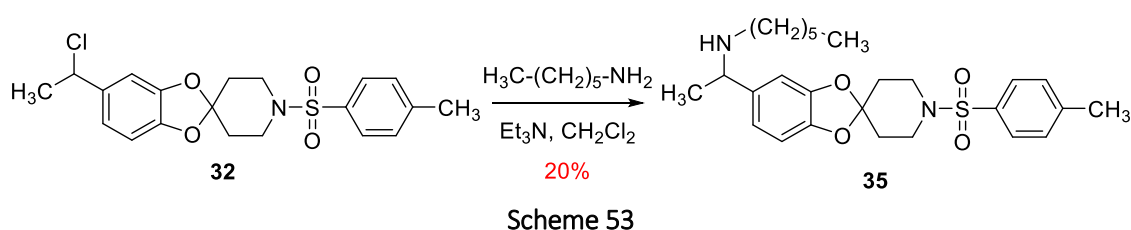
Alternatively, the alkylation of alcohol **29** with *N,N*-diethyl-2-chloroethylamine in DMF and with the presence of potassium carbonate was attempted (Scheme 52).



The characteristic signals in the <sup>1</sup>H-NMR spectrums of **33** and **34** that enable the structural assign, will be the next ones: for **33**, the presence of a quadruplet signals at 4.23 ppm attributable to the benzylic proton, the quadruplet at 2.51 ppm and the triplet at 0.97 ppm, both signals attributable to the ethylene groups. While for the diamine **34**, there is a quadruplet at 3.54 ppm attributable to benzylic proton and a singlet at 2.08 ppm integrating six protons attributable to the two methyl of the tertiary amine (Figure 44).



In order to obtain a more lipophilic compound than diamine **34**, the preparation of amine **35** was carried out by treatment of chloro-derivative **32** with hexylamine, using the same conditions previously indicated for the preparation of diamine **34** (Scheme 53).



Thus, the corresponding alkylated hexylamine is obtained in 20% yield. In this case, the presence of different signals in the <sup>1</sup>H-NMR spectrum attributable to the lineal chain of hexylamine, allow to confirm the proposed structure for **35** (Figure 45).

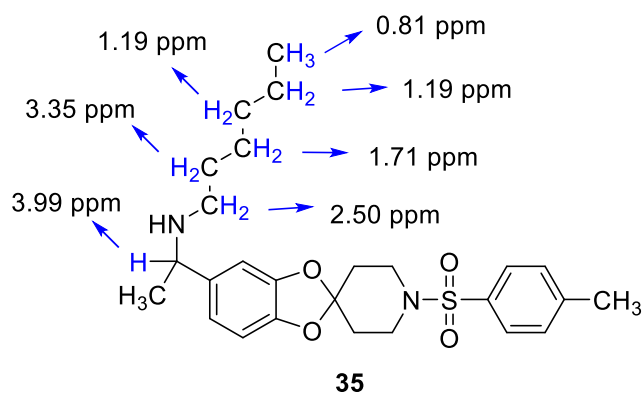
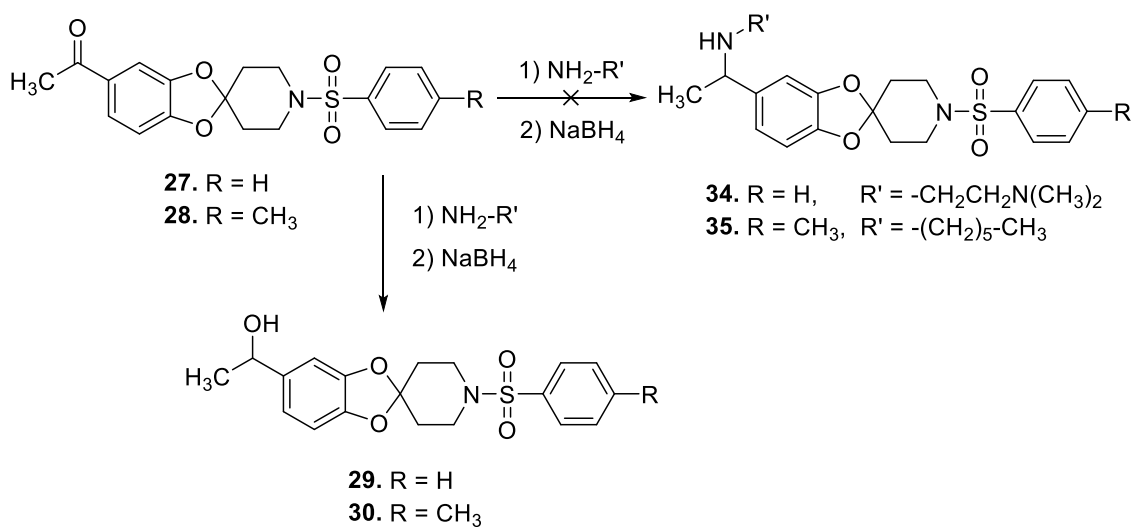


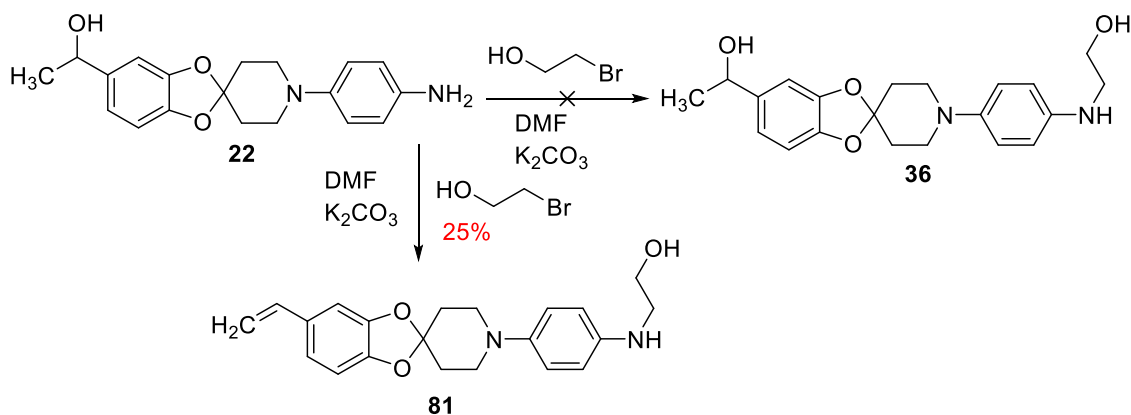
Figure 45.  $^1\text{H}$ -spectroscopy data of compound **35**

In a first moment, the amine **34** and **35** were tried to prepare through reductive amination, starting from the methylketones **27** and **28**. Different conditions were tested, changing both the temperature and the used acid catalyst, even a Dean-Stark system was used in order to facilitate the elimination of water when the used solvent was toluene. In none of these conditions it was possible to isolate the expected amine after the corresponding reduction with  $\text{NaBH}_4$ . In all the assays the alcohols **29** and **30** obtained from the reduction of ketones, were detected (Scheme 54).



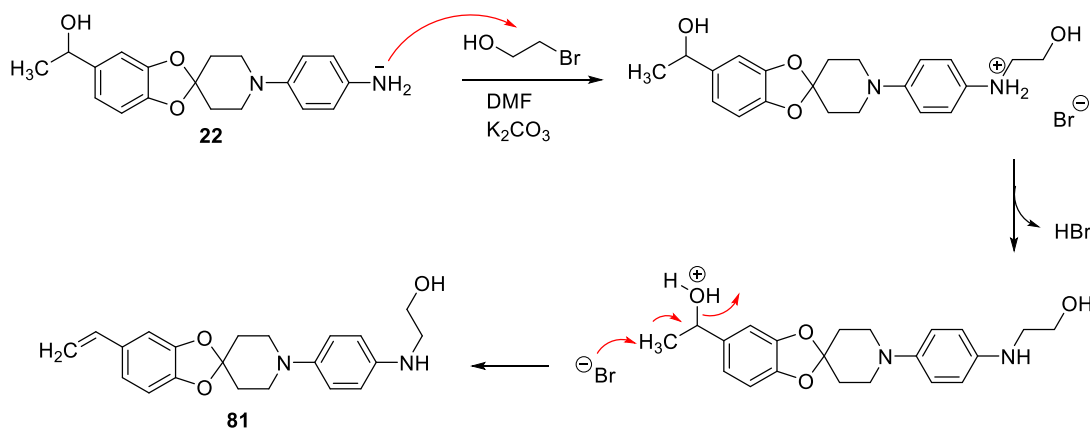
Scheme 54

The treatment of aniline **22** with 2-bromoethanol in presence of potassium carbonate in DMF, do not allow to isolate the dialcohol **36** coming from the alkylation of the aniline function. However, it was isolated in 25% yield an alkylate derivative but with a vinyl group instead of the secondary alcohol in position 5 (Scheme 55).



Scheme 55

A possible mechanism to explain the formation of **81** is indicated in the following scheme 56.



Scheme 56

First of all, the alkylation of the aniline would be produced chemoselectivity in presence of  $K_2CO_3$  as a base. Then, the produced hydrobromic acid allows the protonation of alcohol, converting said group into a good leaving group which could be substituted by bromide through nucleophile substitution, that by elimination would drive to the corresponding alkene. Alternatively, it could be protonated and removed directly.

The emergence doublets in the proton NMR spectrum at 5.10 and 5.58 ppm attributable to the alkene protons, together with the double doublet at 6.58 ppm corresponding to the proton of the benzylic position, enable to confirm the presence of a vinyl group in the structure **81**. Also, it results essential the triplets at 3.80 and 3.91 ppm attributable to hydroxyethylamine chain.

These data, together with other analytical data allow to confirm the proposed structure for **81** (Figure 46).

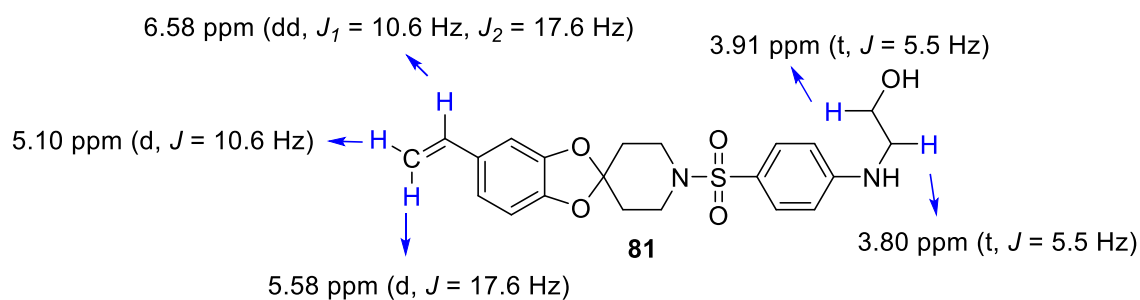


Figure 46.  $^1\text{H-NMR}$  spectroscopy data of compound **81**

### 3.1.1.15. Preparation of ureas **37-42**

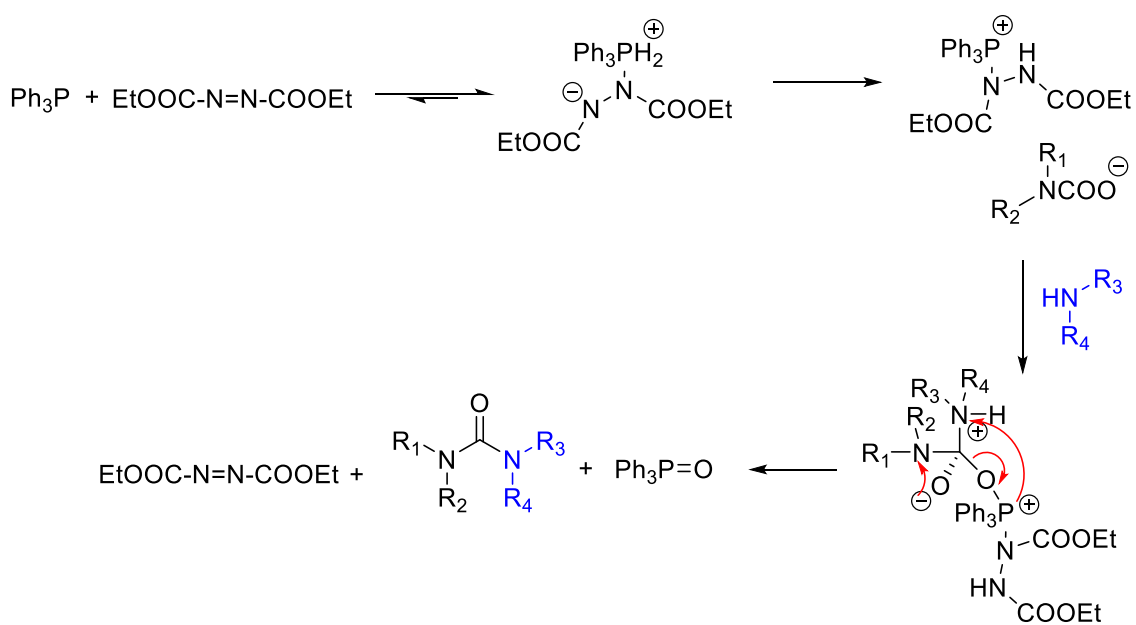
Ureas are present in many compounds of both industrial chemistry and chemistry applied to drug synthesis. Regarding the preparation of ureas it is possible to differentiate between symmetric ureas and no symmetric. The methodology to prepare them is diverse, some of these methods are explain hereunder:

#### ·No symmetric ureas

These are some of the methods to obtain no symmetric ureas:

#### a) Mitsunobu reaction

This method allows to obtain ureas using  $\text{PPh}_3$  and DEAD (diethyl azodicarboxylate), at room temperature and  $\text{CO}_2$  stream, softly conditions that leads to the ureas with good yields. As a result of the treatment of urea with  $\text{CO}_2$ , the carbamic acid is obtained and reacts with the zwitterion derivative of  $\text{PPh}_3$ , making a stable zwitterion species, which reacts with another amine molecule. The resultant intermediate is restructured forming the desired substituted ureas (Scheme 57).<sup>164</sup>

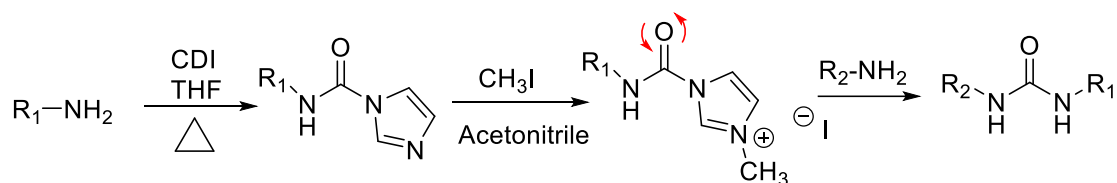


Scheme 57

<sup>164</sup> H. Wang; Z. Xim; Y. Li. *Top. Curr. Chem.* **2017**, 375, 49-75

b) Carbonyldiimidazole salts<sup>165,166</sup>

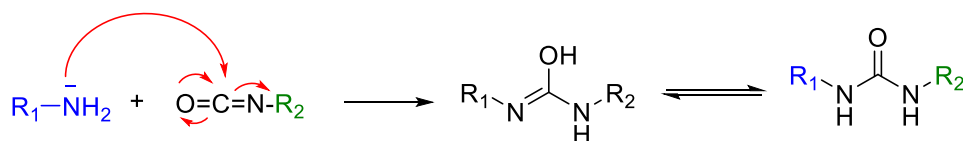
The reaction of carbonyldiimidazole (CDI) with amines or anilines gives as a result the *N*-(aminocarbonyl)imidazole, which through reaction with methyl iodide becomes carbonylimidazole iodide, an intermediate salt, that treat it with another amine leads to the corresponding urea (Scheme 58).



Scheme 58

c) Isocyanates<sup>167,168</sup>

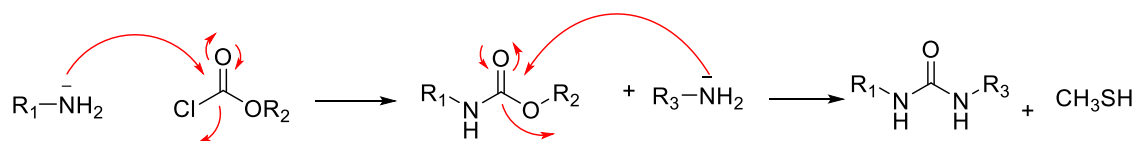
When amines or anilines are added to isocyanates, asymmetric ureas are obtained (Scheme 59). It is necessary to highlight that the transformation of ammonium isocyanate to urea, carried out by Wöhler in 1824, constituted the first synthesis of an organic compound coming from an inorganic precursor. This method affords the best results regarding the previous described methods, allowing the synthesis of ureas in only one step and with softly conditions (room temperature and short times of reaction). It uses solvents as DMSO,<sup>169</sup> ethylic ether<sup>167,168</sup> or THF.<sup>167,168</sup> Most of the isocyanates are commercially available, however its preparation is possible in the laboratory.



Scheme 59

d) Chloroformates<sup>170</sup>

Through the use of chloroformates and amines or anilines it is possible to obtain asymmetric ureas. To explain these reactions the mechanism would be: first the addition to the carbonyl group from the amine or aniline and elimination of chloride, next, the reaction of a second amine which adds again into the carbamate intermediate to generate the urea (Scheme 60).



Scheme 60

<sup>165</sup> J. A. Grzyb; R. A. Batey. *Tetrahedron Lett.* **2008**, 49, 5279-5282

<sup>166</sup> M. N. Bertrand; J. P. Wolfe. *Tetrahedron* **2005**, 61, 6447-6459

<sup>167</sup> D. P. N. Satchel; R. S. Satchel. *Chem. Soc. Rev.* **1975**, 4, 231-250

<sup>168</sup> E. A. Castro; R. B. Moodle; P. J. Sansom. *Chem. Soc. Perkin Trans. I.* **1985**, 2, 737-742

<sup>169</sup> Y. Zhang; M. Anderson; J. L. Weisman; M. Lu; C. J. Choy; V. A. Boyd; J. Price; M. Sigal; J. Clark; M. Connelly; F. Zhu; W. A. Guiguemde; C. Jeffries; L. Yang; A. Lemoff; A. P. Liou; T. R. Webb; J. L. DeRisi; R. K. Guy. *ACS Med. Chem. Lett.* **2010**, 1, 460-465

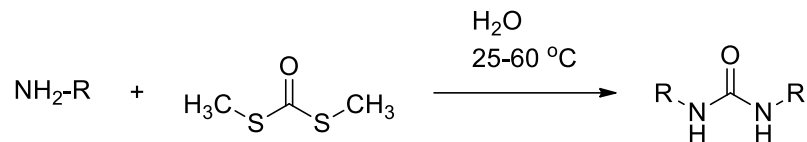
<sup>170</sup> C. Han; J. A. Porco. *Org. Lett.* **2007**, 9, 1517-1520



### Symmetric ureas<sup>171</sup>

These are some of the possible reactions to obtain symmetric ureas:

- a) *S,S*-Dimethyldithiocarbamate with an amine or aniline (addition to the carbonyl group plus elimination of the methyl methanethiol) (Scheme 61).

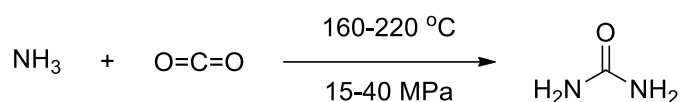


Scheme 61

- b) Ammonia or amines in the presence of CO<sub>2</sub>

Through the addition of ammonia or amines to carbon dioxide the corresponding ureas are afforded (Scheme 62). This synthesis of urea was carried out for first time at 1870 by A. Bazarov.

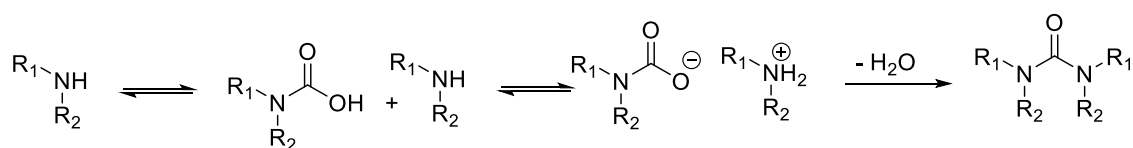
172



Scheme 62

Being a fast method and with simple reagents, it is considered a good option to prepare ureas at industry scale and sustainable with natural environment. Thanks to the low acidity of CO<sub>2</sub> and the softly conditions of the reaction, the carbamic acid is made together with the carbamate salt. The conversion between the carbamate salt, the carbamic acid and CO<sub>2</sub> is reversible, therefore the efficiency of the synthesis lies in the dehydration of the carbamate salt which leads to the corresponding urea.

This reaction can be carried out as well with secondary or tertiary amines as indicated in the following scheme 63.<sup>164</sup>



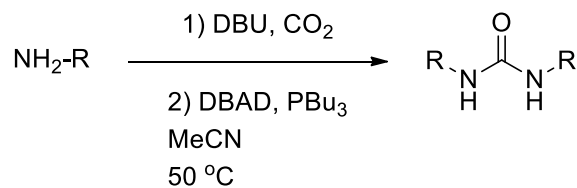
Scheme 63

From the Bazarov, Li and col.<sup>173</sup> methodology, it was proposed changes to improve the dehydration (Scheme 64). It was used assays of radioactive labeling with DBU (1,8-diazabicyclo[5.4.0]undec-7-ene) as a base, in presence of di-*tert*-butyl azodicarboxylate, in order to label the ureas in only one step.

<sup>171</sup> E. Artuso; I. Degani; R. Fochi; C. Magistris. *Synthesis* **2007**, 3497-3506

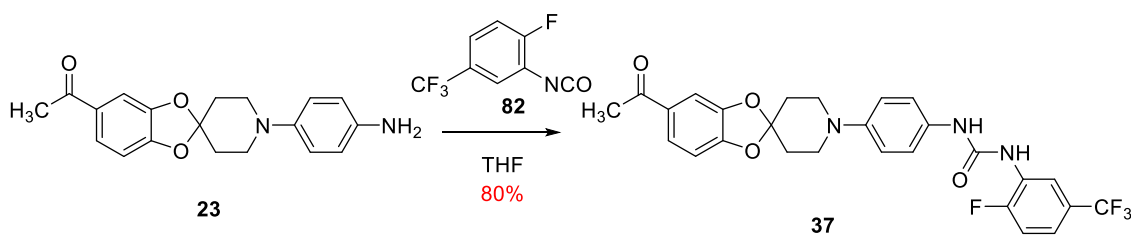
<sup>172</sup> A. I. Bazarov. *J. Prakt. Chem.* **1870**, 2, 283-312

<sup>173</sup> A. K. H. Dheere; S. Bongarzone; C. Taddei; R. Yan; A. D. Gee. *Synlett* **2015**, 26, 2257-2260



Scheme 64

In our research group, the urea **37** was prepared by addition of the amine **23** to the corresponding isocyanate under the conditions reported before (Scheme 65).



Scheme 65

The used solvent was THF, which under stirring at room temperature allows to achieve **37** in 80% yield. The data corresponding to the  $^1\text{H-NMR}$  spectroscopy signals as the pics at 7.07, 7.18 and 8.54 ppm attributable to the protons of positions 4''', 3''' and 6''' and the signal at 154 ppm (d,  $J = 247$  Hz) that appears in the  $^{13}\text{C-NMR}$  spectroscopy, attributable to C-2''' and bringing out the C-F coupling, allow to confirm the proposed structure for urea **37** (Figure 47).

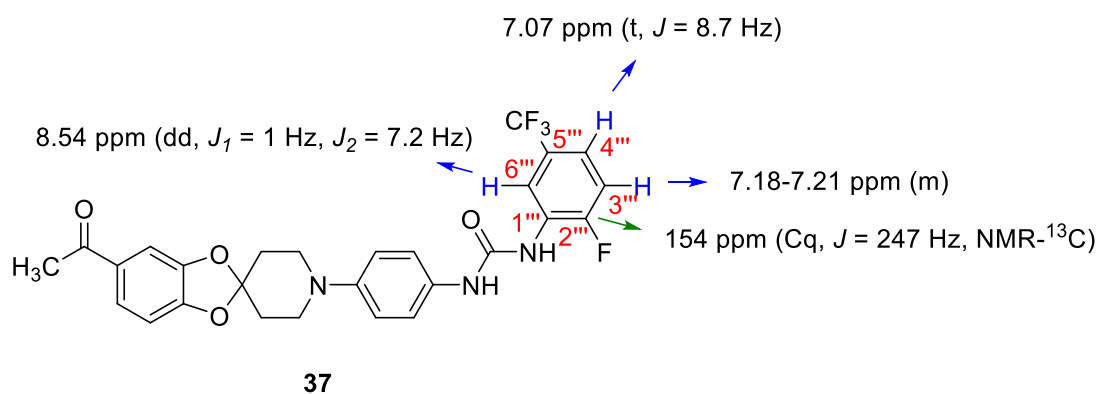
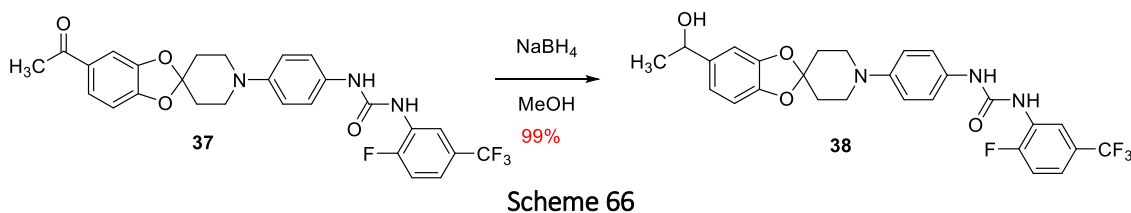


Figure 47.  $^1\text{H-NMR}$  and  $^{13}\text{C-NMR}$  spectroscopy data of compound **37**

The reduction with  $\text{NaBH}_4$  of urea **37** leads to secondary alcohol **38** in 99% yield (Scheme 66).



Scheme 66

The step from **37** to **38** was confirmed by the presence of a doublet signal at 1.23 ppm (CH<sub>3</sub>) and a quadruplet at 4.63 ppm (CH-OH) (Figure 48).

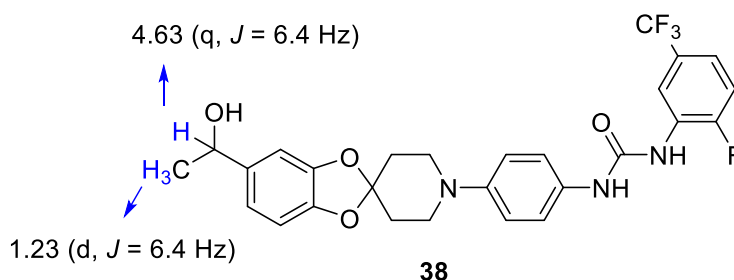
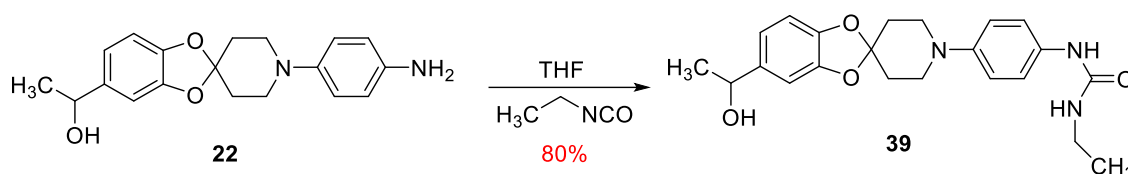


Figure 48. <sup>1</sup>H-NMR spectroscopy data of compound **38**

Following the indicated methodology for the anilines addition to isocyanates, at room temperature, in THF, it arrives to the obtention of urea **39** in 80% yield (Scheme 67).



Scheme 67

In this case, the presence of signals in the <sup>1</sup>H-NMR spectrum corresponding to -CH<sub>2</sub>-CH<sub>3</sub> group, it allows to confirm the proposed structure for the arylalkylurea **39** (Figure 49).

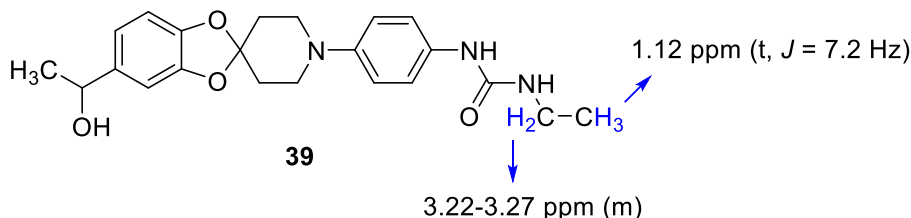
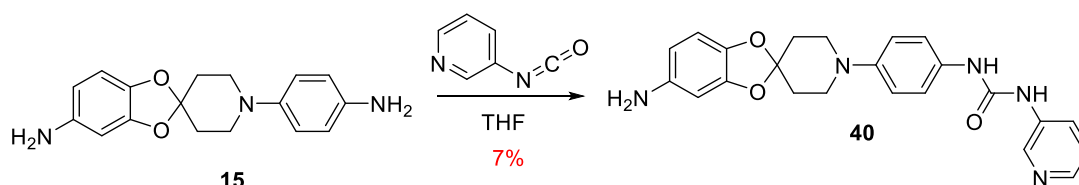


Figure 49. <sup>1</sup>H-NMR spectroscopy data of compound **39**

The treatment of diamine **15** with pyridyl-3-isocyanate leads to the monourea **40** in only 7% yield. (Scheme 68).

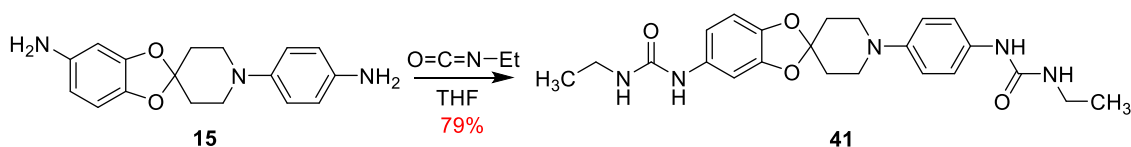


Scheme 68

The structure of monourea **40** was confirmed by mass spectroscopy (mass found: 418.1883 g/mol) being the theoretical mass of 418.1834 g/mol for C<sub>23</sub>H<sub>23</sub>N<sub>5</sub>O<sub>3</sub> applying ESI (+) method. In this case, the urea from the reaction of amino group at C-4'' position is obtained regioselectively. The main reactivity of this NH<sub>2</sub> group regarding the position C-5, it can be

attributed to the major nucleophile power of this group due to the higher electron donating character of the amine function in *para* position. While the amino group of position 5 account with an -O- group in *para* position presenting electron donor character and other -O- in *meta* position, acting as electron withdrawing group through inductive effect.

Alternatively, the treatment of dianiline **15** with an excess of ethyl-isocyanate leads to the bis-urea **41** in 79% yield (Scheme 69).



Scheme 69

The presence of signals in  $^1\text{H-NMR}$  spectrum attributable to the ethyl groups of the ureas **41**, and as well the integral corresponding to the exact number of protons, allow to confirm the proposed structure for this compound (Figure 50).

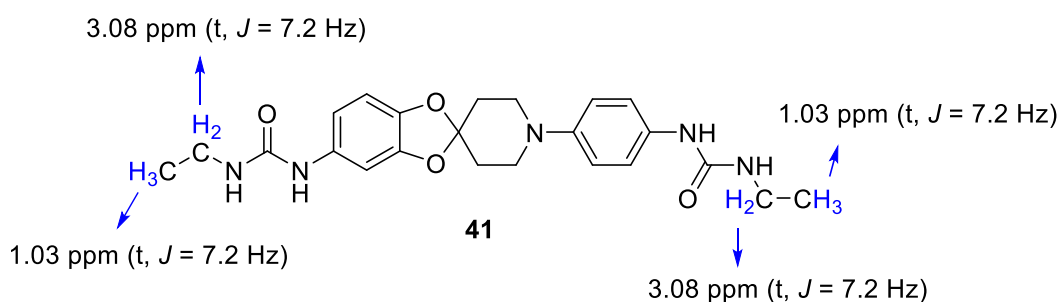
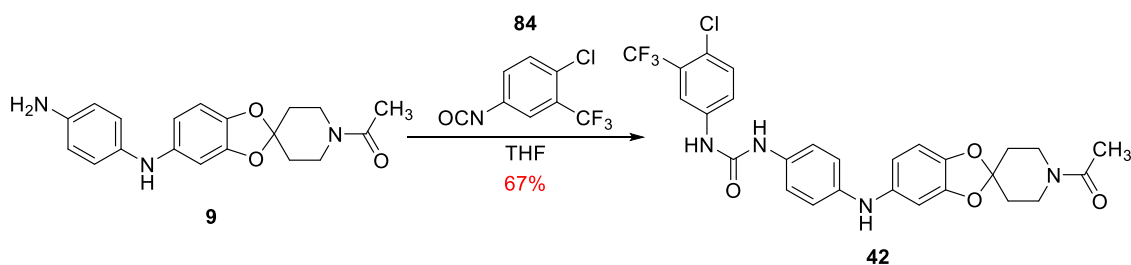


Figure 50.  $^1\text{H-NMR}$  spectroscopy data of compound **41**

The urea **42** was prepared by addition of aniline **9** to isocyanate **84**, in THF and under stirring at room temperature (Scheme 70).



Scheme 70

In the NMR proton spectrum are distinguishable signals at 2.08, at 7.52, at 7.72 and at 8.14 ppm, attributable to protons of  $\text{CH}_3$  group of acetyl function and positions C-5''', C-6''' and C-2''' respectively (Figure 51).

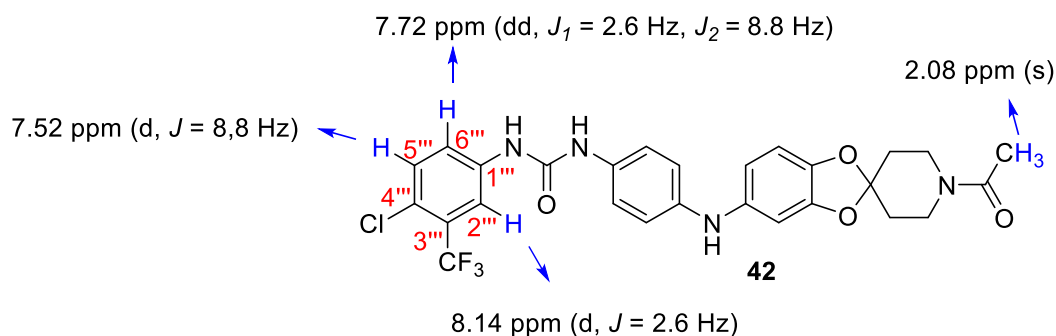
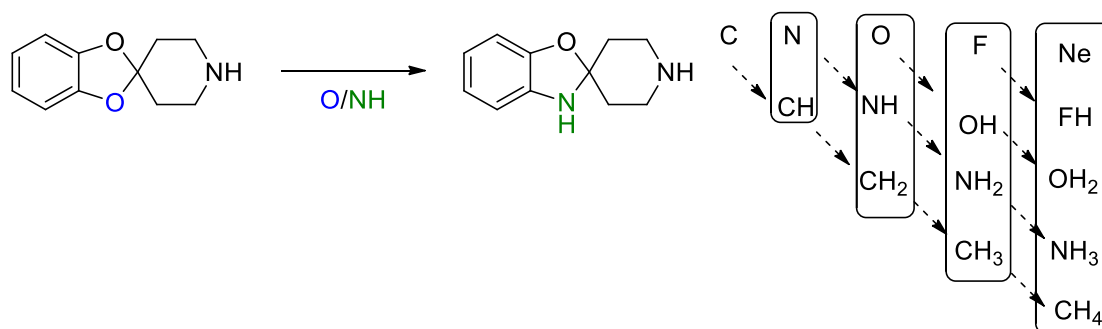


Figure 51. <sup>1</sup>H-NMR spectroscopy data of compound **42**

### 3.1.1.16. Preparation of 1'-acetyl-1-(3H-spiro[benzoxazole-2,4'-piperidine]) (**43**) and 1',3,6-triacetyl-1-(spiro[benzoxazole-2,4'-piperidine]) (**44**)

The system spiro[benzoxazole-2,4'-piperidine] is not found described in the bibliography. This nucleus is considered a bioisostere of the spiro[benzodioxole-2,4'-piperidine] nucleus, previously commented in this memory, regarding the Grimm's hydride displacement law (Scheme 71).

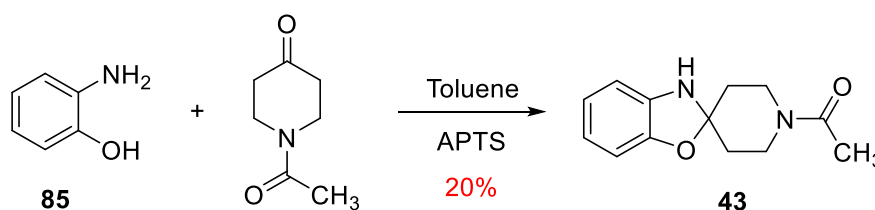
The addition of hydrogen atom to an atom of atomic number "n" gives as a result a specie with the same properties than the atom with a superior atomic number n+1.<sup>174</sup>



Scheme 71

The condensation of aminoalcohols with aldehydes or ketones in acidic media and elimination of the produced water is proposed for the preparation of 1,3-benzoxazoles.<sup>175</sup>

In this work, it was carried out the condensation of 2-aminophenol (**85**) with 4-piperidone in toluene and in presence of APTS as a catalyst. In the reaction system the crystal device of Dean-Stark was introduced to facilitate the elimination of water (Scheme 72).

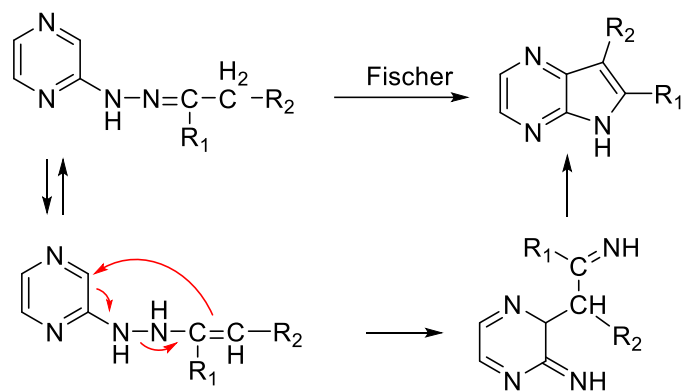


Scheme 72

<sup>174</sup> H. G. Grimm. *Electrochem.* **1925**, *31*, 474-480

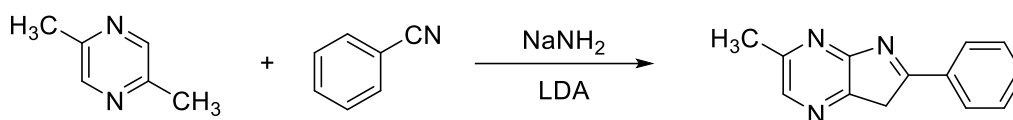
<sup>175</sup> A. I. Moskalenko; V. I. Boev. *Russ. J. Org. Chem.* **2009**, *45*, 1018-1023





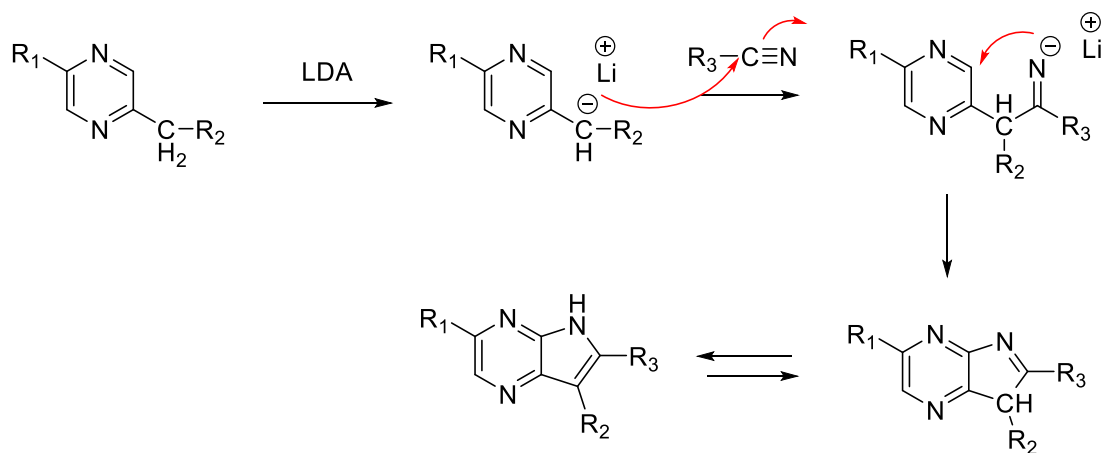
Scheme 75

Another described method<sup>177</sup> to prepare the pyrrole[2,3-*b*]pyrazines implies the addition of alkylpyrazines to nitriles using basic media (Scheme 76).



Scheme 76

Next, a mechanism to explain the previous reaction is proposed (Scheme 77):



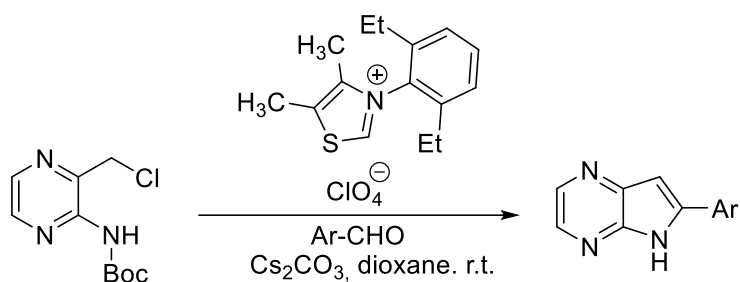
Scheme 77

The LDA takes a proton of the benzylic position and the resultant anion was added to the nitrile derivative. Next, the formed imine was added at position 3 of pyrazine ring.

Scheidt and col.<sup>178</sup> describe the synthesis of indole derivatives and pyrrolepyrazines starting from 2-(2-chloromethyl)-3-aminopyrazines, aromatic aldehydes in basic media and using as a catalyst compounds containing heavy metals (Scheme 78).

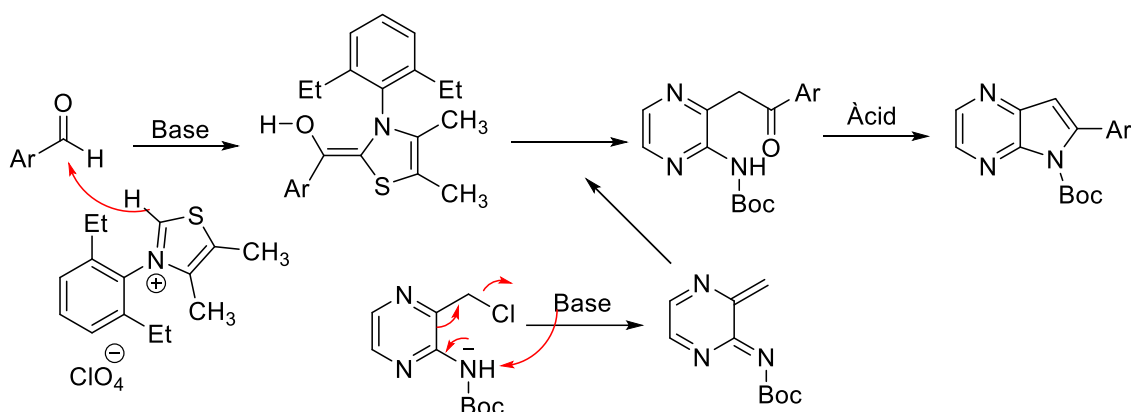
<sup>177</sup> J. M. Vierfond; Y. Mettey; L. Mascrier-Demagny; M. Miocque. *Tetrahedron Lett.* **1981**, 22, 1219-1222

<sup>178</sup> H. A. Sharma; M. T. Hovey; K. A. Scheidt. *Chem. Comm.* **2016**, 52, 9283-9286



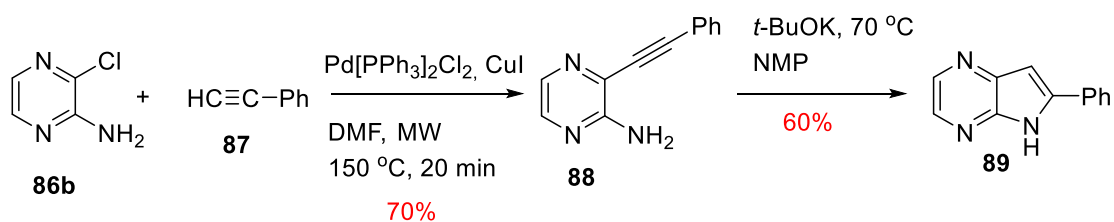
Scheme 78

The authors of this work afford as possible reaction mechanism the detailed below in the scheme 79.



Scheme 79

In 2004, Hopkins and col. describe the use of Sonogoshira reaction to prepare pyrrole[2,3-*b*]pyrazines.<sup>179</sup> Starting from 2-amino-3-chloropyrazine, to which phenylacetylene is added and using CuI and Pd[(PPh<sub>3</sub>)<sub>2</sub>]Cl<sub>2</sub> as a catalyst in DMF, leads to the alkyne intermediate. Later, the addition of *t*-BuOK heating at 70 °C allows to access to the expected pyrrole[2,3-*b*]pyrazine in 42% global yield (Scheme 80).

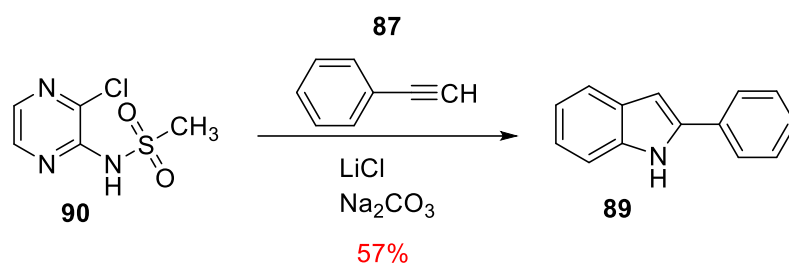


Scheme 80

The same authors reported<sup>179</sup> on other procedure to prepare the pyrrolepyrazine in only one step, starting from the 3-chloro-2-methylsulfonamidepyrazine, using for the cross-coupling reaction and the following cyclization Pd(dppf)Cl<sub>2</sub> as a catalyst and Na<sub>2</sub>CO<sub>3</sub> as a base (Scheme 81).

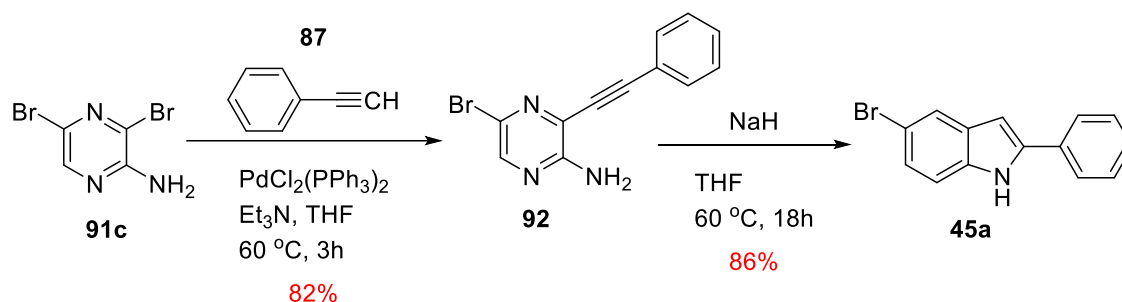
<sup>179</sup> C. R. Hopkins; N. Collar. *Tetrahedron Lett.* **2004**, *45*, 8631-8633





Scheme 81

Whittaker and col.<sup>180</sup> indicate a procedure that implies to use the Sonogoshira reaction conditions followed by intramolecular cyclization of an alkyne intermediate, as in the previous case, but in this work it starts from 2-amino-3,5-dibromopyrazine (Scheme 82).

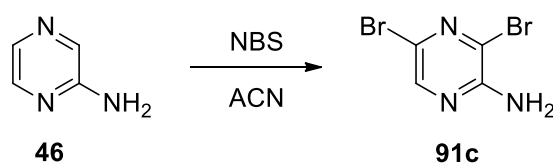


Scheme 82

In this work, the synthesis of **45a** starting from 2-amino-3,5-dibromopyrazine (**91c**) applying similar conditions of the mentioned work from Whittaker was carried out.<sup>180</sup>

### 3.1.2.1. Preparation of 2-amino-3,5-dibromopyrazine (**91c**)

The treatment of 2-aminopyrazine, commercially available, with an excess of NBS (*N*-bromosuccinimide) leads to dibrominated pyrazine **91c** (Scheme 83).



Scheme 83

Previous studies, indicate different methods to halogenate the 2-aminopyrazine collected in Table 9.

<sup>180</sup> I. Simpson; S. A. St-Gallay; S. Stokes; D. T. E. Whittaker; R. Wiewiora. *Tetrahedron Lett.* **2015**, *56*, 1492-1495

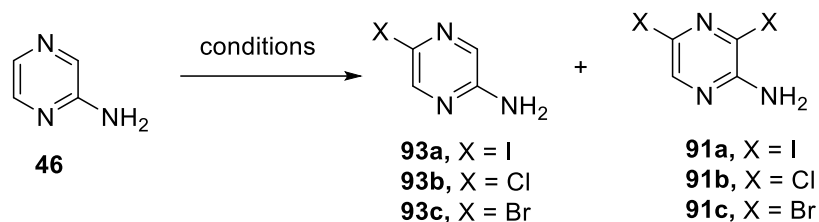


**Table 9.** Halogenation of 2-aminopyrazine. Bibliographic data

ENTRY	CONDITIONS	93 (YIELD %)	91 (YIELD %)	REFERENCES
1	NBS, DMF 0 °C, overnight	88		181
2	NIS, DMF 28 °C, overnight	61		181
3	NBS, CH <sub>2</sub> Cl <sub>2</sub> , r.t. 4 h	50		182
4	NBS, CH <sub>2</sub> Cl <sub>2</sub> , r.t. 1.5 h	52		183
5	DBH, DMF-MeCN, r.t. 0.5 h	65		184
6 <sup>a</sup>	Br <sub>2</sub> /HBr/H <sub>2</sub> O 5 °C		82	185
7	Br <sub>2</sub> , Piridina, CHCl <sub>3</sub> , r.t.		36	186
8	NBS, CH <sub>2</sub> Cl <sub>2</sub>		63	187
9	NBS, DMSO-H <sub>2</sub> O, 15 °C, 6 h		85	188
10	NBS, DMSO-H <sub>2</sub> O, 15 °C, 16 h		77	189
11	NBS, DMSO-H <sub>2</sub> O, r.t. 6 h		90	190

a) From 2-amino-3-bromopyrazine

In our research group, the halogenation conditions of 2-aminopyrazine (**46**) were studied in detail with the intention to optimize the yields of the reaction. The obtained conditions and results are reviewed on Table 10.<sup>191</sup> It is necessary to highlight that it can be obtained in a regioselective manner the compound **93**, the dihalogenated **91** or a mixture of both.

<sup>181</sup> C. M. Chou; Y. W. Tung; M. I. Ling; D. Chan; W. Phakhodee; M. Isobe. *Heterocycles* **2012**, *86*, 1323-1329

<sup>182</sup> Y. Younis; F. Douelle; D. González-Cabrera; C. Le Manach; A. T. Nchinda; T. Paquet; L. Street; K. L. White; M. Zabiulla; J. T. Joseph; S. Bashyam; D. Waterson; M. J. Witty; S. Wittlin; S. A. Charman; K. J. Chibale. *Med. Chem.* **2013**, *56*, 8860-8871

<sup>183</sup> C. Le Manach; A. T. Nchinda; T. Paquet; D. González-Cabrera; Y. Younis; Z. Han; S. Bashyam; M. Zabiulla; D. Taylor; N. Lawrence; K. L. White; S. A. Charman; D. Waterson; M. J. Witty; S. Wittlin; M. E. Botha; S. H. Nondaba; J. Reader; L. M. Birkholtz; M. B. Jiménez-Díaz; M. Santos-Martínez; S. Ferrer; I. Angulo-Barturen; S. Meister; Y. Antonova-Koch; E. A. Winzeler; L. Street; J. K. Chibale. *J. Med. Chem.* **2016**, *59*, 9890-9905

<sup>184</sup> T. Itho; S. Kato; N. Nonoyama; T. Wada; K. Maeda; T. Mase; M. M. Zhao; J. Z. Song; D. M. Tschaen; J. M. McNamara. *Org. Process Res. Dev.* **2006**, *10*, 822

<sup>185</sup> H. J. Brachwitz. *Prakt. Chem.* **1969**, *311*, 40

<sup>186</sup> S. Martínez-González; A. I. Hernández; C. Varela; S. Rodríguez- Arístegui; J. Pastor. *Bioorg. Med. Chem. Lett.* **2012**, *22*, 1874-1878

<sup>187</sup> P. J. Zimmermann; C. Brehm; W. Buhr; A. M. Palmer; W. A. Simon. *Bioorg. Med. Chem.* **2008**, *16*, 536-541

<sup>188</sup> B. Jiang; C. G. Yang; W. N. Xiong; J. Wang. *Bioorg. Med. Chem.* **2001**, *9*, 1149-1154

<sup>189</sup> J. J. Caldwell; N. Veillard; I. Collins. *Tetrahedron* **2012**, *68*, 9713-9728

<sup>190</sup> R. Goel; V. Luxami; K. Paul. *R.S.C. Adv.* **2014**, *4*, 9885-9892

<sup>191</sup> E. Lizano; J. Grima; M. D. Pujol. *Synlett* **2019**, *30*, 2000-2003

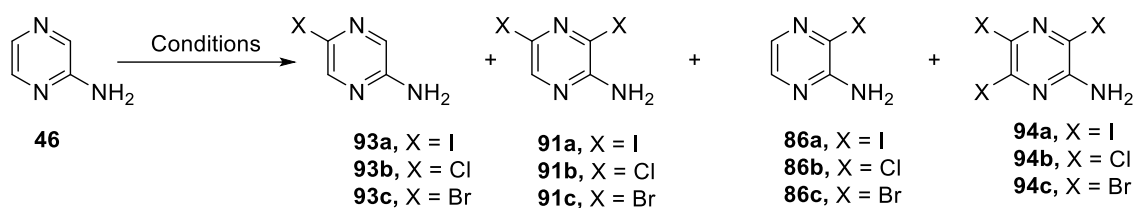


**Table 10.** Halogenation of 2-aminopyrazine. Experimental data

ENTRY	CONDITIONS	X	93 (%)	91 (%)	86 (%)	94 (%)
1	NIS (3 eq), ACN, 100 °C, 20 h	I	9	-	-	-
2	NIS (3 eq), ACN, r.t., 3 h	I	11	-	-	-
3	NIS (1.1 eq), ACN, r.t., 6 h	I	14	28	-	-
4	NIS (1.1 eq), MeOH, r.t., 3 h	I	13	-	-	-
5	NIS (1.1 eq), MeOH, 100 °C, 3 h	I	34	-	-	-
6	NIS (1.1 eq), DMF, r.t., 3 h	I	25	-	-	-
7	NIS (1.1 eq), DMF, 100 °C, 3 h	I	22	-	-	-
8	NIS (1.1 eq), DMF, -30 °C, 3 h	I	15	-	-	-
9	I <sub>2</sub> (1.1 eq), LDA (1.5 eq), THF, -78 °C, 3 h	I	39	-	-	-
10	NCS (2.2 eq), ACN, r.t., 72 h	Cl	-	12	-	14
11	NCS (1.1 eq), ACN, 100 °C, 3 h	Cl	57	13	17	-
12	NCS (1.1 eq), ACN, r.t. 3 h	Cl	89	-	-	-
13	NBS (3 eq), ACN, r.t., 3 h	Br	-	38	-	-
14	NBS (1.1 eq), ACN, 100 °C, 6 h	Br	22	11	-	-
15	NBS (1.1 eq), ACN, r.t., 3 h	Br	89	-	-	-
16	NBS (1.1 eq), ACN, MW, 5 min	Br	88	6	-	-
17	NBS (2.2 eq), ACN, MW, 5 min	Br	-	98	-	-
18 <sup>a</sup>	NBS (2.2 eq), MeOH, r.t., 3 h	Br	-	78	-	-
19	NBS (1.1eq), MeOH, r.t., 3 h	Br	26	19	-	-
20	NBS (1.1 eq), MeOH, 100 °C, 3 h	Br	28	25	-	-
21	NBS (1.1 eq), DMF, MW, 100 °C, 1 h	Br	5	15	-	-
22	NBS (1.1 eq), CuBr, ACN, r.t., 3 h	Br	41	-	-	-
23	NBS (1.1 eq), AIBN, CCl <sub>4</sub> , hv, 3 h	Br	46	-	9	-
24	NBS (2.2 eq.), DMSO, H <sub>2</sub> O, 0 °C to r.t., 16 h <sup>189</sup>	Br	-	48	-	-
				(77) <sup>189</sup>		
25	Bromodioxà (1.1 eq), Dioxane, 0 °C to r.t., 3 h	Br	-	6	-	-
26	Bromodioxà (0.5 eq), Dioxane, 0 °C to r.t., 3 h	Br	32	-	5	-
27	Bromodioxà (1 eq), Dioxane, 100 °C, 30 min	Br	48	-	6	-

a) From 2-amino-5-bromopyrazine

The treatment of aminopyrazine **46** with NIS leads to the mono-iodinated product, but in yields below 35%. Only when the time of the reaction was elongated from 3 to 6 hours, it was possible to isolate in addition of the mono-reaction, the dihalogenated derivative in 28% yield, practically double than the mono-reaction product, which was obtained in 14% (entry 3, Table 10).

The use of molecular iodine instead of NIS, leads in a regioselective manner to the mono-halogenated product in 39% yield (entry 9, Table 10).

The treatment of **46** with NCS (*N*-chlorosuccinimide) at room temperature for 3 hours, leads to mono-chlorinated pyrazine **93b** in 57% yield, together with the dihalogenated product **91b** (13%) and the derivative selectively halogenated in C-3 **86b** (17%) (entry 11, Table 10).

The halogenation reaction with an excess of NCS (2.2 eq) leads to the dihalogenated product **91b** (12%) along with the trihalogenated derivative **94b** (14%) (entry 10, Table 10).

These unsatisfying results bring us to consider the bromination of aminopyrazines, thus the treatment of **46** with NBS, in acetonitrile, leads to different products depending on the applied conditions in each assay. With an excess of NBS (3 eq) it obtains selectively the dihalogenated **91c** in 38% yield (entry 13, Table 10).

Diminishing the quantity of NBS at 1.1 eq and heating to 100 °C for 6 hours, it obtains a mixture of **93c** and **91c** in 22 and 11% yields respectively (entry 14, Table 10).

When these mentioned conditions are applied but the crude of reaction stirs at room temperature for 3 hours, it obtains exclusively **93c** in 89% yield (entry 15, Table 10).

The application of assistance by microwave irradiation leads to **93c** (88% yield) and **91c** (6% yield), using 1.1 eq of NBS (entry 16, Table 10), while when NBS quantities are increased double, it achieves the preparation of **91c** in 98% yield (entry 17, Table 10). These results are obtained after heating for 5 minutes the crude of reaction at 100 °C.

It must be indicated, that the assistance by microwave irradiation allows to reduce considerably the time of reaction and also it achieves a notably improvement in the outcomes.<sup>192</sup>

When instead of acetonitrile, methanol is used as a solvent and 1.1 eq of NBS at room temperature or heating at 100 °C, it obtains a mixture of mono-brominated and dibrominated compounds **93c** and **91c** in yields of the same order (entry 19 and 20, Table 10). However, when it works at room temperature but adding double quantity of halogenating agent (NBS), it obtains selectively the dihalogenated derivative **91c** in 78% yield (entry 18, Table 10). Other solvents as DMF (entry 21, Table 10) lead to a mixture of **91c** and **93c** in low yields.

The addition of a catalyst as CuBr (entry 22, Table 10) leads to mono-brominated pyrazine **91c** in 41% yield. The application of radical conditions in this reaction, using NBS as halogenating agent, AIBN as radical indicator in carbon tetrachloride, keeping the reaction system under radiation of a 100 W lamp, drives to mono-brominated derivative **93c** (46%) in yields slightly higher regarding the previous mentioned conditions. Along with it, it obtains derivative **86c** brominated at position 3 (entry 23, Table 10).

---

<sup>192</sup> a) D. Bogdal; M. Lukasiewicz; A. Pielichowski; A. Miciak; Sz. Bednarz. *Tetrahedron* **2003**, *59*, 649-653 b) E. Buxaderas; D. A. Alonso; C. Nájera. *Eur. J. Org. Chem.* **2013**, 5864-5870 c) G. Broggini; V. Barbera; E. M. Beccalli; U. Chiacchio; A. Fasana; S. Galli; S. Gazzola. *Adv. Synth. Catal.* **2013**, *355*, 1640-1648 d) H. H. Nguyen; M. J. Kurth. *Org. Lett.* **2013**, *15*, 362-365 e) W. Qian; L. Zhang; H. Sun; H. Jiang; H. Liu. *Adv. Synth. Catal.* **2012**, *354*, 3231-3236 f) M. Baghbanzadeh; C. Pilger; C. O. Kappe. *J. Org. Chem.* **2011**, *76*, 8138-8142 g) J. F. Cívicos; D. A. Alonso; C. Nájera. *Adv. Synth. Catal.* **2011**, *353*, 1683-1687 h) E. M. Beccalli; A. Bernasconi; E. Borsini; G. Broggini; M. Rigamonti; G. Zecchi. *J. Org. Chem.* **2010**, *75*, 6923-6932 i) D. Liptrot; G. Alcaraz; B. Roberts. *Adv. Synth. Catal.* **2010**, *352*, 2183-2188

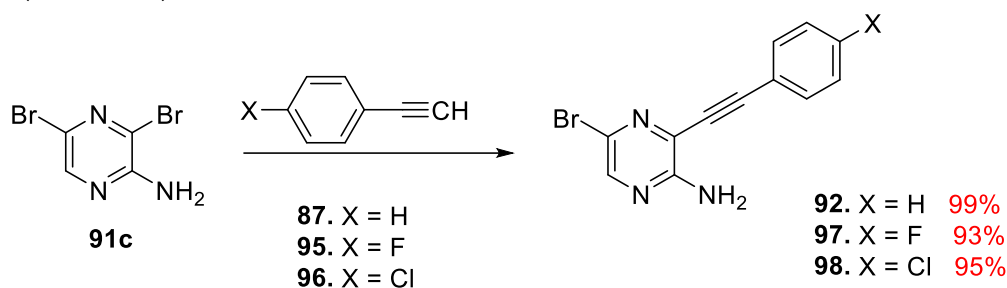
It is of interest the halogenation of 2-aminopyrazine **46** using NBS and DMSO-H<sub>2</sub>O as a solvent, which are the most described conditions in the literature for the obtention of 3,5-dihalogenated pyrazine, which is obtained in 48% yield (entry 24, Table 10).

The reaction was assayed several times but it was not possible to achieve the described yield of 77%.<sup>189</sup>

Also, in this work, the halogenation of 2-aminopyrazine **46** was assayed, using bromodioxane as halogenating agent. The best results, of this reaction, were obtained by heating to 100 °C for 30 minutes the mixture of reaction, which contains 2-aminopyrazine and bromodioxane (1 eq) (entry 25, 26 and 27, Table 10).

### 3.1.2.2. Preparation of pyrrole[2,3-b]pyrazine

The alkylation of 2-amino-3,5-dibromopyrazine (**91c**) with phenylacetylene, was achieved with success using the conditions of Sonogoshira reaction catalyzed by palladium complexes in basic media (Scheme 84).

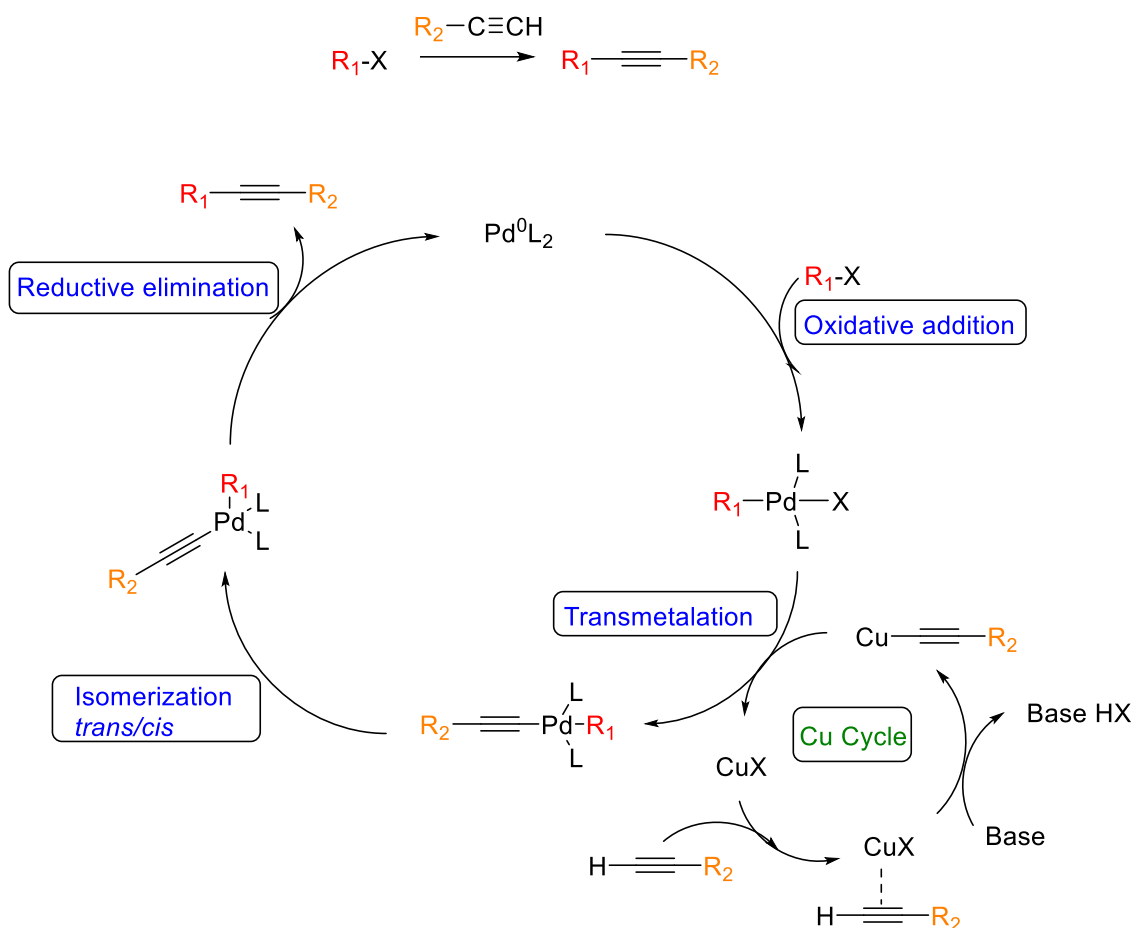


Scheme 84

The Sonogoshira reaction is based in a cross-coupling reaction between bromoaryl and alkyne, allowing the formation of C-C bonds, with high utility for the formation of aromatic systems with potential industrial application.<sup>193</sup> This reaction was presented by K. Sonogoshira and N. Hagihara in 1975.<sup>194</sup> The advantage lies on the fact that the cross-coupling is produced in softly conditions, using palladium as a catalyst, CuI as a co-catalyst and an organic salt as triethylamine, which in most cases acts as a solvent as well. The mechanism of this reaction can be represented through the cycle of cross-coupling reaction catalyzed by palladium complex (Scheme 85).

<sup>193</sup> a) M. Bakherad. *Appl. Organomet. Chem.* **2013**, 27, 125-140 b) C. Torborg; M. Beller. *Adv. Synth. Catal.* **2009**, 351, 3027-3043 c) J. W. B. Cooke; R. Bright; M. J. Coleman; K. P. Jenkins. *Org. Process Res. Dev.* **2001**, 5, 383-386

<sup>194</sup> K. Sonogoshira; Y. Tohda; N. Hagihara. *Tetrahedron Lett.* **1975**, 16, 4467-4470



Scheme 85

This mechanism is sustained by the following points:

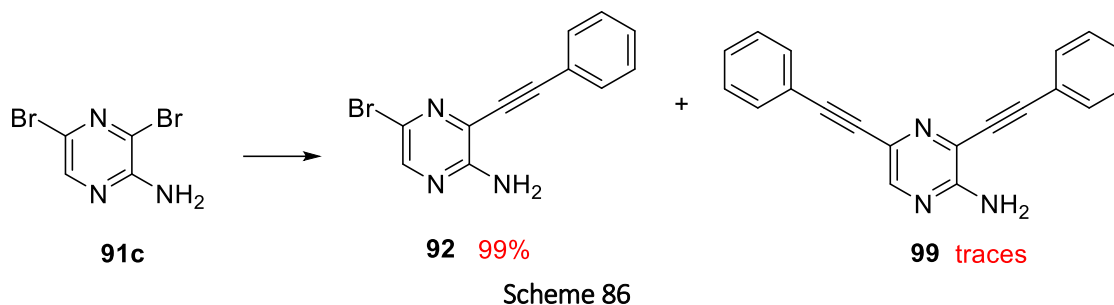
- Pd (II) is reduced to Pd (0) when it loses the two substituents, in this case the chlorides.
- The oxidative addition of the halogenated aryl to the palladium complex (changing to Pd (II)).
- The transmetalation allows the exchange and the salt generation. The copper acetylide fixes into the palladium, with release of the corresponding halogenated copper.
- An isomerization *trans-cis* occurs, making to change the configuration of the ligands from *trans* to *cis*.
- Finally, the *cis* complex through reductive elimination allow to form the C-C bond and release the Pd, which changes again from Pd (II) to Pd (0).

Regarding the cycle corresponding to the catalysis of the copper salt (CuI) it is reviewed in the following points:

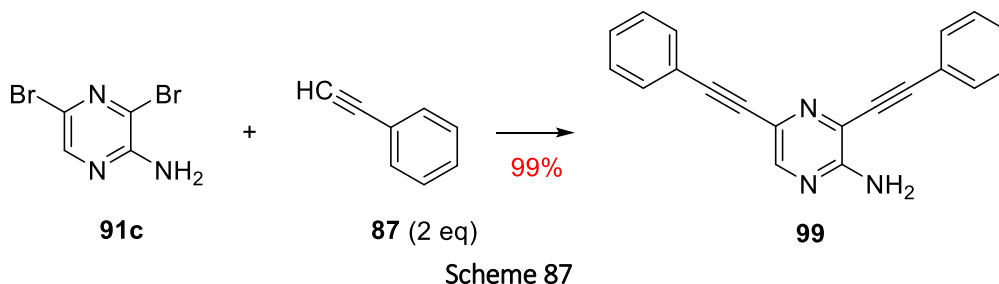
- The alkyne makes a complex with CuI of M-alkyne type, that makes more labile the proton of the acetylene and therefore more reactive.
- The produced copper acetylide reacts with the palladium (II) complex and in that way it is possible the regeneration of the Cu.

In this work, the Sonogoshira reaction allows to obtain in excellent yields compounds **92**, **97** and **98** (Scheme 85). The best conditions found, setting up this reaction, in this work, allow us to obtain good results without using copper salt (CuI) as a co-catalyst.

It must be noted the formation of mono-alkylized and the one coming from the di-alkylation in lower proportion, due to the coupling reaction between the acetylene and the halogenated positions 3 and 5 under the tested conditions (Scheme 86).

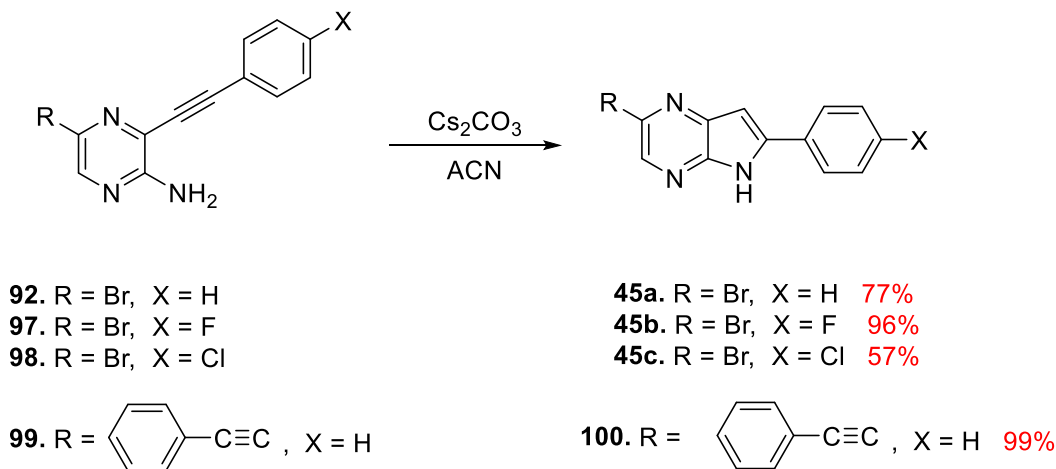


The formation of **99** is minimized by the use of quantities below 1 eq of the corresponding phenylacetylene, obtaining in a regioselective manner the alkylation of position 3 of the pyrazine nucleus. While the use of excess of phenylacetylene leads to the product **99** (Scheme 87).



The derivative **99** results of interest for the formation of new aromatic systems coming from cyclo-additions that will be studied in detail in another work of our research group. Also, it opens the possibility to apply the formation of heterocyclic systems through click-chemistry reactions (click chemistry).<sup>195</sup>

The cyclization of the alkyne derivatives leads to the pyrrole[2,3-*b*]pyrazines (Scheme 88).

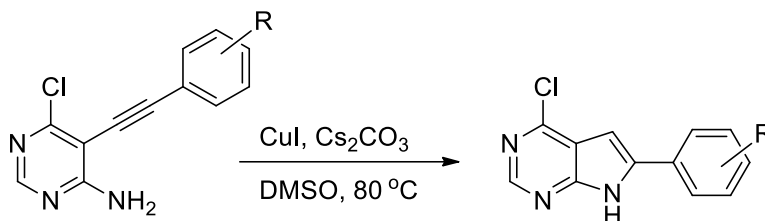


**Scheme 88**

<sup>195</sup> H. C. Kolb; M. G. Finn; K. B. Sharpless. *Angew. Chemie Int. Ed.* **2001**, *40*, 2004-2021

The cyclization of alkynes derivatives **92**, **97-99** to the corresponding **45a-c** and **100** was carried out by treatment of the starting alkynes with Cs<sub>2</sub>CO<sub>3</sub> in acetonitrile.

The cesium carbonate presents better solubility in organic solvents than sodium or potassium carbonate.<sup>196</sup> In similar products to pyrazines, as pyrimidines or pyridinic derivatives, the cyclization is carried out in basic media and using CuI as a catalyst, affording interesting results. (Scheme 89).<sup>197</sup>



In this work, it is not used CuI as a catalyst, only the presence of a base as cesium carbonate at reflux of acetonitrile.

This is a 5-endo-dig cyclisation following the Baldwin rules. The amino group is added to the alkyne without expulsion of any leaving group (endo) and thus, affords a 5 atoms ring<sup>198</sup> and because it is an addition to an alkyne (Sp) it is called dig (diagonal) (Figure 52).

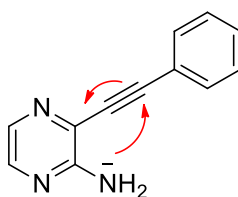


Figure 52. Cyclization 5-endo-dig

The emergence of two singlets in the <sup>1</sup>H-NMR at 6.81 and at 7.93 ppm corresponding to the protons of positions 7 and 3 respectively, confirms the proposed structure for pyrrole[2,3-*b*]pyrazines (Figure 53).

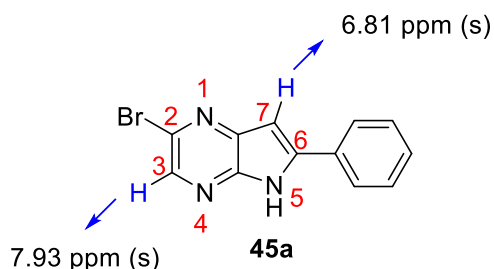


Figure 53. <sup>1</sup>H-NMR spectroscopy data of compound **45a**

### 3.1.2.3. Preparation of derivatives 2,6-diphenyl-5H-pyrrole[2,3-*b*]pyrazines **47-52**

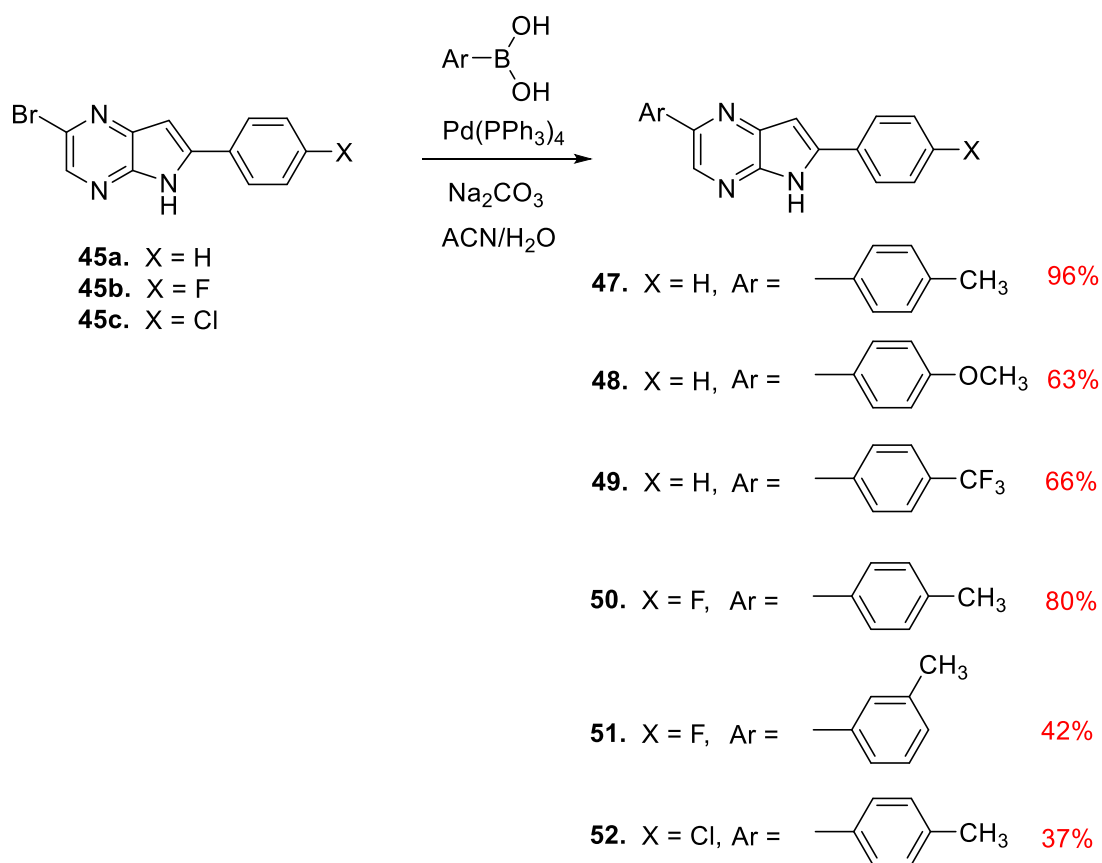
The arylation of derivatives 2-bromopyrrolepyrazines was carried out by reaction of bromo-derivatives with the corresponding boronic acids (Scheme 90).

<sup>196</sup> R. Gujadhur; D. Ven Katarama; J. T. Kintight. *Tetrahedron Lett.* **2001**, 42, 4791-4793

<sup>197</sup> Z. Li; L. Hong; R. Lui; J. Shen; X. Zhou. *Tetrahedron Lett.* **2011**, 52, 1343-1347

<sup>198</sup> J. E. Baldwin *J. Chem. Soc. Chem. Commun.* **1976**, 18, 734-736





Scheme 90

For this cross-coupling reaction it is required the Suzuki-Miyaura conditions, previously mentioned in this work (page 44).

Thus, the pyrrole[2,3-*b*]pyrazines **47-52** are obtained in yields from acceptable to excellent (from 37% to 96%) (Scheme 90).

The proposed structure for this pyrrolepyrazines was confirmed by the presence of  $^1\text{H-NMR}$  signals as the singlets at 7.00 ppm and at 8.50 ppm attributable to the protons of positions C-7 and C-3 respectively for **47** (Figure 54). Also, the presence of doublets at 7.27 and at 7.81 ppm corresponding to the protons of positions C-3'', C-5'' and C-2'', C-6'' respectively, showed the incorporation of the methylphenyl group at position 2 (Figure 54).

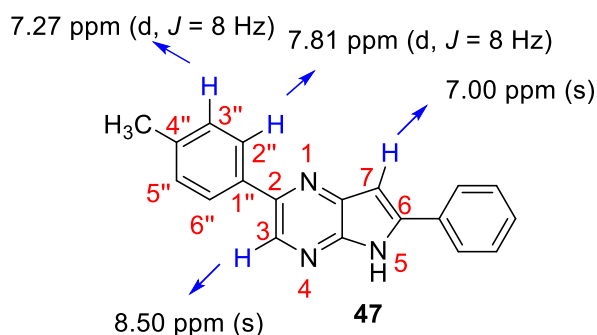
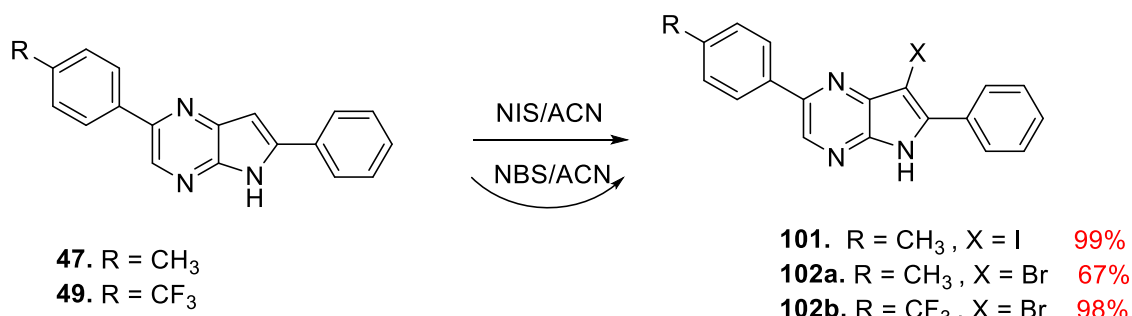


Figure 54.  $^1\text{H-NMR}$  spectroscopy data of compound **47**

### 3.1.2.4. Preparation of arylated derivatives at positions C-3 and C-7

On the first moment, it was carried out the halogenation at the C-7 position of pyrrole[2,3-*b*]pyrazines system through SEAr conditions, using NIS (*N*-iodosuccinimide) or NBS (*N*-bromosuccinimide) (Scheme 91).



Scheme 91

In both cases, it is obtained the corresponding halogenated derivative, in quantitative yields in the case of the iodinated derivative **101**, 67% for the bromo derivative **102a** and 98% for **102b**.

Emphasize that in one of these bromination reactions with NBS it was possible to isolate the 3,7-dibrominated derivative (**103**) (9% yield) from the crude of reaction.

In this case, the absence of signals in the <sup>1</sup>H-NMR spectrum corresponding to the protons of positions C-3 and C-7 indicates the reaction of the heterocyclic system by these positions. The data from mass spectroscopy (ESI +) with a molecular pic found at 443.9490 g/mol (theoretical: 443.9489 g/mol, 442.9456 g/mol, 440.9476 g/mol) allows to confirm the presence of two bromo atoms in the indicated positions (Figure 55).

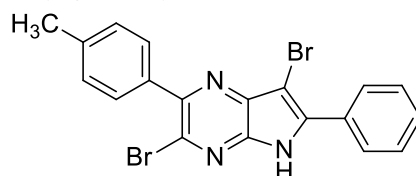
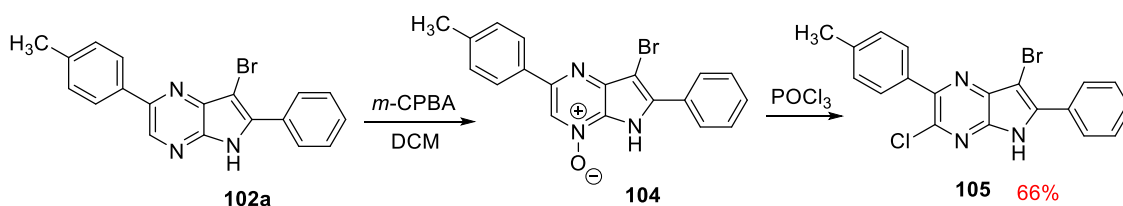


Figure 55. Structure of **103**

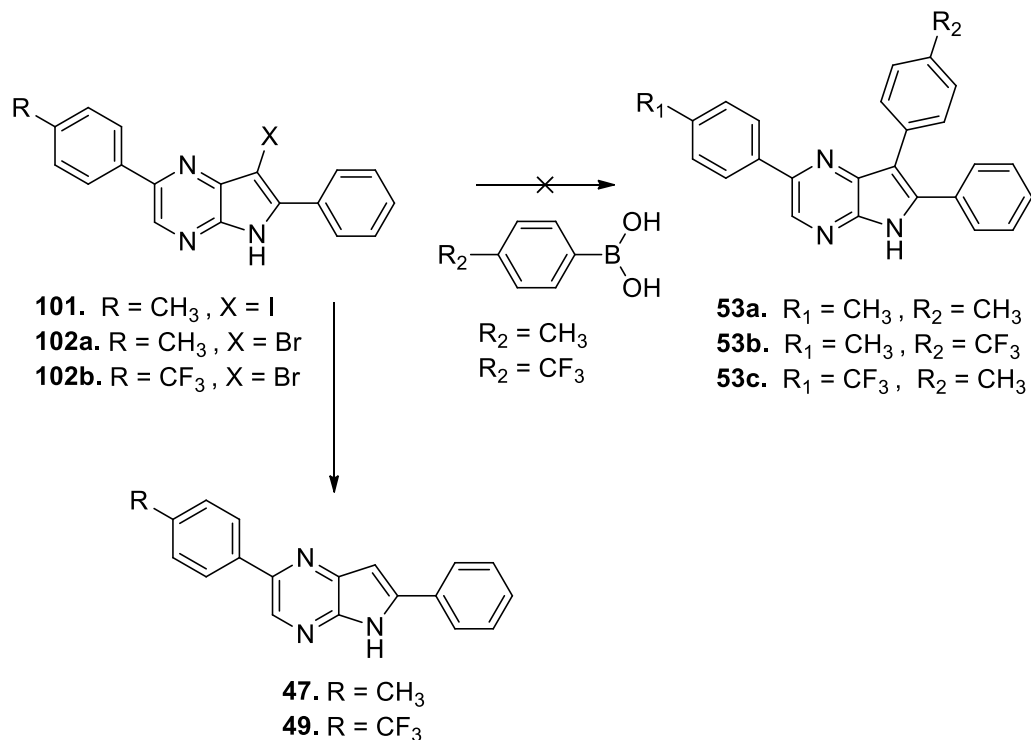
Other assays were carried out to obtain the halogenation at C-3 starting from the mono-halogenated **102**, treating it with an excess of NBS and even with other halogenating agents, but it was not possible to obtain big quantities of the expected dibrominated **103**.

Highlight the treatment of **102**, with *m*-CPBA in DMF, in first instance, to oxidize the nitrogen atom of the pyrazine and then halogenation at C-3 position. This treatment leads in good yields to the corresponding *N*-oxide and then the phosphoryl chloride is added allowing to obtain the chlorinated derivative **105** in 66% yield (Scheme 92).



Scheme 92

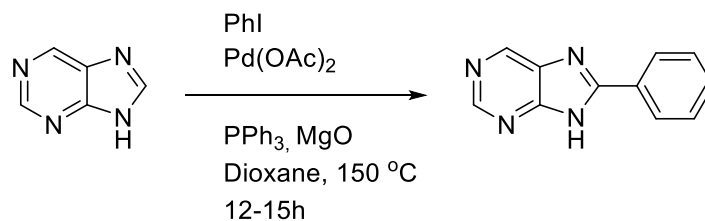
Then, the treatment separately of **101**, **102a** and **102b** with the corresponding boronic acid under Suzuki Miyaura conditions does not lead to the expected triarylated derivatives. In its place was found the compound coming from the C-7 dehalogenation (Scheme 93).



Scheme 93

It looks like the cause of this lack of reactivity is due to the presence of the free NH function (pyrrolopyrazines) and therefore it must interfere with the cross-coupling reaction, mostly for the interactions with the used catalyst. In the bibliography, there is no constancy of arylation reactions in the indole ring of heterocyclic nitrogenated systems with free NH.

Just indicate that Sames and col. that in the beginning published the functionalization at C-5 of purines and derivatives with free NH,<sup>199</sup> then, they ended disproving this reactivity in the indicate position of the indole ring<sup>200</sup>(Scheme 94).

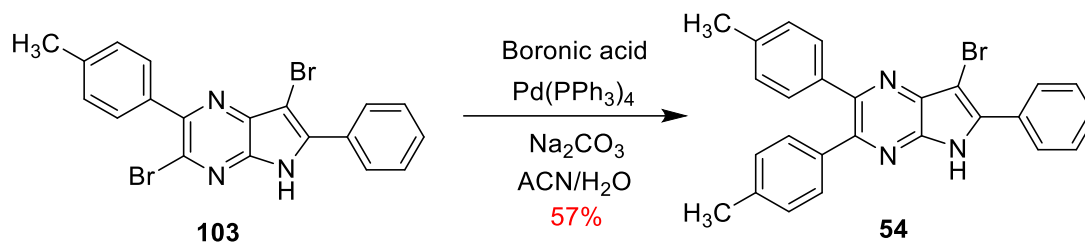


Scheme 94

Back to this work, it was possible the arylation of position 3 of pyrrolepyrazine system, that is, the arylation of the pyrazine ring, as indicated below, under the Suzuki-Miyaura conditions between derivative **103** and *p*-methylboronic acid (Scheme 95).

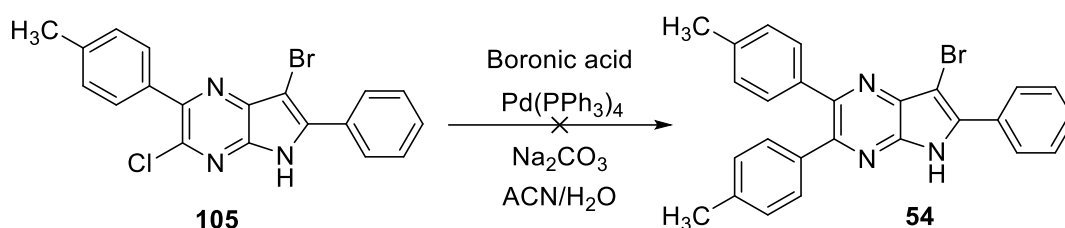
<sup>199</sup> B. Sezen; D. Sames. *J. Am. Chem. Soc.* **2003**, *125*, 5274-5275

<sup>200</sup> M. Tian; D. Sames. *J. Am. Chem. Soc.* **2006**, *128*, 8364-8364



Scheme 95

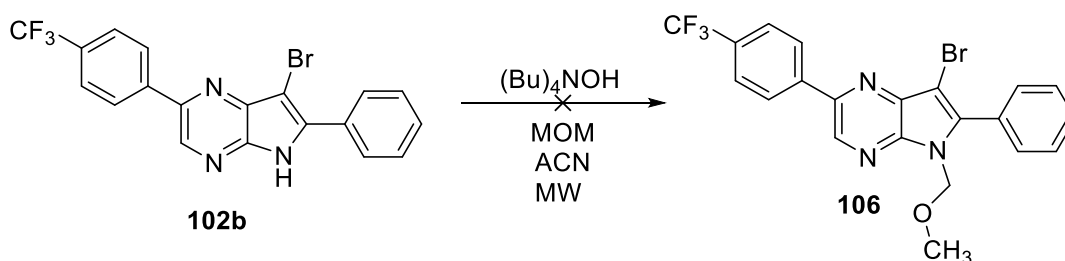
Thus, the triarylated derivative **54** was obtained in 57% yield of purified product. While the cross-coupling reaction between the chloride derivative **105** with *p*-methylboronic acid, under the same conditions of Suzuki-Miyaura previously applied, do not lead to the expected pyrrolopyrazine and the starting material was recovered (Scheme 96).



Scheme 96

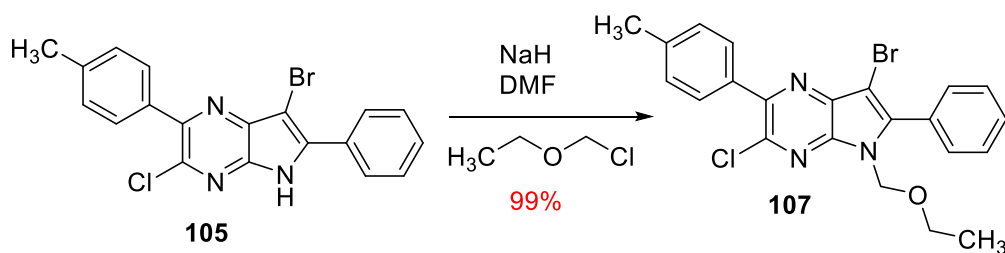
### 3.1.2.5. Protection of pyrrole NH, arylation of pyrrole[2,3-*b*]pyrazines

The last results drive us to consider the possibility to protect the pyrrole-NH. First of all, the protection of **102b** with methoxymethyl chloride (MOMCl), in basic media was tried, but even assaying different conditions, in any case it was possible to obtain the expected compound **106** (Scheme 97).



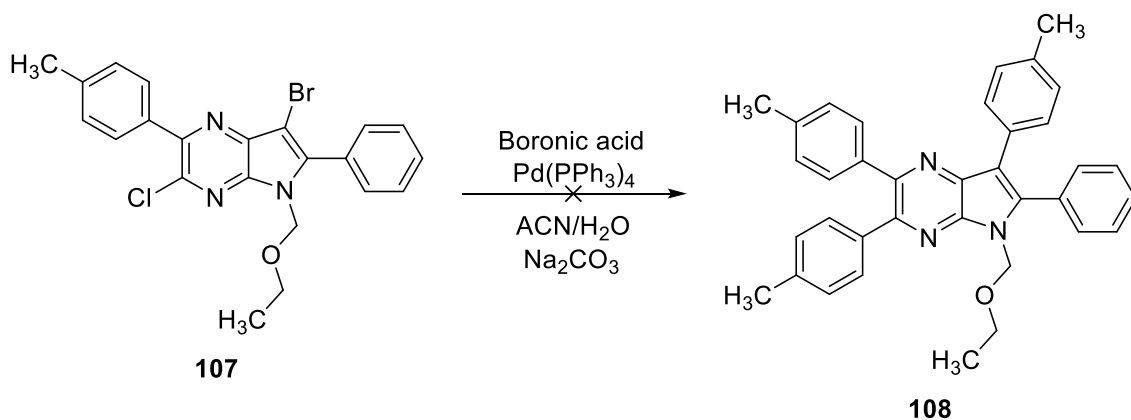
Scheme 97

The pyrrolepyrazine **105** was protected through the use of ethoxymethyl chloride instead of MOM, under the classic conditions of alkylation and the **107** was obtained in quantitative yield (Scheme 98).



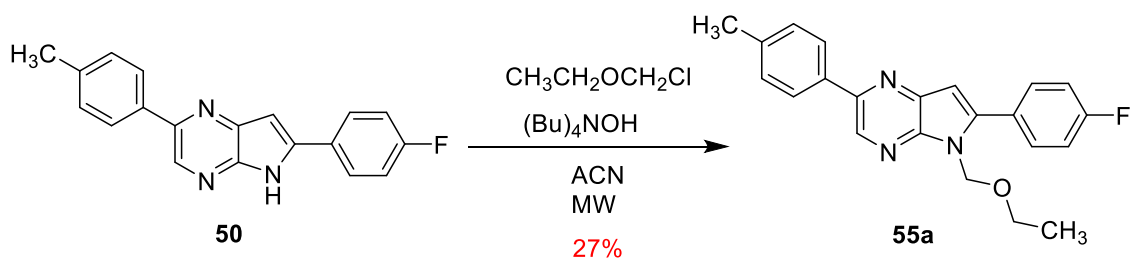
Scheme 98

Once the product with protected NH (**107**) was obtained it was treated with *p*-tolylboronic acid under the Suzuki-Miyaura conditions in order to carry out the cross-coupling reaction between both reagents. But in the assayed conditions the starting material **107** was recovered without reaction of any of both halogens present in the structure (Scheme 99).



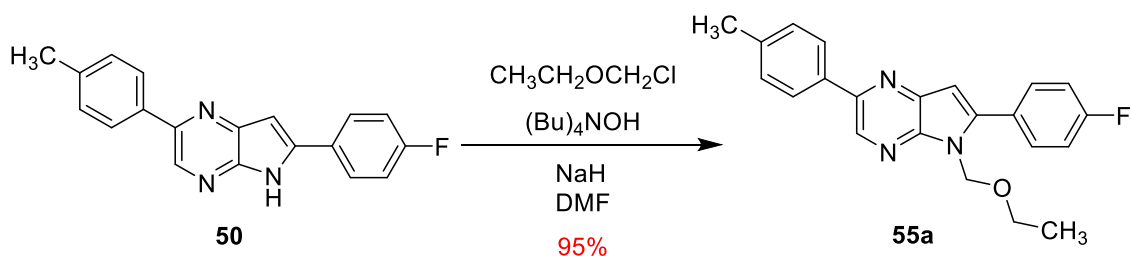
Scheme 99

These results lead us to consider the protection of the non-halogenated derivative in any of the two positions C-3 and C-7. Thus, it was carried out the protection of **50** with ethoxymethyl chloride, in presence of tetrabutylammonium and under microwave irradiation (Scheme 100). Obtaining under these conditions the protected derivative **55a** in 27% yield.



Scheme 100

In order to optimize this procedure, the last reaction was carried out with classic heating, without assistance of microwave irradiation. In addition, the solvent was changed, acetonitrile instead of DMF, and the addition of a stronger base, as NaH was considered. Thus, the expected product was obtained in 95% yield (Scheme 101).



Scheme 101

Among the signals in the  $^1\text{H-NMR}$  spectrum it is necessary to stand out the singlet at 5.57 ppm attributable to the  $-\text{N-CH}_2\text{-O}$  group, the triplet at 1.15 ppm and the quadruplet that resonates at 3.65 ppm, which are attributable to the protons of the methylene and methyl groups of the ethoxy substituent respectively (Figure 56).

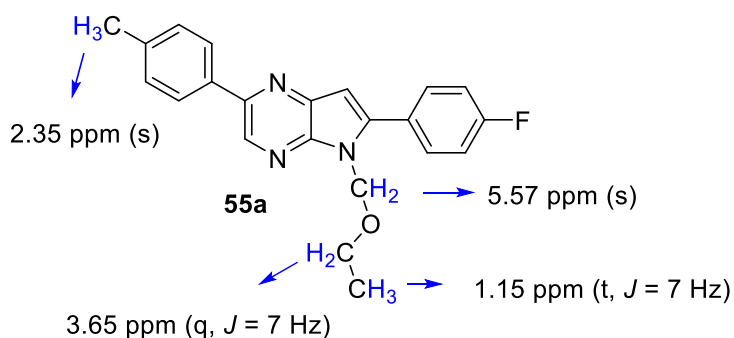
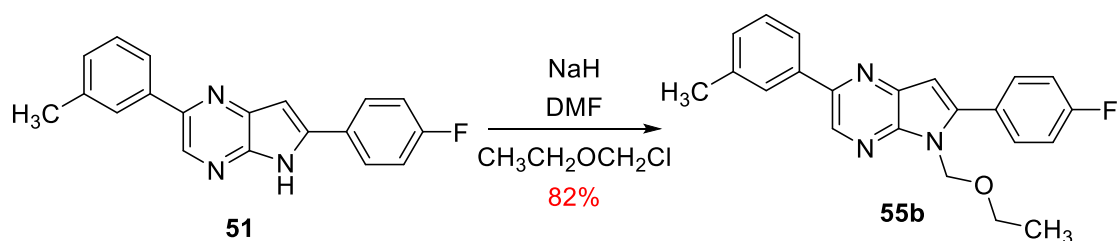


Figure 56.  $^1\text{H-NMR}$  spectroscopy data of compound **55a**

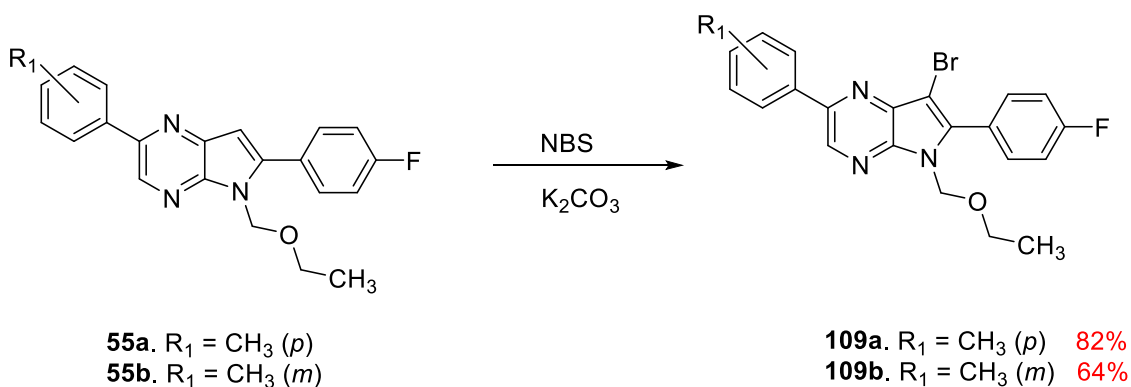
In addition, the molecular pic at 361.1598 g/mol in the mass spectrum (ESI +, theoretical: 361.1590 g/mol), allows to confirm the proposed structure for derivative **55a**.

These reaction conditions of protection were also applied with success for derivative **51**, obtaining the protected pyrrolepyrazine **55b** in 82% yield (Scheme 102).



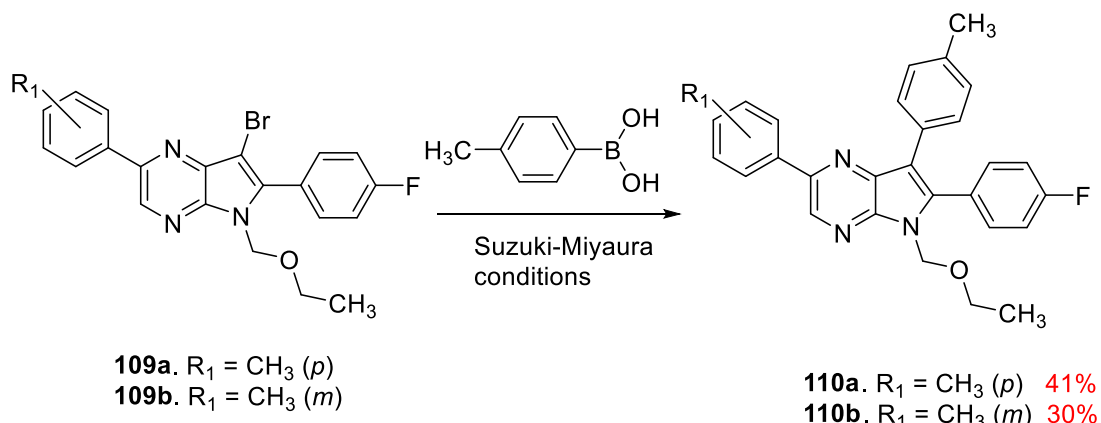
Scheme 102

Then, the bromination of pyrrole[2,3-*b*]pyrazines **55a** and **55b** with NBS and in presence of potassium carbonate leads with success to halogenated derivatives **109a** (82% yield) and **109b** (64% yield) (Scheme 103).



Scheme 103

The addition of *p*-methylphenylboronic acid to each 7-bromo-derivative **109a** and **109b** applying the Suzuki-Miyaura conditions, allows to reach with moderated yields the 2,6,7-triarylated derivatives **110a** and **110b** (Scheme 104).



Scheme 104

The signals appearing at 7.12-7.15 ppm and at 7.49-7.55 ppm in the <sup>1</sup>H-NMR spectrum attributable to the *ortho* and *meta* positions corresponding to the tolyl from position 7 of pyrrolopyrazine system, allow to confirm the proposed structure for **100a** (Figure 57).

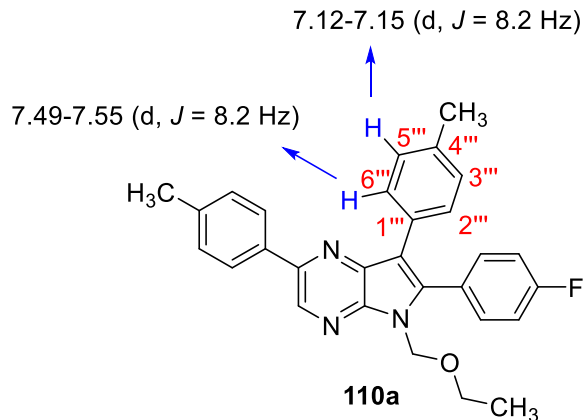
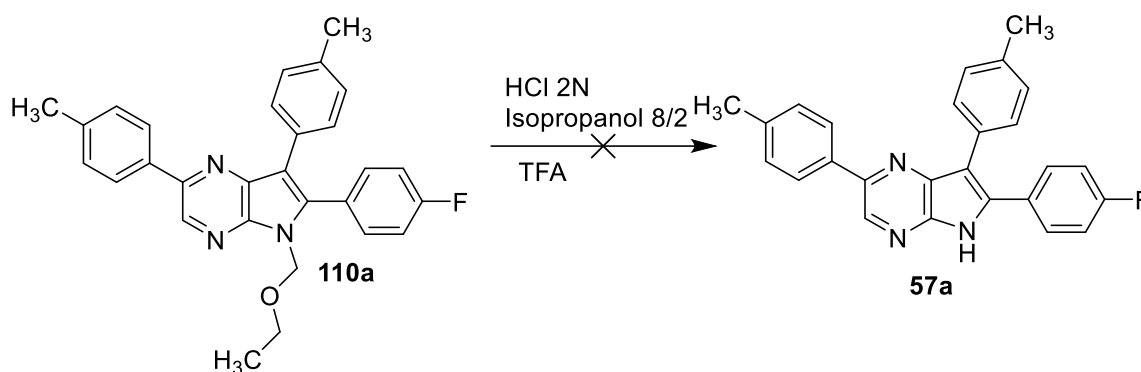


Figure 57. <sup>1</sup>H-NMR spectroscopy data of compound **110a**

In the mass spectrum (ESI +) appears a molecular pic at 452.2099 g/mol (theoretical: 452.2093 g/mol) which supports the structure of **110a**.

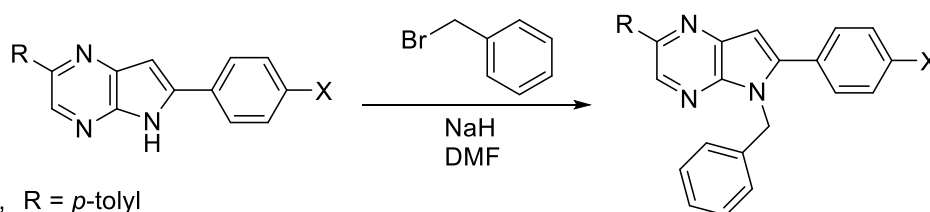
It is recorded that the alkyloxymethyl groups, considered acetalic derivatives, it can be hydrolyzed in acidic conditions.<sup>201</sup> In this work, even different conditions were tried, in any case it was possible to isolate the product with free NH **57a** (Scheme 105).

<sup>201</sup> T. W. Greene; P. G. W. Wuts. *Protective groups in organic synthesis*. John Wiley and Sons, Inc. 2<sup>ona</sup> edició, Harvard **1980**, pg 18



In the reactions carried out at room temperature and in the ones with high temperatures, the unaltered starting material was recovered in all assays, that brings out the good stability of these pyrrolepyrazines.

These difficulties found for the hydrolysis in the EOM (ethoxymethyl) protected derivatives, it was considered to carry out the *N*-benzylation of the pyrrole[2,3-*b*]pyrazines (Scheme 106).



**50.** X = F, R = *p*-tolyl

**100.** X = H, R =  $\text{---}\equiv\text{---C}_6\text{H}_5$

**111.** X = F, R = *p*-tolyl **20%**

**112.** X = H, R =  $\text{---}\equiv\text{---C}_6\text{H}_5$  **77%**

**Scheme 106**

The treatment separately of pyrrole[2,3-*b*]pyrazines **50** and **100** with benzyl bromide and in presence of sodium hydride, allows to obtain the benzylated pyrrolepyrazines **111** and **112** in 20 and 77% yields respectively.

In the proton NMR spectrum, the presence of signals at 5.79 ppm (for **111**) and 5.48 ppm (for **112**) attributable to the benzylic methylene, plus the singlet integrating 5 protons at 7.34 (for **112**) and the doublet plus multiplate at 7.09 and 7.12-7.15 ppm respectively (for **111**) allows to identify the phenyl group introduced into the structure (Figure 58).



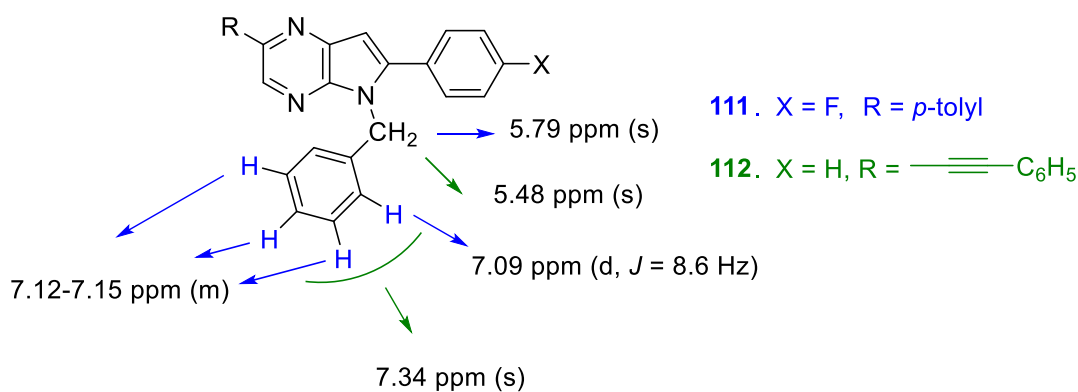
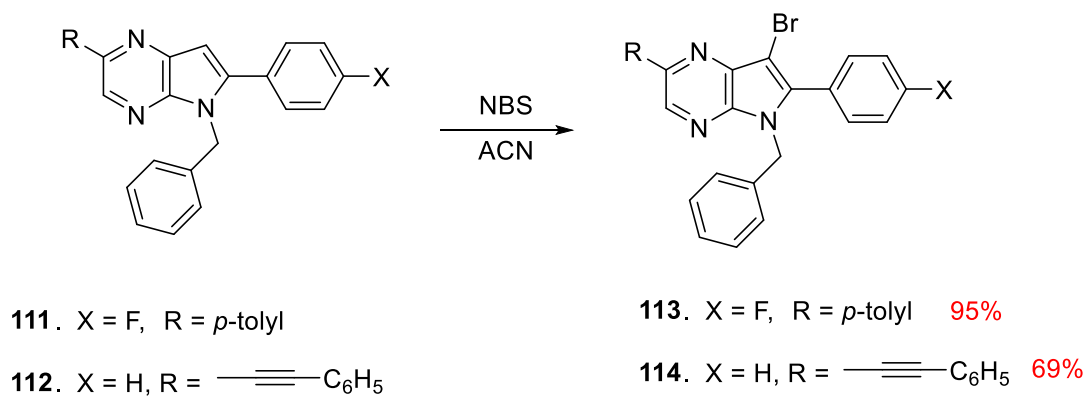


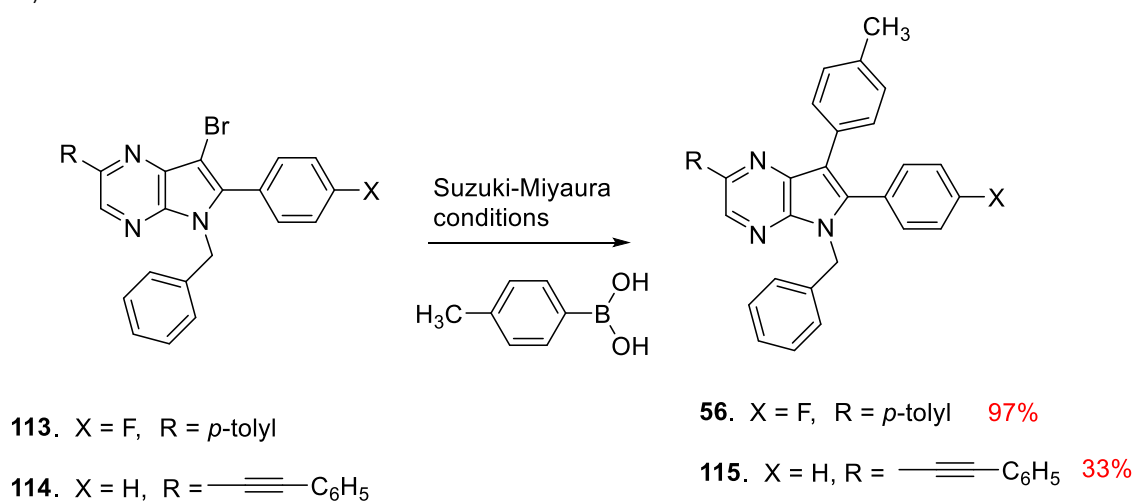
Figure 58.  $^1\text{H-NMR}$  spectroscopy data of compounds **111** and **112**

Then, the intermediates **111** and **112** were halogenated with NBS at room temperature and it enables to obtain with good yields the expected pyrrolepyrazines **113** and **114** (Scheme 107).



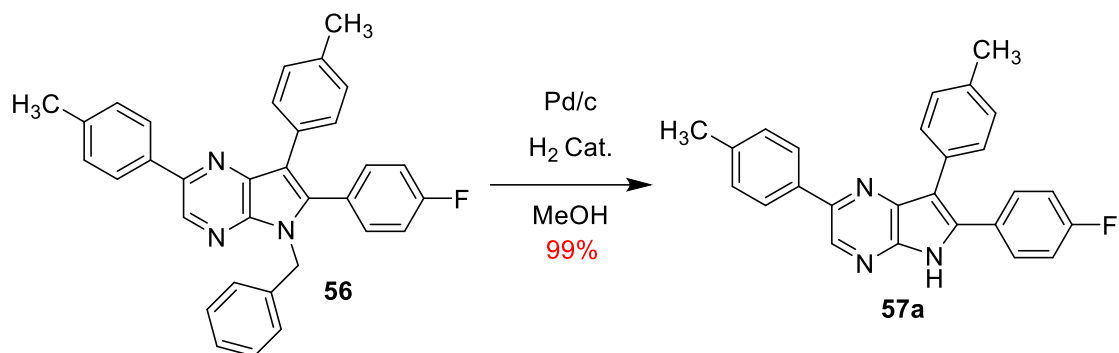
Scheme 107

The brominated derivatives **113** and **114** by reaction with *p*-tolylboronic acid lead to the 2,6,7-triarylated derivatives in good yields, under Suzuki-Miyaura cross-coupling conditions (Scheme 108).

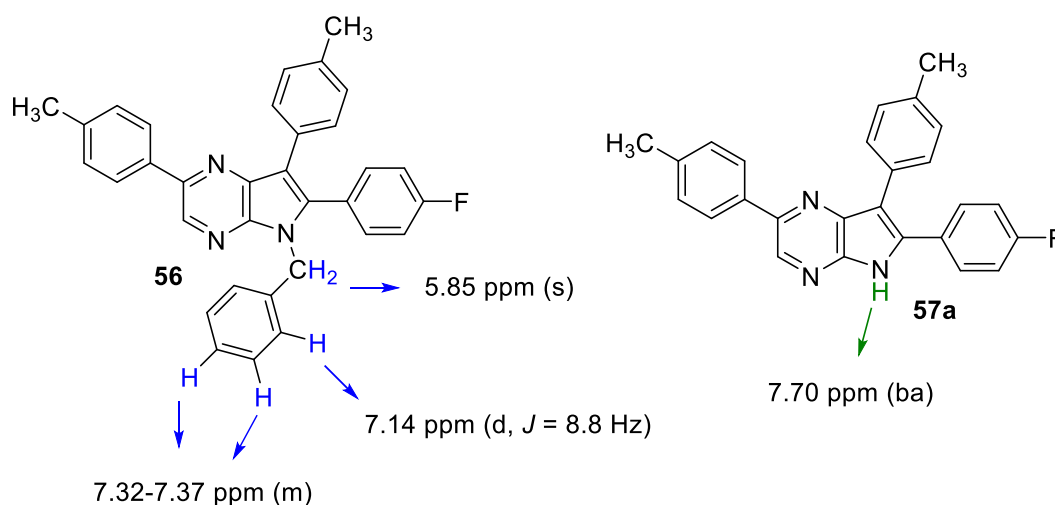


Scheme 108

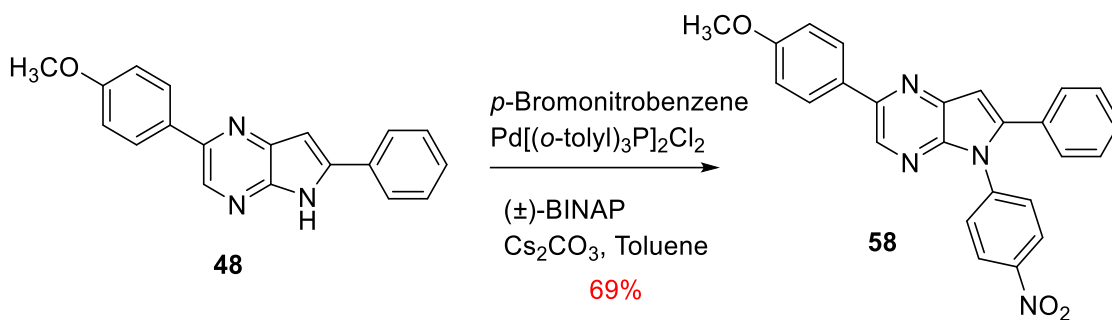
Then, the treatment of **56** under hydrogen stream and in presence of Pd-C as a catalyst, in polar solvents, as methanol or ethanol leads to the debenzylated product **57a** in quantitative yield (Scheme 109).



In the  $^1\text{H-NMR}$  spectrum appears a signal at 7.70 ppm corresponding to the NH group, also the absence of signals at 5.85 ppm (s) attributable to the benzylic- $\text{CH}_2$ - group and the triplet at 7.14 ppm together with the multiplet at 7.32-7.37 ppm which integrated 3 protons for the starting material **56**, it allows to confirm the debenzylated structure of **57a**. In addition, the molecular pic of the mass spectrum (ESI +) at 394.1688 g/mol (theoretical 394.1675 g/mol) supports the proposed structure (Figure 59).



Due to the protection of the pyrrole NH facilitated the functionalization of pyrrolepyrazines, the *N*-arylation of diarylated **48** was carried out (Scheme 110). In order to make the *N*-arylation, pyrrolepyrazine **48** was treated with *p*-bromonitrobenzene and applying the cross-coupling conditions to prepare C-N bonds, previously described, it was possible to obtain the triarylated derivative **58** in 69% yield.



**Scheme 110**

The proton NMR spectrum of **58** shows two doublets at 6.99 ppm (*ortho* position) and at 7.80 ppm (*meta* position) which allow to confirm the introduction of *p*-nitrophenyl group into the pyrrolepyrazine structure **58** (Figure 60).

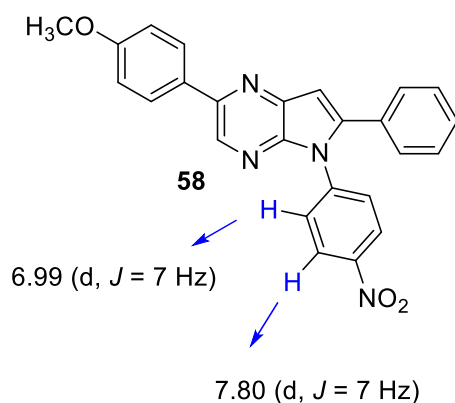
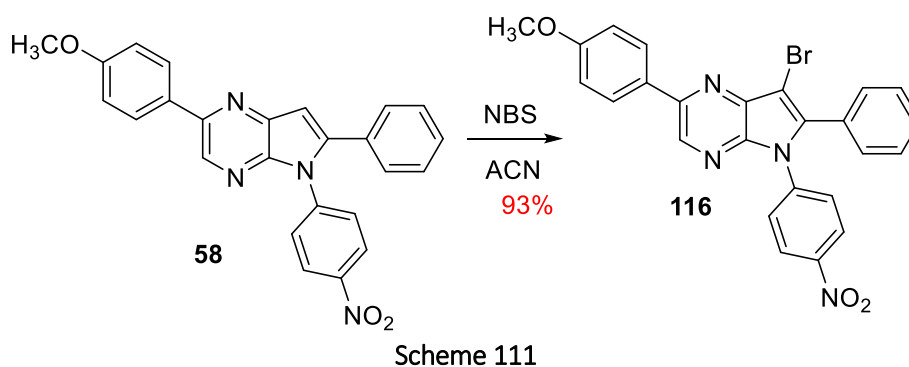


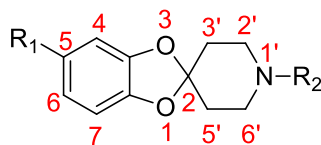
**Figure 60.** <sup>1</sup>H-NMR spectroscopy data of compound **58**

Then, the halogenation of **58** with NBS in acetonitrile allows the obtention of **116** in 93% yield (Scheme 111).



### 3.1.3. Characterization results of the synthesized compounds

#### 3.1.3.1. Analysis of 1-spiro[benzodioxole-2,4'-piperidines]



Compound	PROTONS				
	CH <sub>2</sub> -C	CH <sub>2</sub> -N	4	6	7
<b>1</b>	2.00 (q, $J = 5.8$ Hz)	3.65 (t, $J = 5.8$ Hz ax.) 3.82 (t, $J = 5.8$ Hz eq.)	6.76-6.82 (m)	6.76-6.82 (m)	6.76-6.82 (m)
<b>2</b>	1.96-2.00 (m)	3.63 (t, $J = 6$ Hz ax.) 3.82 (t, $J = 6$ Hz eq.)	7.36 (d, $J = 2$ Hz)	7.51 (dd, $J_1 = 2$ Hz, $J_2 = 8.2$ Hz)	6.79 (d, $J = 8.2$ Hz)
<b>3</b>	1.97 (t, $J = 6$ Hz)	3.04 (t, $J = 6$ Hz)	7.36 (d, $J = 2$ Hz)	7.51 (dd, $J_1 = 2$ Hz, $J_2 = 8.2$ Hz)	6.77 (d, $J = 8.2$ Hz)
<b>4</b>	1.91 (m)	3.58 (t, $J = 6$ Hz, ax.) 3.75 (t, $J = 6$ Hz, eq.)	7.06 (d, $J = 2$ Hz, H-4)	7.00 (dd, $J_1 = 2$ Hz, $J_2 = 8.2$ Hz)	6.68 (d, $J = 8.2$ Hz)
<b>5</b>	1.87-1.95 (m)	3.58 (t, $J = 6$ Hz, ax) 3.73 (t, $J = 6$ Hz eq)	6.78 (s)	6.72 (dd, $J_1 = 2$ Hz, $J_2 = 8$ Hz)	6.64 (d, $J = 8$ Hz)
<b>6</b>	1.86 (t, $J = 5.9$ Hz, ax), 1.92 (t, $J = 5.9$ Hz eq)	3.54 (t, $J = 5.9$ Hz, ax) 3.70 (t, $J = 5.9$ Hz, eq)	6.81 (d, $J = 2$ Hz)	6.82 (dd, $J_1 = 2$ Hz, $J_2 = 8$ Hz)	6.55 (dd, $J_1 = 1$ Hz, $J_2 = 8$ Hz)
<b>7</b>	1.93-1.95 (m)	3.55-3.58 (m, ax) 3.73-3.75 (m, eq)	6.92 (d, $J = 1$ Hz)	6.93 (dd, $J_1 = 1$ Hz, $J_2 = 7.8$ Hz)	6.72 (dd, $J_1 = 1$ Hz, $J_2 = 7.8$ Hz)
<b>8</b>	1.99-2.07 (m)	3.66 (t, $J = 5.9$ Hz ax), 3.80-3.83 (m, eq)	6.67 (d, $J = 2$ Hz)	6.65 (dd, $J_1 = 2$ Hz, $J_2 = 8.4$ Hz)	6.76 (d, $J = 8.4$ Hz)
<b>9</b>	1.90 (t, $J = 6$ Hz)	3.56 (t, $J = 6$ Hz ax) 3.73 (t, $J = 6$ Hz eq)	6.38 (s)	6.55 (d, $J = 7$ Hz)	6.24 (d, $J = 7$ Hz)
<b>10</b>	1.97 (t, $J = 6.5$ Hz ax), 2.04 (t, $J = 6.5$ Hz eq)	3.64 (t, $J = 6.5$ Hz ax), 3.79 (t, $J = 6.5$ Hz eq)	6.67 (d, $J = 2$ Hz)	6.56 (dd, $J_1 = 2$ Hz, $J_2 = 8.2$ Hz)	6.76 (d, $J = 8.2$ Hz)

<b>11</b>	1.91 (t, $J = 5.8$ Hz)	3.55 (t, $J = 5.8$ Hz ax), 3.72 (t, $J = 5.8$ Hz eq)	6.51 (d, $J = 2$ Hz)	6.46 (dd, $J_1 = 2$ Hz, $J_2 = 8$ Hz)	6.36 (dd, $J_1 = 2$ Hz, $J_2 = 8$ Hz)
<b>12</b>	1.97 (t, $J = 6$ Hz ax); 2.02 (t, $J = 6$ Hz eq)	3.62 (t, $J = 6$ Hz ax) 3.75 (t, $J = 6$ Hz eq)	7.54 (d, $J = 2.3$ Hz)	7.79 (dd, $J_1 = 2.3$ , $J_2 = 8.6$ Hz)	6.77 (d, $J = 8.6$ Hz)
<b>13</b>	1.94 (t, $J = 6$ Hz)	2.99 (t, $J = 6$ Hz)	7.52 (d, $J = 2.3$ Hz)	7.77 (dd, $J_1 = 2.3$ , $J_2 = 8.6$ Hz)	6.72 (d, $J = 8.6$ Hz)
<b>14</b>	2.11 (t, $J = 5.7$ Hz)	3.64 (t, $J = 5.7$ Hz)	7.58 (d, $J = 2.3$ Hz)	7.82 (dd, $J_1 = 2.3$ , $J_2 = 8.6$ Hz)	6.77 (d, $J = 8.6$ Hz)
<b>15</b>	2.13 (t, $J = 6$ Hz)	3.25 (t, $J = 6$ Hz)	6.24 (d, $J = 2$ Hz)	6.10 (dd, $J_1 = 2$ Hz, $J_2 = 8$ Hz)	6.56 (d, $J = 8$ Hz)
<b>16</b>	2.11 (t, $J = 6$ Hz)	3.68 (t, $J = 5.7$ Hz)	6.77-6.78 (m)	6.77-6.78 (m)	6.77-6.78 (m)
<b>17</b>	2.07 (t, $J = 6$ Hz)	3.63 (t, $J = 6$ Hz)	7.33 (d, $J = 2$ Hz)	7.47 (dd, $J_1 = 2$ Hz, $J_2 = 8.2$ Hz)	6.74 (d, $J = 8.2$ Hz)
<b>73</b>	2.10-2.12 (m, ax.) 4.15-4.17 (m, eq.)	3.25-3.37 (m)	7.40 (s)	7.51 (dd, $J_1 = 2$ Hz, $J_2 = 8.2$ Hz)	7.62 (d, $J = 8.2$ Hz)
<b>18</b>	2.03 (t, $J = 5$ Hz)	3.69 (q, $J = 5$ Hz)	7.14 (d, $J = 2$ Hz)	7.09 (dd, $J_1 = 2$ Hz, $J_2 = 8.1$ Hz)	6.86 (d, $J = 8.1$ Hz)
<b>19</b>	2.03 (t, $J = 5.7$ Hz)	3.61 (t, $J = 5.7$ Hz)	7.09 (d, $J = 2$ Hz)	7.18-7.19 (m)	6.63-6.64 (m)
<b>20</b>	1.99-2.12 (m)	3.59-3.66 (m)	6.21 (s)	6.08 (d, $J = 7$ Hz)	6.52 (d, $J = 7$ Hz)
<b>21</b>	2.04 (t, $J = 5.7$ Hz)	3.62 (t, $J = 5.7$ Hz)	7.79 (s)	6.74 (dd, $J_1 = 2$ Hz, $J_2 = 8$ Hz)	6.65 (d, $J = 8$ Hz)
<b>22</b>	2.08 (t, $J = 5.5$ Hz)	3.19 (t, $J = 5.5$ Hz)	6.77 (d, $J = 2$ Hz)	6.71 (dd, $J_1 = 2$ Hz, $J_2 = 8$ Hz)	6.64 (d, $J = 8$ Hz)
<b>75</b>	2.12 (t, $J = 6$ Hz)	3.70 (t, $J = 6$ Hz)	6.93 (d, $J = 2$ Hz)	6.83 (dd, $J_1 = 2$ Hz, $J_2 = 8$ Hz)	6.72 (d, $J = 8$ Hz)

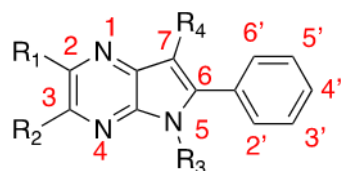
23	2.09 (t, $J = 6$ Hz)	3.19 (t, $J = 6$ Hz)	7.31 (d, $J = 2$ Hz)	7.45 (dd, $J_1 = 2$ Hz, $J_2 = 8.1$ Hz)	6.72 (d, $J = 8.1$ Hz)
24	2.17 (t, $J = 5.8$ Hz)	3.52 (t, $J = 5.8$ Hz)	7.41 (d, $J = 2$ Hz)	7.54 (dd, $J_1 = 2$ Hz, $J_2 = 8.2$ Hz)	6.81 (d, $J = 8.2$ Hz)
25	2.07-2.09 (m)	3.53 (t, $J = 5.8$ Hz)	6.78 (d, $J = 2$ Hz)	6.72 (dd, $J_1 = 2$ Hz, $J_2 = 8$ Hz)	6.65 (d, $J = 8$ Hz)
26	2.08 (t, $J = 6$ Hz)	3.44 (t, $J = 6$ Hz)	6.93 (d, $J = 2$ Hz)	7.47 (dd, $J_1 = 2$ Hz, $J_2 = 8$ Hz)	6.74 (d, 1H, $J = 8$ Hz)
27	2.05 (t, $J = 5.7$ Hz)	3.20-3.26 (m)	7.24 (d, $J = 1.8$ Hz)	7.42 (dd, $J_1 = 1.8$ Hz, $J_2 = 8$ Hz)	6.66 (d, $J = 8$ Hz)
28	2.05 (t, $J = 7$ Hz)	3.16–3.28 (m)	7.26 (s)	7.43 (d, $J = 8$ Hz)	6.67 (d, $J = 8$ Hz)
29	2.02 (t, $J = 5.5$ Hz)	3.22 (t, $J = 5.5$ Hz)	6.71 (s)	6.69 (d, $J = 8$ Hz)	6.58 (d, $J = 8$ Hz)
30	2.00-2.03 (m)	3.27 (t, $J = 5.8$ Hz)	6.78 (d, $J = 2$ Hz)	6.75 (dd, $J_1 = 2$ Hz, $J_2 = 8$ Hz)	6.64 (d, $J = 8$ Hz)
32	2.09 (t, $J = 5.7$ Hz)	3.27 (t, $J = 5.7$ Hz)	6.82 (d, $J = 1.5$ Hz)	6.79 (dd, $J_1 = 1.5$ Hz, $J_2 = 8$ Hz)	6.63 (d, $J = 8$ Hz)
33	2.08 (t, $J = 5.3$ Hz)	3.29 (t, $J = 5.3$ Hz)	6.70 (s)	6.67 (d, $J = 7.9$ Hz)	6.61 (d, $J = 7.9$ Hz)
34	2.02 (t, $J = 5.7$ Hz)	3.22 (t, $J = 5.7$ Hz)	6.65 (s)	6.62 (d, $J = 7.9$ Hz)	6.54 (d, $J = 7.9$ Hz)
35	2.08-2.10 (m)	3.07 (q, $J = 7$ Hz) 3.32 (q, $J = 7$ Hz)	7.08 (s)	6.62 (d, $J = 8$ Hz)	6.81 (d, $J = 8$ Hz)
81	2.14 (q, $J = 6$ Hz)	2.14 (t, $J = 6$ Hz)	6.85 (s)	7.05 (d, $J = 8.8$ Hz)	6.97 (d, $J = 8.8$ Hz)
37	2.12 (t, $J = 5.5$ Hz)	3.52 (t, $J = 5.5$ Hz)	7.40 (d, $J = 2$ Hz)	7.54 (dd, $J_1 = 2$ Hz, $J_2 = 8.2$ Hz)	6.80 (d, $J = 8.2$ Hz)
38	1.98 (t, $J = 5.7$ Hz)	3.26 (t, $J = 5.7$ Hz)	6.74 (d, $J = 2$ Hz)	6.68 (dd, $J_1 = 2$ Hz, $J_2 = 8$ Hz)	6.59 (d, $J = 8$ Hz)
39	2.13-2.14 (m)	3.27-3.40 (m)	6.85 (d, $J = 2$ Hz)	6.79 (dd, $J_1 = 2$ Hz, $J_2 = 8$ Hz)	6.71 (d, $J = 8$ Hz)

40	2.04 (t, $J = 5.8$ Hz)	3.34 (t, $J = 5.8$ Hz)	6.17 (d, $J = 2$ Hz)	6.05 (dd, $J_1 = 2$ Hz, $J_2 = 8$ Hz)	6.50 (d, $J = 8$ Hz)
41	2.04 (t, $J = 5.4$ Hz ax) 3.28 (t, $J = 5.4$ Hz eq)	3.15 (t, $J = 5.4$ Hz)	6.78 (d, $J = 2$ Hz)	6.52 (dd, $J_1 = 2$ Hz, $J_2 = 8.2$ Hz)	6.57 (d, $J = 8.2$ Hz)
42	0.90 (t, $J = 5.8$ Hz, ax), 1.93 (t, $J = 5.8$ Hz eq)	3.70 (q, $J = 5.8$ Hz)	6.62 (d, $J = 2$ Hz)	6.53 (dd, $J_1 = 2$ Hz, $J_2 = 8.3$ Hz)	6.69 (d, $J = 8.3$ Hz)

Compound	Carbons								
	CH <sub>2</sub> -C	CH <sub>2</sub> -N	4 (CH)	6 (CH)	7 (CH)	C-2 (Cq)	C-5 (Cq)	C-3a (Cq)	C-7a (Cq)
4	34.6 35.4	38.8 43.5	106.4	116.3	108.2	120.1	130.8	147.1	147.7
5	34.6 35.4	38.7 43.5	106.2	118.5	108.2	115.8	139.8	147.1	146.1
6	34.5 35.3	38.5 43.3	109.7	112.3	124.0	112.7	117.0	146.2	147.8
7	34.7 35.4	38.7 43.5	108.7	120.1	107.6	116.0	136.6	147.4	146.1
9	34.5 35.3	38.8 43.6	99.9	109.6	108.6	115.5	127.8	147.4	140.8
10	34.6 35.4	38.7 43.5	104.8	109.8	108.7	112.4	134.0	146.2	143.8
11	34.6 35.4	38.7 43.5	108.6	110.7	109.8	113.5	136.3	147.5	146.5
12	34.6 35.4	38.5 43.2	104.6	107.8	119.7	119.3	142.6	147.3	152.3
13	36.1	43.4	104.3	107.4	119.4	120.4	142.4	147.6	152.7
14	34.2	44.8	104.8	107.8	119.7	119.2	142.8	152.3	153.7
15	34.7	49.0	98.1	106.4	108.5	108.2	147.8	140.9	140.1
16	34.2	45.0	113.0	126.1	113.0	115.3	126.1	146.7	146.7
17	34.2	44.9	108.1	124.6	108.2	117.2	132.0	147.4	151.0
18	34.2	44.6	108.6	120.1	106.0	117.1	131.0	147.1	147.4
19	34.1	44.9	103.1	112.9	108.1	116.1	133.3	142.5	146.9
21	34.2	44.9	106.2	118.6	108.2	115.7	138.5	147.1	146.1
22	34.9	48.8	106.0	118.2	108.0	116.5	139.4	147.4	146.5
24	34.4	46.6	107.9	116.7	108.1	117.8	125.5	147.6	151.3
25	25.1	34.3	106.1	117.4	108.1	118.2	131.7	147.2	146.4
26	34.3	46.4	107.9	116.6	108.1	117.8	129.7	147.6	151.2

75	34.2	45.0	105.5	120.9	108.4	111.9	136.3	146.7	147.3
27	34.5	43.5	108.0	124.5	108.2	116.4	131.9	147.2	150.8
28	34.5	43.5	108.0	124.6	108.1	116.5	131.9	147.3	150.9
29	34.4	43.7	106.2	118.5	108.1	114.9	136.4	146.8	145.9
33	34.4	47.5	106.4	119.4	107.2	114.8	136.5	146.9	145.9
34	33.5	44.7	106.8	120.7	107.8	114.9	128.6	146.7	146.5
37	34.5	47.2	108.0	124.7	108.1	117.9	131.6	147.7	147.7
38	34.4	47.3	105.9	118.0	107.6	116.2	131.6	147.0	146.8
39	25.1	34.3	106.1	118.4	108.1	110.2	124.6	147.2	146.4
41	34.3	47.6	104.9	113.8	108.1	116.5	127.5	137.4	138.7
	34.7								
42	34.3	38.4	100.4	109.9	108.4	116.0	141.1	147.5	138.9
	34.9	43.3							

### 3.1.3.1. Analysis of pyrrole[2,3-b]pyrazines

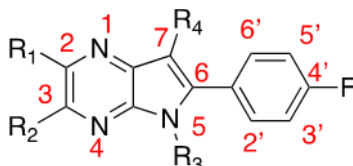


Compound	PROTONS				
	3	7	2', 6'	3', 5'	4'
92	8.04 (s) (H-6)	-	7.57 (dd, $J_1 = 1.5$ Hz, $J_2 = 7.2$ Hz)	7.40 (t, $J = 7.2$ Hz)	7.41 (t, $J = 7.2$ Hz)
45a	7.93 (s)	6.81 (s)	7.02-7.08 (m)	7.02-7.08 (m)	7.02-7.08 (m)
47	8.50 (s)	7.00 (s)	7.83 (d, $J = 7.7$ Hz)	7.46 (t, $J = 7.7$ Hz)	7.38 (t, $J = 7.7$ Hz)
48	8.35 (s)	6.99 (s)	7.15 (dd, $J_1 = 1.7$ Hz, $J_2 = 7$ Hz)	7.09 (d, $J = 7$ Hz)	7.00-7.02 (m)
49	8.93 (s)	7.24 (s)	8.04 (d, $J = 7.4$ Hz)	7.53 (t, $J = 7.4$ Hz)	7.44 (t, $J = 7.4$ Hz)
100	8.43 (s)	6.98 (s)	7.88 (d, $J = 7.5$ Hz)	7.53 (t, $J = 7.5$ Hz)	7.53 (t, $J = 7.5$ Hz)
101	8.17 (bs)	Iode	7.88 (d, $J = 7.2$ Hz)	7.50 (t, $J = 7.2$ Hz)	7.50 (t, $J = 7.2$ Hz)
102a	8.83 (s)	Brom	8.55 (dd, $J_1 = 1.3$ Hz, $J_2 = 7.6$ Hz)	7.51 (t, $J = 7.6$ Hz)	7.54 (t, $J = 7.6$ Hz)
102b	8.88 (s)	Brom	8.54 (d, $J = 7.3$ Hz)	7.52 (t, $J = 7.3$ Hz)	7.56-7.58 (m)
103	Brom	Brom	7.64 (d, $J = 8$ Hz)	7.54 (t, $J = 8$ Hz)	7.51-7.52 (m)
105	Clor	Brom	7.53 (t, $J = 7.8$ Hz)	7.30 (d, $J = 7.8$ Hz)	7.44-7.47 (m)
107	Clor	Brom	7.48 (d, $J = 7.3$ Hz)	7.16-7.20 (m)	7.16-7.20 (m)
54	Aril	Brom	7.71 (d, $J = 7.2$ Hz)	7.48 (t, $J = 7.2$ Hz)	7.41-7.43 (m)
112	8.42 (s)	6.70 (s)	7.57 (m) (H-2'', H- 6'')	6.86-6.89 (m) (H- 3'', H-5'')	7.30-7.32 (m) (H- 4'')



114	8.48 (s)	Brom	7.42 (dd, $J_1 = 1.2$ Hz, $J_2 = 7$ Hz) (H-2'', H-6'')	6.79-6.81 (m) (H-3'', H-5'')	7.29-7.34 (m) (H-4'')
115	8.47 (s)	Aril	7.11-7.13 (m) (H-2'', H-6'')	7.11-7.13 (m) (H-3'', H-5'')	7.11-7.13 (m) (H-4'')
58	8.46 (s)	6.68 (s)	7.45 (d, $J = 7.2$ Hz)	7.19 (t, $J = 7.2$ Hz)	7.36 (t, $J = 7.2$ Hz)
116	8.66 (s)	Brom	7.94 (d, $J = 7.7$ Hz)	7.57 (t, $J = 7.7$ Hz)	7.43 (t, $J = 7.7$ Hz)
59	8.58 (s)	Aril	7.95 (d, $J = 7.2$ Hz)	7.50 (t, $J = 7.2$ Hz)	7.56-7.58 (m)

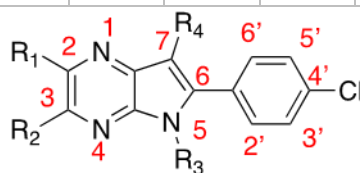
Compound	Carbons									
	2	3	4a	6	7	7a	1'	2', 6'	3', 5'	4'
92	121.1 (C-5)	143.6 (C-6)	154.2 (C-2)	-	-	125.9 (C-3)	124.5	128.6	132.0	129.8
45a	133.4	137.6	146.0	139.3	102.9	129.4	141.4	128.2	128.0	129.2
47	-	142.6	-	-	106.1	-	-	133.0	133.5	138.0
102a	152.0	142.2	152.8	132.8	103.5	128.7	140.4	128.6	129.9	133.5
102b	153.9	142.8	148.1	128.0	102.1	128.3	134.1	127.4	130.6	133.9
105	152.9	144.5	147.4	130.6	96.7	118.4	134.4	128.1	129.5	128.7
112	137.2	139.4	147.7	140.4	101.5	122.4	133.6	126.6 (C-2'', C-6'')	128.7 (C-3'', C-5'')	129.4 (C-4'')



Compound	Protons			
	3	7	2', 6'	3', 5'
97	8.06 (s) (H-6)	-	7.57 (dd, $J_1 = 5$ Hz, $J_2 = 8.5$ Hz)	7.09 (t, $J = 8.5$ Hz)
45b	8.18 (s)	6.80 (s)	7.66 (dd, $J_1 = 5$ Hz, $J_2 = 8.5$ Hz)	6.95 (dd, $J_1 = 5$ Hz, $J_2 = 8.5$ Hz)
50	8.18 (s)	6.81 (s)	7.77 (dd, $J_1 = 5$ Hz, $J_2 = 8.6$ Hz)	7.15 (d, $J = 8.5$ Hz)
51	8.00 (s)	7.00 (s)	7.78 (d, $J = 9$ Hz)	7.25 (d, $J = 9$ Hz)
55a	8.62 (s)	6.77 (s)	7.73 (dd, $J_1 = 5.3$ Hz, $J_2 = 8.6$ Hz)	7.13 (t, $J = 8.6$ Hz)
55b	8.63 (s)	6.77 (s)	7.74 (d, $J = 9$ Hz)	7.16 (d, $J = 9$ Hz)
109a	8.69 (s)	Brom	7.68 (dd, $J_1 = 5.3$ Hz, $J_2 = 8.6$ Hz)	7.19 (t, $J = 8.6$ Hz)
109b	8.76 (s)	Brom	7.75 (d, $J = 9$ Hz)	7.26 (d, $J = 9$ Hz)
110a	8.76 (s)	Aril	7.74 (dd, $J_1 = 5.3$ Hz, $J_2 = 8.5$ Hz)	7.26 (t, $J = 8.5$ Hz)

111	7.38 (s)	7.01 (s)	7.23 (d, $J = 8$ Hz rotamer), 7.64 (dd, $J_1 = 5$ Hz, $J_2 = 8$ Hz), 7.69 (d, $J = 8$ Hz rotamer)	7.35 (t, $J = 6$ Hz)
113	7.49 (s)	Brom	7.78 (bs), 7.81 (dd, $J_1 = 5$ Hz, $J_2 = 8.4$ Hz)	7.40 (sc)
56	7.71 (s)	Aril	7.57 (d, $J = 7$ Hz)	7.56 (d, $J = 7$ Hz)
57	8.63 (bs)	Aril	7.54 (dd, $J_1 = 5.5$ Hz, $J_2 = 8.5$ Hz), 7.76-7.80 (m)	7.21 (d, $J = 8.5$ Hz)

Compound	Carbons									
	2	3	4a	6	7	7a	1'	2', 6'	3', 5'	4'
55a	148.3	135.1	145.9	142.2	101.9	127.3	135.2	131.3 ( $J = 8.2$ Hz)	115.9 ( $J = 21.5$ Hz)	163 ( $J = 248.6$ Hz)
109b	149.2	136.6	142.1	137.5	91.8	124.8	127.7	132.8 ( $J = 9$ Hz)	115.7 ( $J = 22$ Hz)	163.7 ( $J = 254$ Hz)
110a	149.1	136.4	148.0	134.8	129.2	115.1	124.9 ( $J = 3.5$ Hz)	132.8 ( $J = 8.5$ Hz)	115.7 ( $J = 21.7$ Hz)	163.0 ( $J = 249.9$ Hz)
113	151.4	120.3	150.0	139.7	98.6	123.7	126.4	131.3 ( $J = 8.4$ Hz)	115.4 ( $J = 21.5$ Hz)	163.8 ( $J = 250$ Hz)



Compound	Protons			
	3	7	2', 6'	3', 5'
98	8.06 (s) (H-6)	-	7.50 (d, $J = 8.5$ Hz)	7.36 (d, $J = 8.5$ Hz)
45c	8.27 (s)	6.90 (s)	7.66 (d, $J = 8.4$ Hz)	7.49 (d, $J = 8.4$ Hz)
52	8.05 (s)	6.91 (s)	7.63 (d, $J = 7.7$ Hz)	7.22 (d, $J = 7.7$ Hz)

Compound	Carbons									
	2	3	4a	6	7	7a	1'	2', 6'	3', 5'	4'
52	143,7	137,6	141,1	128,5	97,9	120,1	133,0	129,4	129,4	135,6

## 3.2. BIOLOGICAL DISCUSSION

Eli Lilly & Company laboratories (Indianapolis, USA) have carried out a biological assays for a selected compounds described in this doctoral thesis. A high throughput screening for several biological targets related with different diseases, such as cancer, tropical diseases, autoimmune diseases and others, was made in order to acquire a potential drugs. Therefore, a review of the tested compounds and their activities is described hereunder.

It is necessary to highlight that some assays were interrupted along this work due to Eli Lilly interest. Hence, even one of the aims of this thesis was to evaluate synthesized compounds in targets like hNNMT (nicotinamide *N*-methyl transferase), arginase or CD73 (all three with important roles in MDR), as well as in malaria, chagas or tuberculosis, it was not possible to obtain all the desired results.

### 3.2.1. ONCOLOGY

#### *INHIBITION OF NNMT*

As it has been described in the introduction of this work memory, the *N*-nicotinamide *N*-methyl transferase (NNMT), cytosolic enzyme that is expressed in the adipose tissue and in the liver, catalyzes the transfer of methyl groups from the methyl donor (S)-adenosyl-L-methionine (SAM) to nicotinamide (vitamin B3), generating (S)-adenosyl-L-homocysteine (SAH) and *N*<sup>1</sup>-methylnicotinamide (MNAM). Previous reports have connected the increased expression levels of NNMT in cancer cells with chemotherapy and radiation resistance as well as with increased tumor aggressiveness. Metabolic changes driven by activation of oncogenes, inactivation of tumor suppressors, and protumorigenic mutations are considered a hallmark of cancer. So, downregulation or silencing of NNMT has been shown to increase the sensitivity of carcinoma cells to radiation therapy and the decrease of tumorigenicity, providing key support for the role of NNMT in promoting treatment resistance and tumorigenesis in cancer cells. Thus, compounds able to modulate the activity of NNMT in the setting oncology may have therapeutic utility.<sup>202</sup> NNMT is also implicated in others diseases including obesity, diabetes and neurodegenerative diseases.<sup>203</sup>

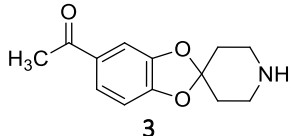
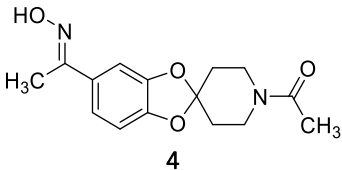
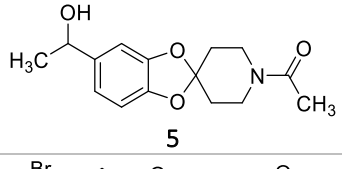
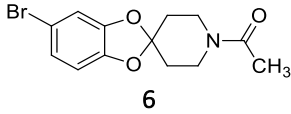
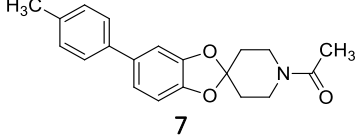
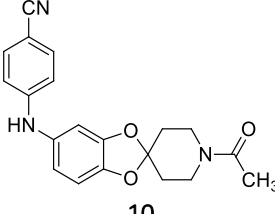
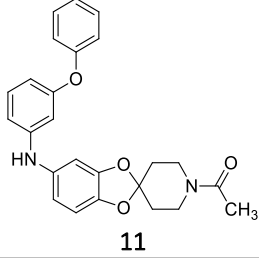
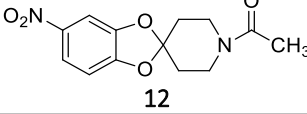
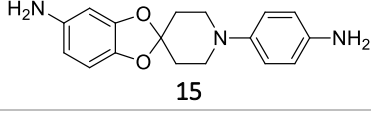
In order to identify possible NNMT inhibitors, the Open Innovation Drug Discovery (OIDD) from Eli Lilly carry out an evaluation of the enzymatic modulation of the human NNMT (hNNMT) through liquid chromatography and mass spectrometry (LC/MS), obtaining as a result the percentage of inhibited enzyme (Table 11).

---

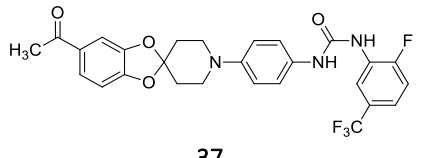
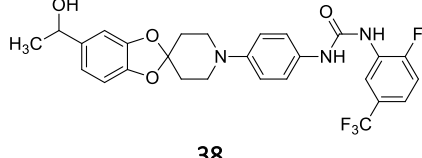
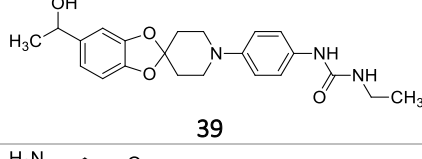
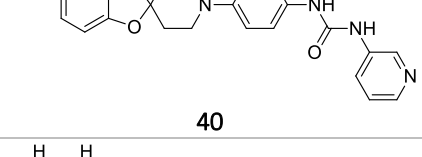
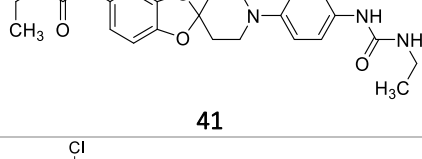
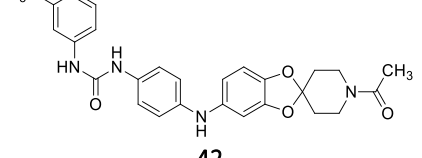
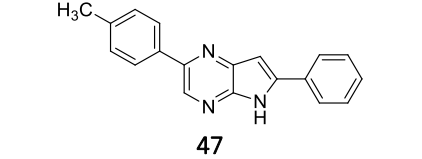
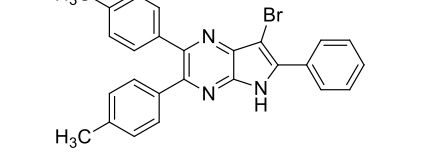
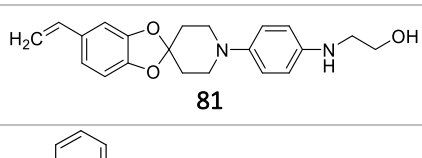
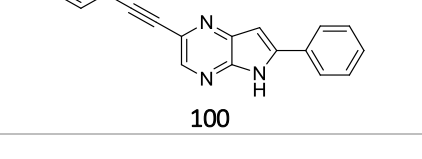
<sup>202</sup> J. V. Haren; J. S. Toraño; D. Sartini; M. Emanuelli; R. B. Parsons; N. I. Martin. *Biochemistry* **2016**, *55*, 5307-5315

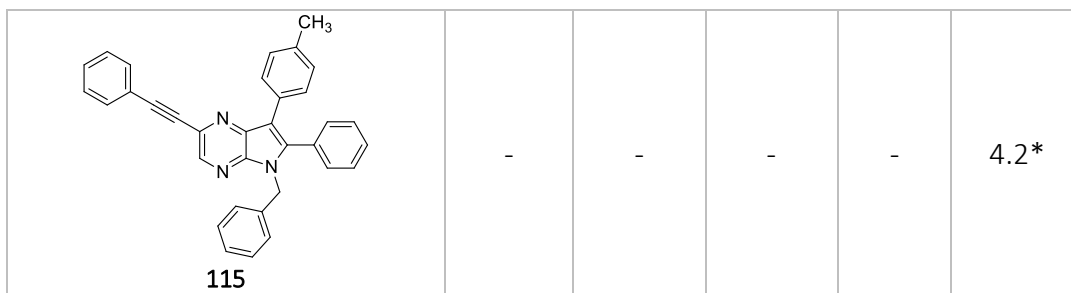
<sup>203</sup> D. Kraus; Q. Yang; D. Kong; A. S. Banks; L. Zhang; J. T. Rodgers; E. Pirinen. *Nature* **2014**, *508*, 258-262

**Table 11.** Determination of hNNMT inhibition

hNNMT INHIBITORS					
COMPOUNDS	Primary SP		Primary CRC		Secondary
	NNMT MNAN SP	NNMT SAH SP	NNMT MNAN CRC	NNMT SAH CRC	NV-NNMT (10 nM) MNAM 120min MS CRC
	% Inh. @ 10 $\mu$ M	% Inh. @ 10 $\mu$ M	Rel IC50 ( $\mu$ M)	Rel IC50 ( $\mu$ M)	Rel IC50 ( $\mu$ M)
 3	2.2	0	-	-	-
 4	-10.6	25.5 -1.2	-	-	-
 5	-11.5	-	-	-	-
 6	-1.6	-	-	-	-
 7	-3.5	-	-	-	-
 10	4.8	-	-	-	-
 11	12.5	-	-	-	-
 12	29.1	-	-	-	-
 15	6.5	24.7 -8.9	-	-	-

<p style="text-align: center;"><b>17</b></p>	18.2	-7.9	-	-	-
<p style="text-align: center;"><b>18</b></p>	19.6	27	-	-	-
<p style="text-align: center;"><b>19</b></p>	20.5	0.7	-	-	-
<p style="text-align: center;"><b>20</b></p>	10.5	47.3 8.9	170.1*	192*	-
<p style="text-align: center;"><b>21</b></p>	-16	3.5	-	-	-
<p style="text-align: center;"><b>22</b></p>	33.8	-	-	-	-
<p style="text-align: center;"><b>23</b></p>	14.4	14.9	-	-	-
<p style="text-align: center;"><b>24</b></p>	8.6	-	-	-	-
<p style="text-align: center;"><b>25</b></p>	22.4	-	-	-	-
<p style="text-align: center;"><b>28</b></p>	-	-	-	-	>20*
<p style="text-align: center;"><b>30</b></p>	-	-	-	-	>20*
<p style="text-align: center;"><b>33</b></p>	-5.1	1.6	-	-	-

 <p><b>37</b></p>	15.3	-	-	-	-
 <p><b>38</b></p>	16.9	-	-	-	-
 <p><b>39</b></p>	-5.3	-	-	-	-
 <p><b>40</b></p>	2.9	-	-	-	-
 <p><b>41</b></p>	19.8	-	-	-	-
 <p><b>42</b></p>	-	-	-	-	15.7*
 <p><b>47</b></p>	99.7	103	-	-	11.8 * >20*
 <p><b>54</b></p>	3.6	5.6	-	-	-
 <p><b>81</b></p>	13.4	-	-	-	-
 <p><b>100</b></p>	2.3	-	-	-	-



SP: single point. CRC: concentration response curve. \* The CRC is showed hereunder

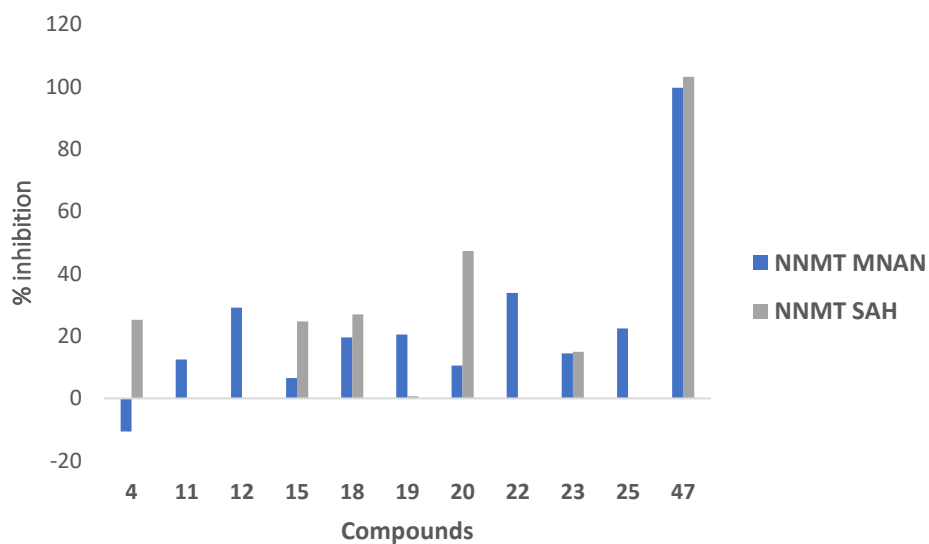


**Figure 61.** Graphic of the most significant products with their hNNMT inhibitory percentage

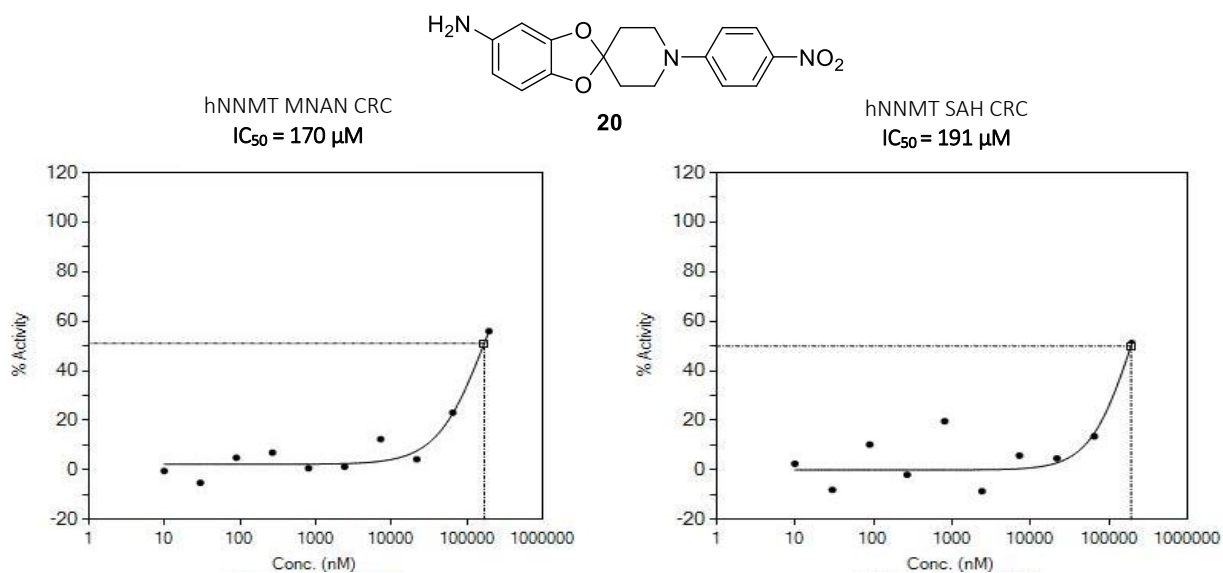
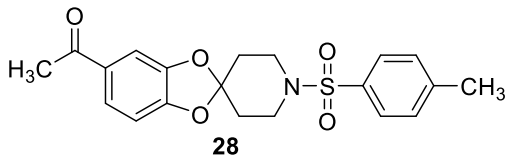
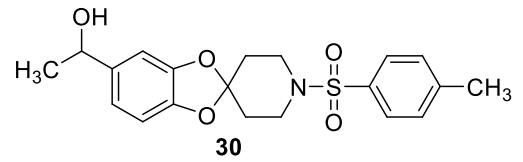
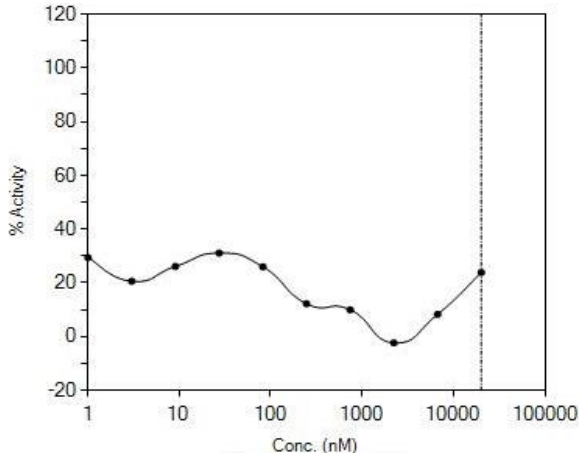


**Figure 62.** Concentration response curve of product 20 in hNNMT inhibition



NV-hNNMT (10nM) MNAN 120 min MS CRC  
 $IC_{50} > 20 \mu M$



NV-hNNMT (10nM) MNAN 120 min MS CRC  
 $IC_{50} > 20 \mu M$

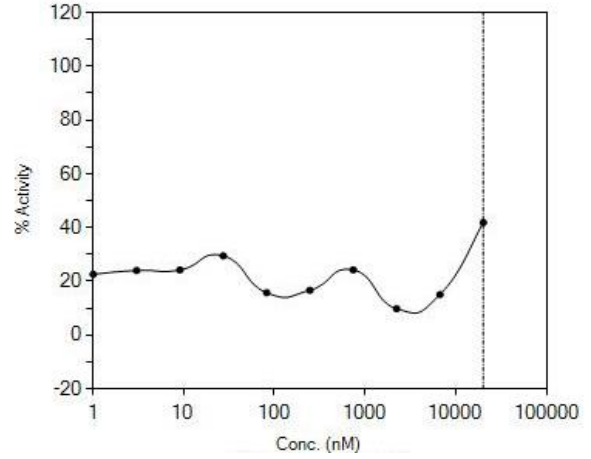
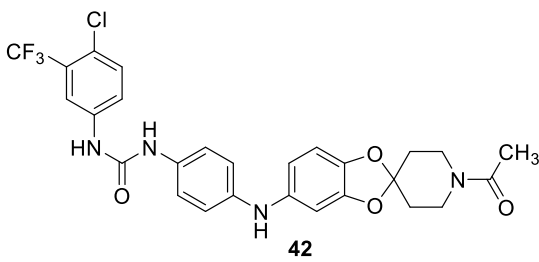
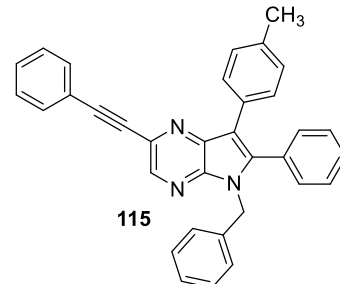
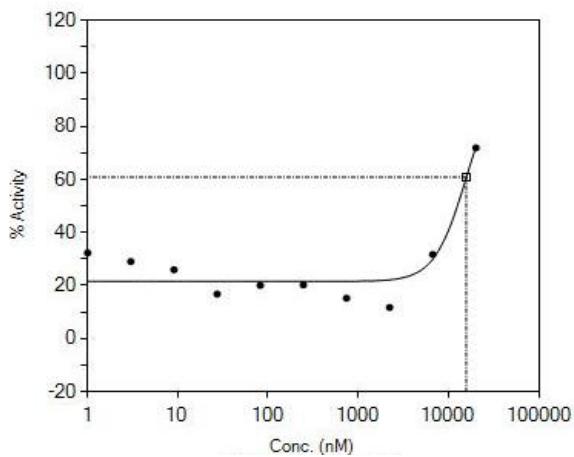


**Figure 63.** Concentration response curve of products **28** and **30** in hNNMT inhibition



NV-hNNMT (10nM) MNAN 120 min MS CRC  
 $IC_{50} = 15 \mu M$



NV-hNNMT (10nM) MNAN 120 min MS CRC  
 $IC_{50} = 4.2 \mu M$

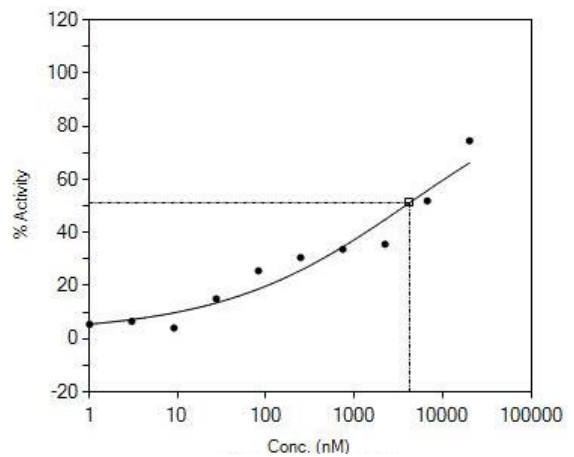


**Figure 64.** Concentration response curve of product **42** and **115** in hNNMT inhibition



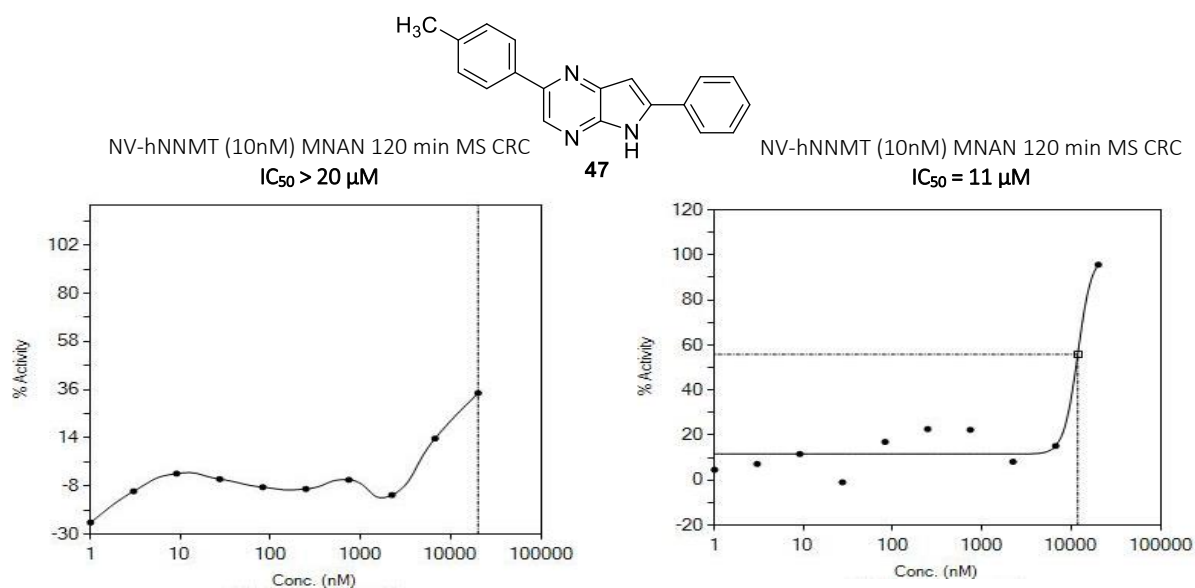


**Figure 65.** Concentration response curve of product **47** in hNNMT inhibition

From the results obtained, it can be extracted that the pyrrolopyrazine nucleus allows to obtain better NNMT inhibitors than the spiranic nucleus. The introduction of a sulfonyl substituent in spiranic derivatives (compounds **28** and **30**) on piperidine nitrogen is less effective than *p*-nitrophenyl (**20**) or acetyl (**42**). In the other hand, the introduction of a urea function on C-5 is an effective modification since it leads to compound **42**, that has an  $IC_{50} = 15 \mu M$ . Regarding pyrrolopyrazines, it seems clear that the phenylacetylene substituent favors the NNMT inhibitory activity (compare **47** and **115**) (Figure 66).

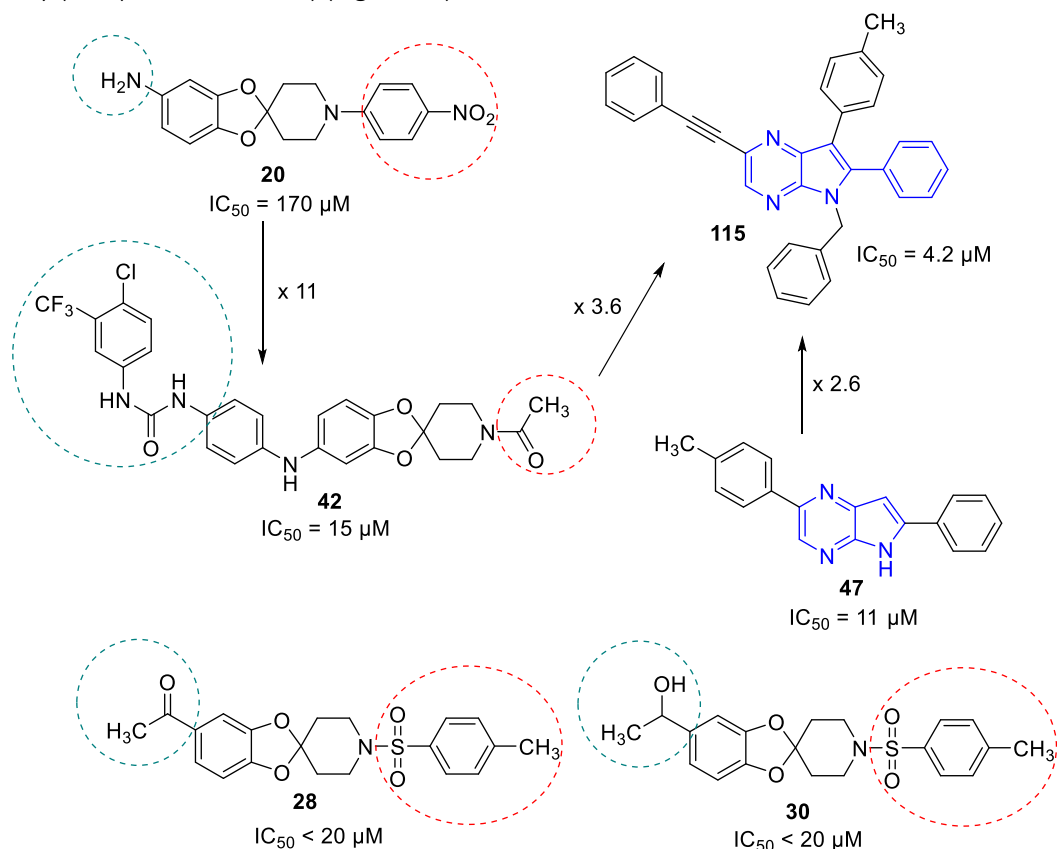


**Figure 66.** Activity relationships of compounds **20**, **28**, **30**, **42**, **47** and **115**

Potent and selective NNMT inhibitors are valuable tools to investigate the role of its biological activity and to know the catalytic function.

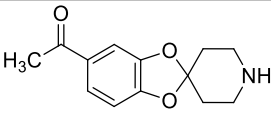
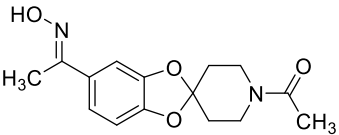
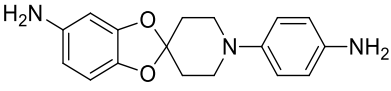
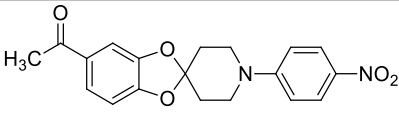
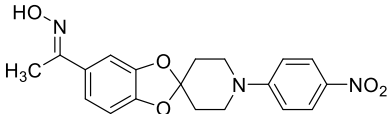
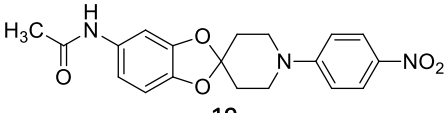
### ARGINASE INHIBITION

Arginase is an intracellular enzyme that hydrolyses L-arginine to ornithine and urea. In mammals there are two arginase isoenzymes which differ in their subcellular location. ARG1 is cytoplasmic and ARG2 is mitochondrial. Arginase plays an important role in the immune response with high ARG1 expression and activity seen in both M2 macrophages and myeloid-derived suppressor cells (MDSC). Arginase has become a target of interest for oncology to stimulate the immune system when used in combination with checkpoint inhibitors.<sup>204</sup>

Eli Lilly carry out an evaluation of the enzymatic modulation of the human arginase through liquid chromatography and mass spectrometry (LC/MS), obtaining as a result the percentage of inhibited enzyme (Table 12).

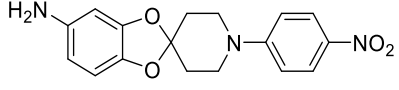
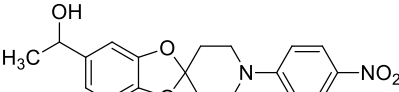
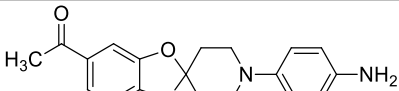
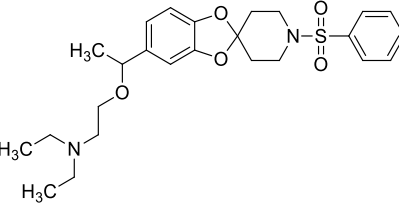
Small molecules as arginase inhibitors are described as promising compounds for the treatment of several diseases such as cardiovascular, cancer, immune disorders, asthma and others.<sup>205</sup>

**Table 12.** Determination of arginase inhibition

ARGINASE	
COMPOUND	Primary SP
	hARG1 MassSpec_No Metal or BSA_384 SP
	% inh. @ 100 $\mu$ M
 <p><b>3</b></p>	15.5
 <p><b>4</b></p>	-10.4
 <p><b>15</b></p>	57.3
 <p><b>17</b></p>	74.5
 <p><b>18</b></p>	28.8
 <p><b>19</b></p>	11

<sup>204</sup> V. Bronte; P. Zanovello. *Nat. Rev. Immunol.* **2005**, 5, 641-654

<sup>205</sup> M. Pudio; C. Demougeot; C. Girard-Thernier. *Med. Res. Rev.* **2017**, 37, 475-513

 <p style="text-align: center;"><b>20</b></p>	48.5
 <p style="text-align: center;"><b>21</b></p>	13
 <p style="text-align: center;"><b>23</b></p>	38.7
 <p style="text-align: center;"><b>33</b></p>	35.4

SP: single point

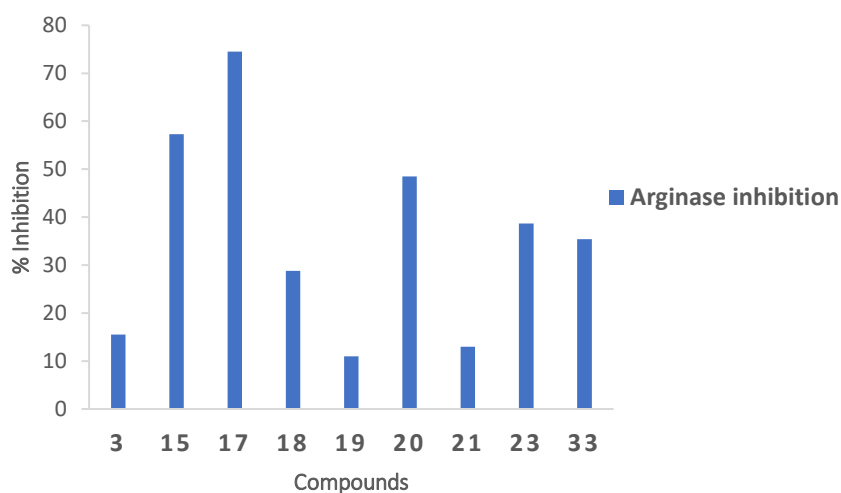


**Figure 67.** Graphic of the most significant products with their arginase inhibition percentage

The evaluated compounds show a slight arginase inhibitory activity at 100  $\mu$ M. Compounds **15**, **17** and **20** are those with the greatest inhibitory power of the enzyme. The spiranic derivative **17** turns out to be the most powerful in these tests. The simple reduction of the nitro group to amino leads to a 50% reduction of inhibitory activity (Table 12, compare **17** and **23**).

Comparing the results of **17** and **20** it is demonstrated that the change of acetyl group of C-5 by an amino group leads to a decrease in the inhibitory capacity of arginase.

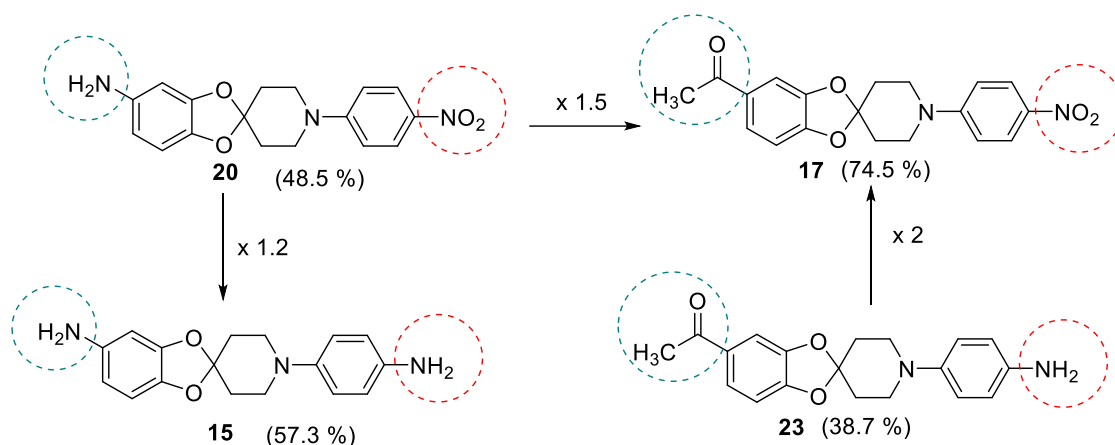


Figure 68. Comparison of the results of 15, 17, 20 and 23

### CD73 INHIBITION

CD73 is an enzyme in human encoded *NT5E* gene. It is an extracellular enzyme that catalyzes a rate-limiting step in the conversion of ATP to adenosine. It serves as an immune suppressant that impairs antitumor immune responses and enhances tumor immune escape via activation of adenosine receptors. It generates immunosuppressive adenosine within hypoxic tumor microenvironment which leads to abnormality in immune cell infiltration, tumor progression, metastasis and poor disease outcomes. Knock-out in mice has shown a significantly protection against development of tumor and metastasis. Therapies targeting CD73 may lead to novel cancer immune therapy.<sup>206</sup> Eli Lilly runs a RapidFire Mass Spectrometry as a primary assay, giving as a result a percentage of inhibition, to discover new potential anti CD73 compounds (Table 13).<sup>206</sup> None of the compounds (**3**, **33**) tested showed activity.

Table 13. Determination of CD73 inhibition

CD73 INHIBITOR	
COMPOUND	Primary SP
	CD73 MassSpec SP
	% Inh. @ 50 $\mu$ M
<p><b>3</b></p>	-1.1
<p><b>33</b></p>	-

SP: single point

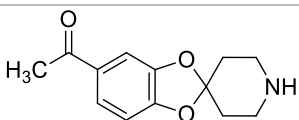
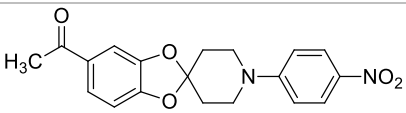
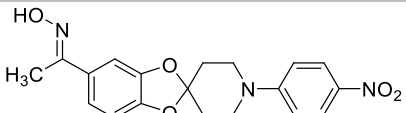
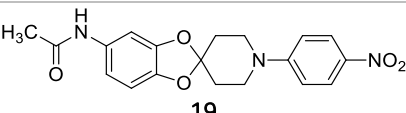
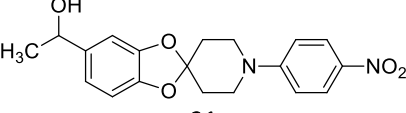
<sup>206</sup> B. Allard; S. Pomme; M. J. Smyth; J. Stagg. *Clin. Cancer Res.* **2013**, *19*, 5626-5635

### 3.2.2. IMMUNOLOGY

#### INHIBITION OF IL-17

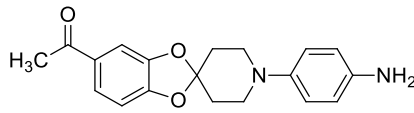
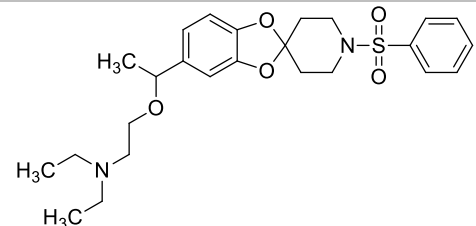
The IL-17A (Th17/ interleukin) has three main roles: host defense against extracellular bacteria and fungi, neutrophil homeostasis and chronic pathogenic inflammation. It is expressed by a subset of T cells, called Th17 cells, at inflammatory sites. The IL-17 family includes 6 cytokines: IL-17A, IL-17B, IL-17C, IL17-D, IL-17E and IL-17F. Most type of cells can respond to the local production of IL-17A because of the near ubiquitous expression of IL-17A receptors, IL17-AR and IL17-RC. IL-17A plays a role in maintaining a proinflammatory state in the site of injury or inflammation through stimulating the release of cytokines and chemokines, designed to recruit and activate both, neutrophils and memory T cells. IL-17A producing “pathogenic” T cells contribute to the pathogenesis of autoimmune diseases, including psoriasis, psoriatic arthritis, rheumatoid arthritis and ankylosing spondylitis. Neutralizing antibodies to IL-17A have demonstrated profound clinical efficacy in patients with plaque psoriasis.<sup>207</sup> The assay carried out by Eli Lilly measures the interaction protein-protein between the IL-17A and its specific antibody through AlphaLisa IL-17A (Table 14).<sup>207</sup> There are currently three antibodies approved for the treatment of psoriasis, two monoclonal antibodies targeting IL-17A (*secukinumab* and *ixekizumab*) and one against IL-17 receptor (*brodalumab*).<sup>208</sup>

**Table 14.** Determination of IL-17 inhibition

IL-17 PROTEIN-PROTEIN INTERACTION	
COMPOUND	Primary SP
	IL-17A AlphaLisa SP % Inh. @ 100 $\mu$ M
 <p style="text-align: center;"><b>3</b></p>	5.8
 <p style="text-align: center;"><b>17</b></p>	61.8
 <p style="text-align: center;"><b>18</b></p>	30
 <p style="text-align: center;"><b>19</b></p>	26.4
 <p style="text-align: center;"><b>21</b></p>	21.4

<sup>207</sup> S. L. Gaffen. *Nat. Rev. Immunol.* **2009**, 9, 556-567

<sup>208</sup> M. Amin; K. Darji; D. J. No; T. Bhutani; J. J. Wu. *J. Dermatol. Treat.* **2018**, 29, 347-352

 <p style="text-align: center;"><b>23</b></p>	39.6
 <p style="text-align: center;"><b>33</b></p>	6.7

SP: single point

These compounds **3**, **17**, **18**, **19**, **21**, **23** and **33** were tested at a concentration of 100  $\mu$ M and the results of interaction with the protein were moderate. The nitro derivative **17** was the most active with 62% inhibition. The reduction of the nitro to amino group and the reduction of the ketone to alcohol lead to a notable decrease in activity (compare **17** and **23**). The other compounds (**3**, **18**, **19**, **21** and **33**) showed poor activity on this target.

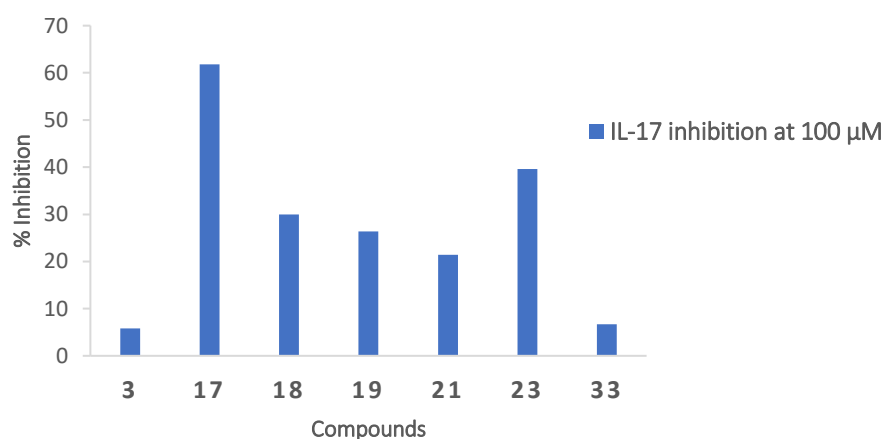


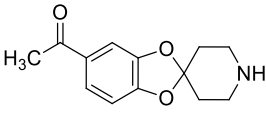
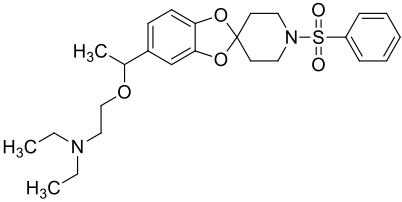
**Figure 69.** Graphic of the most significant products with their IL-17 inhibition percentage

IL-17 is produced and secreted by at least two classes of lymphocytes, CD4<sup>+</sup> T cells (Th17) and  $\delta\gamma$ . The IL17 phenotypic drug discovery module seeks to identify inhibitors of IL-17 secretion from human peripheral blood mononuclear cells (PBMCs) following stimulation of memory T cells by IL-23, anti-CD3, and anti-CD28.<sup>209</sup> Eli Lilly performed an assay to find inhibitor compounds of IL-17 secretion without overt cytotoxicity and without affecting secretion of INF $\gamma$  and IL-5, cytokine markers for Th1 and Th2 T cell subset, respectively (Table 15).<sup>210</sup>

<sup>209</sup> O. Ouyang; J. K. Kolls; Y. Zheng. *Immunity* **2008**, 28, 454-467

<sup>210</sup> <https://openinnovation.lilly.com> (20/12/2018)

**Table 15.** Determination of IL-17 secretion inhibition

IL-17 SECRETION	
COMPOUND	Primary SP
	antiCD3/antiCD28/IL23_PBMC ELISA IL-17 sec Inh.
	% Inh. @ 10 $\mu$ M
 <p><b>3</b></p>	17.8
 <p><b>34</b></p>	38.5

SP: single point

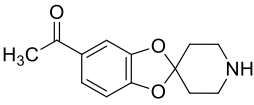
Regarding the inhibition of the secretion of IL-17, it should be noted that the spiro-derivative **34** shows a 38.5% inhibition at 10  $\mu$ M, while the derivative **3** of simplified structure has a significant decrease of the inhibition activity.

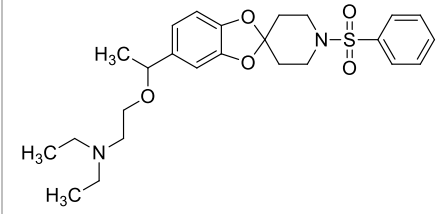
### 3.2.3. TROPICAL DISEASES AND NEGLECTED

#### MALARIA

Malaria is a disease caused by the parasite *Plasmodium*. Eli Lilly working with Medicines for Malaria Venture (MMV) are partnering to find compounds that can play an important role in the fight to eradicate malaria. The screening module is designed to test compounds in primary assays that target activity against liver stages of the parasitic strain of *Plasmodium berghei* (Pb), in particular, against the sporozoite infection and the viability of liver schizonts of liver cells. To evaluate parasitic growth, activity in the asexual blood stages of the parasite *Plasmodium falciparum* (DD2 strain) will be tested as well as non-specific cytotoxicity screen (Table 16).<sup>210</sup> The treatment of malaria depends of type of infection, severity of infection, status of the host and other performed conditions.

**Table 16.** Determination of malaria inhibition

MALARIA			
COMPOUND	Primary SP		
	<i>P. falciparum</i> DD2 (Malaria parasite) Inh.	NV- <i>P. berghei</i> EEF parasite viability HepG2 SP	HepG2 cytotox SP MMV
	% Inh. @ 12.5 $\mu$ M	% Inh. @ 10 $\mu$ M	% Inh. @ 10 $\mu$ M
 <p><b>3</b></p>	2.6 -13.2 -6.7 5.3	22.1 52.3 35.7 -2.2	2.2 -2.2

 <p style="text-align: center;"><b>33</b></p>	10.4	87.7	
	51.4	89.5	12.9
	19.3	82	4.4
	65.3	87.2	

SP: single point

Of the two products evaluated for the treatment of malaria, compound **33** shows better activity than derivative **3**. Structural simplification, in this case, has reduced antimalarial activity. Regarding the obtained results, **33** reduces the viability of *P. berghei* more than that of *P. falciparum*.

It should be noted that **33** has an interesting antimalarial activity and minimal toxicity. These results lead to **33** being taken as a model for the design of new compounds.

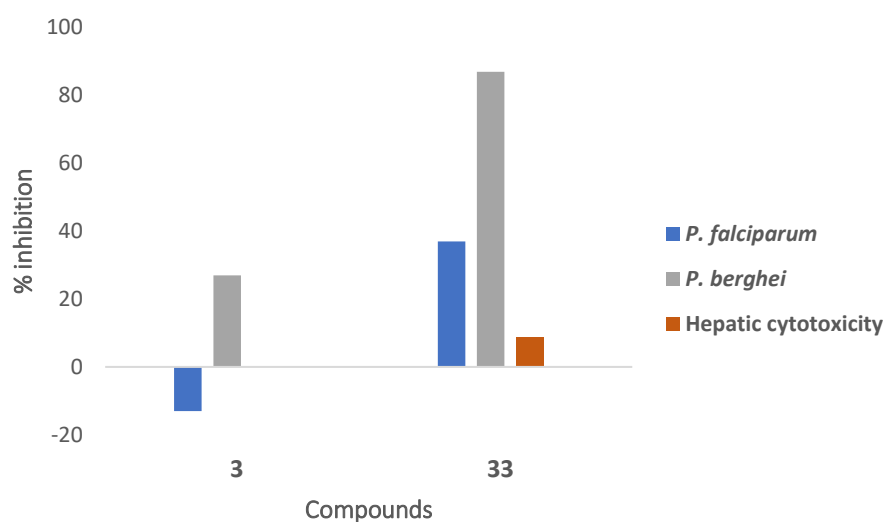


**Figure 70.** Graphic of the malaria average inhibitory percentage for products **3** and **33**

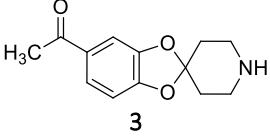
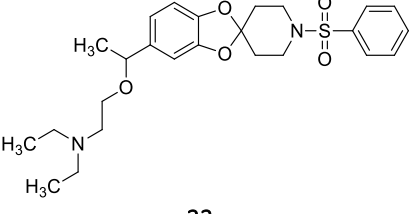
### CHAGAS

Eli Lilly performs a growth inhibition (in NIH-3T3 cells), a trypomastigote luciferin-based and a cytotoxicity test as a primary assay. Then, *T. cruzi* CYP51 inhibition and *T. cruzi* intracellular Imaging Rate of Kill (RoK) kinetic as a secondary assay (Table 17 and 18).<sup>211</sup>

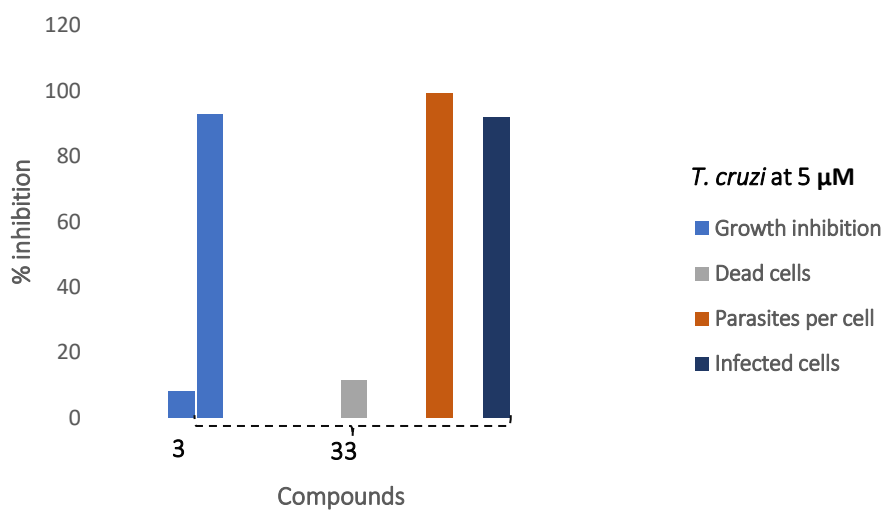
<sup>211</sup> J. A. Padilla; I. Cotillo; J. Presa; J. Cantizani; I. Peña; A. I. Bardera; J. J. Martín; A. Rodriguez. *PLoS Negl. Trop. Dis.* **2015**, *9*, e0003493



**Table 17.** Determination of chagas inhibition with primary SP

CHAGAS DISEASE					
COMPOUND	Primary SP				
	<i>T. cruzi</i> Growth Inh.	NV- Basal_Viability <i>T.</i> <i>cruzi</i> CTG Inh.	NV- <i>T. cruzi</i> m. Dead Cells	NV- <i>T. cruzi</i> m. Parasites per Cell	NV- <i>T. cruzi</i> m. Infected Cells
	% Inh. @ 5 $\mu$ M	% Inh. @ 5 $\mu$ M	% Inh. @ 5 $\mu$ M	% Inh. @ 5 $\mu$ M	% Inh. @ 5 $\mu$ M
 <p><b>3</b></p>	8.2	-	-	-	-
 <p><b>33</b></p>	92.1 93.6 92.4	-15.7 -24.4	18.6 4.1	99.2 99.3	90.9 92.6

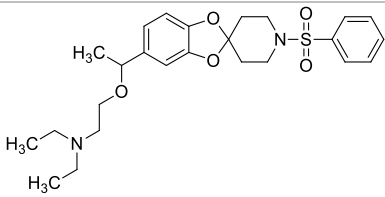
SP: single point. m: myocardiocyte



**Figure 71.** Graphic of the *T. cruzi* average inhibitory percentage for products **3** and **33**

As in previous cases, compound **33** has more activity against *T. cruzi* than analog **3**. The high growth inhibitory activity of *T. cruzi* at 5  $\mu$ M opens the door to other complementary studies that are currently being carried out.

**Table 18.** Determination of chagas inhibition with primary CRC and secondary assay for compound **33**

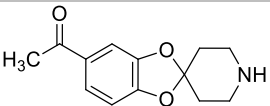
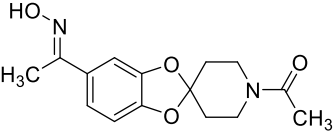
COMPOUND	CHAGAS DISEASE			
	Primary CRC			Secondary
	NV- <i>T. cruzi</i> m. Dead Cells	NV- <i>T. cruzi</i> m. Infected Cells	NV- <i>T. cruzi</i> m. Parasites per Cell	NV-Basal_Viability HepG2 CTG Inh. CRC
	pIC50 (M)	pIC50 (M)	pIC50 (M)	pIC50 (M)
 <p style="text-align: center;"><b>33</b></p>	<4.3	5.8	6.2	4.6
	<4.3	6.5	6.2	4.7

CRC: concentration response curve. m: myocardiocyte

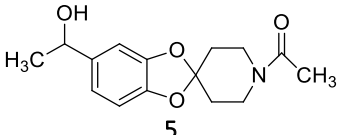
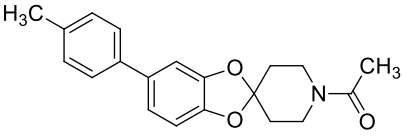
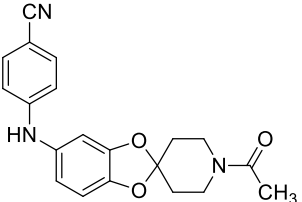
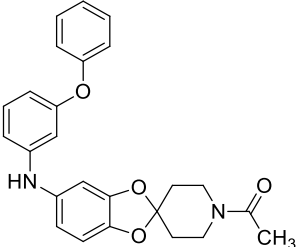
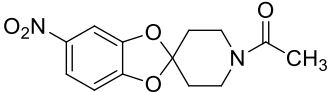
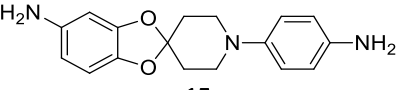
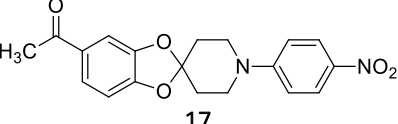
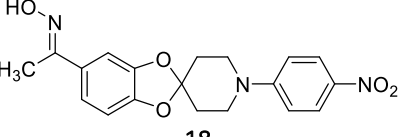
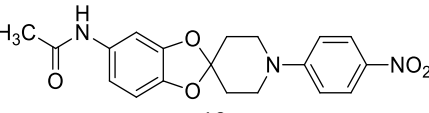
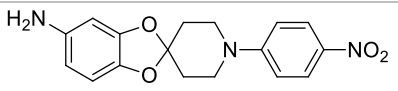
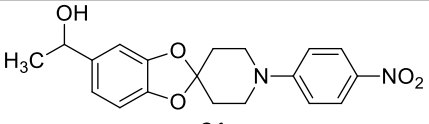
### TUBERCULOSIS

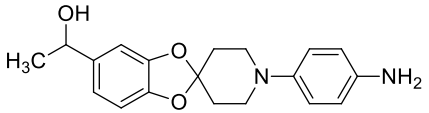
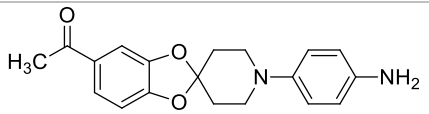
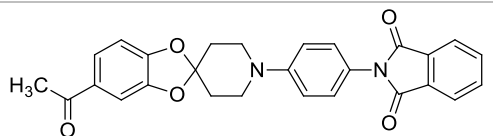
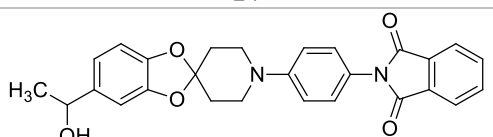
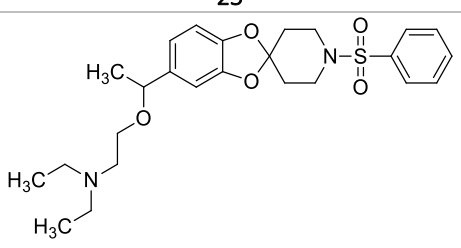
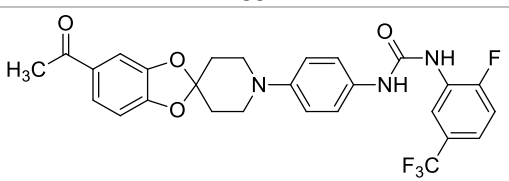
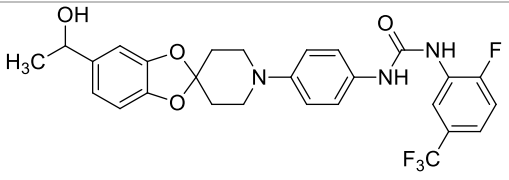
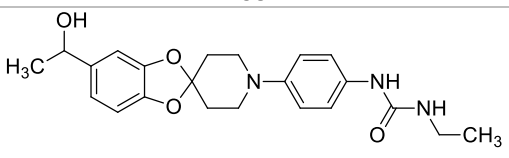
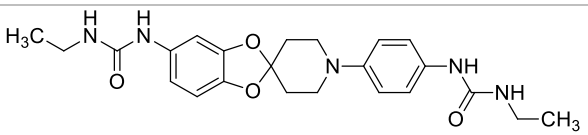
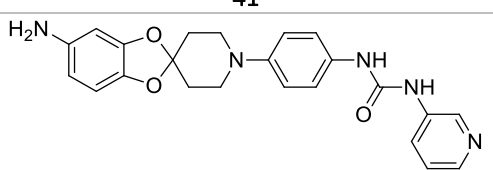
Screening chemical libraries is the first crucial step in the antimicrobial discovery process. Potential antimycobacterial agents are identified by testing chemicals for the ability to inhibit *M. tuberculosis* growth under *in vitro* growth conditions in culture medium. However, *in vitro* screening results are often misleading, as the culture broth does not reflect the environment *M. tuberculosis* encounters *in vivo* during the natural course of the disease, neglecting important factors such as compound activation, membrane permeability, removal by efflux pump, and toxicity to mammalian cells. Also, metabolic changes that *M. tuberculosis* undergoes within the host may affect the compound activity. *Ex vivo* screening, in the macrophage, may represent physiological conditions that mimic the disease and take into consideration the favorable contribution of host cells in the process of eradicating MTB.<sup>212</sup> In order to discover new active compounds against intracellular *M. tuberculosis*, the OIDD compounds will be screened using the protocol developed at Tres Cantos, which uses THP-1 human monocytes infected with MTB strains expressing luciferase (Table 19).<sup>212</sup>

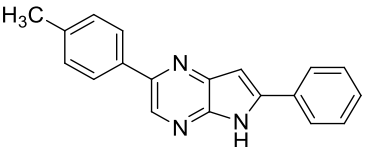
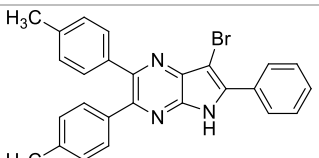
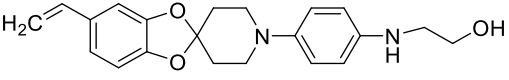
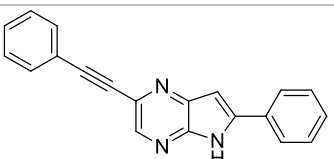
**Table 19.** Determination of tuberculosis inhibition

COMPOUND	TUBERCULOSIS	
	Primary SP	
	TB MIC SP IDRI OIDD	% Inh. @ 20 $\mu$ M
 <p style="text-align: center;"><b>3</b></p>		20.1
 <p style="text-align: center;"><b>4</b></p>		7.8

<sup>212</sup> E. Sorrentino; R. G. del Rio; X. Zheng; J. P. Matilla; P. T. Gomez; M. M. Hoyos; M. E. P. Herran; A. M. Losana; Y. Av-Gay. *Antimicrob. Agents Chemother.* **2016**, *60*, 640-645

 <p style="text-align: center;"><b>5</b></p>	6.3
 <p style="text-align: center;"><b>7</b></p>	3.8
 <p style="text-align: center;"><b>10</b></p>	6.8
 <p style="text-align: center;"><b>11</b></p>	13.2
 <p style="text-align: center;"><b>12</b></p>	-2.7
 <p style="text-align: center;"><b>15</b></p>	-2.1
 <p style="text-align: center;"><b>17</b></p>	7.7 -1.8
 <p style="text-align: center;"><b>18</b></p>	6.6 1.7
 <p style="text-align: center;"><b>19</b></p>	23.6 5.1
 <p style="text-align: center;"><b>20</b></p>	1.6
 <p style="text-align: center;"><b>21</b></p>	18.3 12.7

 <p style="text-align: center;"><b>22</b></p>	-4.3
 <p style="text-align: center;"><b>23</b></p>	5.6 -1
 <p style="text-align: center;"><b>24</b></p>	2
 <p style="text-align: center;"><b>25</b></p>	5.9
 <p style="text-align: center;"><b>33</b></p>	32.4 19.2
 <p style="text-align: center;"><b>37</b></p>	10.2
 <p style="text-align: center;"><b>38</b></p>	6.3
 <p style="text-align: center;"><b>39</b></p>	2.7
 <p style="text-align: center;"><b>41</b></p>	1.7
 <p style="text-align: center;"><b>46</b></p>	-3.3

 <p style="text-align: center;"><b>47</b></p>	6.5
 <p style="text-align: center;"><b>54</b></p>	-4.4
 <p style="text-align: center;"><b>81</b></p>	-8.3
 <p style="text-align: center;"><b>100</b></p>	2

SP: single point. MIC: minimum inhibitory concentration

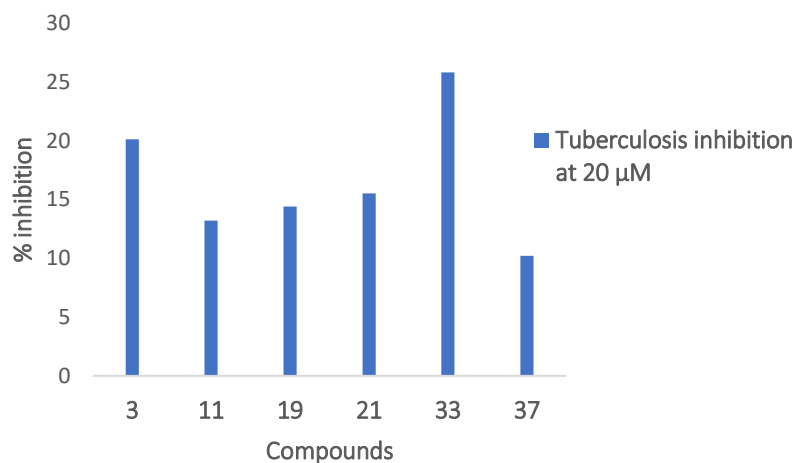


**Figure 72.** Graphic of the most significant products with their tuberculosis inhibition percentage

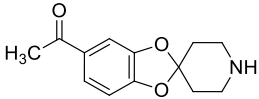
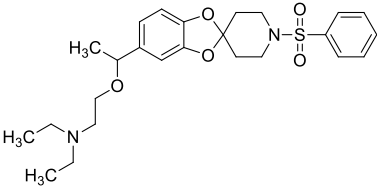
The results of growth inhibitory *M. tuberculosis* at 20 μM of the evaluated compounds show a low to moderate activity. In this case, compound **33** is again the one that shows the best activity. The pyrrolopyrazines show almost no activity against *M. tuberculosis*.

### 3.2.4. NEURODEGENERATION AND PAIN

#### TRK-A

Tropomyosin-related kinase A is one of the two receptors identified for Nerve Growth Factor (NGF). The mechanism of action of the anti-NGF drug class has been largely attributed to a reduction in signaling through Trk-A receptors on nociceptive sensory neurons. Hereditary sensory and autonomic neuropathy type IV (HSANIV) has been linked to defective mutations in Trk-A, and is characterized by mental retardation, reduced sweating, and profound loss of pain sensitivity. Trk-A receptors have been implicated in the acute effects of NGF on the sensitization of peripheral nerves, contributing to allodynia and hyperalgesia, particularly associated with thermal stimuli.<sup>213</sup> These data suggest that Trk-A receptor antagonist or Trk-A kinases inhibitors may provide a novel therapeutic approach to chronic pain. In order to identify compounds with high potency and selectivity for blocking Trk-A receptor Eli Lilly runs a Pathhunter ANT (antibody therapeutics) as a primary assay (Table 20).

**Table 20.** Determination of TRK-A inhibition

TRK-A	
COMPOUND	Primary SP
	hTrka-P75 Pathhunter ANT SP
	% Inh. @ 15 $\mu$ M
 <b>3</b>	-10.6
 <b>33</b>	-21.1

SP: single point

The compounds evaluated in this case do not show any type of TRK-A inhibition. Both **3** and **33** enhance the activity of the protein TRK-A at 15  $\mu$ M.

#### PROTEIN TRANSLATION INHIBITION FOR ALZHEIMER DISEASE

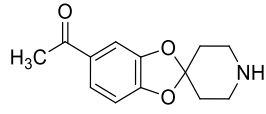
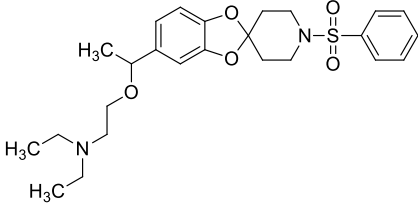
The Alzheimer disease is characterized by the extracellular accumulation of amyloid plaques and intracellular formation of neurofibrillary tangles (NFTs). The former is composed by A $\beta$  protein and the latter are composed of tau protein. The actual strategies to fight the disease are focused on removing or preventing the accumulation of these disease-associated proteins, because regulating or inhibiting the expression of such proteins, at a protein translation level, may also have therapeutic benefit.<sup>214</sup>

<sup>213</sup> P. W. Manthy; M. Koltzenburg; L. M. Mendell; L. Tive; D. L. Shelton. *Anesthesiology* **2011**, *115*, 189-204

<sup>214</sup> S. L. Devos; R. L. Miller; K. M. Schoch; B. B. Holmes; C. S. Kebodeaux; A. J. Wegener; G. Chen; T. Shen; H. Tran; B. Nichols; T. A. Zanardi; H. B. Kordasiewicz; E. E. Swayze; C. F. Bennett; M. I. Diamond; T. M. Miller. *Sci. Tranl. Med.* **2017**, *9*, eaag0481

Eli Lilly runs a reporter inhibition assay in Huh7 (human liver cells) giving as a result a percentage of inhibition (Table 21).

**Table 21.** Determination of TAU protein inhibition

TAU PROTEIN TRANSLATION INHIBITOR	
COMPOUND	Primary SP
	hTau Huh7 TT Inh. SP
	% Inh. @ 40 $\mu$ M
 <p><b>3</b></p>	24.7
 <p><b>33</b></p>	100.6

SP: single point

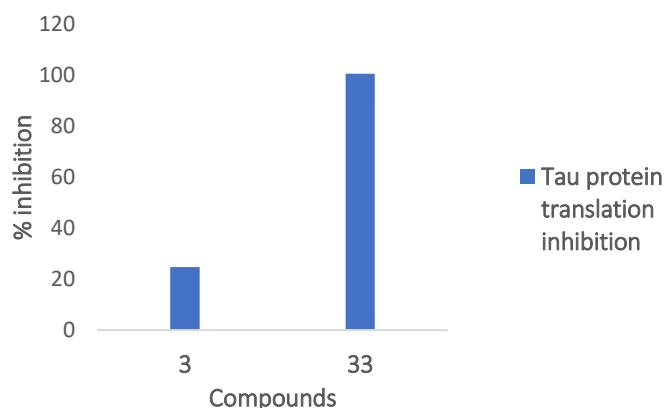


**Figure 7.** Graphic of the tau protein translation inhibition percentage for products **3** and **33**

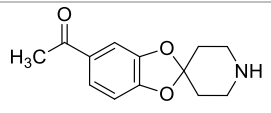
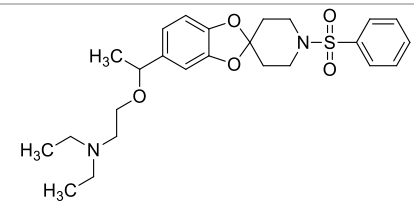
Compound **33** has shown excellent inhibitory activity of the TAU protein at 40  $\mu$ M. Derivative **3** shows an activity five times lower. It would be of interest to submit the spiroderivative **33** to other trials to confirm the excellent activity.

#### *CALCITONIN GENE-RELATED PEPTIDE (CGRP) RECEPTOR ANTAGONIST*

CGRP is a 37 aminoacid neuropeptide that plays a key role in the patho-physiology of migraine. CGRP levels in venous plasma have been reported to be elevated during a migraine attack and infusion of it into individuals with a past history of migraine attacks can induce an attack. Receptor antagonist of CGRP have successfully treated migraine attacks. Eli Lilly runs the CGRP cAMP assay test for compounds that inhibit the activation of CGRP receptor and the resulting generation of cAMP by CGRP (Table 22).<sup>215</sup>

<sup>215</sup> N. T. Redpath; Y. Xu; N. J. Wilson; L. J. Fabri; M. Baca; A. E. Andrews; H. Braley; P. Lu; C. Ireland; R. E. Ernst; A. Woods; G. Forrest; Z. An; D. M. Zaller; W. R. Strohl; C. S. Luo; P. E. Czabotar; T. P. Garrett; D. J. Hilton; A. D. Nash; J. G. Zhang; N. A. Nicola. *Structure* **2010**, *18*, 1083-1093

**Table 22.** Determination of CGRP inhibition

CGRP ANTAGONIST			
COMPOUND	Primary SP	Primary CRC	
	hCGRP1 cAMP	hCGRP1 cAMP	
	% Inh. @ 30 $\mu$ M	IC <sub>50</sub> ( $\mu$ M)	Kb ( $\mu$ M)
 <p><b>3</b></p>	-80.6	-	-
 <p><b>33</b></p>	76.3	>30 10.7*	7570.1 2690.7

SP: single point. CRC: concentration response curve. \* The CRC is showed hereunder

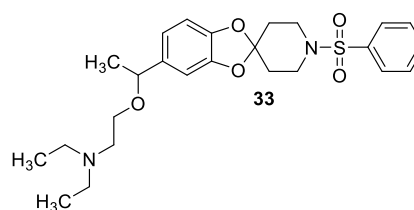
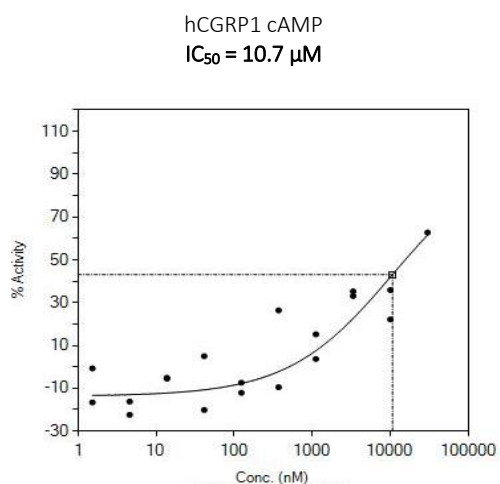


**Figure 74.** Concentration response curve of product **33** in hCGRP1 inhibition

It is repeated again that compound **33** has an interesting activity profile, in this case it is an antagonist activity on the receptors of CGRP.

### NAV1.7 ANTAGONIST

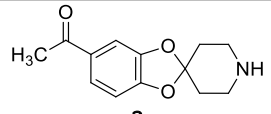
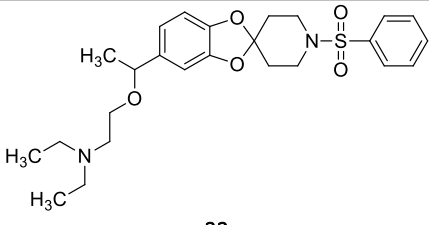
Nav1.7 is encoded by the SCN9A gene and is one of nine currently described voltage-gated sodium ion channels. All sodium channels in this family are involved in action potential generation, propagation, and/or neurotransmitter release in excitable tissues. Interest in Nav1.7 as a potential therapeutic target for pain comes from several converging lines of evidence. Patients with activating or gain function mutations in Nav1.7 display varying degrees of chronic and intermittent pain.<sup>216</sup> Together, the efficacy of nonselective sodium channel inhibitors combined with the wealth of genetic information strongly suggest that selective Nav1.7 inhibitors may provide a novel therapeutic approach to chronic pain of different etiologies without significant safety/tolerability side-effects. Hence, Eli Lilly performs an Ion Works Quattro electrophoresis assay in HEK293 cell line (from human embryonic kidney) and a target based

<sup>216</sup> S. D. Dib-Hajj; Y. Yang; J. A. Black; S. G. Waxman. *Nat. Rev. Neurosci.* **2013**, *14*, 49-62



inhibitory assay in Huh7 cell line (human hepatocyte-derived carcinoma), to identify compounds with high potency and selectivity for blocking Nav1.7 channels (Table 23).<sup>210</sup>

**Table 23.** Determination of NAV 1.7. inhibition

NAV 1.7. ANTAGONIST		
COMPOUND	Primary SP	
	hNav1.7 IWQ	hNav1.7 Huh7 TT Inh. SP
	% Inh. @ 3 $\mu$ M	% Inh. @ 40 $\mu$ M
 <p><b>3</b></p>	9.7	25.6
 <p><b>33</b></p>	40.6	98.2

SP: single point

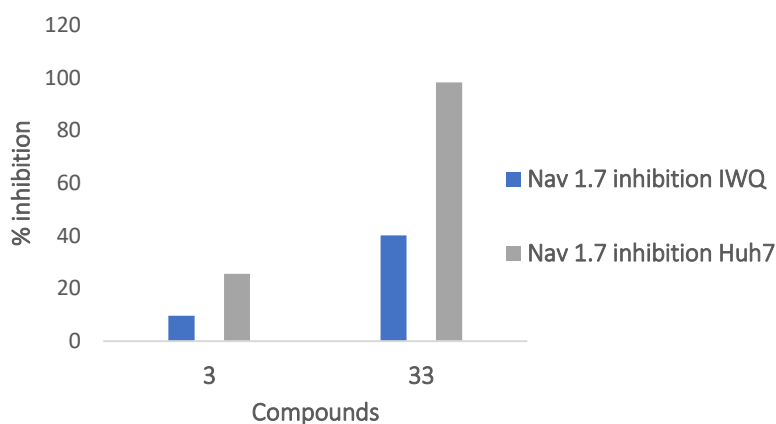


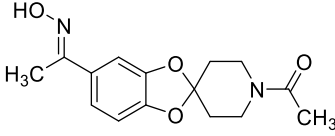
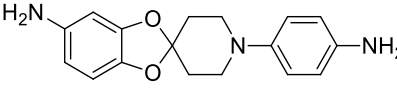
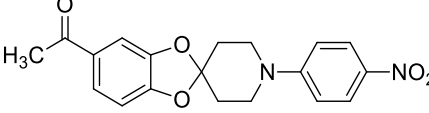
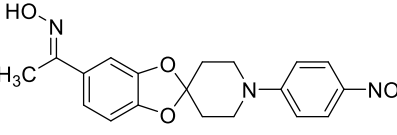
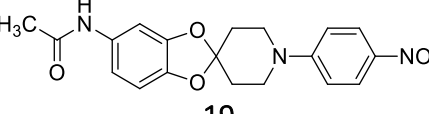
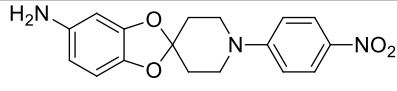
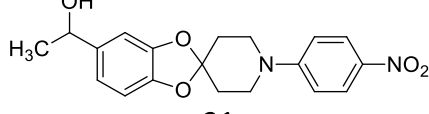
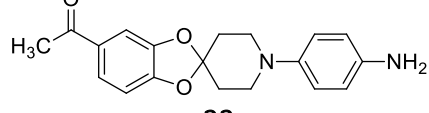
**Figure 75.** Graphic of the Nav 1.7 inhibition percentage for products **3** and **33**

#### KCNQ2/3 AGONIST

KCNQ2/3 is a heteromeric voltage-gated potassium channel. Together with other members of the Kv7 subfamily of voltage-gated potassium channels, KCNQ2/3 underlies the neuronal M-current that modulates excitability in many neurons of the central and peripheral nervous system. It is exclusively expressed in the nervous system, and it is the predominant subtype in pain sensing neurons in the dorsal root ganglion (DRG) and spinal cord. Agonist of KCNQ2/3 hyperpolarize sensory neurons, reduce excitability and show efficacy in rodent models of persist pain. The fluorescence-based thallium flux FLIPR assay carried by Eli Lilly measures functional activity of ligand and voltage-gated potassium channels in a HEK293 cell type (Table 24).<sup>217</sup>

<sup>217</sup> X. Du; H. Hao; S. Gigout; D. Huang; Y. Yang; L. Li; C. Wang; D. Sundt; D. B. Jaffe; H. Zhang; N. Gamper. *Pain* **2014**, *155*, 2306-2322

**Table 24.** Determination of KCNQ2-3 stimulation

KCNQ2-3 AGONIST	
COMPOUND	Primary SP
	hKCNQ2/3 FluxOR Ag SP % Stim @ 10 $\mu$ M
 <b>4</b>	-6.7 5
 <b>15</b>	-5.4 2
 <b>17</b>	-3 -1.4
 <b>18</b>	-1.1 6.5
 <b>19</b>	-2.6 -2.5
 <b>20</b>	-1.6 -8.2
 <b>21</b>	-2.9 -5.9
 <b>23</b>	-2.3 18.2

SP: single point

None of the evaluated compounds have shown stimulatory activity of KCNQ2/3. The results indicate, in some cases, a slight inhibitory activity.

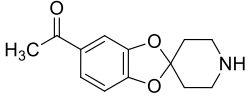
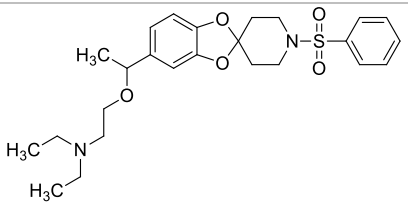
### 3.2.5. ENDOCRINE/CARDIOVASCULAR

#### GLP-1 SECRETION

Glucagon like peptide 1 is derived from transcription of the proglucagon gene. Its secretion by ileal L cells is dependent on the presence of nutrients in the lumen of the small intestine. It is a potent anti-hyperglycemic hormone inducing glucose-dependent insulin secretion and suppressing glucagon secretion. When the glucose in the plasma is in the fasting range stage, the

GLP-1 does not stimulate the secretion of insulin. Diabetes phenotypic module identifies compounds that stimulate secretion of GLP-1 in mouse and human cell lines derived from gastrointestinal tract tissue.<sup>210</sup> GLP-1 secretion is measured by Eli Lilly using ELISA assay that was specifically designed to detect the appropriate forms of GLP-1 secreted from these cells (Table 25).

**Table 25.** Determination of GLP-1 stimulation

GLP-1 SECRETION				
COMPOUND	Primary SP			
	mSTC-1 GLP1 Sec SP		hNCI-H716 GLP1 Sec SP	
	% Stim @ 20 $\mu$ M	% Stim @ 2 $\mu$ M	% Stim @ 20 $\mu$ M	% Stim @ 2 $\mu$ M
 <p><b>3</b></p>	-0.8	-3.5	0.1	-0.4
 <p><b>33</b></p>	-5.2	-0.9	3.5	0.2

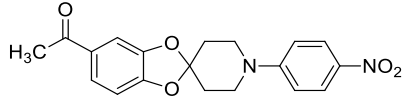
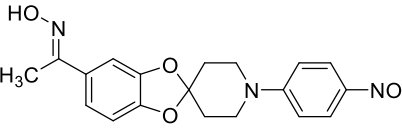
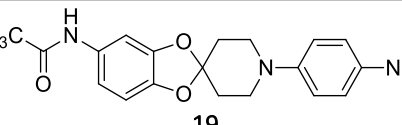
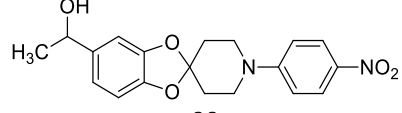
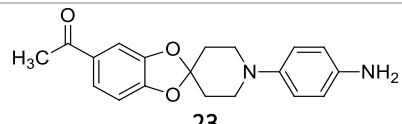
SP: single point

### PCSK9 INHIBITION

Proprotein convertase subtilisin kexin type 9 (PCSK9) belongs to the proteinase K subfamily of secretory proteases. This protein plays a major regulatory role in cholesterol homeostasis. It regulates plasma LDL-cholesterol (LDL-C) levels by directing LDL receptor (LDLR) to lysosomal degradation, resulting in reduced LDL clearance and accumulation of LDL in circulation. So, gain function mutations of PCSK9 lead to hyperlipidemia and premature coronary artery disease (CAD) in humans, whereas loss of function mutations of PCSK9 are associated with lower levels of LDL and protection from CAD. Therapeutic antibodies are demonstrating impressive efficacy in LDL lowering either as a monotherapy or combination therapy with statins. After this strong clinical validation, small molecule inhibitors of PCSK9 are being actively sought. PCSK9 protein expression is actively regulated at transcription and post transcriptional levels. The PCSK9 phenotypic module is designed to identify compounds that inhibit expression of PCSK9 protein multiple cell systems, including human hepatoma cell lines (Huh7), HeLa cells, and primary human hepatocytes. Eli Lilly runs an Alphascreen and a CellTiter-Glo<sup>®</sup> luminescent cell viability assay in Huh7 cell lines as a primary assay to identify possible inhibitors (Table 26 and 27).<sup>218</sup>

<sup>218</sup> S. Crunkhorn. *Nat. Rev. Drug Discov.* **2012**, *11*, 189-189

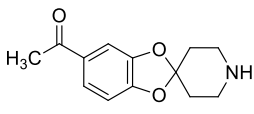
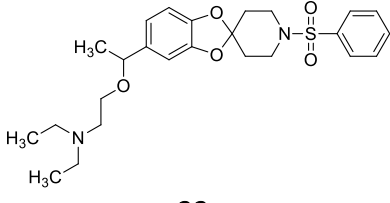
**Table 26.** Determination of PCSK-9 inhibition

PCSK9 Inhibition		
COMPOUND	Primary SP	
	PCSK9 AlphaLisa Huh7 SP	PCSK9 Huh7 Viability CellTiter-Glo SP
	% Inh. @ 5 $\mu$ M	% Inh. @ 5 $\mu$ M
 <p><b>17</b></p>	-6.7	6
 <p><b>18</b></p>	-1.2	18.4
 <p><b>19</b></p>	9.2	7.7
 <p><b>20</b></p>	1.2	17
 <p><b>23</b></p>	-74.2	0.3

SP:

single point

**Table 27.** Determination of PCSK-9 inhibition

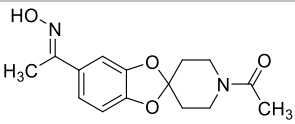
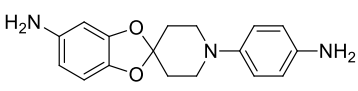
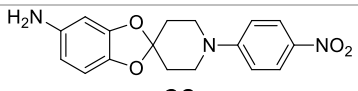
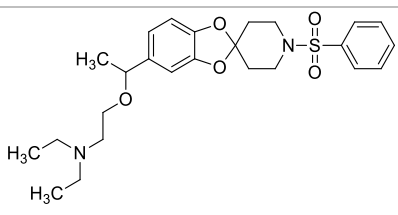
PCSK9 INHIBITOR (EFFORT-1)						
COMPOUND	Primary SP		Primary CRC		Confirmatory	
	Basal_PCS K9 HepG2 SP	Basal_PCS K9 HepG2 Cell Health	Basal_PCS K9 HepG2 Cell Health	Metridia luc HepG2 Non Specific Secretion Inh.	PCSK9 ELISA RPH SP	
	% Inh. @ 5 $\mu$ M	% Inh. @ 5 $\mu$ M	IC50 ( $\mu$ M)	IC50 ( $\mu$ M)	% Inh. @ 100 $\mu$ M	% Inh. @ 20 $\mu$ M
 <p><b>3</b></p>	42.3	-0.7	>50	>50	4.5 -22.1	-5.7 -0.8 -9.6 1.6
 <p><b>33</b></p>	-80.7	0.79	-	-	-	-

SP: single point

### 3.2.6. ELANCO ANIMAL HEALTH

Animal welfare is highly compromised by parasites. Because of the growing issue about the resistance to existing antiparasitic treatments the options are limited. Synergic with human welfare exist due to zoonotic potential and overlapping spectrums with human diseases. Eli Lilly performs an assay with the whole organism motility phenotypic screening that enables the quick and highly relevant assessment of antiparasitic potential (Table 28).<sup>210</sup>~~Error! No s'ha definit el marcador.~~

**Table 28.** Determination of antiparasitic potential

ELANCO HEALTH ANIMAL						
COMPOUND	Primary SP					Primary CRC
	NV-D. immitis Mobility Inh. SP Elanco	NV-H. contortus Mobility Inh. SP Elanco		NV-A. aegypti Mobility Inh. SP Elanco		NV-A. aegypti Mobility Inh. CRC Elanco
	%Inh. @ 5 $\mu$ M	%Inh. @ 5 $\mu$ M	%Inh. @ 8 $\mu$ M	%Inh. @ 10 $\mu$ M	%Inh. @ 5 $\mu$ M	Rel IC50 ( $\mu$ M)
 <p><b>4</b></p>	-4 0	10 -1	-	2 -5	-	-
 <p><b>15</b></p>	-1 0	11 1	-	1 3	-	-
 <p><b>20</b></p>	0 0	7 1	-	14 56	-	-
 <p><b>33</b></p>	32 34	-	34 31	-4 -5	-11 69	>10 >10

SP: single point

Finally, these last tests show, in most of the cases, results with a lower than per cent of inhibition, so even they are not significant to continue its studies in such targets, the results have been included in order to highlight the importance of relationship between structure-activity, a preliminary activity that helps to continue our work.

### 3.3. DISCOVERING NEW TARGETS- Quantitative Biology in Eli Lilly & Company

The work accomplished in Eli Lilly & Company was focused on a family of drug targets known as G-protein coupled receptors (GPCRs). An untapped subfamily of GPCRs is exemplified by the 33 adhesion receptors that exist in mammals.<sup>219</sup> This adhesion family of GPCRs is considered 'dark' due to the fact that very few small or large molecule ligands are known for these proteins. This is primarily due to a lack of assay approaches to investigate their cellular pharmacology as commented before in the introduction of this work.

GPCRs are found ubiquitously in the human body. GPCRs are important drug targets to attenuate inflammation, cancer, cardiac dysfunction, diabetes, and others.<sup>220,221</sup> Therefore, it is important to describe and summarize their structure, mechanisms, roles and other important concepts as a basis for understanding the GPCRs experiments conducted.

#### 3.3.1. G-PROTEIN COUPLED RECEPTORS (GPCRs)

The GPCRs, also called seven transmembrane receptors, are proteins located in the cell membrane, coupled to heterotrimeric G proteins.<sup>221</sup> The GPCRs are the largest and most diverse membrane receptors in eukaryotes. The exact size of the GPCR superfamily in humans is unknown,<sup>222</sup> but from genome sequence analysis is deduced that at least 810 human genes encoding GPCRs exist.

The existence of GPCRs was demonstrated along the twentieth century by several scientist such as Robert J. Lefkowitz, Martin Rodbell, Alfred G. Gilman, amongst others.<sup>223,224</sup>

#### STRUCTURE

GPCRs have a conserved tertiary structure: seven  $\alpha$ -helices form transmembrane domains, acting as a recognition and connection site and allowing extracellular ligands to modulate intracellular physiology. GPCRs canonically interact with heterotrimeric G-proteins, which are composed by three subunits: alpha, beta and gamma. Physiologically, several ligands bind these receptors: peptide hormones, neurotransmitters, lipids, nucleotides, ions, varying from small molecules to peptides and proteins. Also, the sensation of external stimuli as odor, light or taste is mediated through them. Those receptors with unknown ligand are named as orphan.<sup>225</sup>

Once the receptor has been activated by an agonist ligand it acts as a guanine-nucleotide exchange factor, producing a conformational change in the associated G protein, specifically in  $\alpha$ -subunit, leading to release of GDP subsequent GTP binding on this subunit. Thereafter the  $\alpha$ -subunit-GTP is disassociated from the receptor and from the  $\beta\gamma$ -dimer, and both subunits are able to modulate several intracellular signal transduction pathways.<sup>226</sup>

---

<sup>219</sup> T. Xiao-long; W. Ying; L. Da-li; L. Jian; L. Ming-yao. *Acta Pharmacol. Sin.* **2012**, *33*, 363–371

<sup>220</sup> J. Wang; G. Clarice; A. H. Rockman. *Circ. Res.* **2018**, *123*, 716–735

<sup>221</sup> S. P. Alexander; A. Christopoulos. *Br. J. Pharmacol.* **2019**, *176*, 21–141

<sup>222</sup> <https://www.guidetopharmacology.org> (20/05/2019)

<sup>223</sup> <https://www.britannica.com> (20/05/2019)

<sup>224</sup> M. Rodbell. *Environ Health Perspect.* **1995**, *103*, 338–345

<sup>225</sup> V. V. Gurevich; E. V. Gurevich. *Int. J. Mol. Sci.* **2017**, *18*, e2519

<sup>226</sup> C. J. Folts; S. Giera; T. Li; X. Piao. *Trends Pharmacol. Sci.* **2019**, *40*, 278-293

Based on these features, many GPCRs have been detected in the human genome and many of them are well described in the literature (distribution in human body, ligands, functions and others) and also their roles in diseases. For example, beta-adrenergic receptors<sup>227</sup> and their antagonist (i.e. *bisoprolol*) for the treatment of hypertension and cardiac diseases.<sup>228</sup> GPCRs are involved in Systems as diverse as neurotransmitter and hormonal signaling.

#### CLASSIFICATION

The GPCR superfamily has been sub-divided into classes based on evolutionary homology and with common physiological ligands.

The G protein-coupled receptors (GPCRs) consist in five main families in mammal:<sup>229</sup>

- *Rhodopsin family* (class A): 284 members (plus 380 olfactory receptors)
- *Secretin family* (class B1): 15 members
- *Adhesion GPCR* (class B2): 33 members
- *Glutamate family* (class C): 22 members
- *Frizzled family*: 11 members

#### GPCRS IN DRUG DISCOVERY

GPCRs, due to their wide role in the human body regulating diverse physiological processes and due to their accessible ligand binding sites in the cell membrane have been a point of interest as pharmacological targets. In fact, the GPCRs are the most studied drug targets because of their relevant role in human pathophysiology and their understood and reproduceable pharmacology. It is claimed that 25-50% of approved drugs target GPCRs in different diseases such as cancer, endocrinology, psychiatric conditions, cardiovascular pathologies, among others (Table 29).<sup>230</sup> The untapped potential of the drug-discovery in the GPCR field is thought to be vast.

**Table 29.** Few examples of drugs in different diseases with GPCRs as a targets

Substance	Tradename	Indications	Targets	Approval year
<i>Propranolol</i>	<i>Inderal</i>	Cardiovascular diseases	$\beta$ -adrenergic R	1965
<i>Cimetidine</i>	<i>Tagamet</i>	Heartburn	Histamine H2 R	1977
<i>Clozapine</i>	<i>Clozaril</i>	Antipsychotic	5-HT2A	1972
<i>Dulaglutide</i>	<i>Trulicity</i>	Type 2 diabetes	GLP1R	2014
<i>Suvorexant</i>	<i>Belsomra</i>	Insomnia	OX2R and OX1R	2015
<i>Aripiprazole</i>	<i>Aristada</i>	Schizophrenia	5HT1A, 5HT2A	2015
<i>Sonidegib</i>	<i>Odomzo</i>	Basal cell carcinoma	SMO	2015
<i>Abaloparatide</i>	<i>Tymlos</i>	Osteoporosis	PTH1R	2017
<i>Etelcalcetide</i>	<i>Parsabiv</i>	Hyperparathyroidism	CASR	2017

R: receptor

<sup>227</sup> T. Warne; R. Moukhametzianov; J. G. Baker; R. Nehmé; P. C. Edwards; A. G. Leslie; *Nature* **2011**, 469, 241-244

<sup>228</sup> J. P. Vilardaga; M. Búnemann; T. N. Feinstein; N. Lambert; V. O. Nikolaev; S. Engelhardt; M. J. Lohse; C. Hoffmann. *Mol. Endocrinol.* **2009**, 23, 590-599

<sup>229</sup> O. Civelli; R. K. Reinscheid; Y. Zhang; Z. Wang; R. Fredriksson; H. B. Schiöth. *Annu. Rev. Pharmacol. Toxicol.* **2013**, 53, 127-146

<sup>230</sup> A. S. Hauser; M. M. Attwood; M. Rask-Andersen; H. B. Schiöth; D. E. Gloriam. *Nat. Rev. Drug. Discov.* **2017**, 6, 829-842

Historically, GPCRs drugs have been developed in the absence of structural information for a variety of reasons. Currently, the crystal structures of 44 receptors and 205 ligand-receptor complexes gives a large potential for structure-based drug discovery and design.<sup>231</sup>

For example, modulation in receptor allosteric sites can increase the selectivity and improve the therapeutic potential because these receptors support a wide pharmacological profile, such as biased agonisms which can activate the desired intracellular signaling pathway and silence the side effects.

The previously mentioned orphan GPCRs represent novel targets to treat several diseases. Approximately, more than 300 agents are in clinical trials, and around 70 of them are targeting novel GPCRs,<sup>230</sup> even when their endogenous ligands have not been discovered yet, indicating that drug discovery process can proceed even if receptors are not well known. Research on orphan GPCRs, in different clinical trials and research laboratories can afford new hints and targets to focus on. For example, in the subfamily of the adhesion GPCRs, where the main part are orphan receptors and recent literature has shown the important role that they are playing in some pathologies.<sup>232,233</sup> The druggability of GPCRs and their role in pathologies, highlights the importance of continuing the research in this field.

### 3.3.2. ADHESION GPCRs

The adhesion GPCRs are a recently characterized family of receptors that were firstly classified as part of the secretin family, but due to the difference between them, as the autocatalytic process (secretin family do not have autocatalytic process), the *N*-terminal domains, the evolutionary conservation and the important role that they play in cell-cell and cell-matrix adhesion, they can be considered as an independent family.<sup>234</sup> In fact, from the last 20 years the number of articles related with aGPCRS has grown considerably (Figure 76). In the annex 1 a review of each aGPCR with its NTF architecture, its described functions, its implications in some disorders, such as tumorigenesis, amongst others are collected.

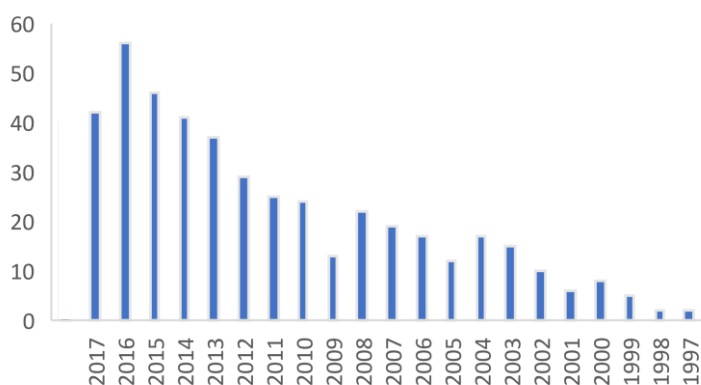


Figure 76. Timeline of aGPCRs articles in the last 22 years

<sup>231</sup> Y. Lee; S. Basith; S. Choi. *J. Med. Chem.* **2018**, *61*, 1-46

<sup>232</sup> F. Bassilana; M. Nash; M. G. Ludwig. *Nat. Rev. Drug Discov.* **2019**, *18*, 869-884

<sup>233</sup> G. Aust; D. Zhu; E. G. Van Meir; L. Xu L. *Handb. Exp. Pharmacol.* **2016**, *234*, 369-396

<sup>234</sup> J. Hamann; G. Aust; D. Araç; F. B. Engel; C. Formstone; R. Fredriksson; R. A. Hall; B. L. Harty; C. Kirchhoff; B. Knapp. *Pharmacol. Rev.* **2015**, *67*, 338-367



The subfamilies of the adhesion GPCRs were decided based on previous phylogenetic classifications according to their 7TM regions and their extracellular regions.<sup>235,236</sup>

#### TAXONOMY

Adhesion GPCRs are found in all vertebrates and high efforts to sequence the genomes of invertebrates provided a wide dataset to classify aGPCRs. Earlier literature, that looks to determine aGPCRs in these species, found homologs of select human aGPCR subfamilies. Additionally, aGPCRs have been identified in fungi, which indicates that aGPCRS were developed before the split of unikonts (members of a taxonomic group), from the common ancestor of eukaryotes, about 1275 million years ago.<sup>237,238</sup>

Another argument to reinforce this idea, is the fact that they are the most complex among GPCRs in terms of molecular genetics as they have: multiple introns, a complex genomic size, and multiple functional domains present in other proteins.<sup>237,238</sup>

#### NOMENCLATURE

The initial names for the adhesion GPCRs were established by the pioneers of the research field without a common harmonization, like BAI (brain-specific angiogenesis inhibitor), VLGR (very large GPCR), and others. Then, with the collaboration of the Human Genome Organization (HUGO) and the Gene Nomenclature Committee (HGNC), most of the aGPCRs were named after GPR# names (where GPR stands for G-Protein coupled Receptor).<sup>239</sup>

All these names were kept as identifiers until a better nomenclature could be devised. Subsequently, the field has expanded and aGPCRs are being studied in many areas and therefore common names are needed for researchers.<sup>234</sup>

The Adhesion GPCR Consortium working with HGNC and the IUPHAR Committee on Receptor Nomenclature and Drug Classification (NC-IUPHAR) established a prefix that identifies any aGPCR homolog, independent of the family or even the species. That prefix is ADGR (Adhesion G protein-coupled receptor). Then, for each family a letter to relate them with the previous names was assigned (for example, B for the BAIs) and for the subfamilies with receptors called after GPR#, were recalled with a letter (following alphabetic order, A, D, F, G). Before this agreed, the subfamilies were indicated with Roman numbers I-IX. Finally, for each member, 33 receptors, a number was given to each one in a similar order to the previous names (Table 30).

The HGNC as well as the NC-IUPHAR are agreement about the use of this new nomenclature to promote easier research.<sup>240</sup>

---

<sup>235</sup> T. K. Bjarnadóttir; K. Geirardsdóttir; M. Ingemansson; M. A. Mirza; R. Fredriksson; H. B. Schiöth. *Gene* **2007**, *387*, 38-48

<sup>236</sup> M. C. Lagerström; H. B. Schiöth. *Nat. Rev. Drug Discov.* **2008**, *7*, 339-357

<sup>237</sup> N. Kamesh; G. K. Aradhyam; N. Manoj. *BMC Evol. Biol.* **2008**, *8*, 129-129

<sup>238</sup> A. Krishnan; M. S. Almén; R. Fredriksson; H. B. Schiöth. *PLoS One* **2012**, *7*, e29817

<sup>239</sup> R. Fredriksson; M. C. Lagerström; L. G. Lundin; H. B. Schiöth. *Mol. Pharmacol.* **2003**, *63*, 1256-1272

<sup>240</sup> <https://www.adhesiongpcr.org> (20/05/2019)

**Taola 30.** Classification of aGPCRs

Subfamilies	Proposed names for subfamilies	Previous gene names	Currently accepted nomenclature
I	Letrophilin (L)	LPHN1	ADGRL1
		LPHN2	ADGRL2
		LPHN3	ADGRL3
		ELTD1	ADGRL4
II	EGF-TM7 (E)	EMR1	ADGRE1
		EMR2	ADGRE2
		EMR3	ADGRE3
		EMR4	ADGRE4
		CD97	ADGRE5
III	A	GPR123	ADGRA1
		GPR124	ADGRA2
		GPR125	ADGRA3
IV	CELSR (C)	CELSR1	ADGRC1
		CELSR2	ADGRC2
		CELSR3	ADGRC3
V	D	GPR133	ADGRD1
		GPR144	ADGRD2
VI	F	GPR110	ADGRF1
		GPR111	ADGRF2
		GPR113	ADGRF3
		GPR115	ADGRF4
		GPR116	ADGRF5
VII	BAI (B)	BAI1	ADGRB1
		BAI2	ADGRB2
		BAI3	ADGRB3
VIII	G	GPR56	ADGRG1
		GPR64	ADGRG2
		GPR97	ADGRG3
		GPR112	ADGRG4
		GPR114	ADGRG5
		GPR126	ADGRG6
		GPR128	ADGRG7
IX	V	GPR98	ADGRV1

BAI: Brain-specific angiogenesis inhibitor, CD: Cluster of differentiation, CELSR: Cadherin EGF LAG seven-pass G-type receptor, EGF-7TM: epiderma growth factor-seven-span transmembrane, ELTD: EGF, letrophilin, and seven-transmembrane domain-containing protein, EMR: EGF-like molecule-containing mucin-like hormone receptor.

### STRUCTURAL ASPECTS

As has been explained, the 33 aGPCRs can be split into nine subfamilies based on their 7TM sequence, but all subfamilies share some similarities in extracellular domains. The structure of the receptor can be divided in two parts, extracellular domain (ECD) and intracellular domain (ID). Within the ECD, the G-protein-coupled receptor autoproteolytic-inducing domain (GAIN) bears a conserved GPCR proteolytic site (GPS) where aGPCRs are autoproteolytically cleaved into N-terminal fragment (NTF) and C-terminal fragment (CTF). Previous to GPS motif, a region called “Stalk”, B-Strand-13 or “Stachel” is revealed when GAIN domain is cleaved. This region can directly activate the receptor as a tethered agonist (Figure 77).<sup>241</sup>

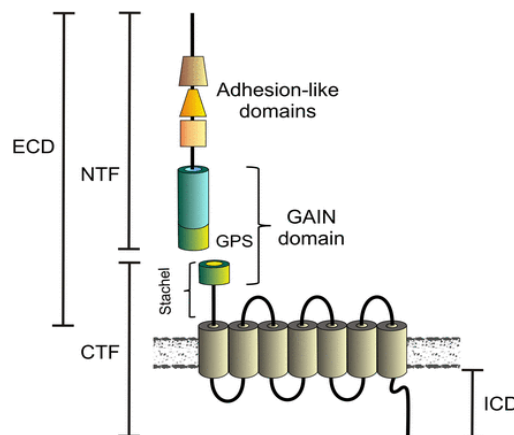


**Figure 77.** Structural aspects of aGPCRS. ECD: Extracellular domain; ICD: Intracellular domain; NTF: N-terminal fragment; CTF: C-terminal fragment; GPS: GPCR proteolytic site<sup>241</sup>

### EXTRACELLULAR DOMAIN

All the Adhesion GPCRs have a unique and typically large N-terminal extracellular domain (ECD) that contains specific features from subfamilies (like different adhesion domains) and features the GAIN domain, typically for all the aGPCRs.

### GAIN DOMAIN

The GAIN domain is present in 32 of the 33 human aGPCRs (ADGRA1/GPR123 does not have it), it is located after the 7-TM. It is formed by two domains, the A domain, which contains 6 alpha-helices and B domain, which has a beta-sandwich with 13 beta-strands and 2 alpha-helices.<sup>242</sup> The GAIN domain is defined as 320 residues and inside the B domain there are 40 residues defined as the proteolytic GPS motif. GPS motif is described as an integral element for aGPCR receptor function.<sup>243</sup> Crystallographic studies indicate that the GPS motif requires the rest of the GAIN domain for auto-proteolysis. It is hypothesized that self-cleavage occurs at the GPS site and takes place in the endoplasmic reticulum.<sup>244</sup>

### 7TM DOMAIN

The 33 aGPCRs have the seven transmembrane spanning architecture common to the GPCR superfamily and it has been found a conserved evolutionary relation between extracellular domains and seven transmembrane function.<sup>245,234</sup>

<sup>241</sup> K. R. Monk; J. Hamann; T. Langenhan; S. Nijmeijer; S. Schöneberg; T. Liebscher. *J. Mol. Pharmacol.* **2015**, *88*, 617-623

<sup>242</sup> D. Araç; A. A. Boucard; M. F. Bolliger; J. Nguyen; S. M. Soltis; T. C. Südhof; A. T. Brunger. *EMBO J.* **2012**, *31*, 1364-1378

<sup>243</sup> H. M. Stoveken; A. G. Hajduczuk; L. Xu; G. G. Tall. *Proc. Natl. Acad. Sci. USA.* **2015**, *112*, 6194-61499

<sup>244</sup> V. Krasnoperov; Y. Lu; L. Buryanovsky; T. A. Neubert; K. Ichtchenko; A. G. Petrenko. *J. Biol. Chem.* **2002**, *277*, 46518-46526

<sup>245</sup> T. Langenhan; G. Aust; J. Hamann. *Sci. Signal.* **2013**, *6*, 1-21

Recently, a mechanism by which aGPCRs are activated has been proposed that utilizes the *N*-terminal of the 7-TM region. After proteolysis at the GPS site, this *N*-terminus (Stachel part) is free to stimulate the 7TM as tethered agonist and therefore to induce activation. It is remarkable that all aGPCRS keep this conserved motif.<sup>243,246,247,248</sup>

Actually, it is similar to how thrombin receptors work (PAR1). When thrombin binds to its receptor and cleaves a part of its exodomain a new *N*-terminus appears, which acts as a tethered ligand activating the receptor.<sup>249</sup>

#### HETEROTRIMERIC G-PROTEINS

Another characteristic in aGPCRs is the associated G protein that mediates the intracellular pathways. The heterotrimeric G protein complex, as has been described, consist of an  $\alpha$ -subunit that binds and hydrolyzes GTP and also a  $\beta\gamma$ -subunit that forms a non-dissociable complex.<sup>250</sup>

In one hand,  $\beta\gamma$  complex usage does not appear to be significantly different among the 33 aGPCRs. In the other hand, the alpha subunit, can be, sorted in four types:  $G\alpha_s$ ,  $G\alpha_{i/o}$ ,  $G\alpha_q$ ,  $G\alpha_{12}$ . In humans 16 genes encode for  $G\alpha$ -subunits, five genes encode for  $G\beta$ -subunits, and 12 genes encode for  $G\gamma$ -subunits.<sup>251</sup> Most GPCRs are able to activate more than one  $G\alpha$  subunit, but each receptor has selectivity towards particular  $G\alpha$  families. For example, a ligand binding in a receptor can produces a specific conformation which can activate a specific G protein pathway. G-protein coupling selectivity is known to depend on local physiological conditions and thus may change in different cell lines, tissues, or experimental conditions.

#### G PROTEIN SIGNAL TRANSDUCTION MECHANISMS

The heterotrimeric G protein coupled to the aGPCRs undergoes a cycle of activation and inactivation. When the receptor is in basal state, the  $\alpha$ -GDP, and  $\beta\gamma$ -subunits form a tight trimeric complex that does not signal. Once the GPCR has been activated, the conformational changes in the receptor promote an exchange of the GDP to GTP by  $G\alpha$ , followed by a disassociation of  $\alpha$ -GTP from both the receptor and the  $\beta\gamma$ -complex. The two complexes are freed, so are able to independently modulate effector proteins. The activity is terminated by GTP hydrolysis and reformation of the G-protein heterotrimer. This can be enhanced by effector proteins or by regulators of G protein signaling (RGS), promoting hydrolysis of GTP by the intrinsic GTPase activity of  $G\alpha$  (Figure 78).<sup>252</sup>

---

<sup>246</sup> G. S. Salzman; S. Zhang; A. Gupta; A. Koide; S. Koide; D. Araç. *Proc. Natl. Acad. Sci. USA*. **2017**, *114*, 10095-10100

<sup>247</sup> L. M. Demberg; J. Winkler; C. Wilde; K. U. Simon; J. Schön; S. Rothemund; T. Schöneberg; S. Prömel; I. Liebscher. *J. Biol. Chem.* **2017**, *292*, 4383-4394

<sup>248</sup> I. Liebscher; T. Schöneberg. *Handb. Exp. Pharmacol.* **2016**, *234*, 111-125

<sup>249</sup> S.R. Coughlin. *Proc. Natl. Acad. Sci.* **1999**, *96*, 11023-11027

<sup>250</sup> H. E. Hamm. *J. Biol. Chem.* **1998**, *273*, 669-672

<sup>251</sup> G. B. Downes; N. Gautam. *Genomics* **1999**, *62*, 544-552

<sup>252</sup> T. M. Cabrera-Vera; J. Vanhauwe; T. O. Thomas; M. Medkova; A. Preininger; M. R. Mazzoni; H. E. Hamm. *Endocr. Rev.* **2003**, *24*, 765-781

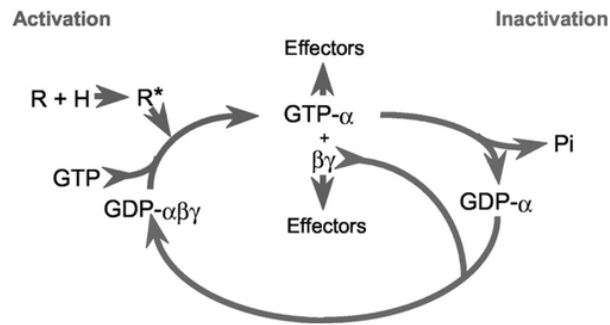


Figure 78. G protein activation and inactivation cycle<sup>253</sup>

#### a) G $\alpha$ mediated signal transduction

G alpha subunit can be classified based on their primary sequence and functions: G $\alpha_s$ , G $\alpha_i$ , G $\alpha_q$  and G $\alpha_{12}$  (Figure 79).<sup>254</sup> The G $\alpha_s$  subunit stimulates membrane-bound adenylyl cyclase (AC), increasing the intracellular cyclic adenosine monophosphate (cAMP). In contrast, G $\alpha_i$  subunits inhibit AC, diminishing the intracellular cAMP. The levels of cytosolic cAMP regulate (binding) the PKA (cAMP-dependent protein kinase) which can go to the nucleus and phosphorylates the CREB (cAMP response element-binding), which is a transcriptional factor that binds to CRE (cAMP response element) and activates the transcription of determinate genes.<sup>255</sup>

The PKA can be downregulated through the cAMP hydrolyzing phosphodiesterase, transforming cAMP to ATP, therefore the amount of activated PKA will be less. Also, different phosphorylation pathways downregulate the PKA. The G $\alpha_i$  can activate the PKC (phospholipase C) as well.<sup>256,257</sup> Various other proteins such as ion channels and small GTPase exchange factors (EPAC) are also modulated by cAMP binding. Then, there is the G $\alpha_q$ , which once it is activated directly interacts and stimulates the enzyme activity of several PLC $\beta$  (phospholipase C-B) isoforms which promotes the cleavage of the membrane lipid PIP2 (phosphatidylinositol 4,5-diphosphate) producing IP3 (1,4,5-triphosphate) and DAG (diacylglycerol).

IP3 interacts with its receptors in the endoplasmic reticulum to activate the release of intracellular calcium stores and DAG activates PKC (protein kinase C) isozymes.<sup>258</sup>

The calcium is able, as well, to activate PKC and the Ca<sup>2+</sup>/calmodulin-dependent protein kinase (CaMK) which transfers phosphates groups from the ATP to transcriptional factors and therefore, activating them.<sup>259</sup> Finally, activated G $\alpha_{12}$  modulates RGS-domain containing RhoGEF proteins (guanine nucleotide exchange factors). When there is an allosteric interaction between G12 and RhoGEF, the GTPase Rho is activated and then Rho activated by GTP and subsequently promotes a cascade where different proteins are implicated, such as Rho-kinase that regulates migration and adhesion contractibility of the cytoskeleton. It is known that most of the receptors that activate G12 also activate Gq.<sup>260</sup>

<sup>253</sup> T. B. Patel. *Pharmacol. Rev.* **2004**, *56*, 371-385

<sup>254</sup> T. R. Dorsam; J. S. Gutkind. *Nat. Rev. Cancer* **2007**, *7*, 79–94

<sup>255</sup> S. R. Sprang. *Biopolymers* **2016**, *105*, 449-456

<sup>256</sup> J. Wu; N. Xie; X. Zhao; E. C. Nice; C. Huang. *Cancer Genomics Proteomics* **2012**, *9*, 37-50

<sup>257</sup> J. P. Mahoney; R. K. Sunahara. *Curr. Opin. Struct. Biol.* **2016**, *41*, 247-254

<sup>258</sup> I. Litosch. *Life Sci.* **2016**, *152*, 99-106

<sup>259</sup> D. Kankanamge; M. Tennakoon; A. Weerasinghe; L. Cedeno-Rosario; D. N. Chadee; A. Karunaratne. *Cell Signal.* **2019**, *58*, 34-43

<sup>260</sup> T. M. Seasholtz; M. Majumdar; J. H. Brown. *Mol. Pharmacol.* **1999**, *55*, 949-956

## b) Gβγ mediated signaling

The Gα-signaling mechanisms explained above are independent of the Gβγ complex, but this complex is required for GPCR catalyzed nucleotide exchange.<sup>261</sup>

As has been discussed before, when subunits are in the heterotrimeric complex, βγ-subunits acts as an inhibitor of the α-subunit, trapping the α-subunit in the GDP form (inactive state).<sup>262</sup>

It is generally thought that βγ subunits do not change conformation upon GPCR activation as they are rigid β-sheet proteins.<sup>263</sup> Once βγ complex is free from Gα, it acts as a dimer, interacting with several proteins and activating or inhibiting various pathways (synergistic or contrary to the Gα subunit). For example, βγ subunits can activate phospholipase C (PLC), inhibit adenylyl cyclase (AC), and modulate ion channel (Figure 79).<sup>264</sup>

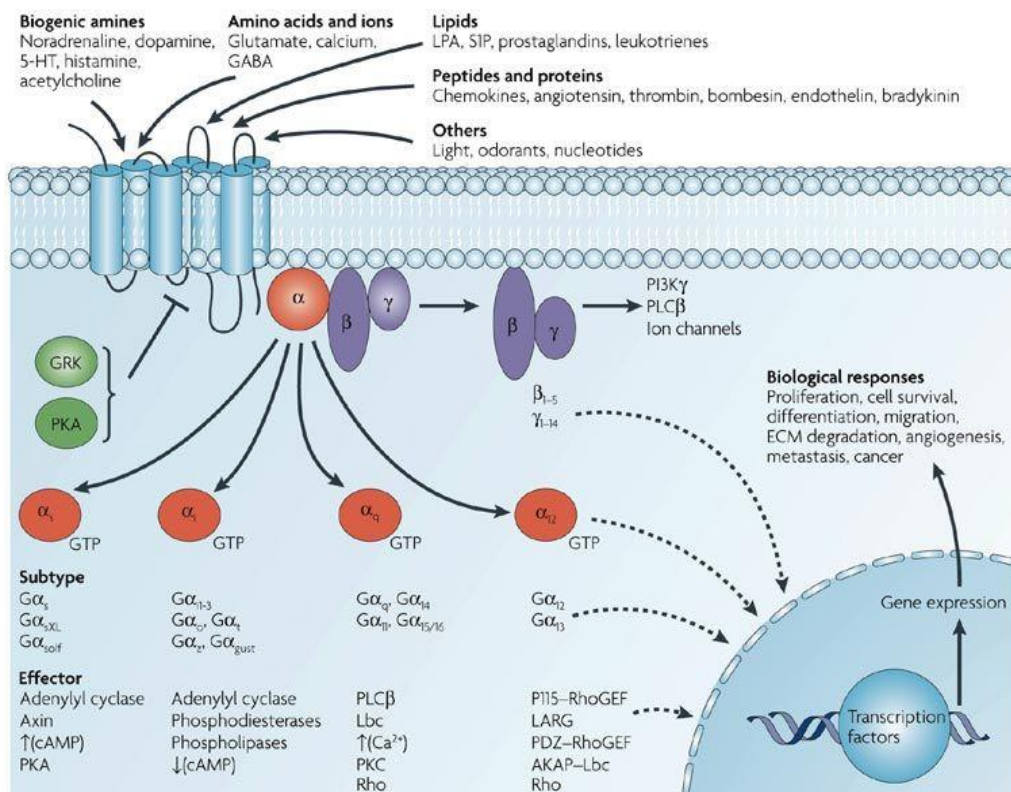


Figure 79. G proteins signal pathways<sup>254</sup>

## SIGNAL TERMINATION

Signaling of GPCRs can be ended by different means. When the ligand is removed or degraded from the receptor the downstream signaling time life is limited by the RGS (regulators of G protein signaling), as explained previously. In addition, there are other mechanisms to end the signal, the GRKs and arrestins. GRKs characteristically phosphorylate activated GPCRs on serine/threonine residues present in their C-terminal (3<sup>rd</sup> loop).<sup>265</sup> GPCR phosphorylation by GRKs drives to binding of the receptors to arrestin proteins. It has been shown that selectivity between GPCRs and GRKs

<sup>261</sup> B. K. Fung. *J. Biol. Chem.* **1983**, 258, 10495-10502

<sup>262</sup> V. A. Florio; P. C. Sternweis. *J. Biol. Chem.* **1989**, 264, 3909-3915

<sup>263</sup> D. G. Lambright; J. Sondek; A. Bohm; N. P. Skiba; H. E. Hamm; P. B. Sigler. *Nature* **1996**, 379, 311-319

<sup>264</sup> S. M. Khan; J. Y. Sung; T. E. Hébert. *Pharmacol. Res.* **2016**, 111, 434-441

<sup>265</sup> V. V. Gurevich; E. V. Gurevich. *Crit. Rev. Biochem. Mol. Biol.* **2015**, 50, 440-452

is more controlled by the activation and the situation of this activation (quantity of GRKs, quantity of agonist, amongst others) rather than a specific phosphorylation site.<sup>266</sup> Arrestins recognize activated GPCRs and the affinity for them is increased by GRKs phosphorylation. Depending on the pattern of the phosphorylation, arrestins act to terminate signal transduction signal by two mechanisms, desensitization and receptor sequestration. One arrestin is able to regulate one receptor, playing an important homeostasis role.<sup>265</sup>

Activated arrestin-GPCR complexes recruit the proteins adaptin and clathrin to endocytosis and receptor internalization (vesicular traffic), diminishing the amount of cell surface receptors. The endocytic process may occur in different ways based on the affinity of arrestins to GPCR phosphorylation sites. Weak affinity interactions induce a state where arrestins disassociate fast and receptors are recycled and back to the cell surface.<sup>267</sup> It is important to remark on the role of conformational changes in GPCRs in which the dynamics and the different states can result in different functional outcomes. For example, some drugs (biased drugs) activate a conformational state where arrestin pathway is activated but the G protein pathway is not.<sup>268</sup>

### 3.3.3. CHARACTERIZATION of 33 ADHESION GPCRs

Given that the physiological basics of these receptors and their promise as drug targets for human disease are established, the executed procedures to characterize them are explained hereunder.

The project involved design of cellular assay systems to measure the signal transduction of recombinant adhesion family receptors. It has involved transient transfection of mammalian cells and the measurement of various second messengers (cAMP, IP<sub>3</sub>, kinase activity) in response to activated receptor point mutants and literature-described peptides. Analysis of the mechanism of receptor activation and G-protein signal- transduction pathway will be quantified. The receptors were mutated in order to be cleavable by the bovine enterokinase enzyme, generating an agonist neo-epitope through the proteolysis of their GPS sequence. Then, the free Stachel sequence of the receptors will be available to bind the transmembrane domains of the receptor and promote the conformational changes that causes activation (Figure 80). Also, recent literature described how aGPCRs can be activated by peptides containing the aminoacid sequence of the  $\beta$ -strand.<sup>269</sup>

Thus, a peptide sequenced by the aminoacids present in the GPS of GPR126 were tested as well. Since they were able to be activated, the next step was to quantify the G-protein signal-transduction pathways in every aGPCR. So, it was necessary to transfect each receptor in HEK293 cells (human embryonic kidney cells), to incubate them, and finally, to measure second messengers activated through G protein activity.

---

<sup>266</sup> C. A. Moore; S. K. Milano; J. L. Benovic. *Annu. Rev. Physiol.* **2007**, *69*, 451-482

<sup>267</sup> S. M. DeWire; S. Ahn; R. J. Lefkowitz; S. K. Shenoy. *Annu. Rev. Physiol.* **2007**, *69*, 483-510

<sup>268</sup> Y. K. Peterson; L. M. Luttrell. *Pharmacol. Rev.* **2017**, *69*, 256-297

<sup>269</sup> H. M. Stoveken; L. L. Bahr; M. W. Anders; A. P. Wojtovich; A. V. Smrcka; G. G. Tall. *Mol. Pharmacol.* **2016**, *90*, 214-222

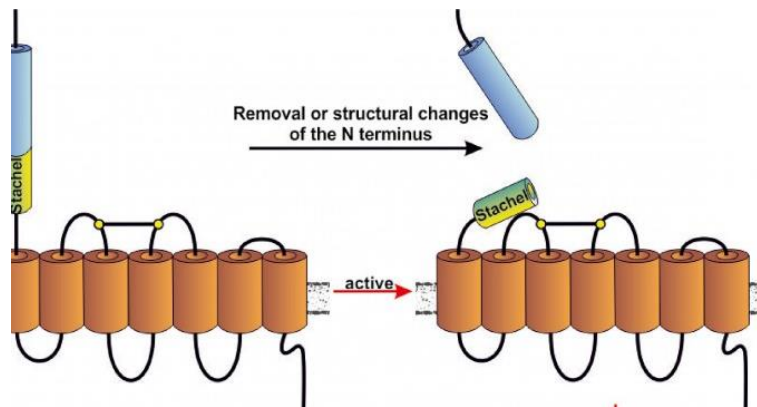
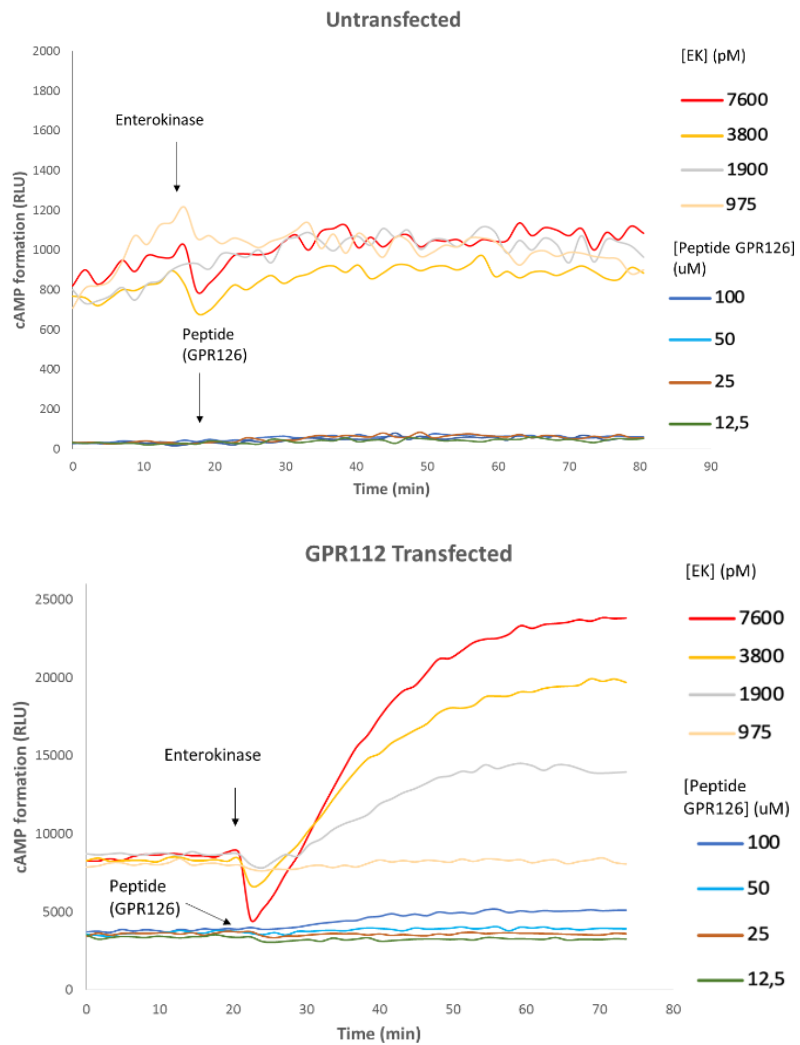


**Figure 80.** Activation of the receptor through the free stachel part after proteolysis<sup>270</sup>

In that way, it was possible to quantify the preferred G protein associated in each receptor. As a negative control, untransfected cells were used to assure that response was due to receptor activation (Figure 81).



<sup>270</sup> <http://www.adhesiongpcr.de> (09/01/2020)



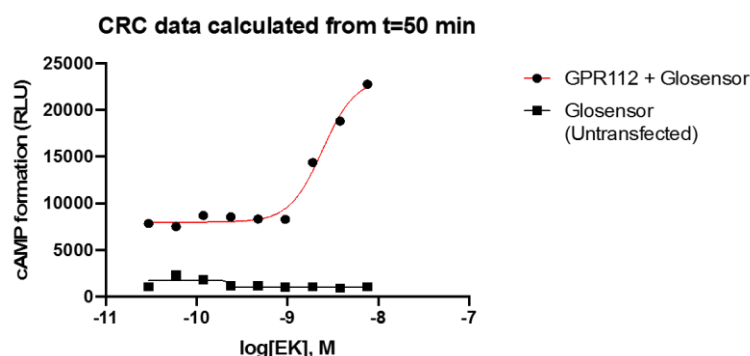


**Figure 81.** cAMP formation before and after activation through enterokinase or peptide (containing the sequence of GPR126  $\beta$ -strand) in untransfected cells (negative control) and transfected cells with GPR112

For each  $G\alpha$  protein a different assay (using different procedures and devices) was accomplished:

- a)  $G\alpha_s$ : cAMP was measured with luminescence using the Glosensor system (Promega)
- b)  $G\alpha_i$ : the decrease of Forskolin-induced cAMP<sup>271</sup> was measured using the Glosensor approach. Pertussis toxin,<sup>272,273</sup> as an inhibitor of  $G\alpha_i$ , was used to confirm the results.
- c)  $G\alpha_q$ : intracellular calcium was measured using calcium sensitive fluorescent dyes. YM-254890<sup>274,275</sup> was used as an inhibitor of  $G\alpha_q$  to confirm the results.
- d)  $G\alpha_{12}$ : the intracellular calcium was measured after stimulation of RhoA (increases intracellular calcium) through PLC- $\epsilon$ . YM-254890 was used as an inhibitor of  $G\alpha_q$  to characterized any false positive results.
- e) Reporter assay: transcription factor response elements (CRE-  $G\alpha_s$ , SRE-  $G\alpha_i$ , NFAT-RE-  $G\alpha_q$ , SRF-RE- $G\alpha_{12}$ ) were measured after receptor activation. These response elements encoding DNAs coupled activate to the production of luciferase. If the signal transduction pathway is activated through CRE, SRE, NFAT or SRF, luciferase expression increases and it can be detected with luminescence (Figure 82).

<sup>271</sup> J. Gilissen; P. Geubelle; N. Dupuis; C. Laschet; B. Pirotte; J. Hanson. *Biochem. Pharmacol.* **2015**, *98*, 381-391

<sup>272</sup> S. Mangmool; H. Kurose. *Toxins* **2011**, *3*, 884-899

<sup>273</sup> T. Katada. *Biol. Pharm. Bull.* **2012**, *35*, 2103-2111

<sup>274</sup> H. Zhang; A. L. Nielsen; K. Strømgaard. *Med. Res. Rev.* **2020**, *40*, 135-157

<sup>275</sup> A. Nishimura; K. Kitano; J. Takasaki; M. Taniguchi; N. Mizuno; K. Tago; T. Hakoshima; H. Itoh. *Proc. Natl. Acad. Sci. USA* **2010**, *107*, 13666-13671

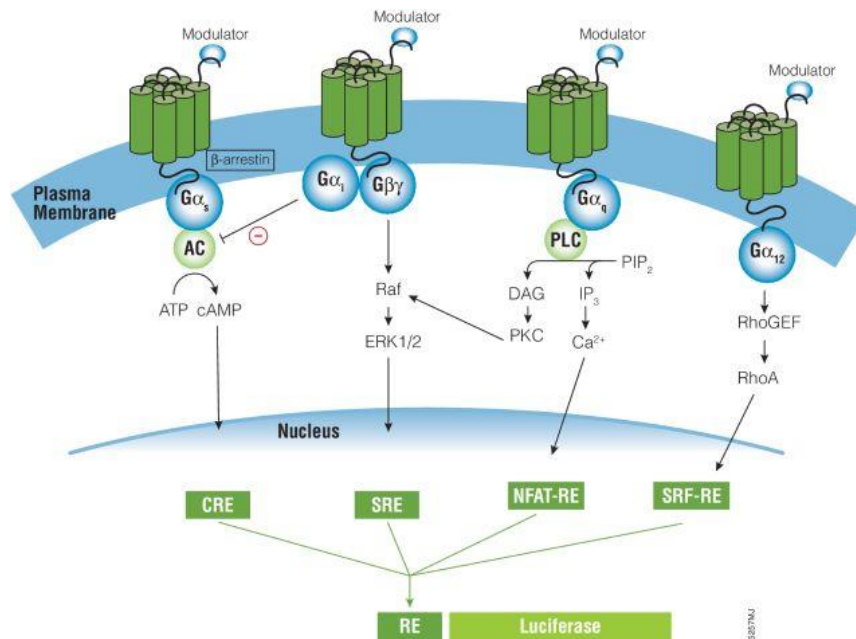


Figure 82. Pathways undertaken through G alpha subunit<sup>276</sup>

Very little information exists as to the G-protein coupling specificities of aGPCRs. Accordingly, most of the aGPCRs have the theoretical potential to be associated with several different G $\alpha$  proteins.

The used methods and materials are described in the experimental part.

After several assays and repetitions the obtained results for the 33 receptors are summarized in the following table, where the number of independent repetitions of each experiment are shown (Table 31).

Table 31. Number of independent repetitions of each experiment for each receptor.

G-protein	Significant	Possible
Gs		
Gi		
Gq		
G12		
Gq + Gs		
Gi + Gq		

The concluded coupled G protein for each receptor is showed in different colors depending if the results were significant, possible or null.

	G <sub>s</sub>		G <sub>i</sub>			G <sub>q</sub>		G <sub>12</sub>	
	cAMP	CRE	cAMP	G.F.	SRE	Ca <sup>2+</sup>	NFAT	plc-Ca <sup>2+</sup>	SRF
BAI 1	3	2 (1 PT)	3 (1 PT)	1	4 (1 PT, 1 YM)	5 (2 YM)	-	1	3
BAI2	2	1	3 (1PT)	1	4 (1 PT, 1 YM)	5 (1 YM)	-	1	3
BAI 3	1	1	2 (1PT)	1	3 (1YM)	5 (1 YM)	-	1	2
CD97	2	2 (1PT)	3 (1PT)	1	4 (1 PT, 1 YM)	5 (2 YM)	-	1	3
CELSR1	3	2 (1PT)	3 (1PT)	1	4 (1 PT, 1 YM)	5 (2 YM)	-	1	3
CELSR2	2	1	3 (1PT)	1	4 (1 PT, 1 YM)	5 (2 YM)	-	1	3
CELSR3	2	1	3 (1PT)	1	4 (1 PT, 1 YM)	5 (2 YM)	-	1	3
ELTD1	2	1	4 (2 PT)	1	4 (1 PT, 1 YM)	5 (1 YM)	-	1	3

<sup>276</sup> www.promega.es (25/05/2019)

EMR1	2	2 (1 PT)	4 (2 PT)	1	4 (1 PT, 1 YM)	6 (2 YM)	-	1	3
EMR2	2	2 (1 PT)	3 (1 PT)		4 (1 PT, 1 YM)	6 (2 YM)	-	1	3
EMR3	2	1	3 (2 PT)	1	3 (1 YM)	5 (1 YM)	-	1	3
EMR4	4	1	3 (1PT)		4 (1 PT, 1 YM)	4 (1 YM)	-	1	3
GPR56	3	2 (1 PT)	4 (1 PT, 1 PEPTIDE)	1	4 (1 PT, 1 YM)	4 (2 YM, 1 PEPTIDE)	-	1	3
GPR64	4 (1 PEPTIDE)	2	2		4 (1 PT, 1 YM)	5 (2 YM, 1 PEPTIDE)	-	1	3
GPR97	3	2 (1 PT)	3 (1 PT)	1	2	4 (2 YM)	-	1	2
GPR98	2	2 (1PT)	3 (1 PT)		3 (1 YM)	4 (1 YM)	-	1	3
GPR110	4	2 (1PT)	3 (1 PT)	1	4 (1 PT, 1 YM)	5 (1 YM)	-	1	3
GPR111	3	1	3 (1 PT)		3 (1 YM)	4 (1 YM)	-	1	2
GPR112	4 (1 PEPTIDE)	1	3		4 (1 PT, 1 YM)	5 (1 YM, 1 PEPTIDE)	-	1	3
GPR113	3	1	3 (1 PT)		4 (1 PT, 1 YM)	5 (2 YM)	-	1	2
GPR114	4 (1 PEPTIDE)	1	2		2	5 (1 YM, 1 PEPTIDE)	-	1	2
GPR115	3	2 (1PT)	3 (1PT)	1	3 (1 YM)	4 (1 YM)	-	1	2
GPR116	3	2 (1PT)	3 (1PT)	1	4 (1 PT, 1 YM)	3 (2 YM)	-	1	3
GPR123	2	1	3 (1PT)		4 (1 PT, 1 YM)	6 (2 YM)	-	1	2
GPR124	2	2 (1PT)	2 (1PT)		3 (1 YM)	4 (1 YM)	-	1	2
GPR125	3	2 (1 PT)	4 (2 PT)	1	4 (1 PT, 1 YM)	6 (1 YM)	-	1	3
GPR126	4 (1 PEPTIDE)	2	2		4 (1 PT, 1 YM)	4 (2 YM, 1 PEPTIDE)	-	3	3
GPR128	4 (1 PEPTIDE)	1	2		4 (1 PT, 1 YM)	4 (1 YM)	-	1	3
GPR133	4 (1 PEPTIDE)	1	2		4 (1 PT, 1 YM)	4 (1 YM)	-	1	2
GPR144	4 (1 PEPTIDE)	1	1		2	4 (1 YM)	-	1	2
LPHN1	3	1 (1 PT)	4 (2 PT)	1	2	5 (1 YM)	-	1	2
LPHN2	2	1 (1 PT)	3 (1 PT)	1	4 (1 PT, 1 YM)	5 (1 YM)	-	1	2
LPHN3	2	2 (1 PT)	3 (1 PT)	1	4 (1 PT, 1 YM)	5 (1 YM)	-	1	2

PT: pertussis toxin, YM: YM-254890, GLO: Glosensor experiment, CRE: cAMP response element, G.F.: Gradual forskolin, SRE: serum response element, NFAT: nuclear factor of activated T-cells, SRF: serum response factor

- 1) It is concluded that under the described assays conditions GPR64, GPR112, GPR114, GPR126, GPR128, GPR133, GPR144 were coupled with Gs.
- 2) It is concluded that under the described assays conditions EMR2, GPR56, GPR110 and GPR116 were coupled with Gi.
- 3) It is concluded that under the described assays conditions BAI2, GPR64 and GPR126 were coupled with Gq.
- 4) It is concluded that under the described assays conditions GPR56, GPR64, GPR112, GPR126 and GPR128 were coupled with G12.

The proposed and undertaken assays were reproducible and efficient to analyze the coupled G proteins and the intracellular mechanisms related with adhesion GPCRs.

## 4. EXPERIMENTAL PART

### 4.1. ORGANIC CHEMISTRY LABORATORY MATERIALS AND METHODS

Proton and carbon nuclear magnetic spectroscopy ( $^1\text{H}$  and  $^{13}\text{C}$  NMR, respectively) spectrums have been performed with a Mercury-400 spectrophotomer (400 and 100.6 MHz, respectively) using  $\text{CDCl}_3$ ,  $(\text{CD}_3)_2\text{CO}$ ,  $\text{DMSO-d}_6$  or other deuterated solvents with TMS as a reference. Chemical shifts are expressed as parts per million (ppm).

ESI Mass spectrums have been carried out with Agilent LC/MSD-ToF mass spectrophotomer (Faculty of Chemistry, University of Barcelona).

Melting points have been determined with a Gallenkamp model MFB.595.010M device with an internal thermometer and have been adjusted with an external thermometer.

Column chromatography has been performed manually on silica gel Merck 60 (40-60 cm) eluting with mixtures of different solvents or through an automatic CombiFlash<sup>®</sup> R<sub>f</sub> system equipped with UV-Vis (PN 68-5230-008) and silica gel RediSep R<sub>f</sub> (4 and 12 grams).

TLC plate 60 F<sub>254</sub> Merck has been used as thin layer chromatography.

The microwaves reactions have been carried out with CEM Discover LabMate and the temperature have been adjuster by an external IR sensor.

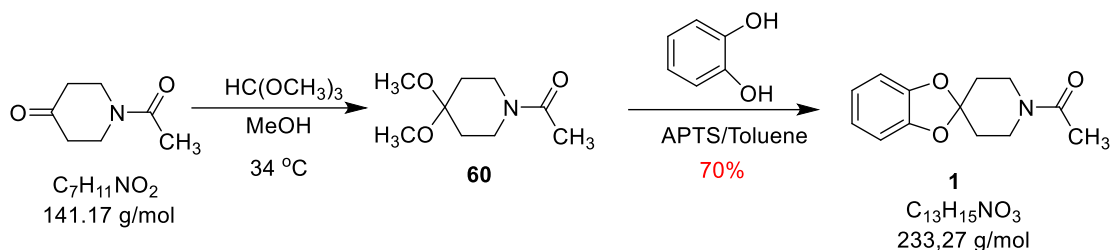
All reagents and organic used have recognized analytical grade or have been purified before their use. Commercial products have been obtained from Sigma-Aldrich (Merck).

The experimental part has been sorted in:

- 4.2. Preparation of 1-spiro[benzodioxole-2,4'-piperidine]
- 4.3. Preparation of pyrrolo[2,3-*b*]pyrazines

## 4.2. Preparation of 1-spiro[benzodioxole-2,4'-piperidine]

### 4.2.1. Preparation of *N*-acetyl-spiro[1,3-benzodioxole-2,4'-piperidine] (**1**)



#### · Procedure

In a 25 mL round bottom flask the *N*-acetyl-4-piperidone (0.78 mL, 6.37 mmol) was dissolved in 8 mL of methanol. The trimethyl orthoformate (0.83 mL, 7.6 mmol) and *p*-toluenesulfonic acid (catalytic quantity) were also added.

The reaction was stirred at 34 °C until distillation of methyl formate was observed. Then, the reaction was stopped, cooled (0 °C) and 5 mL of sodium methoxide 10% were added. Methanol was evaporated to obtain the crude of reaction. The crude of reaction was extracted with dichloromethane (3 x 20 mL) and water (1 x 20 mL) was made. The organic phases were collected, dried over anhydrous  $\text{Na}_2\text{SO}_4$ , filtered and concentrated under reduced pressure to obtain the acetal intermediate. Then, it was dissolved in a round bottom flask with toluene (10 mL) and catechol (2.1 g, 19 mmol) was added. The mixture was stirred at 120 °C until distillation of toluene was observed. After this time, the reaction was cooled at 60 °C in order to add APTS (catalytic quantity). Soon after, the reaction crude was heated at 120 °C. The reaction control was carried out by TLC (hexane/ethyl acetate 4:6).

#### · Work-Up

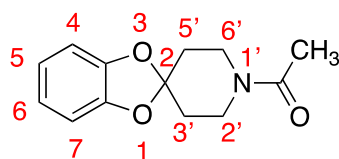
The residue of reaction obtained was cooled below 0 °C and 3 mL of triethylamine were added. The solvent was concentrated *in vacuo* giving as a result the crude of reaction, which was dissolved in dichloromethane (20 mL) and washed with water (3 x 20 mL). The organic phase was dried over anhydrous  $\text{Na}_2\text{SO}_4$ , filtered and concentrated under reduced pressure. A mixture of expected compound and starting catechol was obtained.

#### · Purification

An automatic flash column chromatography was carried out to afford the expected compound. The desired product eluted with a mixture of hexane/ethyl acetate 40:60.

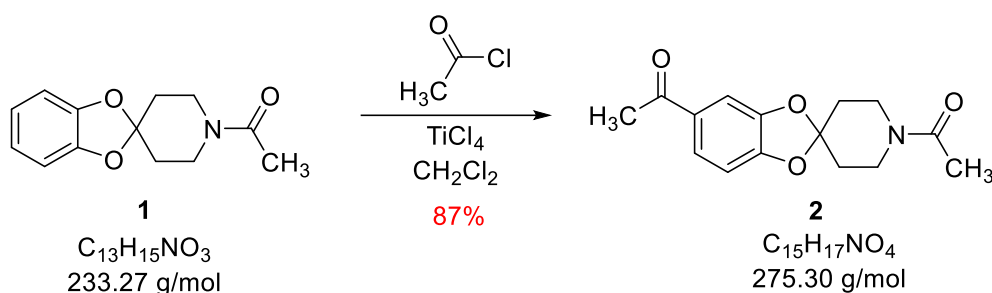
#### · Analytical data

Product aspect	Mass obtained	Yield	$R_f$ (hexane/ethyl acetate 4:6)	Melting point
White solid	1 g	70%	0.32	162-163 °C (ethanol)



$^1\text{H NMR}$  ( $\text{CDCl}_3$ , 400 MHz)  $\delta$ (ppm), 2.00 (q,  $J = 5.8$  Hz, 4H,  $\text{CH}_2\text{-C}$  (x2)); 2.15 (s, 3H,  $\text{CH}_3$ ); 3.65 (t,  $J = 5.8$  Hz, 2H,  $\text{CH-N}$  axial (x2)); 3.82 (t,  $J = 5.8$  Hz, 2H,  $\text{CH-N}$  equatorial (x2)); 6.76 – 6.82 (m, 4H, Ar).

#### 4.2.2. Preparation of 1',5-diacetyl-spiro[benzo[1,3]dioxole-2,4'-piperidine] (2)



· Procedure (general acetylation procedure)

In a 50 mL round bottom flask the spiro derivative **1** (0.4 g, 1.71 mmol) was dissolved in dichloromethane (15 mL). Then, acetyl chloride (0.83 mL, 7.6 mmol) and titanium tetrachloride were added (0.18 mL, 2.4 mmol) dropwise at 0 °C (keeping the reaction submerged in an ice bath). The reaction mixture was stirred for 6 hours at 0 °C to room temperature.

· Work-up

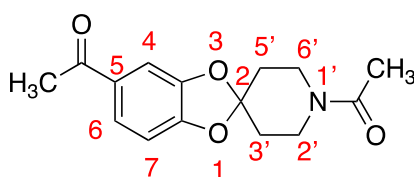
A thin layer chromatography (TLC) of reaction (hexane/ethyl acetate 7:3) indicated a formation of a new compound. Thus, 3 mL of water were added in order to hydrolyze the crude of reaction. The mixture was washed with water (3 x 20 mL) and diluted with dichloromethane (20 mL). The organic phase was dried over anhydrous sodium sulfate, filtered and concentrated *in vacuo*.

· Purification

No purification of the obtained residue by column chromatography was performed since the product was obtained with enough purity.

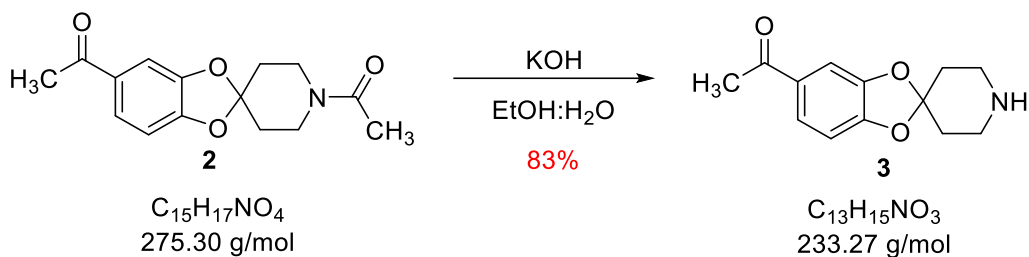
· Analytical data

Product aspect	Mass obtained	Yield	$R_f$ (hexane/ethyl acetate 7:3)
White solid	0.4 g	87%	0.18



$^1H$  NMR ( $CDCl_3$ , 400 MHz)  $\delta$ (ppm), 1.96-2.00 (m, 4H,  $CH_2-C$  (x2)); 2.03 (s, 3H,  $CH_3-CO-N$ ); 2.50 (s, 3H,  $CH_3-CO-C$ ); 3.63 (t,  $J = 6$  Hz, 2H,  $CH-N$  axial (x2)); 3.82 (t,  $J = 6$  Hz, 2H,  $CH-N$  equatorial (x2)); 6.79 (d,  $J = 8.2$  Hz, 1H, H-7); 7.36 (d,  $J = 2$  Hz, 1H, H-4); 7.51 (dd,  $J_1 = 2$  Hz,  $J_2 = 8.2$  Hz, 1H, H-6).

#### 4.2.3. Preparation of 5-acetyl-spiro[benzo[1,3]dioxole-2,4'-piperidine] (3)



· Procedure (general hydrolysis procedure)

The compound **2** (0.4 g, 1.45 mmol) was dissolved in a mixture of ethanol/water (75:25) and potassium hydroxide (1.3 g, 23 mmol) was added. The mixture was stirred at 100 °C and the course of the reaction was controlled by TLC (hexane/ethyl acetate 5:5).

· Work-up

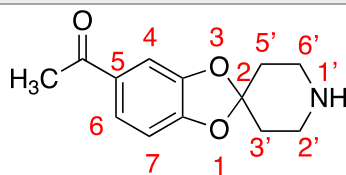
After 24 hours of reaction, when no more starting material was observed in TLC, ethanol was removed under reduced pressure. Next, an extraction with dichloromethane was made (20 mL x 3) and the organic phases were collected, dried over anhydrous  $\text{Na}_2\text{SO}_4$ , filtered and concentrated *in vacuo*.

· Purification

No purification of the obtained residue by column chromatography was performed since product was obtained with enough purity.

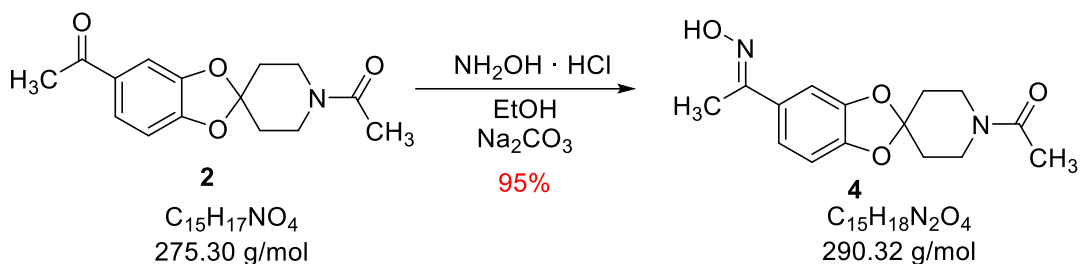
· Analytical data

Product aspect	Mass obtained	Yield	$R_f$ (hexane/ethyl acetate 5:5)
Brownish semisolid	0.280 g	83%	0.02



$^1\text{H NMR}$  ( $\text{CDCl}_3$ , 400 MHz)  $\delta$ (ppm), 1.59 (m, 1H, NH); 1.97 (t,  $J = 6$  Hz, 4H,  $\text{CH}_2\text{-C}$  (x2)); 2.51 (s, 3H,  $\text{CH}_3$ ); 3.04 (t,  $J = 6$  Hz, 4H,  $\text{CH}_2\text{-N}$ (x2)); 6.77 (d,  $J = 8.2$  Hz, 1H, H-7); 7.36 (d,  $J = 2$  Hz, 1H, H-4); 7.51 (dd,  $J_1 = 2$  Hz,  $J_2 = 8.2$  Hz, 1H, H-6).

4.2.4. Preparation of 1'-acetyl-5-(1-(hydroxyimino)ethyl)spiro[benzo[1,3]dioxole-2,4'-piperidine] (4)



· Procedure

In a 50 mL round bottom flask the compound **2** (0.2 g, 0.73 mmol) was dissolved in ethanol (10 mL). Then, hydroxylamine hydrochloride (0.065 g, 0.90 mmol) and sodium carbonate (0.06 g, 0.56 mmol), dissolved in 5 mL of water, were added. The reaction was stirred for 22 h at room temperature. At this time, starting material was still present in TLC, therefore, reaction was heated at 80 °C.

· Work-up

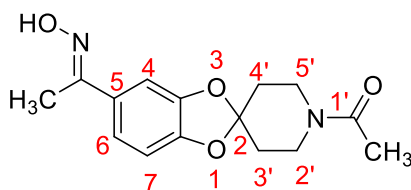
After 20 hours of reaction, a TLC of reaction indicated consumption of starting material (hexane/ethyl acetate 5:5). The ethanol was removed under reduced pressure and the crude was extracted with dichloromethane (20 mL x 3). The organic phases were collected, dried over anhydrous  $\text{Na}_2\text{SO}_4$ , filtered and concentrated *in vacuo*.

· Purification

No purification of the obtained residue by column chromatography was performed since product was obtained with enough purity.

· Analytical data

Product aspect	Mass obtained	Yield	$R_f$ (hexane/ethyl acetate 5:5)	Melting point
Yellow solid	0.1 g	95%	0.25	180-182 °C (DCM)

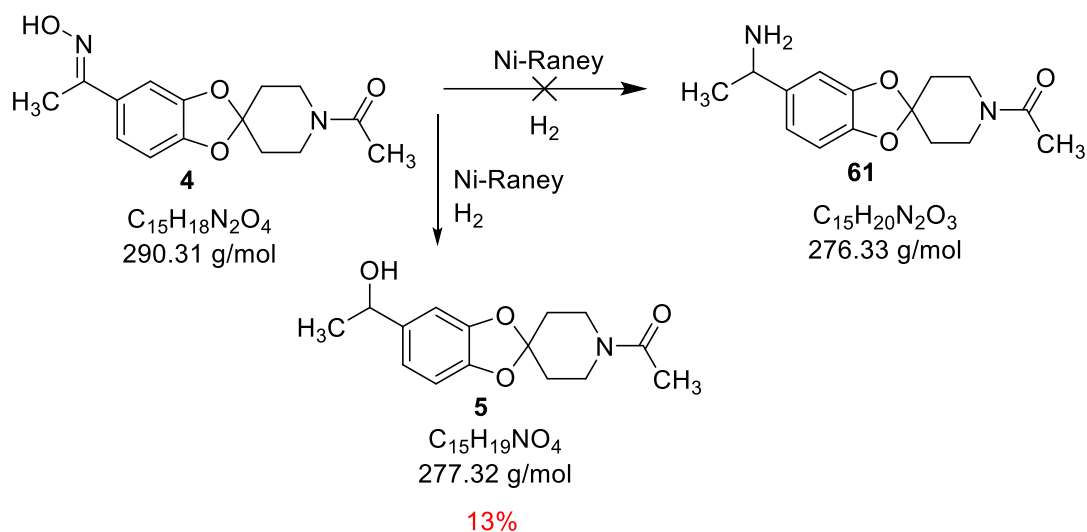


$^1\text{H NMR}$  ( $\text{CDCl}_3$ , 400 MHz)  $\delta$ (ppm), 1.91 (m, 4H,  $\text{CH}_2\text{-C}$  (x2)); 2.09 (s, 3H,  $\text{CH}_3\text{-CO}$ ); 2.17 (s, 3H,  $\text{CH}_3$ ); 3.58 (t,  $J = 6$  Hz, 2H, CH-N axial (x2)); 3.75 (t,  $J = 6$  Hz, 2H, CH-N equatorial (x2)); 6.68 (d,  $J = 8.2$  Hz, 1H, H-7); 7.00 (dd,  $J_1 = 2$  Hz,  $J_2 = 8.2$  Hz, 1H, H-6); 7.06 (d,  $J = 2$  Hz, 1H, H-4).

$^{13}\text{C NMR}$  ( $\text{CDCl}_3$ , 100.6 MHz)  $\delta$ (ppm), 12.2 ( $\text{CH}_3$ ); 21.3 ( $\text{CH}_3$ ); 34.6 (CH-C); 35.4 (CH-C); 38.8 (CH-N); 43.5 (CH-N); 106.4 (CH, C-4); 108.2 (CH, C-7); 116.3 (CH, C-6); 120.1 (Cq, C-2); 130.8 (Cq, C-5); 147.1 (Cq, C-3a); 147.7 (Cq, C-7a); 151.1 (Cq,  $\text{C}\equiv\text{N}$ ); 169.2 (Cq, C=O).



#### 4.2.5. Preparation of 1'-acetyl-5-(1-hydroxyethyl)spiro[benzo[1,3]dioxole-2,4'-piperidine](5)



##### · Procedure

In a 100 mL round-bottomed flask, specific for catalytic hydrogenations, equipped with a magnetic stirring bar, the oxime **4** (0.160 g, 0.55 mmol) and Ni-Raney (0.06 mmol) were added suspended in methanol (10 mL) and ethyl acetate (3 mL). The reaction was stirred at room temperature for 5 days under hydrogen stream.

##### · Work-up

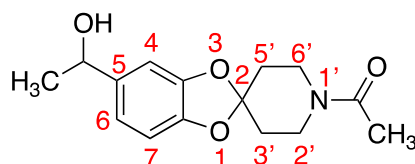
The theoretical required volume for the reaction was 25 mL. Given that hydrogenation apparatus was not completely hermetical, the consumed volume was 40 mL, higher than expected. The analysis of TLC showed consumption of starting material (hexane/ethyl acetate 7:3). The reaction crude was filtered by means of a pleated filter and washed with 20 mL of methanol and was then collected in a 100 mL round-bottomed flask. Finally, the solvent was removed under reduced pressure. The residue was dissolved in ethyl ether (15 mL x 1) and washed with a solution of HCl 3N (10 mL x 3). The aqueous phase was basified with NaOH 2N and extracted with dichloromethane (3 x 20 mL). The last organic phases were collected, dried over anhydrous sodium sulfate, filtered and concentrated *in vacuo*.

##### · Purification

No purification of the obtained residue by column chromatography was performed. The  $^1\text{H}$  NMR and  $^{13}\text{C}$  NMR signals indicated formation of alcohol **5**.

##### · Analytical data

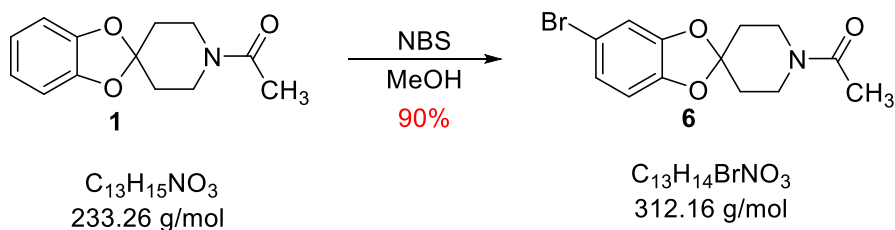
Product aspect	Mass obtained	Yield	$R_f$ (hexane/ethyl acetate 7:3)
Brown oil	0.02 g	13%	0.05



$^1\text{H}$  NMR ( $\text{CDCl}_3$ , 400 MHz)  $\delta(\text{ppm})$ , 1.38 (d,  $J = 6.5$  Hz, 3H,  $\text{CH}_3\text{-CH}$ ); 1.87-1.95 (m, 4H,  $\text{CH}_2\text{-C}$  (x2)); 2.08 (s, 3H,  $\text{CH}_3$ ); 3.58 (t,  $J = 6$  Hz, 2H,  $\text{CH-N}$  axial (x2)); 3.73 (t,  $J = 6$  Hz, 2H,  $\text{CH-N}$  equatorial (x2)); 4.73 (q,  $J = 6.5$  Hz, 1H,  $\text{CH-O}$ ); 6.64 (d,  $J = 8$  Hz, 1H, H-7); 6.72 (dd,  $J_1 = 2$  Hz,  $J_2 = 8$  Hz, 1H, H-6); 6.78 (s, 1H, H-4).

$^{13}\text{C}$  NMR ( $\text{CDCl}_3$ , 100.6 MHz)  $\delta(\text{ppm})$ , 21.4 ( $\text{CH}_3\text{-CH}$ ); 25.2 ( $\text{CH}_3\text{-CO}$ ); 34.6 ( $\text{CH}_2$ ,  $\text{CH}_2\text{-C}$ ); 35.4 ( $\text{CH}_2$ ,  $\text{CH}_2\text{-C}$ ); 38.7 ( $\text{CH}_2\text{-N}$ ); 43.5 ( $\text{CH}_2$ ,  $\text{CH}_2\text{-N}$ ); 70.2 ( $\text{CH}$ ,  $\text{CH-O}$ ); 106.2 ( $\text{CH}$ , C-4); 108.2 ( $\text{CH}$ , C-7); 115.8 (Cq, C-2); 118.5 ( $\text{CH}$ , C-6); 139.8 (Cq, C-5); 146.1 (Cq, C-7a); 147.1 (Cq, C-3a); 168.9 (C=O).

#### 4.2.6. Preparation of 1'-acetyl-5-bromospiro[benzo[1,3]dioxole-2,4'-piperidine] (6)



##### · Procedure

In a 50 mL round bottom flask, the spiro **1** (0.5 g, 2.1 mmol) was dissolved in methanol (12 mL) and NBS (0.42 g, 2.3 mmol) was added slowly. The reaction was vigorously stirred at room temperature.

##### · Work-up

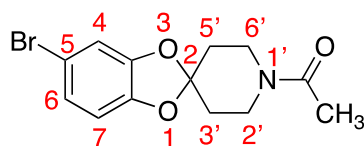
After 3 hours of reaction, analysis of TLC showed a formation of a new product (hexane/ethyl acetate 6:4). The solvent was removed *in vacuo* affording the crude mixture, which was dissolved in dichloromethane (20 mL x 1) and washed with a basic solution of NaOH 2N (20 mL x 3). The organic phase was dried over anhydrous sodium sulfate, filtered and concentrated under reduced pressure.

##### · Purification

Finally, the crude of reaction was purified by a flash automatic column chromatography. The desired product eluted with a mixture of hexane/ethyl acetate 60:40.

##### · Analytical data

Product aspect	Mass obtained	Yield	$R_f$ (hexane/ethyl acetate 6:4)	Melting point
White solid	0.6 g	90%	0.17	253-255 °C (DCM)

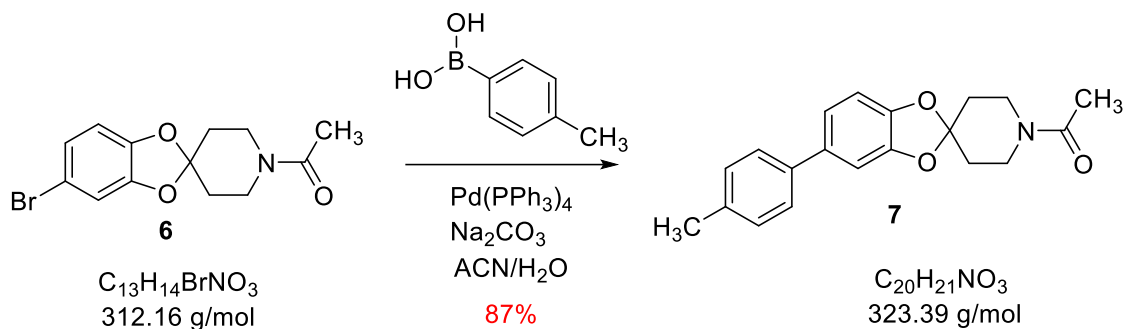


$^1\text{H}$  NMR ( $\text{CDCl}_3$ , 400 MHz)  $\delta(\text{ppm})$ , 1.86 (t,  $J = 5.9$  Hz, 2H,  $\text{CH-C}$  axial (x2)); 1.92 (t,  $J = 5.9$  Hz, 2H,  $\text{CH-C}$  equatorial (x2)); 3.54 (t,  $J = 5.9$  Hz, 2H,  $\text{CH-N}$  axial (x2)); 3.70 (t,  $J = 5.9$  Hz, 2H,  $\text{CH-N}$  equatorial

(x2)); 6.55 (dd,  $J_1 = 1$  Hz,  $J_2 = 8$  Hz, 1H, H-7); 6.81 (d,  $J = 2$  Hz, 1H, H-4); 6.82 (dd,  $J_1 = 2$  Hz,  $J_2 = 8$  Hz, 1H, H-6).

$^{13}\text{C}$  NMR ( $\text{CDCl}_3$ , 100.6 MHz)  $\delta$ (ppm), 21.3 ( $\text{CH}_3$ ); 34.5 ( $\text{CH}_2\text{-C}$ ); 35.3 ( $\text{CH}_2$ ,  $\text{CH}_2\text{-C}$ ); 38.5 ( $\text{CH}_2$ ,  $\text{CH}_2\text{-N}$ ); 43.3 ( $\text{CH}_2$ ,  $\text{CH}_2\text{-N}$ ); 109.7 ( $\text{CH}$ , C-4); 112.3 ( $\text{CH}$ , C-6); 112.7 (Cq, C-2); 117.0 (Cq, C-5); 124.0 ( $\text{CH}$ , C-7); 146.2 (Cq, C-3a); 147.8 (Cq, C-7a); 168.8 (C=O).

#### 4.2.7. Preparation of 1'-acetyl-5-(p-tolyl)spiro[benzo[1,3]dioxole-2,4'-piperidine] (7)



##### · Procedure

In a Pyrex glass tube with screw cap, previously flame-dried under argon atmosphere, the bromo spiro **6** (0.1 g, 0.32 mmol) was dissolved in acetonitrile (10 mL). Then, aryl boronic acid (0.05 g, 0.37 mmol), sodium carbonate (0.068 g, 0.61 mmol), tetrakis(triphenylphosphine)palladium (0.06 mmol) and water (0.6 mL) were added under argon atmosphere. The reaction was stirred at 150 °C for 24 hours.

##### · Work-up

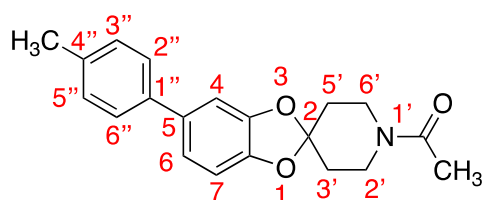
A TLC of reaction mixture showed a formation of a new product and consumption of starting material (hexane/ethyl acetate 7:3). The toluene was removed under reduced pressure to afford the crude, which was dissolved in dichloromethane (20 mL x 1) and washed with water (20 mL x 3). The organic layer was dried over anhydrous  $\text{Na}_2\text{SO}_4$ , filtered and concentrated *in vacuo*.

##### · Purification

Finally, the crude of reaction was purified by a flash automatic column chromatography. The desired product eluted with a mixture of hexane/ethyl acetate 65:45.

##### · Analytical data

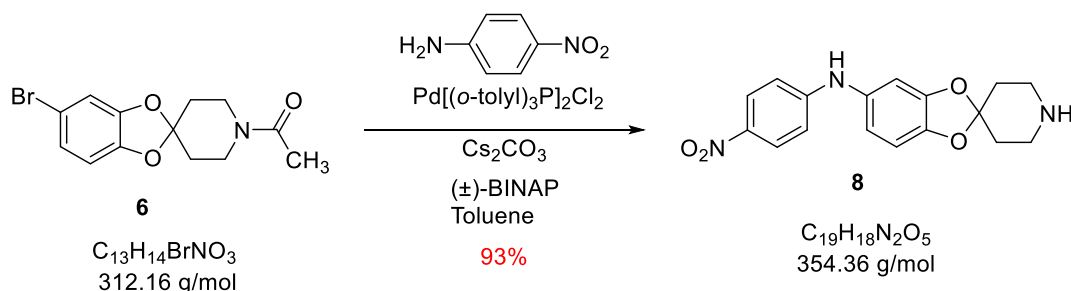
Product aspect	Mass obtained	Yield	$R_f$ (hexane/ethyl acetate 7:3)
Grey oil	0.09 g	87%	0.11



$^1\text{H}$  NMR ( $\text{CDCl}_3$ , 400 MHz)  $\delta$ (ppm), 1.93-1.95 (m, 4H,  $\text{CH}_2\text{-C}$  (x2)); 2.06 (s, 3H,  $\text{CH}_3\text{-CO}$ ); 2.28 (s,  $\text{CH}_3\text{-Ar}$ ); 3.55-3.58 (m, 2H,  $\text{CH-N}$  axial (x2)); 3.73-3.75 (m, 2H,  $\text{CH-N}$  equatorial (x2)); 6.72 (dd,  $J_1 = 1$  Hz,  $J_2 = 7.8$  Hz, 1H, H-7); 6.92 (d,  $J = 1$  Hz, 1H, H-4); 6.93 (dd,  $J_1 = 1$  Hz,  $J_2 = 7.8$  Hz, 1H, H-6); 7.11 (d,  $J = 8$  Hz, 2H, H-3'', H-5''); 7.30 (d,  $J = 8$  Hz, 2H, H-2'', H-6'').

$^{13}\text{C}$  NMR ( $\text{CDCl}_3$ , 100.6 MHz)  $\delta$ (ppm), 21.0 ( $\text{CH}_3\text{-CO}$ ); 21.4 ( $\text{CH}_3\text{-Ar}$ ); 34.7 ( $\text{CH}_2$ ,  $\text{CH}_2\text{-C}$ ); 35.4 ( $\text{CH}_2$ ,  $\text{CH}_2\text{-C}$ ); 38.7 ( $\text{CH}_2$ ,  $\text{CH}_2\text{-N}$ ); 43.5 ( $\text{CH}_2$ ,  $\text{CH}_2\text{-N}$ ); 107.6 ( $\text{CH}$ , C-7); 108.7 ( $\text{CH}$ , C-4); 116.0 (Cq, C-2); 120.1 ( $\text{CH}$ , C-6); 126.6 ( $\text{CH}$ , C-2'', C-6''); 129.1 ( $\text{CH}$ , C-3'', C-5''); 135.4 (Cq, C-4''); 136.6 (Cq, C-5); 138.0 (Cq, C-1''); 146.1 (Cq, C-7a); 147.4 (Cq, C-3a); 168.9 (C=O).

#### 4.2.8. Preparation of 1'-acetyl-5-(4-nitrophenyl)spiro[benzo[1,3]dioxole-2,4'-piperidine] (8)



· Procedure (Buchwald-Hartwig cross-coupling reaction general procedure)

In a Pyrex glass tube with screw cap, previously flame-dried under argon, the spiro compound **6** (0.1 g, 0.32 mmol) was suspended in toluene (5 mL). The 4-nitroaniline (0.05 g, 0.32 mmol), cesium carbonate (0.150 g, 0.48 mmol), BINAP (0.06 mmol) and the  $\text{Pd}[(o\text{-tolil})_3\text{P}]_2\text{Cl}_2$  (0.06 mmol) were added carefully under argon atmosphere. Once the tube is tightly closed the reaction was stirred at 150 °C for 24 h.

· Work-up

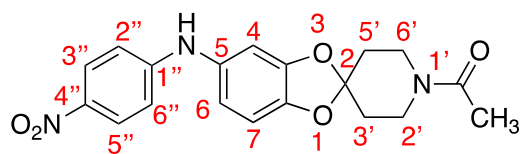
After 24 hours of reaction, in the analysis of TLC, a new yellow compound was observed (hexane/ethyl acetate 6:4). Therefore, toluene was removed under reduced pressure. Then, the crude mixture was dissolved in dichloromethane (20 mL x 1) and washed with water (20 mL x 3). The organic phase was dried over anhydrous  $\text{Na}_2\text{SO}_4$ , filtered and concentrated *in vacuo*.

· Purification

Finally, the obtained residue was purified by manual silica gel column chromatography. The desired product eluted with a mixture of hexane/ethyl acetate 60:40.

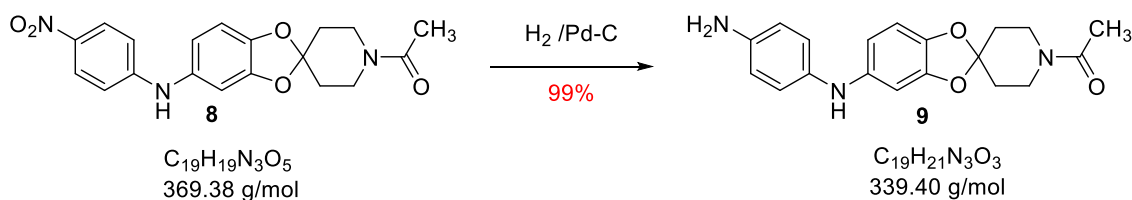
· Analytical data

Product aspect	Mass obtained	Yield	$R_f$ (hexane/ethyl acetate 6:4)
Brownish oil	0.105 g	93%	0.10



$^1\text{H NMR}$  ( $\text{CDCl}_3$ , 400 MHz)  $\delta$ (ppm), 1.99-2.07 (m, 4H,  $\text{CH}_2\text{-C}$  (x2)); 2.16 (s, 3H,  $\text{CH}_3$ ); 3.66 (t,  $J = 5.9$  Hz, 4H,  $\text{CH-N}$  axial (x2)); 3.80-3.83 (m, 2H,  $\text{CH-N}$  equatorial (x2)); 6.24 (bs, 1H,  $\text{NH}$ ); 6.65 (dd,  $J_1 = 2$  Hz,  $J_2 = 8.4$  Hz, 1H, H-6); 6.67 (d,  $J = 2$  Hz, 1H, H-4); 6.76 (d,  $J = 8.4$  Hz, 1H, H-7); 6.78 (d,  $J = 9.3$  Hz, 2H, H-2'', H-6''); 8.07 (d,  $J = 9.3$  Hz, 2H, H-3'', H-5'').

#### 4.2.9. Preparation of 1'-acetyl-5-((4-aminophenyl)amino)spiro[benzo[1,3]dioxole-2,4'-piperidine] (9)



##### · Procedure

The compound from the previous reaction (0.1 g, 0.27 mmol) was dissolved in a mixture of methanol and ethyl acetate in a specific hydrogenation round bottom flask. Then, Pd-C (10% w/w) (0.01 g, 0.094 mmol) suspended in methanol (5 mL) and 0.2 mL of HCl 5N were added. The reaction was stirred under  $\text{H}_2$  stream for 16 hours at room temperature.

##### · Work-up

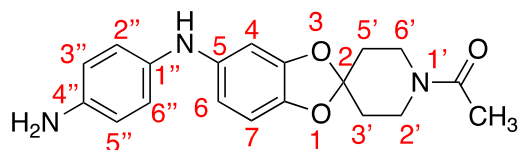
After 24 hours of reaction, a TLC of reaction showed a formation of a new compound (hexane/ethyl acetate 4:6). The crude mixture was filtered by means of a pleated filter and washed with 20 mL of methanol and was then collected in a 100 mL round-bottom flask. Finally, solvent was removed under reduced pressure.

##### · Purification

No purification of the obtained residue by column chromatography was performed since desired product was obtained with enough purity.

##### · Analytical data

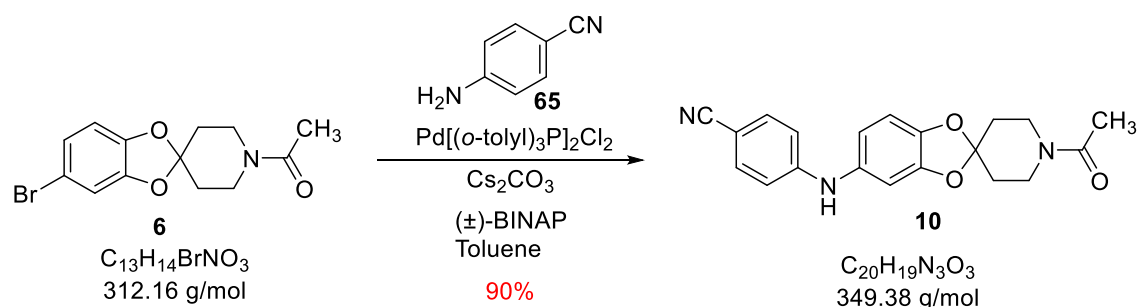
Product aspect	Mass obtained	Yield	$R_f$ (hexane/ethyl acetate 4:6)
Black semisolid	0.064 g	99%	0.13



$^1\text{H}$  NMR ( $\text{CDCl}_3$ , 400 MHz)  $\delta(\text{ppm})$ , 1.90 (t,  $J = 6$  Hz, 4H,  $\text{CH}_2\text{-C}$  (x2)); 2.08 (s, 3H,  $\text{CH}_3$ ); 3.56 (t,  $J = 6$  Hz, 2H,  $\text{CH-N}$  axial (x2)); 3.73 (t,  $J = 6$  Hz, 2H,  $\text{CH-N}$  equatorial (x2)); 6.24 (d,  $J = 7$  Hz, 1H, H-7); 6.38 (s, 1H, H-4); 6.55 (d,  $J = 7$  Hz, 1H, H-6); 6.57 (d,  $J = 7$  Hz, 2H, H-3'', H-5''); 6.80 (d,  $J = 7$  Hz, 2H, H-2'', H-6'').

$^{13}\text{C}$  NMR ( $\text{CDCl}_3$ , 100.6 MHz)  $\delta(\text{ppm})$ , 21.0 ( $\text{CH}_3\text{-CO}$ ); 34.5 ( $\text{CH}_2$ ,  $\text{CH}_2\text{-C}$ ); 35.3 ( $\text{CH}_2$ ,  $\text{CH}_2\text{-C}$ ); 38.8 ( $\text{CH}_2$ ,  $\text{CH}_2\text{-N}$ ); 43.6 ( $\text{CH}_2$ ,  $\text{CH}_2\text{-N}$ ); 99.9 (CH, C-4); 108.6 (CH, C-7); 109.6 (CH, C-6); 115.5 (Cq, C-2); 117.7 (CH, C-3'', C-5''); 120.5 (CH, C-2'', C-6''); 127.8 (Cq, C-5); 137.2 (Cq, C-4''); 138.0 (Cq, C-1''); 140.8 (Cq, C-7a); 147.4 (Cq, C-3a); 168.9 (C=O).

#### 4.2.10. Preparation of 4-((1'-acetylspiro[benzo[1,3]dioxole-2,4'-piperidine]-5-yl)amino) benzonitrile (**10**)



##### · Procedure

Starting from **6** (0.32 mmol), the conditions of Buchwald-Hartwig cross coupling reaction previously described in the synthesis of **8** were applied in this reaction.

##### · Work-up

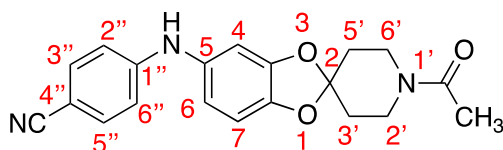
After 24 hours of reaction, the analysis of reaction showed a formation of a new product (hexane/ethyl acetate 7:3). Therefore, toluene was removed under reduced pressure. Then, the crude mixture was dissolved in dichloromethane (20 mL x 1) and washed with water (20 mL x 3). The organic layer was dried over anhydrous  $\text{Na}_2\text{SO}_4$ , filtered and concentrated *in vacuo*.

##### · Purification

Finally, the residue obtained was purified by flash automatic column chromatography. The desired product eluted with a mixture of hexane/ethyl acetate 0:100.

##### · Analytical data

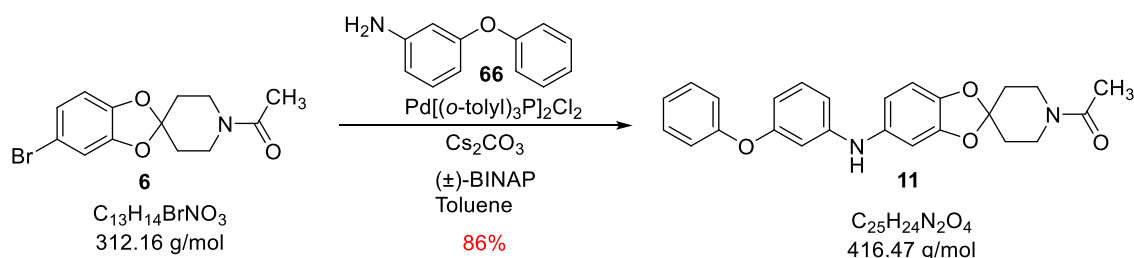
Product aspect	Mass obtained	Yield	$R_f$ (hexane/ethyl acetate 7:3)
Brownish oil	0.1 g	90%	0.09



$^1\text{H}$  NMR ( $\text{CDCl}_3$ , 400 MHz)  $\delta$ (ppm), 1.97 (t,  $J$  = 6.5 Hz, 4H, CH-C axial (x2)); 2.04 (t,  $J$  = 6.5 Hz, 2H, CH-C equatorial (x2)); 2.14 (s, 3H,  $\text{CH}_3$ ); 3.64 (t,  $J$  = 6.5 Hz, 2H, CH-N axial (x2)); 3.79 (t,  $J$  = 6.5 Hz, 2H, CH-N equatorial (x2)); 6.50 (bs, 1H, NH); 6.56 (dd,  $J_1$  = 2 Hz,  $J_2$  = 8.2 Hz, 1H, H-6); 6.67 (d,  $J$  = 2 Hz, 1H, H-4); 6.76 (d,  $J$  = 8.2 Hz, 1H, H-7); 6.78 (d,  $J$  = 8.8 Hz, 2H, H-2'', H-6''); 7.37 (d,  $J$  = 8.8 Hz, 2H, H-3'', H-5'').

$^{13}\text{C}$  NMR ( $\text{CDCl}_3$ , 100.6 MHz)  $\delta$ (ppm), 21.4 ( $\text{CH}_3$ -CO); 34.6 ( $\text{CH}_2$ ,  $\text{CH}_2$ -C); 35.4 ( $\text{CH}_2$ ,  $\text{CH}_2$ -C); 38.7 ( $\text{CH}_2$ ,  $\text{CH}_2$ -N); 43.5 ( $\text{CH}_2$ ,  $\text{CH}_2$ -N); 104.8 (CH, C-4); 108.7 (CH, C-7); 109.8 (CH, C-6); 112.4 (Cq, C-2); 114.0 (CH, C-2'', C-6''); 116.4 (Cq, C $\equiv$ N); 117.0 (Cq, C-4''); 133.6 (CH, C-3'', C-5''); 134.0 (Cq, C-5); 143.8 (Cq, C-7a); 146.2 (Cq, C-3a); 147.8 (Cq, C-1''); 168.9 (Cq, C=O).

#### 4.2.11. Preparation of 1'-acetyl-5-((3-phenoxyphenyl)amino)spiro[benzo[1,3]dioxole-2,4'-piperidine] (**11**)



##### · Procedure

Starting from **6** (0.33 mmol) the Buchwald-Hartwig cross-coupling reaction conditions described in the synthesis of **8**, were applied.

##### · Work-up

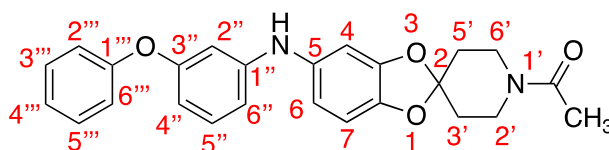
After 24 hours of reaction, the analysis of reaction showed a formation of a new product (hexane/ethyl acetate 6:4). Therefore, toluene was removed under reduced pressure to obtain the crude mixture, which was dissolved in dichloromethane (20 mL x 1) and washed with water (20 mL x 3). The organic layer was dried over anhydrous  $\text{Na}_2\text{SO}_4$ , filtered and concentrated *in vacuo*.

##### · Purification

Finally, the residue obtained was purified by flash automatic column chromatography. The desired product eluted with a mixture of hexane/ethyl acetate 25:75.

##### · Analytical data

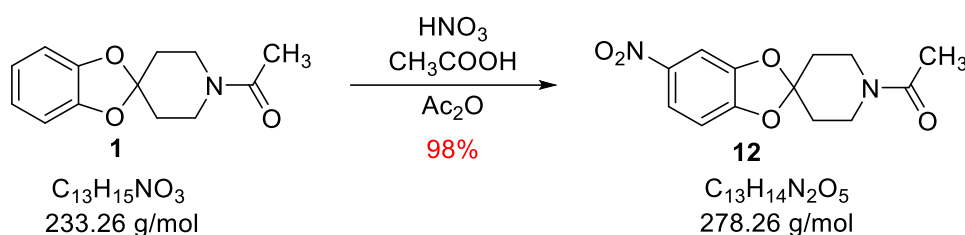
Product aspect	Mass obtained	Yield	$R_f$ (hexane/ethyl acetate 6:4)
Brownish oil	0.120 g	86%	0.14



$^1\text{H}$  NMR ( $\text{CDCl}_3$ , 400 MHz)  $\delta(\text{ppm})$ , 1.91 (t,  $J = 5.8$  Hz, 4H,  $\text{CH-CH}_2$  (x2)); 2.06 (s,  $\text{CH}_3$ , 3H); 3.55 (t,  $J = 5.8$  Hz, 2H,  $\text{CH-N}$  axial (x2)); 3.72 (t,  $J = 5.8$  Hz, 2H,  $\text{CH-N}$  equatorial (x2)); 6.36 (dd,  $J_1 = 2$  Hz,  $J_2 = 8$  Hz, 1H, H-7); 6.46 (dd,  $J_1 = 2$  Hz,  $J_2 = 8$  Hz, 1H, H-6); 6.51 (d,  $J = 2$  Hz, 1H, H-4); 6.55 (d,  $J = 2$  Hz, 1H, H-2''); 6.58 (d,  $J = 8.2$  Hz, 2H, H-4'', H-6''); 6.92 (d,  $J = 7.6$  Hz, 2H, H-2''', H-6'''); 6.98 (t,  $J = 7.6$  Hz, 1H, H-4'''); 7.05 (t,  $J = 8.2$  Hz, 1H, H-5''); 7.23 (t,  $J = 7.6$  Hz, 2H, H-3''', H-5''').

$^{13}\text{C}$  NMR ( $\text{CDCl}_3$ , 100.6 MHz)  $\delta(\text{ppm})$ , 21.4 ( $\text{CH}_3$ ); 34.6 ( $\text{CH}_2$ ,  $\text{CH}_2\text{-C}$ ); 35.4 ( $\text{CH}_2$ ,  $\text{CH}_2\text{-C}$ ); 38.7 ( $\text{CH}_2$ ,  $\text{CH}_2\text{-N}$ ); 43.5 ( $\text{CH}_2$ ,  $\text{CH}_2\text{-N}$ ); 103.3 ( $\text{CH}$ , C-2''); 106.2 ( $\text{CH}$ , C-4''); 108.6 ( $\text{CH}$ , C-4); 109.8 ( $\text{CH}$ , C-7); 110.7 ( $\text{CH}$ , C-6); 113.5 (Cq, C-2); 116.1 ( $\text{CH}$ , C-6''); 118.9 ( $\text{CH}$ , C-2''', C-6'''); 123.1 ( $\text{CH}$ , C-4'''); 129.6 ( $\text{CH}$ , C-3''', C-5'''); 130.3 ( $\text{CH}$ , C-5''); 136.3 (Cq, C-5); 142.6 (Cq, C-1''); 146.5 (Cq, C-7a); 147.5 (Cq, C-3a); 157.1 (Cq, C-1'''); 158.3 (Cq, C-3''); 168.9 (C=O).

#### 4.2.12. Preparation of 1'-acetyl-5-nitrospiro[benzo[1,3]dioxole-2,4'-piperidine] (**12**)



##### · Procedure

In a 10 mL beaker, a mixture between acetic acid and nitric acid was prepared (1:1). Then, in a 25 mL round bottom flask the spiro compound **1** (0.1 g, 0.43 mmol) was dissolved in acetic anhydride (2 mL). A bath with acetone and dry ice was introduced to keep the reaction at  $-15$  °C. At the time the temperature was reached, the mixture of acids was added dropwise into the reaction. Soon after, the bath was removed, and the reaction was stirred for 24 hours at room temperature.

##### · Work-up

A TLC analysis of the crude of reaction showed a formation of a new product and the consumption of the starting material (hexane/ethyl acetate 7:3). Thus, 5 mL of water were added into the mixture. Next, an extraction with dichloromethane (20 mL x 3) and a wash with water (20 mL x 1) was done. Organic layers were collected, dried over anhydrous sodium sulfate, filtered and concentrated under reduced pressure. To remove acetic anhydride traces a co-evaporation with toluene was accomplished.

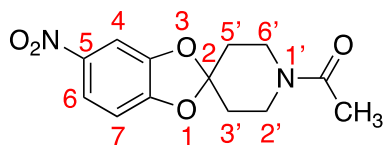
##### · Purification

No purification of the obtained residue by column chromatography was performed since the desired product was obtained with enough purity.

##### · Analytical data

Product aspect	Mass obtained	Yield	$R_f$ (hexane/ethyl acetate 7:3)	Melting point
Yellow solid	0.098 g	98%	0.1	175-177°C (DCM)

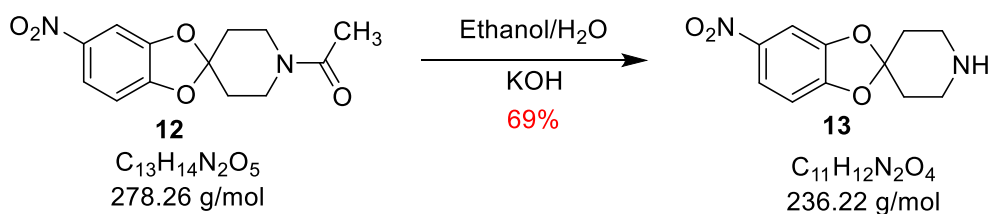




$^1\text{H}$  NMR ( $\text{CDCl}_3$ , 400 MHz)  $\delta$ (ppm), 1.97 (t,  $J = 6$  Hz, 2H, CH-C axial (x2)); 2.02 (t,  $J = 6$  Hz, 2H, CH-C equatorial (x2)); 2.03 (s, 3H,  $\text{CH}_3$ ); 3.62 (t,  $J = 6$  Hz, 2H, CH-N axial (x2)); 3.75 (t,  $J = 6$  Hz, 2H, CH-N equatorial (x2)); 6.77 (d,  $J = 8.6$  Hz, H-7); 7.54 (d,  $J = 2.3$  Hz, 1H, H-4); 7.79 (dd,  $J_1 = 2.3$  Hz,  $J_2 = 8.6$  Hz, 1H, H-6).

$^{13}\text{C}$  NMR ( $\text{CDCl}_3$ , 100.6 MHz)  $\delta$ (ppm), 21.3 ( $\text{CH}_3$ ); 34.6 (CH, CH-C); 35.4 (CH, CH-C); 38.5 (CH, CH-N); 43.2 (CH, CH-N); 104.6 (CH, C-4); 107.8 (CH, C-6); 119.3 (Cq, C-2); 119.7 (CH, C-7); 142.6 (Cq, C-5); 147.3 (Cq, C-3a); 152.3 (Cq, C-7a); 169.0 (Cq, C=O).

#### 4.2.13. Preparation of 5-nitrospiro[benzo[1,3]dioxole-2,4'-piperidine] (**13**)



· Procedure

Starting from **12** (0.43 mmol), the general hydrolysis procedure described in the synthesis of **3** was applied in this reaction. After 24 hours at room temperature, in TLC of reaction (ethyl acetate 100%) starting material was observed. In order to accelerate the hydrolysis, reaction was stirred for 5 hours at 100 °C.

· Work-up

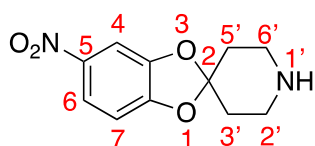
After this time, ethanol was removed under reduced pressure. The obtained crude mixture was dissolved in dichloromethane (20 mL x 1) and washed with water (20 mL x 3). The organic layer was dried over anhydrous sodium sulfate, filtered and concentrated under reduced pressure.

· Purification

No purification of the obtained residue by column chromatography was performed since desired spiro-compound was obtained with enough purity.

· Analytical data

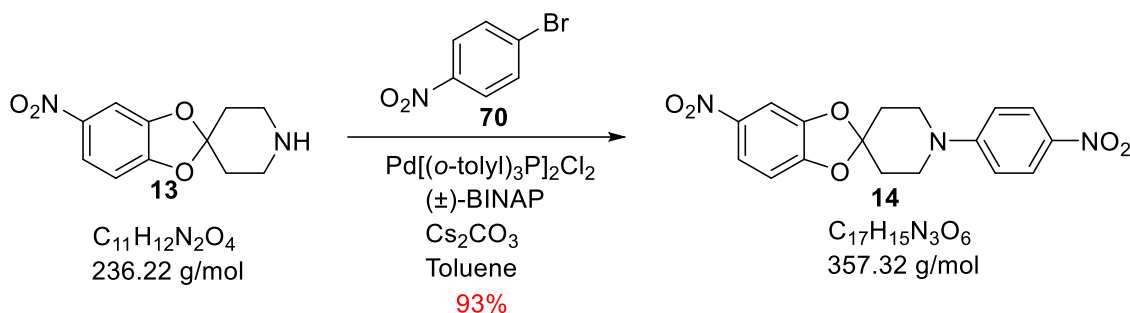
Product aspect	Mass obtained	Yield	$R_f$ (hexane/ethyl acetate 0:1)
Yellow solid	0.070 g	69%	0.05



$^1\text{H}$  NMR ( $\text{CDCl}_3$ , 400 MHz)  $\delta(\text{ppm})$ , 1.94 (t,  $J = 6$  Hz, 4H,  $\text{CH}_2\text{-C}$  (x2)); 2.99 (t,  $J = 6$  Hz, 4H,  $\text{CH}_2\text{-N}$  (x2)); 6.72 (d,  $J = 8.6$  Hz, H-7); 7.52 (d,  $J = 2.3$  Hz, 1H, H-4); 7.77 (dd,  $J_1 = 2.3$  Hz,  $J_2 = 8.6$  Hz, 1H, H-6).

$^{13}\text{C}$  NMR ( $\text{CDCl}_3$ , 100.6 MHz)  $\delta(\text{ppm})$ , 36.1 ( $\text{CH}_2\text{-C}$  (x2)); 43.4 ( $\text{CH}_2\text{-N}$  (x2)); 104.3 (CH, C-4); 107.4 (CH, C-6); 119.4 (CH, C-7); 120.4 (Cq, C-2); 142.4 (Cq, C-5); 147.6 (Cq, C-3a); 152.7 (Cq, C-7a).

#### 4.2.14. Preparation of 5-nitro-1'-(4-nitrophenyl)spiro[benzo[1,3]dioxole-2,4'-piperidine] (14)



##### · Procedure

Starting from **13** (0.027 mmol), the conditions of Buchwald-Hartwig cross-coupling reaction described in synthesis of the spiro derivative **8**, were applied in this reaction.

##### · Work-up

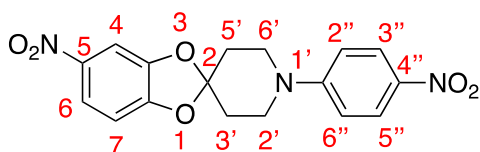
A TLC analysis showed a formation of a new product and consumption of starting material (hexane/ethyl acetate 7:3). The toluene was removed *in vacuo* to afford a crude mixture, which was dissolved in dichloromethane (20 mL x 1) and washed with water (20 mL x 3). The organic layer was dried over anhydrous Na $_2$ SO $_4$ , filtered and concentrated under reduced pressure.

##### · Purification

The crude of reaction was purified by flash automatic column chromatography to afford the expected compound. The desired spiro-compound eluted with a mixture of hexane/ethyl acetate 70:30.

##### · Analytical data

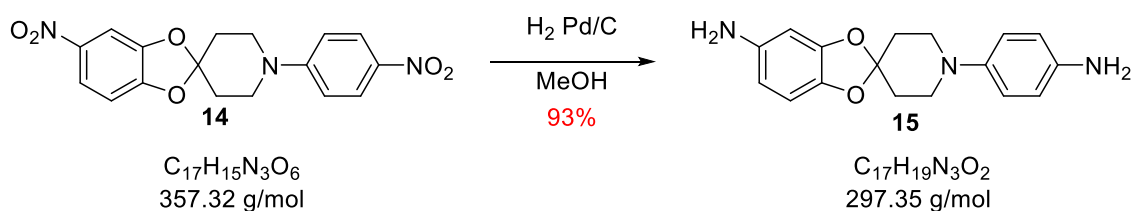
Product aspect	Mass obtained	Yield	R $_f$ (hexane/ethyl acetate 7:3)	Melting point
Yellowish solid	0.097 g	93%	0.67	210-212 °C (DCM)



$^1\text{H}$  NMR ( $\text{CDCl}_3$ , 400 MHz)  $\delta(\text{ppm})$ , 2.11 (t,  $J = 5.7$  Hz, 4H,  $\text{CH}_2\text{-C}$  (x2)); 3.64 (t,  $J = 5.7$  Hz, 4H,  $\text{CH}_2\text{-N}$  (x2)); 6.77 (d,  $J = 8.6$  Hz, 1H, H-7); 6.83 (d,  $J = 9.3$  Hz, 2H, H-2'', H-6''); 7.58 (d,  $J = 2.3$  Hz, 1H, H-4); 7.82 (dd,  $J_1 = 2.3$  Hz,  $J_2 = 8.6$  Hz, 1H, H-6); 8.08 (d,  $J = 9.3$  Hz, 2H, H-3'', H-5'').

$^{13}\text{C}$  NMR ( $\text{CDCl}_3$ , 100.6 MHz)  $\delta(\text{ppm})$ , 34.2 ( $\text{CH}_2$ ,  $\text{CH}_2\text{-C}$  (x2)); 44.8 ( $\text{CH}_2$ ,  $\text{CH}_2\text{-N}$  (x2)); 104.8 (CH, C-4); 107.8 (CH, C-6); 113.2 (CH, C-2'', C-6''); 119.2 (Cq, C-2); 119.7 (CH, C-7); 126.1 (CH, C-3'', C-5''); 138.9 (Cq, C-4''); 142.8 (Cq, C-5); 147.3 (Cq, C-1''); 152.3 (Cq, C-3a); 153.7 (Cq, C-7a).

#### 4.2.15. Preparation of 1'-(4-aminophenyl)spiro[benzo[1,3]dioxole-2,4'-piperidine]-5-amine (**15**)



##### · Procedure

Starting from **14** (0.77 mmol) the catalytic hydrogenation conditions described in synthesis of the spiro derivative **9** were also applied in this case.

##### · Work-up

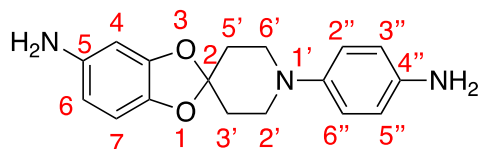
After 24 hours, a TLC confirmed consumption of starting material (hexane/ethyl acetate 6:4). The crude reaction was filtered by means of a pleated filter and washed with 20 mL of methanol and was then collected in a 100 mL round-bottomed flask. Finally, solvent was removed under reduced pressure.

##### · Purification

The crude of reaction was purified by flash automatic column chromatography to afford the expected compound. The desired product eluted with a mixture of hexane/ethyl acetate 30:70.

##### · Analytical data

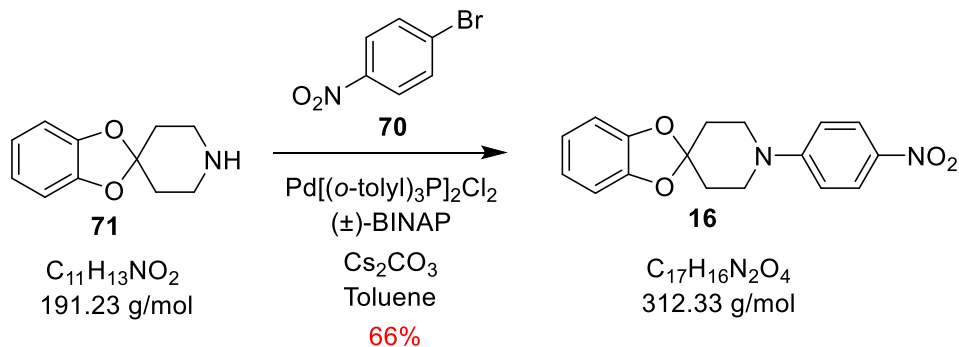
Product aspect	Mass obtained	Yield	$R_f$ (hexane/ethyl acetate 6:4)
Greenish semisolid	0.230 g	93%	0.06



$^1\text{H}$  NMR ( $\text{CDCl}_3$ , 400 MHz)  $\delta(\text{ppm})$ , 2.13 (t,  $J = 6$  Hz, 4H,  $\text{CH}_2\text{-C}$  (x2)); 3.25 (t,  $J = 6$  Hz, 4H,  $\text{CH}_2\text{-N}$  (x2)); 3.46 (bs, 4H,  $\text{NH}_2$  (x2)); 6.10 (dd,  $J_1 = 2$  Hz,  $J_2 = 8$  Hz, 1H, H-6); 6.24 (d,  $J = 2$  Hz, 1H, H-4); 6.56 (d,  $J = 8$  Hz, 1H, H-7); 6.65 (d,  $J = 8.7$  Hz, 2H, H-3'', H-5''); 6.86 (d,  $J = 8.7$  Hz, 2H, H-2'', H-6'').

$^{13}\text{C}$  NMR ( $\text{CDCl}_3$ , 100.6 MHz)  $\delta$ (ppm), 34.7 ( $\text{CH}_2\text{-C}$  (x2)); 49.0 ( $\text{CH}_2\text{-N}$  (x2)); 98.1 (CH, C-4); 106.4 (CH, C-6); 108.2 (Cq, C-2); 108.5 (CH, C-7); 116.1 (CH, C-2'', C-6''); 119.5 (CH, C-3'', C-5''); 140.1 (Cq, C-7a); 140.9 (Cq, C-3a); 141.0 (Cq, C-4''); 144.1 (CH, C-1''); 147.8 (Cq, C-5).

#### 4.2.16. Preparation of 1'-(4-nitrophenyl)spiro[benzo[1,3]dioxole-2,4'-piperidine] (**16**)



##### · Procedure

Starting from **71** (1.79 mmol), the conditions of Buchwald-Hartwig cross-coupling reaction described in the synthesis of **8**, were applied in this reaction.

##### · Work-up

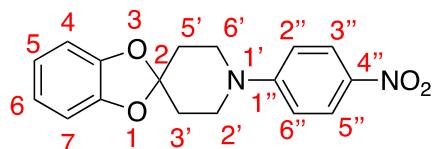
A TLC of reaction (hexane/ethyl acetate 8:2) showed formation of a characteristic yellowish product. The toluene was removed *in vacuo*. The crude mixture was dissolved in dichloromethane and washed with water (20 mL x 3). The organic phase was dried over anhydrous Na<sub>2</sub>SO<sub>4</sub>, filtered and concentrated *in vacuo*.

##### · Purification

Finally, the crude reaction was purified by flash automatic column chromatography. The desired product eluted with a mixture of hexane/ethyl acetate 80:20.

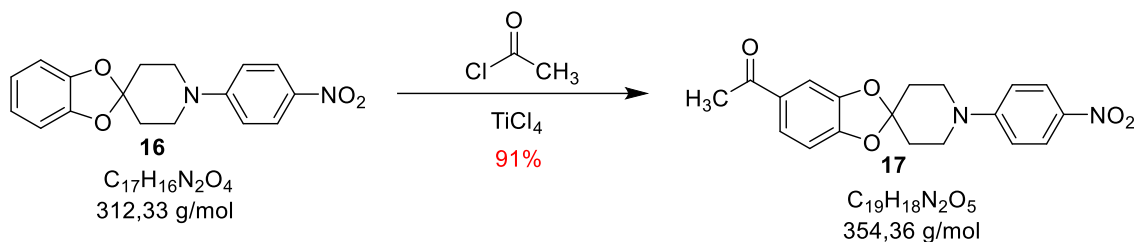
##### · Analytical data

Product aspect	Mass obtained	Yield	R <sub>f</sub> (hexane/ethyl acetate 8:2)
Yellow solid	0.560 g	66%	0.68



$^1\text{H}$  NMR ( $\text{CDCl}_3$ , 400 MHz)  $\delta$ (ppm), 2.11 (t,  $J$  = 6 Hz, 4H,  $\text{CH}_2\text{-C}$  (x2)); 3.68 (t,  $J$  = 5.7 Hz, 4H,  $\text{CH}_2\text{-N}$  (x2)); 6.77-6.78 (m, 4H, H-4, H-5, H-6, H-7); 6.87 (d,  $J$  = 9.4 Hz, 2H, H-2'', H-6''); 8.12 (d,  $J$  = 9.4 Hz, 2H, H-3'', H-5'').

4.2.17. Preparation of 5-acetyl-1'-(4-nitrophenyl)spiro[benzo[1,3]dioxole-2,4'-piperidine] (17)



· Procedure

Starting from **16** (1.6 mmol), the general acetylation procedure described previously by us, was applied in this case.

· Work-up

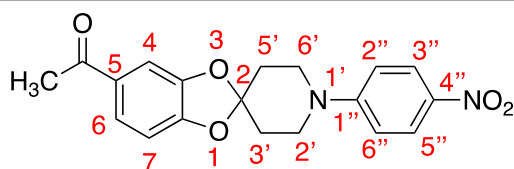
In TLC analysis (hexane/ethyl acetate 7:3) a new yellow compound was observed. The mixture was washed with water (3 x 20 mL) and the organic phase was dried over anhydrous  $\text{Na}_2\text{SO}_4$ , filtered and concentrated *in vacuo*.

· Purification

No purification of the obtained residue by column chromatography was performed since the spiro-compound was obtained with enough purity.

· Analytical data

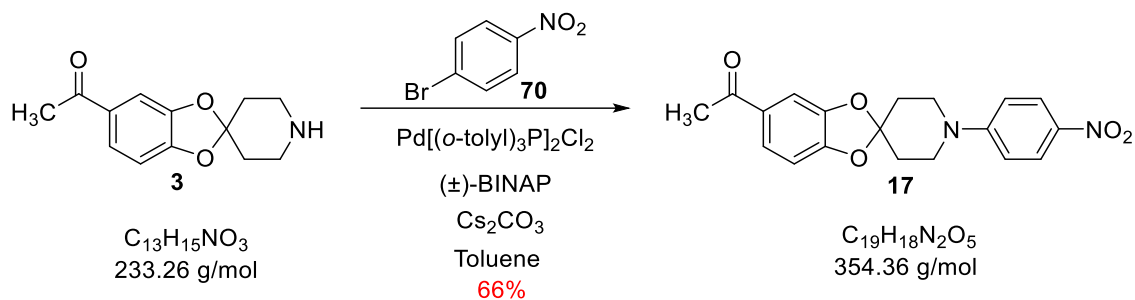
Product aspect	Mass obtained	Yield	$R_f$ (hexane/ethyl acetate 7:3)	Melting point
Yellow solid	0.550 g	91%	0.63	153-155 °C (DCM)



$^1\text{H NMR}$  ( $\text{CDCl}_3$ , 400 MHz)  $\delta$ (ppm), 2.07 (t,  $J = 6$  Hz, 4H,  $\text{CH}_2\text{-C}$  (x2)); 2.46 (s, 3H,  $\text{CH}_3$ ); 3.63 (t,  $J = 6$  Hz, 4H,  $\text{CH}_2\text{-N}$  (x2)); 6.74 (d,  $J = 8.2$  Hz, 1H, H-7); 6.81 (d,  $J = 9.4$  Hz, 2H, H-2'', H-6''); 7.33 (d,  $J = 2$  Hz, 1H, H-4); 7.47 (dd,  $J_1 = 2$  Hz,  $J_2 = 8.2$  Hz, 1H, H-6); 8.05 (d,  $J = 9.4$  Hz, 2H, H-3'', H-5'').

$^{13}\text{C NMR}$  ( $\text{CDCl}_3$ , 100.6 MHz)  $\delta$ (ppm), 26.4 ( $\text{CH}_3$ ); 34.2 ( $\text{CH}_2$ ,  $\text{CH}_2\text{-C}$  (x2)); 44.9 ( $\text{CH}_2$ ,  $\text{CH}_2\text{-N}$  (x2)); 108.1 (CH, C-4); 108.2 (CH, C-7); 113.1 (CH, C-2'', C-6''); 117.2 (Cq, C-2); 124.6 (CH, C-6); 126.1 (CH, C-3'', C-5''); 132.0 (Cq, C-5); 138.6 (Cq, C-4''); 147.4 (Cq, C-3a); 151.0 (Cq, C-7a); 153.0 (Cq, C-1'').

#### 4.2.18. Preparation of 5-acetyl-1'-(4-nitrophenyl)spiro[benzo[1,3]dioxole-2,4'-piperidine] (17)



##### · Procedure

Starting from **3** (0.3 mmol), the general procedure of Buchwald-Hartwig cross-coupling reaction for the formation of C-N bond was applied.

##### · Work-up

In TLC analysis (hexane/ethyl acetate 7:3) the described yellow product **17** was observed. The toluene was removed under reduced pressure to afford the crude, which was dissolved in dichloromethane (10 mL) and washed with water (20 mL x 3). Organic phase was dried over anhydrous sodium sulfate, filtered and concentrated *in vacuo*.

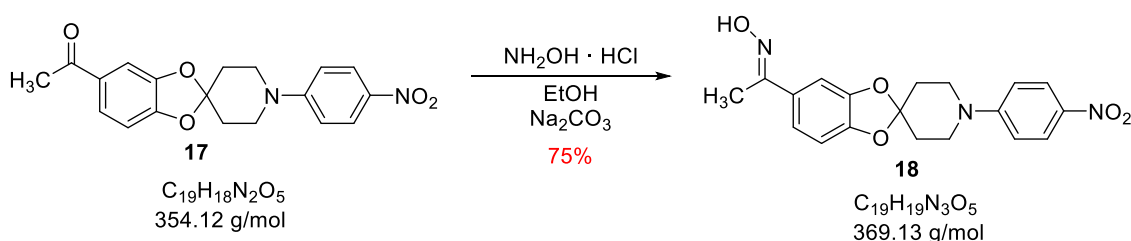
##### · Purification

The crude of the reaction was purified by flash automatic column chromatography. The desired spiro-compound eluted with a mixture of hexane/ethyl acetate 62:38.

##### · Analytical data

The analytical data (product aspect,  $^1\text{H}$  NMR,  $R_f$ , and others) was coincident with those previously described for **17**.

#### 4.2.19. Preparation of 1-(1'-(4-nitrophenyl)spiro[benzo[1,3]dioxole-2,4'-piperidine]-5-yl)ethanone oxime (18)



##### · Procedure

In a 50 mL round bottom flask, the nitro derivative **17** (0.2 g, 0.56 mmol) was dissolved in ethanol (10 mL). Then, hydroxylamine hydrochloride (0.05 g, 0.71 mmol) and sodium carbonate (0.03 g, 0.28 mmol), dissolved in 5 mL of water, were added. The reaction was stirred for 22 h at room temperature. At this time, the starting material was still present on the TLC, therefore, reaction was heated to 80 °C during 20 h.

· Work-up

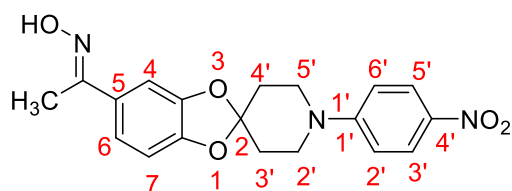
Once this time has passed, a TLC of crude reaction indicated consumption of starting material (hexane/ethyl acetate 6:4). The ethanol was removed under reduced pressure and the obtained crude mixture was extracted with dichloromethane (20 mL x 3). The organic phases were collected, dried over anhydrous Na<sub>2</sub>SO<sub>4</sub>, filtered and concentrated *in vacuo*.

· Purification

The crude of reaction was purified by manual silica gel flash column chromatography. The desired product eluted with a mixture of hexane/ethyl acetate 80:20.

· Analytical data

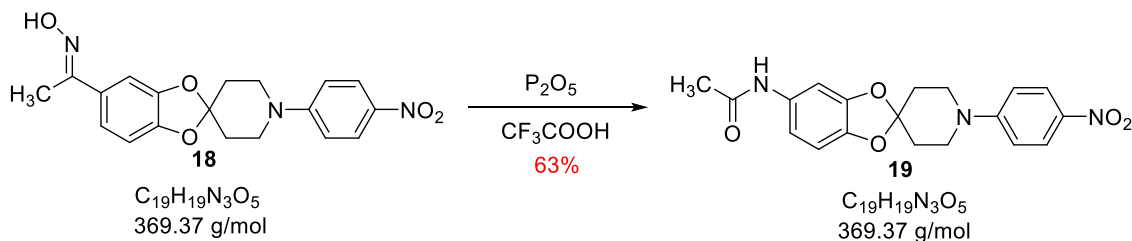
Product aspect	Mass obtained	Yield	R <sub>f</sub> (hexane/ethyl acetate 6:4)	Melting point
Yellow solid	0.156 g	75%	0.88	160-162 °C (DCM)



<sup>1</sup>H NMR (Acetone-d<sub>6</sub>, 400 MHz) δ(ppm), 2.03 (t, *J* = 5 Hz, 4H, CH<sub>2</sub>-C (x2)); 2.06 (s, 3H, CH<sub>3</sub>); 3.69 (q, *J* = 5 Hz, 4H, CH<sub>2</sub>-N (x2)); 6.86 (d, *J* = 8.1 Hz, 1H, H-7); 7.08 (d, *J* = 9.4 Hz, 2H, H-2'', H-6''); 7.09 (dd, *J*<sub>1</sub> = 2 Hz, *J*<sub>2</sub> = 8.1 Hz, 1H, H-6); 7.14 (d, *J* = 2 Hz, 1H, H-4); 8.03 (d, *J* = 9.4 Hz, 2H, H-3'', H-5''); 10.99 (s, 1H, -OH).

<sup>13</sup>C NMR (Acetone-d<sub>6</sub>, 100.6 MHz) δ(ppm), 12.1 (CH<sub>3</sub>); 34.2 (CH<sub>2</sub>, CH<sub>2</sub>-C (x2)); 44.6 (CH<sub>2</sub>, CH<sub>2</sub>-N (x2)); 106.0 (CH, C-7); 108.6 (CH, C-4); 113.5 (CH, C-2'', C-6''); 117.1 (Cq, C-2); 120.1 (CH, C-6); 126.3 (CH, C-3'', C-5''); 131.0 (Cq, C-5); 137.1 (Cq, C-4''); 147.1 (Cq, C-3a); 147.4 (Cq, C-7a); 152.9 (Cq, C-1''); 154.2 (Cq, C≡N).

#### 4.2.20. Preparation of *N*-(1'-(4-nitrophenyl)spiro[benzo[1,3]dioxole-2,4'-piperidine]-5-yl)acetamide (**19**)



· Procedure

In a 5 mL round bottom flask, the oxime **18** (0.08 g, 0.22 mmol) was added. The diphosphorus pentoxide (0.061 g, 0.43 mmol) and TFA (1 mL) were also added. Reaction was stirred under reflux (80 °C) for 12 h.

· Work-up

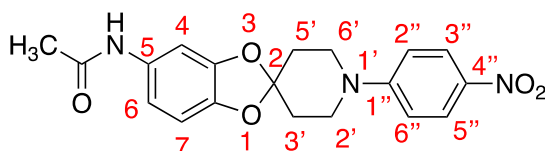
A TLC analysis of crude reaction (hexane/ethyl acetate 6:4) indicated a formation of a new yellow compound. Thus, the mixture was dissolved in dichloromethane and washed with water (20 mL x 3). Organic phase was dried over anhydrous Na<sub>2</sub>SO<sub>4</sub>, filtered and concentrated under reduced pressure.

· Purification

The crude of reaction was purified by manual silica gel column chromatography. The desired product eluted with a mixture of hexane/ethyl acetate 50:50.

· Analytical data

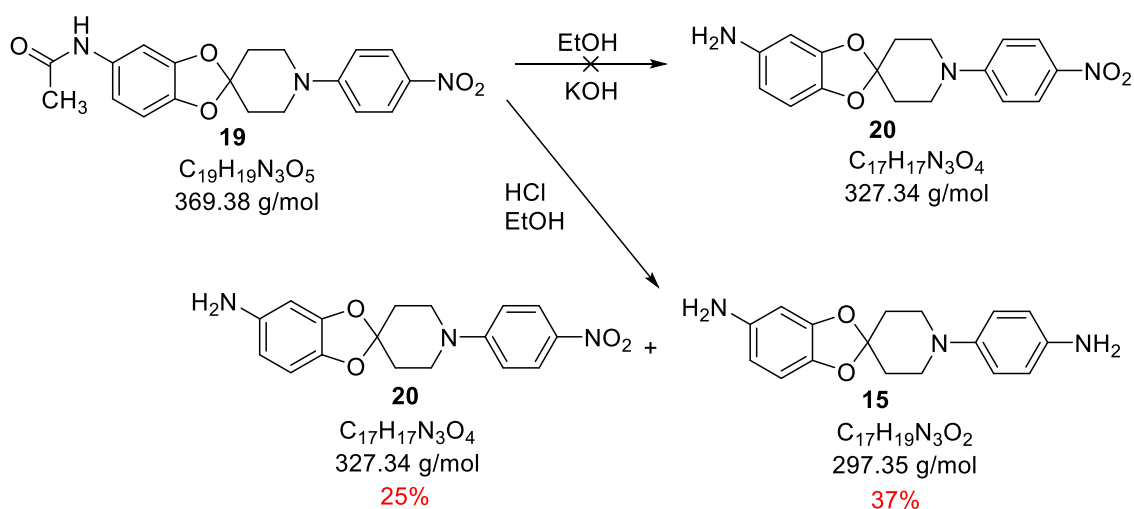
Product aspect	Mass obtained	Yield	R <sub>f</sub> (hexane/ethyl acetate 6:4)
Yellowish semisolid	0.050 g	63%	0.36



<sup>1</sup>H NMR (CDCl<sub>3</sub>, 400 MHz) δ(ppm), 2.03 (t, *J* = 5.7 Hz, 4H, CH<sub>2</sub>-C (x2)); 2.11 (s, 3H, CH<sub>3</sub>); 3.40 (bs, 1H, NH); 3.61 (t, *J* = 5.7 Hz, 4H, CH<sub>2</sub>-N (x2)); 6.63-6.64 (m, 1H, H-7); 6.81 (d, *J* = 9.4 Hz, 2H, H-2'', H-6''); 7.09 (d, *J* = 2 Hz, 1H, H-4); 7.18-7.19 (m, 1H, H-6); 8.07 (d, *J* = 9.4 Hz, 2H, H-3'', H-5'')

<sup>13</sup>C NMR (CDCl<sub>3</sub>, 100.6 MHz) δ(ppm), 23.8 (CH<sub>3</sub>); 34.1 (CH<sub>2</sub>, CH<sub>2</sub>-C (x2)); 44.9 (CH<sub>2</sub>, CH<sub>2</sub>-N (x2)); 103.1 (CH, C-4); 108.1 (CH, C-7); 112.9 (CH, C-6); 113.0 (CH, C-2'', C-6''); 116.1 (Cq, C-2); 126.1 (CH, C-3'', C-5''); 133.3 (Cq, C-5); 133.6 (Cq, C-4''); 142.5 (Cq, C-3a); 146.9 (Cq, C-7a); 153.8 (Cq, C-1'')

#### 4.2.21. Preparation of 1'-(4-nitrophenyl)spiro[benzo[1,3]dioxole-2,4'-piperidine]-5-amine (20)





· Procedure

In a 25 mL round bottom flask the acetamide **19** (0.05 g, 0.14 mmol) was dissolved in a mixture of ethanol (4 mL) and KOH 2N (8 mL). Reaction was stirred at room temperature for 24 hours. After this time, a TLC of the reaction showed starting material and no traces from new products. Therefore, temperature was increased to 60-70 °C. After 24 h, a new TLC indicated same results. The reaction was set up again in a round bottom flask with the product dissolved in a mixture of ethanol and HCl 2N (5:5). Reaction was stirred at 70 °C for 24 hours.

· Work-up

In the TLC analysis (hexane/ethyl acetate 7:3) two new products were observed. Thus, ethanol was removed under reduced pressure to afford a crude mixture, which was dissolved in ethyl ether (1 x 20 mL) and washed with HCl 2N (10 mL x 3). The aqueous phases were collected and basified by means of NaOH 2N. Next, the product was extracted with dichloromethane (20 x 3 mL). Organic phases were collected, dried over anhydrous sodium sulfate, filtered and concentrated under reduced pressure.

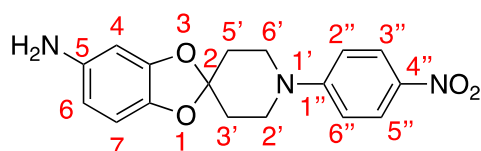
· Purification

Finally, the crude reaction was purified by flash automatic column chromatography. The products **20** and **15** eluted with a mixture of hexane/ethyl acetate 70:30 and 65:35 respectively.

· Analytical data

**20.**

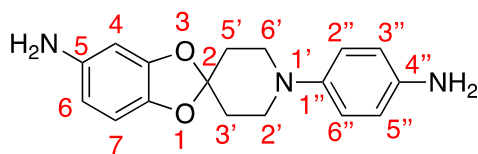
Product aspect	Mass obtained	Yield	R <sub>f</sub> (hexane/ethyl acetate 7:3)	Melting point
Brownish solid	0.01 g	25%	0.51	225-227 °C (DCM)



<sup>1</sup>H NMR (CDCl<sub>3</sub>, 400 MHz) δ(ppm), 1.99-2.12 (m, 4H, CH<sub>2</sub>-C (x2)); 3.59-3.66 (m, 4H, CH<sub>2</sub>-N (x2)); 6.02 (d, J = 7 Hz, 1H, H-6 rotamer m); 6.08 (d, J = 7 Hz, 1H, H-6 rotamer M); 6.15 (s, 1H, H-4, rotamer m); 6.21 (s, 1H, H-4, rotamer M); 6.46 (d, J = 7 Hz, 0.5H, H-7, rotamer m); 6.52 (d, J = 7 Hz, 1H, H-7, rotamer M); 6.79 (d, J = 9 Hz, 1H, H-2'', H-6'' rotamer m); 6.83 (d, J = 9 Hz, 2H, H-2'', H-6'' rotamer M); 8.02 (d, J = 9 Hz, 1H, H-3'', H-5'' rotamer m); 8.09 (d, J = 9 Hz, 2H, H-3'', H-5'' rotamer M). **M rotamer: majority, m rotamer: minority.**

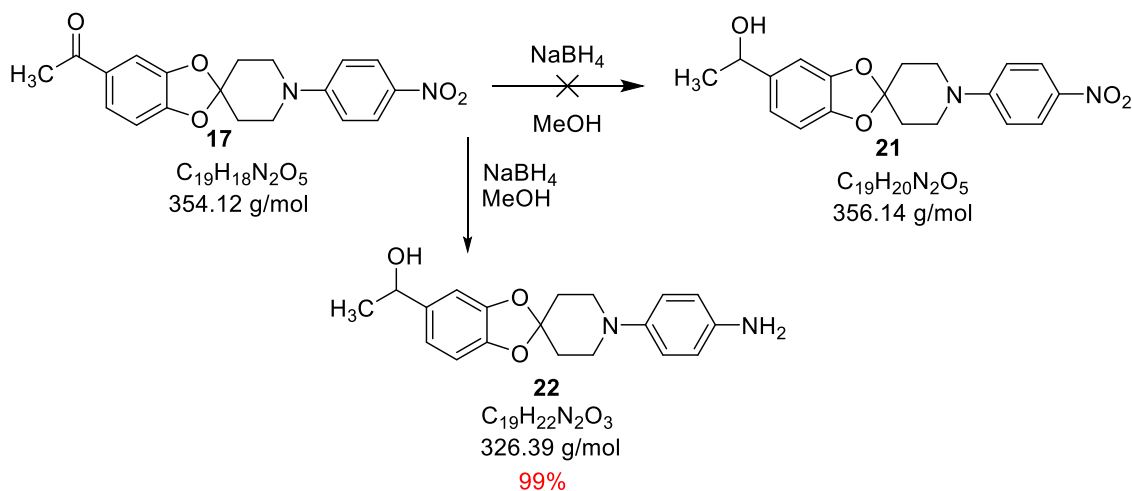
**15.**

Product aspect	Mass obtained	Yield	R <sub>f</sub> (hexane/ethyl acetate 7:3)
Brownish solid	0.015 g	37%	0.33



The analytical data (product aspect,  $^1\text{H}$  NMR,  $R_f$ , and others) was coincident with those previously described for **15**.

#### 4.2.22. Preparation of 1-(1'-(4-nitrophenyl)spiro[benzo[1,3]dioxole-2,4'-piperidine]-5-yl)ethanol (**21**)



##### · Procedure

In a 25 mL round bottom flask, the spiro-derivative **17** (0.06 g, 0.22 mmol) was dissolved in methanol (10 mL) and sodium borohydride (0.01 g, 0.22 mmol) was slowly added. The reaction was stirred for 2 hours at room temperature. After this time, a TLC of reaction (hexane/ethyl acetate 6:4) showed a formation of two new products. As well, a remaining quantity of starting material was observed. Therefore, one more equivalent of NaBH<sub>4</sub> was added and the color of reaction turned from yellow to brownish.

##### · Work-up

A new TLC indicated a presence of one compound and complete consumption of starting material. To proceed with hydrolysis of the reaction, 2 mL of water were added. Finally, methanol was evaporated *in vacuo*.

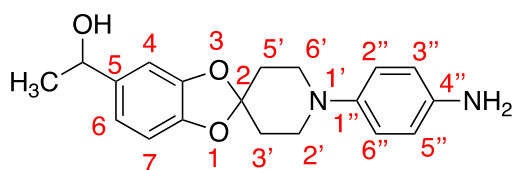
The crude mixture was dissolved in ethyl ether (10 mL) and washed with HCl 2N (10 mL x 3). Aqueous phases were collected and basified by means of NaOH 2N. Then, the product was extracted with dichloromethane (20 mL x 3). Organic phases were collected, dried over anhydrous sodium sulfate, filtered and concentrated *in vacuo*.

##### · Purification

No purification of the obtained residue by column chromatography was performed since the product was obtained with enough purity. The  $^1\text{H}$  NMR and the  $^{13}\text{C}$  NMR confirmed formation of 1-(1'-(4-aminophenyl)spiro[benzo[1,3]dioxole-2,4'-piperidine]-5-yl)ethanol (**22**).

· Analytical data

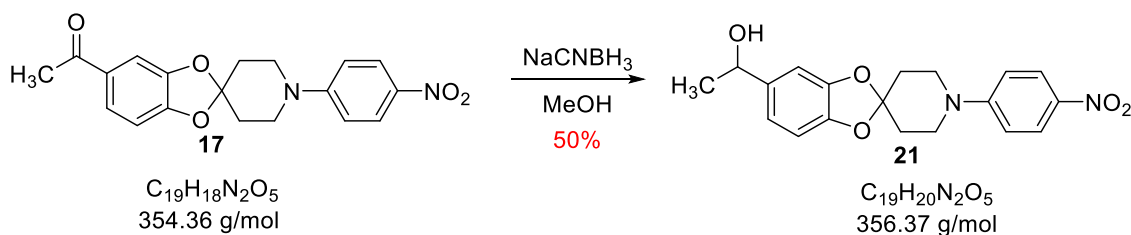
Product aspect	Mass obtained	Yield	$R_f$ (hexane/ethyl acetate 6:4)	Melting point
Brownish solid	0.055 g	99%	0.16	180-182 °C (DCM)



$^1\text{H}$  NMR ( $\text{CDCl}_3$ , 400 MHz)  $\delta$ (ppm), 1.38 (d,  $J = 6.4$  Hz, 3H,  $\text{CH}_3$ ); 2.08 (t,  $J = 5.5$  Hz, 4H,  $\text{CH}_2\text{-C}$  (x2)); 3.19 (t,  $J = 5.5$  Hz, 4H,  $\text{CH}_2\text{-N}$  (x2)); 4.73 (q,  $J = 6.4$  Hz, 1H,  $\text{CH-OH}$ ); 6.59 (d,  $J = 8.9$  Hz, 2H, H-3'', H-5''); 6.64 (d,  $J = 8$  Hz, 1H, H-7); 6.71 (dd,  $J_1 = 2$  Hz,  $J_2 = 8$  Hz, 1H, H-6); 6.77 (d,  $J = 2$  Hz, 1H, H-4); 8.79 (d,  $J = 8.9$  Hz, 2H, H-2'', H-6'').

$^{13}\text{C}$  NMR ( $\text{CDCl}_3$ , 100.6 MHz)  $\delta$ (ppm), 25.0 ( $\text{CH}_3$ ); 34.9 ( $\text{CH}_2$ ,  $\text{CH}_2\text{-C}$  (x2)); 48.8 ( $\text{CH}_2$ ,  $\text{CH}_2\text{-N}$  (x2)); 70.3 ( $\text{CH}$ ,  $\text{CH-O}$ ); 106.0 ( $\text{CH}$ , C-4); 108.0 ( $\text{CH}$ , C-7); 116.2 ( $\text{CH}$ , C-2'', C-6''); 116.5 (Cq, C-2); 118.2 ( $\text{CH}$ , C-6); 119.5 ( $\text{CH}$ , C-3'', C-5''); 139.4 (Cq, C-5); 140.3 (Cq, C-4''); 143.9 (Cq, C-1''); 146.5 (Cq, C-7a); 147.4 (Cq, C-3a).

#### 4.2.23. Preparation of 1-(1'-(4-aminophenyl)spiro[benzo[1,3]dioxole-2,4'-piperidine]-5-yl)ethanol (**21**)



· Procedure

The spiro-compound **17** (0.065 g, 0.28 mmol) was dissolved in methanol (10 mL) and sodium cyanoborohydride (0.005 g, 0.04 mmol) was added instead of sodium borohydride. Also, the reaction was set up keeping temperature at 0 °C. After 3 hours of stirring, a TLC (hexane/ethyl acetate 6:4) showed starting material. Thus, the iced bath was removed in order to keep the reaction at room temperature.

· Work-up

After 6 hours of reaction, in TLC analysis (hexane/ethyl acetate 6:4) a formation of expected compound without any traces of reduced amino was observed. To proceed with reaction work-up, 5 mL of water were added. The methanol was removed under reduced pressure and the

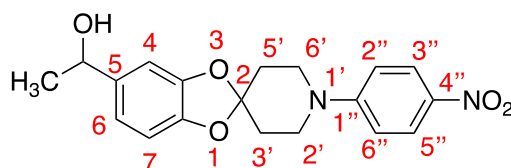
resultant crude mixture was extracted with dichloromethane (20 mL x 3). Organic phases were collected, dried over anhydrous sodium sulfate, filtered and concentrated *in vacuo*.

· Purification

Finally, the crude reaction was purified by flash automatic column chromatography. The desired product (**21**) eluted with a mixture of hexane/ethyl acetate 60:40.

· Analytical data

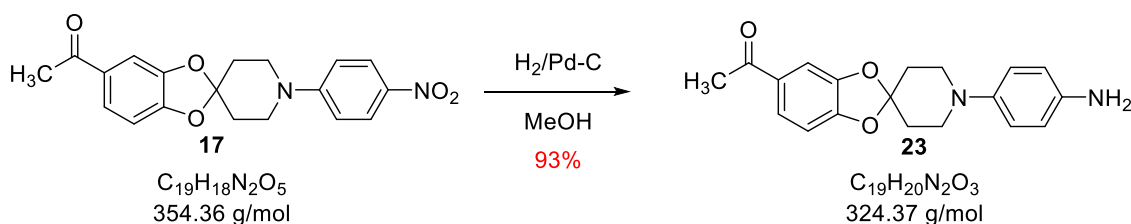
Product aspect	Mass obtained	Yield	R <sub>f</sub> (hexane/ethyl acetate 6:4)
Yellow semisolid	0.030 g	50%	0.47



<sup>1</sup>H NMR (CDCl<sub>3</sub>, 400 MHz) δ(ppm), 1.39 (d, *J* = 6.4 Hz, 3H, CH<sub>3</sub>); 2.04 (t, *J* = 5.7 Hz, 4H, CH<sub>2</sub>-C (x2)); 2.10 (s, 1H, OH); 3.62 (t, *J* = 5.7 Hz, 4H, CH<sub>2</sub>-N (x2)); 4.75 (q, *J* = 6.4 Hz, 1H, CH); 6.65 (d, *J* = 8 Hz, 1H, H-7); 6.74 (dd, *J*<sub>1</sub> = 2 Hz, *J*<sub>2</sub> = 8 Hz, 1H, H-6); 6.80 (d, *J* = 9.5 Hz, 2H, H-2'', H-6''); 7.79 (s, 1H, H-4); 8.06 (d, *J* = 9.5 Hz, 2H, H-3'', H-5'').

<sup>13</sup>C NMR (CDCl<sub>3</sub>, 100.6 MHz) δ(ppm), 25.1 (CH<sub>3</sub>); 34.2 (CH<sub>2</sub>, CH<sub>2</sub>-C (x2)); 44.9 (CH<sub>2</sub>, CH<sub>2</sub>-N (x2)); 70.2 (CH, CH-O); 106.2 (CH, C-4); 108.2 (CH, C-7); 113.0 (CH, C-2'', C-6''); 115.7 (Cq, C-2); 118.6 (CH, C-6); 126.1 (CH, C-3'', C-5''); 138.5 (Cq, C-5); 139.8 (Cq, C-4''); 146.1 (Cq, C-7a); 147.1 (Cq, C-3a); 153.9 (Cq, C-1'').

#### 4.2.24. Preparation of 5-acetyl-1'--(4-aminophenyl)spiro[benzo[1,3]dioxole-2,4'-piperidine] (**23**)



· Procedure

The spiro derivative **17** (0.1 g, 0.26 mmol) was added, dissolved in a mixture of methanol and ethyl acetate, in a specific hydrogenation round bottom flask. Then, Pd-C (10%) (0.01 g, 0.094 mmol) in methanol and 0.2 mL of HCl 5N were added. The mixture of reaction was stirred vigorously under H<sub>2</sub> stream at atmospheric pressure for 16 hours.

· Work-up

The theoretical required volume for the reaction was 10 mL. Given that hydrogenation apparatus was not completely hermetical, the consumed volume was 30 mL, higher than expected. TLC (hexane/ethyl acetate 7:3) of reaction indicated a formation of a new compound. The mixture

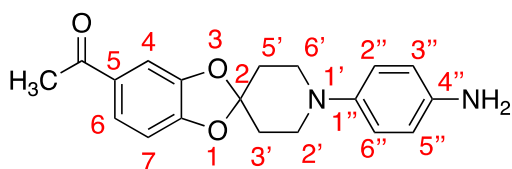
was filtered by means of a pleated filter and washed with 20 mL of methanol and was then collected in a 100 mL round-bottomed flask. The solvent was removed under reduced pressure to afford a residue that was dissolved in dichloromethane (10 mL) and washed with a solution of NaOH 8N (20 mL x 3). Organic phase was dried over anhydrous Na<sub>2</sub>SO<sub>4</sub>, filtered and concentrated under reduced pressure.

· Purification

Finally, the crude reaction was purified by flash automatic column chromatography. The desired product eluted with a mixture of hexane/ethyl acetate 80:20.

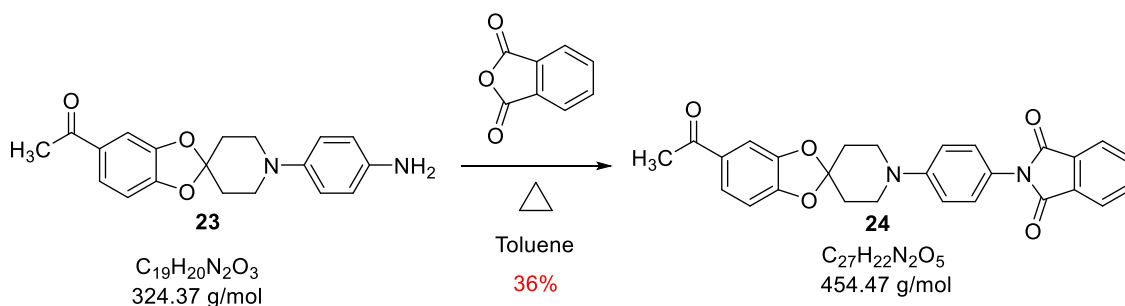
· Analytical data

Product aspect	Mass obtained	Yield	R <sub>f</sub> (hexane/ethyl acetate 7:3)	Melting point
Brownish solid	0.085 g	93%	0.29	200-202 °C (DCM)



<sup>1</sup>H NMR (CDCl<sub>3</sub>, 400 MHz) δ(ppm), 2.09 (t, *J* = 6 Hz, 4H, CH<sub>2</sub>-C (x2)); 2.45 (s, 3H, CH<sub>3</sub>); 3.19 (t, *J* = 6 Hz, 4H, CH<sub>2</sub>-N (x2)); 3.40 (bs, 2H, NH<sub>2</sub>); 6.58 (d, *J* = 8.9 Hz, 2H, H-3'', H-5''); 6.72 (d, *J* = 8.1 Hz, 1H, H-7); 6.78 (d, *J* = 8.9 Hz, 2H, H-2'', H-6''); 7.31 (d, *J* = 2 Hz, 1H, H-4); 7.45 (dd, *J*<sub>1</sub> = 2 Hz, *J*<sub>2</sub> = 8.1 Hz, 1H, H-6).

#### 4.2.25. Preparation of 2-(4-(5-acetylspiro[benzo[1,3]dioxole-2,4'-piperidine]-1'-yl)phenyl)-isoindoline-1,3-dione (**24**)



· Procedure

In a Pyrex glass tube, previously flame-dried under argon, aniline **23** (0.08 g, 0.462 mmol) dissolved in toluene (6 mL) and phthalic anhydride (0.05 g, 0.35 mmol) were added under argon atmosphere. After 6 hours of reaction, a catalytic quantity of APTS (0.06 mmol) was added. The tube closes tightly and the mixture was stirred overnight at 120-130 °C.

· Work-up

After 18 hours of reaction, a TLC analysis showed consumption of starting material (hexane/ethyl acetate 7:3). Thus, toluene was removed *in vacuo* and the resultant crude mixture was diluted

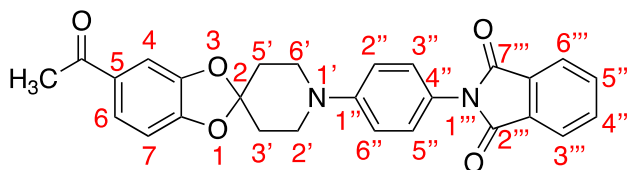
with water (20 mL) and extracted with ethyl acetate (3 x 20 mL). The combined organic phases were dried over anhydrous Na<sub>2</sub>SO<sub>4</sub>, filtered and concentrated under reduced pressure.

· Purification

Finally, the crude reaction was purified by flash automatic column chromatography. The desired product (**24**) eluted with a mixture of hexane/ethyl acetate 30:70.

· Analytical data

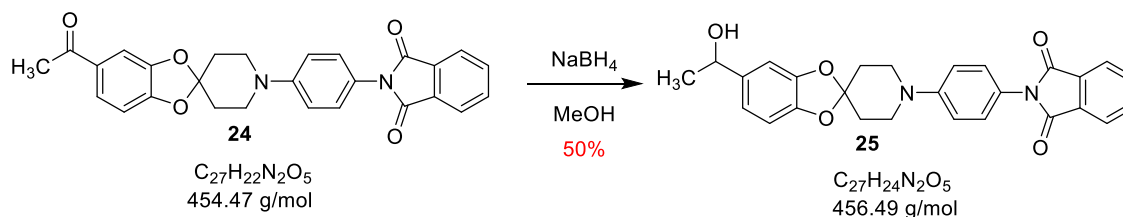
Product aspect	Mass obtained	Yield	R <sub>f</sub> (hexane/ethyl acetate 3:7)	Melting point
Whitish solid	0.036 g	36%	0.78	223-225 °C (DCM)



<sup>1</sup>H NMR (CDCl<sub>3</sub>, 400 MHz) δ(ppm), 2.17 (t, *J* = 5.8 Hz, 4H, CH<sub>2</sub>-C (x2)); 2.54 (s, 3H, CH<sub>3</sub>); 3.52 (t, *J* = 5.8 Hz, 4H, CH<sub>2</sub>-N (x2)); 6.81 (d, *J* = 8.2 Hz, 1H, H-7); 7.06 (d, *J* = 8.9 Hz, 2H, H-2'', H-6''); 7.32 (d, *J* = 8.9 Hz, 2H, H-3'', H-5''); 7.41 (d, *J* = 2 Hz, 1H, H-4); 7.54 (dd, *J*<sub>1</sub> = 2 Hz, *J*<sub>2</sub> = 8.2 Hz, 1H, H-6); 7.78 (dd, *J*<sub>1</sub> = 3 Hz, *J*<sub>2</sub> = 5.5 Hz, 2H, H-4''', H-5'''); 7.94 (dd, *J*<sub>1</sub> = 3 Hz, *J*<sub>2</sub> = 5.5 Hz, 2H, H-3''', H-6''').

<sup>13</sup>C NMR (CDCl<sub>3</sub>, 100.6 MHz) δ(ppm), 26.4 (CH<sub>3</sub>); 34.4 (CH<sub>2</sub>, CH<sub>2</sub>-C (x2)); 46.6 (CH<sub>2</sub>, CH<sub>2</sub>-N (x2)); 107.9 (CH, C-4); 108.1 (CH, C-7); 116.7 (CH, C-6); 117.8 (Cq, C-2); 123.6 (CH, C-2'', C-6''); 123.8 (Cq, C-4''); 124.4 (CH, C-3''', C-6'''); 125.5 (Cq, C-5); 127.6 (CH, C-3'', C-5''); 131.8 (Cq, C-C=O (x2)); 134.3 (CH, C-4''', C-5'''); 147.6 (Cq, C-3a); 149.8 (Cq, C-1''); 151.3 (Cq, C-7a); 167.6 (Cq, C=O (x2)); 196.3 (Cq, C=O).

#### 4.2.26. Preparation of 2-(4-(5-(1-hydroxyethyl)spiro[benzo[1,3]dioxole-2,4'-piperidine]-1'-yl)phenyl)isoindoline-1,3-dione (**25**)



· Procedure

In a 50 mL round-bottom flask, the compound **24** (0.03 g, 0.07 mmol) and sodium borohydride (0.005 g, 0.07 mmol) were added. Reaction was stirred for 3 hours at room temperature. Along this time, a color change was observed, white to colorless.

· Work-up

Analysis of TLC showed a formation of a new product (hexane/ethyl acetate 7:3). Therefore, 5 mL of water were added. Methanol was removed under reduced pressure and the obtained crude

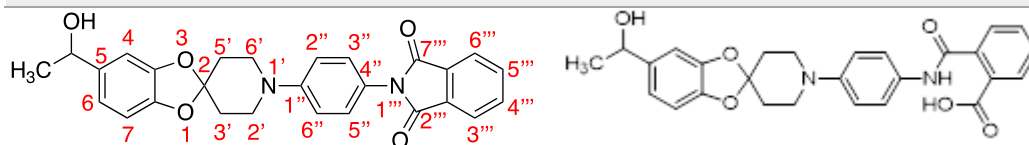
mixture was extracted with dichloromethane (20 mL x 3). The combined organic layers were dried over anhydrous Na<sub>2</sub>SO<sub>4</sub>, filtered and concentrated under reduced pressure.

· Purification

Finally, the reaction mixture was purified by flash automatic column chromatography. The desired product eluted with a mixture of hexane/ethyl acetate 70:30. A co-evaporation with toluene was done in order to dry the product and to close phthalimide ring.

· Analytical data

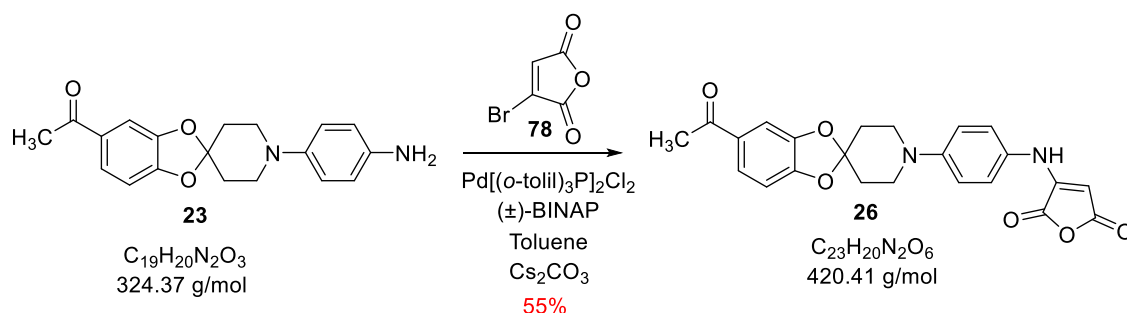
Product aspect	Mass obtained	Yield	R <sub>f</sub> (hexane/ethyl acetate 7:3)	Melting point
White solid	0.030 g	50%	0.16	193-195 °C (DCM)



<sup>1</sup>H NMR (CDCl<sub>3</sub>, 400 MHz) δ(ppm), 1.39 (d, *J* = 6.4 Hz, 3H, CH<sub>3</sub>); 2.07-2.09 (m, 4H, CH<sub>2</sub>-C (x2)); 3.53 (t, *J* = 5.8 Hz, 4H, CH<sub>2</sub>-N (x2)); 4.74 (q, *J* = 6.4 Hz, 1H, CH-O); 6.65 (d, *J* = 8 Hz, 1H, H-7); 6.72 (dd, *J*<sub>1</sub> = 2 Hz, *J*<sub>2</sub> = 8 Hz, 1H, H-6); 6.78 (d, *J* = 2 Hz, 1H, H-4); 6.93 (d, *J* = 8 Hz, 2H, H-2'', H-6''); 7.44 (dt, *J*<sub>1</sub> = 1.5 Hz, *J*<sub>2</sub> = 7.2 Hz, 1H, C-H phthalimide); 7.50 (d, *J* = 8 Hz, 2H, H-3'', H-5''); 7.54 (dt, *J*<sub>1</sub> = 1.5 Hz, *J*<sub>2</sub> = 7.2 Hz, 1H, C-H phthalimide); 7.58 (d, *J* = 7.2 Hz, 1H, C-H phthalimide); 7.73 (d, *J* = 7.2 Hz, 1H, C-H phthalimide); (Due to the multiplicity observed in phthalimide protons it has been concluded that imide ring was open during the time of spectrum acquisition).

<sup>13</sup>C NMR (CDCl<sub>3</sub>, 100.6 MHz) δ(ppm), 22.7 (CH<sub>3</sub>); 25.1 (CH<sub>2</sub>, CH<sub>2</sub>-C (x2)); 34.3 (CH<sub>2</sub>, CH<sub>2</sub>-N (x2)); 70.3 (CH-O); 106.1 (CH, C-4); 108.1 (CH, C-7); 117.4 (CH, C-6); 118.2 (Cq, C-2); 118.4 (CH, C-2'', C-6''); 122.2 (CH, phthalimide); 123.8 (CH, phthalimide); 124.2 (CH, C-3'', C-5''); 130.1 (CH, phthalimide); 131.7 (Cq, C-5); 132.6 (CH, phthalimide); 134.7 (Cq, phthalimide); 136.2 (Cq, phthalimide); 139.5 (Cq, C-4''); 142.8 (Cq, C-1''); 146.4 (Cq, C-7a); 147.2 (Cq, C-3a); 166.2 (Cq, C=O (x2)).

#### 4.2.27. Preparation of 3-((4-(5-acetylspiro[benzo[1,3]dioxole-2,4'-piperidine]-1'-yl)phenyl)amino)furan-2,5-dione (**26**)



· Procedure

The general procedure of Buchwald-Hartwig cross-coupling reaction previously described, was applied to spiro-compound **23** (0.15 mmol)

· Work-up

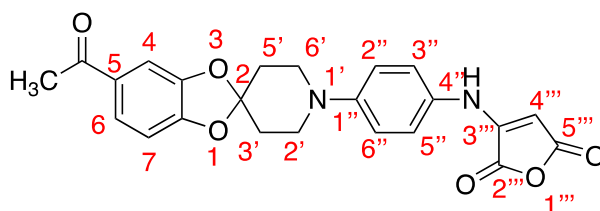
In TLC analysis (hexane/ethyl acetate 7:3) a new yellow product was observed. Thus, toluene was removed under reduced pressure to afford a crude mixture which was dissolved in dichloromethane (20 mL x 1) and washed with water (20 mL x 3). Organic phase was dried over anhydrous sodium sulfate, filtered and concentrated *in vacuo*.

· Purification

Finally, the crude of reaction was purified by flash automatic column chromatography. The desired product eluted with a mixture of hexane/ethyl acetate 70:30.

· Analytical data

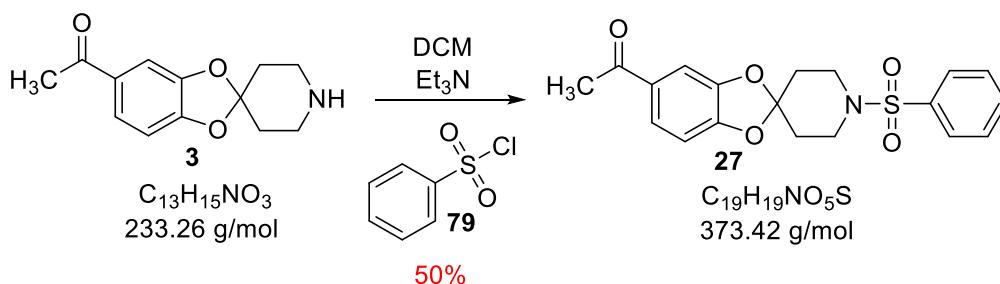
Product aspect	Mass obtained	Yield	R <sub>f</sub> (hexane/ethyl acetate 7:3)	Melting point
White solid	0.050 g	55%	0.40	225-227 °C (DCM)



<sup>1</sup>H NMR (CDCl<sub>3</sub>, 400 MHz)  $\delta$ (ppm), 2.08 (t, *J* = 6 Hz, 4H, CH<sub>2</sub>-C (x2)); 2.47 (s, 3H, CH<sub>3</sub>); 3.44 (t, *J* = 6 Hz, 4H, CH<sub>2</sub>-N (x2)); 6.74 (d, *J* = 8 Hz, 1H, H-7); 6.93 (d, *J* = 2 Hz, 1H, H-4); 6.94 (d, *J* = 9 Hz, 2H, H-2'', H-6''); 7.12 (d, *J* = 9 Hz, 2H, H-3'', H-5''); 7.34 (s, 1H, CH=); 7.47 (dd, *J*<sub>1</sub> = 2 Hz, *J*<sub>2</sub> = 8 Hz, 1H, H-6).

<sup>13</sup>C NMR (CDCl<sub>3</sub>, 100.6 MHz)  $\delta$ (ppm), 26.4 (CH<sub>3</sub>); 34.3 (CH<sub>2</sub>, CH<sub>2</sub>-C (x2)); 46.4 (CH<sub>2</sub>, CH<sub>2</sub>-N (x2)); 107.9 (CH, C-4); 108.1 (CH, C-7); 116.6 (CH, C-6); 117.8 (Cq, C-2); 124.4 (CH, C-4'''); 127.2 (CH, C-2'', C-6''); 129.7 (Cq, C-5); 131.80 (Cq, C-4''); 131.82 (CH, C-3'', C-5''); 147.6 (Cq, C-3a); 150.0 (Cq, C-1''); 151.2 (Cq, C-7a); 164.5 (Cq, C-3''); 167.8 (Cq, C=O (x2)); 196.2 (Cq, C=O).

#### 4.2.28. Preparation of 5-acetyl-1<sup>1</sup>-(phenylsulfonyl)spiro[benzo[1,3]dioxole-2,4<sup>1</sup>-piperidine] (**27**)





· Procedure

In a 50 mL round bottom flask, spiro derivative **3** (0.080 g, 0.34 mmol) was dissolved in dichloromethane (4 mL). By means of an ice bath, temperature was kept at 0 °C, while addition of triethylamine (0.096 mL, 0.69 mmol) and *p*-toluenesulfonyl chloride (0.66 g, 0.38 mmol) was done. The reaction was stirred for 2 hours at room temperature.

· Work up

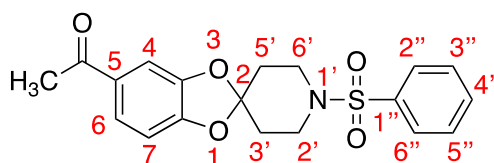
In TLC analysis, consumption of starting material was observed (8:2 hexane/ethyl acetate). Therefore, the mixture was extracted with dichloromethane (20 mL x 3) and water (20 mL x 1). Organic phases were collected and washed with acid chloride 2N (20 mL x 3). The organic layer was dried over anhydrous Na<sub>2</sub>SO<sub>4</sub>, filtered and concentrated *in vacuo*.

· Purification

Finally, the crude reaction was purified by flash automatic column chromatography. The desired product eluted with a mixture of hexane/ethyl acetate 65:45.

· Analytical data

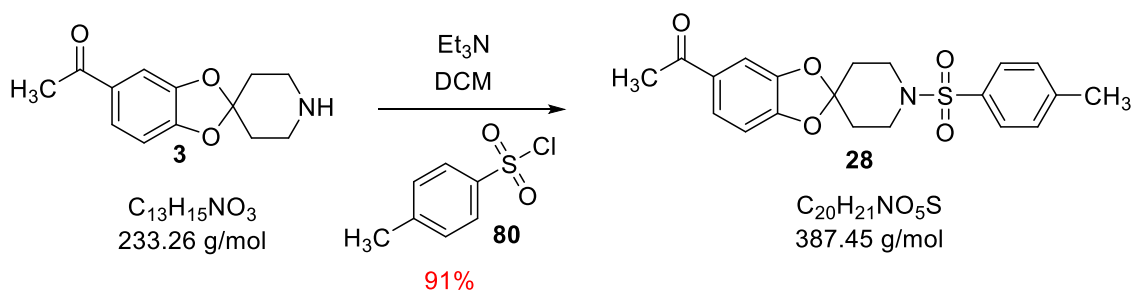
Product aspect	Mass obtained	Yield	R <sub>f</sub> (hexane/ethyl acetate 8:2)	Melting point
Yellowish solid	0.186 g	50%	0.31	147-149 °C (DCM)



<sup>1</sup>H NMR (CDCl<sub>3</sub>, 400 MHz) δ(ppm), 2.05 (t, *J* = 5.7 Hz, 4H, CH<sub>2</sub>-C-(x2)); 2.42 (s, 3H, CH<sub>3</sub>); 3.20-3.26 (m, 4H, CH<sub>2</sub>-N (x2)); 6.66 (d, *J* = 8 Hz, 1H, H-7); 7.24 (d, *J* = 1.8 Hz, 1H, H-4); 7.42 (dd, *J*<sub>1</sub> = 1.8 Hz, *J*<sub>2</sub> = 8 Hz, 1H, H-6); 7.51 (t, *J* = 8 Hz, 2H, H-3'', H-5''); 7.58 (t, *J* = 8 Hz, 1H, H-4''); 7.72 (d, *J* = 8 Hz, 2H, H-2'', H-6'').

<sup>13</sup>C NMR (CDCl<sub>3</sub>, 100.6 MHz) δ(ppm), 26.4 (CH<sub>3</sub>); 34.5 (CH<sub>2</sub>, CH<sub>2</sub>-C (x2)); 43.5 (CH<sub>2</sub>, CH<sub>2</sub>-N (x2)); 108.0 (CH, C-4); 108.2 (CH, C-7); 116.4 (Cq, C-2); 124.5 (CH, C-6); 127.5 (CH, C-2'', C-6''); 129.3 (CH, C-3'', C-5''); 131.9 (Cq, C-5); 133.1 (CH, C-4''); 136.4 (Cq, C-1''); 147.2 (Cq, C-3a); 150.8 (Cq, C-7a); 196.1 (Cq, C=O).

4.2.29. Preparation of 5-acetyl-1'-tosylspiro[benzo[1,3]dioxole-2,4'-piperidine] (**28**)



· Procedure

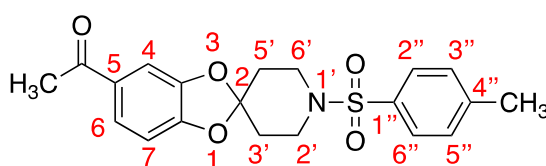
The conditions described in synthesis of spiro-derivative **27** were also applied to the reaction of **3** (0.30 mmol).

· Purification

The crude reaction obtained was purified by flash automatic column chromatography. The desired product eluted with a mixture of hexane/ethyl acetate 65:45.

· Analytical data

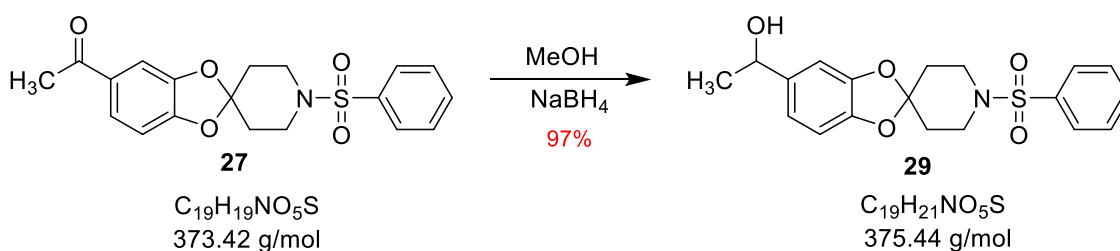
Product aspect	Mass obtained	Yield	R <sub>f</sub> (hexane/ethyl acetate 8:2)	Melting point
Yellowish solid	0.117 g	91%	0.29	155-157 °C (DCM)



<sup>1</sup>H NMR (CDCl<sub>3</sub>, 400 MHz)  $\delta$ (ppm), 2.05 (t,  $J = 7$  Hz, 4H, CH<sub>2</sub>-C-(x2)); 2.39 (s, 3H, CH<sub>3</sub>-Ar); 2.43 (s, 3H, CH<sub>3</sub>-C-O-); 3.16–3.28 (m, 4H, CH<sub>2</sub>-N (x2)); 6.67 (d,  $J = 8$  Hz, 1H, H-7); 7.26 (s, 1H, H-4); 7.29 (d,  $J = 8$  Hz, 2H, H-3'', H-5''); 7.43 (d,  $J = 8$  Hz, 1H, H-6); 7.61 (d,  $J = 8$  Hz, 2H, H-2'', H-6'').

<sup>13</sup>C NMR (CDCl<sub>3</sub>, 100.6 MHz)  $\delta$ (ppm), 21.6 (CH<sub>3</sub>-Ar); 26.4 (CH<sub>3</sub>-CO); 34.5 (CH<sub>2</sub>, CH<sub>2</sub>-C (x2)); 43.5 (CH<sub>2</sub>, CH<sub>2</sub>-N (x2)); 108.0 (CH, C-4); 108.1 (CH, C-7); 116.5 (Cq, C-2); 124.6 (CH, C-6); 127.6 (CH, C-2'', C-6''); 129.9 (CH, C-3'', C-5''); 131.9 (Cq, C-5); 133.6 (Cq, C-4''); 143.9 (Cq, C-1''); 147.3 (Cq, C-3a); 150.9 (Cq, C-7a); 196.1 (Cq, CO).

#### 4.2.30. Preparation of 1-(1'-(phenylsulfonyl)spiro[benzo[1,3]dioxole-2,4'-piperidine]-5-yl)ethan-1-ol (**29**)



· Procedure

in a 25 mL round bottom flask the sulfonyl derivative (**27**) (0.186 g, 0.5 mmol) was dissolved in methanol (5 mL). Next, NaBH<sub>4</sub> (0.03 mmol) was gently added along 5-10 minutes. The crude reaction was stirred at room temperature.

· Work up

After 2 hours of reaction, a TLC showed a formation of a new product and consumption of starting material (8:2 hexane/ethyl acetate). Hence, methanol was concentrated *in vacuo* to afford a residue, which was dissolved in ethyl acetate (20 mL x 1) and washed with water (20 mL x 3). The

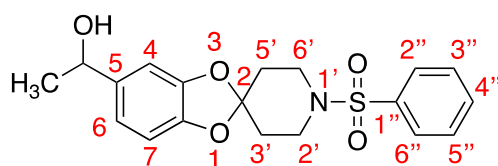
organic layer was dried over anhydrous sodium sulfate, filtered and concentrated under reduced pressure.

· Purification

No purification of the obtained residue by column chromatography was performed since desired product was obtained with enough purity.

· Analytical data

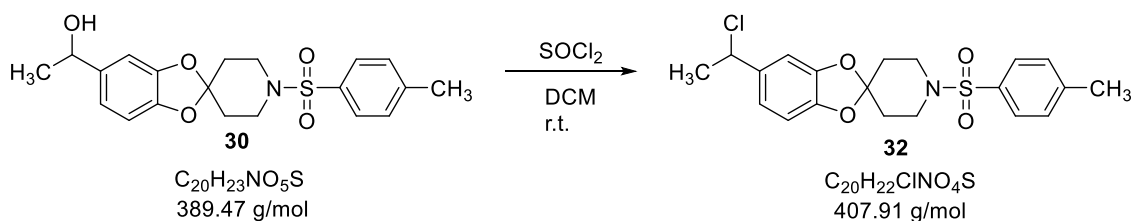
Product aspect	Mass obtained	Yield	R <sub>f</sub> (hexane/ethyl acetate 8:2)	Melting point
Yellowish solid	0.181 g	97%	0.01	165-167 °C (DCM)



<sup>1</sup>H NMR (CDCl<sub>3</sub>, 400 MHz) δ(ppm), 1.32 (d, *J* = 6.4 Hz, 3H, CH<sub>3</sub>); 2.02 (t, *J* = 5.5 Hz, 4H, CH<sub>2</sub>-C (x2)); 3.22 (t, *J* = 5.5 Hz, 4H, CH<sub>2</sub>-N (x2)); 4.68 (q, *J* = 7 Hz, 1H, CH-OH); 6.58 (d, *J* = 8 Hz, 1H, H-7); 6.69 (d, *J* = 8 Hz, 1H, H-6); 6.71 (s, 1H, H-4); 7.49 (t, *J* = 7.8 Hz, 2H, H-3'', H-5''); 7.54 (t, *J* = 7.8 Hz, 1H, H-4''); 7.73 (d, *J* = 7.8 Hz, 2H, H-2'', H-6'').

<sup>13</sup>C NMR (CDCl<sub>3</sub>, 100.6 MHz) δ(ppm), 25.2 (CH<sub>3</sub>); 34.4 (CH<sub>2</sub>, CH<sub>2</sub>-C (x2)); 43.7 (CH<sub>2</sub>, CH<sub>2</sub>-N (x2)); 70.0 (CH, CH-O); 106.2 (CH, C-4); 108.1 (CH, C-7); 114.9 (Cq, C-2); 118.5 (CH, C-6); 127.5 (CH, C-2'', C-6''); 129.2 (CH, C-3'', C-5''); 132.9 (CH, C-4''); 136.4 (Cq, C-5); 139.9 (Cq, C-1''); 145.9 (Cq, C-7a); 146.8 (Cq, C-3a).

#### 4.2.31. Preparation of 5-(1-chloroethyl)-1'-tosylspiro[benzo[1,3]dioxole-2,4'-piperidine] (**32**)



· Procedure

In a round bottom flask, the spiro-derivative alcohol **30** (0.05 g, 0.13 mmol) was dissolved in dichloromethane (8 mL) and thionyl chloride (0.5 mL) was added carefully. The crude reaction was stirred at room temperature.

· Work up

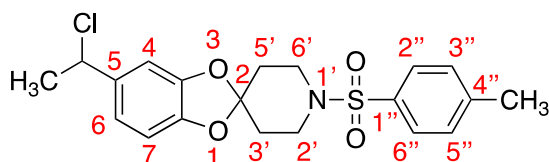
After 2 hours of reaction no more starting material was observed in TLC (hexane/ethyl acetate 8:2). The mixture was washed with water (3 x 20 mL), dried over anhydrous sodium sulfate and concentrated under reduced pressure to afford the chloro derivative **32**.

· Purification

No purification was necessary since product was obtained with enough purity.

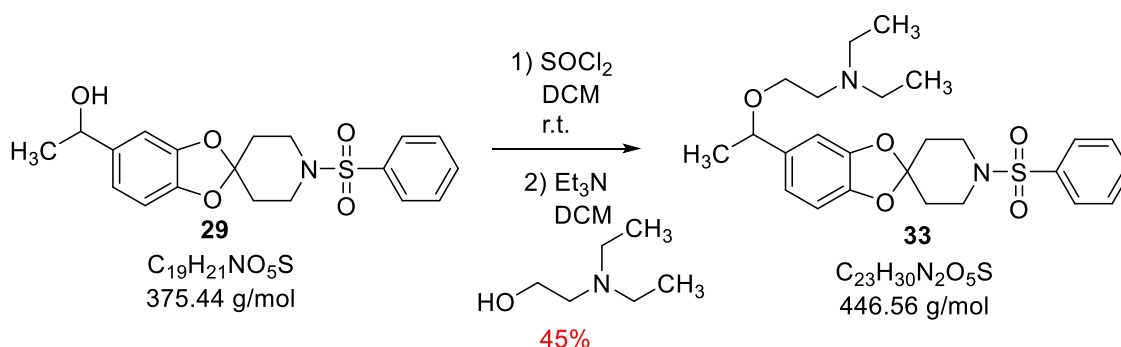
· Analytical data

Product aspect	Mass obtained	Yield	R <sub>f</sub> (hexane/ethyl acetate 8:2)	Melting point
Brown solid	0.052 g	Quantitative	0.68	154-156 °C (DCM)



<sup>1</sup>H NMR (CDCl<sub>3</sub>, 400 MHz) δ(ppm), 1.77 (d, *J* = 6.8 Hz, 3H, CH<sub>3</sub>-CH); 2.09 (t, *J* = 5.7 Hz, 4H, CH<sub>2</sub>-C (x2)); 2.46 (s, 3H, CH<sub>3</sub>-Ar); 3.27 (t, *J* = 5.7 Hz, 4H, CH<sub>2</sub>-N (x2)); 5.00 (q, *J* = 6.8 Hz, 1H, CH-Cl); 6.63 (d, *J* = 8 Hz, 1H, H-7); 6.79 (dd, *J*<sub>1</sub> = 1.5 Hz, *J*<sub>2</sub> = 8 Hz, 1H, H-6); 6.82 (d, *J* = 1.5 Hz, 1H, H-4); 7.35 (d, *J* = 8.5 Hz, 2H, H-3'', H-5''); 7.68 (d, *J* = 8.5 Hz, 2H, H-2'', H-6'').

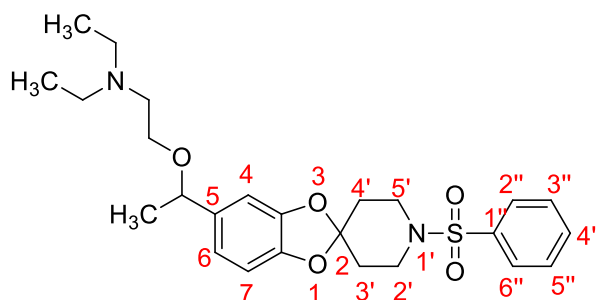
#### 4.2.32. Preparation of *N,N*-diethyl-2-(1-(1'-(phenylsulfonyl)spiro[benzo[*d*][1,3]dioxole-2,4'-piperidine]-5-yl)ethoxy)ethan-1-amine (**33**)



· Procedure

Starting from **29** (0.04 mmol), the same procedure indicated for the synthesis of the spiro-derivative **34** was applied.

Product aspect	Mass obtained	Yield	R <sub>f</sub> (hexane/ethyl acetate/methanol 7:2:1)
Brown semisolid	0.02 g	45%	0.15

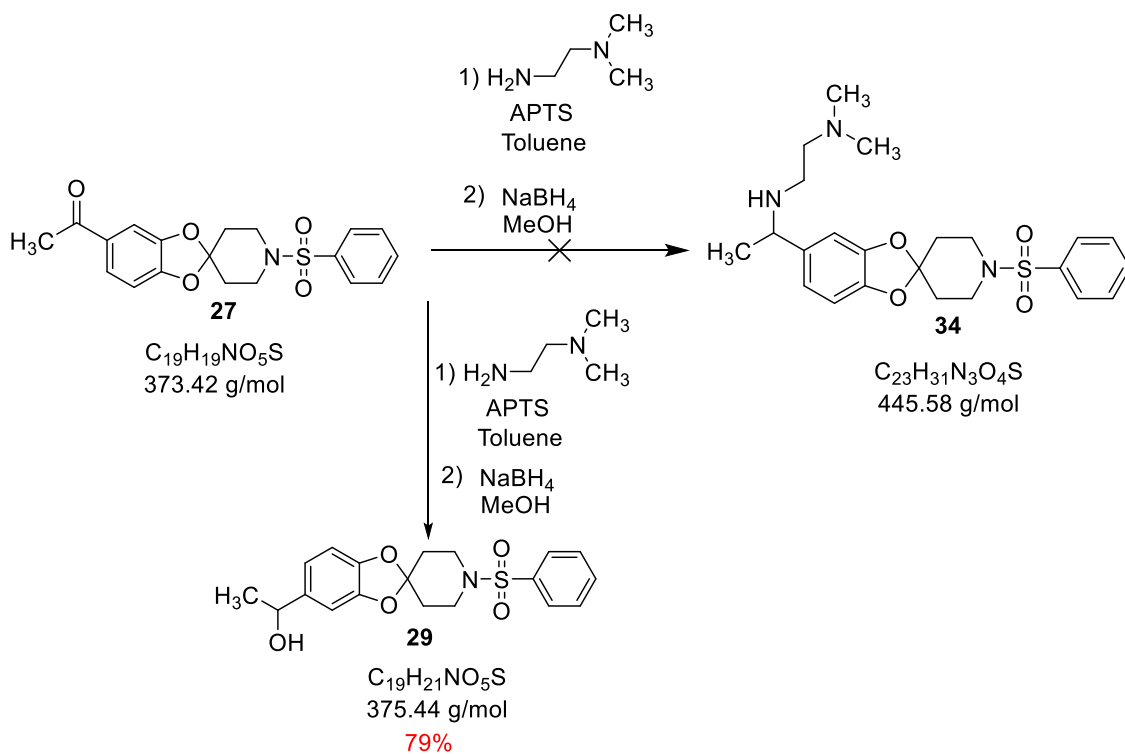


<sup>1</sup>H NMR (CDCl<sub>3</sub>, 400 MHz) δ(ppm), 0.97 (t, *J* = 7.2 Hz, 6H, CH<sub>3</sub>-CH<sub>2</sub> (x2)); 1.33 (d, *J* = 6.4 Hz, 3H, CH<sub>3</sub>-CH); 2.08 (t, *J* = 5.3 Hz, 4H, CH<sub>2</sub>-C (x2)); 2.51 (q, *J* = 7.2 Hz, 4H, CH<sub>2</sub>-N (x2)); 2.61 (q, *J* = 6.7 Hz, 2H,

CH<sub>2</sub>-N); 3.29 (t, *J* = 5.3 Hz, 4H, CH<sub>2</sub>-N piperidine (x2)); 3.33 (t, *J* = 6.7 Hz, 2H, CH<sub>2</sub>-O); 4.27 (q, *J* = 6.4 Hz, 1H, CH-CH<sub>3</sub>); 6.61 (d, *J* = 7.9 Hz, 1H, H-7); 6.67 (d, *J* = 7.9 Hz, 1H, H-6); 6.70 (s, 1H, H-4); 7.56 (t, *J* = 7.7 Hz, 2H, H-3'', H-5''); 7.63 (t, *J* = 7.7 Hz, 1H, H-4''); 7.78 (d, *J* = 7.7 Hz, 2H, H-2'', H-6'').

<sup>13</sup>C NMR (CDCl<sub>3</sub>, 100.6 MHz) δ(ppm), 11.4 (CH<sub>3</sub>, CH<sub>3</sub>-CH<sub>2</sub>); 11.6 (CH<sub>3</sub>, CH<sub>3</sub>-CH<sub>2</sub>); 24.1 (CH<sub>3</sub>, CH<sub>3</sub>-CH); 34.4 (CH<sub>2</sub>-C (x2)); 43.7 (CH<sub>2</sub>, CH<sub>2</sub>-N); 47.5 (CH<sub>2</sub>-N piperidine (x2)); 52.4 (CH<sub>2</sub>, CH<sub>2</sub>-N (x2)); 66.6 (CH<sub>2</sub>, CH<sub>2</sub>-O); 78.0 (CH, CH-O); 106.4 (CH, C-4); 107.2 (Cq, C-7); 114.8 (Cq, C-2); 119.4 (CH, C-6); 127.5 (CH, C-4''); 129.2 (CH, C-2'', C-6''); 132.9 (CH, C-3'', C-5''); 136.5 (Cq, C-5); 137.8 (Cq, C-1''); 145.9 (Cq, C-7a); 146.9 (Cq, C-3a).

#### 4.2.33. Preparation of *N,N*-dimethyl-*N*-(1-(1'-tosylspiro[benzo[1,3]dioxole-2,4'-piperidine]-5-yl)ethyl)ethane-1,2-diamine (**34**)



#### · Procedure

In a round bottom flask the spiro-compound **27** (0.065 g, 0.17 mmol) was dissolved in toluene (8 mL). Then *N,N*-dimethylethylenediamine (0.027 mL, 0.25 mmol) and *p*-toluenesulfonic acid were added. A Dean-Stark system was used in order to remove the resultant water from reaction. The mixture was stirred overnight at 140 °C.

After 30 hours of reaction, toluene was removed under reduced pressure and the mixture was extracted with ethyl acetate (20 mL x 3) and water (20 mL x 1). Organic phases were collected, filtered and concentrated under reduced pressure, giving an intermediary product as a result.

That intermediary product (0.074 g, 0.02 mmol) was dissolved in methanol (8 mL) and NaBH<sub>4</sub> (0.002 g, 0.05 mmol) was slowly added. Reaction was stirred at room temperature during 1 hour.

· Work up

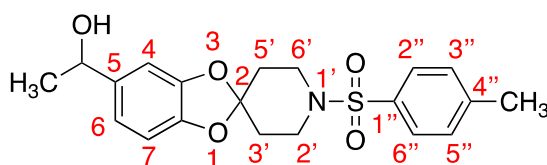
After this time, a TLC of reaction showed a formation of a new compound (8:2 hexane/ethyl acetate). Hence, methanol was removed under reduced pressure and the obtained crude mixture was extracted with ethyl acetate (20 mL x 3) and water (20 mL x 1). Organic phases were collected, dried over anhydrous sodium sulfate, filtered and concentrated *in vacuo*.

· Purification

The crude of reaction was purified by flash automatic column chromatography. The product eluted with a mixture of hexane/ethyl acetate 50:50. The <sup>1</sup>H NMR signals showed the alcohol 1-(1'-tosylspiro[benzo[1,3]dioxole-2,4'-piperidine]-5-yl)ethanol (**29**).

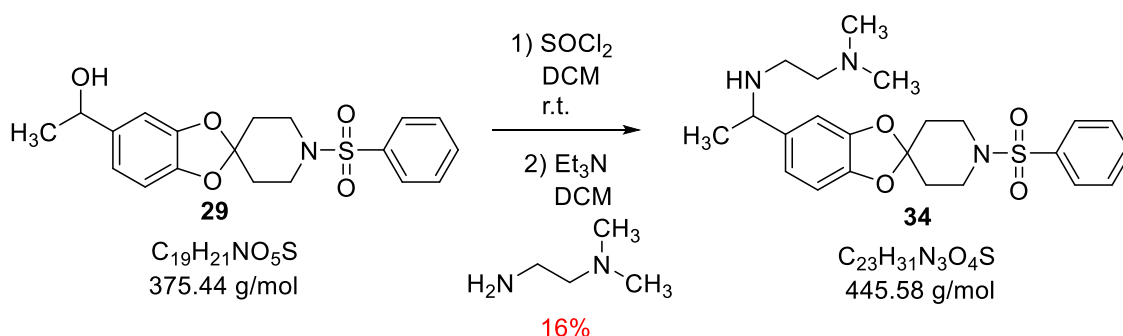
· Analytical data

Product aspect	Mass obtained	Yield	R <sub>f</sub> (hexane/ethyl acetate 5:5)	Melting point
White solid	0.059 g	79%	0.30	150-152 °C (DCM)



<sup>1</sup>H NMR (CDCl<sub>3</sub>, 400 MHz) δ(ppm), 1.42 (d, *J* = 6.4 Hz, 3H, CH<sub>3</sub>-CH); 2.00-2.03 (m, 4H, CH<sub>2</sub>-C (x2)); 2.46 (s, 3H, CH<sub>3</sub>-Ar); 3.27 (t, *J* = 5.8 Hz, 4H, CH<sub>2</sub>-N (x2)); 4.77 (q, *J* = 6.4 Hz, 1H, CH-OH); 6.64 (d, *J* = 8 Hz, 1H, H-7); 6.75 (dd, *J*<sub>1</sub> = 2 Hz, *J*<sub>2</sub> = 8 Hz, 1H, H-6); 6.78 (d, *J* = 2 Hz, 1H, H-4); 7.35 (d, *J* = 8 Hz, 2H, H-3'', H-5''); 7.68 (d, *J* = 8 Hz, 2H, H-2'', H-6'').

#### 4.2.34. Preparation of *N,N*-dimethyl-*N*-(1-(1'-(phenylsulfonyl)spiro[benzo[*d*][1,3]dioxole-2,4'-piperidine]-5-yl)ethyl)ethane-1,2-diamine (**34**)



· Procedure

In a round bottom flask, alcohol **29** (0.05 g, 0.13 mmol) was dissolved in dichloromethane (8 mL) and thionyl chloride (0.5 mL). The reaction was stirred at room temperature for 2 hours. At this time no more starting material was observed in TLC (hexane/ethyl acetate 8:2). The resulting mixture was washed with water (3 x 20 mL), dried over anhydrous sodium sulfate and concentrated under reduced pressure to afford the chloro derivative **31**, which was diluted with

dichloromethane (7 mL) in a 25 mL round bottom flask. Then, triethylamine (0.03 mL, 0.2 mmol) and *N,N*-dimethylethylenediamine (0.02 mL, 0.15 mmol) were added. The crude reaction was stirred at 100 °C.

· Work up

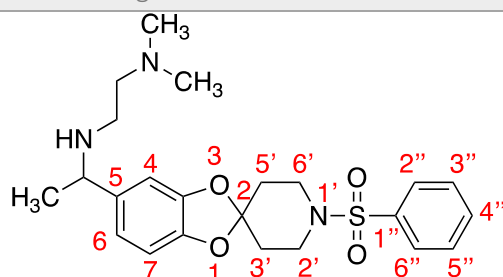
The reaction was stirred for 4 days, when no more starting material was observed in TLC (hexane/ethyl acetate/methanol 7:2:1). Therefore, the mixture was washed with water (20 mL x 3), dried over anhydrous sodium sulfate, filtered off and concentrated *in vacuo*.

· Purification

The crude of the reaction was purified by flash automatic column chromatography. The product eluted with a mixture of ethyl acetate/methanol 0:100.

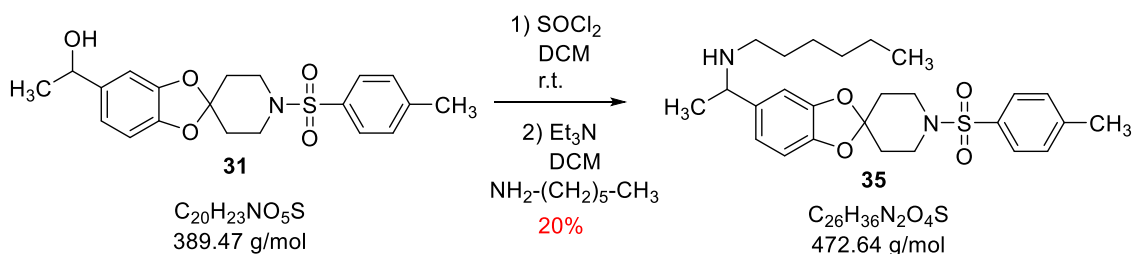
· Analytical data

Product aspect	Mass obtained	Yield	R <sub>f</sub> (hexane/ethyl acetate/methanol 7:2:1)
Brown semisolid	0.01 g	16%	0.1



<sup>1</sup>H NMR (CDCl<sub>3</sub>, 400 MHz) δ(ppm), 1.21 (d, *J* = 6.4 Hz, 3H, CH<sub>3</sub>-CH); 2.02 (t, *J* = 5.7 Hz, 4H, CH<sub>2</sub>-C (x2)); 2.08 (s, 3H, CH<sub>3</sub>-N (x2)); 2.22-2.29 (m, 2H, CH<sub>2</sub>-N(CH<sub>3</sub>)<sub>2</sub>); 2.39-2.42 (m, 2H, CH<sub>2</sub>-NH); 3.22 (t, *J* = 5.7 Hz, 4H, CH<sub>2</sub>-N (x2)); 3.54 (q, *J* = 6.4 Hz, 1H, CH-NH); 6.54 (d, *J* = 7.9 Hz, 1H, H-7); 6.62 (d, *J* = 7.9 Hz, 1H, H-6); 6.65 (s, 1H, H-4); 7.50 (t, *J* = 7.8 Hz, 2H, H-3'', H-5''); 7.48 (t, *J* = 7.8 Hz, 1H, H-4''); 7.73 (d, *J* = 7.8 Hz, 2H, H-2'', H-6'').

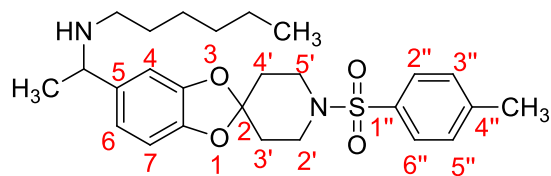
#### 4.2.35. Preparation of *N*-(1-(1'-tosylspiro[benzo[*d*][1,3]dioxole-2,4'-piperidine]-5-yl)ethyl)hexan-1-amine (**35**)



· Procedure

Starting from **30** (0.04 mmol), the same procedure indicated for the synthesis of the spiro-compound **34** was applied.

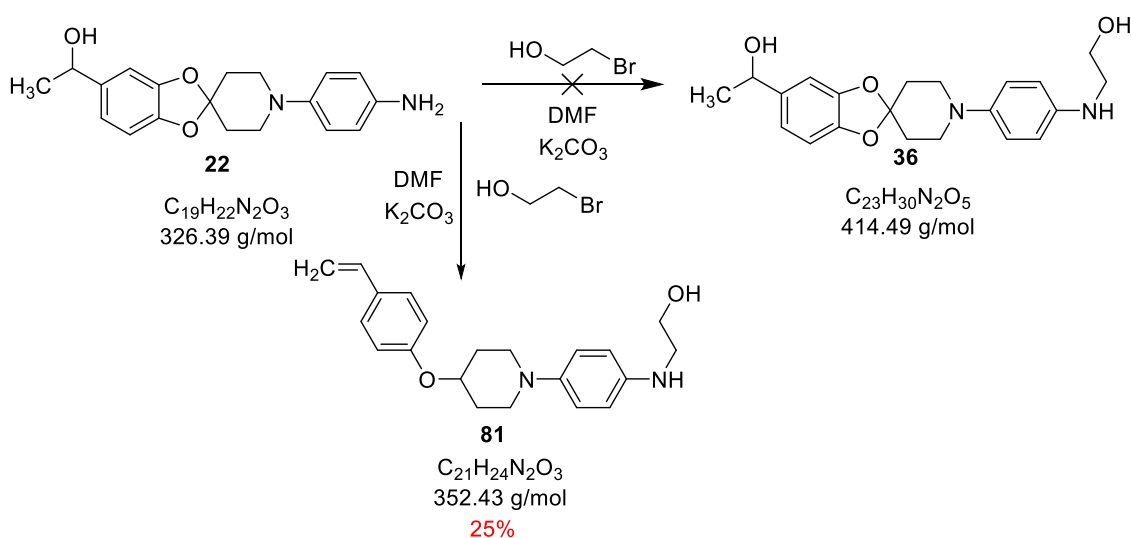
Product aspect	Mass obtained	Yield	R <sub>f</sub> (hexane/ethyl acetate/methanol 7:2:1)
Brown semisolid	0.02 g	20%	0.1



$^1\text{H NMR}$  ( $\text{CDCl}_3$ , 400 MHz)  $\delta$ (ppm), 0.74 (t,  $J = 6.4$  Hz, 3H,  $\text{CH}_3\text{-CH}_2$ ); 1.12-1.19 (m, 4H,  $\text{CH}_2\text{-}$  (x2)); 1.55 (q,  $J = 6.4$  Hz, 2H,  $\text{CH}_2\text{-}$ (x2)); 1.72 (d,  $J = 7$  Hz, 3H,  $\text{CH}_3\text{-CH}$ ); 2.08-2.10 (m, 4H,  $\text{CH}_2\text{-C}$  (x2)); 2.40 (s, 3H,  $\text{CH}_3\text{-Ar}$ ); 2.51-2.54 (m, 2H,  $\text{CH}_2\text{-}$ ); 3.07 (q,  $J = 7$  Hz, 2H,  $\text{CH}_2\text{-N}$ ); 3.23 (q,  $J = 6.4$  Hz, 2H,  $\text{CH}_2\text{-}$ ); 3.32 (q,  $J = 7$  Hz, 2H,  $\text{CH}_2\text{-N}$ ); 3.98-3.99 (m, 1H,  $\text{CH-CH}_3$ ); 6.62 (d,  $J = 8$  Hz, 1H, H-6); 6.81 (d,  $J = 8$  Hz, 1H, H-7); 7.08 (s, 1H, H-4); 7.29 (d,  $J = 8.2$  Hz, 2H, H-3'', H-5''); 7.60 (d,  $J = 8.2$  Hz, 2H, H-2'', H-6'').

$^{13}\text{C NMR}$  ( $\text{CDCl}_3$ , 100.6 MHz)  $\delta$ (ppm), 12.9 ( $\text{CH}_3$ ,  $\text{CH}_3\text{-CH}_2$ ); 20.0 ( $\text{CH}_3$ ,  $\text{CH}_3\text{-CH}$ ); 20.6 ( $\text{CH}_3$ ,  $\text{CH}_3\text{-Ar}$ ); 21.4 ( $\text{CH}_2$ ,  $\text{CH}_2\text{-CH}_3$ ); 25.5 ( $\text{CH}_2$ ,  $\text{CH}_2\text{-CH}_2\text{-CH}_3$ ); 30.1 ( $\text{CH}_2$ ,  $\text{CH}_2\text{-CH}_2\text{-CH}_2\text{-CH}_3$ ); 33.5 ( $\text{CH}_2\text{-C}$  (x2)); 42.7 ( $\text{CH}_2$ ,  $\text{CH}_2\text{-CH}_2\text{-CH}_2\text{-CH}_2\text{-CH}_3$ ); 44.7 ( $\text{CH}_2\text{-N}$  (x2)); 46.8 ( $\text{CH}_2$ ,  $\text{CH}_2\text{-NH}$ ); 57.8 ( $\text{CH}$ ,  $\text{CH-NH}$ ); 106.8 ( $\text{CH}$ , C-4); 107.8 (Cq, C-7); 114.9 (Cq, C-2); 120.7 ( $\text{CH}$ , C-6); 126.5 ( $\text{CH}$ , C-2'', C-6''); 128.6 (Cq, C-5); 128.9 ( $\text{CH}$ , C-3'', C-5''); 132.1 (Cq, C-4''); 142.9 (Cq, C-1''); 146.5 (Cq, C-7a); 146.7 (Cq, C-3a).

#### 4.2.36. Preparation of 2-((4-(5-(1-(2-hydroxyethoxy)ethyl)spiro[benzo[1,3]dioxole-2,4'-piperidine]-1'-yl)phenyl)amino)ethanol (**36**)



##### · Procedure

In a 25 mL round-bottom flask equipped with magnetic stirring, the aniline **22** (0.06 g, 0.19 mmol) was dissolved in DMF (10 mL). Then, bromoethanol (0.07 g, 0.56 mmol) and potassium carbonate (0.08 g, 0.56 mmol) were added. The crude reaction was stirred at 120 °C.

##### · Work-up

After 4 days under these conditions following the course of the reaction by TLC, its analysis confirmed consumption of starting material (hexane/ethyl acetate 7:3). The mixture was



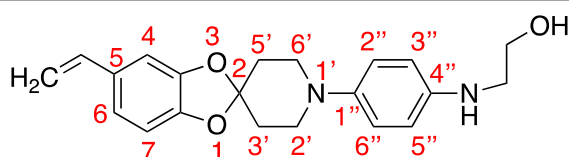
dissolved in ethyl ether (20 mL x 1) and washed with water (20 mL x 3). The organic phase was dried over anhydrous sodium sulfate, filtered and concentrated under reduced pressure.

· Purification

Finally, the crude mixture was purified by flash automatic column chromatography. The product eluted with a mixture of hexane/ethyl acetate 0:100. The  $^1\text{H}$  NMR signals indicated formation of the non-desired 2-((4-(5-vinylspiro[benzo[1,3]dioxole-2,4'-piperidine]-1'-yl)phenyl)amino)-ethanol (**81**).

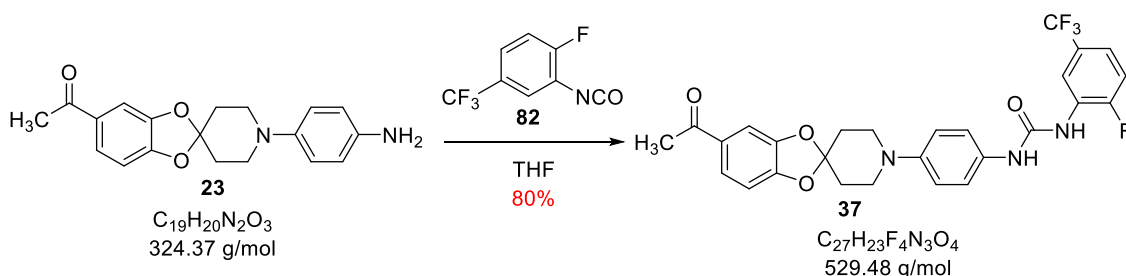
· Analytical data

Product aspect	Mass obtained	Yield	$R_f$ (hexane/ethyl acetate 7:3)
Brown oil	0.015 g	25%	0.14



$^1\text{H}$  NMR ( $\text{CDCl}_3$ , 400 MHz)  $\delta$ (ppm), 2.14 (q,  $J = 6$  Hz, 8H,  $\text{CH}_2\text{-C}$  (x2),  $\text{CH}_2\text{-N}$  (x2)); 3.40 (t,  $J = 5.5$  Hz, 2H,  $\text{CH}_2\text{-N}$  chain); 3.80 (m, 2H,  $\text{CH}_2\text{-O}$ ); 5.04 (d,  $J = 10.6$  Hz, 1H,  $\text{C}=\text{CH}$  *cis*); 5.48 (d,  $J = 17.6$  Hz, 1H,  $\text{C}=\text{CH}$  *trans*); 6.54 (dd,  $J_1 = 10.6$  Hz,  $J_2 = 17.6$  Hz, 1H,  $\text{CH}=\text{C}$ ); 6.64 (d,  $J = 8$  Hz, 2H, H-3'', H-5''); 6.74 (d,  $J = 8$  Hz, 2H, H-2'', H-6''); 6.85 (s, 1H, H-4); 6.97 (d,  $J = 8.8$  Hz, 1H, H-7); 7.05 (d,  $J = 8.8$  Hz, 1H, H-6).

#### 4.2.37. Preparation of 1-(4-(5-acetylspiro[benzo[1,3]dioxole-2,4'-piperidine]-1'-yl)phenyl)-3-(2-fluoro-5-(trifluoromethyl)phenyl)urea (**37**)



· Procedure (general urea synthesis procedure)

In a 50 mL round bottom flask equipped with magnetic stirring, the compound **23** (0.07 g, 0.22 mmol) was dissolved in THF (8 mL) and 2-fluoro-5-(trifluoromethyl)phenyl isocyanate (0.031 mL, 0.22 mmol) was added. The mixture reaction was stirred during 48 hours at room temperature.

· Work-up

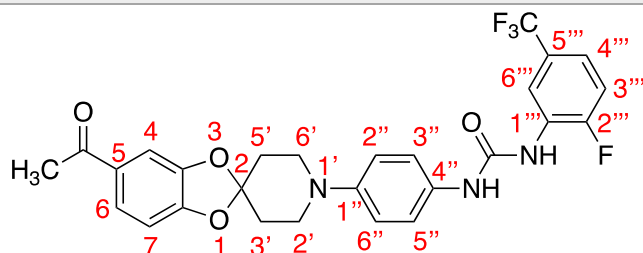
A control of the reaction by TLC (hexane/ethyl acetate 7:3) showed consumption of starting material. Thus, solvent was removed under reduced pressure to afford a crude mixture.

· Purification

The crude product obtained was purified by flash automatic column chromatography. The desired product eluted with a mixture of hexane/ethyl acetate 58:42.

· Analytical data

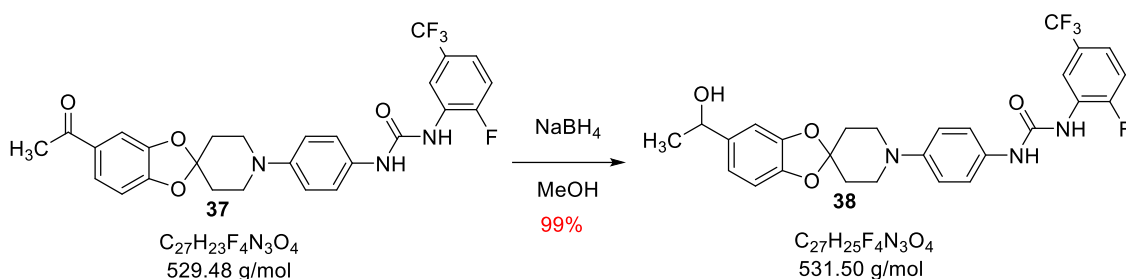
Product aspect	Mass obtained	Yield	R <sub>f</sub> (hexane/ethyl acetate 7:3)	Melting point
White solid	0.09 g	80%	0.26	200-202 °C (DCM)



<sup>1</sup>H NMR (CDCl<sub>3</sub>, 400 MHz) δ(ppm), 2.12 (t, *J* = 5.5 Hz, 4H, CH<sub>2</sub>-C (x2)); 2.58 (s, 3H, CH<sub>3</sub>); 3.52 (t, *J* = 5.5 Hz, 4H, CH<sub>2</sub>-N (x2)); 6.80 (d, *J* = 8.2 Hz, 1H, H-7); 6.87 (d, *J* = 8.4 Hz, 2H, H-2'', H-6''); 7.07 (t, *J* = 8.7 Hz, 1H, H-4'''); 7.18-7.21 (m, 1H, H-3'''); 7.24 (d, *J* = 8.4 Hz, 2H, H-3'', H-5''); 7.40 (d, *J* = 2 Hz, 1H, H-4); 7.54 (dd, *J*<sub>1</sub> = 2 Hz, *J*<sub>2</sub> = 8.2 Hz, 1H, H-6); 7.69 (ba, 2H, NH (x2)); 8.54 (dd, *J*<sub>1</sub> = 1 Hz, *J*<sub>2</sub> = 7.2 Hz, 1H, H-6''').

<sup>13</sup>C NMR (CDCl<sub>3</sub>, 100.6 MHz) δ(ppm), 26.4 (CH<sub>3</sub>); 34.5 (CH<sub>2</sub>-C (x2)); 47.2 (CH<sub>2</sub>-N (x2)); 108.0 (CH, C-4); 108.1 (CH, C-7); 115.0 (CH, *J* = 20.8 Hz, C-3'''); 117.5 (CH, C-2'', C-6''); 117.9 (Cq, C-2); 118.4 (CH, *J*<sub>1</sub> = 4 Hz, *J*<sub>2</sub> = 7 Hz, C-6'''); 119.8 (CH, *J*<sub>1</sub> = 4 Hz, *J*<sub>2</sub> = 9 Hz, C-4'''); 123.2 (Cq, *J* = 271 Hz, CF<sub>3</sub>); 123.3 (CH, C-3'', C-5''); 124.7 (CH, C-6); 127.0 (Cq, *J*<sub>1</sub> = 3 Hz, *J*<sub>2</sub> = 32 Hz, C-5'''); 127.9 (Cq, *J* = 11 Hz, C-1'''); 128.8 (Cq, C-4''); 131.6 (Cq, C-5); 147.7 (Cq, C-3a, C-7a); 151.5 (Cq, C-1''); 153.4 (Cq, NH-C=O); 154.0 (Cq, *J* = 247 Hz, C-2'''); 197.1 (Cq, C=O).

4.2.38. Preparation of 1-(2-fluoro-5-(trifluoromethyl)phenyl)-3-(4-(5-(1-hydroxyethyl)-spiro[benzo[1,3]dioxole-2,4'-piperidine]-1'-yl)phenyl)urea (**38**)



· Procedure

In a 50 mL round bottom flask equipped with magnetic stirring, the urea **37** (0.06 g, 0.11 mmol) was dissolved in methanol (10 mL) and sodium borohydride (0.005 g, 0.11 mmol) was added. The crude reaction was stirred at room temperature for 12 hours.

· Work-up

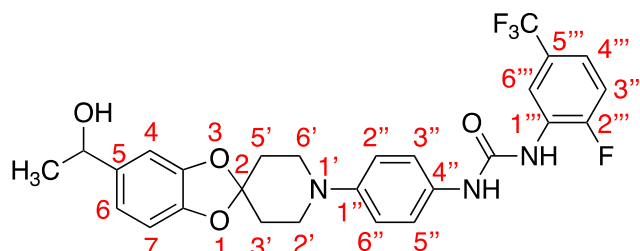
After this time, a TLC of reaction (hexane/ethyl acetate 7:3) showed a new product and consumption of starting material. Then, 5 mL of water were added, methanol was removed *in vacuo* and the obtained crude was extracted with dichloromethane (20 mL x 3) and water (20 mL x 1). Organic phases were dried over anhydrous Na<sub>2</sub>SO<sub>4</sub>, filtered and concentrated under reduced pressure to afford the expected compound.

· Purification

No purification of the obtained residue by column chromatography was performed since product was obtained with enough purity.

· Analytical data

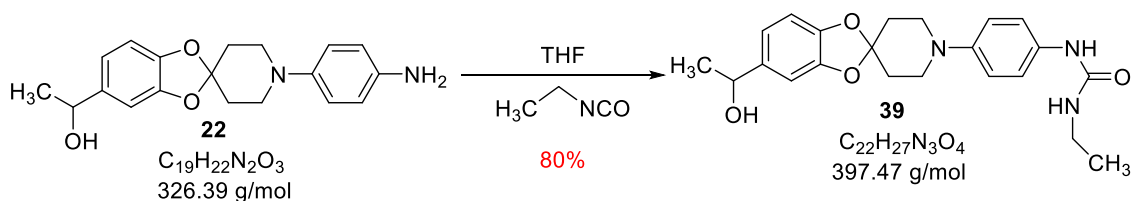
Product aspect	Mass obtained	Yield	R <sub>f</sub> (hexane/ethyl acetate 7:3)	Melting point
White solid	0.06 g	99%	0.23	195-197 °C (DCM)



<sup>1</sup>H NMR (Acetone-d<sub>6</sub>, 400 MHz) δ(ppm), 1.23 (d, *J* = 6.4 Hz, 3H, CH<sub>3</sub>); 1.98 (t, *J* = 5.7 Hz, 4H, CH<sub>2</sub>-C (x2)); 3.26 (t, *J* = 5.7 Hz, 4H, CH<sub>2</sub>-N (x2)); 3.96 (d, *J* = 4 Hz, 1H, OH); 4.63 (q, *J* = 6.4 Hz, 1H, CH-O); 6.59 (d, *J* = 8 Hz, 1H, H-7); 6.68 (dd, *J*<sub>1</sub> = 2 Hz, *J*<sub>2</sub> = 8 Hz, 1H, H-6); 6.74 (d, *J* = 2 Hz, 1H, H-4); 6.88 (d, *J* = 9 Hz, 2H, H-2'', H-6''); 7.30 (d, *J* = 9 Hz, 2H, H-3'', H-5''); 8.13 (d, *J* = 3 Hz, 1H, H-3'''); 8.31 (s, 1H, H-6'''); 8.67 (dd, *J*<sub>1</sub> = 3 Hz, *J*<sub>2</sub> = 7.6 Hz, 1H, H-4''').

<sup>13</sup>C NMR (Acetone-d<sub>6</sub>, 100.6 MHz) δ(ppm), 25.4 (CH<sub>3</sub>); 34.4 (CH<sub>2</sub>, CH<sub>2</sub>-C (x2)); 47.3 (CH<sub>2</sub>, CH<sub>2</sub>-N (x2)); 68.9 (CH-OH); 105.9 (CH, C-4); 107.6 (CH, C-7); 115.4 (CH, *J* = 20.8 Hz, C-3'''); 116.2 (Cq, C-2); 117.0 (CH, *J*<sub>1</sub> = 4 Hz, *J*<sub>2</sub> = 9 Hz, C-6'''); 117.2 (CH, C-2'', C-6''); 118.0 (CH, C-6); 118.9 (CH, *J*<sub>1</sub> = 4 Hz, *J*<sub>2</sub> = 7 Hz, C-4'''); 120.2 (CH, C-3'', C-5''); 124.2 (Cq, *J* = 271 Hz, CF<sub>3</sub>); 126.4 (Cq, *J*<sub>1</sub> = 1.3 Hz, *J*<sub>2</sub> = 32.5 Hz, C-5'''); 128.8 (Cq, C-4''); 129.3 (Cq, *J* = 11 Hz, C-1'''); 131.6 (Cq, C-5); 145.9 (Cq, C-1''); 146.8 (Cq, C-7a); 147.0 (Cq, C-3a); 152.1 (Cq, C=O); 153.5 (Cq, *J*<sub>1</sub> = 1.3 Hz, *J*<sub>2</sub> = 246 Hz, C-2''').

#### 4.2.39. Preparation of 1-ethyl-3-(4-(5-(1-hydroxyethyl)spiro[benzo[1,3]dioxole-2,4'-piperidine]-1'-yl)phenyl)urea (39)



· Procedure

In a 25 mL round-bottom flask equipped with magnetic stirring, the spiro derivative **22** (0.1 g, 0.31 mmol) was dissolved in THF and then ethyl isocyanate (0.02 mL, 0.31 mmol) was added. The crude reaction was stirred at room temperature for 24 hours.

· Work-up

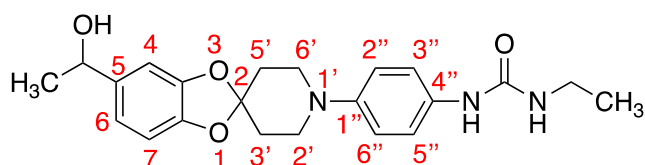
Analysis by TLC (hexane/ ethyl acetate 5:5) showed consumption of starting material. Therefore, THF was evaporated under reduced pressure to afford the crude mixture.

· Purification

The crude was purified by flash automatic column chromatography. The desired product eluted with a mixture of hexane/ethyl acetate 20:80.

· Analytical data

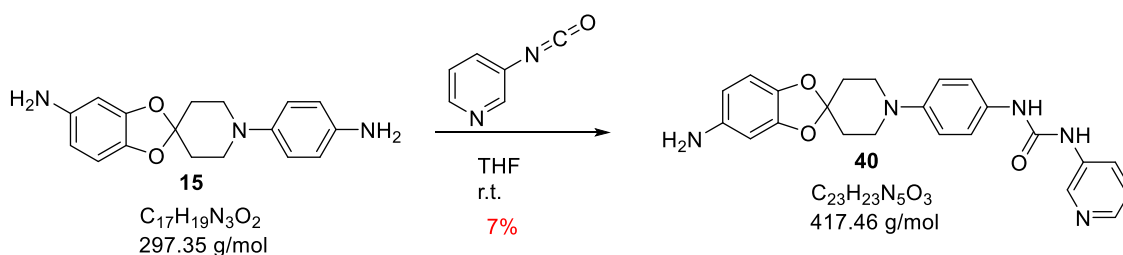
Product aspect	Mass obtained	Yield	R <sub>f</sub> (hexane/ethyl acetate 5:5)	Melting point
Whitish solid	0.1 g	80%	0.13	175-177 °C (DCM)



<sup>1</sup>H NMR (CDCl<sub>3</sub>, 400 MHz) δ(ppm), 1.12 (t, *J* = 6.4 Hz, 3H, CH<sub>3</sub>); 1.46 (d, *J* = 6.4 Hz, 3H, CH<sub>3</sub>-CH) 2.13-2.14 (m, 4H, CH<sub>2</sub>-C (x2)); 3.20-3.26 (m, 2H, CH<sub>2</sub>-NH); 3.27-3.40 (m, 4H, CH<sub>2</sub>-N (x2)); 4.74 (bs, 1H, OH); 4.82 (q, *J* = 6.4 Hz, 1H, CH-O); 6.71 (d, *J* = 8 Hz, 1H, H-7); 6.79 (dd, *J*<sub>1</sub> = 2 Hz, *J*<sub>2</sub> = 8 Hz, 1H, H-6); 6.85 (d, *J* = 2 Hz, 1H, H-4); 6.91-6.94 (m, 2H, H-2'', H-6''); 7.15 (d, *J* = 8 Hz, 2H, H-3'', H-5'').

<sup>13</sup>C NMR (CDCl<sub>3</sub>, 100.6 MHz) δ(ppm), 14.01 (CH<sub>3</sub>-CH<sub>2</sub>); 22.7 (CH<sub>3</sub>, CH<sub>3</sub>-CH); 25.1 (CH<sub>2</sub>, CH<sub>2</sub>-C (x2)); 34.3 (CH<sub>2</sub>, CH<sub>2</sub>-N (x2)); 70.3 (CH-O); 106.1 (CH, C-4); 108.1 (CH, C-7); 110.2 (Cq, C-2); 118.4 (CH, C-6); 124.6 (Cq, C-5); 127.1 (Cq, C-4''); 139.6 (Cq, C-1''); 146.4 (Cq, C-7a); 147.2 (Cq, C-3a); 154.8 (Cq, CO); (The C-2'', C-6'' and C-3'', C-5'' carbons were not detected).

4.2.40. Preparation of 1-(pyridin-3-yl)-3-(4-(5-(3-(pyridin-3-yl)ureido)spiro[benzo[1,3]-dioxole-2,4'-piperidine]-1'-yl)phenyl)urea (**40**)



· Procedure

Starting from **15** (3 mmol), the general procedure for urea synthesis described previously in this work was applied in this case.

· Work-up

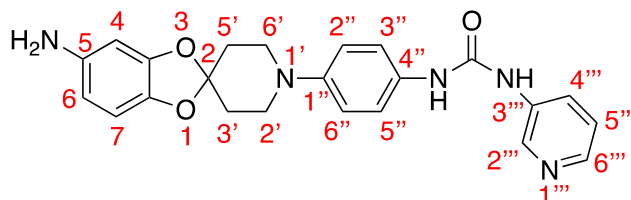
At 76 hours of reaction, a TLC of reaction showed the formation of a new product (ethyl acetate 100%). THF was removed *in vacuo*.

· Purification

The crude mixture was purified by flash automatic column chromatography to afford the product. The desired product eluted with a mixture of hexane/ethyl acetate 0:100.

· Analytical data

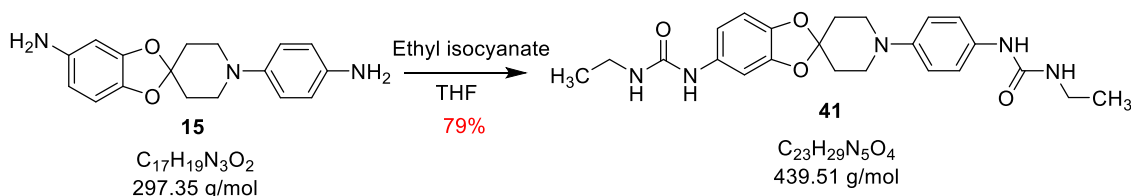
Product aspect	Mass obtained	Yield	R <sub>f</sub> (hexane/ethyl acetate 0:1)
Grey semisolid	0.01 g	7%	0.15



<sup>1</sup>H NMR (CDCl<sub>3</sub>, 400 MHz) δ(ppm), 2.04 (t, *J* = 5.8 Hz, 4H, CH<sub>2</sub>-C (x2) rotamer M); 2.25 (t, 1H, CH<sub>2</sub>-C rotamer m); 2.48 (t, 1.7H, CH<sub>2</sub>-C rotamer m); 3.18 (t, 1.3H, CH<sub>2</sub>-N, rotamer m); 3.34 (t, *J* = 5.8 Hz, 4H, CH<sub>2</sub>-N (x2) rotamer M); 3.50 (t, 1.5H, CH<sub>2</sub>-N, rotamer m); 6.05 (dd, *J*<sub>1</sub> = 2 Hz, *J*<sub>2</sub> = 8 Hz, 1H, H-6); 6.17 (d, *J* = 2 Hz, 1H, H-4); 6.50 (d, *J* = 8 Hz, 1H, H-7); 6.60 (t, *J* = 8.8 Hz, 1H, H-5'''); 6.79 (d, *J* = 8.8 Hz, 1H, H-4'''); 6.88 (d, *J* = 9 Hz, 2H, H-2'', H-6''); 7.14 (d, *J* = 9 Hz, 2H, H-3'', H-5''); 7.96 (d width, *J* = 8 Hz, 2H, H-6''', NH); 8.20 (bs, 2H, H-2''', NH); 8.28 (bs, 2H, NH<sub>2</sub>). **M rotamer: majority, m rotamer: minority.**

HRMS (ESI +): Calculated for C<sub>23</sub>H<sub>23</sub>N<sub>5</sub>O<sub>3</sub> [M+H]<sup>+</sup>: 418.1834, found 418.1883.

#### 4.2.41. Preparation of 1-ethyl-3-(4-(5-(3-ethylureido)spiro[benzo[1,3]dioxole-2,4'-piperidine]-1'-yl)phenyl)urea (**41**)



· Procedure

Starting from **15** (0.18 mmol), the general procedure for urea synthesis described previously in this work was applied in this case. An excess of ethyl isocyanate was used (2 eq).

· Work-up

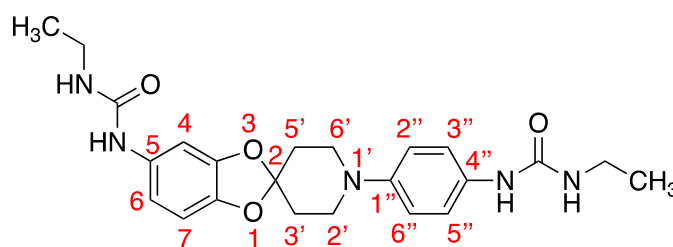
After 24 hours of stirring at room temperature, a TLC of reaction confirmed consumption of starting material (ethyl acetate 100%). THF was removed *in vacuo*.

· Purification

The crude mixture obtained was purified by flash automatic column chromatography to afford the expected compound. The desired product eluted with a mixture of hexane/ethyl acetate 0:100.

· Analytical data

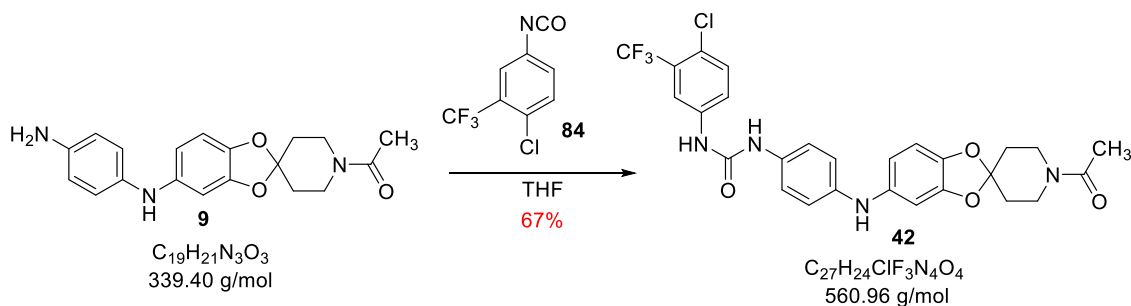
Product aspect	Mass obtained	Yield	R <sub>f</sub> (hexane/ethyl acetate 0:1)	Melting point
White solid	0.074 g	79%	0.15	205-207 °C (DCM)



<sup>1</sup>H NMR (CDCl<sub>3</sub>, 400 MHz) δ(ppm), 1.03 (t, *J* = 7.2 Hz, 6H, CH<sub>3</sub> (x2)); 2.04 (t, *J* = 5.4 Hz, 2H, CH-C axial (x2)); 3.08 (t, *J* = 7.4 Hz, 4H, CH<sub>2</sub>-NH (x2)); 3.15 (t, *J* = 5.4 Hz, 4H, CH<sub>2</sub>-N (x2)); 3.28 (t, *J* = 5.4 Hz, 2H, CH-C equatorial (x2)); 6.52 (dd, *J*<sub>1</sub> = 2 Hz, *J*<sub>2</sub> = 8.2 Hz, 1H, H-6); 6.57 (d, *J* = 8.2 Hz, 1H, H-7); 6.78 (d, *J* = 2 Hz, 1H, H-4); 6.83 (d, *J* = 8.6 Hz, 2H, H-2'', H-6''); 7.09 (d, *J* = 8.6 Hz, 2H, H-3'', H-5'').

<sup>13</sup>C NMR (CDCl<sub>3</sub>, 100.6 MHz) δ(ppm), 15.2 (CH<sub>3</sub>, (x2)); 34.3 (CH<sub>2</sub>, CH<sub>2</sub>-C); 34.5 (CH<sub>2</sub>, CH<sub>2</sub>-NH); 34.7 (CH<sub>2</sub>, CH<sub>2</sub>-C); 47.5 (CH<sub>2</sub>, CH<sub>2</sub>-NH); 47.6 (CH<sub>2</sub>, CH<sub>2</sub>-N (x2)); 104.9 (CH, C-4); 108.1 (CH, C-7); 113.8 (CH, C-6); 116.5 (Cq, C-2); 117.7 (CH, C-2'', C-6''); 122.7 (CH, C-3'', C-5''); 127.5 (Cq, C-5); 128.4 (Cq, C-4''); 137.4 (Cq, C-3a); 138.7 (Cq, C-7a); 147.3 (Cq, C-1''); 155.3 (Cq, C=O); 156.9 (Cq, C=O).

#### 4.2.42. Preparation of 1-(4-((1'-acetylspiro[benzo[1,3]dioxole-2,4'-piperidine]-5-yl)-amino)phenyl)-3-(4-chloro-3-(trifluoromethyl)phenyl)urea (**42**)



##### · Procedure

Starting from **9** (0.18 mmol), the general procedure for urea synthesis described previously in this work was applied in this case.

##### · Work-up

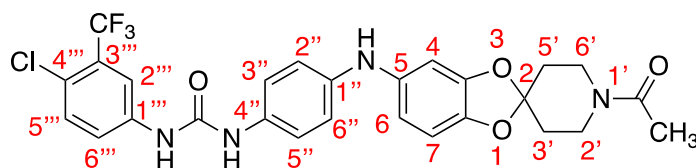
At 24 hours of stirring, a precipitate in the mixture and analysis by TLC confirmed a formation of a new product (hexane/ethyl acetate 5:5).

##### · Purification

The crude reaction was purified by flash automatic column chromatography. The desired product eluted with a mixture of hexane/ethyl acetate 20:80.

##### · Analytical data

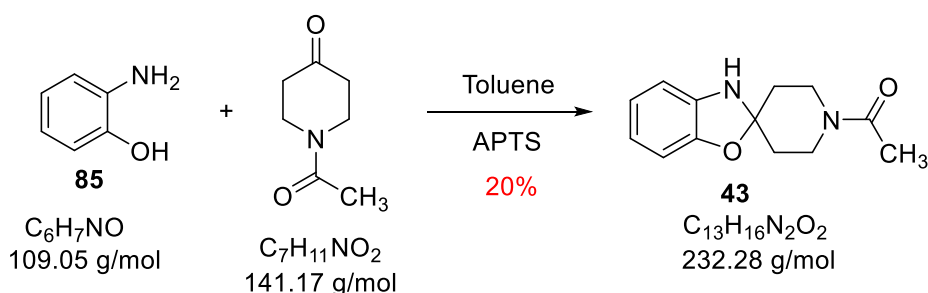
Product aspect	Mass obtained	Yield	R <sub>f</sub> (hexane/ethyl acetate 5:5)
Greenish semisolid	0.065 g	67%	0.5



<sup>1</sup>H NMR (Acetone-d<sub>6</sub>, 400 MHz) δ(ppm), 0.90 (t, *J* = 5.8 Hz, 2H, CH-C axial (x2)); 1.93 (t, *J* = 5.8 Hz, 2H, CH-C equatorial (x2)); 2.08 (s, 3H, CH<sub>3</sub>); 3.70 (q, *J* = 5.8 Hz, 4H, CH<sub>2</sub>-N(x2)); 6.53 (dd, *J*<sub>1</sub> = 2 Hz, *J*<sub>2</sub> = 8.3 Hz, 1H, H-6); 6.62 (d, *J* = 2 Hz, 1H, H-4); 6.69 (d, *J* = 8.3 Hz, 1H, H-7); 6.97 (d, *J* = 8.7 Hz, 2H, H-2'', H-6''); 7.36 (dd, *J*<sub>1</sub> = 1 Hz, *J*<sub>2</sub> = 8.7 Hz, 2H, H-3'', H-5''); 7.52 (d, *J* = 8.8 Hz, 1H, H-5'''); 7.72 (dd, *J*<sub>1</sub> = 2.6 Hz, *J*<sub>2</sub> = 8.8 Hz, 1H, H-6'''); 8.07 (bs, 1H, NH); 8.14 (d, *J* = 2.6 Hz, 1H, H-2'''); 8.49 (bs, 1H, NH).

<sup>13</sup>C NMR (Acetone-d<sub>6</sub>, 100.6 MHz) δ(ppm), 20.5 (CH<sub>3</sub>); 34.3 (CH<sub>2</sub>, CH-C); 34.9 (CH<sub>2</sub>, CH-C); 38.4 (CH<sub>2</sub>, CH-N); 43.3 (CH<sub>2</sub>, CH-N); 100.4 (CH, C-4); 108.4 (CH, C-7); 109.9 (CH, C-6); 116.0 (Cq, C-2); 117.3 (CH, C-2'', C-6''); 120.7 (CH, C-3'', C-5''); 122.6 (CH, C-2'''); 122.8 (Cq, C-4'''); 123.2 (Cq, *J* = 272 Hz, CF<sub>3</sub>); 125.9 (Cq, C-4'''); 127.2 (Cq, *J* = 33.6 Hz, C-3'''); 131.7 (CH, C-5''', C-6'''); 138.9 (Cq, C-7a); 139.9 (Cq, C-1''); 141.0 (Cq, C-1'''); 141.1 (Cq, C-5); 147.5 (Cq, C-3a); 151.7 (Cq, N-C=O); 170.0 (Cq, NH-CO).

#### 4.2.43. Preparation of 1'-acetyl-3H-spiro[benzoxazole-2,4'-piperidine] (43)



##### · Procedure

In a 50 mL round bottom-flask the 1-acetyl-piperidine-4-one (0.17 mL, 0.92 mmol) was dissolved in 10 mL of toluene and *o*-aminophenol (0.14 g, 0.91 mmol) was added in the mixture. A Dean-Stark system was used to remove resultant water. The reaction was stirred for 24 hours at 130-140 °C.

##### · Work-up

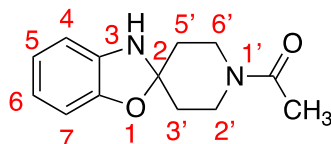
In a TLC analysis a new product was observed (hexane/ethyl acetate 6:4). Reaction was cooled down and toluene was removed to afford the crude mixture, which was dissolved in ethyl acetate (20 mL x 1) and washed with water (20 mL x 3). Organic phase was dried over anhydrous Na<sub>2</sub>SO<sub>4</sub>, filtered and concentrated under reduced pressure.

##### · Purification

Finally, the crude residue obtained was purified by flash automatic column chromatography. The obtained product eluted with a mixture of hexane/ethyl acetate 0:100.

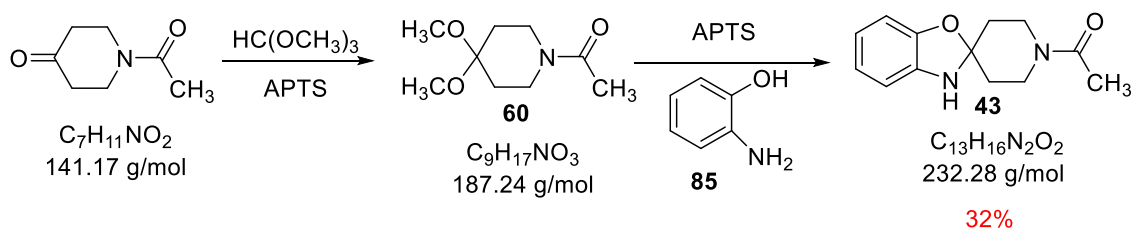
· Analytical data

Product aspect	Mass obtained	Yield	R <sub>f</sub> (hexane/ethyl acetate 6:4)
Brown oil	0.05 g	20%	0.14



<sup>1</sup>H NMR (CDCl<sub>3</sub>, 400 MHz) δ(ppm), 2.10 (s, 3H, CH<sub>3</sub>); 2.47 (dd, *J*<sub>1</sub> = 6.3 Hz, *J*<sub>2</sub> = 15.8 Hz, 4H, CH<sub>2</sub>-C (x2)); 3.74 (t, *J* = 6.3 Hz, 2H, CH-N axial (x2)); 3.87 (t, *J* = 6.3 Hz, 2H, CH-N equatorial (x2)); 6.57 (dt, *J*<sub>1</sub> = 1.5 Hz, *J*<sub>2</sub> = 8 Hz, 1H, H-6); 6.63 (dd, *J*<sub>1</sub> = 1.5 Hz, *J*<sub>2</sub> = 8 Hz, 1H, H-4); 6.77 (dt, *J*<sub>1</sub> = 1.5 Hz, *J*<sub>2</sub> = 8 Hz, 1H, H-5); 6.79 (d, *J* = 8 Hz, 1H, H-7).

#### 4.2.44. Preparation of 1'-acetyl-3H-spiro[benzoxazole-2,4'-piperidine] (**43**)



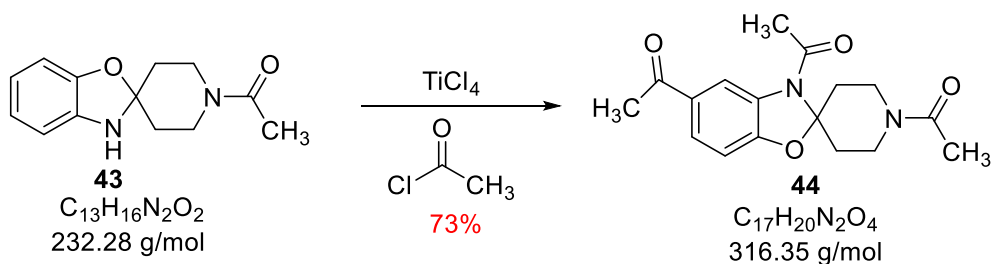
· Procedure

The general procedure of transacetylation described previously in this work to the synthesis of the spiro derivative **1** was applied (0.09 mmol of 1-acetylpiperidine-4-one).

· Purification

Finally, the crude mixture obtained was purified by flash automatic column chromatography. The desired product eluted with a mixture of hexane/ethyl acetate 0:100.

#### 4.2.45. Preparation of 1,1'-(3H-spiro[benzoxazole-2,4'-piperidine]-1',5-diyl)bis(ethanone) (**44**)



· Procedure

General acetylation procedure described previously in this work was applied in this case (0.43 mmol of **43**).



· Work-up

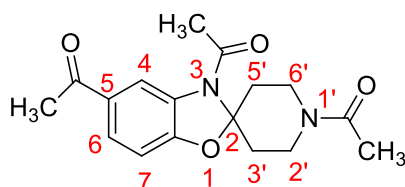
A TLC of reaction showed a new product (hexane/ethyl acetate 7:3). To proceed with hydrolysis of the reagents, 5 mL of water were added. Then, an extraction with dichloromethane (20 mL x 3) was carried out and the organic phases were collected, dried over anhydrous sodium sulfate and concentrated under reduced pressure.

· Purification

No purification of the crude of reaction by column chromatography was performed since product was obtained with enough purity.

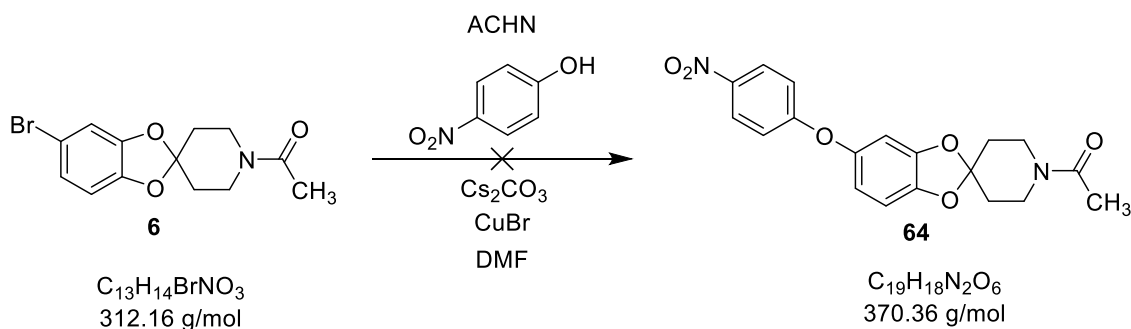
· Analytical data

Product aspect	Mass obtained	Yield	R <sub>f</sub> (hexane/ethyl acetate 7:3)
Brown oil	0.1 g	73%	0.13



<sup>1</sup>H NMR (CDCl<sub>3</sub>, 400 MHz) δ(ppm), 1.79 (s, 3H, CH<sub>3</sub>-O); 2.04 (s, 3H, CH<sub>3</sub>-O); 2.14-2.17 (m, 2H, CH-C axial (x2)); 2.19 (s, 3H, CH<sub>3</sub>-CO); 2.45-2.51 (m, 2H, CH-C equatorial (x2)); 3.09-3.19 (m, 2H, CH-N axial (x2)); 3.73-3.77 (m, 2H, CH-N equatorial (x2)); 6.83-6.87 (m, 1H, H-4); 7.02 (m, 1H, H-7); 7.19-7.23 (m, 1H, H-5).

#### 4.2.46. Preparation of 1'-acetyl-5-(4-nitrophenoxy)spiro[benzo[1,3]dioxole-2,4'-piperidine] (**64**)



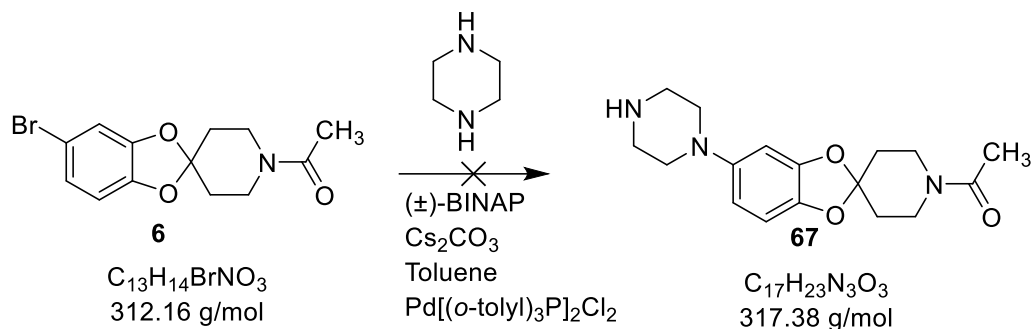
· Procedure

In a Pyrex glass tube with screw cap, previously flame-dried under argon atmosphere, the compound **6** (0.04 g, 0.11 mmol) was dissolved in DMF (7 mL). Then, 4-nitrophenol (0.015 g, 0.11 mmol), cesium carbonate (0.036 g, 0.11 mmol) and CuBr (0.06 mmol) were added under argon atmosphere. Once the tube is closed the reaction was stirred for 24 hours at 120 °C.

After this time, a TLC showed no reaction progress (hexane/ethyl acetate 7:3). The temperature was increased to 150 °C for 76 hours more. At this time, no new products were observed in TLC. The starting material was obtained. The reaction was set up again under microwave irradiation, in a glass tube (10 mL) sealed with a silicon septum under magnetic stirring. The tube was introduced in oven microwave and heated at 100 °C and subjected to a variable MW power until

300 W (an IR sensor measured the temperature of glass tube surface). The same results were obtained.

#### 4.2.47. Preparation of 1'-acetyl-5-(piperazin-1-yl)spiro[benzo[1,3]dioxole-2,4'-piperidine] (**67**)



· Procedure

The Buchwald-Hartwig cross-coupling reaction conditions described in the synthesis of **8**, were applied in this reaction (0.033 mmol of **6**).

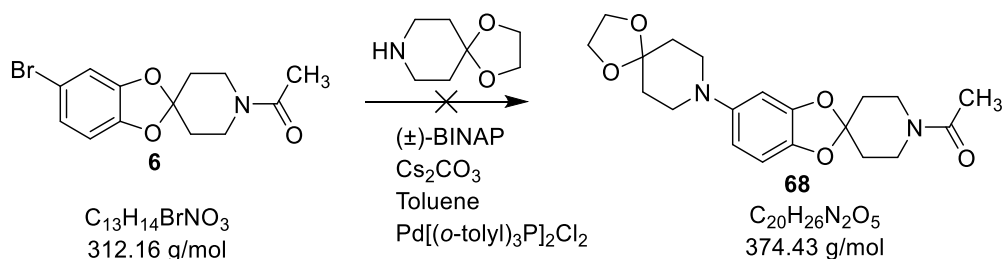
· Work-up

After 48 hours of reaction, a TLC of reaction showed consumption of starting material (hexane/ethyl acetate 5:5). The toluene was evaporated under reduced pressure. Then, the crude residue was dissolved in dichloromethane (20 mL x 1) and washed with water (20 mL x 3). The organic phase was dried over anhydrous sodium sulfate, filtered and concentrated *in vacuo*.

· Purification

Finally, the obtained mixture was purified by flash automatic column chromatography. The main product eluted with a mixture of hexane/ethyl acetate 45:55. The  $^1\text{H}$  NMR signals showed formation of **6**.

#### Preparation of 1'-acetyl-5-(1,4-dioxo-8-azaspiro[4.5]decan-8-yl)spiro[benzo[1,3]dioxole-2,4'-piperidine] (**68**)



· Procedure

The conditions of Buchwald-Hartwig cross-coupling reaction were applied to **6** (0.033 mmol) in this reaction.

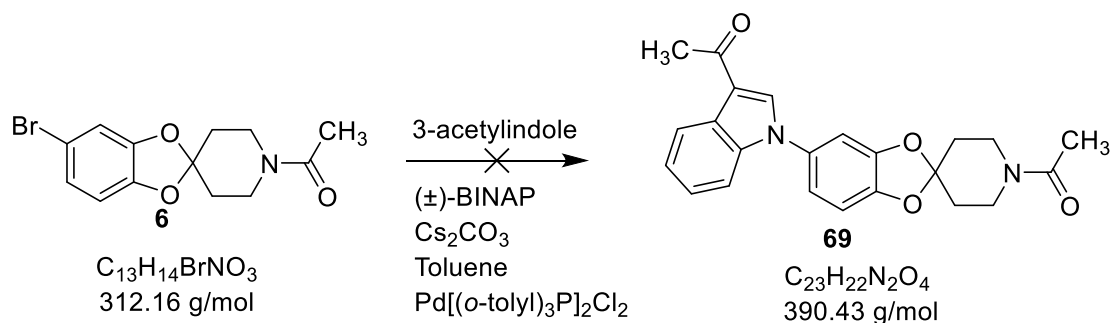
· Work-up

After 76 hours of reaction, the TLC of reaction showed consumption of starting material (hexane/ethyl acetate 7:3). The toluene was evaporated under reduced pressure. Then, the crude residue was dissolved in dichloromethane (20 mL x 1) and washed with water (20 mL x 3). The organic phase was dried over anhydrous sodium sulfate, filtered and concentrated *in vacuo*.

· Purification

Finally, the obtained mixture was purified by flash automatic column chromatography. The product eluted with a mixture of hexane/ethyl acetate 45:55. The  $^1\text{H}$  NMR signals showed the starting material **6**.

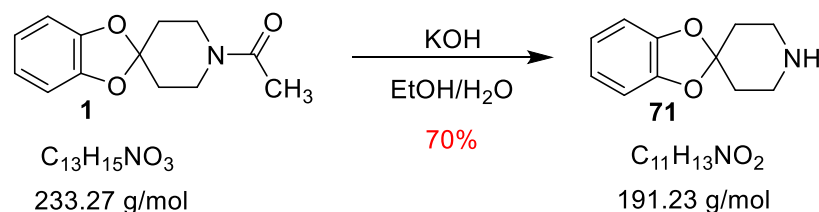
#### 4.2.48. Preparation of 1'-acetyl-5-(3-acetyl-1H-indol-1-yl)spiro[benzo[1,3]dioxole-2,4'-piperidine] (**69**)



· Procedure

The conditions of Buchwald-Hartwig cross-coupling reaction described in the synthesis of **8**, were applied in this reaction (0.033 mmol of **6**). After 76 hours at 160 °C, no progression was seen in TLC. The starting materials were recuperated, and no traces of expected compound was observed under these conditions.

#### 4.2.49. Preparation of spiro[benzo[1,3]dioxole-2,4'-piperidine] (**71**)



· Procedure

Starting from **1** (6.4 mmol), the general hydrolysis procedure described in synthesis of **3** was also applied. The reaction was stirred for 24 hours.

· Work-up

After this time, in TLC analysis (hexane/ethyl acetate 5:5) a new product was observed. The ethanol was removed under reduced pressure. Then, the crude reaction was extracted with

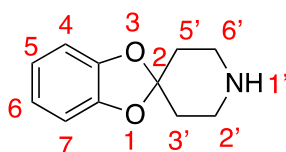
dichloromethane (20 mL x 3) and the organic phases were dried over anhydrous Na<sub>2</sub>SO<sub>4</sub>, filtered and concentrated *in vacuo* to afford the desired compound.

· Purification

No purification of the obtained residue by column chromatography was performed since the product was obtained with enough purity.

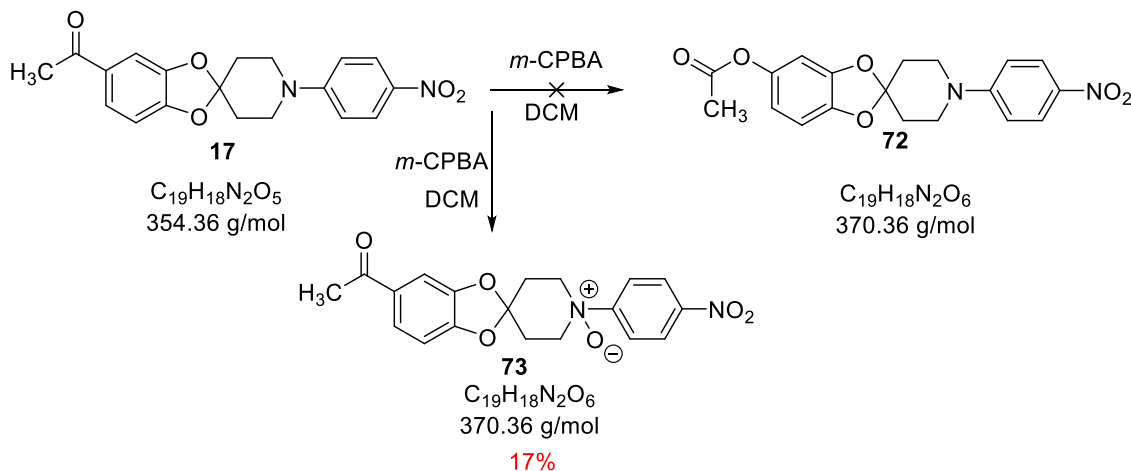
· Analytical data

Product aspect	Mass obtained	Yield	R <sub>f</sub> (hexane/ethyl acetate 5:5)	Melting point
Brownish solid	0.850 g	70%	0.02	244-246 °C (ethanol)



<sup>1</sup>H NMR (CDCl<sub>3</sub>, 400 MHz) δ(ppm), 1.96 (t, *J* = 6 Hz, 4H, CH<sub>2</sub>-C (x2)); 2.78 (bs, 1H, NH); 3.04 (t, *J* = 6 Hz, 4H, CH<sub>2</sub>-N (x2)); 6.75-6.77 (m, 4H, Ar).

#### 4.2.50. Preparation of 1'-(4-nitrophenyl)spiro[benzo[1,3]dioxole-2,4'-piperidine]-5-yl acetate (**72**)



· Procedure

In a 50 mL round bottom flask the spiro-compound **17** (0.185 g, 0.52 mmol) was dissolved in dichloromethane (10 mL) and *m*-CPBA (0.2 g, 1.2 mmol) was added. Reaction was stirred at room temperature for 16 hours.

· Work-up

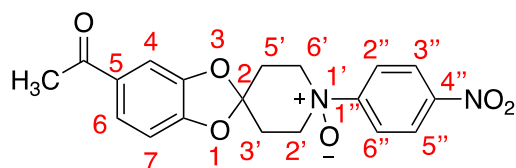
A TLC analysis of the crude reaction showed consumption of starting material (hexane/ethyl acetate 7:3). The mixture was washed first with saturated NaCl aqueous solution (10 mL x 1) and then with saturated NaHCO<sub>3</sub> aqueous solution (10 mL x 1). The organic phase was dried over anhydrous sodium sulfate, filtered and concentrated under reduced pressure.

· Purification

Finally, the crude reaction was purified by flash automatic column chromatography. The product eluted with a mixture of methanol/ethyl acetate 100:0. The  $^1\text{H}$  NMR signals and the HRMS showed a secondary product identified as 5-acetyl-1'-(4-nitrophenyl)spiro[benzo[1,3]dioxole-2,4'-piperidine]-1'-oxide (**73**).

· Analytical data

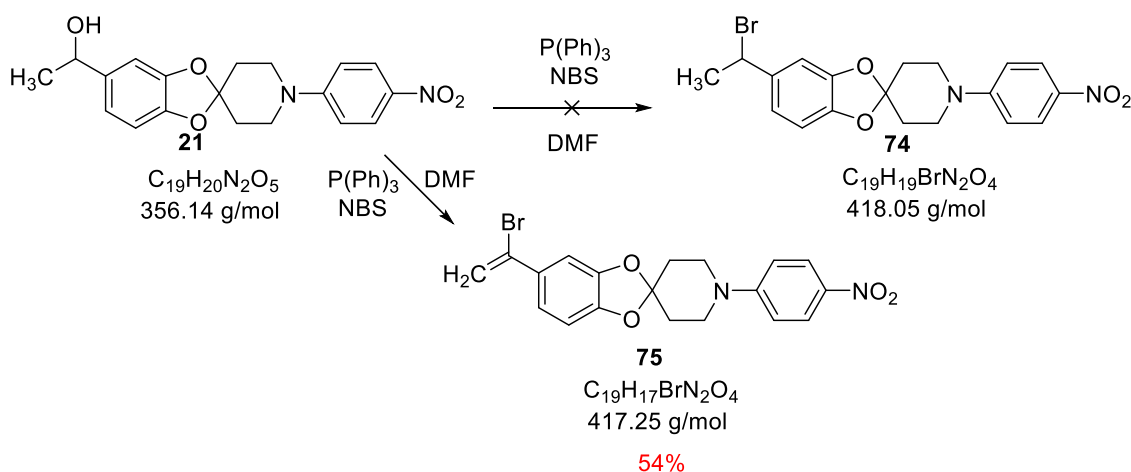
Product aspect	Mass obtained	Yield	$R_f$ (hexane/ethyl acetate 1:9)
Brownish semisolid	0.03 g	17%	0.01



$^1\text{H}$  NMR ( $\text{CDCl}_3$ , 400 MHz)  $\delta$ (ppm), 2.07 (t,  $J = 5.6$  Hz, 1H, CH-C axial (x2) m rotamer); 2.10-2.12 (m, 2H, CH-C axial (x2) M rotamer); 2.48 (s, 1H,  $\text{CH}_3$ , m rotamer); 2.49 (s, 3H,  $\text{CH}_3$ , M rotamer) 3.25-3.37 (m, 4H,  $\text{CH}_2\text{-N}$  (x2)); 3.63 (t,  $J = 5.5$  Hz, 1H, CH-C equatorial (x2) m rotamer); 4.15-4.17 (m, 2H,  $\text{CH}_2\text{-C}$  equatorial (x2), M rotamer); 6.78 (d,  $J = 9$  Hz, 1H, H-2'', H-6'' m rotamer); 6.82 (d,  $J = 8$  Hz, 2H, H-2'', H-6'', M rotamer); 7.40 (s, 1H, H-4); 7.51 (dd,  $J_1 = 2$  Hz,  $J_2 = 8.2$  Hz, 1H, H-6); 7.62 (d,  $J = 8.2$  Hz, 1H, H-7); 8.03 (d,  $J = 9$  Hz, 1H, H-3'', H-5'' m rotamer); 8.08 (d,  $J = 9$  Hz, 2H, H-3'', H-5'' M rotamer); 8.34 (cs, 1H, OH). **M rotamer: majority, m rotamer: minority.**

HRMS (ESI +): Calculated  $\text{C}_{19}\text{H}_{18}\text{N}_2\text{O}_6$   $[\text{M}+\text{H}]^+$ : 371.1200, found 371.1243.

#### 4.2.51. Preparation of 5-(1-bromoethyl)-1'-(4-nitrophenyl)spiro[benzo[1,3]dioxole-2,4'-piperidine] (**74**)



· Procedure

In a 50 mL round bottom flask, the alcohol **21** (0.11 g, 0.3 mmol) was dissolved in 20 mL of DMF. Then, NBS (0.08 g, 0.46 mmol) and triphenylphosphine (0.121 g, 0.46 mmol) were added. The reaction was stirred at 40 °C. After 6 hours of reaction, a TLC analysis (hexane/ethyl acetate 7:3)

showed a mixture between starting material and new product. The reaction mixture was stirred for 24 hours.

· Work-up

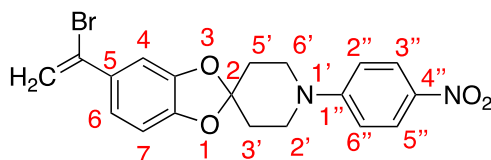
After this time, an extraction with ethyl ether (20 mL x 3) and water (20 mL x 1) was carried out in order to remove DMF from organic phase. Organic phases were collected, dried over anhydrous  $\text{Na}_2\text{SO}_4$ , filtered and concentrated under reduced pressure.

· Purification

Finally, the obtained residue was purified by flash automatic column chromatography. The product eluted with a mixture of hexane/ethyl acetate 80:20. The  $^1\text{H}$  NMR and  $^{13}\text{C}$  NMR confirmed that 5-(1-bromovinyl)-1'-(4-nitrophenyl)spiro[benzo[1,3]dioxole-2,4'-piperidine] (**75**) was obtained.

· Analytical data

Product aspect	Mass obtained	Yield	$R_f$ (hexane/ethyl acetate 7:3)
Brown semisolid	0.07 g	54%	0.80



$^1\text{H}$  NMR ( $\text{CDCl}_3$ , 400 MHz)  $\delta$ (ppm), 2.12 (t,  $J = 6$  Hz, 4H,  $\text{CH}_2\text{-C}$  (x2)); 3.70 (t,  $J = 6$  Hz, 4H,  $\text{CH}_2\text{-N}$  (x2)); 5.12 (d,  $J = 10.8$  Hz, 1H, H *cis*-Br); 5.57 (d,  $J = 17.5$  Hz, 1H, H *trans*-Br); 6.72 (d,  $J = 8$  Hz, 1H, H-7); 6.83 (dd,  $J_1 = 2$  Hz,  $J_2 = 8$  Hz, 1H, H-6); 6.88 (d,  $J = 9.4$  Hz, 2H, H-2'', H-6''); 6.93 (d,  $J = 2$  Hz, 1H, H-4); 8.14 (d,  $J = 9.4$  Hz, 2H, H-3'', H-5'').

$^{13}\text{C}$  NMR ( $\text{CDCl}_3$ , 100.6 MHz)  $\delta$ (ppm), 34.2 ( $\text{CH}_2$ ,  $\text{CH}_2\text{-C}$  (x2)); 45.0 ( $\text{CH}_2$ ,  $\text{CH}_2\text{-N}$  (x2)); 105.5 (CH, C-4); 108.4 (CH, C-7); 111.9 (Cq, C-2); 113.0 (CH, C-2'', C-6''); 115.9 (Cq, CH-Br); 120.9 (CH, C-6); 126.1 (CH, C-3'', C-5''); 132.0 ( $\text{CH}_2$ ,  $\text{CH}_2\text{=Br}$ ); 136.3 (Cq, C-5); 138.5 (Cq, C-4''); 146.7 (Cq, C-3a); 147.3 (Cq, C-7a); 153.9 (Cq, C-1'').

### 4.3. Preparation of pyrrolo[2,3-*b*]pyrazines

#### *General procedure A (Sonogoshira coupling)*

In a Pyrex glass tube equipped with a magnetic stirring, previously flame-dried under argon atmosphere, 2-amino-3,5-dibromopyrazine (1.0 mmol), the appropriate aryl acetylene (0.95 mmol), Pd(dba)<sub>2</sub> (0.03 mmol) and tri(2-furyl)phosphine (0.06 mmol) were added. Then, THF (3 mL) and triethylamine (0.45 mL), previously outgassed were added as well. The reaction mixture was stirred for 16 hours. When control of reaction through TLC confirmed consumption of starting material, 20 mL of NH<sub>4</sub>Cl solution were added and the obtained crude was extracted with ethyl acetate (15 mL x 3). Organic phases were collected, dried over anhydrous sodium sulfate, filtered and concentrated under reduced pressure to afford a solid which was purified by means of a flash automatic silica gel column chromatography, using as an eluent an ascending polarity from hexane to ethyl acetate.

#### *General procedure B (Cyclization)*

In a Pyrex glass tube equipped with a magnetic stirring, previously flame-dried under argon atmosphere, the pyrazine obtained previously from Sonogoshira reaction (1.0 mmol), 6-8 mL of acetonitrile and cesium carbonate (1.0 mmol) were added. The mixture was stirred at 130-140 °C for 16 hours. When control of reaction through TLC confirmed consumption of starting material, solvent was evaporated *in vacuo*, 20 mL of water were added, and the obtained crude of reaction was extracted with ethyl acetate (15 mL x 3). If needed a warm extraction was carried out to facilitate layers separation. Organic phases were collected, dried over anhydrous sodium sulfate, filtered and concentrated under reduced pressure affording the desired product.

#### *General procedure C (Suzuki-Miyaura coupling)*

In a Pyrex glass tube equipped with a magnetic stirring, previously flame-dried under argon atmosphere, the appropriate 5*H*-pyrrolo[2,3-*b*]pyrazine (1.0 mmol), acetonitrile (4 mL), previously outgassed under argon, appropriate boronic acid (1.0 mmol), dried sodium carbonate (2.0 mmol), Pd(P(C<sub>6</sub>H<sub>5</sub>)<sub>3</sub>)<sub>4</sub> (0.02 mmol) and 0.6 mL of distilled water were added. The reaction was stirred at 140 °C until no more starting material was observed in TLC. Then, a saturated NaCl aqueous solution was added (20 mL) and the obtained crude was extracted with ethyl acetate (20 mL x 3). Organic phases were collected, dried over anhydrous sodium sulfate, filtered and concentrated under reduced pressure affording a solid, which was purified by means of a flash automatic silica gel column chromatography, using as an eluent an ascending polarity from hexane to ethyl acetate.

#### *General procedure D (halogenation of C-7)*

In a Pyrex glass tube equipped with a magnetic stirring, previously flame-dried under argon atmosphere, the appropriate 5*H*-pyrrolo[2,3-*b*]pyrazine in acetonitrile and *N*-bromosuccinimide (NBS) were added under argon atmosphere. The reaction mixture was stirred at room temperature until no starting material could be detected by TLC. Solvent was removed under reduced pressure and the obtained crude extracted with ethyl acetate (20 mL x 1) and water (20 mL x 3). Organic phases were dried over sodium sulfate, filtered and solvent removed to dryness affording the desired characteristic yellow brominated product.

#### 4.3.1. Halogenation of 2-aminopyrazine

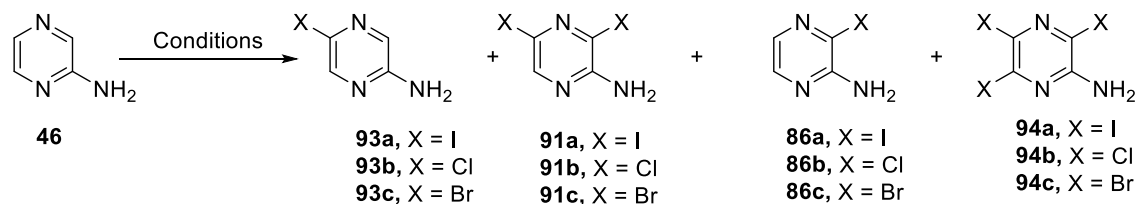


**Table 32.** Halogenation of 2-aminopyrazine. Conditions and results

Entry	Conditions	X	93 (%)	91 (%)	86 (%)	94 (%)
1	NIS (3 eq), ACN, 100 °C, 20 h	I	9	-	-	-
2	NIS (3 eq), ACN, r.t., 3 h	I	11	-	-	-
3	NIS (1.1 eq), ACN, r.t., 6 h	I	14	28	-	-
4	NIS (1.1 eq), MeOH, r.t., 3 h	I	13	-	-	-
5	NIS (1.1 eq), MeOH, 100 °C, 3 h	I	34	-	-	-
6	NIS (1.1 eq), DMF, r.t., 3 h	I	25	-	-	-
7	NIS (1.1 eq), DMF, 100 °C, 3 h	I	22	-	-	-
8	NIS (1.1 eq), DMF, -30 °C, 3 h	I	15	-	-	-
9	I <sub>2</sub> (1.1 eq), LDA (1.5 eq), THF, -78 °C, 3 h	I	39	-	-	-
10	NCS (2.2 eq), ACN, r.t., 72 h	Cl	-	12	-	14
11	NCS (1.1 eq), ACN, 100 °C, 3 h	Cl	57	13	17	-
12	NCS (1.1 eq), ACN, r.t. 3 h	Cl	89	-	-	-
13	NBS (3 eq), ACN, r.t., 3 h	Br	-	38	-	-
14	NBS (1.1 eq), ACN, 100 °C, 6 h	Br	22	11	-	-
15	NBS (1.1 eq), ACN, r.t., 3 h	Br	89	-	-	-
16	NBS (1.1 eq), ACN, MW, 5 min	Br	88	6	-	-
17	NBS (2.2 eq), ACN, MW, 5 min	Br	-	98	-	-
18 <sup>A</sup>	NBS (2.2 eq), MeOH, r.t., 3 h	Br	-	78	-	-
19	NBS (1.1eq), MeOH, r.t., 3 h	Br	26	19	-	-
20	NBS (1.1 eq), MeOH, 100 °C, 3 h	Br	28	25	-	-
21	NBS (1.1 eq), DMF, MW, 100 °C, 1 h	Br	5	15	-	-
22	NBS (1.1 eq), CuBr, ACN, r.t., 3 h	Br	41	-	-	-
23	NBS (1.1 eq), AIBN, CCl <sub>4</sub> , hv, 3 h	Br	46	-	9	-
24	NBS (2.2 eq), DMSO, H <sub>2</sub> O, 0 °C to r.t., 16 h	Br	-	48 (77)	-	-
25	Bromodioxane (1.1 eq), Dioxane, 0 °C to r.t., 3 h	Br	-	6	-	-
26	Bromodioxane (0.5 eq), Dioxane, 0 °C to r.t., 3 h	Br	32	-	5	-
27	Bromodioxane (1 eq), Dioxane, 100 °C, 30 min	Br	48	-	6	-



· General procedure

General procedure using conventional heating: To a solution of pyrazine-2-amine (1.0 mmol) in methanol, acetonitrile, dimethylformamide or lithium diisopropylethylamine (5-10 mL) the *N*-iodosuccinimide (NIS) (procedure E) (1.1 mmol – 3.0 mmol) or I<sub>2</sub> (1.1 mmol) or *N*-chlorosuccinimide (NCS) (procedure F) or *N*-bromosuccinimide (NBS) (procedure G) were added (in the reaction with I<sub>2</sub> also LDA (1.5 mmol) was added). The obtained reaction mixture was stirred until no starting material could be detected by thin-layer chromatography. Then solvent was removed under reduced pressure to give the crude product, which was purified by silica gel column chromatography.

General procedure with microwaves radiation assistance: To a solution of the pyrazine-2-amine (1.0 mmol) in acetonitrile (5 mL) the *N*-iodosuccinimide (NIS) (procedure E) (1.1 mmol – 3.0 mmol) or I<sub>2</sub> (1.1 mmol) or *N*-chlorosuccinimide (NCS) (procedure F) or *N*-bromosuccinimide (NBS) (procedure G) (1.1 mmol – 2.2 mmol) were added to the glass tube (10 mL) sealed with a silicon septum equipped with magnetic stirring. The tube was introduced in the oven microwave and was heated to 100 °C (external temperature) and subjected to a variable MW power until 300 W (an IR sensor measured the temperature of glass tube surface) until total consumption of starting material could be detected by thin-layer chromatography. Then the solvent was removed under reduced pressure to give the crude product, which was purified by silica gel column chromatography. Alternatively, the residue of reaction can be extracted with ethyl ether and water (3 x 15 mL), dried over sodium sulfate, filtered and the solvent removed to dryness.

· Analytical data

a) 2-Amino-5-iodopyrazine

<sup>1</sup>H NMR (CDCl<sub>3</sub>, 400 MHz) δ(ppm), 7.83 (s, 1H, H-3); 8.21 (s, 1H, H-6).

Mp: 110-113 °C (DCM)

b) 2-Amino-3,5-diiodopyrazine

<sup>1</sup>H NMR (CDCl<sub>3</sub>, 400 MHz) δ(ppm), 7.99 (s, 1H, H-3); 8.21 (s, 1H, H-6).

c) 2-Amino-5-chloropyrazine

<sup>1</sup>H NMR (CDCl<sub>3</sub>, 400 MHz) δ(ppm), 7.77 (s, 1H, H-3); 8.00 (s, 1H, H-6).

Mp: 122-124 °C (DCM)

d) 2-Amino-3,5-dichloropyrazine

<sup>1</sup>H NMR (CDCl<sub>3</sub>, 400 MHz) δ(ppm), 5.12 (bs, 2H, NH<sub>2</sub>); 7.97 (s, 1H, H-6).

Mp: 115-118 °C (DCM)

e) 2-Amino-5-bromopyrazine

<sup>1</sup>H NMR (CDCl<sub>3</sub>, 400 MHz) δ(ppm), 7.76 (s, 1H, H-3); 8.10 (s, 1H, H-6).

Mp: 113-115 °C (DCM)

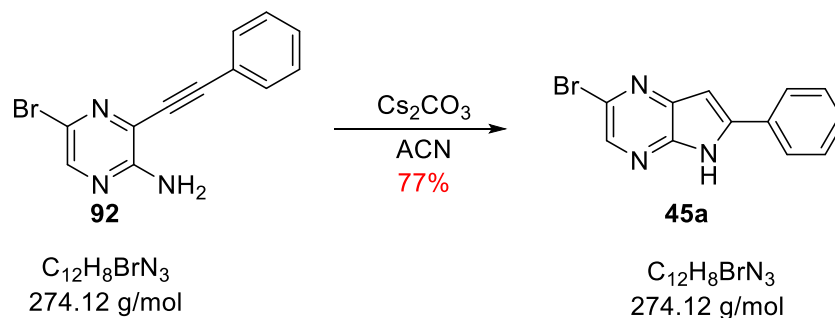
f) 2-Amino-3,5-dibromopyrazine

$^1\text{H}$  NMR ( $\text{CDCl}_3$ , 400 MHz)  $\delta(\text{ppm})$ , 5.18 (bs, 2H,  $\text{NH}_2$ ); 8.04 (s, 1H, H-6).

$^{13}\text{C}$  NMR ( $\text{CDCl}_3$ , 100.6 MHz)  $\delta(\text{ppm})$ , 123.6 (CH, C-3); 124.0 (Cq, C-5); 143.1 (CH, C-6); 151.9 (Cq, C-2).

Mp: 118-120 °C (DCM)

#### 4.3.2. Preparation of 2-bromo-6-phenyl-5H-pyrrolo[2,3-b]pyrazine (45a)

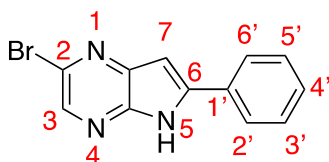


Procedure

Starting from **92** (0.75 mmol), the general procedure **B** described above was followed in this case (cyclization).

Analytical data

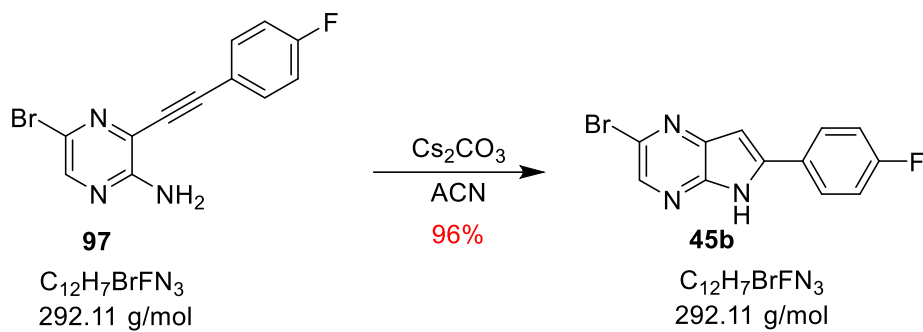
Product aspect	Mass obtained	Yield	$R_f$ (hexane/ethyl acetate 8:2)	Melting point
Yellowish solid	0.120 g	92%	0.46	289-291 °C (DCM)



$^1\text{H}$  NMR ( $\text{CDCl}_3$ , 400 MHz)  $\delta(\text{ppm})$ , 6.34 (s, 1H, NH); 6.81 (s, 1H, H-7); 7.02-7.08 (m, 5H, Ar); 7.93 (s, 1H, H-3).

$^{13}\text{C}$  NMR ( $\text{CDCl}_3$ , 100.6 MHz)  $\delta(\text{ppm})$ , 102.9 (CH, C-7); 128.0 (CH, C-3', C-5'); 128.2 (CH, C-2', C-6'); 129.2 (CH, C-4'); 129.4 (Cq, C-7a); 133.4 (Cq, C-2); 137.6 (CH, C-3); 139.3 (Cq, C-6); 141.4 (Cq, C-1'); 146.0 (Cq, C-4a).

#### 4.3.3. Preparation of 2-bromo-6-(4-fluorophenyl)-5H-pyrrolo[2,3-b]pyrazine (**45b**)



##### · Procedure

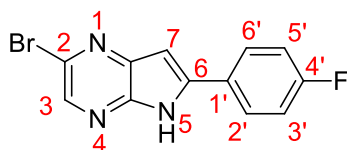
Starting from **97** (1 mmol), the general procedure **B** described above was followed in this case (cyclization).

##### · Purification

The crude mixture obtained was purified by flash automatic silica gel column chromatography. The desired product eluted with a mixture of hexane/ethyl acetate 80:20.

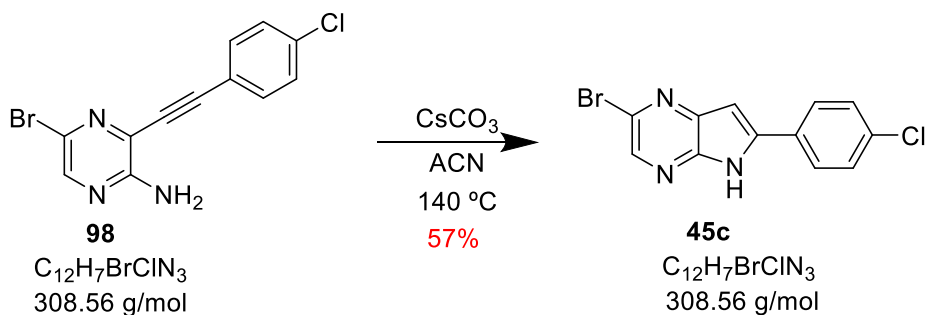
##### · Analytical data

Product aspect	Mass obtained	Yield	R <sub>f</sub> (hexane/ethyl acetate 8:2)	Melting point
Yellowish solid	0.280 g	96%	0.46	> 300 °C (DCM)



<sup>1</sup>H NMR (CDCl<sub>3</sub>, 400 MHz) δ(ppm), 6.80 (s, 1H, H-7); 6.95 (dd, *J*<sub>1</sub> = 5 Hz, *J*<sub>2</sub> = 8.5 Hz, 2H, H-3', H-5'); 7.66 (dd, *J*<sub>1</sub> = 5 Hz, *J*<sub>2</sub> = 8.5 Hz, 2H, H-2', H-6'); 8.18 (s, 1H, H-3).

#### 4.3.4. Preparation of 2-bromo-6-(4-chlorophenyl)-5H-pyrrolo[2,3-b]pyrazine (**45c**)



##### · Procedure

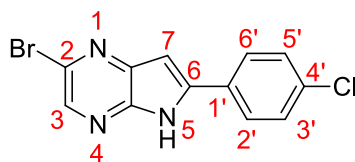
Starting from **98** (1.28 mmol), the general procedure **B** described above was followed in this case (cyclization).

##### · Purification

No purification was performed since the product was obtained with enough purity.

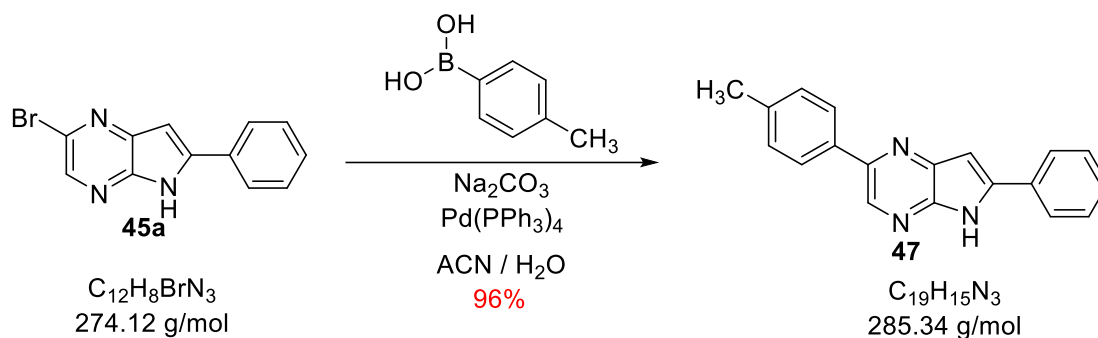
· Analytical data

Product aspect	Mass obtained	Yield	R <sub>f</sub> (hexane/ethyl acetate 8:2)	Melting point
Yellow solid	0.227 g	57%	0.66	> 300 °C (DCM)



<sup>1</sup>H NMR (CDCl<sub>3</sub> + Acetone-D<sub>6</sub> drop, 400 MHz) δ(ppm), 6.90 (s, 1H, H-7); 7.49 (d, *J* = 8.4 Hz, 2H, H-3', H-5'); 7.66 (d, *J* = 8.4 Hz, 2H, H-2', H-6'); 8.27 (s, 1H, H-3).

#### 4.3.5. Preparation of 6-phenyl-2-(*p*-tolyl)-5H-pyrrolo[2,3-*b*]pyrazine (**47**)

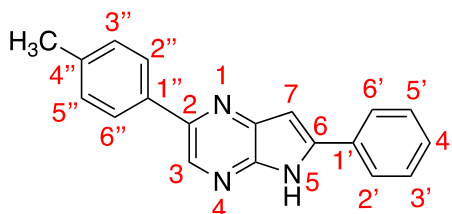


· Procedure

Starting from **45a** (0.33 mmol), the general procedure **C** described previously in this work was followed in this case (Suzuki-Miyaura coupling reaction).

· Analytical data

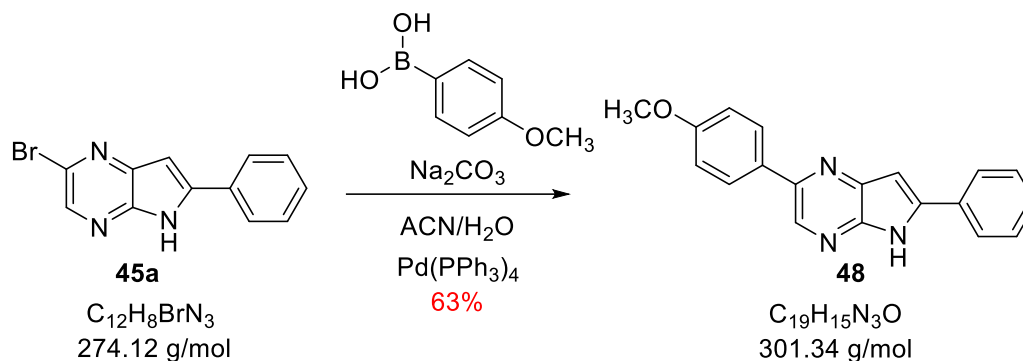
Product aspect	Mass obtained	Yield	R <sub>f</sub> (hexane/ethyl acetate 8:2)	Melting point
Yellow solid	0.090 g	96%	0.47	150-152°C (DCM)



<sup>1</sup>H NMR (CDCl<sub>3</sub>, 400 MHz) δ(ppm), 2.38 (s, 3H, CH<sub>3</sub>); 7.00 (s, 1H, H-7); 7.27 (d, *J* = 8 Hz, 2H, H-3'', H-5''); 7.38 (t, *J* = 7.7 Hz, 1H, H-4''); 7.46 (t, *J* = 7.7 Hz, 2H, H-3', H-5'); 7.81 (d, *J* = 8 Hz, 2H, H-2'', H-6''); 7.83 (d, *J* = 7.7 Hz, 2H, H-2', H-6'); 8.50 (s, 1H, H-3).

<sup>13</sup>C NMR (CDCl<sub>3</sub>, 100.6 MHz) δ(ppm), 33.5 (CH<sub>3</sub>); 106.1 (CH, C-7); 129.7 (CH, C-2'', C-6''); 130.7 (CH, C-3'', C-5''); 133.0 (CH, C-2', C-6'); 133.5 (CH, C-3', C-5'); 138.0 (CH, C-4'); 142.6 (CH, C-3); Quaternary carbons were not observed, in this spectrum.

#### 4.3.6. Preparation of 2-(4-methoxyphenyl)-6-phenyl-5H-pyrrolo[2,3-b]pyrazine (**48**)



· Procedure

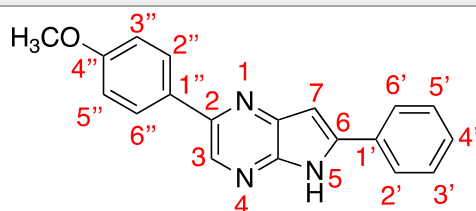
Starting from **45a** (0.96 mmol), the general procedure **C** described previously was also applied in this case (Suzuki-Miyaura coupling reaction).

· Purification

The crude mixture obtained was purified by flash automatic silica gel column chromatography. The desired product eluted with a mixture of hexane/ethyl acetate 75:25.

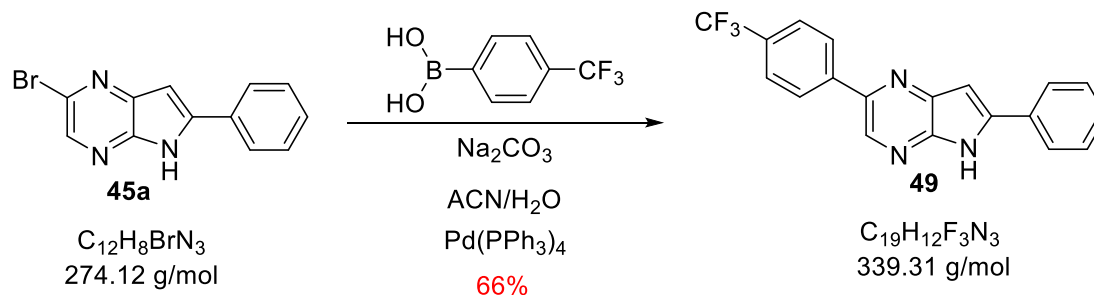
· Analytical data

Product aspect	Mass obtained	Yield	$R_f$ (hexane/ethyl acetate 8:2)	Melting point
Yellowish solid	0.182 g	63%	0.46	153-155 °C (DCM)



$^1\text{H NMR}$  ( $\text{CDCl}_3$ , 400 MHz)  $\delta$ (ppm), 3.89 (s, 3H,  $\text{CH}_3\text{-O}$ ); 6.53 (bs, 1H, NH); 6.99 (s, 1H, H-7); 7.00-7.02 (m, 1H, H-4'); 7.05 (d,  $J = 8.8$  Hz, 2H, H-3'', H-5''); 7.09 (d,  $J = 7$  Hz, 2H, H-3', H-5'); 7.15 (dd,  $J_1 = 1.7$  Hz,  $J_2 = 7$  Hz, 2H, H-2', H-6'); 7.91 (d,  $J = 8.8$  Hz, 2H, H-2'', H-6''); 8.35 (s, 1H, H-3).

#### 4.3.7. Preparation of 6-phenyl-2-(4-(trifluoromethyl)phenyl)-5H-pyrrolo[2,3-b]pyrazine (**49**)



· Procedure

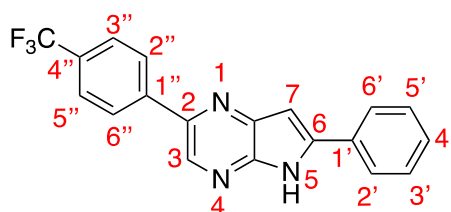
Starting from **45a** (0.68 mmol), the general procedure **C** described previously in this work was applied in this case (Suzuki-Miyaura coupling reaction).

· Purification

The crude mixture obtained was purified by flash automatic silica gel column chromatography. The desired product eluted with a mixture of hexane/ethyl acetate 85:15.

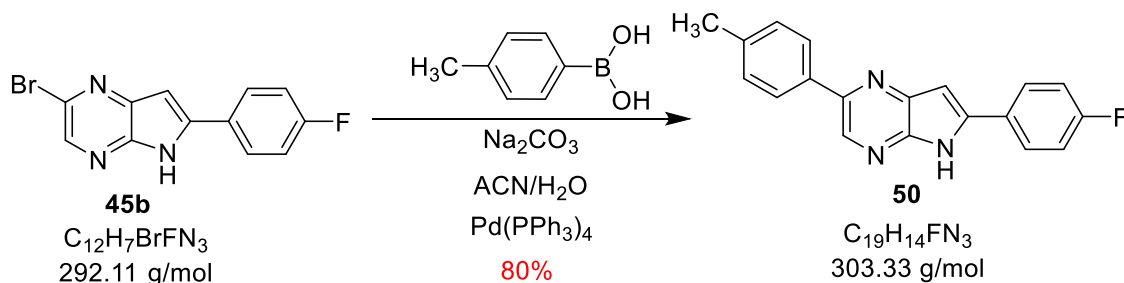
· Analytical data

Product aspect	Mass obtained	Yield	R <sub>f</sub> (hexane/ethyl acetate 8:2)
Yellowish solid	0.153 g	66%	0.37



<sup>1</sup>H NMR (DMSO-d<sub>6</sub>, 400 MHz) δ(ppm), 7.24 (d, *J* = 2 Hz, 1H, H-7); 7.44 (t, *J* = 7.4 Hz, 1H, H-4'); 7.53 (t, *J* = 7.4 Hz, 2H, H-3', H-5'); 7.85 (d, *J* = 8.2 Hz, 2H, H-3'', H-5''); 8.04 (d, *J* = 7.4 Hz, 2H, H-2', H-6'); 8.36 (d, *J* = 8.2 Hz, 2H, H-2'', H-6''); 8.93 (s, 1H, H-3).

#### 4.3.8. Preparation of 6-(4-fluorophenyl)-2-(*p*-tolyl)-5H-pyrrolo[2,3-*b*]pyrazine (**50**)



· Procedure

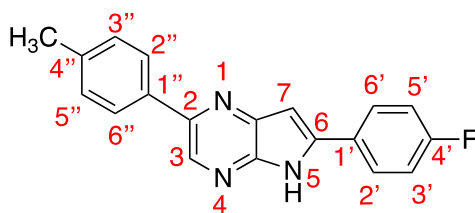
Starting from **45b** (1.02 mmol), the general procedure **C** described above was followed in this case (Suzuki-Miyaura coupling reaction).

· Purification

The crude reaction was purified by flash automatic silica gel column chromatography. The desired product eluted with a mixture of hexane/ethyl acetate 80:20.

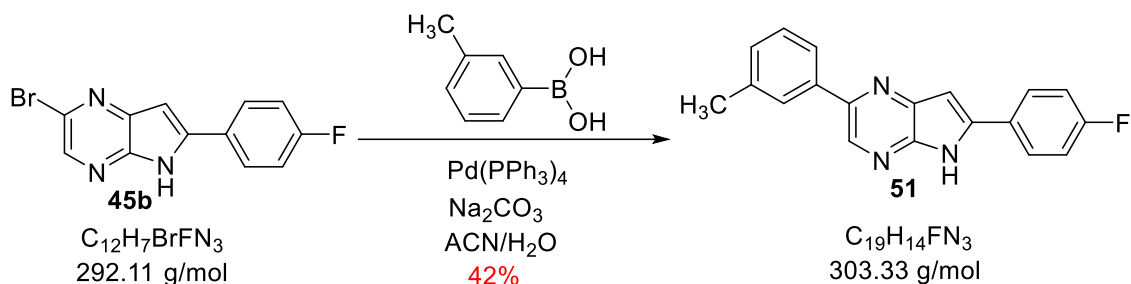
· Analytical data

Product aspect	Mass obtained	Yield	R <sub>f</sub> (hexane/ethyl acetate 8:2)	Melting point
Yellowish solid	0.257 g	80%	0.20	293-295 °C (DCM)



$^1\text{H NMR}$  ( $\text{CDCl}_3$ , 400 MHz)  $\delta$ (ppm), 2.37 (s, 3H,  $\text{CH}_3$ ); 6.81 (s, 1H, H-7); 7.15 (d,  $J = 8.5$  Hz, 2H, H-3', H-5'); 7.28 (d,  $J = 7.8$  Hz, 2H, H-3'', H-5''); 7.77 (dd,  $J_1 = 5$  Hz,  $J_2 = 8.6$  Hz, 2H, H-2', H-6'); 7.86 (d,  $J = 7.8$  Hz, 2H, H-2'', H-6''); 8.18 (s, 1H, H-3); 9.88 (bs, 1H, NH).

#### 4.3.9. Preparation of 6-(4-fluorophenyl)-2-(m-tolyl)-5H-pyrrolo[2,3-b]pyrazine (**51**)



· Procedure

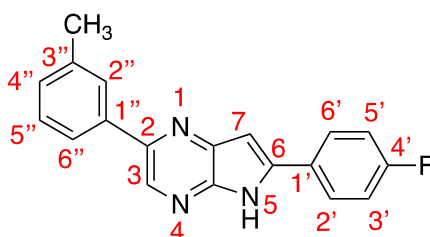
Starting from **45b** (1.03 mmol), the general procedure **C** described above was followed in this case (Suzuki-Miyaura coupling reaction).

· Purification

A purification of the residue obtained to remove excess of boronic acid was carried out by flash automatic silica gel column chromatography. The desired product eluted with a mixture of hexane/ethyl acetate 80:20.

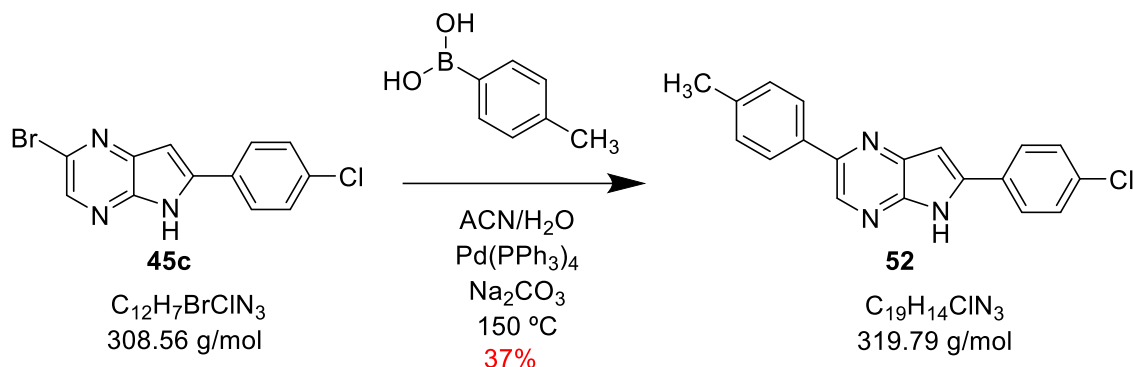
· Analytical data

Product aspect	Mass obtained	Yield	$R_f$ (hexane/ethyl acetate 8:2)	Melting point
Yellowish solid	0.131 g	42%	0.31	292-294 °C (DCM)



$^1\text{H NMR}$  ( $\text{CDCl}_3$ , 400 MHz)  $\delta$ (ppm), 2.46 (s, 3H,  $\text{CH}_3$ ); 4.88 (s, 1H, NH); 7.00 (s, 1H, H-7); 7.25 (d,  $J = 9$  Hz, 2H, H-3', H-5'); 7.29-7.31 (m, 1H, H-4''); 7.38-7.40 (m, 1H, H-5''); 7.78 (d,  $J = 9$  Hz, 2H, H-2', H-6'); 8.00 (s, 1H, H-3); 7.98-8.03 (m, 2H, H-2'', H-6''); 10.4 (bs, 1H, NH).

#### 4.3.10. Preparation of 6-(4-chlorophenyl)-2-(p-tolyl)-5H-pyrrolo[2,3-b]pyrazine (**52**)



##### · Procedure

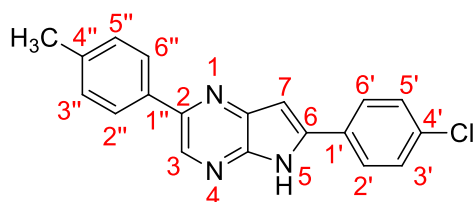
Starting from **45c** (0.73 mmol), the general procedure **C** described above was followed in this case (Suzuki-Miyaura coupling reaction).

##### · Purification

A purification of the crude reaction was carried out by flash automatic silica gel column chromatography. The desired product eluted with a mixture of hexane/ethyl acetate 85:15.

##### · Analytical data

Product aspect	Mass obtained	Yield	R <sub>f</sub> (hexane/ethyl acetate 8:2)	Melting point
Yellow solid	0.086 g	37%	0.40	> 300 °C (DCM)

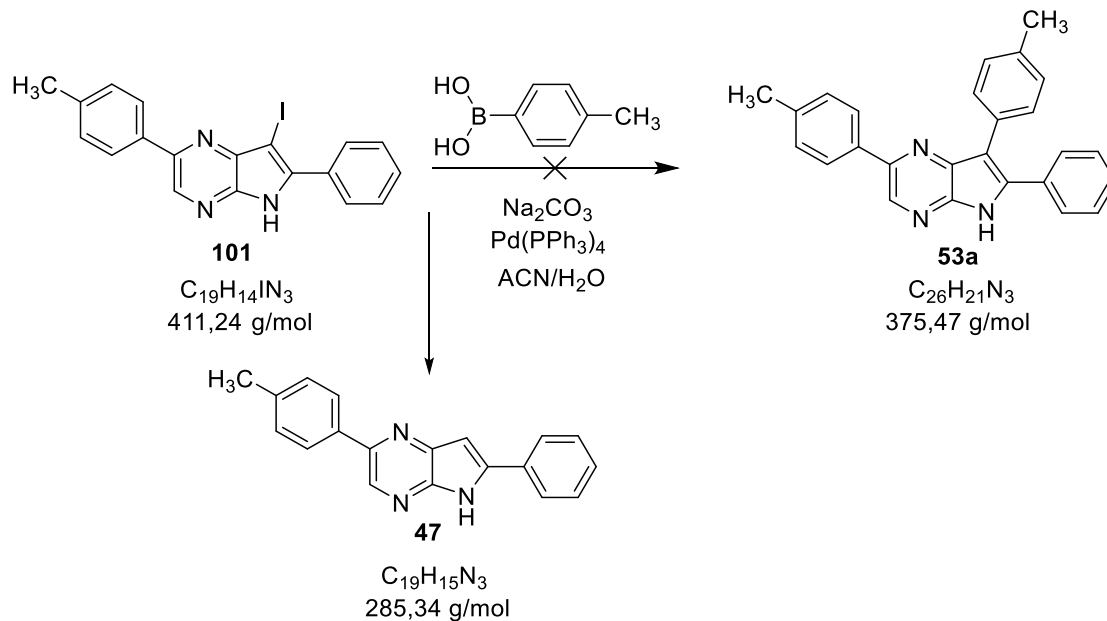


<sup>1</sup>H NMR (CDCl<sub>3</sub> + Acetone-d<sub>6</sub> drop, 400 MHz) δ(ppm), 2.38 (s, 3H, CH<sub>3</sub>); 4.66 (bs, 1H, NH); 7.22 (d, *J* = 7.7 Hz, 2H, H-3', H-5'); 7.31 (d, *J* = 7.7 Hz, 2H, H-3'', H-5''); 7.63 (d, *J* = 7.7 Hz, 2H, H-2', H-6'); 8.12 (d, *J* = 7.7 Hz, 2H, H-2'', H-6''); (H-7 appears at 6.91 ppm and H-3 at 8.05 ppm, both width and barely visible signals).

<sup>13</sup>C NMR (CDCl<sub>3</sub> + CD<sub>3</sub>OD drop, 100.6 MHz) δ(ppm), 20.7 (CH<sub>3</sub>); 97.9 (CH, C-7); 120.1 (Cq, C-7a); 126.8 (Cq, C-1''); 127.2 (CH, C-2'', C-6''); 128.5 (Cq, C-6); 129.4 (CH, C-2', C-3', C-3'', C-5', C-5'', C-6'); 131.6 (Cq, C-4''); 133.0 (Cq, C-1'); 135.6 (Cq, C-4'); 137.6 (CH, C-3); 141.1 (Cq, C-4a); 143.7 (Cq, C-2).



#### 4.3.11. Preparation of 6-phenyl-7-(*m*-tolyl)-2-(*p*-tolyl)-5H-pyrrolo[2,3-*b*]pyrazine (**53a**)



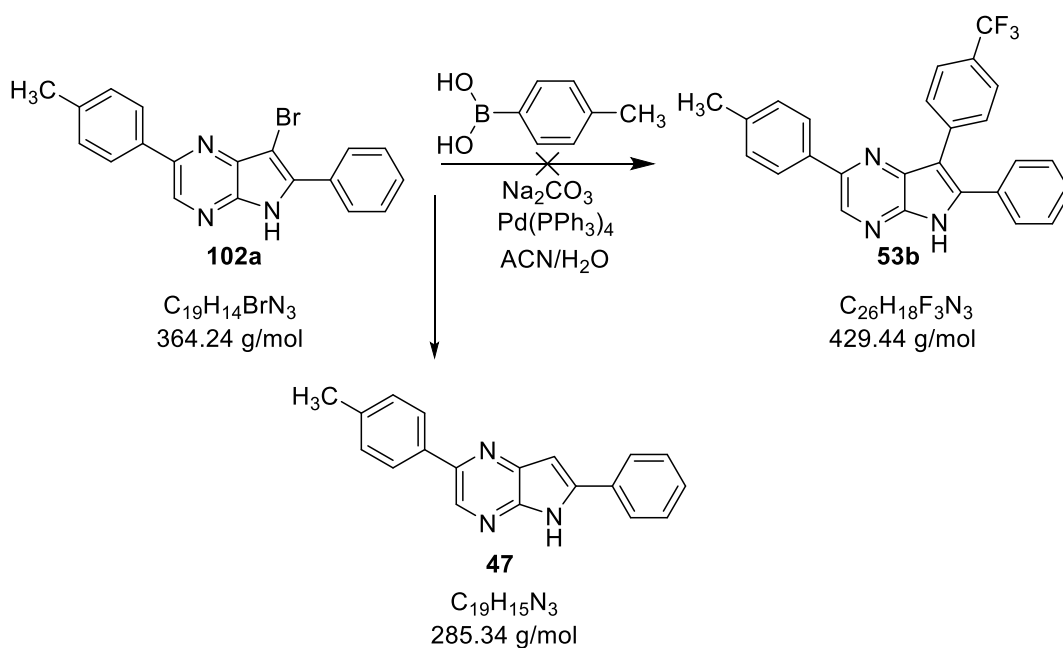
#### · Procedure

Starting from **101** (0.5 mmol), the general procedure **C** described previously was followed (Suzuki-Miyaura coupling reaction). The  $^1\text{H}$  NMR signals of crude mixture showed a formation of the described diarylated product **47**.

The analytical data (product aspect,  $^1\text{H}$  NMR,  $R_f$ , and others) was coincident with those previously described for **47**.

HRMS, ESI(+)  $m/z$ : Calculated for  $\text{C}_{19}\text{H}_{15}\text{N}_3$   $[\text{M}+\text{H}]^+$ : 286.1300, found 286.1342.

#### 4.3.12. Preparation of 6-phenyl-2,7-di-*p*-tolyl-5H-pyrrolo[2,3-*b*]pyrazine (**53b**)



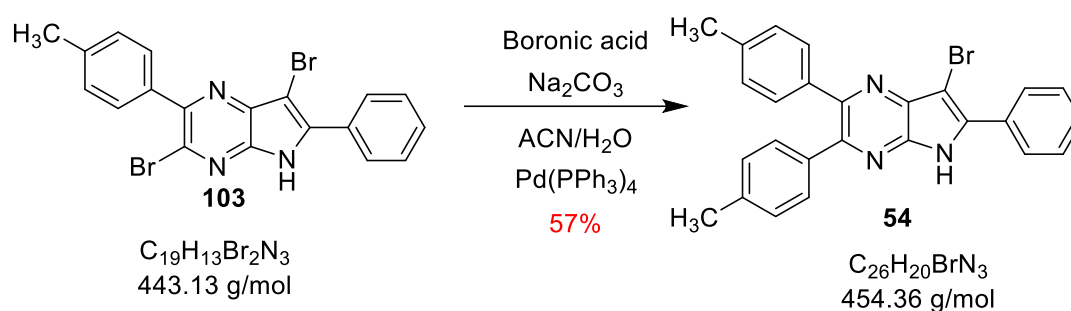
· Procedure

The general procedure **C** described previously was followed in this case (Suzuki-Miyaura coupling reaction). The <sup>1</sup>H NMR signals and the HRMS of the crude mixture showed a formation of **47** and the bromo derivative **102a**.

The analytical data (product aspect, <sup>1</sup>H NMR, R<sub>f</sub>, and others) match completely with those previously described for **47** and **102a**.

**HRMS, ESI(+)** m/z: Calculated for C<sub>19</sub>H<sub>15</sub>N<sub>3</sub> [M+H]<sup>+</sup>: 286.1300, major found 286.1340 and 364.0457 (bromo derivative).

4.3.13. Preparation of 7-bromo-6-phenyl-2,3-di-p-tolyl-5H-pyrrolo[2,3-b]pyrazine (**54**)



· Procedure

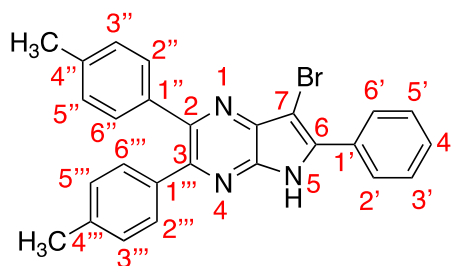
Starting from **103** (0.04 mmol), the general procedure **C** described above was also followed in this case (Suzuki-Miyaura coupling reaction).

· Purification

The residue mixture was purified by flash automatic silica gel column chromatography. The product eluted with a mixture of hexane/ethyl acetate 90:10.

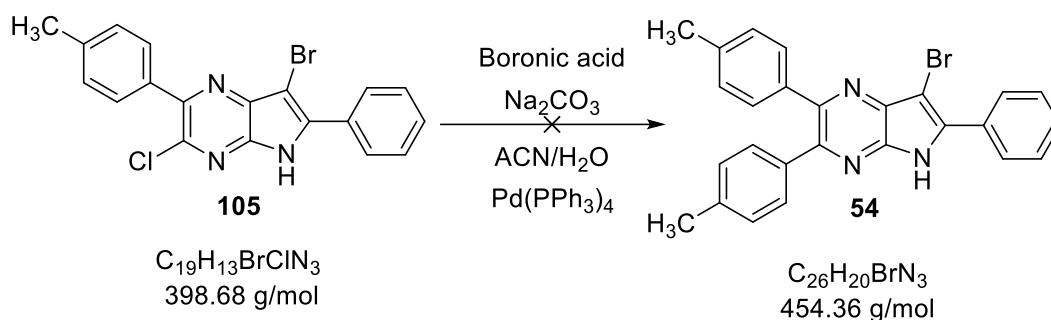
· Analytical data

Product aspect	Mass obtained	Yield	R <sub>f</sub> (hexane/ethyl acetate 7:3)	Melting point
Yellow solid	0.01 g	57%	0.75	> 300 °C (DCM)



<sup>1</sup>H NMR (CDCl<sub>3</sub>, 400 MHz) δ(ppm), 2.32 (s, 3H, CH<sub>3</sub>-Ar); 2.34 (s, 3H, CH<sub>3</sub>-Ar); 7.05 (d, *J* = 8.2 Hz, 2H, H-3''', H-5'''); 7.10 (d, *J* = 8.2 Hz, 2H, H-3'', H-5''); 7.30 (d, *J* = 8.2 Hz, 2H, H-2'', H-6''); 7.34 (d, *J* = 8.2 Hz, 2H, H-2''', H-6'''); 7.41-7.43 (m, 1H, H-4'); 7.48 (t, *J* = 7.2 Hz, H-3', H-5'); 7.71 (d, *J* = 7.2 Hz, 2H, H-2', H-6').

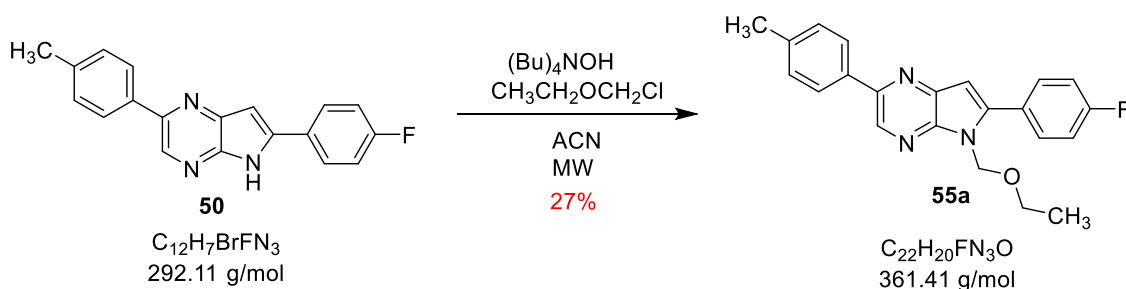
#### 4.3.14. Preparation of 7-bromo-6-phenyl-2,3-di-*p*-tolyl-5H-pyrrolo[2,3-*b*]pyrazine (**54**)



##### · Procedure

Starting from **105** (0.1 mmol), the general procedure **C** described previously was followed in this case (Suzuki-Miyaura coupling). The expected compound was not obtained and starting material was recuperated under these conditions.

#### 4.3.15. Preparation of 5-(ethoxymethyl)-6-(4-fluorophenyl)-2-(*p*-tolyl)-5H-pyrrolo[2,3-*b*]pyrazine (**55a**)



##### · General procedure

In a microwave tub, the pyrrolo-pyrazine **50** (0.1 g, 0.33 mmol) was diluted in acetonitrile (3 mL) and chloromethyl ethyl ether (0.033 mL, 0.40 mmol) was added. Finally, a catalytic amount of tetrabutylammonium hydroxide (0.06 mmol) was also added.

##### · Work up

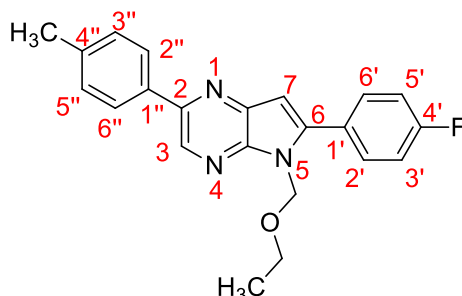
The reaction was heated under MW radiation and stirred for 60 minutes, when no more starting material was observed in TLC (hexane/ ethyl acetate 8:2). The color of reaction changed from orange to greenish. Due to the acid pH of the mixture, 5 mL of NaOH 2N were added in order to neutralize it. Then, an extraction with ethyl acetate (20 mL x 3) and water (10 mL x 1) was done. The organic phases were collected, dried over Na<sub>2</sub>SO<sub>4</sub>, filtered and concentrated under reduced pressure.

##### · Purification

The residue obtained was purified by flash automatic silica gel column chromatography. The desired product eluted with a mixture of hexane/ethyl acetate 80:20.

· Analytical data

Product aspect	Mass obtained	Yield	R <sub>f</sub> (hexane/ethyl acetate 8:2)
Yellowish semisolid	0.03 g	27%	0.10

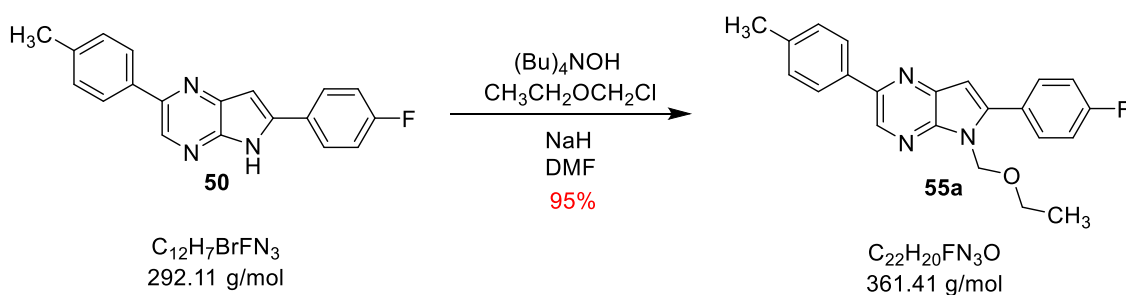


<sup>1</sup>H NMR (CDCl<sub>3</sub>, 400 MHz) δ(ppm), 1.15 (t, *J* = 7 Hz, 3H, CH<sub>3</sub>-CH<sub>2</sub>-O); 2.35 (s, 3H, CH<sub>3</sub>-Ar); 3.65 (q, *J* = 7 Hz, 2H, CH<sub>2</sub>-O); 5.57 (s, 2H, N-CH<sub>2</sub>-O); 6.77 (s, 1H, H-7); 7.13 (t, *J* = 8.6 Hz, 2H, H-3', H-5'); 7.24 (d, *J* = 8 Hz, 2H, H-3'', H-5''); 7.73 (dd, *J*<sub>1</sub> = 5.3 Hz, *J*<sub>2</sub> = 8.6 Hz, 2H, H-2', H-6'); 7.86 (d, *J* = 8 Hz, 2H, H-2'', H-6''); 8.62 (s, 1H, H-3).

<sup>13</sup>C NMR (CDCl<sub>3</sub>, 100.6 MHz) δ(ppm), 15.1 (CH<sub>3</sub>, CH<sub>3</sub>-CH<sub>2</sub>); 21.2 (CH<sub>3</sub>, CH<sub>3</sub>-Ar); 64.9 (CH<sub>2</sub>, CH<sub>2</sub>-O); 71.1 (CH<sub>2</sub>, N-CH<sub>2</sub>-O); 101.9 (CH, C-7); 115.9 (CH, *J* = 21.5 Hz, C-3', C-5'); 126.9 (CH, C-2', C-6'); 127.3 (Cq, C-7a); 129.6 (CH, C-3'', C-5''); 131.3 (CH, *J* = 8.2 Hz, C-2', C-6'); 135.1 (CH, C-3); 135.2 (Cq, C-1'); 138.7 (Cq, C-1''); 138.9 (Cq, C-4''); 142.2 (Cq, C-6); 145.9 (Cq, C-4a); 148.3 (Cq, C-2); 163.0 (Cq, *J* = 248.6 Hz, C-4').

HRMS, ESI(+) *m/z*: Mass calculated for C<sub>22</sub>H<sub>20</sub>FN<sub>3</sub>O: 362.1600 g/mol [M+H]<sup>+</sup>. Mass found: 362.1598 g/mol.

4.3.16. Preparation of 5-(ethoxymethyl)-6-(4-fluorophenyl)-2-(p-tolyl)-5H-pyrrolo[2,3-*b*]pyrazine (**55a**)



· Procedure (general procedure for 5H-pyrrolo[2,3-*b*]pyrazine protection)

In a 50 mL round bottom flask, NaH (60% vaseline) (0.015 g, 0.59 mmol) was washed with hexane in order to remove vaseline. The compound **50** (0.150 g, 0.50 mmol) was suspended in DMF and chloromethyl ethyl ether (0.07 mL, 0.67 mmol) was added. Finally, a catalytic amount of tetrabutylammonium hydroxide (0.01 mL, 0.1 mmol) was added as well.

· Work up

The reaction was stirred at room temperature until no more starting material was observed in TLC (hexane/ethyl acetate 8:2). The mixture of reaction was diluted with ethyl acetate (15 mL) and washed with water (3 x 20 mL). The organic phase was dried over sodium sulfate, filtered and concentrated under reduced pressure. When ethyl acetate was removed, a few amount of toluene was added to co-evaporate and facilitate the removal of DMF residues.

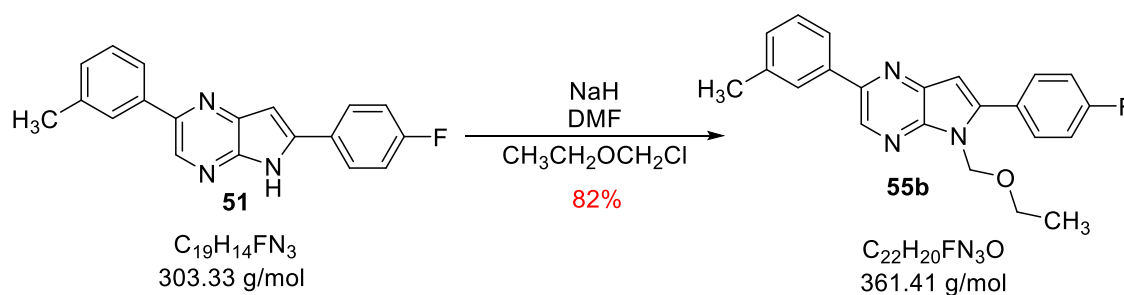
· Purification

The desired product was obtained with enough purity.

· Analytical data

Product aspect	Mass obtained	Yield	R <sub>f</sub> (hexane/ethyl acetate 8:2)
Yellowish semisolid	0.170 g	95%	0.10

#### 4.3.17. Preparation of 5-(ethoxymethyl)-6-(4-fluorophenyl)-2-(*m*-tolyl)-5H-pyrrolo[2,3-*b*]pyrazine (**55b**)



· Procedure

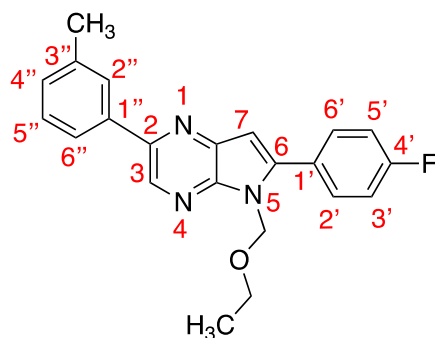
Starting from **51** (0.36 mmol), the general procedure described previously for 5H-pyrrolo[2,3-*b*]pyrazine protection was followed.

· Purification

The desired product was obtained with enough purity.

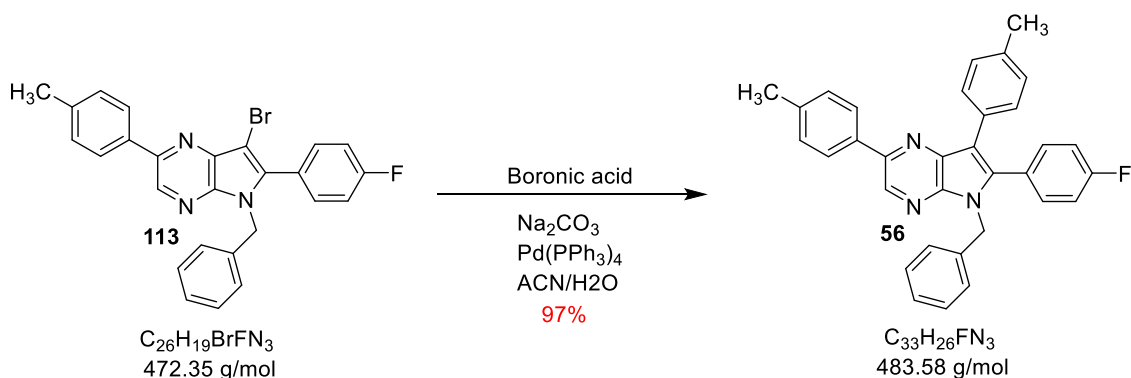
· Analytical data

Product aspect	Mass obtained	Yield	R <sub>f</sub> (hexane/ethyl acetate 8:2)
Greenish semisolid	0.107 g	82%	0.59



$^1\text{H NMR}$  ( $\text{CDCl}_3$ , 400 MHz)  $\delta$ (ppm), 1.15 (t,  $J = 7$  Hz, 3H,  $\text{CH}_2\text{-CH}_3$ ); 2.40 (s, 3H,  $\text{CH}_3\text{-Ar}$ ); 3.66 (q,  $J = 7$  Hz, 2H,  $\text{CH}_2\text{-O-}$ ); 5.58 (s, 2H,  $\text{N-CH}_2\text{-O-}$ ); 6.77 (s, 1H, H-7); 7.15 (t,  $J = 7$  Hz, 1H, H-4''); 7.16 (d,  $J = 9$  Hz, 2H, H-3', H-5'); 7.49 (m, 1H, H-5''); 7.74 (d,  $J = 9$  Hz, 2H, H-2', H-6'); 7.77 (d,  $J = 7$  Hz, 1H, H-6''); 7.81 (m, 1H, H-2''); 8.63 (s, 1H, H-3).

#### 4.3.18. Preparation of 5-benzyl-6-(4-fluorophenyl)-2,7-di-p-tolyl-5H-pyrrolo[2,3-b]pyrazine (**56**)



##### · Procedure

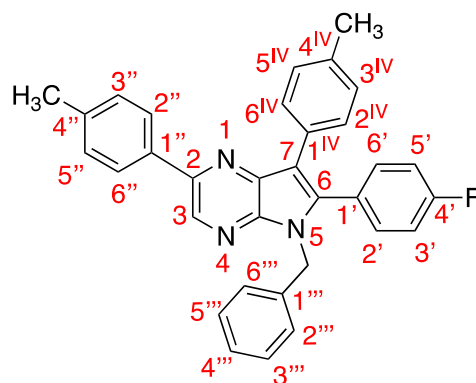
Starting from **113** (0.14 mmol) the general procedure **C** described previously in this same work was followed in this case (Suzuki-Miyaura coupling reaction).

##### · Purification

A purification to remove excess of boronic acid was carried out by flash automatic column chromatography. The desired product eluted with a mixture of hexane/ethyl acetate 70:30.

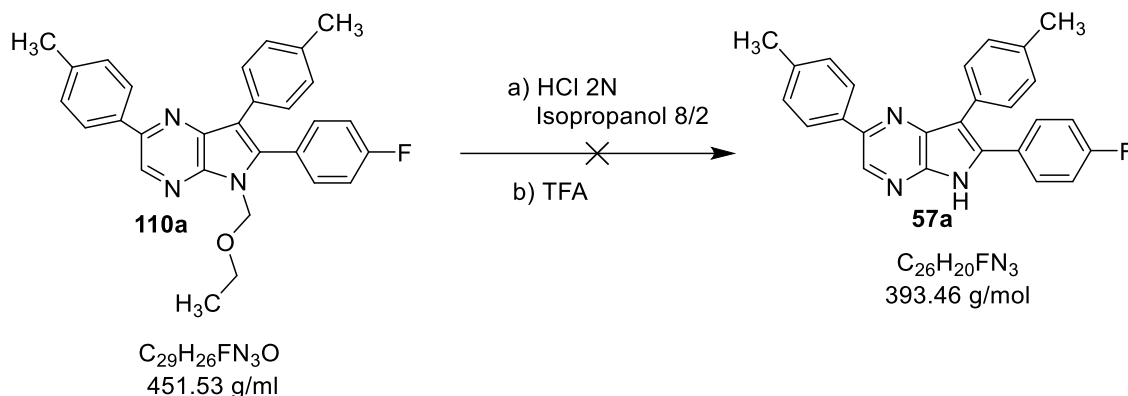
##### · Analytical data

Product aspect	Mass obtained	Yield	$R_f$ (hexane/ethyl acetate 7:3)	Melting point
Yellowish solid	0.068 g	97%	0.80	> 300 °C (DCM)



$^1\text{H NMR}$  ( $\text{CDCl}_3$ , 400 MHz)  $\delta$ (ppm), 2.32 (s, 3H,  $\text{CH}_3\text{-Ar}$  (x2)); 5.85 (s, 2H,  $\text{CH}_2\text{-N}$ ); 7.14 (t,  $J = 8.8$  Hz, 2H, H-2''', H-6'''); 7.32-7.37 (m, 3H, H-3''', H-4''', H-5'''); 7.39 (dd,  $J_1 = 2$  Hz,  $J_2 = 7.8$  Hz, 2H, H-3<sup>IV</sup>, H-5<sup>IV</sup>); 7.46 (dd,  $J_1 = 2$  Hz,  $J_2 = 7.8$  Hz, 2H, H-2<sup>IV</sup>, H-6<sup>IV</sup>); 7.56 (d,  $J = 7$  Hz, 2H, H-3', H-5'); 7.57 (d,  $J = 7$  Hz, 2H, H-2', H-6'); 7.71 (s, 1H, H-3); 7.74 (t,  $J = 8$  Hz, 2H, H-3'', H-5''); 8.41 (dd,  $J_1 = 5.5$  Hz,  $J_2 = 8$  Hz, 2H, H-2'', H-6'').

#### 4.3.19. Preparation of 6-(4-fluorophenyl)-2,7-di-p-tolyl-5H-pyrrolo[2,3-b]pyrazine (**57a**)

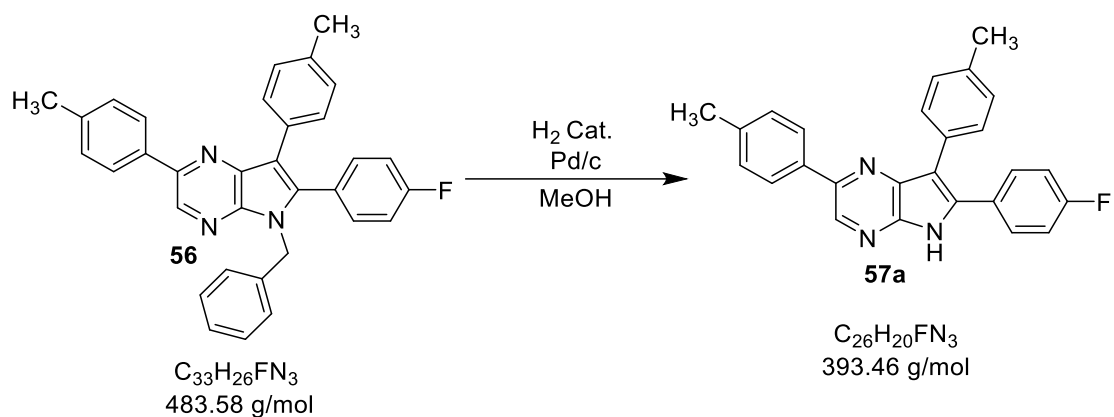


#### · Procedure

In order to remove the protecting group, different conditions were tried. In a round bottom flask the product **110a** was dissolved in methanol or THF and HCl 2N was added. After 24 hours at room temperature, TLC of reaction showed the presence of starting material. Therefore, the reaction was heated at 60 °C. After 48 hours of reaction, no new product was observed in TLC.

Different conditions were tried as TFA at room temperature, heating at 60 °C or using a mixture of HCl 2N and isopropanol (8:2), but same results were obtained in all reactions, starting material.

#### 4.3.20. Preparation of 6-(4-fluorophenyl)-2,7-di-*p*-tolyl-5H-pyrrolo[2,3-*b*]pyrazine (**57a**)



##### · Procedure

In a specific catalytic hydrogenation round bottom flask equipped with a magnetic stirring, the compound **56** (0.068 g, 0.14 mmol) was added with a mixture of methanol and ethyl acetate (2:1). Then Pd-C 10% (0.01 g, 0.094 mmol) and 0.3 mL of HCl 5N were added. The reaction was stirred under H<sub>2</sub> stream for 16 hours.

##### · Work-up

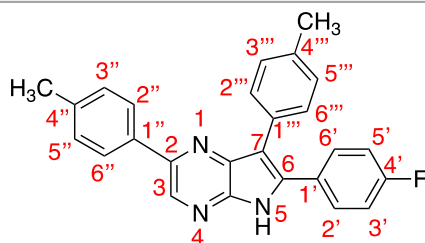
Given that the hydrogenation apparatus was not completely hermetical, the consumed volume was higher than expected. A TLC indicated consumption of starting material (hexane/ethyl acetate 7:3). The crude reaction was filtered by means of a pleated filter and washed with 20 mL of methanol and was then collected in a 100 mL round-bottomed flask. The solvent was removed under reduced pressure. The crude was dissolved in dichloromethane (10 mL) and washed with a solution of NaOH 8N (20 mL x 3). The organic phase was dried over anhydrous Na<sub>2</sub>SO<sub>4</sub>, filtered and concentrated under reduced pressure.

##### · Purification

The desired product was obtained with enough purity.

##### · Analytical data

Product aspect	Mass obtained	Yield	R <sub>f</sub> (hexane/ethyl acetate 7:3)	Melting point
Yellowish solid	0.04 g	Quantitative	0.45	233-235 °C (DCM)

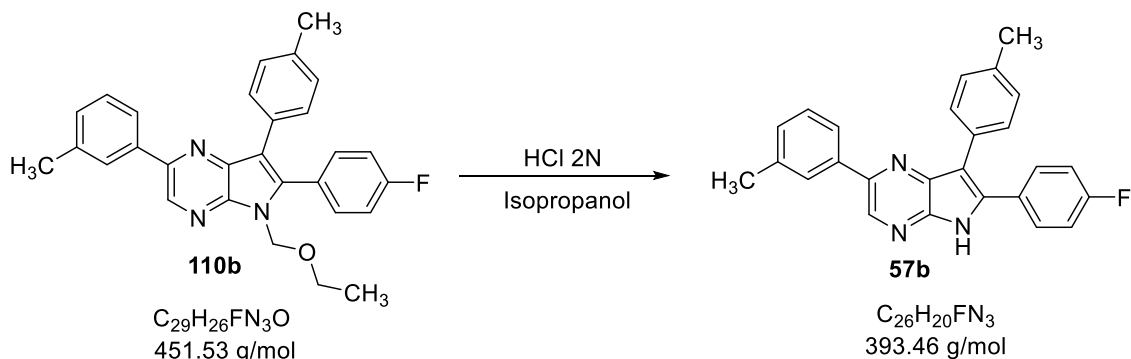


<sup>1</sup>H NMR (CDCl<sub>3</sub>, 400 MHz) δ(ppm), 2.07 (s, 3H, CH<sub>3</sub>-Ar); 2.37 (s, 3H, CH<sub>3</sub>-Ar); 7.12-7.17 (m, 2H, H-3'', H-5''); 7.18 (d, *J* = 7.2 Hz, 2H, H-3''', H-5'''); 7.21 (d, *J* = 8.5 Hz, 2H, H-3', H-5'); 7.27 (d, *J* = 7.2 Hz, 2H, H-2''', H-6'''); 7.54 (dd, *J*<sub>1</sub> = 5.5 Hz, *J*<sub>2</sub> = 8.5 Hz, 1H, H-2'); 7.76-7.80 (m, 1H, H-6'); 7.95 (q, *J* = 7.7 Hz, 3H, H-2'', H-6'', NH); 8.63 (bs, 1H, H-3); (H-2' and H-6' are interchangeable protons).



HRMS, ESI(+)  $m/z$ : Mass calculated for  $C_{26}H_{20}FN_3$ : 394.1675 g/mol  $[M+H]^+$ . Mass found: 394.1688 g/mol.

#### 4.3.21. Preparation of 6-(4-fluorophenyl)-2-(*m*-tolyl)-7-(*p*-tolyl)-5H-pyrrolo[2,3-*b*]pyrazine (**57b**)



##### · Procedure

In a 25 mL round bottom flask the triarylated **110b** (0.025 g, 0.06 mmol) was dissolved in isopropanol (2 mL) and HCl 2N (8 mL). The reaction was stirred at room temperature for two days. The control of reaction by TLC (a sample of reaction was neutralized with NaOH 2N and extracted with ether) showed no consumption of starting material (hexane/ethyl acetate 8:2). Then, 5 mL of methanol were added, and the reaction was stirred for 24 hours more at reflux.

##### · Work up

At this time, no more starting material was observed in TLC. Therefore, 5 mL of NaOH 2N were added in the mixture until basic pH was reached. Then, methanol and isopropanol were evaporated under reduced pressure. The obtained crude mixture was diluted with water (15 mL) and extracted with dichloromethane (3 x 20 mL). The organic layers were dried over anhydrous sodium sulfate, filtered and concentrated under reduced pressure.

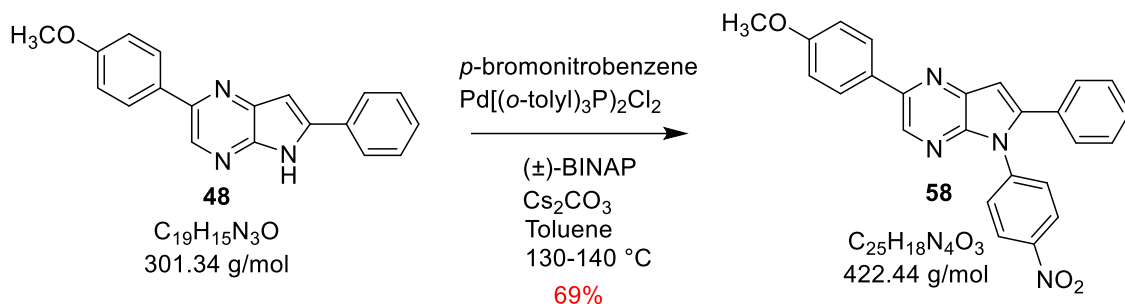
##### · Purification

No purification was necessary since product was obtained with enough purity. The  $^1H$  NMR of the crude showed the 6-(4-fluorophenyl)-2-(*m*-tolyl)-5H-pyrrolo[2,3-*b*]pyrazine, the diarylated **50** instead of the expected compound.

##### · Analytical data

The analytical data (product aspect,  $^1H$  NMR,  $R_f$ , and others) was completely coincident with the previously described for **50**.

4.3.22. Preparation of 2-(4-methoxyphenyl)-5-(4-nitrophenyl)-6-phenyl-5H-pyrrolo[2,3-b]pyrazine (**58**)



· Procedure

In a Pyrex glass tube, previously flame-dried under argon atmosphere, the diarylated pyrazine **48** (0.120 g, 0.4 mmol) was dissolved in toluene (7 mL). Then, *p*-bromonitrobenzene (0.08 g, 0.04 mmol), cesium carbonate (0.155 g, 0.048 mmol), palladium (0.06 mmol) and BINAP (0.06 mmol) were added under argon atmosphere. The reaction mixture was stirred at 140 °C ± 5 °C.

· Work up

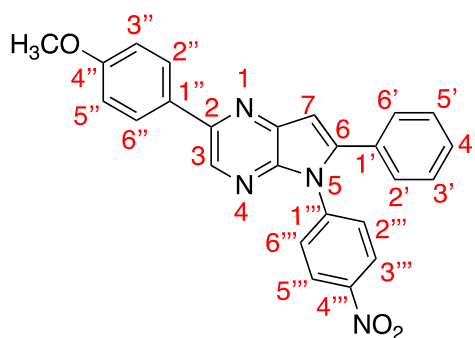
After 24 hours of reaction no more starting material was observed in a TLC of reaction (hexane/ethyl acetate 8:2). Therefore, the mixture was diluted with ethyl acetate and washed with water (3 x 20 mL) and brine (3 x 5 mL). The organic phase was dried over anhydrous sodium sulfate, filtered and concentrated under reduced pressure.

· Purification

No purification was carried out since the product was obtained with enough purity.

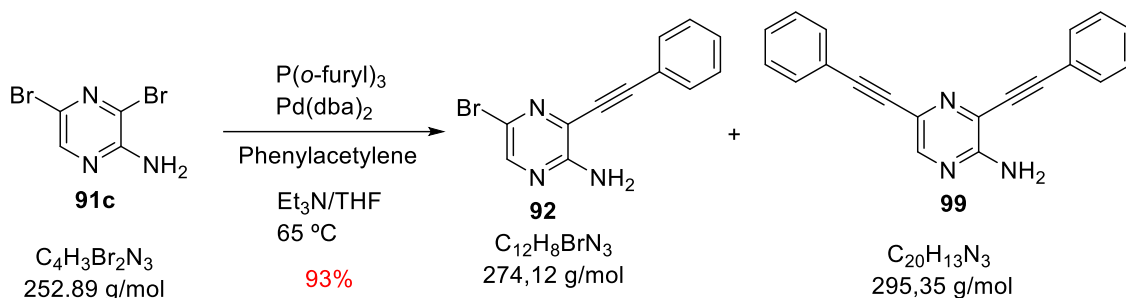
· Analytical data

Product aspect	Mass obtained	Yield	R <sub>f</sub> (hexane/ethyl acetate 8:2)	Melting point
Yellow solid	0.116 g	69%	0.25	230-235 °C (DCM)



$^1\text{H}$  NMR ( $\text{CDCl}_3$ , 400 MHz)  $\delta$ (ppm), 3.83 (s, 3H, O-CH<sub>3</sub>); 6.68 (s, 1H, H-7); 6.97 (d,  $J$  = 9.0 Hz, 2H, H-3'', H-5''); 6.99 (d,  $J$  = 7.0 Hz, 2H, H-2''', H-6'''); 7.19 (t,  $J$  = 7.2 Hz, 2H, H-3', H-5'); 7.36 (t,  $J$  = 7.2 Hz, 1H, H-4'); 7.45 (d,  $J$  = 7.2 Hz, 2H, H-2', H-6'); 7.80 (d,  $J$  = 7.0 Hz, 2H, H-3''', H-5'''); 7.87 (d,  $J$  = 9.0 Hz, 2H, H-2'', H-6''); 8.46 (s, 1H, 3-H).

#### 4.3.23. Preparation of 5-bromo-3-(phenylethynyl)pyrazin-2-amine (**92**)

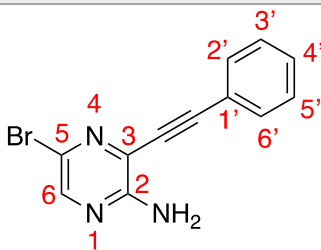


· Procedure

Starting from **91c** (0.52 mmol) the general procedure **A** described above was followed (Sonogoshira coupling reaction). The  $^1\text{H}$  NMR showed a subproduct, the 3,5-*bis*(phenylethynyl)pyrazin-2-amine (**99**).

· Analytical data of **92**

Product aspect	Mass obtained	Yield	$R_f$ (hexane/ethyl acetate 8:2)	Melting point
Yellowish solid	0.140 g	Quantitative	0.40	140-142 °C (DCM)



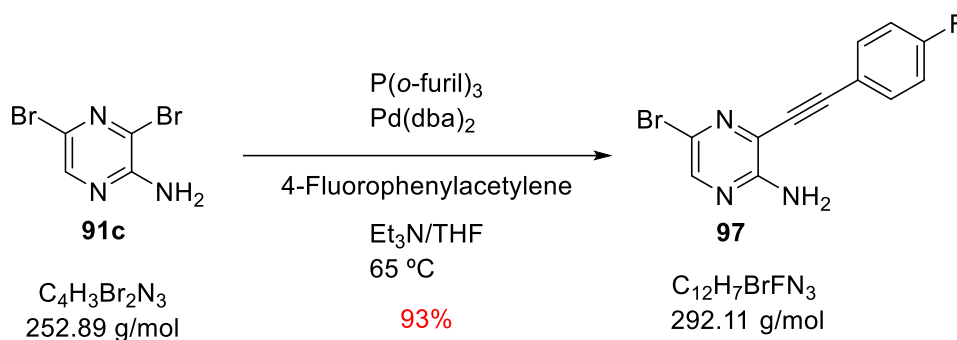
$^1\text{H}$  NMR ( $\text{CDCl}_3$ , 400 MHz)  $\delta$ (ppm), 5.18 (bs, 2H,  $\text{NH}_2$ ); 7.40 (t,  $J = 7.2$  Hz, 2H, H-3', H-5'); 7.41 (t,  $J = 7.2$  Hz, 1H, H-4'); 7.57 (dd,  $J_1 = 1.5$  Hz,  $J_2 = 7.2$  Hz, 2H, H-2', H-6'); 8.04 (s, 1H, H-6).

$^{13}\text{C}$  NMR ( $\text{CDCl}_3$ , 100.6 MHz)  $\delta$ (ppm), 83.2 (Cq, C $\equiv$ Bn); 97.4 (Cq, C $\equiv$ Pyrazine); 121.1 (Cq, C-5); 124.5 (Cq, C-1'); 125.9 (Cq, C-3); 128.6 (CH, C-2', C-6'); 129.8 (CH, C-4'); 132.0 (CH, C-3', C-5'); 143.6 (CH, C-6); 154.2 (Cq, C-2).

· Analytical data of **99**

$^1\text{H}$  NMR ( $\text{CDCl}_3$ , 400 MHz)  $\delta$ (ppm), 5.30 (bs, 2H,  $\text{NH}_2$ ); 7.40 (m, 6H, H-3', H-4', H-5', H-3'', H-4'', H-5''); 7.60 (m, 4H, H-2', H-6', H-2'', H-6''); 8.20 (s, 1H, H-6).

#### 4.3.24. Preparation of 5-bromo-3-((4-fluorophenyl)ethynyl)pyrazin-2-amine (**97**)



· Procedure

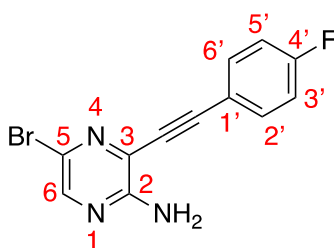
Starting from **91c** (1 mmol), the general procedure **A** described above was followed (Sonogoshira coupling reaction).

· Purification

No purification of the obtained residue by column chromatography was performed since desired product was obtained with enough purity.

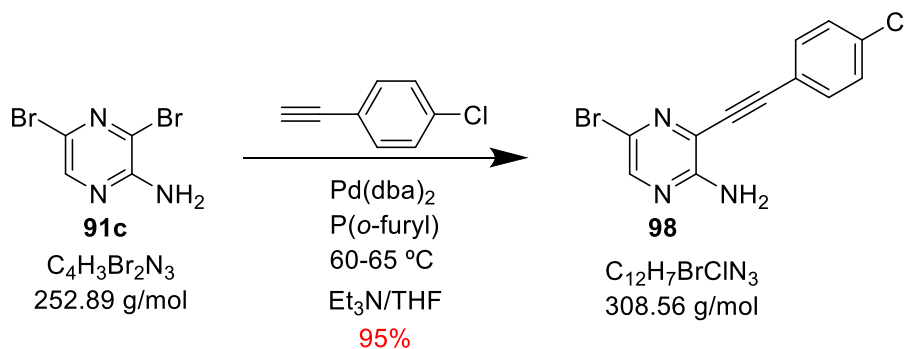
· Analytical data

Product aspect	Mass obtained	Yield	$R_f$ (hexane/ethyl acetate 8:2)	Melting point
Yellowish solid	0.268 g	93%	0.14	160-162 $^\circ\text{C}$ (Hexane/AcOEt)



$^1\text{H NMR}$  ( $\text{CDCl}_3$ , 400 MHz)  $\delta$ (ppm), 5.20 (bs, 2H,  $\text{NH}_2$ ); 7.09 (t,  $J = 8.5$  Hz, 2H, H-3', H-5'); 7.57 (dd,  $J_1 = 5$  Hz,  $J_2 = 8.5$  Hz, 2H, H-2', H-6'); 8.06 (s, 1H, H-6).

#### 4.3.25. Preparation of 5-bromo-3-((4-chlorophenyl)ethynyl)pyrazin-2-amine (**98**)



· Procedure

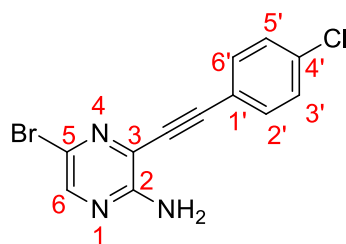
Starting from **91c** (1.3 mmol), the general procedure **A** described above was followed (Sonogoshira coupling reaction).

· Purification

No purification was performed since the product was obtained with enough purity.

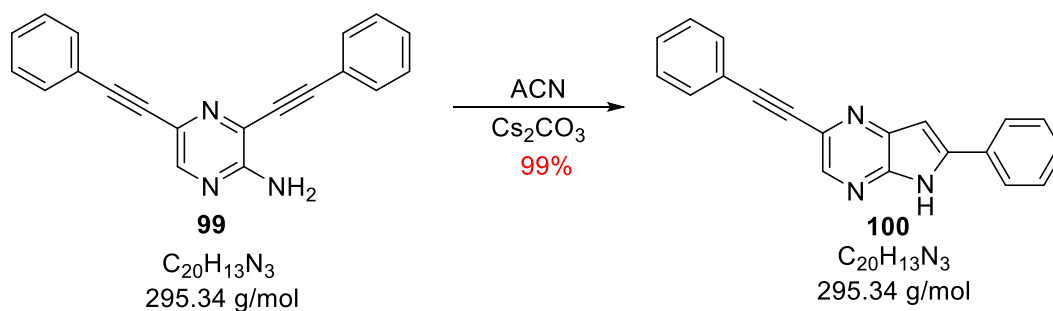
· Analytical data

Product aspect	Mass obtained	Yield	R <sub>f</sub> (hexane/ethyl acetate 8:2)	Melting point
Yellow solid	0.400 g	95%	0.50	168-170 °C (DCM)



<sup>1</sup>H NMR (CDCl<sub>3</sub>, 400 MHz) δ(ppm), 5.12 (bs, 2H, NH<sub>2</sub>); 7.36 (d, *J* = 8.5 Hz, 2H, H-3', H-5'); 7.50 (d, *J* = 8.5 Hz, 2H, H-2', H-6'); 8.06 (s, 1H, H-6).

#### 4.3.26. Preparation of 6-phenyl-2-(phenylethynyl)-5H-pyrrolo[2,3-b]pyrazine (**100**)

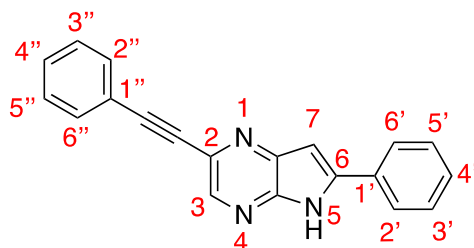


· Procedure

Starting from **99** (0.27 mmol), the general procedure **B** described above was followed in this case (cyclization).

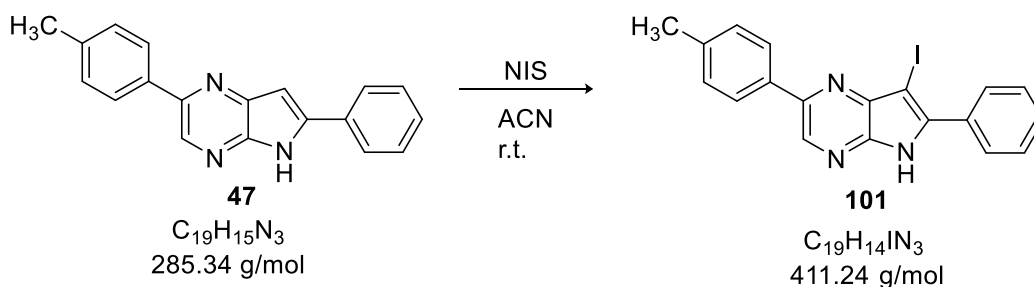
· Analytical data

Product aspect	Mass obtained	Yield	R <sub>f</sub> (hexane/ethyl acetate 8:2)
Yellow solid	0.08 g	99%	0.30



$^1\text{H NMR}$  ( $\text{CDCl}_3$ , 400 MHz)  $\delta$ (ppm), 6.98 (s, 1H, H-7); 7.38-7.39 (m, 2H, H-3'', H-5''); 7.45-7.47 (m, 1H, H-4''); 7.53 (t,  $J = 7.5$  Hz, 3H, H-3', H-4', H-5'); 7.63-7.65 (m, 2H, H-2'', H-6''); 7.88 (d,  $J = 7.5$  Hz, 2H, H-2', H-6'); 8.43 (s, 1H, H-3'); 10.92 (s, 1H, NH).

#### 4.3.27. Preparation of 7-iodo-6-phenyl-2-(p-tolyl)-5H-pyrrolo[2,3-b]pyrazine (**101**)

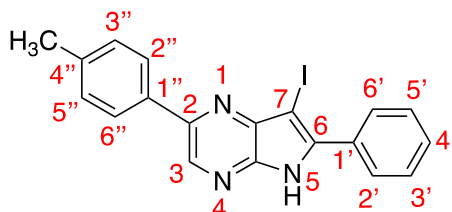


· Procedure

Starting from **47** (0.17 mmol), the general procedure **D** described previously in this same work (halogenation of C-7), using *N*-iodosuccinimide (NIS) instead of *N*-bromosuccinimide (NBS).

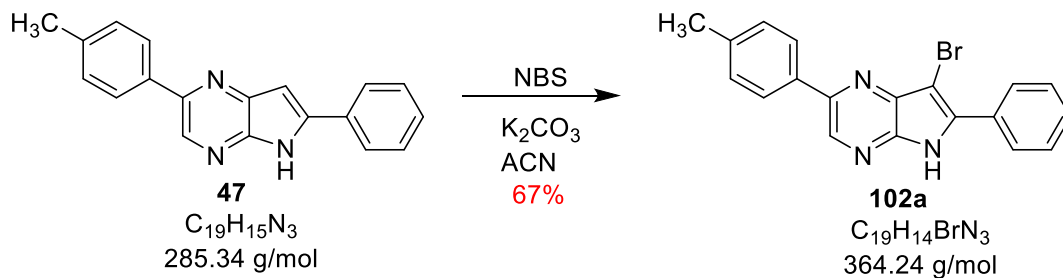
· Analytical data

Product aspect	Mass obtained	Yield	$R_f$ (hexane/ethyl acetate 8:2)
Brown semisolid	0.07 g	Quantitative	0.47



$^1\text{H NMR}$  ( $\text{CDCl}_3$ , 400 MHz)  $\delta$ (ppm), 2.70 (s, 3H,  $\text{CH}_3$ ); 7.26 (d,  $J = 8$  Hz, 2H, H-3'', H-5''); 7.50 (t,  $J = 7.2$  Hz, 3H, H-3', H-4', H-5'); 7.88 (d,  $J = 7.2$  Hz, 2H, H-2', H-6'); 7.95 (d,  $J = 7.2$  Hz, 2H, H-2'', H-6''); 8.17 (bs, 1H, H-3); 8.55 (bs, 1H, NH).

4.3.28. Preparation of 7-bromo-6-phenyl-2-(*p*-tolyl)-5H-pyrrolo[2,3-*b*]pyrazine (**102a**)



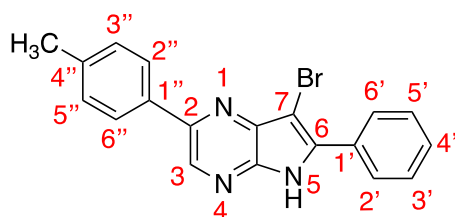
· Procedure

Starting from **47** (0.25 mmol), the general procedure **D** described previously in this work (halogenation of C-7). In one assay the 3,7-dibromo derivative **103** was obtained.

· Analytical data

a) For compound **102a**

Product aspect	Mass obtained	Yield	R <sub>f</sub> (hexane/ethyl acetate 8:2)
Yellow solid	0.060 g	67%	0.8

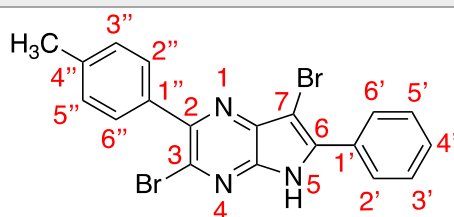


<sup>1</sup>H NMR (CDCl<sub>3</sub>, 400 MHz) δ(ppm), 2.37 (s, 3H, CH<sub>3</sub>); 7.27 (d, *J* = 8 Hz, 2H, H-3'', H-5''); 7.51 (t, *J* = 7.6 Hz, 2H, H-3', H-5'); 7.54 (t, *J* = 7.6 Hz, 1H, H-4'); 7.95 (d, *J* = 8 Hz, 2H, H-2'', H-6''); 8.35 (bs, 1H, NH); 8.55 (dd, *J*<sub>1</sub> = 1.3 Hz, *J*<sub>2</sub> = 7.6 Hz, 2H, H-2', H-6'); 8.83 (s, 1H, H-3).

<sup>13</sup>C NMR (CDCl<sub>3</sub>, 100.6 MHz) δ(ppm), 21.4 (CH<sub>3</sub>); 103.5 (CH, C-7); 127.0 (CH, C-2'', C-6''); 128.6 (CH, C-2', C-6'); 128.7 (Cq, C-7a); 129.9 (CH, C-3', C-5'); 130.4 (CH, C-3'', C-5''); 132.8 (Cq, C-6); 133.5 (CH, C-4'); 140.4 (Cq, C-4''); 140.5 (Cq, C-1'); 142.2 (CH, C-3); 151.2 (Cq, C-1''); 152.0 (Cq, C-2); 152.8 (Cq, C-4a).

b) For compound **103**

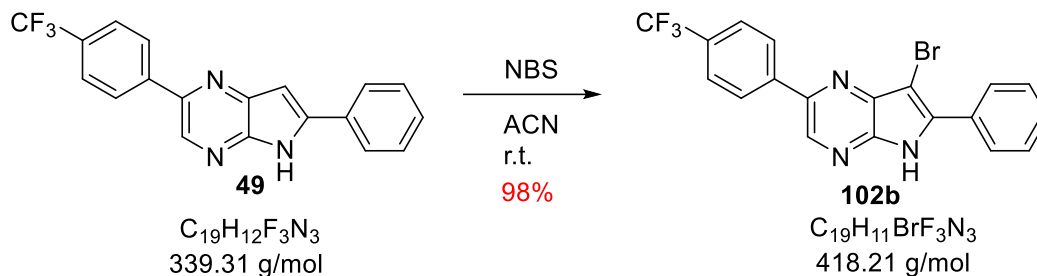
Product aspect	Mass obtained	Yield	R <sub>f</sub> (hexane/ethyl acetate 8:2)	Melting point
Yellow solid	0.01 g	9%	0.62	> 300 °C (DCM)



<sup>1</sup>H NMR (CDCl<sub>3</sub>, 400 MHz) δ(ppm), 2.44 (s, H, CH<sub>3</sub>); 7.29 (d, *J* = 8 Hz, H-3'', H-5''); 7.51-7.52 (m, 1H, H-4'); 7.54 (t, *J* = 8 Hz, 2H, H-3', H-5'); 7.64 (d, *J* = 8 Hz, 2H, H-2', H-6'); 7.88 (dd, *J*<sub>1</sub> = 1.6 Hz, *J*<sub>2</sub> = 8 Hz, 2H, H-2'', H-6''); 9.01 (bs, 1H, NH).

HRMS, ESI(+) m/z: Calculated for C<sub>19</sub>H<sub>13</sub>Br<sub>2</sub>N<sub>3</sub> [M+H]<sup>+</sup>: 443.9489, found 443.9490.

#### 4.3.29. Preparation of 7-bromo-6-phenyl-2-(4-(trifluoromethyl)phenyl)-5H-pyrrolo[2,3-b]pyrazine (**102b**)



##### · Procedure

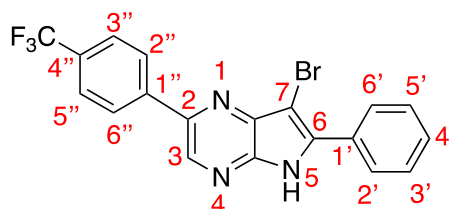
Starting from **49** (0.29 mmol), the general procedure **D** described above was followed in this case (halogenation of C-7).

##### · Purification

A manual column chromatography was made. The desired product eluted with a mixture of hexane/ethyl acetate 80:20.

##### · Analytical data

Product aspect	Mass obtained	Yield	R <sub>f</sub> (hexane/ethyl acetate 8:2)	Melting point
Yellowish solid	0.080 g	65%	0.47	288-290 °C (DCM)

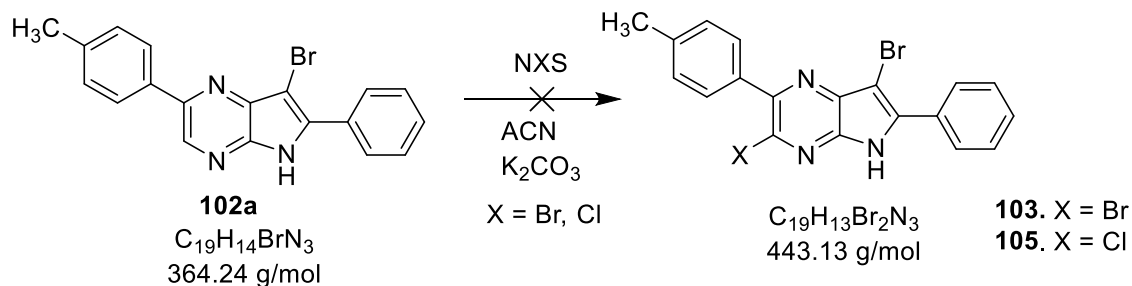


<sup>1</sup>H NMR (CDCl<sub>3</sub>, 400 MHz) δ(ppm), 7.52 (t, *J* = 7.3 Hz, 2H, H-3', H-5'); 7.56-7.58 (m, 1H, H-4'); 7.72 (d, *J* = 8.2 Hz, 2H, H-3'', H-5''); 8.17 (d, *J* = 8.2 Hz, 2H, H-2'', H-6''); 8.54 (d, *J* = 7.3 Hz, 2H, H-2', H-6'); 8.88 (s, 1H, H-3).

<sup>13</sup>C NMR (CDCl<sub>3</sub>, 100.6 MHz) δ(ppm), 102.1 (Cq, C-7); 123.2 (Cq, *J* = 270.7 Hz, CF<sub>3</sub>); 126.0 (CH, *J* = 7.5 Hz, C-3'', C-5''); 127.4 (CH, C-2', C-6'); 128.0 (Cq, C-6); 128.3 (Cq, C-7a); 128.7 (CH, *J* = 3 Hz, C-2'', C-6''); 130.6 (CH, C-3', C-5'); 131.8 (Cq, *J* = 32.5 Hz, C-4''); 133.9 (CH, C-4'); 134.1 (Cq, C-1'); 138.9 (Cq, *J* = 1.2 Hz, C-1''); 142.8 (CH, C-3); 148.1 (Cq, C-4a); 153.9 (Cq, C-2).



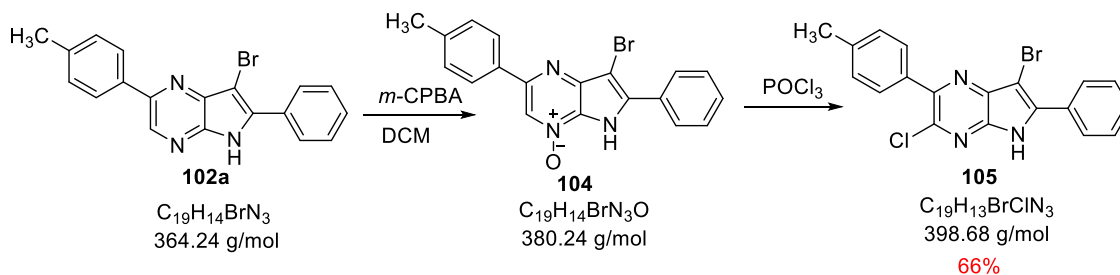
4.3.30. Preparation of 3,7-dibromo-6-phenyl-2-(p-tolyl)-5H-pyrrolo[2,3-b]pyrazine and the 7-bromo-3-chloro-6-phenyl-2-(p-tolyl)-5H-pyrrolo[2,3-b]pyrazine (**103** and **105**)



· Procedure

Starting from **102a** (0.03 mmol), the general procedure **D**, halogenating with NBS or NCS in C-3 instead of C-7, described previously in the same work was followed. The halogenation afforded starting material under these conditions.

4.3.31. Preparation of 7-bromo-3-chloro-6-phenyl-2-(p-tolyl)-5H-pyrrolo[2,3-b]pyrazine (**105**)



· Procedure

In a 50 mL round bottom-flask, the bromo derivative **102a** (0.07 g, 0.19 mmol) and *m*-CPBA (0.036 g, 0.2 mmol) were dissolved in dichloromethane (10 mL). The reaction was stirred at room temperature for 48 hours.

The end of this reaction was confirmed by TLC (hexane/ethyl acetate 7:3 (*R<sub>f</sub>* = 0.38)), showing consumption of starting material. Then, the mixture was cooled to 0-5 °C and POCl<sub>3</sub> (0.04 mL, 0.4 mmol) was added carefully. The reaction stirred until no more starting material was observed.

· Work-up

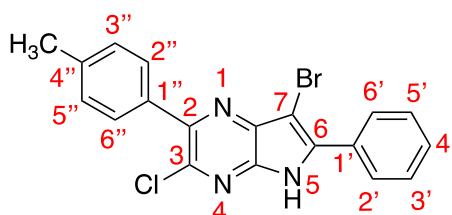
Then, 10 mL of water were added in the reaction. After 5 minutes, the mixture was diluted with dichloromethane (20 mL x 1) and washed with water (20 mL x 3). The obtained organic phase was dried over anhydrous sodium sulfate, filtered and concentrated under reduced pressure to afford a crude mixture.

· Purification

Finally, the crude mixture obtained was purified by flash automatic column chromatography. The desired product eluted with a mixture of hexane/ethyl acetate 78:22.

· Analytical data

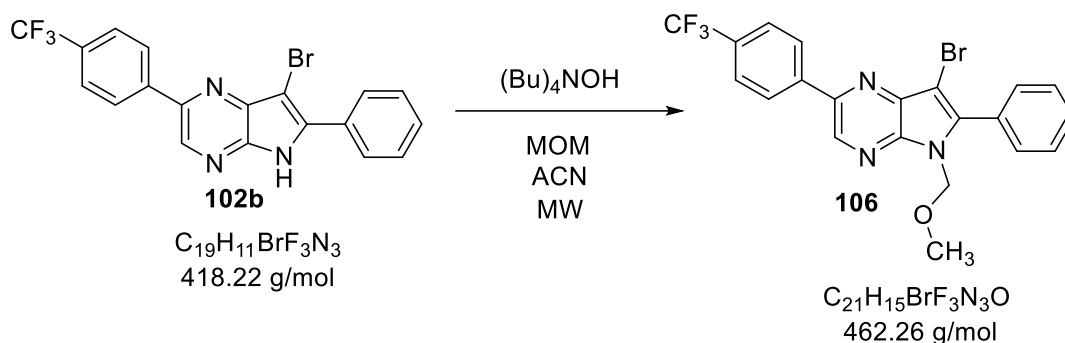
Product aspect	Mass obtained	Yield	R <sub>f</sub> (hexane/ethyl acetate 7:3)
Yellowish solid	0.04 g	66%	0.66



<sup>1</sup>H NMR (CDCl<sub>3</sub>, 400 MHz) δ(ppm), 2.42 (s, 3H, CH<sub>3</sub>); 7.30 (d, *J* = 7.8 Hz, 2H, H-3', H-5'); 7.44-7.47 (m, 1H, H-4'); 7.53 (t, *J* = 7.8 Hz, 2H, H-2', H-6'); 7.95 (d, *J* = 8 Hz, 2H, H-2'', H-6''); 7.97 (d, *J* = 8 Hz, 2H, H-3'', H-5''); 8.61 (bs, 1H, NH).

<sup>13</sup>C NMR (CDCl<sub>3</sub>, 100.6 MHz) δ(ppm), 21.2 (CH<sub>3</sub>); 96.7 (CH, C-7); 118.4 (Cq, C-7a); 126.9 (CH, C-2'', C-6''); 128.1 (CH, C-2', C-6'); 128.7 (CH, C-4'); 129.5 (CH, C-3', C-5'); 129.6 (CH, C-3'', C-5''); 130.6 (Cq, C-6); 130.9 (Cq, C-1''); 132.6 (Cq, C-4''); 134.4 (Cq, C-1'); 144.5 (Cq, C-3); 147.4 (Cq, C-4a); 152.9 (Cq, C-2).

4.3.32. Preparation of 7-bromo-5-(methoxymethyl)-6-phenyl-2-(4-(trifluoromethyl)phenyl)-5H-pyrazolo[2,3-b]pyrazine (**106**)



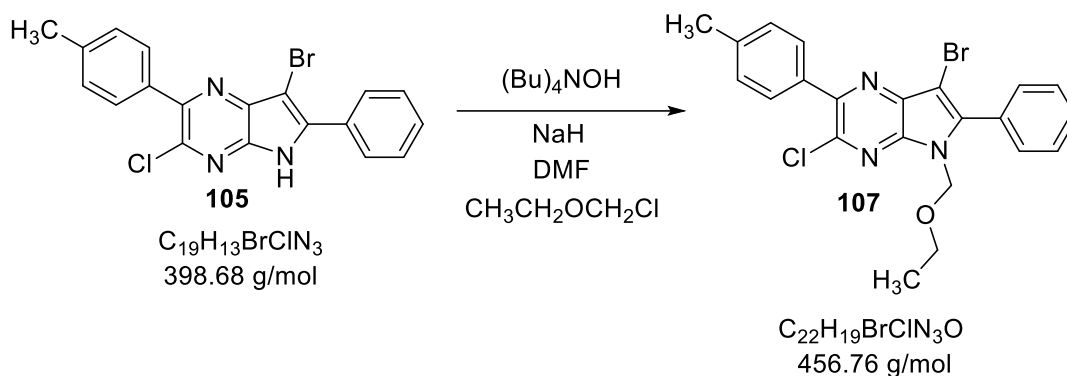
· Procedure

In a microwave glass tube (10 mL) sealed with a silicon septum under magnetic stirring, the bromo derivative **102b** (0.09 g, 0.22 mmol) diluted in acetonitrile (3 mL) and methoxymethyl acetal (MOM) (0.033 mL, 0.44 mmol) were added. Finally, a catalytic quantity of tetrabutylammonium hydroxide (0.06 mmol) was added in the mixture. The tube was introduced in oven microwave and heated to 100 °C (external temperature) and subjected to a variable MW power until 300 W (an IR sensor measured the temperature of glass tube surface).

· Work up

A TLC of the reaction showed consumption of starting material (hexane/ethyl acetate 6:4). The mixture was extracted with ethyl acetate (20 mL x 3) and water (20 mL x 1). The organic phases were collected, dried over sodium sulfate, filtered and concentrated under reduced pressure to afford the crude mixture. The <sup>1</sup>H NMR of the obtained residue showed the diarylated **49**.

4.3.33. Preparation of 7-bromo-3-chloro-5-(ethoxymethyl)-6-phenyl-2-(p-tolyl)-5H-pyrrolo[2,3-b]pyrazine (**107**)



· Procedure

In a 50 mL round bottom flask the NaH (60% in vaseline) (0.015 g, 0.59 mmol) was washed with hexane to remove vaseline. The dihalogenated product **105** (0.150 g, 0.50 mmol) was dissolved in DMF and chloromethyl ethyl ether (0.07 mL, 0.67 mmol) was added. Then, a catalytic quantity of tetrabutylammonium hydroxide (0.01 mL, 0.1 mmol) was added. The reaction was stirred for 24 hours.

· Work up

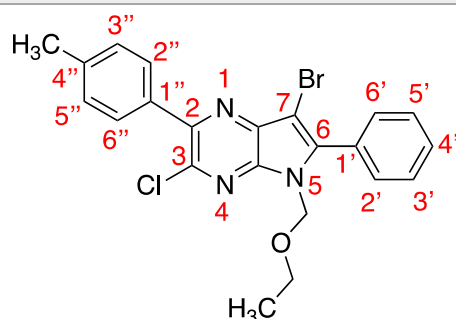
A TLC analysis showed consumption of starting material (hexane/ethyl acetate 8:2). The mixture of reaction was diluted with ethyl acetate (10 mL) and washed with water (20 mL x 3). The organic layer was dried over anhydrous sodium sulfate, filtered and concentrated under reduced pressure. When ethyl acetate was removed, a few quantity of toluene was added to co-evaporate and facilitate the removal of DMF residues.

· Purification

The desired product was obtained with enough purity to characterize and continue the following steps.

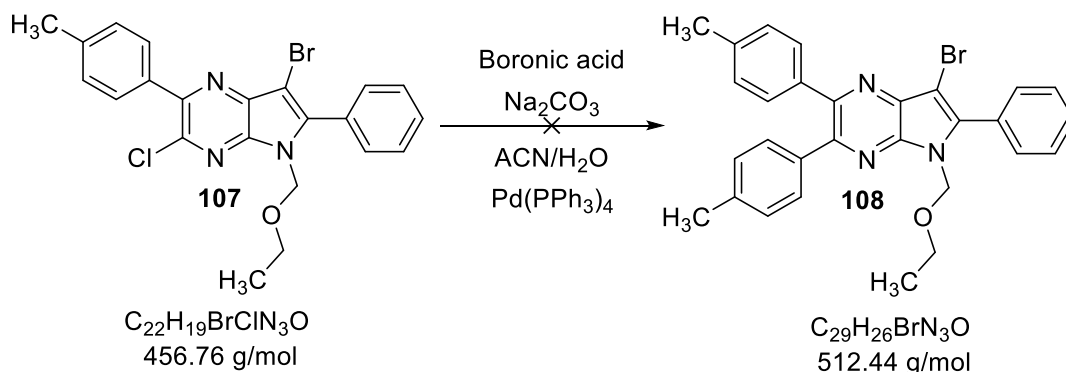
· Analytical data

Product aspect	Mass obtained	Yield	$R_f$ (hexane/ethyl acetate 8:2)
Yellowish semisolid	0.04 g	Quantitative	0.80



$^1\text{H NMR}$  ( $\text{CDCl}_3$ , 400 MHz)  $\delta$ (ppm), 1.11 (t,  $J = 7.3$  Hz,  $\text{CH}_3\text{-CH}_2\text{-O}$ ); 2.36 (s, 3H,  $\text{CH}_3\text{-Ar}$ ); 3.52 (q,  $J = 7.3$  Hz, 2H,  $\text{CH}_2\text{-O}$ ); 5.52 (s, 2H,  $\text{N-CH}_2\text{-O}$ ); 7.08-7.10 (m, 2H, H-3'', H-5''); 7.16-7.20 (m, 3H, H-3', H-5', H-4'); 7.48 (d,  $J = 7.3$  Hz, 2H, H-2', H-6'); 7.94 (d,  $J = 8.0$  Hz, 2H, H-2'', H-6'').

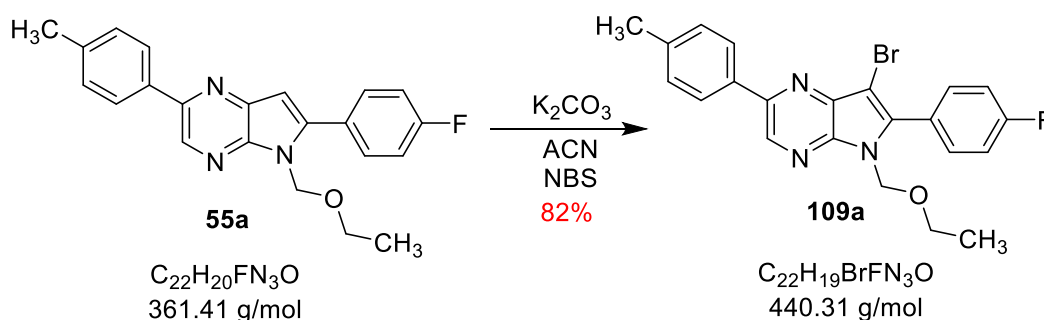
4.3.34. Preparation of 7-bromo-5-(ethoxymethyl)-6-phenyl-2,3-di-(p-tolyl)-5H-pyrrolo[2,3-b]pyrazine (**108**)



· Procedure

Starting from **107** (0.05 mmol), the general procedure **C** described previously in this same work was followed in this case (Suzuki-Miyaura coupling reaction). The expected compound was not obtained and starting material was recuperated under these conditions.

4.3.35. Preparation of 7-bromo-5-(ethoxymethyl)-6-(4-fluorophenyl)-2-(p-tolyl)-5H-pyrrolo[2,3-b]pyrazine (**109a**)



· Procedure

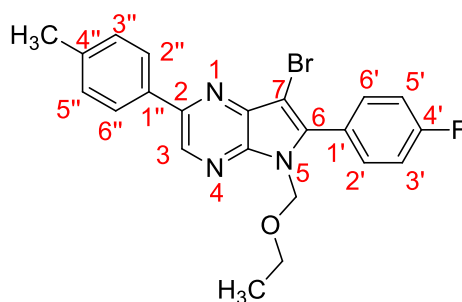
Starting from **55a** (0.49 mmol) the general procedure **D** described above was followed in this case (halogenation of C-7).

· Purification

The desired product was obtained with enough purity.

· Analytical data

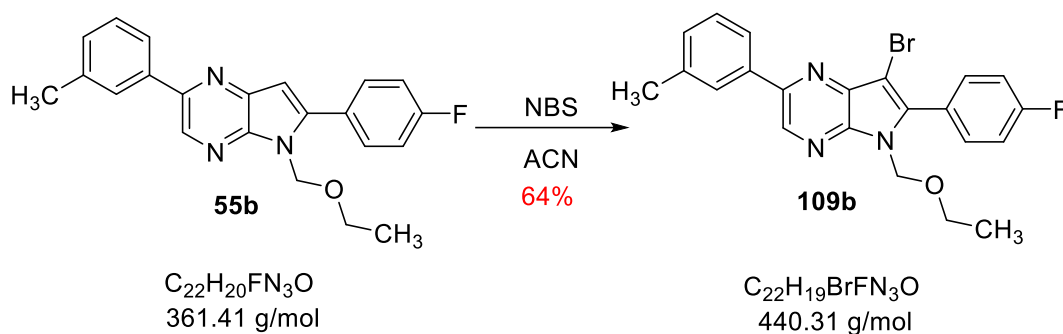
Product aspect	Mass obtained	Yield	R <sub>f</sub> (hexane/ethyl acetate 8:2)
Yellow semisolid	0.178 g	82%	0.70



$^1\text{H NMR}$  ( $\text{CDCl}_3$ , 400 MHz)  $\delta$ (ppm), 1.12 (t,  $J = 7$  Hz, 3H,  $\text{CH}_3\text{-CH}_2\text{-O}$ ); 2.36 (s, 3H,  $\text{CH}_3\text{-Ar}$ ); 3.55 (q,  $J = 7$  Hz, 2H,  $\text{CH}_2\text{-O}$ ); 5.50 (s, 2H,  $\text{N-CH}_2\text{-O}$ ); 7.19 (t,  $J = 8.6$  Hz, 2H, H-3', H-5'); 7.25 (d,  $J = 8$  Hz, 2H, H-3'' H-5''); 7.68 (dd,  $J_1 = 5.3$  Hz,  $J_2 = 8.6$  Hz, 2H, H-2', H-6'); 7.94 (d,  $J = 8$  Hz, 2H, H-2'', H-6''); 8.69 (s, 1H, H-3).

HRMS,ESI(+)  $m/z$ : Mass calculated for  $\text{C}_{22}\text{H}_{19}\text{BrFN}_3\text{O}$ : 440.0729 g/mol  $[\text{M}+\text{H}]^+$ . Mass found: 440.0800 g/mol.

#### 4.3.36. Preparation of 7-bromo-5-(ethoxymethyl)-6-(4-fluorophenyl)-2-(*m*-tolyl)-5H-pyrrolo[2,3-*b*]pyrazine (**109b**)



· Procedure

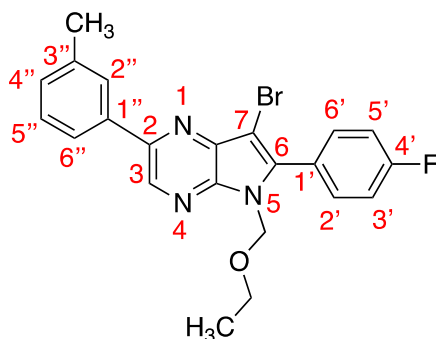
Starting from **55b** (0.29 mmol) the general procedure **D** described above was followed in this case (halogenation of C-7).

· Purification

The desired product was obtained with enough purity.

· Analytical data

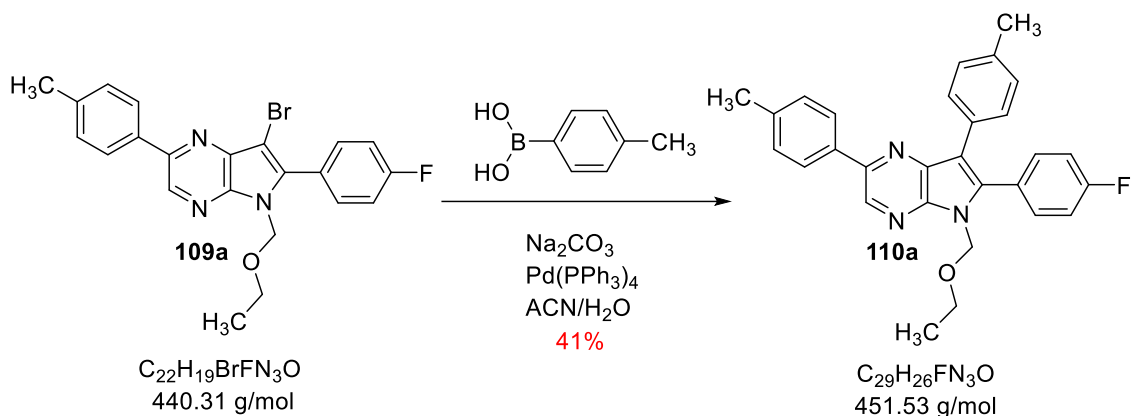
Product aspect	Mass obtained	Yield	$R_f$ (hexane/ethyl acetate 8:2)
Yellow semisolid	0.083 g	64%	0.65



$^1\text{H NMR}$  ( $\text{CDCl}_3$ , 400 MHz)  $\delta$ (ppm), 1.19 (t,  $J = 7$  Hz, 3H,  $\text{CH}_2\text{-CH}_3$ ); 2.48 (s, 3H,  $\text{CH}_3\text{-Ar}$ ); 3.62 (q,  $J = 7$  Hz, 2H,  $\text{CH}_2\text{-O}$ ); 5.58 (s, 2H,  $\text{-N-CH}_2\text{-O}$ ); 7.26 (d,  $J = 9$  Hz, 2H, H-3', H-5'); 7.28 (d,  $J = 7$  Hz, 1H, H-4''); 7.41 (t,  $J = 7$  Hz, 1H, H-5''); 7.75 (d,  $J = 9$  Hz, 2H, H-2', H-6'); 7.88 (d,  $J = 7$  Hz, 1H, H-2''); 8.76 (s, 1H, H-3)

$^{13}\text{C}$  NMR ( $\text{CDCl}_3$ , 100.6 MHz)  $\delta$ (ppm), 15.0 ( $\text{CH}_3$ ,  $\text{CH}_3\text{-CH}_2$ ); 21.6 ( $\text{CH}_3$ ,  $\text{CH}_3\text{-Ar}$ ); 65.0 ( $\text{CH}_2$ ,  $\text{CH}_2\text{-O-}$ ); 71.5 ( $\text{CH}_2\text{-O-CH}_2\text{-O-}$ ); 91.8 (Cq, C-7); 115.7 ( $\text{CH}$ ,  $J = 22$  Hz, C-3', C-5'); 124.2 ( $\text{CH}$ , C-6''); 124.8 (Cq, C-7a); 127.7 (Cq, C-1'); 127.9 ( $\text{CH}$ , C-4''); 128.8 ( $\text{CH}$ , C-5''); 129.7 ( $\text{CH}$ , C-2''); 132.8 ( $\text{CH}$ ,  $J = 9$  Hz, C-2', C-6'); 136.6 ( $\text{CH}$ , C-3); 137.5 (Cq, C-6); 138.6 (Cq, C-1''); 140.7 (Cq, C-3''); 142.1 (Cq, C-4a); 149.2 (Cq, C-2); 163.7 (Cq,  $J = 254$  Hz, C-4')

#### 4.3.37. Preparation of 5-(ethoxymethyl)-6-(4-fluorophenyl)-2,7-di-p-tolyl-5H-pyrrolo[2,3-b]pyrazine (**110a**)



· Procedure

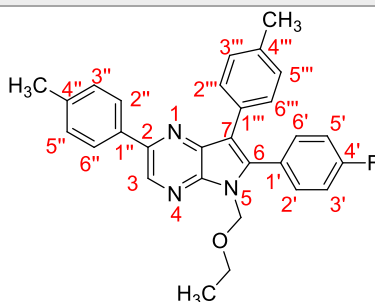
Starting from **109a** (0.41 mmol) the general procedure **C** described previously in the same work was followed in this case (Suzuki-Miyaura coupling reaction).

· Purification

A purification to remove excess of boronic acid was done by flash automatic silica gel column chromatography. The desired product eluted with a mixture of hexane/ethyl acetate 70:30.

· Analytical data

Product aspect	Mass obtained	Yield	R <sub>f</sub> (hexane/ethyl acetate 7:3)
Yellowish semisolid	0.075 g	41%	0.57

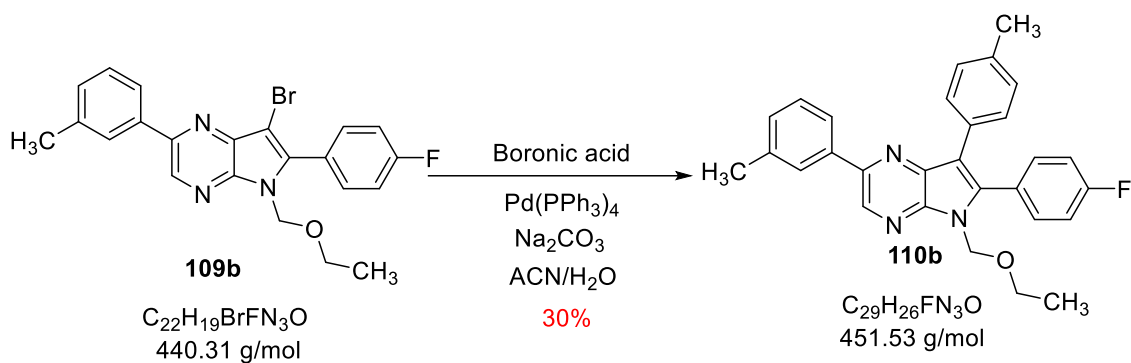


$^1\text{H}$  NMR ( $\text{CDCl}_3$ , 400 MHz)  $\delta$ (ppm), 1.20 (t,  $J = 7$  Hz, 3H,  $\text{CH}_3\text{-CH}_2\text{-O}$ ); 2.43 (s, 3H,  $\text{CH}_3\text{-Ar}$  (x2)); 3.63 (q,  $J = 7$  Hz, 2H,  $\text{CH}_2\text{-O}$ ); 5.57 (s, 2H,  $\text{N-CH}_2\text{-O}$ ); 7.12 (d,  $J = 8.4$  Hz, 2H, H-3''', H-5''', rotamer m); 7.15 (d,  $J = 8.4$  Hz, 2H, H-3''', H-5''', rotamer M); 7.26 (t,  $J = 8.5$  Hz, 2H, H-3', H-5'); 7.32 (d,  $J = 8$  Hz, 2H, H-3'' H-5''); 7.49 (d,  $J = 8.2$  Hz, 2H, H-2''', H-6''', rotamer m); 7.55 (d,  $J = 8.2$  Hz, 2H, H-2''', H-6''' rotamer M); 7.74 (d,  $J = 8.5$  Hz, 2H, H-2', H-6' rotamer M); 7.76 (d,  $J = 8.4$  Hz, 2H, H-2', H-6', rotamer m); 8.01 (d,  $J = 8$  Hz, 2H, H-2'', H-6''); 8.76 (s, 1H, H-3).

$^{13}\text{C}$  NMR ( $\text{CDCl}_3$ , 100.6 MHz)  $\delta$ (ppm), 15.0 ( $\text{CH}_3$ ,  $\text{CH}_3\text{-CH}_2$ ); 21.3 ( $\text{CH}_3$ ,  $\text{CH}_3\text{-Ar}$  (x2)); 64.7 ( $\text{CH}_2$ ,  $\text{CH}_2\text{-O}$ , rotamer m); 65.0 ( $\text{CH}_2$ ,  $\text{CH}_2\text{-O}$ , rotamer M); 70.9 ( $\text{CH}_2$ ,  $\text{N-CH}_2\text{-O}$ , rotamer m); 71.5 ( $\text{CH}_2$ ,  $\text{N-CH}_2\text{-O}$ , rotamer M); 115.1 (Cq, C-7a); 115.7 (CH,  $J = 21.7$  Hz, C-3', C-5'); 124.9 (Cq,  $J = 3.5$  Hz, C-1'); 127.0 (CH, C-2'', C-6''); 128.9 (CH, C-2''', C-6'''); 129.2 (Cq, C-7); 129.6 (CH, C-3'', C-5'', C-3''', C-5'''); 132.8 (CH,  $J = 8.5$  Hz, C-2', C-6', rotamer M); 133.0 (CH,  $J = 8.5$  Hz, C-2', C-6', rotamer m); 134.8 (Cq, C-6); 136.4 (CH, C-3); 138.5 (Cq, C-1''); 139.0 (Cq, C-4'', C-4'''); 140.65 (Cq, C-1'''); 148.0 (Cq, C-4a); 149.1 (Cq, C-2); 163.0 (Cq,  $J = 249.9$  Hz, C-4'). **M rotamer: majority, m rotamer: minority.**

HRMS, ESI(+)  $m/z$ : Mass calculated for  $\text{C}_{29}\text{H}_{26}\text{FN}_3\text{O}$ : 452.2093 g/mol  $[\text{M}+\text{H}]^+$ . Mass found: 452.2099 g/mol.

4.3.38. Preparation of 5-(ethoxymethyl)-6-(4-fluorophenyl)-2-(*m*-tolyl)-7-(*p*-tolyl)-5H-pyrrolo[2,3-*b*]pyrazine (**110b**)



· Procedure

Starting from **109b** (0.18 mmol) the general procedure **C** described in this research work was followed in this case (Suzuki-Miyaura coupling reaction).

· Purification

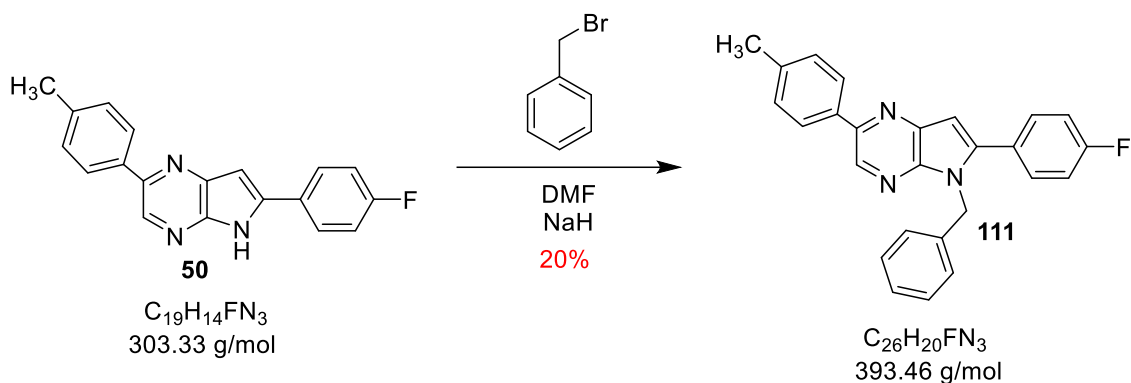
A purification to remove excess of boronic acid was carried out by flash automatic column chromatography. The desired product eluted with a mixture of hexane/ethyl acetate 80:20.

· Analytical data

Due to the obtained quantity and solubility problems the  $^1\text{H}$  NMR was not accomplished.

Product aspect	Mass obtained	Yield	$R_f$ (hexane/ethyl acetate 8:2)
Yellow semisolid	0.025 g	30%	0.74

4.3.39. Preparation of 5-benzyl-6-(4-fluorophenyl)-2-(p-tolyl)-5H-pyrrolo[2,3-b]pyrazine (111)



· Procedure

In a round bottom flask the diarylated pyrrolopyrazine **50** (0.070 g, 0.23 mmol) was dissolved in DMF (6 mL). NaH (60% in vaseline) (0.012 g, 0.35 mmol) was washed with hexane in order to remove vaseline and was then added into the mixture. The reaction was stirred at room temperature for 30 minutes. After this time the benzyl bromide was also added (0.042 mL, 0.43 mmol).

· Work up

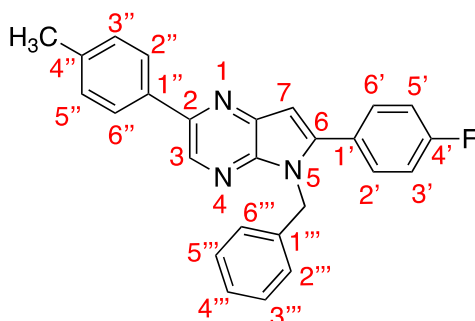
The reaction was stirred until no more starting material was observed in TLC (hexane/ethyl acetate 7:3). The mixture was diluted with ethyl ether (15 mL) and washed with water (3 x 20 mL). The organic phases were collected, dried over sodium sulfate, filtered off and concentrated under reduced pressure.

· Purification

A purification to remove excess of boronic acid was done by flash automatic column chromatography. The desired product eluted with a mixture of hexane/ethyl acetate 70:30.

· Analytical data

Product aspect	Mass obtained	Yield	$R_f$ (hexane/ethyl acetate 7:3)
Yellow solid	0.041 g	20%	0.45

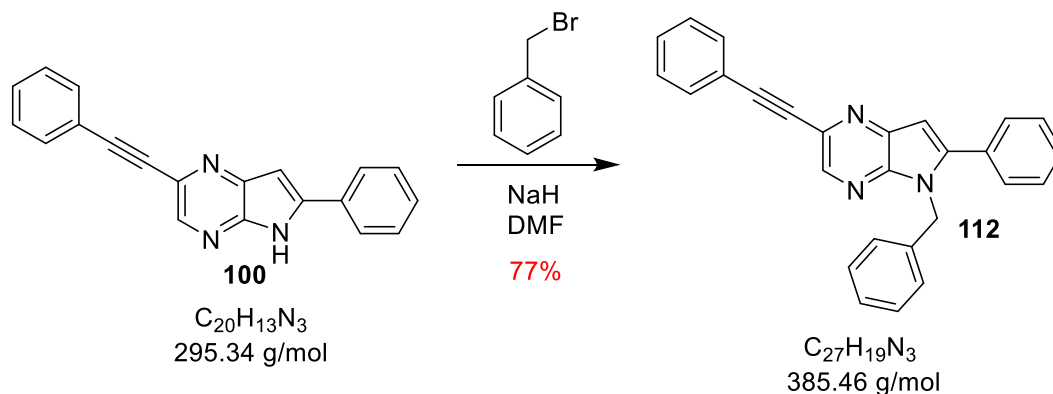


$^1H$  NMR ( $CDCl_3$ , 400 MHz)  $\delta$ (ppm), 2.34 (s, 3H,  $CH_3$ ); 5.79 (s, 2H,  $CH_2-Ar$ ); 7.01 (s, 1H, H-7); 7.09 (d,  $J = 8.6$  Hz, 2H, H-2''', H-6'''); 7.12-7.15 (m, 3H, H-3''', H-4''', H-5'''); 7.23 (d,  $J = 8$  Hz, 1H, H-2' rotamer); 7.35 (t,  $J = 6$  Hz, 2H, H-3', H-5'); 7.38 (s, 1H, H-3); 7.42-7.44 (m, 2H, H-3'', H-5'');



(dd,  $J_1 = 5$  Hz,  $J_2 = 8$  Hz, 1H, H-6'); 7.69 (d,  $J = 8$  Hz, 1H, H-2' rotamer); 8.18 (dd,  $J_1 = 5.5$  Hz,  $J_2 = 8.9$  Hz, 2H, H-2'', H-6''); (H-2' and H-6' are interchangeable protons).

#### 4.3.40. Preparation of 5-benzyl-6-phenyl-2-(phenylethynyl)-5H-pyrrolo[2,3-b]pyrazine (**112**)



##### · Procedure

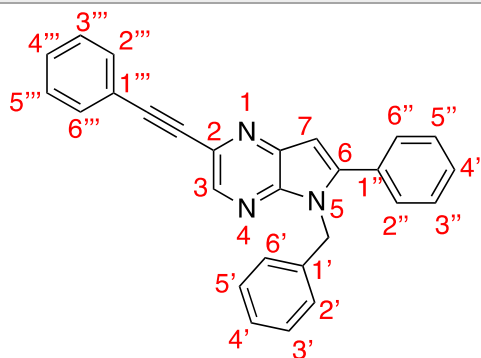
Starting from **100** (0.2 mmol) the general procedure described in the previous reaction of this work was applied for preparation of **112**.

##### · Purification

The crude of reaction was purified by flash automatic column chromatography to remove excess of benzyl bromide. The desired product eluted with a mixture of hexane/ethyl acetate 60:40.

##### · Analytical data

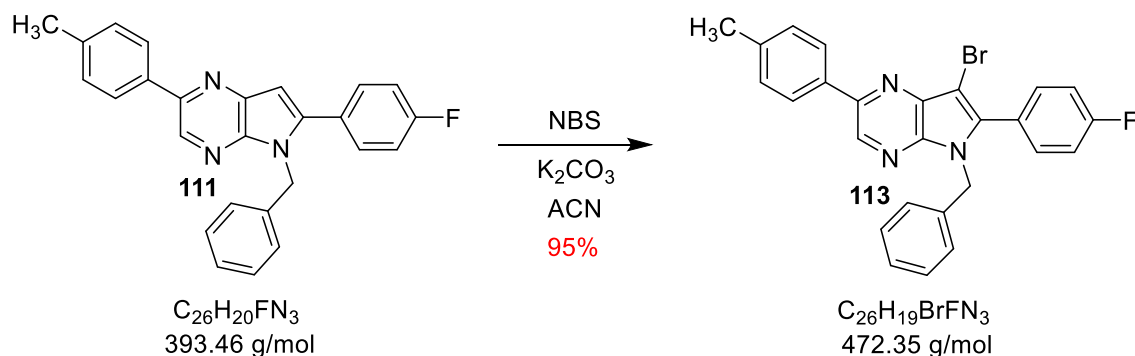
Product aspect	Mass obtained	Yield	$R_f$ (hexane/ethyl acetate 7:3)
Yellow solid	0.060 g	77%	0.83



$^1H$  NMR ( $CDCl_3$ , 400 MHz)  $\delta$ (ppm), 5.48 (s, 2H,  $CH_2$ -Ar); 6.70 (s, 1H, H-7); 6.86-6.89 (m, 2H, H-3'', H-5''); 7.15 (dd,  $J_1 = 2$  Hz,  $J_2 = 5$  Hz, 2H, H-3''', H-5'''); 7.30-7.32 (m, 4H, H-2''', H-4''', H-4'', H-6'''); 7.34 (s, 5H, phenyl); 7.57 (m, 2H, H-2'', H-6''); 8.42 (s, 1H, H-3).

$^{13}C$  NMR ( $CDCl_3$ , 100.6 MHz)  $\delta$ (ppm), 46.1 ( $CH_2, CH_2-N$ ); 87.2 (Cq, Ar-C $\equiv$ ); 90.6 (Cq,  $\equiv C$ -Pyrzine); 101.5 (CH, C-7); 122.4 (Cq, C-7a); 126.6 (CH, C-2'', C-6''); 127.5 (CH, C-4''); 127.7 (Cq, C-1'''); 128.4 (CH, C-2', C-6'); 128.5 (Cq, C-1''); 128.6 (CH, C-3''', C-5'''); 128.7 (CH, C-3'', C-5''); 128.8 (CH, C-4'); 129.2 (CH, C-3', C-5'); 129.4 (CH, C-4''); 131.9 (CH, C-2''', C-6'''); 133.6 (Cq, C-1'); 137.2 (Cq, C-2); 139.4 (CH, C-3); 140.4 (Cq, C-6); 147.7 (Cq, C-4a).

4.3.41. Preparation of 5-benzyl-7-bromo-6-(4-fluorophenyl)-2-(p-tolyl)-5H-pyrrolo[2,3-b]pyrazine (**113**)



· Procedure

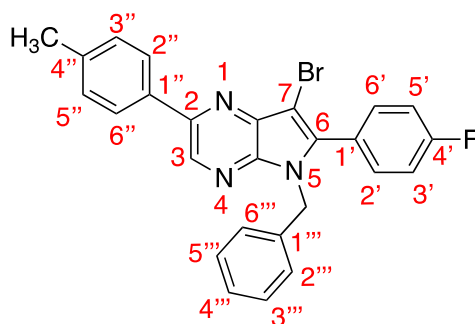
Starting from **111** (0.11 mmol) the general procedure **D** described previously in this work was followed in this case (halogenation of C-7).

· Purification

The desired product was obtained with enough purity.

· Analytical data

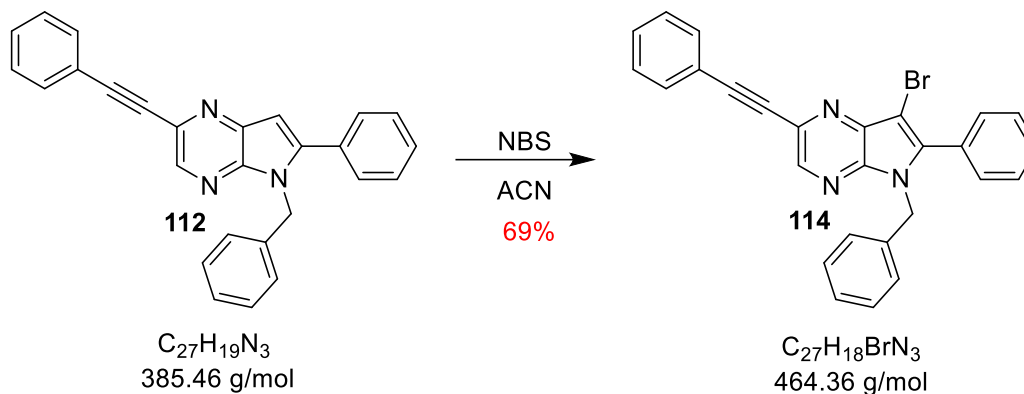
Product aspect	Mass obtained	Yield	R <sub>f</sub> (hexane/ethyl acetate 8:2)	Melting point
Yellow solid	0.048 g	95%	0.40	> 300 °C (DCM)



$^1H$  NMR ( $CDCl_3$ , 400 MHz)  $\delta$ (ppm), 2.70 (s, 3H,  $CH_3$ -Ar) ; 5.78 (s, 2H,  $CH_2$ -N); 7.13 (t,  $J = 8.7$  Hz, 2H, H-2''', H-6'''); 7.15-7.21 (m, 3H, H-3''', H-5''', H-4'''); 7.36 (sc, 2H, H-3'', H-5''); 7.40 (sc, H-3', H-5'); 7.49 (s, 1H, H-3); 7.78 (bs, 1H, H-2'); 7.81 (dd,  $J_1 = 5$  Hz,  $J_2 = 8.4$  Hz, 1H, H-6'); 8.42 (dd,  $J_1 = 5.6$  Hz,  $J_2 = 8.8$  Hz, 2H, H-2'', H-6''); (H-2' and H-6' are interchangeable protons).

$^{13}C$  NMR ( $CDCl_3$ , 100.6 MHz)  $\delta$ (ppm), 21.2 ( $CH_3$ ); 55.4 ( $CH_2$ ,  $CH_2$ -N) ; 115.4 ( $CH$ ,  $J = 21.5$  Hz, C-3', C-5'); 98.6 (Cq, C-7); 120.3 ( $CH$ , C-3); 123.7 (Cq, C-7a); 126.4 (Cq, C-1'); 129.0 ( $CH$ , C-2''); 129.2 ( $CH$ , C-2''', C-6'''); 129.3 ( $CH$ , C-6''); 129.5 ( $CH$ , C-3''', C-5'''); 129.7 ( $CH$ , C-4'''); 130.1 ( $CH$ , C-3''); 130.2 ( $CH$ , C-5''); 131.0 (Cq, C-1''); 131.3 ( $CH$ ,  $J = 8.4$  Hz, C-2', C-6'); 132.9 (Cq, C-4''); 138.7 (Cq, C-1'''); 139.7 (Cq, C-6); 150.0 (Cq, C-4a); 151.4 (Cq, C-2); 163.8 ( $CH$ ,  $J = 250$  Hz, C-4'); (C-2'' and C-6'' are interchangeable carbons; C-3'' and C-5'' are interchangeable carbons).

4.3.42. Preparation of 5-benzyl-7-bromo-6-phenyl-2-(phenylethynyl)-5H-pyrrolo[2,3-b]pyrazine (**114**)



· Procedure

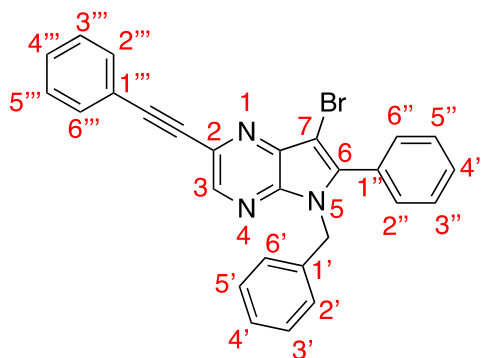
Starting from **112** (0.16 mmol) the general procedure **D** described previously was followed in this case (halogenation of C-7).

· Purification

The desired product was obtained with enough purity.

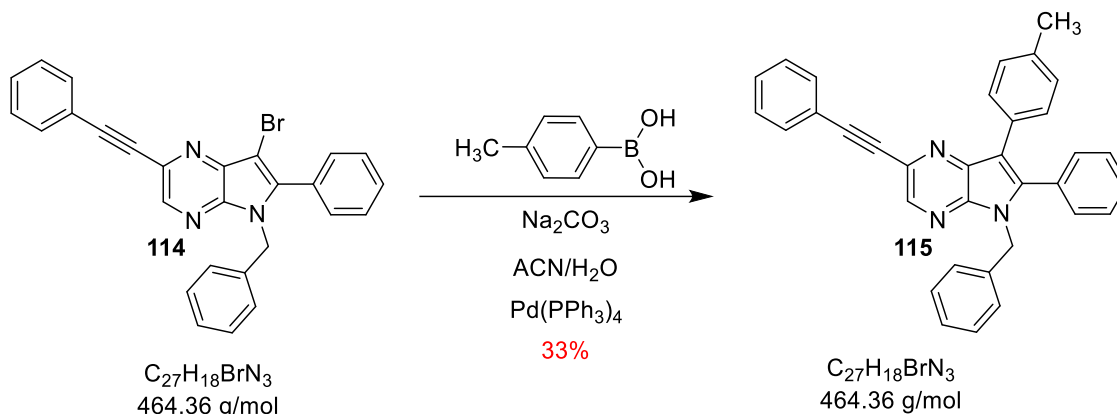
· Analytical data

Product aspect	Mass obtained	Yield	R <sub>f</sub> (hexane/ethyl acetate 7:3)
Yellow solid	0.050 g	69%	0.83



$^1\text{H NMR}$  ( $\text{CDCl}_3$ , 400 MHz)  $\delta$ (ppm), 5.41 (s, 2H,  $\text{CH}_2\text{-Ar}$ ); 6.79-6.81 (m, 2H, H-3'', H-5''); 7.12 (dd,  $J_1 = 2$  Hz,  $J_2 = 5$  Hz, 2H, H-3''', H-5'''); 7.29-7.34 (m, 6H, phenyl + H-4'') 7.42 (dd,  $J_1 = 1.2$  Hz,  $J_2 = 7$  Hz, 3H, H-2'', H-4''', H-6''); 7.57-7.59 (m, 2H, H-2''', H-6''); 8.48 (s, 1H, H-3).

4.3.43. Preparation of 5-benzyl-6-phenyl-2-(phenylethynyl)-7-(p-tolyl)-5H-pyrrolo[2,3-b]pyrazine (**115**)



· Procedure

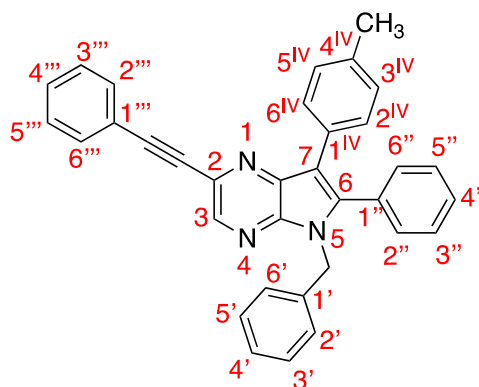
Starting from **114** (0.06 mmol) The general procedure **C** described previously in this same work was followed in this case (Suzuki-Miyaura coupling reaction).

· Purification

The crude of reaction was purified by flash automatic silica gel column chromatography. The desired product eluted with a mixture of hexane/ethyl acetate 90:10.

· Analytical data

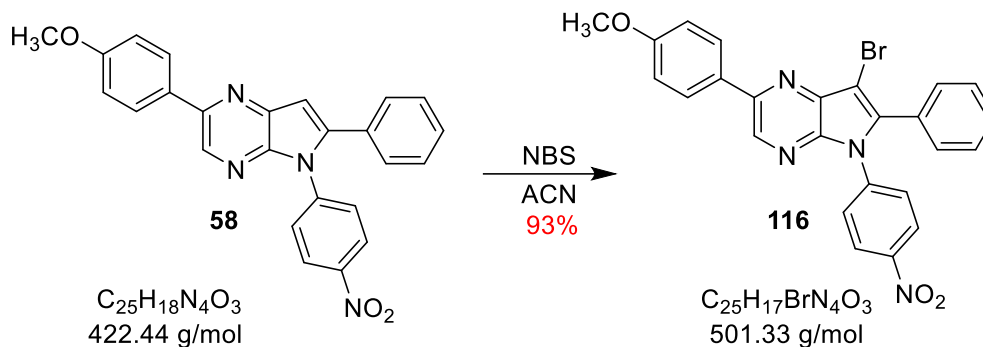
Product aspect	Mass obtained	Yield	$R_f$ (hexane/ethyl acetate 9:1)	Melting point
Yellowish solid	0.01 g	33%	0.58	>300 °C (DCM)



$^1\text{H NMR}$  ( $\text{CDCl}_3$ , 400 MHz)  $\delta$ (ppm), 2.29 (s, 3H,  $\text{CH}_3$ ); 5.38 (s, 2H,  $\text{CH}_2\text{-Ar}$ ); 6.83-6.85 (m, 2H, H-3''', H-5'''); 7.00 (d,  $J = 8$  Hz, 2H, H-3<sup>IV</sup>, H-5<sup>IV</sup>); 7.11-7.13 (m, 5H, H-2'', H-3'', H-4'', H-5'', H-6''); 7.29-7.30 (m, 6H, phenyl + H-4'''); 7.33 (d,  $J = 8$  Hz, 2H, H-2<sup>IV</sup>, H-6<sup>IV</sup>); 7.56-7.58 (m, 2H, H-2''', H-6'''); 8.47 (s, 1H, H-3).

**HRMS, ESI (+)  $m/z$** : Mass calculated for  $\text{C}_{27}\text{H}_{18}\text{BrN}_3$ : 476.2082 g/mol  $[\text{M}+\text{H}]^+$ . Mass found: 476.2091 g/mol.

4.3.44. Preparation of 7-bromo-2-(4-methoxyphenyl)-5-(4-nitrophenyl)-6-phenyl-5H-pyrrolo[2,3-b]pyrazine (**116**)



· Procedure

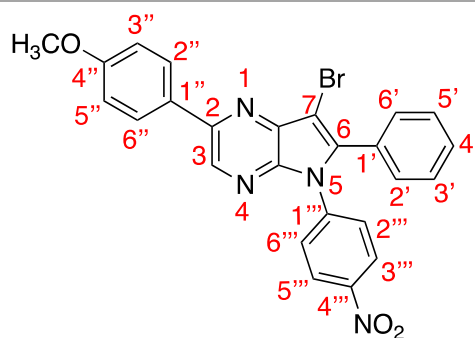
Starting from **58** (0.28 mmol) the general procedure **D** described previously in this work was followed in this case (halogenation of C-7).

· Purification

No purification was made since the product was obtained with enough purity.

· Analytical data

Product aspect	Mass obtained	Yield	$R_f$ (hexane/ethyl acetate 8:2)	Melting point
Yellow solid	0.128 g	93%	0.75	> 300 °C (DCM)



$^1H$  NMR ( $CDCl_3$ , 400 MHz)  $\delta$ (ppm), 3.89 (s, 3H, O-CH<sub>3</sub>); 7.04 (d,  $J = 8.7$  Hz, 2H, H-3'', H-5''); 7.43 (t,  $J = 7.7$  Hz, 1H, H-4'); 7.57 (t,  $J = 7.7$  Hz, 2H, H-3', H-5'); 7.69 (d,  $J = 8.9$  Hz, 2H, H-2''', H-6'''); 7.94 (d,  $J = 7.7$  Hz, 2H, H-2', H-6'); 8.06 (d,  $J = 8.7$  Hz, 2H, H-2'', H-6''); 8.10 (d,  $J = 8.9$  Hz, 2H, H-3''', H-5'''); 8.66 (s, 1H, H-3).

## 4.4. MATERIALS AND METHODS OF QUANTITATIVE BIOLOGY LABORATORY

### Materials

MATERIAL	DESCRIPTION
FUGENE	Multicomponent reagent (non-liposomal) that forms a complex with DNA in order to transfect it into a wide variety of cells. <sup>276</sup>
OPTIMEM	Medium containing insulin, transferrin, hypoxanthine, thymidine, and trace elements. <sup>277</sup>
PGLOSENSOR™-22F	Plasmid encoding a cAMP biosensor known as the Glosensor <sup>276</sup>
GLOSENSOR REAGENT	The GloSensor cAMP reagent is composed of Luciferin. Which is the luciferase substrate that works in the presence of cAMP produced after receptor activation. <sup>278</sup> The magnitude of the luminescence increase is directly proportional to the amount of analyte present. <sup>276</sup>
DMEM	Modification of Basal Medium Eagle (BME) which contains a higher concentration of amino acids and vitamins, as well as additional supplementary components. <sup>277</sup>
DYE REAGENT-FLUO 3	Labeled calcium indicators are molecules that exhibit an increase in fluorescence upon binding Ca <sup>2+</sup> . Fluo-3 is used to image the spatial dynamics of Ca <sup>2+</sup> signaling in flow cytometry experiments. <sup>277</sup>
HBSS	Hank's Balanced Salt Solution, to maintain the pH and osmotic balance. <sup>277</sup>
HEPES	A buffering agent (sulfonic acid) to keep a physiological pH <sup>277</sup>
LUCIFERASE REAGENT	Lysis buffer, lysing the cells in order to detect the generated luciferase through luminescence. <sup>276</sup>

### Cell Culture preparation

The cell line HEK293E were grown in a cell media containing DMEM/F-12 (7.5 g/kg), sodium bicarbonate (1.1 g/kg), sodium hydroxide solution (50%, 0.4 g/kg), L-glutamine (1.022 g/kg), dextrose (1.8 g/kg), tropolone (0.0002 g/kg), Kolliphor P188 (0.5 g/kg). Charged with 80% of the required make up weight of purified water and then the DMEM were added and mixed for 15 minutes. Sodium bicarbonate and sodium hydroxide were added and mixed for 10 minutes. The rest of the components were added. The solution was filtered (0.22-0.1) into final container as a master stock.

<sup>277</sup> <https://www.thermofisher.com> (25/05/2019)

<sup>278</sup> M. Buccioni; G. Marucci; D. Dal Ben; D. Giacobbe; C. Lambertucci; L. Soverchia; A. Thomas; R. Volpini; G. Cristalli. *Purinergic Signal*. **2011**, 7, 463-468

### Transfection (general procedure)

The FuGENE was mixed with OptiMEM and incubated at room temperature for 5 minutes. When the ratio FuGENE:DNA was established (6:1), the DNA of each receptor plus reporter vectors or pGlosensor-22F or PLC- $\epsilon$ , depending on the assay, were added and mixed with 0.2 mL of FuGENE-OptiMEM. These mixtures were incubated for 20 minutes at room temperature.

At this time, 1 mL aliquot from the master HEK293 cells stock was quantified through Vicell (counting cells device). The viability of the cells oscillates between 95-100%. Dilutions were made to obtain the desired quantity of cells/mL.

Finally, 0.2 mL of the DNA complexes with a total amount of 1.5  $\mu$ g of DNA (FuGENE:OptiMEM containing aGPCRs DNA (0.75  $\mu$ g) + reporter vectors DNA/ pGlosensor-22F/ PLC- $\epsilon$  (0.75  $\mu$ g) were added into a solution of 250,000 cells/mL in a 50 mL culture tubs. The tubes were left incubating in a shaker at 150 rpm.

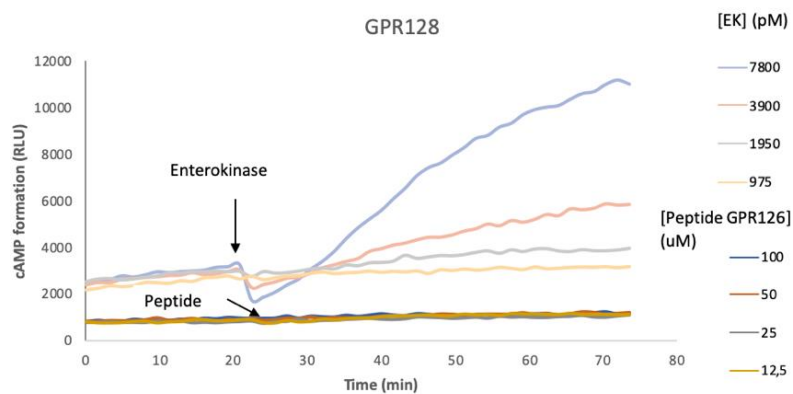
In all assays, a culture tube with untransfected cells was used as a negative control. As well, in each assay an appropriate positive control was conducted.

### a) cAMP assay - Gas quantification- pGlosensor-22F

After 48h in suspension in a rotating shaker, according to standard protocols, HEK293 transfected cells, with aGPCRs DNA and pGlosensor-22F, were pelleted by gentle centrifugation (1500 rpm/ 5 min) and resuspended by tituration in 5 mL of assay media (CO<sub>2</sub> Independent Media + 0.1% casein + 2% Glosensor reagent). 1 mL of each sample was quantified by Vicell to control the viability and the number of cells/mL.

Samples were plated into a 96 well assay plate (costar 3917, 200  $\mu$ L cells/well), and luminescence was measured to stablish a baseline (Envision Luminescence mode). Then a series of enterokinase dilutions were made in order to create a dose-response curve. 20  $\mu$ L of enterokinase light chain stock (2  $\mu$ g/mL, 7.6 nM) were added to 200  $\mu$ L assay buffer and dilutions 1:2 were created with assay buffer. 20  $\mu$ L were added in each well, obtaining a starting concentration of 76 pM.

For the custom peptide GPR126, (peptide with the GPS sequence of GPR126) a gradient of concentrations was created as well. 20  $\mu$ L from the stock (1 mM) were added to 200  $\mu$ L assay buffer. 1:2 dilutions were created with assay buffer. The starting concentration was 0.1 mM. Luminescence was measured in real time for 45 minutes (Figure 83).



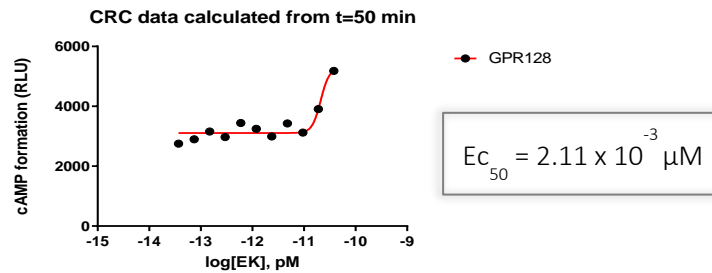


**Figure 83.** Example of cAMP assay for  $G\alpha_s$  quantification

*b) cAMP assay –  $G_{i/o}$  quantification- pGlosensor-22F*

In these assays, pertussis toxin (from *Bordetella pertussis*) was used and the experiment was doubled in size to allow the comparison of samples with and without pertussis toxin.

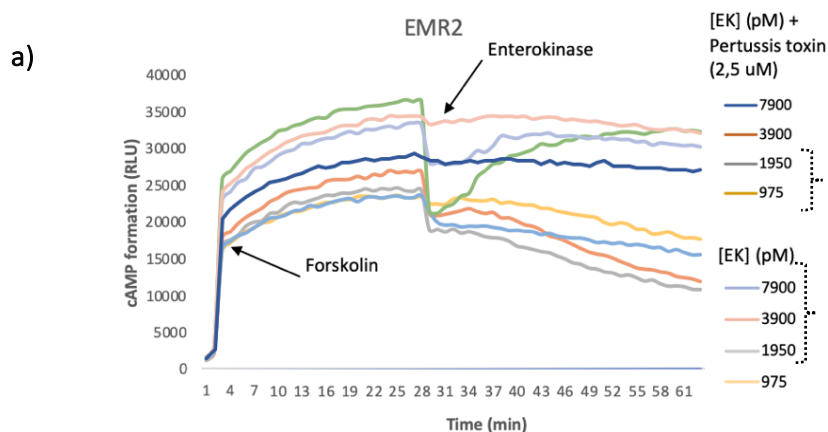
At 24h after transfection every sample of cells was split in 2 tubes and 10  $\mu\text{L}$  of pertussis toxin (100 ng/mL) was added in one of them. Therefore, 2 samples were created: one of transfected cells with receptor and pGlosensor and other sample with the same plus pertussis toxin. The samples were incubated in the shaker at 150 rpm for a further 24 hours. Subsequently, the samples were pelleted by gentle centrifugation (1500 rpm/ 5 min) and resuspended by titration in 5 mL of assay media (CO<sub>2</sub> independent media + 0.1% casein + 2% Glosensor reagent). 1 mL of each sample was quantified with a Vicell cytometer to determine the viability of the cells/mL.

Using an assay plate (costar 3917), cells were placed (200  $\mu\text{L}$  cells/well), and luminescence was measured to establish a baseline (Envision Luminescence mode).

Because the  $G\alpha_i$  is an inhibitor of adenylate cyclase, an increase of intracellular cAMP has to be induced prior to receptor activation in order to be able to observe this effect. If a decrease of cAMP is observed after receptor activation through enterokinase, it is probable that the receptor is coupled to  $G\alpha_i$ . Hence, 20  $\mu\text{L}$  Forskolin, a natural diterpene that activates adenylate cyclase (cAMP rises)<sup>271</sup> was added with the same concentration (2  $\mu\text{M}$ ) in each well.

Luminescence was measured in real time for 25 minutes (cAMP levels upswing to 25.000-200.000 RLU).

Then, a series of enterokinase dilutions were made in order to create a dose-response curve (same dilutions applied for  $G_s$  assay). Luminescence was measured in real time for 45 minutes (Figure 84).





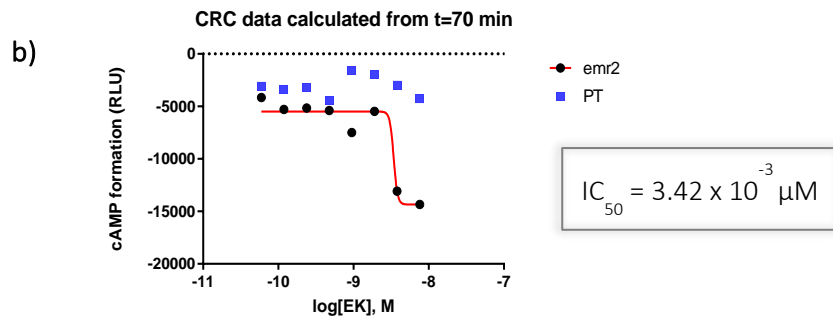


Figure 84. a) Example of cAMP assay for  $G\alpha_i$  quantification b)  $IC_{50}$  calculated with and without PT.

c) *Calcium mobilization assay*

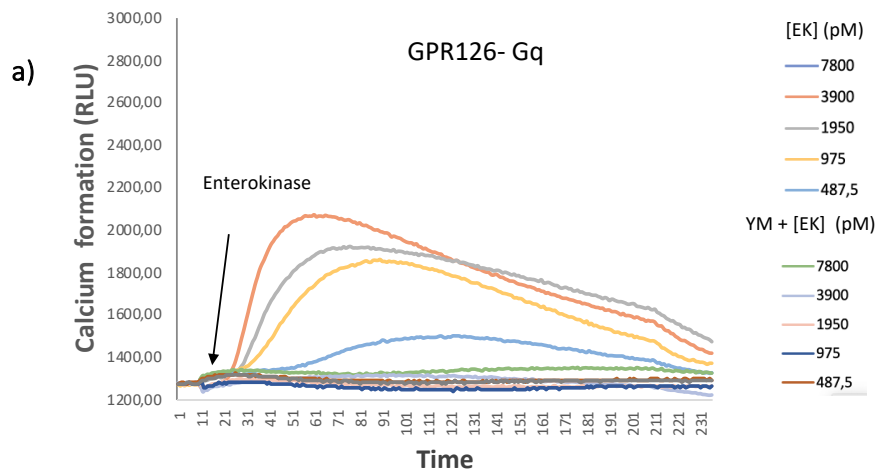
After 24 hours post-transfection (general procedure), assay plates were coated with 20  $\mu$ L of poly-L-lysine for 2 hours at 37  $^{\circ}$ C. Then, the buffer was removed and with 50  $\mu$ L of DMEM, plates were rinsed.

The HEK293E transfected cells with the aGPCRs DNA (and PLC- $\epsilon$  for  $G\alpha_{12}$  assays) were pelleted by gentle centrifugation (1500 rpm/ 5 min) and resuspended by titration in 5 mL assay media (DMEM 500mL + 10% FBS + Glutamax 6 mL + MEM 6 mL + Ampicilin 6 mL + Hepes 12 mL). One mL of each sample was quantified by Vicell to quantify viability and concentration.

Cells were plated in an assay plate (corning 354663, 40  $\mu$ L/well, that is 12000 to 16000 cells/well) and incubated for 24 hours at 37 $^{\circ}$ C in the tissue culture incubator. Every sample was plated twice in order to compare the sample with YM-254890 with the one without it.

After this time, a dye reagent Fluo-3 was diluted with HBSS/Hepes. 20  $\mu$ L of this mixture was added in each well and the cells were incubated at room temperature for two hours. The  $G\alpha_q$  inhibitor YM-254890, was added (1.04  $\mu$ M) 30 minutes before running the assay in one of the rows of each sample. Meanwhile, in an assay plate, dilutions of enterokinase were created with assay buffer (same dilutions applied for Gs assay). For the custom peptide (with GPS sequence of GPR126), dilutions were created as well.

Through the FLIPR (Fluorescent Imaging Plate Reader), the fluorescence baseline was measured (10 seconds). Then, enterokinase dilutions were added automatically into the samples and the fluorescence was measured for 300 seconds (Figure 85 and Figure 86).



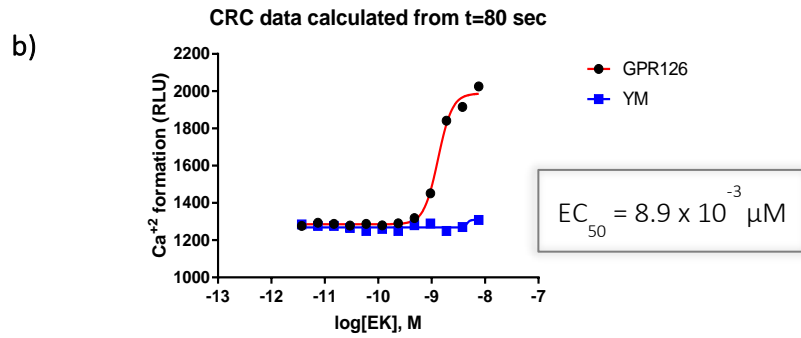


**Figure 85.** a) Example of calcium assay for  $G\alpha_q$  quantification. b)  $IC_{50}$  calculated with and without YM.

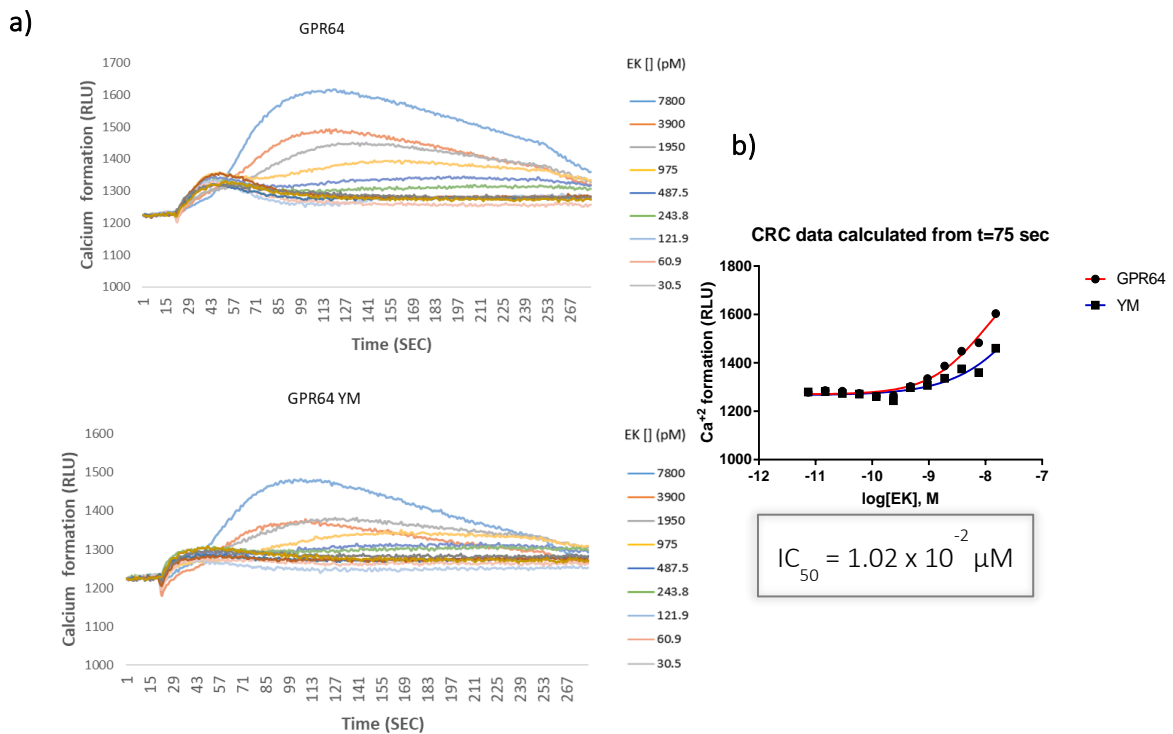


**Figure 86.** a) Example of calcium assay for  $G\alpha_{12}$  quantification b)  $IC_{50}$  calculated with and without YM

*d) Reporter vectors assay- CRE, SRE, NFAT, SRF*

At 24 hours of transfection, the transfected cells with CRE, SRE, NFAT or SRF, were placed in an assay plate (costar 3917). 1 mL of sample was quantified by Vicell. The plates were incubated for 2 hours at 37 °C in the cell tissue incubator.

Meanwhile, dilutions of enterokinase were created with buffer (starting concentration 76  $\mu\text{M}$ ) and the same dilutions were done for forskolin (2  $\mu\text{M}$ , positive control for CRE), serum 100% (10%, positive control for SRF), ATP (100  $\mu\text{M}$ , positive control for NFAT) and PAM (protein associated with Myc, inhibitor of adenylate cyclase) (10  $\mu\text{M}$ , positive control for

SRE). These dilutions were added and plates were placed again for incubation at 37 °C for 6 hours. After this time, 50  $\mu\text{L}$  of luciferase reagent were added in each well and luminescence was measured one time (Envision Luminescence mode) (Figure 87).

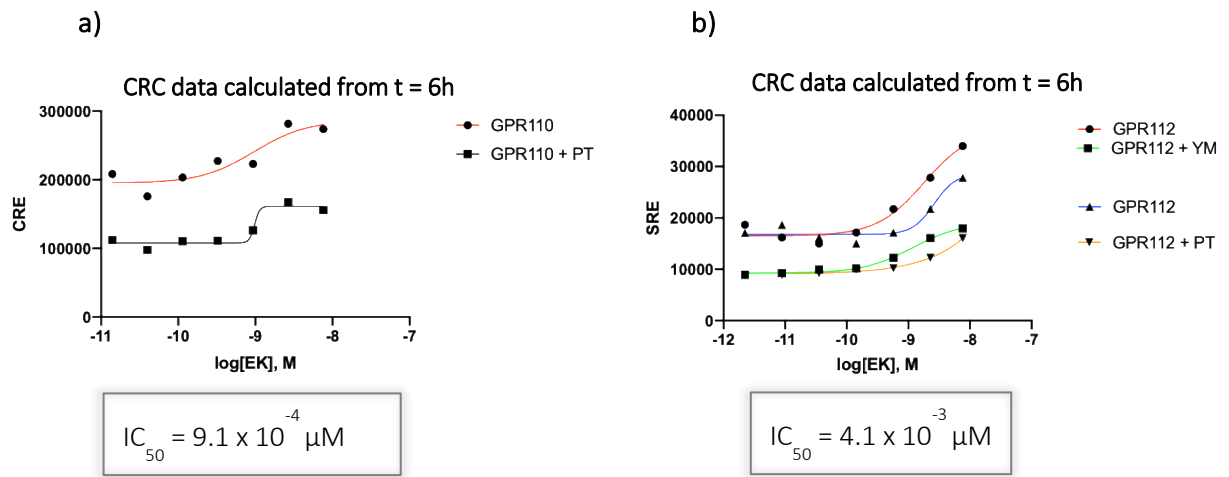


**Figure 87.** a) Example of reporter vector CRE with and without PT for GPR110. b) Example of reporter vector SRE with and without PT and YM for GPR112.

## 5. CONCLUSIONS

The most relevant conclusions of this work are indicated below:

1. The transacetylation reaction between *N*-methyl-4-piperidone and catechol or 2-aminophenol affords the best yields to obtain the spirobenzodioxole (**1**) and spirobenzoxazole (**43**) systems respectively. Between them, the preparation of **1** provides better yield (70%) than that which leads **43** (32%), probably due to lower reactivity of 2-aminophenol compared with catechol. Since the main nucleus is obtained, the formation of the spiro-piperidines **2**, **3**, **4**, **5**, **6** and **12** are prepared with high yields (80-98%) through classical reactions: alkylation, hydrolysis of amida, oxime formation with hydroxylamine, reduction, halogenation and nitration, respectively.
2. The 1'-acetyl-5-bromospiro[benzo[1,3]dioxole-2,4'-piperidine] (**6**) is a good scaffold to add aryl groups into position 5 of spiro derivatives through coupling reactions (Suzuki-Miyaura and Buchwald-Hartwig), affording compounds **7**, **8**, **9**, **10** and **11** with high yields (86-93%). Also, from the nitrospiro derivative **12**, the consequent basic hydrolysis, followed by a coupling reaction using Pd[(*o*-tolil)<sub>3</sub>P]<sub>2</sub>Cl<sub>2</sub>, cesium carbonate, BINAP and toluene affords the compound **14** which is reduced to the diamino **15**, a desirable compound to synthesize the corresponding diaryl or arylalkyl ureas.
3. The 5-acetyl-1'-(4-nitrophenyl)spiro[benzo[1,3]dioxole-2,4'-piperidine] (**17**) is a good intermediate for the synthesis of the following spiro derivatives: 1-(1'-(4-nitrophenyl)spiro[benzo[1,3]dioxole-2,4'-piperidine]-5-yl)ethanone oxime (**18**) with a *Z* conformation confirmed by NOE experiments, the 1-(1'-(4-nitrophenyl)spiro[benzo[1,3]dioxole-2,4'-piperidine]-5-yl)ethanol (**21**) and the 5-acetyl-1'-(4-aminophenyl)spiro[benzo[1,3]dioxole-2,4'-piperidine] (**23**). The amide **19** was obtained with 63% of yield from the oxime **18** by Beckmann rearrangement. Then, the amide **19** was reduced with chloride acid and ethanol to amine **20** with 25% of yield. When the amino **23** was treated with phthalic anhydride in toluene, the imide **24** was obtained with 24% of yield. Then, when **23** was treated with bromomaleic anhydride and coupling reaction conditions (Buchwald-Hartwig), the anhydride **26** was obtained with 55% of yield.
4. The activation of hydroxyl group by treatment with thionyl chloride is a good method for functionalization of spiro-piperidines **29** and **30** allowing the nucleophile substitution reaction with *N,N*-diethyl-2-aminoethanol, *N,N*-diethylethylenediamine and hexylamina given as a result the final compounds **33**, **34** and **35** respectively. The reductive aminations of the methylketones **27** and **28** were tried as a first pathway to obtain these final spiro derivatives (**33**, **34** and **35**), but in all assays, with different conditions, the alcohol derivatives **29** and **30** were obtained.
5. The addition of isocyanate to the anilines dissolved in THF constitutes an excellent method for the preparation of ureas. Thus, the ureas **37**, **39**, **40**, **41** and **42** were successfully prepared. The addition of aniline **22** to ethylisocyanate allows the formation of urea **39** with 50% yield. The treatment of diamina **15** with the same isocyanate afforded the diurea **41** with 79% yield. By contrast, the treatment of **15** with pyridine-3-isocyanate afforded the monourea **40** with only 7% of yield, due to the lower reactivity of the isocyanate. The treatment of amina **23** with 2-fluoro-5-(trifluoromethyl)phenyl isocyanate afforded as a result the urea **37** with 80% yield and the treatment of **9** with 4-chloro-3-(trifluoromethyl)phenyl isocyanate afforded the urea **42** with 62% yield.

6. A new method for the preparation of 2-amino-5-bromopyrazine (**93c**) and 2-amino-3,5-dibromopyrazine (**91c**) has developed. The yields obtained are in function of the amount of halogenating agent added. Acetonitrile has proved to be the ideal solvent and the assistance of microwave irradiation is essential to obtain halogenated 2-aminopyrazine. 3,5-Dibromo-2-aminopyrazine (**91c**) is an excellent functionalized starting material for the synthesis of nitrogen heterocycles.
7. The Sonogoshira reaction conditions between 2-amino-3,5-dibromopyrazine (**91c**) and different phenylacetylenes, using a proportion of base (Et<sub>3</sub>N)/solvent (THF) 1:7 and without CuI, afforded the pyrazine derivatives **92**, **97** and **98** with the best yields 99%, 93% and 95% respectively. These derivatives were cyclized through an *endo-dig* cyclization and followed by Suzuki Miyaura cross-coupling reaction in order to arylate at position 2 using different boronic acids and given as a result the diarylated pyrazines **47-52** with considerable yields (36%-96%).
8. The halogenation at the position 7 of the pyrrolo[2,3-*b*]pyrazine system was a success, using NBS and acetonitrile, but the followed Suzuki Miyaura reaction to arylate the same position was never achieved due to the interactions of catalyst with unprotected NH of the pyrrolo ring. Then, protecting this position with MOM or benzyl groups the halogenation and the Suzuki Miyaura reaction were accomplished given as a result the triarylated compounds, at (positions 2, 6 and 7) **110a** (41%), **110b** (30%), both protected with MOM and **56** (95%) and **115** (69%) both protected with benzyl group.
9. The halogenation of 6-(4-fluorophenyl)-2-(*p*-tolyl)-5*H*-pyrrolo[2,3-*b*]pyrazine in carbon 3 was achieved through oxidation of the pyrazine ring followed by halogenation with POCl<sub>3</sub> affording the product **105** with 66% yield. When the halogenation of this position was tried directly with NBS and NCS was not obtained, only once, the dibromide derivative was achieved with 9% yield (**103**). For the following arylation of position 3, only with the bromo derivative, the triarylated pyrrolo[2,3-*b*]pyrazine **54** was found with 56% yield.
10. The hydrolysis of the *NH*- protecting group of the pyrrolopyrazine system was only possible through catalytic hydrogenation of **54**, given as a result the 6-(4-fluorophenyl)-2,7-di-*p*-tolyl-5*H*-pyrrolo[2,3-*b*]pyrazine with quantitative yields. The hydrolysis of acetal group of compounds **110a** and **110b** were not possible, even trying different reaction conditions.
11. Of the biological assays performed at Eli Lilly & Company in oncology field, it is interesting to note that compounds **20**, **28**, **30**, **42** show the best therapeutic profile in hNNT inhibition, compared with its spiro analogues. While compounds **47** and **115** are the best ones for the pyrrolo[2,3-*b*]pyrazine family. In fact, compound **47** is the most potent among all tested compounds with an IC<sub>50</sub> of 4.2 μM. For arginase inhibition, a change in the amino group in the product **20** for an acetyl group, compound **17**, increases the activity x 1.5. Also, when the nitro group of **17** is reduced to amino, compound **23**, the activity is reduced 2 times.
12. The results of preliminary tests on other targets also reveal interesting information. In the field of tropical diseases, comparing products **3** and **33** stands out the importance of the substituents groups, *N,N*-diethyl-2-aminoethoxy chain and sulfonamide, because a 65% of inhibition of *P. falciparum* at 12 μM of concentration and 90% of inhibition of *P. Bergheri* at 10 μM, with low hepatic cytotoxicity, shows the potential of compound **33** in malaria treatment, not as 5-acetyl-spiro[benzo[1,3]dioxole-2,4'-piperidine] (**3**) that

shows low inhibitory activity for both parasites. Concerning [chagas disease](#), compound **33** shows an outstanding inhibitory activity in front of the grow of *T. cruzi* with 93% of inhibition and 99% when the number of parasites per cell is evaluated, both at 5  $\mu$ M. Again, compound **3** showed no activity.

13. In [neurodegeneration and pain](#), spiro-sulfonamide **33** is highlighted due to an inhibitory activity in front Tau protein of 100% at 40  $\mu$ M, with interest in Alzheimer disease and 76% of inhibitory activity at 30  $\mu$ M in front of calcitonin gene-related peptide (CGRP) related with migraine attacks.
14. The project undertaken at Eli Lilly & Company, designing cellular assay systems to measure the signal transduction of recombinant adhesion family receptors involved transient transfection of mammalian cells and the measurement of various second messengers (cAMP, IP3, kinase activity) in response to activated receptor point mutants and literature-described peptides. The analysis of the mechanism of receptor activation and G-protein signal- transduction pathway has been quantified and the proposed and accomplished assays are reproducible and efficient to analyze the coupled G proteins and the intracellular mechanisms related with adhesion GPCRs.

## 6. REFERENCES AND NOTES

- <sup>1</sup> <https://www.cancer.gov> (07/08/2019)
- <sup>2</sup> C. Alibert; B. Goud; J. B. Manneville. *Biol. Cell.* **2017**, *109*, 167-189
- <sup>3</sup> <https://www.who.int> (07/08/2019)
- <sup>4</sup> <https://www.cancer.org> (07/10/2019)
- <sup>5</sup> R. D. Wood; M. Mitchell; J. Sgouros; T. Lindahl. *Science* **2001**, *291*, 1284-1289
- <sup>6</sup> S. I. Hajdu. *Cancer* **2011**, *117*, 1097-1102
- <sup>7</sup> <https://gco.iarc.fr> (08/10/2019)
- <sup>8</sup> <https://www.iqvia.com> (08/10/2019)
- <sup>9</sup> <https://www.aecc.es> (08/10/2019)
- <sup>10</sup> <https://seom.org> (08/10/2019)
- <sup>11</sup> F. T. Kolligs. *Visc. Med.* **2016**, *32*, 158–164
- <sup>12</sup> <https://ghr.nlm.nih.gov> (09/10/2019)
- <sup>13</sup> F. Zijl; G. Krupitza; W. Mikulitsa. *Mutat. Res.* **2011**, *728*, 23–34
- <sup>14</sup> T. N. Seyfried; L. C. Huysentruyt. *Crit. Rev. Oncog.* **2013**, *18*, 43–73
- <sup>15</sup> J. Rueff; A. S. Rodrigues. *Methods Mol. Biol.* **2016**, *1395*, 1-18
- <sup>16</sup> S. Turajlic; A. Sottoriva; T. Graham; C. Swanton. *Nat. Rev. Genet.* **2019**, *20*, 404-416
- <sup>17</sup> M. Najafi; B. Farhood; K. Mortezaee. *J. Cell. Physiol.* **2019**, *234*, 8381-8395
- <sup>18</sup> D. Huang; H. Duan; H. Huang; X. Tong; Y. Han; G. Ru; L. Qu; C. Shou; Z. Zhao. *Sci. Rep.* **2016**, *6*, 1-12
- <sup>19</sup> M. Kartal-Yandim; A. Adan-Gokbulut; Y. Baran. *Crit. Rev. Biotechnol.* **2016**, *36*, 716-726
- <sup>20</sup> C. Holohan; S. Van Schaeybroeck; D. B. Longley; P.G. Johnston. *Nat. Rev. Cancer* **2013**, *13*, 714-726
- <sup>21</sup> M. Akada; T. Crnogorac-Jurcevic; S. Lattimore; P. Mahon; R. Lopes; M. Sunamura; S. Matsuno; N.R. Lemoine. *Clin. Cancer. Res.* **2005**, *11*, 3094-3101
- <sup>22</sup> J. R. Bertino; E. Göker; R. Gorlick; W. W. Li; D. Banerjee. *Stem Cells* **1996**, *14*, 5-9
- <sup>23</sup> W. Guo; J. H. Healey; P. A. Meyers; M. Ladanyi; A. G. Huvos; J. R. Bertino; R. Gorlick. *Clin. Cancer Res.* **1999**, *51*, 621-627
- <sup>24</sup> D. S. Hsu; W. L. H. Wang; C. H. Yuh; C. H. Chu; Y. H. Ho; P. B. Chen; H. S. Lin; H. K. Lin; S. P. Wu; C. Y. Lin; W. H. Hsu; H. Y. Lan; H. J. Wang; S. K. Tai; M. C. Hung; M. H. Yang. *Clin. Cancer Res.* **2017**, *23*, 4388-4401
- <sup>25</sup> H. J. Choi; H. S. Joo; H. Y. Won; K. W. Min; H. Y. Kim; T. Son; Y. H. Oh; J. Y. Lee; G. Kong. *J. Nat. Cancer Inst.* **2018**, *110*, 400-410
- <sup>26</sup> D. Yan; J. Kowal; L. Akkari; A. J. Schuhmacher; J. T. Huse; B. L. West; J. A. Joyce. *Oncogene* **2017**, *36*, 6049-6058
- <sup>27</sup> R. R. Begicevic; M. Falasca. *Int. J. Mol. Sci.* **2017**, *18*, 2362-2386
- <sup>28</sup> Y. H. Choi; A. M. Yu. *Curr. Pharm. Des.* **2014**, *20*, 793–807
- <sup>29</sup> A. Lucci; W. I. Cho; T. Y. Han; A. E. Giuliano; D. L. Morton; M. C. Cabot. *Anticancer Res.* **1998**, *18*, 475-480
- <sup>30</sup> L. H. Matherly; M. R. Wilson; Z. Hou. *Drug Metab. Dispos.* **2014**, *42*, 632-649
- <sup>31</sup> D. T. Manallack. *Perspect. Medicin. Chem.* **2007**, *17*, 25-38
- <sup>32</sup> F. J. Sharom. *Pharmacogenomics* **2008**, *9*, 105-127
- <sup>33</sup> A. Adamska; M. Falasca. *World J. Gastroenterol.* **2018**, *24*, 3222–3238
- <sup>34</sup> X. X. Peng; K. T. Amit; H. C. Wu; Z. S. Chen. *Chin. J. Cancer* **2012**, *31*, 110–118

- <sup>35</sup> Z. Lin; M. Chen; X. Yang; Z. Cui; X. Zhang; L. Yuan; Q. Zhang. *Int. J. Nanomedicine* **2014**, *9*, 3425-3437
- <sup>36</sup> J. Gao; H. R. Li; C. Jin; J. H. Jiang; J. Y. Ding. *Clin. Transl. Oncol.* **2019**, *21*, 1287-1301
- <sup>37</sup> M. Kacevska; M. Ivanov; M. Ingelman-Sundberg. *Pharmacogenomics* **2012**, *13*, 1373-1385
- <sup>38</sup> M. D. Wyatt; D. M. Wilson. *Cell. Mol. Life Sci.* **2009**, *66*, 788-799
- <sup>39</sup> G. Sharma; S. Mirza; R. Parshad; A. Srivastava; S. D. Gupta; P. Pandya; R. Ralhan. *Clin. Biochem.* **2010**, *43*, 373-379
- <sup>40</sup> A. A. Mugggerud; J. A. Rønneberg; F. Wärnberg; J. Botling; F. Busato; J. Jovanovic; H. Solvang; I. Bukholm; A. L. Børresen-Dale; V. N. Kristensen; T. Sørli; J. Tost. *Breast Cancer Res.* **2010**, *12*, 1-10
- <sup>41</sup> J. Jung; L. J. Kim; X. Wang; Q. Wu; T. Sanvoranart; C. G. Hubert; B. C. Prager; L. C. Wallace; X. Jin; S. C. Mack; J. N. Rich; *J.C.I. Insight* **2017**, *2*, e90019
- <sup>42</sup> F. P. Andrea; A. Safwat; M. Kassem; L. Gautier; J. Overgaard; M. R. Horsman. *Radiother. Oncol.* **2011**, *99*, 373-378
- <sup>43</sup> Y. Wang; J. Zeng; W. Wu; S. Xie; H. Yu; G. Li; T. Zhu; F. Li; J. Lu; G. Y. Wang; X. Xie; J. Zhang. *Breast Cancer Res.* **2019**, *21*, 1-17
- <sup>44</sup> <https://www.proteinatlas.org> (11/10/2019)
- <sup>45</sup> X. Xinyou; L. Huixing; W. Yanzhong; Z. Yanwen; Y. Haitao; L. Guiling; R. Zhi; L. Fengying; W. Xiuhong; Z. Jun. *Oncotarget* **2016**, *7*, 45837-45848
- <sup>46</sup> M. A. Eckert; F. Coscia; A. Chryplewicz; J. W. Chang; K. M. Hernandez; S. Pan; S. M. Tienda; D. A. Nahotko; G. Li; I. Blaženović; R. R. Lastra; M. Curtis; S. D. Yamada; R. Perets; S. M. McGregor; J. Andrade; O. Fiehn; R. E. Moellering; M. Mann; E. Lengyel. *Nature* **2019**, *569*, 723-728
- <sup>47</sup> S. Qu; Y. Zhong; R. Shang; X. Zhang; W. Song; J. Kjems; H. Li. *RNA Biol.* **2017**, *14*, 992-999
- <sup>48</sup> J. S. Mattick. *EMBO Rep.* **2001**, *2*, 986-991
- <sup>49</sup> E. Anastasiadou; L. S. Jacob; F. J. Slack. *Nature Reviews Cancer* **2018**, *18*, 5-18
- <sup>50</sup> W. Z. Hu; C. L. Tan; Y. J. He; G. Q. Zhang; Y. Xu; J. H. Tang. *Onco. Targets Ther.* **2018**, *11*, 1529-1541
- <sup>51</sup> I. Berindan-Neagoe; P. Monroig; B. Pasculli; G. A. Calin. *C.A. Cancer J. Clin.* **2014**, *64*, 311-336
- <sup>52</sup> H. Lan; H. Lu; X. Wang; H. Jin. *Biomed. Res. Int.* **2015**, *v2015*, 1-17
- <sup>53</sup> M. Carlo; M. D. Croce. *Nat. Rev. Genet.* **2009**, *10*, 704-714
- <sup>54</sup> H. Hu; S. Li; X. Cui; X. Lv; Y. Jiao; F. Yu; H. Yao; E. Song; Y. Chen; M. Wang; L. Lin. *J. Biol. Chem.* **2013**, *288*, 10973-10985
- <sup>55</sup> S. J. Shi; L. J. Wang; B. Yu; Y. H. Li; Y. Jin; X. Z. Bai. *Oncotarget* **2015**, *6*, 11652-11663
- <sup>56</sup> H. Zhang; J. Yan; X. Lang; Y. Zhuang. *Oncol. Lett.* **2018**, *16*, 5856-5862
- <sup>57</sup> <https://www.nature.com> (14/10/2019)
- <sup>58</sup> M. W. Pickup; J. K. Mouw; V. M. Weaver. *EMBO Rep.* **2014**, *15*, 1243-1253
- <sup>59</sup> A. B. Hanker; M. V. Estrada; G. Bianchini; P. D. Moore; J. Zhao; F. Cheng; J. P. Koch; L. Gianni; D. R. Tyson; V. Sánchez; B. N. Rexer; M. E. Sanders; Z. Zhao; T. P. Stricker; C. L. Arteaga. *Cancer Res.* **2017**, *77*, 3280-3292
- <sup>60</sup> Z. N. Lu; B. Tian; X. L. Guo. *Cancer Chemother. Pharmacol.* **2017**, *80*, 925-937
- <sup>61</sup> M. Wang; J. Zhao; L. Zhang; F. Wei; Y. Lian; Y. Wu; Z. Gong; S. Zhang; J. Zhou; K. Cao; X. Li; W. Xiong; G. Li; Z. Zeng; C. Guo. *J. Cancer* **2017**, *8*, 761-773
- <sup>62</sup> X. Qin; H. Guo; X. Wang; X. Zhu; M. Yan; X. Wang; Q. Xu; J. Shi; E. Lu; W. Chen; J. Zhang. *Genome Biol.* **2019**, *20*, 1-21
- <sup>63</sup> Q. Zhang; J. Yang; J. Bai; J. Ren. *Cancer Sci.* **2018**, *109*, 944-955



- <sup>64</sup> A. J. Petty; Y. Yang. *Immunotherapy* **2017**, *9*, 289–302
- <sup>65</sup> X. T. Fu; K. Song; J. Zhou; Y. H. Shi; W. R. Liu; G. M. Shi; Q. Gao; X. Y. Wang; Z. B. Ding; J. Fan. *Cancer Cell Int.* **2019**, *19*, 1-11
- <sup>66</sup> Y. Zhou; F. Tozzi; J. Chen; F. Fan; L. Xia; J. Wang; G. Gao; A. Zhang; X. Xia; H. Brasher; W. Widger; L. M. Ellis; Z. Weihua. *Cancer Res.* **2012**, *72*, 304-314
- <sup>67</sup> Y. Qian; X. Wang; Y. Liu; Y. Li; R. A. Colvin; L. Tong; S. Wu; X. Chen. *Cancer Lett.* **2014**, *351*, 242-251
- <sup>68</sup> X. Wang; Y. Li; Y. Qian; Y. Cao; P. Shriwas; H. Zhang; X. Chen. *Oncotarget* **2017**, *8*, 87860-87877
- <sup>69</sup> F. D. Virgilio; A. C. Sarti; S. Falzoni; E. De Marchi; E. Adinolfi. *Nat. Rev. Cancer* **2018**, *10*, 601-618
- <sup>70</sup> I. Dagogo-Jack; A. T. Shaw. *Nat. Rev. Clin. Oncol.* **2018**, *15*, 81-94
- <sup>71</sup> N. A. Yousafzai; H. Wang; Z. Wang; Y. Zhu; L. Zhu; H. Jin; X. Wang. *Am. J. Cancer Res.* **2018**, *8*, 2210–2226
- <sup>72</sup> K. Fernald; M. Kurokawa. *Trends. Cell. Biol.* **2013**, *23*, 620–633
- <sup>73</sup> N. Mizushima; M. Komatsu. *Cell.* **2011**, *147*, 728-741
- <sup>74</sup> Z. J. Yang; C. E. Chee; S. Huang; F. A. Sinicrope. *Mol. Cancer. Ther.* **2011**, *10*, 1533–1541
- <sup>75</sup> Y. J. Li; Y. H. Lei; N. Yao; C. R. Wang; N. Hu; W. C. Ye; D. M. Zhang; Z. S. Chen. *Chin. J. Cancer* **2017**, *36*, 1-10
- <sup>76</sup> Y. Cao; Y. Luo; J. Zou. J. Ouyang; Z. Cai; X. Zeng; H. Ling; T. Zeng. *Clin. Chim.* **2019**, *489*, 10-20
- <sup>77</sup> N. Xu; J. Zhang; C. Shen; Y. Luo; L. Xia; F. Xue; Q. Xia. *Biochem. Biophys. Res. Commun.* **2012**, *423*, 826-831
- <sup>78</sup> B. Y. K. Law; V. W. K. Wai. *Intechopen* **2016**, *20*, 435-454
- <sup>79</sup> F. Huang; B. R. Wang; Y. G. Wang. *World J. Gastroenterol.* **2018**, *24*, 4643-4651
- <sup>80</sup> X. Liu; D. Fan. *Curr. Pharm. Des.* **2015**, *21*, 1279-1291
- <sup>81</sup> Z. S. Jiang; Y. Z. Sun; S. M. Wang; J. S. Ruan. *J. Cancer* **2017**, *8*, 2319-2327
- <sup>82</sup> Y. T. Tang; Y. Y. Huang; J. H. Li; S. H. Qin; Y. Xu; T. X. An; C. C. Liu; Q. Wang; L. Zheng. *BMC Genomics* **2018**, *19*, 1-14
- <sup>83</sup> M. Mutlu; U. Raza; Ö. Saatci; E. Eyüpoğlu; E. Yurdusev; Ö. Şahin. *J. Mol. Med.* **2016**, *94*, 629-644
- <sup>84</sup> N. E. Bholia; J. M. Balko; T. C. Dugger; M. G. Kuba; V. Sánchez; M. Sanders; J. Stanford; R. S. Cook; C. L. Arteaga. *J. Clin. Invest.* **2013**, *123*, 1348-1358
- <sup>85</sup> T. B. Steinbichler; J. Dudás; S. Skvortsov; U. Ganswindt; H. Riechelmann; I. I. Skvortsova. *Semin. Cancer Biol.* **2018**, *53*, 156-167
- <sup>86</sup> E. Batlle; H. Clevers. *Nat. Med.* **2017**, *23*, 1124-1134
- <sup>87</sup> S. Skvortsov; P. Debbage; P. Lukas; I. Skvortsova. *Semin. Cancer Biol.* **2015**, *31*, 36-42
- <sup>88</sup> X. Xu; S. Chai; P. Wang; C. Zhang; Y. Yang; Y. Yang; K. Wang. *Cancer Lett.* **2015**, *369*, 50-57
- <sup>89</sup> L. Ponnusamy; P. K. S. Mahalingaiah; Y. W. Chang; K. P. Singh. *Cancer Drug Resist.* **2019**, *2*, 297-312
- <sup>90</sup> X. Wang; H. Zhang; X. Chen. *Cancer Drug Resist.* **2019**, *2*, 141-160
- <sup>91</sup> J. A. DiMasi; H. G. Grabowski; R. W. Hansen. *J. Health Econ.* **2016**, *47*, 20-33
- <sup>92</sup> N. Nosengo. *Nature* **2016**, *534*, 314-316
- <sup>93</sup> S. Pushpakom; F. Iorio; P. A. Eyers; K. J. Escott; S. H. A. Wells; A. Doig; T. Williams; J. Latimer; C. McNamee; A. Norris; P. Sanseau; D. Cavalla; M. Pirmohamed. *Drug Discov.* **2019**, *18*, 41-58
- <sup>94</sup> C. M. Telleria. *J. Cancer Sci. Ther.* **2012**, *4*, 9-11
- <sup>95</sup> H. X. J. Li; H. Xie; Y. Wang. *Int. J. Biol. Sci.* **2018**, *14*, 1232-1244
- <sup>96</sup> A. Saxena; D. Becker; I. Preeshagul; K. Lee; E. Katz; B. Levyc. *Oncologist* **2015**, *20*, 934–945
- <sup>97</sup> E. Damery; D. A. Solimando; J. A. Waddell. *Hosp. Pharm.* **2016**, *51*, 628–632

- <sup>98</sup> <https://www.cancerresearchuk.org> (17/10/2019)
- <sup>99</sup> <https://www.fda.gov> (17/10/2019)
- <sup>100</sup> P. Patrignani; C. Patrono. *J. Am. Coll. Cardiol.* **2016**, *68*, 967-976
- <sup>101</sup> J. An; M. Minie; T. Sasaki; J. J. Woodward; K. B. Elkon. *Annu. Rev. Med.* **2017**, *68*, 317-330
- <sup>102</sup> N. Tidten-Luksch; R. Grimaldi; L. S. Torrie; J. A. Frearson; W. N. Hunter; R. Brenk. *PLoS One* **2012**, *7*, e35792
- <sup>103</sup> M. Cortes-Canteli; A. Kruyer; I. Fernandez-Nueda; A. Marcos-Diaz; C. Ceron; A. T. Richards; V. Fuster. *JACC*, **2019**, *74*, 1910-1923
- <sup>104</sup> S. S. Ou-Yang; J. Y. Lu; X. Kong; Z. Liang; C. Luo; H. Jiang. *Acta Pharmacol. Sin.* **2012**, *33*, 1131-1140
- <sup>105</sup> L. Chen; J. K. Morrow; H. T. Tran; S. S. Phatak; L. Du-Cuny; S. Zhang. *Curr. Pharm. Des.* **2012**, *18*, 1217-1239
- <sup>106</sup> C. H. M. M. P. Rao; R. P. Yejella; S. A. Rehman; C. Rajeswari; S. H. Basha. *J. Peer Sci.* **2018**, *1*, e1000008
- <sup>107</sup> L. Scotti; M. F. J. Junior; H. M. Ishiki; F. F. Ribeiro; R. K. Singla; J. M. Barbosa; M. S. Da Silva; M. T. Scotti. *Curr. Drug Targets* **2017**, *18*, 592-604
- <sup>108</sup> A. S. Hauser; S. Chavali; I. Masuho; L. J. Jahn; K. A. Martemyanov; D. E. Gloriam; M. M. Babu. *Cell.* **2018**, *172*, 41-54
- <sup>109</sup> S. Y. Yang. *Drug Discov. Today* **2010**, *15*, 444-450
- <sup>110</sup> G. Gini. *Methods Mol. Biol.* **2016**, *1425*, 1-20
- <sup>111</sup> J. Verma; V. M. Khedkar; E. C. Coutinho. *Curr. Top. Med. Chem.* **2010**, *10*, 95-115
- <sup>112</sup> J. Y. Trosset; C. Cave. *Methods Mol. Biol.* **2019**, *1953*, 189-103
- <sup>113</sup> <http://www.way2drug.com> (18/10/2019)
- <sup>114</sup> V. Konova; A. Lagunin; P. Pogodin; E. Kolotova; A. Shtil; V. Poroikov. *SAR QSAR Environ. Res.* **2015**, *26*, 595-604
- <sup>115</sup> A. A. Lagunin; V. I. Dubovskaja; A. V. Rudik; P. V. Pogodin; D. S. Druzhilovskiy; T. A. Glorizova; D. A. Filimonov; N. G. Sastry; V. V. Poroikov. *PLoS One* **2018**, *13*, e0191838
- <sup>116</sup> <http://worldpopulationreview.com> (22/10/2019)
- <sup>117</sup> <https://www.cdc.gov> (22/10/2019)
- <sup>118</sup> M. De Rycker; B. Baragaña; S. L. Duce; I. H. Gilbert. *Nature* **2018**, *559*, 498-506
- <sup>119</sup> <https://www.who.int> (22/10/2019)
- <sup>120</sup> <https://unitingtocombatntds.org> (22/10/2019)
- <sup>121</sup> C. Bern. *N. Engl. J. Med.* **2015**, *373*, 456-466
- <sup>122</sup> S. Meymandi; S. Hernandez; S. Park; D. R. Sanchez; C. Forsyth. *Curr. Treat. Opt. Infect. Dis.* **2018**, *10*, 373-388
- <sup>123</sup> J. A. Padilla; I. Cotillo; J. Presa; J. Cantizani; I. Peña; A. I. Bardera; J. J. Martín; A. Rodriguez. *PLoS Negl. Trop. Dis.* **2015**, *9*, e0003493
- <sup>124</sup> <https://data.unicef.org> (23/10/2019)
- <sup>125</sup> N. Vale; L. Aguiar; P. Gomes. *Front. Pharmacol.* **2014**, *5*, 1-1
- <sup>126</sup> G. Berberian; M. T. Rosanova; C. Torroija; M. L. Praino. *Arch. Argent. Pediatr.* **2014**, *112*, 468-473
- <sup>127</sup> J. Talapko; I. Škrlec; T. Alebić; M. Jukić; A. Včev. *Microorganisms* **2019**, *7*, e179
- <sup>128</sup> S. Basu; P. K. Sahi. *Indian. J. Pediatr.* **2017**, *84*, 521-528
- <sup>129</sup> <https://www.europeanpharmaceuticalreview.com> (24/10/2019)
- <sup>130</sup> <https://ec.europa.eu> (22/10/2019)

- <sup>131</sup> K. Dheda; C. E. Barry; G. Maartens. *Lancet*. **2016**, *387*, 1211-1226
- <sup>132</sup> C. J. Cambier; S. Falkow; L. Ramakrishnan. *Cell* **2014**, *159*, 1497-1509
- <sup>133</sup> E. N. Houben; L. Nguyen; J. Pieters. *Curr. Opin. Microbiol.* **2006**, *9*, 76-85
- <sup>134</sup> J. Tang; W. C. Yam; Z. Chen. *Tuberculosis* **2016**, *98*, 30-41
- <sup>135</sup> T. Degen; T. Bregenzer. *Praxis* **2016**, *105*, 457-61
- <sup>136</sup> M. D. Pujol; G. Rosell; G. Guillaumet. *Eur. J. Med. Chem.* **1996**, *31*, 889-894
- <sup>137</sup> L. Yet. *Privileged Structures in Drug Discovery: Medicinal Chemistry and Synthesis* **2018**, 194-236
- <sup>138</sup> Y. Mettey; M. Gompel. V. Thomas, M. Garnier; M. Leost; I. C. Picot; M. Noble; J. Endicott; J. Vierfond; L. Meijer. *J. Med. Chem.* **2003**, *46*, 222-236
- <sup>139</sup> C. Corbel; R. Haddoub; D. Guiffant; O. Lozach; D. Gueyrard; J. Lemoine; M. Ratin; L. Meijer; S. Bach; P. Goekjian. *Bioorg. Med. Chem.* **2009**, *17*, 5572-5582
- <sup>140</sup> F. Padilla; N. Bhagirath; S. Chen; E. Chiao; D. M. Goldstein; J. C. Hermann; J. Hsu; J. J. Kennedy-Smith; A. Kuglstatler; C. Liao; W. Liu; L. E. Lowrie; K. C. Luk; S. M. Lynch; J. Menke; L. Niu; T. D. Owens; C. O-Yang; A. Railkar; R. C. Schoenfeld; M. Slade; S. Steiner; Y. C. Tan; A. G. Villaseñor; C. Wang; J. Wanner; W. Xie; D. Xu; X. Zhang; M. Zhou; M. C. Lucas. *J. Med. Chem.* **2013**, *56*, 1677-1692
- <sup>141</sup> D. J. Burdick; S. Wang; C. Heise; B. Pan; J. Drummond; J. P. Yin; L. Goeser; S. Magnuson; J. Blaney; J. Moffat; W. Wang; H. Chen. *Bioorg. Med. Chem. Lett.* **2015**, *25*, 4728-4732
- <sup>142</sup> J. de Vicente; R. Lemoine; M. Bartlett; J. C. Hermann; M. Hekmat-Nejad; R. Henningsen; S. Jin; A. Kuglstatler; H. Li; A. J. Lovey; J. Menke; L. Niu, V. Patel; A. Petersen; L. Setti; A. Shao; P. Tivitmahaisoon; M. D. Vu, M. Soth. *Bioorg. Med. Chem. Lett.* **2014**, *24*, 4969-4975
- <sup>143</sup> G. C. Senadi; B. C. Guo; Yu. C. Chang; W.P. Hu; J. J. Wang. *Adv. Synth. Catal.* **2017**, *360*, 491-501
- <sup>144</sup> SANOFI. *Una pirrolopirazina como inhibidor de Syk-quinasa*. España; patente de invención; ES2437318; 23-10-2013
- <sup>145</sup> N. Mur. *Disseny i síntesi de nous compostos de naturalesa heterocíclica amb potencial activitat anticancerígena. Síntesi de nous inhibidors de CDKs*. Tesis doctoral. Universitat de Barcelona, **2011**
- <sup>146</sup> A. Vinuesa. *Diseño, síntesis y evaluación biológica de nuevos compuestos nitrogenados potencialmente antitumorales*. Tesis Doctoral. Universidad de Barcelona y Universidad de San Jorge, **2016**
- <sup>147</sup> V. Prieur. *Pyrolo[2,3-d]pyrimidines: Conception, Synthèse, Fonctionnalisation*. Tesis doctoral. Université d'Orléans (Francia). Universitat de Barcelona, **2015**
- <sup>148</sup> L. Navarro. *Síntesis de nuevos compuestos con potencial actividad antitumoral y/o antiinflamatoria*. Tesis doctoral. Universitat de Barcelona, **2018**
- <sup>149</sup> I. A. Khotina; V. A. Izumrudov; N. V. Tchebotareva; A. L. Rusenov. *Macromol. Chem. Phys.* **2001**, *202*, 2360-2366
- <sup>150</sup> A. Williams; M. L. Bender. *J. Am. Chem. Soc.* **1966**, *88*, 2508-2513
- <sup>151</sup> S. Bher; S. Guha. *Synth. Commun.* **2005**, *35*, 1183-1188
- <sup>152</sup> R. F. Heck; J. P. Nolley. *J. Org. Chem.* **1972**, *37*, 2320-2322
- <sup>153</sup> A. O. King; N. Okukado; E. Negishi. *J. Chem. Soc. Chem. Commun.* **1977**, *19*, 683-684
- <sup>154</sup> N. Miyaura; A. Suzuki. *J. Chem. Soc. Chem. Commun.* **1979**, *19*, 866-867
- <sup>155</sup> F. Monnier; M. Taillefer. *Angew. Chem.* **2009**, *48*, 6954-6971
- <sup>156</sup> a) J. P. Wolfe; S. Wagaw; S. L. Buchwald. *J. Am. Chem. Soc.* **1996**, *118*, 7215-7216 b) J. P. Wolfe; S. L. Buchwald. *J. Org. Chem.* **1997**, *62*, 1264-1267 c) J. P. Wolfe; R. A. Rennels; S. L. Buchwald.

*Tetrahedron* **1996**, *52*, 7525-7546 d) J. P. Wolfe; S. L. Buchwald. *J. Org. Chem.* **2000**, *65*, 1144-1157 e) G. Mann; J. F. Hartwig; M. S. Driver; C. Fernández-Rivas. *J. Am. Chem. Soc.* **1998**, *120*, 827-828 f) J. F. Hartwig. *Synlett* **1996**, 329-340 g) M. S. Driver; J. F. Hartwig. *J. Am. Chem. Soc.* **1996**, *118*, 7217-7218 h) J. F. Hartwig. *Angew. Chem. Int. Ed.* **1998**, *37*, 2046-2067 i) J. Ahman; S. L. Buchwald. *Tetrahedron Lett.* **1997**, *38*, 6363-6366 j) J. P. Wolfe; J. Ahman; J. P. Sadighi; R. A. Singer; S. L. Buchwald. *Tetrahedron Lett.* **1997**, *38*, 6367-6370 k) S. L. Buchwald; X. Huang. *Org. Lett.* **2001**, *3*, 3417-3419 l) S. Lee; M. Jorgensen; J. F. Hartwig. *Org. Lett.* **2001**, *3*, 2729-2732 m) D. Y. Lee; J. F. Hartwig. *Org. Lett.* **2005**, *7*, 1169-1172

<sup>157</sup> M. Romero; Y. Harrak; J. Basset; L. Ginet; P. Constants; M. D. Pujol. *Tetrahedron* **2006**, *62*, 9010-9016

<sup>158</sup> a) J. G. Hoggett; R. B. Moodie; J. R. Penton; K. Schofield. *Nitration and Aromatic Reactivity* Cambridge: London, **1971**, p 76. b) Taylor, R. *Electrophilic Aromatic Substitution* Wiley: New York, **1990**, p 269

<sup>159</sup> C. M. Crudden; A. C. Chen; L. A. Calhoun. *Angew. Chimie. Int. Ed.* **2000**, *39*, 2851-2855

<sup>160</sup> N. K. Jana; J. G. Verkade. *Org. Lett.* **2003**, *5*, 3787-3790

<sup>161</sup> a) R. E. Gawly. *Org. React.* **1988**, *35*, 39-40 b) M. B. Smith; J. March. *In Advanced Organic Chemistry* 5th ed., John Wiley & Sons, New York, **2001**, 1415-1416

<sup>162</sup> M. Boruah; D. Konwar. *J. Org. Chem.* **2002**, *67*, 7138-7139

<sup>163</sup> S. Zhao; Y. Wuo; Q. Sun; T. M. Cheng; R. T. Li. *Synthesis* **2015**, *47*, 1154-1162

<sup>164</sup> H. Wang; Z. Xim; Y. Li. *Top. Curr. Chem.* **2017**, *375*, 49-75

<sup>165</sup> J. A. Grzyb; R. A. Batey. *Tetrahedron Lett.* **2008**, *49*, 5279-5282

<sup>166</sup> M. N. Bertrand; J. P. Wolfe. *Tetrahedron* **2005**, *61*, 6447-6459

<sup>167</sup> D. P. N. Satchel; R. S. Satchel. *Chem. Soc. Rev.* **1975**, *4*, 231-250

<sup>168</sup> E. A. Castro; R. B. Moodle; P. J. Sansom. *Chem. Soc. Perkin Trans.* **1985**, *2*, 737-742

<sup>169</sup> Y. Zhang; M. Anderson; J. L. Weisman; M. Lu; C. J. Choy; V. A. Boyd; J. Price; M. Sigal; J. Clark; M. Connelly; F. Zhu; W. A. Guiguemde; C. Jeffries; L. Yang; A. Lemoff; A. P. Liou; T. R. Webb; J. L. DeRisi; R. K. Guy. *ACS Med. Chem. Lett.* **2010**, *1*, 460-465

<sup>170</sup> C. Han; J. A. Porco. *Org. Lett.* **2007**, *9*, 1517-1520

<sup>171</sup> E. Artuso; I. Degani; R. Fochi; C. Magistris. *Synthesis* **2007**, 3497-3506

<sup>172</sup> A. I. Bazarov. *J. Prakt. Chem.* **1870**, *2*, 283-312

<sup>173</sup> A. K. H. Dheere; S. Bongarzone; C. Taddei; R. Yan; A. D. Gee. *Synlett* **2015**, *26*, 2257-2260

<sup>174</sup> H. G. Grimm. *Electrochem.* **1925**, *31*, 474-480

<sup>175</sup> A. I. Moskalenko; V. I. Boev. *Russ. J. Org. Chem.* **2009**, *45*, 1018-1023

<sup>176</sup> B. A. J. Clark; J. Parrick; R. J. J. Roderick. *J. Chem. Soc. Perkin Transactions 1* **1976**, *13*, 1361-1363

<sup>177</sup> J. M. Vierfond; Y. Mettey; L. Mascrier-Demagny; M. Miocque. *Tetrahedron Lett.* **1981**, *22*, 1219-1222

<sup>178</sup> H. A. Sharma; M. T. Hovey; K. A. Scheidt. *Chem. Comm.* **2016**, *52*, 9283-9286

<sup>179</sup> C. R. Hopkins; N. Collar. *Tetrahedron Lett.* **2004**, *45*, 8631-8633

<sup>180</sup> I. Simpson; S. A. St-Galley; S. Stokes; D. T. E. Whittaker; R. Wiewiora. *Tetrahedron Lett.* **2015**, *56*, 1492-1495

<sup>181</sup> C. M. Chou; Y. W. Tung; M. I. Ling; D. Chan; W. Phakhodee; M. Isobe. *Heterocycles* **2012**, *86*, 1323-1329

- <sup>182</sup> Y. Younis; F. Douelle; D. González-Cabrera; C. Le Manach; A. T. Nchinda; T. Paquet; L. Street; K. L. White; M. Zabiulla; J. T. Joseph; S. Bashyam; D. Waterson; M. J. Witty; S. Wittlin; S. A. Charman; K. J. Chibale. *Med. Chem.* **2013**, *56*, 8860-8871
- <sup>183</sup> C. Le Manach; A. T. Nchinda; T. Paquet; D. González-Cabrera; Y. Younis; Z. Han; S. Bashyam; M. Zabiulla; D. Taylor; N. Lawrence; K. L. White; S. A. Charman; D. Waterson; M. J. Witty; S. Wittlin; M. E. Botha; S. H. Nondaba; J. Reader; L. M. Birkholtz; M. B. Jiménez-Díaz; M. Santos-Martínez; S. Ferrer; I. Angulo-Barturen; S. Meister; Y. Antonova-Koch; E. A. Winzeler; L. Street; J. K. Chibale. *J. Med. Chem.* **2016**, *59*, 9890-9905
- <sup>184</sup> T. Itho; S. Kato; N. Nonoyama; T. Wada; K. Maeda; T. Mase; M. M. Zhao; J. Z. Song; D. M. Tschaen; J. M. McNamara. *Org. Process Res. Dev.* **2006**, *10*, 822
- <sup>185</sup> H. J. Brachwitz. *Prakt. Chem.* **1969**, *311*, 40
- <sup>186</sup> S. Martínez-González; A. I. Hernández; C. Varela; S. Rodríguez-Arístegui; J. Pastor. *Bioorg. Med. Chem. Lett.* **2012**, *22*, 1874-1878
- <sup>187</sup> P. J. Zimmermann; C. Brehm; W. Buhr; A. M. Palmer; W. A. Simon. *Bioorg. Med. Chem.* **2008**, *16*, 536-541
- <sup>188</sup> B. Jiang; C. G. Yang; W. N. Xiong; J. Wang. *Bioorg. Med. Chem.* **2001**, *9*, 1149-1154
- <sup>189</sup> J. J. Caldwell; N. Veillard; I. Collins. *Tetrahedron* **2012**, *68*, 9713-9728
- <sup>190</sup> R. Goel; V. Luxami; K. Paul. *R.S.C. Adv.* **2014**, *4*, 9885-9892
- <sup>191</sup> E. Lizano; J. Grima; M. D. Pujol. *Synlett* **2019**, *30*, 2000-2003
- <sup>192</sup> a) D. Bogdal; M. Lukasiewicz; A. Pielichowski; A. Miciak; Sz. Bednarz. *Tetrahedron* **2003**, *59*, 649-653 b) E. Buxaderas; D. A. Alonso; C. Nájera. *Eur. J. Org. Chem.* **2013**, 5864-5870 c) G. Broggin; V. Barbera; E. M. Beccalli; U. Chiacchio; A. Fasana; S. Galli; S. Gazzola. *Adv. Synth. Catal.* **2013**, *355*, 1640-1648 d) H. H. Nguyen; M. J. Kurth. *Org. Lett.* **2013**, *15*, 362-365 e) W. Qian; L. Zhang; H. Sun; H. Jiang; H. Liu. *Adv. Synth. Catal.* **2012**, *354*, 3231-3236 f) M. Baghbanzadeh; C. Pilger; C. O. Kappe. *J. Org. Chem.* **2011**, *76*, 8138-8142 g) J. F. Cívicos; D. A. Alonso; C. Nájera. *Adv. Synth. Catal.* **2011**, *353*, 1683-1687 h) E. M. Beccalli; A. Bernasconi; E. Borsini; G. Broggin; M. Rigamonti; G. Zecchi. *J. Org. Chem.* **2010**, *75*, 6923-6932 i) D. Liptrot; G. Alcaraz; B. Roberts. *Adv. Synth. Catal.* **2010**, *352*, 2183-2188
- <sup>193</sup> a) M. Bakherad. *Appl. Organomet. Chem.* **2013**, *27*, 125-140 b) C. Torborg; M. Beller. *Adv. Synth. Catal.* **2009**, *351*, 3027-3043 c) J. W. B. Cooke; R. Bright; M. J. Coleman; K. P. Jenkins. *Org. Process Res. Dev.* **2001**, *5*, 383-386
- <sup>194</sup> K. Sonogoshira; Y. Tohda; N. Hagihara. *Tetrahedron Lett.* **1975**, *16*, 4467-4470
- <sup>195</sup> H. C. Kolb; M. G. Finn; K. B. Sharpless. *Angew. Chemie Int. Ed.* **2001**, *40*, 2004-2021
- <sup>196</sup> R. Gujadhur; D. Ven Katarama; J. T. Kintight. *Tetrahedron Lett.* **2001**, *42*, 4791-4793
- <sup>197</sup> Z. Li; L. Hong; R. Lui; J. Shen; X. Zhou. *Tetrahedron Lett.* **2011**, *52*, 1343-1347
- <sup>198</sup> J. E. Baldwin. *J. Chem. Soc. Chem. Commun.* **1976**, *18*, 734-736
- <sup>199</sup> B. Sezen; D. Sames. *J. Am. Chem. Soc.* **2003**, *125*, 5274-5275
- <sup>200</sup> M. Tian; D. Sames. *J. Am. Chem. Soc.* **2006**, *128*, 8364-8364
- <sup>201</sup> T. W. Greene; P. G. W. Wuts. *Protective groups in organic synthesis*. John Wiley and Sons, Inc. 2<sup>nd</sup> edition, Harvard **1980**, pg 18
- <sup>202</sup> J. V. Haren; J. S. Toraño; D. Sartini; M. Emanuelli; R. B. Parsons; N. I. Martin. *Biochemistry* **2016**, *55*, 5307-5315
- <sup>203</sup> D. Kraus; Q. Yang; D. Kong; A. S. Banks; L. Zhang; J. T. Rodgers; E. Pirinen. *Nature* **2014**, *508*, 258-262
- <sup>204</sup> V. Bronte; P. Zanovello. *Nat. Rev. Immunol.* **2005**, *5*, 641-654

- <sup>205</sup> M. Pudio; C. Demougeot; C. Girard-Thernier. *Med. Res. Rev.* **2017**, *37*, 475-513
- <sup>206</sup> B. Allard; S. Pommey; M. J. Smyth; J. Stagg. *Clin. Cancer Res.* **2013**, *19*, 5626-5635
- <sup>207</sup> S. L. Gaffen. *Nat. Rev. Immunol.* **2009**, *9*, 556-567
- <sup>208</sup> M. Amin; K. Darji; D. J. No; T. Bhutani; J. J. Wu. *J. Dermatol. Treat.* **2018**, *29*, 347-352
- <sup>209</sup> O. Ouyang; J. K. Kolls; Y. Zheng. *Immunity* **2008**, *28*, 454-467
- <sup>210</sup> <https://openinnovation.lilly.com> (20/12/2018)
- <sup>211</sup> J. A. Padilla; I. Cotillo; J. Presa; J. Cantizani; I. Peña; A. I. Bardera; J. J. Martín; A. Rodriguez. *PLoS Negl. Trop. Dis.* **2015**, *9*, e0003493
- <sup>212</sup> E. Sorrentino; R. G. del Rio; X. Zheng; J. P. Matilla; P. T. Gomez; M. M. Hoyos; M. E. P. Herran; A. M. Losana; Y. Av-Gay. *Antimicrob. Agents Chemother.* **2016**, *60*, 640-645
- <sup>213</sup> P. W. Manthly; M. Koltzenburg; L. M. Mendell; L. Tive; D. L. Shelton. *Anesthesiology* **2011**, *115*, 189-204
- <sup>214</sup> S. L. Devos; R. L. Miller; K. M. Schoch; B. B. Holmes; C. S. Kebodeaux; A. J. Wegener; G. Chen; T. Shen; H. Tran; B. Nichols; T. A. Zanardi; H. B. Kordasiewicz; E. E. Swayze; C. F. Bennett; M. I. Diamond; T. M. Miller. *Sci. Transl. Med.* **2017**, *9*, eaag0481
- <sup>215</sup> N. T. Redpath; Y. Xu; N. J. Wilson; L. J. Fabri; M. Baca; A. E. Andrews; H. Braley; P. Lu; C. Ireland; R. E. Ernst; A. Woods; G. Forrest; Z. An; D. M. Zaller; W. R. Strohl; C. S. Luo; P. E. Czabotar; T. P. Garrett; D. J. Hilton; A. D. Nash; J. G. Zhang; N. A. Nicola. *Structure* **2010**, *18*, 1083-1093
- <sup>216</sup> S. D. Dib-Hajj; Y. Yang; J. A. Black; S. G. Waxman. *Nat. Rev. Neurosci.* **2013**, *14*, 49-62
- <sup>217</sup> X. Du; H. Hao; S. Gigout; D. Huang; Y. Yang; L. Li; C. Wang; D. Sundt; D. B. Jaffe; H. Zhang; N. Gamper. *Pain* **2014**, *155*, 2306-2322
- <sup>218</sup> S. Crunkhorn. *Nat. Rev. Drug Discov.* **2012**, *11*, 189-189
- <sup>219</sup> T. Xiao-long; W. Ying; L. Da-li; L. Jian; L. Ming-yao. *Acta Pharmacol. Sin.* **2012**, *33*, 363-371
- <sup>220</sup> J. Wang; G. Clarice; A. H. Rockman. *Circ. Res.* **2018**, *123*, 716-735
- <sup>221</sup> S. P. Alexander; A. Christopoulos. *Br. J. Pharmacol.* **2019**, *176*, 21-141
- <sup>222</sup> <https://www.guidetopharmacology.org> (20/05/2019)
- <sup>223</sup> <https://www.britannica.com> (20/05/2019)
- <sup>224</sup> M. Rodbell. *Environ Health Perspect.* **1995**, *103*, 338-345
- <sup>225</sup> V. V. Gurevich; E. V. Gurevich. *Int. J. Mol. Sci.* **2017**, *18*, e2519
- <sup>226</sup> C. J. Folts; S. Giera; T. Li; X. Piao. *Trends Pharmacol. Sci.* **2019**, *40*, 278-293
- <sup>227</sup> T. Warne; R. Moukhametzianov; J. G. Baker; R. Nehmé; P. C. Edwards; A. G. Leslie. *Nature* **2011**, *469*, 241-244
- <sup>228</sup> J. P. Vilaradaga; M. Bünemann; T. N. Feinstein; N. Lambert; V. O. Nikolaev; S. Engelhardt; M. J. Lohse; C. Hoffmann. *Mol. Endocrinol.* **2009**, *23*, 590-599
- <sup>229</sup> O. Civelli; R. K. Reinscheid; Y. Zhang; Z. Wang; R. Fredriksson; H. B. Schiöth. *Annu. Rev. Pharmacol. Toxicol.* **2013**, *53*, 127-146
- <sup>230</sup> A.S. Hauser; M. M. Attwood; M. Rask-Andersen; H. B. Schiöth; D. E. Gloriam. *Nat. Rev. Drug Discov.* **2017**, *6*, 829-842
- <sup>231</sup> Y. Lee; S. Basith; S. Choi. *J. Med. Chem.* **2018**, *61*, 1-46
- <sup>232</sup> F. Bassilana; M. Nash; M. G. Ludwig. *Nat. Rev. Drug Discov.* **2019**, *18*, 869-884
- <sup>233</sup> G. Aust; D. Zhu; E. G. Van Meir; L. Xu. *Handb. Exp. Pharmacol.* **2016**, *234*, 369-396
- <sup>234</sup> J. Hamann; G. Aust; D. Araç; F. B. Engel; C. Formstone; R. Fredriksson; R. A. Hall; B. L. Harty; C. Kirchhoff; B. Knapp. *Pharmacol. Rev.* **2015**, *67*, 338-367
- <sup>235</sup> T. K. Bjarnadóttir; K. Geirardsdóttir; M. Ingemansson; M. A. Mirza; R. Fredriksson; H. B. Schiöth. *Gene* **2007**, *387*, 38-48

- <sup>236</sup> M. C. Lagerström; H. B. Schiöth. *Nat. Rev. Drug Discov.* **2008**, *7*, 339-357
- <sup>237</sup> N. Kamesh; G. K. Aradhyam; N. Manoj. *BMC Evol. Biol.* **2008**, *8*, 129-129
- <sup>238</sup> A. Krishnan; M. S. Almén; R. Fredriksson; H. B. Schiöth. *PLoS One* **2012**, *7*, e29817
- <sup>239</sup> R. Fredriksson; M. C. Lagerström; L. G. Lundin; H. B. Schiöth. *Mol. Pharmacol.* **2003**, *63*, 1256-1272
- <sup>240</sup> <https://www.adhesiongpcr.org> (20/05/2019)
- <sup>241</sup> K. R. Monk; J. Hamann; T. Langenhan; S. Nijmeijer; S. Schöneberg; T. Liebscher. *Mol. Pharmacol.* **2015**, *88*, 617-623
- <sup>242</sup> D. Araç; A. A. Boucard; M. F. Bolliger; J. Nguyen; S. M. Soltis; T. C. Südhof; A. T. Brunger. *EMBO J.* **2012**, *31*, 1364-1378
- <sup>243</sup> H. M. Stoveken; A. G. Hajduczuk; L. Xu; G. G. Tall. *Proc. Natl. Acad. Sci. USA.* **2015**, *112*, 6194-61499
- <sup>244</sup> V. Krasnoperov; Y. Lu; L. Buryanovsky; T. A. Neubert; K. Ichtchenko; A. G. Petrenko. *J. Biol. Chem.* **2002**, *277*, 46518-46526
- <sup>245</sup> T. Langenhan; G. Aust; J. Hamann. *Sci. Signal.* **2013**, *6*, 1-21
- <sup>246</sup> G. S. Salzman; S. Zhang; A. Gupta; A. Koide; S. Koide; D. Araç. *Proc. Natl. Acad. Sci. USA.* **2017**, *114*, 10095-10100
- <sup>247</sup> L. M. Demberg; J. Winkler; C. Wilde; K. U. Simon; J. Schön; S. Rothmund; T. Schöneberg; S. Prömel; I. Liebscher. *J. Biol. Chem.* **2017**, *292*, 4383-4394
- <sup>248</sup> I. Liebscher; T. Schöneberg. *Handb. Exp. Pharmacol.* **2016**, *234*, 111-125
- <sup>249</sup> S.R. Coughlin. *Proc. Natl. Acad. Sci.* **1999**, *96*, 11023-11027
- <sup>250</sup> H. E. Hamm. *J. Biol. Chem.* **1998**, *273*, 669-672
- <sup>251</sup> G. B. Downes; N. Gautam. *Genomics* **1999**, *62*, 544-552
- <sup>252</sup> T. M. Cabrera-Vera; J. Vanhauwe; T. O. Thomas; M. Medkova; A. Preininger; M. R. Mazzoni; H. E. Hamm. *Endocr. Rev.* **2003**, *24*, 765-781
- <sup>253</sup> T. B. Patel. *Pharmacol. Rev.* **2004**, *56*, 371-385
- <sup>254</sup> T. R. Dorsam; J. S. Gutkind. *Nat. Rev. Cancer* **2007**, *7*, 79-94
- <sup>255</sup> S. R. Sprang. *Biopolymers* **2016**, *105*, 449-456
- <sup>256</sup> J. Wu; N. Xie; X. Zhao; E. C. Nice; C. Huang. *Cancer Genomics Proteomics* **2012**, *9*, 37-50
- <sup>257</sup> J. P. Mahoney; R. K. Sunahara. *Curr. Opin. Struct. Biol.* **2016**, *41*, 247-254
- <sup>258</sup> I. Litosch. *Life Sci.* **2016**, *152*, 99-106
- <sup>259</sup> D. Kankanamge; M. Tennakoon; A. Weerasinghe; L. Cedeno-Rosario; D. N. Chadee; A. Karunarathne. *Cell Signal.* **2019**, *58*, 34-43
- <sup>260</sup> T. M. Seasholtz; M. Majumdar; J. H. Brown. *Mol. Pharmacol.* **1999**, *55*, 949-956
- <sup>261</sup> B. K. Fung. *J. Biol. Chem.* **1983**, *258*, 10495-10502
- <sup>262</sup> V. A. Florio; P. C. Sternweis. *J. Biol. Chem.* **1989**, *264*, 3909-3915
- <sup>263</sup> D. G. Lambright; J. Sondek; A. Bohm; N. P. Skiba; H. E. Hamm; P. B. Sigler. *Nature* **1996**, *379*, 311-319
- <sup>264</sup> S. M. Khan; J. Y. Sung; T. E. Hébert. *Pharmacol. Res.* **2016**, *111*, 434-441
- <sup>265</sup> V. V. Gurevich; E. V. Gurevich. *Crit. Rev. Biochem. Mol. Biol.* **2015**, *50*, 440-452
- <sup>266</sup> C. A. Moore; S. K. Milano; J. L. Benovic. *Annu. Rev. Physiol.* **2007**, *69*, 451-482
- <sup>267</sup> S. M. DeWire; S. Ahn; R. J. Lefkowitz; S. K. Shenoy. *Annu. Rev. Physiol.* **2007**, *69*, 483-510
- <sup>268</sup> Y. K. Peterson; L. M. Luttrell. *Pharmacol. Rev.* **2017**, *69*, 256-297
- <sup>269</sup> H. M. Stoveken; L. L. Bahr; M. W. Anders; A. P. Wojtovich; A. V. Smrcka; G. G. Tall. *Mol. Pharmacol.* **2016**, *90*, 214-222

- <sup>270</sup> <http://www.adhesionpcr.de> (09/01/2020)
- <sup>271</sup> J. Gilissen; P. Geubelle; N. Dupuis; C. Laschet; B. Pirotte; J. Hanson. *Biochem. Pharmacol.* **2015**, *98*, 381-391
- <sup>272</sup> S. Mangmool; H. Kurose. *Toxins* **2011**, *3*, 884-899
- <sup>273</sup> T. Katada. *Biol. Pharm. Bull.* **2012**, *35*, 2103-2111
- <sup>274</sup> H. Zhang; A. L. Nielsen; K. Strømgaard. *Med. Res. Rev.* **2020**, *40*, 135-157
- <sup>275</sup> A. Nishimura; K. Kitano; J. Takasaki; M. Taniguchi; N. Mizuno; K. Tago; T. Hakoshima; H. Itoh. *Proc. Natl. Acad. Sci. USA* **2010**, *107*, 13666-13671
- <sup>276</sup> [www.promega.es](http://www.promega.es) (25/05/2019)
- <sup>277</sup> <https://www.thermofisher.com> (25/05/2019)
- <sup>278</sup> M. Buccioni; G. Marucci; D. Dal Ben; D. Giacobbe; C. Lambertucci; L. Soverchia; A. Thomas; R. Volpini; G. Cristalli. *Purinergic Signal.* **2011**, *7*, 463-468



## 7. ANNEX 1

### 7.1. A REVIEW OF THE ADHESION GPCRS FROM THE AVAILABLE LITERATURE UNTIL NOW

A review of 33 adhesion GPCRs has carried out in order to collect in tables the available information of these receptors.

Abbreviations:

Calx: Calnexin

CUB: Cs1 and Csr/Uegf/BMP1

EGF\_Ca: Calcium-binding EGF

EPTP: Epitepin

HRM: Hormone receptor motif

I-set: immunoglobulin I-set domain

L\_EGF: laminin\_EGF

LRR: leucine-rich repeat

OLFM: olfactomedin

PTX: pentraxin

RBL: rhamnose-binding lectin

SEA: sperm protein, enterokinase, agrin module

TSP: trombospondin

AM: adhesion and migration

CC: Cell cycle, death and differentiation

CD: Cell development

CNS: Central nervous system

CVS: Cardiovascular system

DS: Digestive system

ESM: Endocrine system and metabolism

HIS: Hematopoietic system and immunity

MS: Musculoskeletal system

MSM: Musculoskeletal system and metabolism

NS: Nervous system

PCP: Planar cell polarity

RO: Reproductive system

RS: Respiratory system

S: Skin

SO: Sensory organs

US: Urinary system

Subfamily		I (L, Latrophilin)			
Gene name		LPHN1	LPHN2	LPHN3	ELTD1
Protein name (alternative names)		ADGRL1	ADGRL2	ADGRL3	ADGRL4
Chromosome <sup>(1)</sup> (human)		19	1	4	6
NTF architecture <sup>(2)</sup> (number of repetitions)		RBL, OLFM, HRM	RBL, OLFM, HRM	RBL, OLFM HRM	EGF, EGF_Ca
Expression <sup>(3)</sup> (human)	Absent in	Hematopoietic system, astrocytes (SNC), oligodendrocytes (SNC), microglia(SNC), schwann cells (PNS)	-	Pancreas exocrine cells, kidney glomerulus (mesangial cells), astrocytes (CNS), oligodendrocytes (CNS), microglia (CNS), schwann cells (PNS)	-
	Present in	Heart Myocytes, lung pneumocytes (alveolar cells), liver hepatocytes, pancreas exocrine cells, kidney glomerulus (mesangial cells), adrenal gland medulla, anterior pituitary gland, pancreas endocrine cells (islets of Langerhans), placenta,skeletal muscle myocytes, neurons (CNS and PNS)	Same than LPHN1 except adrenal gland medulla	Heart myocytes, lung pneumomyocytes (alveolar cells), liver hepatocytes, placenta, breast mammary gland epithelial cells, skeletal muscle myocytes, neurons (CNS)	Heart myocytes, vasculature smooth muscle cells, urinary bladder smooth muscle cells, uterus myometrium
Functional involvement		CVS, NS <sup>(4-7)</sup>	CC, CVS, NS <sup>(8)</sup>	NS <sup>(9)</sup>	CVS <sup>(10)</sup>
Functional specifications		Axon guidance, neuronal connectivity, synapse formation	Expression is required for heart valve formation	Formation and regulation of excitatory synapses	Cardiac development and cardioprotection Regulation of physiological and tumour angiogenesis
Ligands <sup>(3)</sup>		Lasso (PA), LTX (FA), $\alpha$ -latrotoxin (FA), neurexin-1 $\alpha$ , -1 $\beta$ , -2 $\beta$ and -3 $\beta$ proteins*	$\alpha$ -latrotoxin (FA) (commercial)	FLRT3 (FA)	-
Disorders		-	Microcephaly with rhombencephalosynapsis <sup>(11)</sup>	-	-
Knock out		Neuropsychiatric syndromic disorder in humans <sup>(12)</sup>	-	-	-

<b>SNP</b>	-	-	Risk factor for attention deficit/hyperactivity disorder <sup>(13-15)</sup>	-
<b>Tumorigenesis</b>	Expressed in human monocytic leukemia cell lines and in primary human acute myeloid leukemia (AML) cells <sup>(16)</sup>	Cancer cells in GI cancer with lower LPHN2 expression show higher sensitivity to cisplatin <sup>(17)</sup>	Mutation of missense in lung cancer have been predicted to result in loss of function of the receptor – Tumor suppressor <sup>(18)</sup>	ELTD1 protein levels are significantly higher in human gliomas <sup>(19)</sup> High endothelial cell ELTD1 expression was found to correlate with improved overall survival in a number of cancer types <sup>(4)</sup>

\*Neurexins 1 $\beta$ , 2 $\beta$  and 1 $\alpha$  have been reported to bind ADGRL1 but have not been shown to stimulate it or cause any effect, except limited increase in adhesion between ADGRL1-transfected and NRXN-transfected HEK293 cells.

Subfamily		II (E, EGF-TM7)				
Gene name		EMR1	EMR2	EMR3	EMR4	CD97
Protein name (alternative names)		ADGRE1	ADGRE2	ADGRE3	ADGRE4	ADGRE5
Chromosome <sup>(1)</sup> (human)		19	19	19	19	19
NTF architecture <sup>(1)</sup> (number of repetitions)		EGF, EGF_Ca(5)	EGF, EGF_Ca (4)	EGF, EGF_Ca	EGF, EGF_Ca (no span-seven transmembrane region)	EGF, EGF_Ca (4)
Expression <sup>(3)</sup> (human)	Absent in	-	-	-	-	Circulation erythrocytes, thyroid thyrocytes, thyroid C cells, pancreas endocrine cells (islets of Langerhans), skin epidermis keratinocytes, CNS microglia
	Present in	Circulation granulocytes	Bone marrow hematopoietic stem/progenitor cells, circulation granulocytes, circulation/tissue-monocytes/macrophages/ dendritic cells	Circulation granulocytes, circulation/tissue-monocytes/macrophages/ dendritic cells	Circulation/tissue-monocytes/macrophages/dendritic cells	Bone marrow hematopoietic stem/progenitor cells, circulation platelets, circulation lymphocytes, circulation granulocytes, circulation/tissue monocytes/macrophages/dendritic cells, heart myocytes, vasculature smooth muscle cells, trachea bronchi epithelial cells, lung pneumocytes (alveolar cells), intestine epithelial cells (resorptive, goblet, paneth cells), pancreas exocrine cells, kidney glomerulus (mesangial cells), urinary bladder smooth muscle cells, uterus myometrium, skeletal muscle myocytes
Functional involvement		AM, HIS <sup>(20) (21)</sup>	AM, HIS <sup>(22) (23-25)</sup>	HIS <sup>(26, 27)</sup>	Pseudogene (nonfunctional) <sup>(26, 27)</sup>	AM, HIS, CVS, RS, DS <sup>(28-32)</sup>
Functional specifications		Essential for the induction of peripheral immune tolerance from eye derived antigens (in mice)	Enhance neutrophil migration, degranulation, and cytokine secretion, as well as in suppressing lipopolysaccharide induced neutrophil survival Differentiation and inflammatory activation of human monocytic cells Possible requirement of EMR2 in the generation of immune tolerance in humans	-	-	Establishes an osmotic gradient enabling intestinal fluid secretion. This is pivotal in the creation of an ideal environment for effective enzymatic digestion, nutrient absorption, and stool movement Implicated in innate and adaptive immune processes

<b>Ligands</b> <sup>3</sup>	-	-	-	-	CD55, α5β1 integrin, chondroitin sulfate B and CD90 (Thy1) *
<b>Disorders</b>	Eosinophilic disorders <sup>(33)</sup>	Vibratory urticarial <sup>(25)</sup>	-	-	-
<b>Knock out</b>	-	-	-	-	-
<b>SNP</b>	-	-	-	-	-
<b>Tumorigenesis</b>	-	Immune suppressing function in tumor cells (breast cancer) <sup>(34)</sup> Upregulation of EMR2 in GBM is associated with poor survival <sup>(35)</sup> A significant but low number of colorectal carcinomas are positive for EMR2 <sup>(36)</sup> Lung cancer (adenocarcinomas) <sup>(37)</sup>	Upregulation of EMR3 in GBM is associated with poor survival <sup>(169)</sup>	-	CD97 and CD55 are involved in the dedifferentiation, migration, invasiveness and metastasis of tumors, examples: In thyroid cancer, expression levels correlate with dedifferentiation. <sup>(38)</sup> In colorectal cancer is overexpressed in the invasion front. <sup>(39) (40)</sup> In Gall bladder carcinoma and glioblastoma expression is inversely related to overall survival. <sup>(41) (42)</sup> Has been identified as a leukemic stem cell marker in acute myeloid leukemia. <sup>(41)</sup> Marker for minimal residual disease in acute lymphoblastic leukemia <sup>(43)</sup> CD97 promotes gastric cancer cell proliferation and invasion in vitro <sup>(44)</sup>

\* Each was able to bind to the receptor as a ligand but none were found to have agonist activity at the receptor

Subfamily	III (A)		
Gene name	GPR123	GPR124	GPR125
Protein name (alternative names)	ADGRA1	ADGRA2	ADGRA3
Chromosome <sup>(1)</sup> (human)	10	8	4
NTF architecture <sup>(1)</sup> (number of repetitions)	No specific domain (No GPS)	LRR-8, HRM	LRR-8, I-set, HRM
Expression <sup>(3)</sup> (human)	Absent in	-	-
	Present in	Vasculature endothelial cells, CNS	Eye retina, CNS, placenta, prostate, ovary, heart, skeletal muscle, small intestine, colon, lung, liver, kidney, pancreas, spleen, testis
Functional involvement	Unknown	CVS, RS ,CNS <sup>(5, 39, 41, 42, 45)</sup>	RS <sup>(46)</sup>
Functional specifications	-	In CNS endothelial cells to regulate sprouting and migration Controls CNS angiogenesis and blood-brain barrier integrity	Role in repopulating spermatogonial stem cells (SSCs) in the adult human testes
Ligands <sup>(3)</sup>	-	Several GAGs <sup>+</sup>	-
Disorders	-	CNS related vascular pathologies* <sup>(5, 41, 45)</sup>	-
Knock out	-	Embryonic lethality (mouse) <sup>(5, 45)</sup> Reduced lung size (mouse) <sup>(5, 45)</sup>	-
SNP	-	-	-
Tumorigenesis	-	Highly expressed in tumor vasculature: GPR124 is required for VEGF induced tumor angiogenesis <sup>(45)</sup>	Overexpression suppress colorectal cancer formation by interacting with the Wnt pathway <sup>(47)</sup> Up-regulation of GPR125 promoted cell adhesion and contributed to myeloid sarcoma formation <sup>(48)</sup> Highly expressed in human brain cancer tissues (detected as oncogene) <sup>(41)</sup>

\* Vascular overexpression results in CNS specific hyperproliferative vascular malformations, suggesting relevance for GPR124 in various CNS related vascular pathologies.

+ Gpr124 physically interact to synergistically stimulate Wnt7-specific responses in the brain.

Subfamily		IV (C,CELSR)		
Gene name		CELSR1	CELSR2	CELSR3
Protein name (alternative names)		ADGRC1	ADGRC2	ADGRC3
Chromosome <sup>(1)</sup> (human)		22	1	3
NTF architecture <sup>(2)</sup> (number of repetitions)		C (9),EGF_Ca (2), L_G/Ptx, EGF_Ca, L_G/Ptx, EGF_Ca, L_EGF (No proteolysis in GPS)	C (9),EGF_Ca (2), L_G/Ptx, EGF_Ca, L_G/Ptx, EGF_Ca, L_EGF	C (9),EGF_Ca (2), L_G/Ptx, EGF_Ca, L_G/Ptx, EGF_Ca, L_EGF
Expression <sup>(3)</sup> (human)	Absent in			Neural stem cells
	Present in	Neural stem cell	CNS neurons, eye retina (CNS), neural stem cell, intermediate progenitors (IP)	Neurons
Functional involvement		CD (Cell development), PCP, CVS, RS, US, S, NS, SO <sup>(49)</sup> (48, 50-63)	CD, PCP, CC, CVS, ESM,NS <sup>(50-53),(48, 60-67)</sup> (68)	CD, PCP, CC, ESM, NS, RS <sup>(49)</sup> (50-52),(48, 61-67) (68-73)
Functional specifications *		Regulates epithelial planar cell polarity (PCP) in several organs (abates postnatally in parallel to decreasing numbers of NSC) Ex: plays a critical role for PCP establishment in the developing skin and hair follicles Facilitates neural tube closure via core PCP signaling Role in the planar polarity of vestibular hair cells during inner ear development Important in mammalian kidney development and role in rostrocaudal patterning during organogenesis	Development and maintenance of the nervous system Regulate dendrite morphogenesis Regulate axonal navigation in the forebrain and in the limbs (with Fzd3) Ciliogenesis and neural development, especially neuron migration and axon guidance in the central, peripheral and enteric nervous systems	Neuronal maturation Regulate dendrite morphogenesis Regulate axonal navigation in the forebrain and in the limbs (with Fzd3) Ciliogenesis and neural development, especially neuron migration and axon guidance in the central, peripheral and enteric nervous systems Is required for the fine mapping of sensory fibers in the spinal cord
Ligands <sup>(3)</sup>		Vangl2 (core PCP protein), VhaPRR (accessory unit of the proton pump V-ATPase) via HRM domain of CELSR1	Unknown <sup>+</sup>	Unknown <sup>+</sup>
Disorders		Neural tube defects: caudal agenesis type II, chiari II malformation, craniorachischisis, hydrocephalus, hydromyelia, lipoma, lipomyelocele, lipomyelomeningocele, myelomeningocele <sup>(74)</sup> ischemic stroke, possible risk factor for chronic obstructive pulmonary disease risk among women <sup>(75)</sup>	Idiopathic scoliosis in the Swedish-Danish population <sup>(76)</sup> May be related with Joubert Syndrome <sup>(77)</sup> Associated with myocardial infraction <sup>(42, 64)</sup>	Associated with Tourette disorder <sup>(78)</sup> Hirschsprung disease <sup>(79)</sup>

<b>Knock out</b>	<p>Defects in the orientation of hair outgrowth in the adult (mice) <sup>(80)</sup></p> <p>Defects in hindbrain neuron migration (mouse) <sup>(81)</sup></p> <p>Defects in vestibular hair cells during inner ear development (mice) <sup>(59)</sup></p> <p>Induced missense mutations develop the severe neural tube defect <sup>(82)</sup></p> <p>Induced missense mutation develop lung branching defects <sup>(57)</sup></p>	<p>Simplification of dendritic arbors of cortical pyramidal neurons and Purkinje neurons (rat brain) <sup>(83)</sup></p> <p>Defects in the migration of hindbrain neurons (mouse) <sup>(84)</sup></p> <p>Reduced quiescence of haemopoietic stem cells (mice) <sup>(85)</sup></p> <p>Defects in the development and planar organization of ependymal cilia are compromised, leading to a fatal hydrocephalus (mice) <sup>(86)</sup></p> <p>Mice deficient for ADGRC 2/3 had severe defects in pancreatic beta cell differentiation, resulting in decreased glucose clearance <sup>(66)</sup></p>	<p>Mice deficient for ADGRC 2/3 had severe defects in pancreatic beta cell differentiation, resulting in decreased glucose clearance <sup>(66)</sup></p> <p>Defects in tangential cortical interneuron migration (mouse) <sup>(87)</sup></p> <p>Dysfunction of hippocampal connectivity and maturation and forebrain wiring (mouse) <sup>(88)</sup></p> <p>Defects in forebrain connections such as the anterior commissure and thalamocortical and corticospinal tracts (mouse) <sup>(89)</sup></p> <p>Impaired axonal development (mouse)</p> <p>Marked malformation in the forebrain, absence of anterior commissure, and abnormalities in major axonal tracts (mouse) <sup>(90)</sup></p>
<b>SNP</b>	-	Correlated with decreased low density lipoprotein levels (risk for coronary artery disease) <sup>(91)</sup>	-
<b>Tumorigenesis</b>	<p>Associated with glioma and glioblastoma (up-regulated) <sup>(92) (93)</sup></p> <p>May act as an invasion suppressor in ductal carcinoma <sup>(94)</sup></p> <p>mRNA expressed in gastrointestinal tumor <sup>(95)</sup></p>	Cytoplasmic expression significantly stronger in breast cancer <sup>(96)</sup>	<p>Associated with colorectal cancer metastasis <sup>(97)</sup></p> <p>In pancreatic, bladder, renal, hepatic and oral carcinogenesis CELSR3 was identified as a hypermethylated marker <sup>(98) (99) (84) (100) (101)</sup></p>

\* Subfamily ADGRC (CELSR) receptors recruit Rho- GEFs during PCP signaling to control the size and shape of asymmetric epithelial membrane domains. It is nearly believed that ADGRC (CELSR) proteins form homodimeric molecular bridges between neighboring cells. ADGRCs (CELSRs) are therefore fundamental to local PCP transmission, and their asymmetric enrichment at both interfaces of opposing cell membranes is unique (Strutt et al., 2002; Devenport et al., 2011).

+ CELSR/FZD receptors are probably activated by WNT ligands but no ligand receptor-binding interaction was clearly identified.



Subfamily		V (D)	
Gene name		GPR133	GPR144
Protein name (alternative names)		ADGRD1	ADGRD2
Chromosome <sup>(1)</sup> (human)		12	9
NTF architecture <sup>(2)</sup> (number of repetitions)		Laminin_G/Ptx	Laminin_G/Ptx
Expression <sup>(3)</sup> (human)	Absent in	Pons, hippocampus, thalamus, medulla, midbrain, hypothalamus, amygdala and frontal cortex	-
	Present in	Anterior pituitary gland	CNS neurons
Functional involvement		CVS <sup>(102)</sup> , MS <sup>(103-106)</sup>	-
Functional specifications		Heart rate control, associated locus with human height and weight	-
Ligands <sup>3</sup>		Tethered peptide from its ECD (Stachel sequence)	-
Disorders		-	-
Knock out		-	-
SNP		May cause clinically relevant phenotypes (approximately 9000 single nucleotide polymorphisms (SNPs) in the human ADGRD1) <sup>(103)</sup> SNPs associated with RR duration leading to an increase of one beat per second in heart rate <sup>(102)</sup> Association of ADGRD1 with the postprandial levels of very low density lipoproteins (VLDL) <sup>(107)</sup>	-
Tumorigenesis		Is expressed within hypoxic regions of GBM, promotes tumor growth In Vitro and In Vivo and It's expression correlates with poor prognosis in GBM <sup>(108)</sup> Up-regulated in a murine model of gastrointestinal stromal tumors <sup>(109)</sup>	-

Subfamily	VI (F)				
Gene name	GPR110	GPR111	GPR113	GPR115	GPR116
Protein name (alternative names)	ADGRF1	ADGRF2	ADGRF3	ADGRF4	ADGRF5
Chromosome <sup>(1)</sup> (human)	6	6	2	6	6
NTF architecture <sup>(2)</sup> (number of repetitions)	SAE	No specific domain (No GPS)	HRM	No specific domain (No GPS)	SEA, I-set, Ig_2
Expression <sup>(3)</sup> (human)	Absent in				
	Present in	Kidney glomerulus (mesangial cells), kidney tubules (proximal, distal, collecting), prostate epithelial cells, trachea, mouth and lungs		Kidney (cortex and medulla), small bowel and pancreas	Skin epidermis keratinocytes, mouth, heart, uterus, vascular
Functional involvement	US	S (mouse)			RS, S
Functional specifications	-	Suggesting hypothesis that play a function in skin specialization that is essential for life in land <sup>(110)</sup>	-	Suggesting hypothesis that play a function in skin specialization that is essential for life in land <sup>(110)</sup>	Pulmonary surfactant production, essential for surfactant homeostasis <sup>(111-114)</sup>
Ligands <sup>(3)</sup>	Tethered peptide from its ECD (Stachel sequence) <sup>(115)</sup> Synaptamide * (mouse) <sup>(116, 117)</sup>				Surfactant protein D <sup>(113, 118)</sup>
Disorders					
Knock out	Decelerates carcinogen-induced hepatocarcinogenesis via activation of the IL-6/STAT3 pathway (mouse) <sup>(119)</sup> Loss of Gpr110, Gpr111, or Gpr115 function did not result in detectable defects <sup>(110)</sup>	Loss of Gpr110, Gpr111, or Gpr115 function did not result in detectable defects <sup>(110)</sup>		Loss of Gpr110, Gpr111, or Gpr115 function did not result in detectable defects <sup>(110)</sup>	Local inflammation in the lung (emphysema symptoms) (mice) <sup>(42)</sup> Glucose intolerance and insulin resistance (mice) <sup>(120)</sup> Loss of the both GPR116 and ELTD1 results in malformation of the cardiac outflow tract and the aortic arch arteries as well in the postnatal development of a thrombotic microangiopathy (mice) <sup>+(121)</sup>
SNP	-	-	-	-	-

<b>Tumorigenesis</b>	<p>Overexpression of GPR110 was correlated with the advanced stage of osteosarcoma.<sup>(122)</sup> Correlated with cell malignant transformation and tumor metastasis in glioma.<sup>(122, 123)</sup> Oncogene in prostate and lung cancer.<sup>(124)</sup> Potential role of GPR110 in tumorigenicity and in tumor cell dissemination in HER2+ breast cancer.<sup>(125)</sup> Overexpressed in papillary thyroid cancer while underexpressed in anaplastic thyroid and follicular thyroid cancer.<sup>(126)</sup> High expression predicts a poor prognosis of gastric cancer patients<sup>(127)</sup></p>	<p>-</p>	<p>Its expression could serve as a useful marker for distinguishing gastric duodenal neuroendocrine tumors (down regulated) from small bowel neuroendocrine tumor and pancreatic neuroendocrine tumor.<sup>(128) (33) (33)</sup></p>	<p>Potential prognostic biomarker in lung squamous cell carcinoma<sup>(129)</sup></p>	<p>High expression has been significantly associated with poor overall survival of colorectal carcinoma patients<sup>(130)</sup> Recurrent mutations in early gastric cancer so it may be involved in early carcinogenesis<sup>(131)</sup> Associated with progression, metastasis, and poor prognosis in breast cancer patients. In breast cancer cell lines modulates motility and morphology<sup>(132)</sup> Overexpressed in lung adenocarcinoma<sup>(133)</sup></p>
----------------------	--	----------	--	---	--

\* Metabolite of the omega-3 fatty acid docosahexanoic (N-docosahexaenylethanolamine, synaptamide), potently promotes neurogenesis, neuritogenesis and synaptogenesis. Mediating synaptamide-induced bioactivity in a cAMP-dependent manner.  
+ Knockout alone of the receptors had no obvious effect in the CV or renal system.

Subfamily		VII (B,BAI)		
Gene name		BAI1	BAI2	BAI3
Protein name (alternative names)		ADGRB1	ADGRB2	ADGRB3
Chromosome <sup>(1)</sup> (human)		8	1	6
NTF architecture <sup>(2)</sup> (number of repetitions)		TSP1(5), HRM	TSP1 (4), HRM	CUB, TSP1(4), HRM
Expression <sup>(3)</sup> (human)	Absent in	Placenta, lung, liver, skeletal muscle, kidney, pancreas, spleen, thymus, prostate, testis, ovary, intestines, leukocytes		
	Present in	Circulation/tissue monocytes/macrophages/DCs, brain tissues (hippocampus, basal ganglia, cerebral cortex, and olfactory bulb), neurons and glia, skeletal muscle myoblasts, peritoneal exudate cells, bone marrow, the spleen, the colon, and testes	Brain (adult and neonatal), different embryonically cells types in brain, heart, skeletal muscle, intestine, thymus	Brain (adult and neonatal <sup>™</sup> ) (abundance in the postsynaptic neuron part), in various adult human tissues: the heart, testis, and small intestinal tissues
Functional involvement		CD, CC, HIS, CVS, MSM, NS <sup>(100, 134-148) (145, 149, 150)</sup>	CC, MS, NS <sup>(151) (152) (153) (154) (155) (144)</sup>	CVS, NS <sup>(156-159) (140, 160, 161)</sup>
Functional specifications		Inhibition of angiogenesis/tumorigenesis <sup>♠</sup> Synaptogenesis* Phagocytosis (Engulfment receptor) (especially involved in the clearance of dying neurons by promoting phagosome formation in microglia) <sup>x</sup> . Pattern recognition receptor, interacting with bacterial (Gram -) lipopolysaccharide (LPS) for innate immunity and inflammation in host cells (macrophages) (Pattern recognition receptor) (bacterial cell clearance). Promotes phagosomal reactive oxygen species (ROS) production. <sup>α</sup> Mediator of myoblast function (myogenesis) <sup>+</sup> . Role for BAI1 in facilitating macrophage anti-viral responses <sup>(135)</sup>	Inhibition of angiogenesis	Myoblast fusion <sup>♠</sup> Regulation of dendrite morphogenesis <sup>β</sup> Regulation of synaptogenesis <sup>Ω</sup> Inhibition of angiogenesis Involved in the inhibition of Insulin secretion from pancreatic $\beta$ -cells <sup>Σ</sup>
Ligands <sup>(3)</sup>		p53-binding site <sup>#</sup> , CD36 (inhibition angiogenesis), $\alpha\beta$ 5 integrin (inhibition of proliferation of endothelial cells), phosphatidylserine (clearance apoptotic cells). BAI1-associated protein 1 (Magi 1) (involved in cell adhesion and signal transduction in brain), BAI1-associated protein 2 (link between membrane and cytoskeleton in the process of neuronal growth), BAI1-associated protein 3 (involved in neuronal function (regulating release of neurotransmitters)), BAI1-associated protein 4. Its C terminus can interact with several PDZ domain-containing synaptic proteins (MAGI-1, MAGI-3, and PSD-95), which can regulate various signaling cascades downstream	GA-binding protein gamma (GABP $\gamma$ ), GABP $\alpha/\gamma$ or GABP $\alpha/\beta$ <sup>¥</sup> Cytoplasmic region binds to glutaminase interacting protein (GIP)	Complement component 1, q subcomponent-like 1 (C1q1), C1q2, C1q3 and C1q4
Disorders		Decreased in Parkinson disease <sup>(162)</sup> Involved in neurological diseases <sup>(163)</sup>	Expression decreases in the ischemic cerebral	Downregulated in the early phase of ischemia-induced brain injury <sup>(157)</sup>

	<p>BAI1-ELMO1-Rac1 pathway may be a therapeutic target for raising HDL levels to combat cardiovascular disease <sup>±(164)(165)</sup></p> <p>Involved in the suppression of angiogenesis and neuronal differentiation for revascularization of the damaged brain tissue (ischemia)<sup>(166)</sup></p>	<p>cortex after ischemia induction<sup>(151)</sup></p> <p>Could play an important role in mood disorders<sup>(151)</sup></p> <p>Implicated in a neurological disorder, specifically, in progressive spastic paraparesis<sup>(167)</sup></p>	<p>Could be linked with type 2 diabetes<sup>(168)</sup></p> <p>Psychiatric and neurological disorders (bipolar disorder, schizophrenia <sup>v</sup>, amongst others)<sup>(169) (170)</sup></p>
<b>Knock out</b>	<p>Increased tumor progression (mice) <sup>(171)</sup></p> <p>Pronounced colitis and lower survival (mice) <sup>(172)</sup></p> <p>Increased numbers of apoptotic cells in mice aortic roots, which correlated with altered lipid profiles (Relation BAI1-ABCA1) <sup>(164)</sup></p>	<p>Mice lacking BAI2 were found to have no gross deficits, but did exhibit increased hippocampal neurogenesis and a resilience to learned-helplessness behavior (important role related to depression)<sup>(151)</sup></p>	-
<b>SNP</b>	-	-	<p>Significantly associated with the disorganization symptom of schizophrenia <sup>(173)</sup></p> <p>Associated with early-onset venous thromboembolism<sup>(45)</sup></p>
<b>Tumorigenesis</b>	<p>Expression is absent or downregulated in glioblastoma <sup>(141, 144)</sup>, colorectal cancer <sup>(174)</sup>, metastatic brain tumors derived from lung <sup>(175)</sup> renal cell carcinoma, <sup>(176)</sup> astrocitoma,<sup>(177)</sup> meduloblastomas,<sup>(96)</sup> lung adenocarcinoma, <sup>(178)</sup> bladder transitional cell carcinoma, <sup>(179)</sup> and breast cancer <sup>(180)</sup>. The expression levels are inversely correlated with tumor vascularization <sup>(174)(181) (96, 131, 178, 182, 183)</sup></p> <p>Mutations in ADGRB1 are associated with squamous cell carcinoma of the lung and ovarian cancer <sup>(184)</sup></p> <p>Restoration of BAI1 expression has been reported to decrease proliferation and vascularization of tumors associated with renal carcinomas and gliomas<sup>(182, 185, 186)</sup></p> <p>BAI1 expression that was lost in a selection of human cancer cell lines could be restored by wild-type p53 adenoviral transfection<sup>(181)</sup></p>	<p>Mutations in ADGRB2 are associated with HER2+, HR+ and triple-negative forms of breast cancer, squamous cell carcinoma of the lung, other forms of lung cancer and ovarian cancer <sup>(18)</sup></p>	<p>Mutations in BAI3 are associated with lung adenocarcinoma, squamous cell carcinoma, small cell carcinoma and ovarian cancer<sup>(84)</sup></p> <p>Expression decreased in malignant glioma compared to the normal<sup>(157)</sup></p>

	Antitumor effects of Vstat120 (cleaved and secreted extracellular fragment of BAI1) delivery into established tumors and supports the further development of Rapid Antiangiogenesis Mediated By Oncolytic virus as a possible cancer therapy <sup>(183)</sup>		
--	---	--	--

⌘ BAI1 contains 5 TSP that can be cleaved by matrix metalloproteinase 14 (MMP14) to release Vstat40 (vasculostatin 40), which inhibits angiogenesis

\* Through PAR3/TIAM1/RAC1

± BAI1-ELMO1-Rac1 signaling pathway was found to contribute to the upregulation of ATP-binding cassette transporter 1 (ABCA1), which is known to be a critical cholesterol transporter that is essential for high-density lipoprotein (HDL). Higher HDL levels strongly correlate with a lower incidence of cardiovascular disease

+ Apoptotic myoblasts expose phosphatidylserine which activates BAI 1 signaling on healthy myoblasts to promote fusion with myoblast and myotubes.

α Via activation of the Rho family guanosine triphosphate (GTPase) Rac1, improving the microbicidal activity of the macrophages. BAI 1 is necessary not only clearance via macrophages, but also for activation of the phagosomal nicotinamide adenine dinucleotide phosphate (NADPH) oxidase complex.

X Binding phosphatidylserine mediate the uptake of apoptotic cells by numerous cell types, including macrophages and microglia, operating with the upstream of the signaling comprised of ELMO/Dock180/Rac proteins, facilitating the clearance.

# The regulatory role of p53 in BAI1 is not clear. Some studies show that BAI1 is transcriptionally regulated by p53<sup>(144, 187)</sup> meanwhile others have shown that the level of BAI1 messenger RNA (mRNA) does not correlate with the p53 status.<sup>(141)</sup>

¥ Expression of BAI2 inversely correlates with the vascular endothelial growth factor (VEGF) expression, which is a key mediator of angiogenesis. GA-binding protein gamma (GABPgamma) associates with the cytoplasmic domain of BAI2, and GABPalpha/gamma or GABPalpha/beta works as a transcriptional repressor of VEGF. The C-terminal fragment cleaved at the GPS domain specifically activated the nuclear factor of activated T-cells (NFAT) pathway. Furin prohormone convertase cleaved BAI2 at a different site of the GPS in the ECR.<sup>(188)</sup>

Π During embryonic stages, the expression of BAI3 mRNA is limited to the central nervous system unlike the other members of BAI family.

B The C-terminal region binds to ELMO, resulting in the regulation of dendrite morphogenesis via the activation of small GTPase Rac1.

μ Regulated by C1qL4 and stabillin 2, ligand of BAI3 and its binding partner, respectively. BAI1 and BAI3 can promote myoblast fusion via binding to ELMO-Dock1 in muscle development and repair.

Ω BAI3 binds to the C1ql protein that is expressed and secreted in the brain, and this interaction is important for the regulation of synapse formation and maintenance. It has been demonstrated that the expression of BAI3 is enhanced in Purkinje cells, and C1ql1, as a ligand of BAI3, regulates the spinogenesis of Purkinje cells in a BAI3-dependent manner<sup>(159)</sup>

∑ As a receptor of Clq3.

γ Its expression is changed by treatment with lithium carbonate, an effective drug for bipolar disorder.

Subfamily		VIII (G)		
Gene name		GPR56	GPR64	GPR97
Protein name (alternative names)		ADGRG1	ADGRG2	ADGRG3
Chromosome <sup>(1)</sup> (human)		16	X	16
NTF architecture <sup>(2)</sup> (number of repetitions)		Pentraxin/Laminin/neurexin/sex-hormone-binding-globulin-Like (PLL) <sup>(189)</sup>	No specific domains	No specific domains
Expression <sup>(3)</sup> (human)	Absent in	Circulation granulocytes, circulation/tissue monocytes/macrophages/DCs		
	Present in	Circulation lymphocytes, liver hepatocytes, thyroid thyrocytes, testis, sertoli cells, heart, placenta, lung, brain (hippocampus and hypothalamic nuclei CNS microglia, PNS schwann cells, hematopoietic and mesenchymal stem cells	Parathyroid, testis sertoli cells, epididymis epithelial cells, fibroblasts	Circulation granulocytes, vasculature endothelial cells, marrow, blood, lung, liver, leukemia cells
Functional involvement		AM, HSI, RO, MS, NS <sup>(39, 41, 77, 115, 173, 189-207)</sup>	RS <sup>(208-212)</sup>	HSI, CVS <sup>(213)</sup> (200, 208, 214-216)
Functional specifications		Critical for the frontal cortex development. <sup>α</sup> Oligodendrocyte development and CNS myelination. <sup>β</sup> Regulator in the development and maintenance of peripheral myelin. Myoblast differentiation. <sup>γ</sup> Testis development and male fertility Regulates cytotoxic NK cells. <sup>Ω</sup>	Is mainly expressed in the non-ciliated principal cells of the proximal ex-current ducts which are implicated in testicular fluid reabsorption and sperm concentration. Crucial for male fertility. The role in the female reproductive tract is unclear.	Regulates migration and adhesion of human lymphatic endothelial cells in vitro <sup>†</sup> Regulates B-cell development. <sup>‡</sup> Potential functional involvement in tissue homeostasis and inflammation. Pan-granulocyte aGPCR in humans that triggers antimicrobial effector functions. <sup>2</sup>
Ligands <sup>(3)</sup>		Collagen III <sup>Σ</sup> Transglutaminase 2 <sup>δ</sup>	-	Beclometasone dipropionate <sup>(214)</sup> (commercial)
Disorders		Bilateral frontoparietal polymicrogyria (BFPP) <sup>U</sup> <sup>(198, 217) (218) (201) (219, 220)</sup>  Soluble GPR56 (sGPR56) is elevated in certain chronic inflammatory diseases such as rheumatoid arthritis. <sup>ψ</sup> <sup>(221)</sup>	Disruption led to severe subfertility or complete infertility in male, female unaffected. <sup>W</sup> <sup>(191, 211, 212)</sup> Identified as another disease-causing gene of Congenital Bilateral Absence of Vas Deferens (CBAVD). <sup>(222)</sup>	GPR97 contributes to renal injury and inflammation in an acute kidney injury animal model by controlling the expression and activity of human antigen R (HuR), which is a RNA binding protein to regulate the stability of pro-inflammatory cytokine mRNAs <sup>(223)</sup> Insignificant for inflammation in an ovalbumin-induced asthma model (mice). <sup>(224)</sup>
Knock out		Loss of ADGRG1 (GPR56) resulted in decreased granule cell adhesion to laminin and fibronectin (mice) <sup>π</sup> <sup>(196)</sup>	Infertility due to sperm stasis and duct obstruction by abnormal fluid reabsorption (mice) <sup>(211)</sup>	Important role in experimental autoimmune encephalomyelitis (EAE) (primary animal model of multiple sclerosis). Deficient mice with EAE

	<p>Decreased cellular adhesion of acute myeloid leukemia (AML) cells to fibronectin, laminin-1, and collagen III, corresponding to a significant decrease in the number of hematopoietic stem cells (HSCs) in the bone marrow and, conversely, an increase in HSC number in spleen, liver, and peripheral blood (mice).<sup>μ</sup>(202)</p> <p>Cerebellar malformation (mouse)<sup>(196, 197)</sup></p> <p>Male-specific sterility, malformation of male gonad (mouse)<sup>(191)</sup></p>		<p>exhibited increases in peak severity and the cumulative disease score compared with the control, followed by a notable increase of leukocyte infiltration and more extensive demyelination <sup>(216)</sup></p>
<b>SNP</b>	-	-	-
<b>Tumorigenesis</b>	<p>The function of ADGRG1 (GPR56) in cancer seems to be cell/context specific.</p> <p>Expression inversely correlated with the metastatic potential of melanoma cell lines<sup>(225, 226)</sup> and the re-expression of the receptor led to a reduction in melanoma growth and metastasis.<sup>κ</sup>(227) Found to be upregulated in various cancer types and in tumor cell lines.<sup>(228-230)</sup> Inhibits mesenchymal differentiation and radioresistance in Glioblastoma.<sup>(231)</sup> Promotes proliferation of colorectal cancer cells and enhances metastasis.<sup>ν</sup> (232, 233) Prognostic factor in epithelial ovarian cancer and could promote the progression and invasion.<sup>φ</sup> (234) Associated with tumor progression in non-small-cell lung carcinoma.<sup>(235)</sup> Regulates the proliferation and invasion capacity of osteosarcoma cells.<sup>(192)</sup> Highly expressed in acute myeloid leukemia with poor outcome (significantly associated with high-risk genetic subgroups and poor outcome).<sup>(236)</sup> GPR56 as a novel marker in acute myeloid leukemia (AML) with high ecotropic viral integration site-1 (EVI1) expression.<sup>ρ</sup> (203)</p>	<p>The levels are significantly overexpressed in the Wnt signaling-dependent subgroup of medulloblastoma <sup>(238)</sup> and higher in Ewing sarcomas<sup>N</sup> (239)</p> <p>Overexpressed in parathyroid tumors from patients with primary hyperparathyroidism (PHPT).<sup>F</sup></p> <p>Involved in the adhesion and migration of certain breast cancer cells<sup>θ</sup>(240)</p> <p>Also has been found to be upregulated in various carcinomas, including prostate, kidney, breast and non-small cell lung cancer<sup>(239)</sup></p>	<p>Increases in acute and chronic inflamed and cancerous tissues.</p> <p>Adgrg3 is repressed by the transcription factor Pax5 but activated by the Pax5-Etv6 oncoprotein in B-cell acute lymphoblastic leukemia <sup>(241)</sup> (242)</p> <p>More infiltrating macrophages and higher tumor necrosis factor levels were identified in the liver and kidney of Adgrg3-deficient mice, compared to wild-type animals, in a high-fat diet-induced experimental obesity model<sup>(243)</sup></p>



	<p>Expression detected in human esophageal squamous cell carcinoma.<sup>(237)</sup></p> <p>Expression detected in breast cancer and pancreas carcinoma.<sup>(230)</sup> These studies indicated strongly a role of GPR56 in tumor cell adhesion, migration and survival/apoptosis.</p>		
--	--	--	--

α Regulates the integrity of pial basement membrane (BM) during cortical development<sup>(173)</sup>

β Via the Gα12/13 and RhoA signaling pathways its expression is high in the oligodendrocyte precursor cells and gradually decreased in oligodendrocyte maturation.<sup>(206, 207)</sup>

γ Via the Gα12/13 and mTOR pathways in muscle hypertrophy<sup>(244)</sup>

Ω Restrictively expressed in cytotoxic lymphocytes. Inhibitory receptor on human NK cells through cis-interaction with the tetraspanin CD81.<sup>(190)</sup>

Σ In the basement membrane activates the Gα12/13–RhoA pathway, inhibiting neuronal migration. To regulate cortical development and lamination.

δ Transglutaminase-2 (TG2) signals to ADGRG1 on oligodendrocytes precursor cells (OPC) in the presence of the ECM protein laminin activates of ADGRG1 and promotes OPC proliferation (myelin formation and repair).<sup>(206)</sup> GPR56 inhibits melanoma growth by internalizing and degrading its ligand TG2.<sup>(227)</sup>

ϑ A human brain cortical malformation called bilateral frontoparietal polymicrogyria cortex is associated with one of eleven different mutations of ADGRG1.

ψ The underlying mechanism and physio pathological role of GPR56 shedding are still elusive and the production of sGPR56 in vivo remains undetermined.

π Loss of GPR56 does not affect cell proliferation, migration, or neurite outgrowth

μ These data suggest that ADGRG1 (GPR56) plays a role in the maintenance of HSCs and/or leukemia stem cells in the bone marrow niche.

κ In melanoma, the regulatory mechanisms of GPR56 appear to involve protein kinase C (PKC) activation, vascular endothelial growth factor secretion, and tumor angiogenesis.

ξ Inhibitor of the nuclear factor kappa B (NF-κB) signaling pathway.

ν Metastasis by expediting epithelial-mesenchymal transition by activating PI3K/AKT signaling.

φ Via RhoA-GTP and down regulating the E-cadherin.

ρ GPR56 was found to be associated with high cell adhesion and anti-apoptotic activities in EVI1high AML through activation of RhoA signaling.

ω Signaling complex including ADGRG2, Gq, β-arrestin-1 and the ion channel CFTR, that specifically localizes in non-ciliated cells, is responsible for the regulation of Cl<sup>-</sup> and H<sup>+</sup> homeostasis and fluid reabsorption in the efferent ductules (basic for male fertility).<sup>(129)</sup>

η GPR64 promotes tumor invasion and metastasis through induction of the placental growth factor (PGF) and metalloproteinase (MMP1) expression.<sup>(239)</sup>

θ The truncated constitutively active, but not the full-length GPR64 physically interacts with calcium sensitive receptor (CaSR) and attenuates the CaSR-mediated intracellular Ca<sup>2+</sup> signaling and cAMP suppression in HEK293 cells. GPR64 may be a physiologic regulator of PTH release that is dysregulated in parathyroid tumors, and suggest a role for GPR64 in pathologic calcium sensing in PHPT.<sup>(245)</sup>

ι Via RhoA-SRE (G<sub>12/13</sub>) and Gαq-NFκB pathways.

ϰ Vitro via the small GTPases RhoA and Cdc42

ϱ Regulating Nf-κb activity

ζ Via MAPKs and NF-κB (are well-established signaling molecules involved in inflammatory responses). The majority of GPCR signal transduction in neutrophils is mediated through the Gβγ subunits of Gαi protein.<sup>(215, 246)</sup>

Subfamily		VIII (G)			
Gene name		GPR112	GPR114	GPR126	GPR128
Protein name (alternative names)		ADGRG4	ADGRG5	ADGRG6	ADGRG7
Chromosome <sup>(1)</sup> (human)		X	16	6	3
NTF architecture <sup>(2)</sup> (number of repetitions)		Laminin_G/Ptx	No specific domains	Laminin_G/Ptx, CUB	No specific domains
Expression <sup>(3)</sup> (human)	Absent in	-	-	-	-
	Present in	Mammary gland, kidney, blood vessel, retina, testis	Circulation granulocytes, colon, lung, spleen, thymus, pancreas islets of Langerhans, leukocytes, tonsil	Bone marrow hematopoietic stem/progenitor cells, vasculature endothelial cells, liver hepatocytes, pancreas endocrine cells (islets of Langerhans), placenta, skin epidermis keratinocytes, cartilage chondrocytes, PNS Schwann cells	Liver hepatocytes, small intestine, cervix, skin
Functional involvement		-	HSI	CC, CVS, RS, MS, NSB, SO <sup>(247-254)</sup>	-
Functional specifications		Potential roles in the regulation of secretion, immunity, and epithelial homeostasis (mice) <sup>(255)</sup>	Immune-related functions <sup>(256)</sup>	PNS myelination (important in development) <sup>∪</sup> , adult height (trunk height), pulmonary function, modulates both physiological and pathological angiogenesis <sup>ψ</sup> , regeneration of axons following injuries <sup>φ</sup>	-
Ligands <sup>(3)</sup>		-	Custom peptide GPR126	Collagen IV	
Disorders		-	-	Adolescent idiopathic scoliosis <sup>†</sup> Arthrogryposis multiplex congenita Intellectual disability <sup>(257)</sup>	Can contribute to the cellular events in adolescent idiopathic scoliosis <sup>‡ (258)</sup>
Knock out		-	-	Conditional loss of it in Schwann cells causes increased proliferation of this cell type <sup>(251)</sup> , essential in neural, cardiac, and ear development (mice)	Reduced body weight and increased intestinal contraction frequency (mouse) <sup>(259)</sup>
SNP		-	Differences in the Vitamin D metabolism <sup>(260)</sup>	Impaired pulmonary function in humans <sup>α(261)</sup> Variation in Height <sup>(262)</sup> Candidate genetic risk factor for aggressive periodontitis in the Japanese population <sup>(263)</sup>	-

<b>Tumorigenesis</b>	Upregulated in related primary neuroendocrine carcinoma and liver metastasis <sup>(264)</sup> High expression in ileal carcinoids <sup>(265)</sup>	-	High Prevalence of a Hotspot of Noncoding Somatic Mutations in Intron 6 of GPR126 in Bladder Cancer <sup>(266)</sup> Associated with reduced survival in breast cancer <sup>(267)</sup>	-
----------------------	---	---	--	---

2 The estrogens induced auto-proteolytic mechanism of the GAIN domain and activate via modulated by ESR $\alpha$  (estrogen receptor) and SP1 (specificity protein 1) complex.  
 U GPR126 drives the differentiation of Schwann cells through inducing cAMP levels, which causes Oct6 transcriptional activities to promote myelin gene activity. Domain-specific functions of GPR126 during Schwann cells development: the NTF is necessary and sufficient for axon sorting, while the CTF promotes wrapping through cAMP induction to regulate early and late stages of Schwann cells development.<sup>(268)</sup>  
 T Mouse models have shown GPR126 deletion to affect cartilage biology and spinal column development.<sup>(269)</sup>  
 Ψ GPR126 stimulates VEGF signaling and angiogenesis by modulating VEGF receptor 2 (VEGFR2) expression through STAT5 and GATA2 in endothelial cells.<sup>(247)</sup>  
 α Measured as the ratio of forced expiratory volume in the first second/forced vital capacity (FEV1/FVC), in a meta-analysis of 28,890 participants. May contribute to the physiological adaptations to hypobaric hypoxia, possibly by altering lung function.<sup>(270)</sup>  
 φ GPR126 is not necessary for normal myelin maintenance; knocking out Gpr126 without injuring nerves produced no change in myelination for up to 4 months.<sup>(252)</sup>

<b>Subfamily</b>	IX (V)	
<b>Gene name</b>	GPR98	
<b>Protein name (alternative names)</b>	ADGRV1 (VLGR1)	
<b>Chromosome <sup>(1)</sup> (human)</b>	5	
<b>NTF architecture <sup>(2)</sup> (number of repetitions)</b>	Calnexin beta (9), Laminin_G/Ptx, Calnexin beta (13), epitempin (6), Calnexin beta (13)	
<b>Expression <sup>(3)</sup> (human)</b>	<b>Absent</b>	Spleen, placenta and leukocytes
	<b>Present</b>	Many tissues including ovary, small intestine, colon, gastric mucosa, kidney, adrenal gland, testis, lung, thyroid, skeletal muscle, tongue, heart, brain, eye, cochlea, spinal cord and foreskin fibroblasts
<b>Functional involvement</b>	MS, SO <sup>(207, 271-273)</sup>	
<b>Functional specifications</b>	Necessary for healthy bone mineral density, regulates myelin associated protein (MAG) expression in myelinated regions $\Psi$ , essential for the correct development of mechanosensitive hair bundles (in hair cells is part of the ankle-link complex), required for the assembly of fibrous links communicating between the membranes of the ciliary pocket (photoreceptor cells)	
<b>Ligands <sup>3</sup></b>	-	
<b>Disorders</b>	Usher syndrome, <sup>(274)</sup> low expression is a significant risk factor of epileptic seizures in patients with Low Grade Glioma, <sup>(275, 276) (277) (278)</sup>	
<b>Knock out</b>	Leads to abnormal stereociliary development and hearing loss <sup>(279)</sup>	
<b>SNP</b>	Increased risk of fractures <sup>(271)</sup>	
<b>Tumorigenesis</b>	-	

$\Psi$  MAG is a cell membrane glycoprotein identified as an inhibitor of axon growth in the CNS after injury. Downstream signaling occurs through  $G\alpha_s/G\alpha_q$ , activating PKA and protein kinase C (PKC) respectively. Then post-translational regulation of MAG occurs. Work has shown that elevating cellular levels of cyclic AMP (which activates PKA) can block the inhibitory effects of MAG in the setting of nerve injury and perhaps lead to increased axonal regeneration. <sup>(280-282)</sup>

## 7.2. BIBLIOGRAPHY

- <sup>1</sup> <https://www.ensembl.org> (10/01/2019)
- <sup>2</sup> T. Langenhan; G. Aust; J. Hamann. *Science Signal*. **2013**, *6*, 1-22
- <sup>3</sup> <https://www.guidetopharmacology.org> - Adhesion Class GPCRs (10/01/2019)
- <sup>4</sup> B. Davletov; F. Meunier; A. Ashton; H. Matsushita; W. Hirst; V. Lelianova. *EMBO J*. **1998**, *17*, 3909-3920
- <sup>5</sup> A. C. Ashton; V. Lelianova; E. Orlova; C. Van Renterghem; M. Canepari; M. Seagar. *J. Biol. Chem*. **2001**, *276*, 44695-44703
- <sup>6</sup> M. Capogna; K. Volynski; Y. Ushkaryov. *J. Neurosci*. **2003**, *23*, 4044-4053
- <sup>7</sup> K. Volynski; J. L. Silva; M. A. Rahman; C. Hopkins; Y. Ushkaryov. *EMBO J*. **2004**, *23*, 4423-4433
- <sup>8</sup> S. Doyle; M. Scholz; K. Greer; A. Hubbard; D. Darnell; P. Antin. *Dev. Dyn*. **2006**, *235*, 3213-3221
- <sup>9</sup> M. O'Sullivan; J. de Wit; J. Savas; D. Comoletti; S. Otto-Hitt; J. Yates. *Neuron*. **2012**, *73*, 903-910
- <sup>10</sup> D. Favara; A. Banham; A. Harris. *Biochem Soc Trans*. **2014**, *42*, 1658-1664
- <sup>11</sup> M. Vezain; M. Lecuyer; M. Rubio; V. Dupé; L. Ratié; V. David. *Acta Neuropathol. Commun*. **2018**, *6*, 1-23
- <sup>12</sup> M. Bonaglia; S. Marelli; F. Novara; S. Commodaro; R. Borgatti; G. Minardo. *Eur. J. Hum. Genet*. **2010**, *18*, 1302-139
- <sup>13</sup> M. Arcos-Burgos; D. Wallis. *Mol. Psychiatry*. **2010**, *15*, 1053-1066
- <sup>14</sup> S. Domené; H. Stanescu; D. Wallis; B. Tinloy; D. Pineda; R. Kleta. *Am. J. Med. Genet. B. Neuropsychiatr. Genet*. **2011**, *156*, 11-8
- <sup>15</sup> M. Ribasés; J. Ramos-Quiroga; C. Sánchez-Mora; R. Bosch; V. Richarte; G. Palomar. *Genes Brain Behav*. **2011**, *10*, 149-157
- <sup>16</sup> Z. Kocibalova; M. Guzyova; D. Imrichova; Z. Sulova; A. Breier. *Gen. Physiol. Biophys*. **2018**, *37*, 353-357
- <sup>17</sup> M. Jeon; J. Yun; H. Kim; S. Han. *Cancer Res. Treat*. **2016**, *48*, 676-686
- <sup>18</sup> Z. Kan; B. Jaiswal; J. Stinson; V. Janakiraman; D. Bhatt; H. Stern. *Nature*, **2010**, *466*, 869-873
- <sup>19</sup> J. Ziegler; R. Pody; P. Coutinho; B. Evans; D. Saunders; N. Smith. *Neuro. Oncol*. **2017**, *19*, 175-185
- <sup>20</sup> H. Lin; D. Faunce; M. Stacey, A. Terajewicz; T. Nakamura; J. Zhang-Hoover. *J. Exp. Med*. **2005**, *201*, 1615-1625
- <sup>21</sup> H. Warschkau; A. Kiderlen. *J. Immunol*. **1999**, *163*, 3409-3416
- <sup>22</sup> S. Yona; H. Lin; P. Dri; J. Davies; R. Hayhoe; S. Lewis. *FASEB J*. **2008**, *22*, 741-751
- <sup>23</sup> S. Yona; H. Lin; W. Siu; S. Gordon; M. Stacey. *Trends Biochem. Sci*. **2008**, *33*, 491-500
- <sup>24</sup> Y. Huang; N. Chiang; C. Hu; C. Hsiao; K. Cheng; W. Tsai. *Mol. Cell. Biol*. **2012**, *32*, 1408-1420
- <sup>25</sup> Y. Huang; C. Hu; W. Tseng; C. Cheng; M. Stacey. *Front. Immunol*. **2017**, *373*, 1-13
- <sup>26</sup> J. Hamann; M. Kwakkenbos; E. de Jong; H. Heus; A. Olsen; R. van Lier. *Eur. J. Immunol*. **2003**, *33*, 1365-1371
- <sup>27</sup> I. Caminschi; S. Vandenabeele; M. Sofi; A. McKnight; N. Ward; T. Brodnicki. *DNA seq*. **2006**, *17*, 8-14
- <sup>28</sup> J. Hamann; E. Hartmann; R. van Lier. *Genomics*. **1996**, *32*, 144-147
- <sup>29</sup> J. Leemans; A. te Velde; S. Florquin; R. Bennink; K. de Bruin; R. van Lier. *J. Immunol*. **2004**, *172*, 1125-1131
- <sup>30</sup> M. Capasso; L. Durrant; M. Stacey; S. Gordon; J. Ramage; I. Spendlove. *J. Immunol*. **2006**, *177*, 1070-1077
- <sup>31</sup> M. van Pel; H. Hagoort; M. Kwakkenbos. J. Hamann; W. Fibbe. *Haematologica*. **2008**, *93*, 601-604
- <sup>32</sup> G. Aust; C. Kerner; S. Gonsior; D. Sittig; H. Schneider; P. Buske. *Mol. Bio. Cell*. **2013**, *24*, 2256-2268
- <sup>33</sup> J. C. Carr; S. K. Sherman; D. Wang; F. S. Dahdaleh; A. M. Bellizzi; M. S. O'Dorisio. *Annals of surgical oncology* **2013**, *20*, S739-s46

- <sup>34</sup> J. Davies; H. Lin; M. Stacey; S. Yona; G. Chang; S. Gordon. *Oncol. Rep.* **2011**, *25*, 619-627
- <sup>35</sup> M. Rutkowski; M. Sughrue; A. Kane; J. Kim; O. Bloch; A. Parsa. *J. Neurooncol.* **2011**, *105*, 165-171
- <sup>36</sup> G. Aust; J. Hamann; N. Schilling; M. Wobus. *Virchows Arch.* **2003**, *443*, 32-37
- <sup>37</sup> A. Feliciano; Y. Garcia-Mayea; L. Jubierre; C. Mir; M. Hummel; J. Castellvi. *Cell Death Dis.* **2017**, *8*, e3141
- <sup>38</sup> G. E. Aust; S. Laue; I. Lehmann; N. Heldin; O. Lotz; W. Scherbaum. *Cancer Res.* **1997**, *57*, 1798-1806
- <sup>39</sup> S. D. Ackerman; R. Luo; Y. Poitelon; A. Mogha; B. L. Harty; M. D'Rozario. *J. Exp. Med.* **2018**, *215*, 941-961
- <sup>40</sup> J. Galle; D. Sittig; I. Hanisch; M. Wobus; E. Wandel; M. Loeffler. *Am. J. Pathol.* **2006**, *169*, 1802-1811
- <sup>41</sup> S. D. Ackerman; C. Garcia; X. Piao; D. H. Gutmann; K. R. Monk. *Nature* **2015**, *6*, 1-4
- <sup>42</sup> D. M. Ariestanti; H. Ando; S. Hirose; N. Nakamura. *J. Biol. Chem.* **2015**, *290*, 11032-1140
- <sup>43</sup> E. Coustan-Smith; G. Song; C. Clark; L. Key; P. Liu; M. Mehrpooya. *Blood* **2011**, *117*, 6267-6276
- <sup>44</sup> C. Li; D. Liu; G. Li; H. Wang; X. Li; W. Zhang. *World J. Gastroenterol.* **2015**, *21*, 6215-6228
- <sup>45</sup> G. Antoni; P. E. Morange; Y. Luo; N. Saut; G. Burgos; S. Heath. *JTH.* **2010**, *8*, 2671-2679
- <sup>46</sup> F. Izadyar; J. Wong; C. Maki; J. Pacchiarotti; T. Ramos; K. Howerton. *Hum. Reprod.* **2011**, *26*, 1296-1306
- <sup>47</sup> Y. Wu; W. Chen; L. Gong; C. Ke; H. Wang; Y. Cai. *Med. Sci. Monit.* **2018**, *24*, 6608-6616
- <sup>48</sup> S. Berger-Müller; T. Suzuki. *Mol. Neurobiol.* **2011**, *44*, 313-320
- <sup>49</sup> A. Goffinet; F. Tissir. *Semin. Cell. Dev. Biol.* **2017**, *69*, 102-110
- <sup>50</sup> D. Strutt; R. Johnson; K. Cooper. *Curr. Biol.* **2002**, *12*, 813-824
- <sup>51</sup> D. Devenport; D. Oristian; E. Heller; E. Fuchs. *Nat. Cell. Biol.* **2011**, *13*, 893-902
- <sup>52</sup> S. J. Warrington; H. Strutt; D. Strutt. *Development* **2013**, *5*, 1045-1554
- <sup>53</sup> T. Nishimura; H. Honda; M. Takeichi. *Cell.* **2012**, *149*, 1084-1097
- <sup>54</sup> Y. Zhan; Q. Luo; X. Zhang; N. Xiao; C. Lu; C. Yue. *Biochemistry* **2016**, *81*, 591-599
- <sup>55</sup> Y. Yamada; N. Fuku; M. Tanaka; Y. Aoyagi; M. Sawabe; N. Metoki. *Atherosclerosis* **2009**, *207*, 144-149
- <sup>56</sup> L. Yates; C. Schnatwinkel; J. Murdoch; D. Bogani; C. Formstone; S. Townsend. *Hum. Mol. Genet.* **2010**, *19*, 2251-2267
- <sup>57</sup> L. Yates; J. Papakrivopoulou; D. Long; P. Goggolidou; J. Connolly; A. Woolf. *Hum. Mol. Genet.* **2010**, *19*, 4663-4676
- <sup>58</sup> M. Cetera; L. Leybova; F. Woo; M. Deans; D. Devenport. *Dev. Biol.* **2017**, *428*, 188-203
- <sup>59</sup> J. Duncan; M. Stoller; A. Francl; F. Tissir; D. Devenport; M. Deans. *Dev. Biol.* **2017**, *423*, 126-137
- <sup>60</sup> T. S. Usui; Y. Shimada; S. Hirano; R. Burgess; T. Schwarz; M. Takeichi; T. Uemura. *Cell.* **1999**, *98*, 585-595
- <sup>61</sup> D. Matsubara; S. Horiuchi; K. Shimonono; T. Usui; T. Uemura. *Genes Dev.* **2011**, *25*, 1982-1996
- <sup>62</sup> S. Hakeda; T. Suzuki. *Genes Cells.* **2013**, *18*, 960-973
- <sup>63</sup> E. H. Najjarro; B. Ackley. *Dev. Biol.* **2013**, *377*, 224-235
- <sup>64</sup> S. Kathiresan; B. Voight; S. Purcell; K. Musunuru; D. Ardissino; P. Mannucci. *Nat. Genet.* **2009**, *41*, 334-341
- <sup>65</sup> L. Qi; J. Ma; Q. Qi; J. Hartiala; H. Allayee; H. Campos. *Circulation.* **2011**, *123*, 374-380
- <sup>66</sup> C. Cortijo; M. Gouzi; F. Tissir; A. Grapin-Botton. *Cell. Rep.* **2012**, *2*, 1593-1606
- <sup>67</sup> Y. Shima; S. Kawaguchi; K. Kosaka; M. Nakayama; M. Hoshino; Y. Nabeshima. *Nat. Neurosci.* **2007**, *10*, 963-969
- <sup>68</sup> Y. Qu; Y. Huang; J. Feng; G. Alvarez-Bolado; E. Grove; Y. Yang. *Proc. Natl. Acad. Sci. USA.* **2014**, *111*, e2996-3004
- <sup>69</sup> G. Chai; L. Zhou; M. Manto; F. Helmbacher; F. Clotman; A. Goffinet. *Nat. Neurosci.* **2014**, *17*, 1171-1179
- <sup>70</sup> F. Wang; Q. Wang. C. Li; P. Yu; Y. Qu; L. Zhou. *Neuroscience* **2017**, *359*, 267-276
- <sup>71</sup> F. Tissir; A. Goffinet. *Nat. Rev. Neurosci.* **2013**, *14*, 525-535

- <sup>72</sup> V. Sasselli; W. Boesmans; P. V. Berghe; F. Tissir; A. Goffinet; V. Pachnis. *J. Clin. Investig.* **2013**, *123*, 1763-1772
- <sup>73</sup> J. Feng; Q. Xian; T. Guan; J. Hu; M. Wang; Y. Huang. *Cereb. Cortex.* **2016**, *26*, 3323-3334
- <sup>74</sup> R. Allache; P. De Marco; E. Merello; V. Capra; Z. Kibar. *Birth Defects Res. A Clin. Mol. Teratol.* **2012**, *94*, 176-181
- <sup>75</sup> M. Cho; S. Sharma; K. Glass; P. Castaldi; M. McDonald. *Am. J. Respir. Cell. Mol. Biol.* **2017**, *56*, 332-341
- <sup>76</sup> E. Einarsdottir; A. Grauers; J. Wang; H. Jiao; S. Escher; A. Danielsson. *PLoS One.* **2017**, *12*, e0189591
- <sup>77</sup> B. I. Bae; I. Tietjen; K. D. Atabay; G. D. Evrony; M. B. Johnson; E. Asare. *Science* **2014**, *343*, 764-768
- <sup>78</sup> A. J. Willsey; T. V. Fernandez; D. Yu; R. A. King; A. Dietrich; J. Xing. *Neuron.* **2017**, *94*, 486-499
- <sup>79</sup> L. Su; Z. Zhang; L. Gan; Q. Jiang; P. Xiao; J. Zou. *Exp. mol. pathol.* **2016**, *101*, 241-248
- <sup>80</sup> A. Ravni; Y. Qu; A. M. Goffinet; F. Tissir. *J. inv. dermatol.* **2009**, *129*, 2507-2509
- <sup>81</sup> Y. Qu; D. M. Glasco; L. Zhou; A. Sawant; A. Ravni; B. Fritsch. *J. Neurosci.* **2010**, *30*, 9392-9401
- <sup>82</sup> J. A. Curtin; E. Quint; V. Tsipouri; R. M. Arkell; B. Cattanaach; A. J. Copp. *Curr. Biol.* **2003**, *13*, 1129-1133
- <sup>83</sup> Y. Shima; M. Kengaku; T. Hirano; M. Takeichi; T. Uemura. *Developmental cell.* **2004**, *7*, 205-216
- <sup>84</sup> M. Erkan; N. Weis; Z. Pan; C. Schwager; T. Samkharadze; X. Jiang. *Molecular cancer* **2010**, *9*, 88
- <sup>85</sup> R. Sugimura; X. C. He; A. Venkatraman; F. Arai; A. Box; C. Semerad. *Cell.* **2012**, *150*, 351-365
- <sup>86</sup> F. Tissir; Y. Qu; M. Montcouquiol; L. Zhou; K. Komatsu; D. Shi. *Nat. Neurosci.* **2010**, *13*, 700-707
- <sup>87</sup> G. Ying; S. Wu; R. Hou; W. Huang; M. R. Capecchi; Q. Wu. *Mol. Cell. Biol.* **2009**, *29*, 3045-3061
- <sup>88</sup> J. Feng; Y. Xu; M. Wang; Y. Ruan; K. F. So; F. Tissir. *J. Neurosci.* **2012**, *32*, 13729-13743
- <sup>89</sup> L. Zhou; Y. Qu; F. Tissir; A. M. Goffinet. *Cereb. Cortex.* **2009**, *19*, 114-119
- <sup>90</sup> F. Tissir; I. Bar; Y. Jossin; O. De Backer; A. M. Goffinet. *Nat. Neurosci.* **2005**, *8*, 451-457
- <sup>91</sup> S. Kathiresan; O. Melander; C. Guiducci; A. Surti; N. P. Burt; M. J. Rieder. *Nat. Genet.* **2008**, *40*, 189-197
- <sup>92</sup> B. Vastrad; C. Vastrad; A. Godavarthi; R. Chandrashekar. *Medical oncology* **2017**, *34*, 182
- <sup>93</sup> M. Feve; J. M. Saliou; M. Zeniou; S. Lennon; C. Carapito; J. Dong. *PLoS One.* **2014**, *9*, e91519
- <sup>94</sup> J. Geradts; J. Groth; Y. Wu; G. Jin. *Breast cancer research and treatment* **2016**, *157*, 447-459
- <sup>95</sup> M. Katoh. *Int. J. Mol. Med.* **2007**, *20*, 405-409
- <sup>96</sup> L. Jiang; X. Zhang; C. Xiang; J. Geradts; Q. Wei; Y. Liang. *Histol. and histopathol.* **2018**, *33*, 835-842
- <sup>97</sup> K. Goryca; M. Kulecka; A. Paziewska; M. Dabrowska; M. Grzelak; M. Skrzypczak. *BMC genetics* **2018**, *19*, 85
- <sup>98</sup> G. H. Khor; G. R. Froemming; R. B. Zain; T. M. Abraham; T. K. Lin. *APJCP.* **2016**, *17*, 219-223
- <sup>99</sup> M. R. Morris; C. J. Ricketts; D. Gentle; F. McDonald; N. Carli; H. Khalili. *Oncogene* **2011**, *30*, 1390-1401
- <sup>100</sup> P. Jeong; Y. S. Ha; I. C. Cho; S. J. Yun; E. S. Yoo; I. Y. Kim. *Oncology letters* **2011**, *2*, 679-684
- <sup>101</sup> J. Shen; S. Wang; Y. J. Zhang; M. Kappil; H. C. Wu; M. G. Kibriya. *Hepatology* **2012**, *55*, 1799-1808
- <sup>102</sup> F. Marroni; A. Pfeufer; Y. S. Aulchenko; C. S. Franklin; A. Isaacs; I. Pichler. *Cir. Cardiovascular genet.* **2009**, *2*, 322-328
- <sup>103</sup> L. Fischer; C. Wilde; T. Schoneberg; I. Liebscher. *BMC genomics* **2016**, *17*, 609
- <sup>104</sup> Y. F. Chan; F. C. Jones; E. McConnell; J. Bryk; L. Bunger; D. Tautz. *Curr. Biol.* **2012**, *22*, 794-800
- <sup>105</sup> J. J. Kim; Y. M. Park; K. H. Baik; H. Y. Choi; G. S. Yang; I. Koh. *Human genetics* **2012**, *131*, 471-478
- <sup>106</sup> A. Tonjes; M. Koriath; D. Schleinitz; K. Dietrich; Y. Bottcher; N. W. Rayner. *Hum. Mol. Genet.* **2009**, *18*, 4662-4668
- <sup>107</sup> A. T. Kraja; I. B. Borecki; M. Y. Tsai; J. M. Ordovas; P. N. Hopkins; C. Q. Lai. *Lipids* **2013**, *48*, 155-165

- <sup>108</sup> J. D. Frenster; J. F. Inocencio; Z. Xu; J. Dhaliwal; A. Alghamdi; D. Zagzag. *Neurosurgery* **2017**, *64*, 177-181
- <sup>109</sup> P. Gromova; S. Ralea; A. Lefort; F. Libert; B. P. Rubin; C. Erneux. *J. Cell. Mol. Med.* **2009**, *13*, 1536-1548
- <sup>110</sup> S. Promel; H. Waller-Evans; J. Dixon; D. Zahn; W. H. Colledge; J. Doran. *Dev. Dyn.* **2012**, *241*, 1591-1602
- <sup>111</sup> J. P. Bridges; M. G. Ludwig; M. Mueller; B. Kinzel; A. Sato; Y. Xu. *Am. J. Respir. Cell. Mol. Biol.* **2013**, *49*, 348-357
- <sup>112</sup> K. Brown; A. Filuta; M. G. Ludwig; K. Seuwen; J. Jaros; S. Vidal. *JCI insight* **2017**, *2*, e93700
- <sup>113</sup> T. Fukuzawa; J. Ishida; A. Kato; T. Ichinose; D. M. Ariestanti; T. Takahashi. *PLoS One.* **2013**, *8*, e69451
- <sup>114</sup> M. Y. Yang; M. B. Hilton; S. Seaman; D. C. Haines; K. Nagashima; C. M. Burks. *Cell Rep.* **2013**, *3*, 1457-1464
- <sup>115</sup> H. M. Stoveken; A. G. Hajduczuk; L. Xu; G. G. Tall. *Proc. Natl. Acad. Sci. USA.* **2015**, *112*, 6194-6199
- <sup>116</sup> H. Y. Kim; A. A. Spector. *Mol. Asp. Med.* **2018**, *64*, 34-44
- <sup>117</sup> J. W. Lee; B. X. Huang; H. Kwon; M. A. Rashid; G. Kharebava; A. Desai. *Nature commun.* **2016**, *7*, 13123
- <sup>118</sup> D. Schneberger; J. M. DeVasure; S. A. Kirychuk; T. A. Wyatt. *PLoS One* **2018**, *13*, e0208597
- <sup>119</sup> B. Ma; J. Zhu; J. Tan; Y. Mao; L. Tang; C. Shen. *A. J. Cancer Res.* **2017**, *7*, 433-447
- <sup>120</sup> T. Nie; X. Hui; X. Gao; K. Li; W. Lin; X. Xiang. *FEBS letters* **2012**, *586*, 3618-3625
- <sup>121</sup> S. Lu; S. Liu; A. Wietelmann; B. Kojonazarov; A. Atzberger; C. Tang. *PLoS One.* **2017**, *12*, e0183166
- <sup>122</sup> Z. Liu; G. Zhang; C. Zhao; J. Li. *Med. Sci. Monit.* **2018**, *24*, 5216-5224
- <sup>123</sup> H. Shi; S. Zhang. *Biochem. Biophys. Res. Commun.* **2017**, *491*, 349-354
- <sup>124</sup> A. M. Lum; B. B. Wang; G. B. Beck-Engeser; L. Li; N. Channa; M. Wabl. *BMC cancer* **2010**, *10*, 40
- <sup>125</sup> R. R. Bhat; P. Yadav; D. Sahay; D. K. Bhargava; C. J. Creighton; S. Yazdanfard. *Breast Cancer Res. Treat.* **2018**, *170*, 279-292
- <sup>126</sup> J. Espinal-Enriquez; S. Munoz-Montero; I. Imaz-Rosshandler; A. Huerta-Verde; C. Mejia; E. Hernandez-Lemus. *BMC genomics* **2015**, *16*, 207
- <sup>127</sup> X. Zhu; G. Huang; P. Jin. *Path. Res. Pract.* **2018**, *215*, 539-545
- <sup>128</sup> S. K. Sherman; J. E. Maxwell; J. C. Carr; D. Wang; M. S. O'Dorisio; T. M. O'Dorisio. *J. Surg. Res.* **2014**, *190*, 587-593
- <sup>129</sup> W. Zhang; Q. Cui; W. Qu; X. Ding; D. Jiang; H. Liu. *Oncol. Rep.* **2018**, *40*, 206-216
- <sup>130</sup> L. Yang; X. L. Lin; W. Liang; S. W. Fu; W. F. Lin; X. Q. Tian. *Oncotarget.* **2017**, *8*, 47943-47956
- <sup>131</sup> G. Kang; W. C. Hwang; I. G. Do; K. Wang; S. Y. Kang; J. Lee. *PLoS One* **2013**, *8*, e82770
- <sup>132</sup> X. Tang; R. Jin; G. Qu; X. Wang; Z. Li; Z. Yuan; *Cancer Res.* **2013**, *73*, 6206-6218
- <sup>133</sup> B. Davidson; H. T. Stavnes; B. Risberg; J. M. Nesland; J. Wohlschlaeger; Y. Yang. *Hum. Pathol.* **2012**, *43*, 684-694
- <sup>134</sup> E. A. Billings; C. S. Lee; K. A. Owen; R. S. D'Souza; K. S. Ravichandran; J. E. Casanova. *Sci. Signaling* **2016**, *9*, ra14
- <sup>135</sup> C. Bolyard; W. H. Meisen; Y. Banasavadi-Siddegowda; J. Hardcastle; J. Y. Yoo; E. S. Wohleb. *Cli. Cancer Res. : an official journal of the American Association for Cancer Research* **2017**, *23*, 1809-1819
- <sup>136</sup> S. M. Cork; B. Kaur; N. S. Devi; L. Cooper; J. H. Saltz; E. M. Sandberg. *Oncogene.* **2012**, *31*, 5144-5152
- <sup>137</sup> S. Das; K. A. Owen; K. T. Ly; D. Park; S. G. Black; J. M. Wilson. *Proc. Natl. Acad. Sci. USA.* **2011**, *108*, 2136-2141
- <sup>138</sup> S. Das; A. Sarkar; K. A. Ryan; S. Fox; A. H. Berger; I. J. Juncadella. *Faseb j.* **2014**, *28*, 2214-2224
- <sup>139</sup> J. G. Duman; C. P. Tzeng; Y. K. Tu; T. Munjal; B. Schwechter; T. S. Ho. *J. Neurosci.* **2013**, *33*, 6964-6978



- <sup>140</sup> A. E. Hochreiter-Hufford; C. S. Lee; J. M. Kinchen; J. D. Sokolowski; S. Arandjelovic; J. A. Call *Nature* **2013**, *497*, 263-267
- <sup>141</sup> B. Kaur; D. J. Brat; C.C. Calkins; E. G. Van Meir. *Am. J. Pathol.* **2003**, *162*, 19-27
- <sup>142</sup> J. T. Koh; H. Kook; H. J. Kee; Y. W. Seo; B. C. Jeong; J. H. Lee. *Exp. Cell Res.* **2004**, *294*, 172-184
- <sup>143</sup> K. Mori; Y. Kanemura; H. Fujikawa; A. Nakano; H. Ikemoto; I. Ozaki. *Neurosc. Res.* **2002**, *43*, 69-74
- <sup>144</sup> H. Nishimori; T. Hiratsuchi; T. Urano; Y. Kimura; K. Kiyono; K. Tatsumi. *Oncogene.* **1997**, *15*, 2145-2150
- <sup>145</sup> D. Park; A. C. Tosello-Tramont; M. R. Elliott; M. Lu; L. B. Haney; Z. Ma. *Nature* **2007**, *450*, 430-434
- <sup>146</sup> J. D. Sokolowski; S. L. Nobles; D. S. Heffron; D. Park; K. S. Ravichandran; J. W. Mandell. *Brain, behavior, and immunity.* **2011**, *25*, 915-921
- <sup>147</sup> J. R. Stephenson; K. J. Paavola; S. A. Schaefer; B. Kaur; E. G. Van Meir; R. A. Hall. *J. Biol. Chem.* **2013**, *288*, 22248-22256
- <sup>148</sup> Z. Weng; C. Situ; L. Lin; Z. Wu; J. Zhu; R. Zhang. *Nature commun.* **2019**, *10*, 51
- <sup>149</sup> M. R. Elliott; S. Zheng; D. Park; R. I. Woodson; M. A. Reardon; I. J. Juncadella. *Nature* **2010**, *467*, 333-337
- <sup>150</sup> F. Mazaheri; O. Breus; S. Durdu; P. Haas; J. Wittbrodt; D. Gilmour. *Nature commun.* **2014**, *5*, 4046
- <sup>151</sup> D. Okajima; G. Kudo; H. Yokota. *JPS*, **2011**, *61*, 47-54
- <sup>152</sup> S. Y. Moon; S. A. Shin; Y. S. Oh; H. H. Park; C. S. Lee. *Genes* **2018**, *9*, 597
- <sup>153</sup> H. J. Kee; J. T. Koh; M. Y. Kim; K. Y. Ahn; J. K. Kim; C. S. Bae. *J. Cerebral blood flow and metabolism : official journal of the International Society of Cerebral Blood Flow and Metabolism* **2002**, *22*, 1054-1067
- <sup>154</sup> J. R. Stephenson; R. H. Purcell; R. A. Hall. *Trends Pharmacol. Sci.* **2014**, *35*, 208-215
- <sup>155</sup> B. C. Jeong; M. Y. Kim; J. H. Lee; H. J. Kee; D. H. Kho; K. E. Han. *FEBS letters* **2006**, *580*, 669-676
- <sup>156</sup> W. Kakegawa; N. Mitakidis; E. Miura; M. Abe; K. Matsuda; Y. H. Takeo. *Neuron.* **2015**, *85*, 316-329
- <sup>157</sup> H. J. Kee; K. Y. Ahn; K. C. Choi; J. W. Song; T. Heo; S. Jung. *FEBS letters* **2004**, *569*, 307-316
- <sup>158</sup> V. Lanoue; A. Usardi; S. M. Sigoillot; M. Talleur; K. Iyer; J. Mariani. *Mol. Psychiatry.* **2013**, *18*, 943-950
- <sup>159</sup> S. M. Sigoillot; K. Iyer; F. Binda; I. Gonzalez-Calvo; M. Talleur; G. Vodjdani. *Cell Rep.* **2015**, *10*, 820-832
- <sup>160</sup> N. Hamoud; V. Tran; T. Aimi; W. Kakegawa; S. Lahaie; M. P. Thibault. *Nature commun.* **2018**, *9*, 4470
- <sup>161</sup> N. Hamoud; V. Tran; L. P. Croteau; A. Kania; J. F. Cote. *Proc. Natl. Acad. Sci. U S A.* **2014**, *111*, 3745-3750
- <sup>162</sup> J. S. hoi; W. Y. Bae; S. Nam; J. W. Jeong. *Omics: J. Integr. Biol.* **2018**, *22*, 493-501
- <sup>163</sup> D. Zhu; E. G. Van Meir. *Oncotarget* **2016**, *7*, 17288-17289
- <sup>164</sup> A. M. Fond; C. S. Lee; I. G. Schulman; R. S. Kiss; K. S. Ravichandran. *J. Clin. Invest.* **2015**, *125*, 2748-2758
- <sup>165</sup> J. G. Duman; Y. K. Tu; K. F. Tolias. *Neural plasticity* **2016**, *2016*, 8301737
- <sup>166</sup> J. T. Koh; Z. H. Lee; K. Y. Ahn; J. K. Kim; C. S. Bae; H. H. Kim. *Brain Res. Mol. Brain Res.* **2001**, *87*, 223-237
- <sup>167</sup> R. H. Purcell; C. Toro; W. A. Gahl; R. A. Hall. *Hum. Mut.* **2017**, *38*, 1751-1760
- <sup>168</sup> R. Gupta; D. C. Nguyen; M. D. Schaid; X. Lei; A. N. Balamurugan; G. W. Wong. *J. Biol. Chem.* **2018**, *293*, 18086-18098
- <sup>169</sup> M. J. McCarthy; D. K. Welsh. *J. Biol. Rhyth.* **2012**, *27*, 339-352
- <sup>170</sup> A. McQuillin; M. Rizig; H. M. Gurling. *Pharmacogene. Genomics* **2007**, *17*, 605-617
- <sup>171</sup> D. Zhu; S. Osuka; Z. Zhang; Z. R. Reichert; L. Yang; Y. Kanemura. *Cancer cell* **2018**, *33*, 1004-1016

- <sup>172</sup> C. S. Lee; K. K. Penberthy; K. M. Wheeler; I. J. Juncadella; P. Vandenabeele; J. J. Lysiak. *Immunity* **2016**, *44*, 807-820
- <sup>173</sup> P. DeRosse; T. Lencz; K. E. Burdick; S. G. Siris; J. M. Kane; A. K. Malhotra. *Schizophrenia Bull.* **2008**, *34*, 1047-1053
- <sup>174</sup> Y. Fukushima; Y. Oshika; T. Tsuchida; T. Tokunaga; H. Hatanaka; H. Kijima. *Int. J. Oncol.* **1998**, *13*, 967-970
- <sup>175</sup> V. M. Zohrabian; H. Nandu; N. Gulati; G. Khitrov; C. Zhao; A. Mohan. *Oncol. Rep.* **2007**, *18*, 321-328
- <sup>176</sup> T. Izutsu; R. Konda; J. Sugimura; K. Iwasaki; T. Fujioka. *J. Urol.* **2011**, *185*, 2353-2358
- <sup>177</sup> W. Wang; R. Da; M. Wang; T. Wang; L. Qi; H. Jiang. *Oncol. Lett.* **2013**, *5*, 1513-1518
- <sup>178</sup> H. Hatanaka; Y. Oshika; Y. Abe; Y. Yoshida; T. Hashimoto; A. Handa. *Int. J. Mol. Med.* **2000**, *5*, 181-183
- <sup>179</sup> X. Tian; Q. Wang; Y. Li; J. Hu; L. Wu; Q. Ding. *POR.* **2015**, *21*, 195-201
- <sup>180</sup> W. H. Meisen; S. Dubin; S. T. Sizemore; H. Mathsyaraja; K. Thies; N. L. Lehman. *Mol. Cancer Therap.* **2015**, *14*, 307-314
- <sup>181</sup> D. G. Duda; M. Sunamura; L. Lozonschi; T. Yokoyama; T. Yatsuoka; F. Motoi. *British J. Cancer* **2002**, *86*, 490-496
- <sup>182</sup> S. Kudo; R. Sonda; W. Obara; D. Kudo; K. Tani; Y. Nakamura. *Oncol. Rep.* **2007**, *18*, 785-791
- <sup>183</sup> J. Hardcastle; K. Kurozumi; N. Dmitrieva; M. P. Sayers; S. Ahmad; P. Waterman. *Mol. Therap. : J. Am. Soc. Gene Therapy* **2010**, *18*, 285-294
- <sup>184</sup> Z. Kan; B. S. Jaiswal; J. Stinson; V. Janakiraman; D. Bhatt; H. M. Stern. *Nature* **2010**, *466*, 869-873
- <sup>185</sup> D. H. Nam; K. Park; Y. L. Suh; J. H. Kim. *Oncol. Rep.* **2004**, *11*, 863-869
- <sup>186</sup> V. B. Mathema; K. Na-Bangchang. *Critical reviews in oncology/hematology* **2017**, *111*, 81-86
- <sup>187</sup> T. Shiratsuchi; K. Oda; H. Nishimori; M. Suzuki; E. Takahashi; T. Tokino. *Biochem. Biophys. Res. Commun.* **1998**, *251*, 158-165
- <sup>188</sup> D. Okajima; G. Kudo; H. Yokota. *J. Recept. Signal Transd. Res.* **2010**, *30*, 143-153
- <sup>189</sup> G. S. Salzman; S. D. Ackerman; C. Ding; A. Koide; K. Leon; R. Luo. *Neuron.* **2016**, *91*, 1292-1304
- <sup>190</sup> G. W. Chang; C. C. Hsiao; Y. M. Peng; F. A. Vieira; N. A. Kragten; E. B. Remmerswaal. *Cell Rep.* **2016**, *15*, 1757-1770
- <sup>191</sup> G. Chen; L. Yang; S. Begum; L. Xu. *Dev. Dyn.* **2010**, *239*, 3358-3367
- <sup>192</sup> S. R. Chen; Y. X. Liu. *Biol. Reprod.* **2016**, *94*, 42
- <sup>193</sup> M. Della Chiesa; M. Falco; S. Parolini; F. Bellora; A. Petretto; E. Romeo. *Int. immunology* **2010**, *22*, 91-100
- <sup>194</sup> K. Y. Huang; H. H. Lin. *Front. Oncol.* **2018**, *8*, 304
- <sup>195</sup> S. J. Jeong; R. Luo; K. Singer; S. Giera; J. Kreidberg; D. Kiyozumi. *PLoS One* **2013**, *8*, e68781
- <sup>196</sup> S. Koirala; Z. Jin; X. Piao; G. Corfas. *J. Neurosci.* **2009**, *29*, 7439-7449
- <sup>197</sup> S. Li; Z. Jin; S. Koirala; L. Bu; L. Xu; R. O. Hynes. *J. Neurosci.* **2008**, *28*, 5817-5826
- <sup>198</sup> R. Luo; S. J. Jeong; Z. Jin; N. Strokes; S. Li; X. Piao. *Proc. Natl. Acad. Sci. U S A.* **2011**, *108*, 12925-12930
- <sup>199</sup> R. Luo; S. J. Jeong; A. Yang; M. Wen; D. E. Saslowsky; W. I. Lencer. *PLoS One* **2014**, *9*, e100043
- <sup>200</sup> Y. M. Peng; M. D. van de Garde; K. F. Cheng; P. A. Baars; E. B. Remmerswaal. *J. Leukoc. Biol.* **2011**, *90*, 735-740
- <sup>201</sup> X. Piao; R. S. Hill; A. Bodell; B. S. Chang; L. Basel-Vanagaite; R. Straussberg. *Science* **2004**, *303*, 2033-2036
- <sup>202</sup> Y. Saito; K. Kaneda; A. Suekane; E. Ichihara; S. Nakahata; N. Yamakawa. *Leukemia* **2013**, *27*, 1637-1649
- <sup>203</sup> Y. Saito; K. Morishita. *Jap. J. Clin. Hematol.* **2015**, *56*, 375-383
- <sup>204</sup> K. Singer; R. Luo; S. J. Jeong; X. Piao. *Mol. Neurobiol.* **2013**, *47*, 186-196
- <sup>205</sup> M. P. Wu; J. R. Doyle; B. Barry; A. Beauvais; A. Rozkalne; X. Piao. *The FEBS J.* **2013**, *280*, 6097-6113
- <sup>206</sup> S. Giera; Y. Deng; R. Luo; S. D. Ackerman; A. Mogha; K. R. Monk. *Nature Commun.* **2015**, *6*, 6121

- <sup>207</sup> P. Mehta; X. Piao. *Dev. Dyn.* **2017**, *246*, 275-284
- <sup>208</sup> J. Hamann; G. Aust; D. Arac; F. B. Engel; C. Formstone; R. Fredriksson. *Pharmacol. Rev.* **2015**, *67*, 338-367
- <sup>209</sup> C. Kirchhoff; C. Osterhoff; A. Samalecos. *Reproduction* **2008**, *136*, 235-245
- <sup>210</sup> J. Y. Yoo; J. I. Ahn; T. H. Kim; S. Yu; J. Y. Ahn; J. M. Lim. *Scient. Rep.* **2017**, *7*, 5021
- <sup>211</sup> B. Davies; C. Baumann; C. Kirchhoff; R. Ivell; R. Nubbemeyer; U. F. Habenicht. *Mol. Cell. Biol.* **2004**, *24*, 8642-8648
- <sup>212</sup> D. L. Zhang; Y. J. Sun; M. L. Ma; Y. J. Wang; H. Lin; R. R. Li. *Elife* **2018**, *7*, e33432
- <sup>213</sup> N. Valtcheva; A. Primorac; G. Jurisic; M. Hollmén; M. Detmar. *J. Biol. Chem.* **2013**, *288*, 35736-35748
- <sup>214</sup> J. Gupte; G. Swaminath; J. Danao; H. Tian; Y. Li; X. Wu. *FEBS Lett.* **2012**, *586*, 1214-1219
- <sup>215</sup> C. C. Hsiao; T. Y. Chu; C. J. Wu; M. van den Biggelaar; C. Pabst; J. Hébert. *Front. Immunol.* **2018**, *9*, 2830
- <sup>216</sup> J. J. Wang; L. L. Zhang; H. X. Zhang; C. L. Shen; S. Lu; Y. Kuang. *Cell Death & Disease* **2013**, *4*, e853
- <sup>217</sup> N. Bahi-Buisson; K. Poirier; N. Boddaert; C. Fallet-Bianco; N. Specchio; E. Bertini. *Brain* **2010**, *133*, 3194-3209
- <sup>218</sup> E. Parrini; A. R. Ferrari; T. Dorn; C. A. Walsh; R. Guerrini. *Epilepsia* **2009**, *50*, 1344-1353
- <sup>219</sup> C. C. Quattrocchi; G. Zanni; A. Napolitano; D. Longo; D. M. Cordelli; S. Barresi. *Neurogenet.* **2013**, *14*, 77-83
- <sup>220</sup> R. Santos-Silva; A. Passas; C. Rocha; R. Figueiredo; J. Mendes-Ribeiro; S. Fernandes. *Neuropediatrics* **2015**, *46*, 134-138
- <sup>221</sup> W. Y. Tseng; Y. J. Wu; T. Y. Yang; N. Y. Chiang; W. P. Tsai; S. Gordon. *J. Microbiol. Immunol. Infect.* **2018**, *51*, 485-491
- <sup>222</sup> O. Patat; A. Pagin; A. Siegfried; V. Mitchell; N. Chassaing; S. Faguer. *Am. J. Hum. Genet.* **2016**, *99*, 437-442
- <sup>223</sup> W. Fang; Z. Wang; Q. Li; X. Wang; Y. Zhang; Y. Sun. *J. Am. Soc. Nephrol.* **2018**, *29*, 1475-1489
- <sup>224</sup> J. P. Shi; X. N. Li; X. Y. Zhang; B. Du; W. Z. Jiang; M. Y. Liu. *PloS one* **2015**, *10*, e0131461
- <sup>225</sup> M. W. Millar; N. Corson; L. Xu. *Front. Oncol.* **2018**, *8*, 8
- <sup>226</sup> A. J. Zendman; I. M. Cornelissen; U. H. Weidle; D. J. Ruiter; G. N. van Muijen. *FEBS Lett.* **1999**, *446*, 292-298
- <sup>227</sup> L. Yang; S. Friedland; N. Corson; L. Xu. *Cancer Res.* **2014**, *74*, 1022-1031
- <sup>228</sup> S. Shashidhar; G. Lorente; U. Nagavarapu; A. Nelson; J. Kuo; J. Cummins. *Oncogene* **2005**, *24*, 1673-1682
- <sup>229</sup> T. Kausar; R. Sharma; M. R. Hasan; S. C. Tripathi; A. Saraya; T. K. Chattopadhyay. *Cancer Invest.* **2011**, *29*, 42-48
- <sup>230</sup> N. Ke; H. Ma; G. Diedrich; J. Chionis; G. Liu; D. H. Yu. *Biochem. Biophys Res. Commun.* **2008**, *366*, 314-320
- <sup>231</sup> M. Moreno; L. Pedrosa; L. Paré; E. Pineda; L. Bejarano; J. Martínez. *Cell Rep.* **2017**, *21*, 2183-2197
- <sup>232</sup> B. Ji; Y. Feng; Y. Sun; D. Ji; W. Qian; Z. Zhang. *Oncol. Rep.* **2018**, *40*, 1885-1896
- <sup>233</sup> G. Jin; K. Sakitani; H. Wang; Y. Jin; A. Dubeykovskiy; D. L. Worthley. *Oncotarget* **2017**, *8*, 40606-40619
- <sup>234</sup> Z. Liu; Z. Huang; W. Yang; Z. Li; S. Xing; H. Li. *Neoplasma* **2017**, *64*, 32-39
- <sup>235</sup> Y. Song; A. Li; L. Zhang; L. Duan. *Onco. Targets Ther.* **2016**, *9*, 4105-4112
- <sup>236</sup> H. R. Saha; K. Kaneda-Nakashima; S. Shimosaki; A. Suekane; B. Sarkar; Y. Saito. *Sci. Rep.* **2018**, *8*, 13741
- <sup>237</sup> N. Sud; R. Sharma; R. Ray; T. K. Chattopadhyay; R. Ralhan. *Cancer Lett.* **2006**, *233*, 265-270
- <sup>238</sup> K. L. Whittier; E. A. Boese; K. N. Gibson-Corley; P. A. Kirby; B. W. Darbro; Q. Qian. *Acta. Neuropathol. Commun.* **2013**, *1*, 66
- <sup>239</sup> G. H. S. Richter; A. Fasan; K. Hauer; T. G. P. Grunewald; C. Berns; S. Rössler. *J. Pathol.* **2013**, *230*, 70-81

- <sup>240</sup> M. C. Peeters; M. Fokkelman; B. Boogaard; K. L. Egerod; B. van de Water; A. P. Ijzerman. *Cell Signal*. **2015**, *27*, 579-88
- <sup>241</sup> A. Delogu; A. Schebesta; Q. Sun; K. Aschenbrenner; T. Perlot; M. Busslinger. *Immunity* **2006**, *24*, 269-281
- <sup>242</sup> L. Smeenk; M. Fischer; S. Jurado; M. Jaritz; A. Azaryan; B. Werner. *EMBO J*. **2017**, *36*, 718-735
- <sup>243</sup> J. Shi; X. Zhang; S. Wang; J. Wang; B. Du; Z. Wang. *Sci. Rep*. **2016**, *6*, 24649
- <sup>244</sup> J. P. White; C. D. Wrann; R. R. Rao; S. K. Nair; M. P. Jedrychowski; J. S. You. *Proc. Natl. Acad. Sci. USA*. **2014**, *111*, 15756-15761
- <sup>245</sup> N. Balenga; P. Azimzadeh; J. A. Hogue; P. N. Staats; Y. Shi; J. Koh. *J. Bone Min. Res*. **2017**, *32*, 654-666
- <sup>246</sup> K. Futosi; S. Fodor; A. Mócsai. *Int. Immunopharmacol*. **2013**, *17*, 638-650
- <sup>247</sup> H. Cui; Y. Wang; H. Huang; W. Yu; M. Bai; L. Zhang. *J. Biol. Chem*. **2014**, *289*, 34871-34885
- <sup>248</sup> F. S. Geng; L. Abbas; S. Baxendale; C. J. Holdsworth; A. G. Swanson; K. Slanchev. *Development* **2013**, *140*, 4362-4374
- <sup>249</sup> T. D. Glenn; W. S. Talbot. *Development* **2013**, *140*, 3167-3175
- <sup>250</sup> D. A. Lyons; W. S. Talbot. *Spring. Harb. Perspect. Biol*. **2014**, *7*, a020586
- <sup>251</sup> A. Mogha; A. E. Benesh; C. Patra; F. B. Engel; T. Schöneberg; I. Liebscher. *J. Neurosci.: Off. J. Soc. Neurosci*. **2013**, *33*, 17976-17985
- <sup>252</sup> A. Mogha; B. L. Harty; D. Carlin; J. Joseph; N. E. Sanchez; U. Suter. *J. Neurosci.: Off. J. Soc. Neurosci*. **2016**, *36*, 12351-12367
- <sup>253</sup> K. R. Monk; K. Oshima; S. Jörs; S. Heller; W. S. Talbot. *Development* **2011**, *138*, 2673-2680
- <sup>254</sup> C. Patra; K. R. Monk; F. B. Engel. *Recep. Clin. Invest*. **2014**, *1*, 79
- <sup>255</sup> J. Ito; M. Ito; H. Nambu; T. Fujikawa; K. Tanaka; H. Iwaasa. *Cell. Tissue. Res*. **2009**, *338*, 257-269
- <sup>256</sup> Y. M. Peng; M. D. B. van de Garde; K. F. Cheng; P. A. Baars; E. B. M. Remmerswaal; R. A. W. van Lier. *J. Leukoc. Biol*. **2011**, *90*, 735-740
- <sup>257</sup> M. Hosseini; Z. Fattahi; S. S. Abedini; H. Hu; H. H. Ropers; V. M. Kalscheuer. *Am. J. Med. Gen. Part A* **2019**, *179*, 13-9
- <sup>258</sup> A. Hassan; E. T. Bagu; M. Levesque; S. A. Patten; S. Benhadjeba; L. Edjekouane. *Biol. Open* **2019**, *8*, bio037390
- <sup>259</sup> Y. Y. Ni; Y. Chen; S. Y. Lu; B. Y. Sun; F. Wang; X. L. Wu. *World J. Gastroenterol*. **2014**, *20*, 498-508
- <sup>260</sup> C. D. Engelman; K. J. Meyers; J. T. Ziegler; K. D. Taylor; N. D. Palmer; S. M. Haffner. *J. Steroid. Biochem. Mol. Biol*. **2010**, *122*, 186-192
- <sup>261</sup> D. B. Hancock; M. Eijgelsheim; J. B. Wilk; S. A. Gharib; L. R. Loehr; K. D. Marciante. *Nature genetics* **2010**, *42*, 45-52
- <sup>262</sup> G. Lettre; A. U. Jackson; C. Gieger; F. R. Schumacher; S. I. Berndt; S. Sanna. *Nature genetics* **2008**, *40*, 584-591
- <sup>263</sup> J. Kitagaki; S. Miyauchi; Y. Asano; A. Imai; S. Kawai; I. Michikami. *PloS One* **2016**, *11*, e0160765
- <sup>264</sup> J. Leja; A. Essaghir; M. Essand; K. Wester; K. Oberg; T. H. Tötterman. *Mod. Pathol*. **2009**, *22*, 261-272
- <sup>265</sup> O. Nilsson. *Neuroendocrinology* **2013**, *97*, 7-18
- <sup>266</sup> S. Garinet; G. Pignot; S. Vacher; C. Le Goux; A. Schnitzler; W. Chemlali. *Mol. Cancer Res*. **2019**, *17*, 469-475
- <sup>267</sup> A. Fatima; F. Tariq; M. F. A. Malik; M. Qasim; F. Haq. *J. Breast Cancer*. **2017**, *20*, 246-253
- <sup>268</sup> S. C. Petersen; R. Luo; I. Liebscher; S. Giera; S. J. Jeong; A. Mogha. *Neuron*. **2015**, *85*, 755-769
- <sup>269</sup> C. M. Karner; F. Long; L. Solnica-Krezel; K. R. Monk; R. S. Gray. *Hum. Mol. Genet*. **2015**, *24*, 4365-4373
- <sup>270</sup> C. A. Eichstaedt; L. Pagani; T. Antao; C. E. Inchley; A. Cardona; A. Mörseburg. *Sci. Rep*. **2017**, *7*, 13042
- <sup>271</sup> T. Urano; M. Shiraki; H. Yagi; M. Ito; N. Sasaki; M. Sato. *J. Clin. Endocrinol. Metab*. **2012**, *97*, E565-E574

- <sup>272</sup> J. Yang; X. F. Huang; Y. Tong; Z. B. Jin. *Clinical & Experimental Ophthalmology* **2016**, *44*, 197-199
- <sup>273</sup> D. Shin; S. T. Lin; Y. H. Fu; L. J. Ptáček. *Pro. Nat. Acad. Sci. USA*. **2013**, *110*, 19101-19106
- <sup>274</sup> Q. X. Hu; J. H. Dong; H. B. Du; D. L. Zhang; H. Z. Ren; M. L. Ma. *J. Biol. Chem.* **2014**, *289*, 24215-24225
- <sup>275</sup> Y. Wang; X. Fan; W. Zhang; C. Zhang; J. Wang; T. Jiang. *J. Neuro-oncol.* **2015**, *121*, 609-616
- <sup>276</sup> T. Maerker; E. van Wijk; N. Overlack; F. F. J. Kersten; J. McGee; T. Goldmann. *Hum. Mol. Genet.* **2008**, *17*, 71-86
- <sup>277</sup> J. Reiners; E. van Wijk; T. Märker; U. Zimmermann; K. Jürgens; H. te Brinke. *Hum. Mol. Genet.* **2005**, *14*, 3933-3943
- <sup>278</sup> M. Zallocchi; D. Delimont; D. T. Meehan; D. Cosgrove. *J. Neurosci. : Off. J. Soc. Neurosci.* **2012**, *32*, 13841-13859
- <sup>279</sup> J. P. Sun; R. Li; H. Z. Ren; A. T. Xu; X. Yu; Z. G. Xu. *J. Mol. Neurosci.* **2013**, *50*, 204-214
- <sup>280</sup> M. E. DeBellard; S. Tang; G. Mukhopadhyay; Y. J. Shen; M. T. Filbin. *Mol. Cell. Neurosci.* **1996**, *7*, 89-101
- <sup>281</sup> D. D. Li; S. A. Li. *J. Finance* **1996**, *51*, 691-709
- <sup>282</sup> L. McKerracher; S. David; D. L. Jackson; V. Kottis; R. J. Dunn; P. E. Braun. *Neuron*. **1994**, *13*, 805-811